

Investigations of rapid groundwater flow and karst in the Chalk

by

Louise Maurice

A thesis submitted to University College London for the degree of Doctor of Philosophy

2009

I, Louise Maurice, confirm that the work presented in this thesis is my own. Where information has been derived from other sources, I confirm that this has been indicated in the thesis.

Abstract

This study, with fieldwork undertaken in the Pang and Lambourn catchments in Southern England, investigates the occurrence and distribution of rapid groundwater flow in the Chalk and evaluates the degree of karstification.

A survey of surface karst features revealed a clear spatial pattern in their distribution with three distinctive geomorphological zones. Stream sinks and dolines occur frequently in Zone 1 where there is extensive Palaeogene cover. Only dolines are present in Zone 2 where Clay-with-Flints deposits overlie areas of the Chalk and there is little surface karst, other than dry valleys, in Zone 3 where the Chalk outcrops.

Tracer tests from three stream sinks in Zone 1 demonstrated connections to springs and rapid groundwater flow ($1-6 \text{ km.d}^{-1}$) indicating connected networks of conduits and large fissures over distances up to 5.1 km. Rapid flow was accompanied by variable tracer attenuation. Unsuccessful results at two other stream sinks were probably due to total attenuation. Further investigation at one site using four dyes and one bacteriophage tracer demonstrated the occurrence of diffusion (probably into the Chalk matrix), but indicated that diffusion is only a minor contributor to attenuation. Very high tracer losses ($\sim 75\%$ of dye and $\sim 99\%$ of bacteriophage) appear to be due to transport down multiple flowpaths, many comprising at least one section in which flow is through narrow fissures and fractures.

The Single Borehole Dilution technique was developed to identify the distribution of flowing horizons in all three zones. Flow horizons decrease with depth below ground level but have an average spacing of $\sim 9 \text{ m}$. Comparison with borehole imaging data suggested that solutional enlargement of fractures to form fissures, tubules and small conduits is common in all areas, but that these features may have limited lateral extent. Overall the Chalk appears to be mildly karstic with small-scale karst development resembling the early stages of speleogenesis.

Acknowledgements

Geological and other data from the British Geological Survey (BGS) was used in the construction of many map-based figures in this thesis and these include ^{BGS} in the figure caption. Figures using digital Ordnance Survey data contain the reference “© Crown Copyright. All Rights Reserved”, as stipulated by the license agreement.

The work described in this study was undertaken by the author as part of the NERC LOCAR programme (Lowland Catchment Research) grant NER/T/S/2001/00956.

There are so many people to thank for their help, including:

- Andy Farrant (BGS), who first inspired my interest in Chalk karst and who undertook the initial survey of karst features in the catchments.
- More than a hundred landowners of springs and stream sinks for granting access to their land, often with offers of cups of tea and biscuits.
- In particular the landowners of the Blue Pool for support during many tracer tests.
- Thames Water for granting access to Bradfield and Speen PWS for monitoring during tracer tests.
- John Bloomfield and Alex Gallagher (BGS) for helping with stream sink tracer injections.
- Pete Orton at the Environment Agency for supporting the SBDT work in the EA boreholes.
- Barry Townsend, John Bloomfield, Alex Gallagher, Ann Williams, Kate Griffiths, Magali Moreau, Jude Cobbing, Andrew Hughes (all BGS); Nigel Crooks (Lancaster University); and Tim Guilford for helping with the SBDT hosepipe injections.
- Dave Buckley (BGS) for succeeding in retrieving the jammed hosepipe out of the EA borehole at Great Shefford.
- Alex Gallagher and Dave Buckley (BGS) with whom I had several days in the field learning about geophysical logging, and who provided much of the imaging data used in this thesis.
- Barry Townsend for helping mend the things I broke and finding everything a fieldworker could possibly need from the BGS stores.
- Debbie Allen (BGS) for helping prepare tracers and standards.

- Ned Hughes and Roger Wyatt (CEH) who loaned water samplers and batteries, and helped with access to LOCAR boreholes.
 - The BGS workshop for mending the SBDT point injector kindly donated by Steve Fletcher (Environment Agency)
 - Chris Jackson (BGS) who wrote the macro used to process the raw SBDT data.
 - Simon Quinn (UCL) for great lunchtime chats during the long weeks of dye sample analysis at UCL.
 - Joel Rodet (Rouen University) who took Tim Atkinson and I to visit impressive chalk caves in France.
 - Pete Smart from whom I originally learned how to do catchment scale tracer tests and Single Borehole Dilution Tests at Bristol University.
-
- Ann Williams (BGS) who always had time to advise and support me whilst I was at BGS carrying out the work in this thesis.
 - John Barker (UCL) for his advice and encouragement as a PhD supervisor. John also wrote the SBDT forward modelling code, the tracer breakthrough curve model, and the matrix inversion for dye separation and patiently explained to a non-mathematician how these worked.
 - Tim Guilford, whose patience, moral support, and help during writing up were invaluable.

But I most want to thank Tim Atkinson for his inspiration, dedication and support. There were discussions in caves in Yorkshire and France, and conceptual models drawn on paper towels in cafes. Tim helped with the epic midnight multi-tracer injection at Smithcroft Copse. He read and commented on multiple versions of draft chapters. I came away from our meetings at UCL, which often extended late into the evening, excited by the work and inspired to do more.

Contents

Abstract	3
Acknowledgements	4
Contents	6
List of Figures	14
List of Tables	22
Chapter 1: The Chalk aquifer and karst	26
1.1 Introduction: Objectives and Thesis outline	26
1.2 Introduction to the Chalk	28
1.2.1 Chalk lithology	28
1.2.2 The UK Chalk outcrop	30
1.2.3 Chalk stratigraphy	31
1.3 Chalk Hydrogeology	33
1.3.1 The physical structure of the Chalk aquifer	33
1.3.2 Aquifer properties	35
1.3.2.1 The Chalk matrix	35
1.3.2.2 Hydraulic conductivity and transmissivity	37
1.3.2.3 Storage	41
1.3.3 Groundwater ages	43
1.3.4 Unsaturated zone flow	45
1.3.5 Tracer investigations of groundwater flow in the saturated zone	51
1.3.6 Aquifer contamination	54
1.4 General karst concepts	58
1.4.1 Definition of karst	58
1.4.2 Surface karst geomorphology	59
1.4.3 Epikarst	63
1.4.4 Karst hydrogeology	64
1.4.5 Controls on subsurface karst development	68

1.5 Chalk Karst Geomorphology	71
1.5.1 Introduction	71
1.5.2 Dry valleys and ephemeral streams	71
1.5.3 Dolines	73
1.5.4 Subsurface dissolution features	74
1.5.5 Stream Sinks	76
1.5.6 Springs	77
1.5.7 Chalk caves and conduits	78
1.6 Conclusions	83
Chapter 2: The Pang and Lambourn Study Area	85
2.1 Introduction	85
2.2 General topography	85
2.3 Drainage network	87
2.4 Geology	87
2.4.1 Solid geology	87
2.4.2 Drift geology	91
2.4.3 Geological structure	92
2.5 Springs	92
2.5.1 Springs in the Palaeogene and drift deposits	92
2.5.2 Chalk scarp slope springs	93
2.5.3 River valley chalk springs	94
2.6 Rainfall and evapotranspiration	95
2.7 Surface hydrology	95
2.8 Hydrogeology	103
2.8.1 Previous hydrogeological studies in the catchments	103
2.8.2 Recharge rates	104
2.8.3 Groundwater contours	105
2.8.4 Groundwater abstractions	108
2.8.5 Aquifer properties	111
2.8.5.1 Porosity	111

2.8.5.2 Transmissivity	115
2.8.5.3 Hydraulic conductivity	117
2.8.5.4 Storage properties	118
2.8.6 Groundwater levels in monitoring boreholes	118
2.8.6.1 Seasonal fluctuations in groundwater levels	118
2.8.6.2 Borehole water levels and river elevations	122
2.8.7 Water balance	124
2.9 Conclusions	125

Chapter 3: Karst Geomorphic Features in the Pang and Lambourn

Catchments	127
3.1 Introduction	127
3.2 The distribution of surface karst	128
3.3 Stream sinks	131
3.3.1 Introduction	131
3.3.2 Stream sink hydrology	131
3.3.3 Geomorphological classification of stream sinks	132
3.3.4 The nature and distribution of stream sinks in the Pang and Lambourn	136
3.3.5 Stream sink chemistry	140
3.3.6 Conclusions of stream sink survey	141
3.4 Chalk springs	142
3.4.1 Introduction	142
3.4.2 The River Lambourn	142
3.4.2.1 Introduction	142
3.4.2.2 Major springs	145
3.4.2.3 Smaller springs and groundwater seepages	148
3.4.2.4 The lower reaches of the River Lambourn	149
3.4.2.5 Summary of groundwater inputs to the River Lambourn	150
3.4.3 The River Pang	151
3.4.3.1 Introduction	151

3.4.3.2 Major springs	153
3.4.3.3 Summary of groundwater inputs to the River Pang	156
3.4.4 Springs outside the Pang-Lambourn topographic catchments	157
3.4.5 Spring catchment sizes	158
3.4.6 Conclusions of chalk spring survey	159
3.5 Dolines	160
3.6 Chieveley solution features	162
3.7 Relic Conduits in "Zone 1"	164
3.8 Surface Karst and Groundwater Flow	165
Chapter 4: Investigations of groundwater flowpaths using catchment scale	
tracer tests	167
4.1 Introduction	167
4.2 Tracer selection	170
4.3 Holly Grove, Tylers Lane and Smithcroft Copse	173
4.3.1 Tracer tests from Holly Grove and Tylers Lane stream sinks, 1988	173
4.3.2 Tracer testing from Smithcroft Copse stream sink, 2005	174
4.3.2.1 Objectives	174
4.3.2.2 Methods	174
4.3.2.3 Results	179
4.4 Photine tracer tests from Mirams Copse stream sink, Pang catchment, 2004	182
4.4.1 Introduction	182
4.4.2 Methods	182
4.4.3 Results	188
4.4.3.1 Background samples	188
4.4.3.2 Samples following tracer injections	189
4.4.3.3 Flow conditions and rainfall during tracer injections	189
4.5 Bacteriophage tracer testing from Mirams Copse and Frilsham sinks, Pang Catchment, 2006	192
4.5.1 Introduction	192
4.5.2 Methods	192

4.5.3 Results	196
4.5.3.1 Results of Mirams Copse injection	196
4.5.3.2 Results Frilsham injection	198
4.6 Bacteriophage tracer testing from Honeybottom and Cromwells sinks in the Winterbourne catchment, 2005	198
4.6.1 Introduction	198
4.6.2 Methods	198
4.6.3 Results	202
4.6.3.1 Background samples	202
4.6.3.2 Results of Cromwells injection	203
4.6.3.3 Results of Honeybottom injection	205
4.6.3.4 Comments on sample volumes used in analysis	205
4.7 Groundwater outlets and their catchment areas	205
4.7.1 Bagnor and Jannaways springs	205
4.7.2 The Blue Pool spring	207
4.7.3 Ingle and Jewells springs	211
4.7.4 Connectivity between stream sinks and boreholes	212
4.7.5 River-aquifer interactions	213
4.8 Groundwater velocities from natural gradient tracer tests	214
4.9 Tracer attenuation	216
4.10 Relationship between attenuation and velocity	220
4.11 Conclusions of qualitative tracer testing	221
Chapter 5: Investigations of groundwater flow and contaminant attenuation along the Smithcroft Copse-Blue Pool flowpath	
5.1 Introduction and background	222
5.2 Aims and experimental design	232
5.3 Experimental methods	233
5.3.1 Tracer Methods: Smithcroft Copse 2006 experiment	233
5.3.1.1 Tracer selection	233
5.3.1.2 Tracer quantity	234

5.3.1.3 Tracer injection	234
5.3.1.4 Sampling schedule	235
5.3.1.5 Tracer detection and measurement	236
5.3.2 Flow gauging and discharge monitoring (2005 and 2006 tests)	237
5.4 Results and discussion	238
5.4.1 Flow and stage results	238
5.4.1.1 Smithcroft Copse 2005 experiment	238
5.4.1.2 Smithcroft Copse 2006 experiment	238
5.4.2 Tracer breakthrough curves	239
5.4.2.1 Dye breakthrough curves at the Blue Pool spring	239
5.4.2.2 Breakthrough curves at the Blue Pool outlet	247
5.4.2.3 Dye breakthrough curve in the River Pang at Frogmore Farm	251
5.4.2.4 Comparison of the outlet and the spring monitoring points at the Blue Pool	253
5.4.2.5 Influence of photochemical decay on breakthrough curves	255
5.4.3 Tracer recoveries and mass balance	257
5.4.3.1 Introduction	257
5.4.3.2 Tracer recovery at the Blue Pool outlet	258
5.4.3.3 Tracer recovery at the main Blue Pool spring	261
5.4.3.4 Tracer recovery from the River Pang at Frogmore Farm	263
5.4.3.5 Evidence of diffusion from the tracer recovered in the main and secondary peaks	263
5.4.4 Discussion of sorption of dyes during the 2006 multi-tracer test	267
5.4.5 Advection-dispersion and double porosity modelled breakthrough curves	269
5.5 Summary and Interpretation	271
Chapter 6: Borehole investigations of groundwater flow in the Chalk	276
6.1 Introduction and background	276
6.2 Site selection and testing schedule	280
6.3 Methods	284

6.3.1 Field methods	284
6.3.1.1 Uniform injections	284
6.3.1.2 Point tracer injections	287
6.3.2 Raw data processing	287
6.3.3 Accuracy and precision of depth readings	288
6.3.4 Accuracy and precision of electrical conductance measurements	292
6.3.5 Uniform Injection SBDT data analysis methods	294
6.4 Results of uniform injection SBDTs	295
6.4.1 Tracer efflux times	295
6.4.2 Tracer decline through time	299
6.4.3 Electrical conductance logs	310
6.4.4 Seasonal variations in SBDT results	311
6.5 Identifying flowing features from SBDTs	317
6.5.1 Introduction	317
6.5.2 Forward modelling	317
6.5.2.1 Introduction and methodology	317
6.5.2.2 Simulations of tracer profiles: no vertical flow	320
6.5.2.3 Simulations of tracer profiles with vertical flow	326
6.5.2.4 Summary of borehole simulations	332
6.5.3 Point injection tests	333
6.5.3.1 Introduction	333
6.5.3.2 Point injection results	334
6.5.3.3 Vertical flow rates	356
6.5.3.4 Identifying flow horizons using point injection SBDTs	358
6.5.3.5 Implications of point injection results for interpretation of uniform injection SBDTs	363
6.5.3.6 Conclusions of point injection SBDTs	364
6.5.4 Integrated method of identifying flow horizons	365
6.5.5 Results: flowing features in boreholes from SBDTs	368
6.6 The nature of flow horizons	376
6.6.1 Introduction	376

6.6.2 Visible features on imaging data at class 1 flow horizons	376
6.6.3 Summary	385
6.7 Catchment scale patterns in the distribution of flow horizons	386
6.7.1 Introduction	386
6.7.2 Depth of flowing features below ground level	386
6.7.3 Depth of flowing features below the water table	387
6.7.4 Lateral persistence of flowing features	388
6.7.5 Catchment scale patterns in vertical flow	395
6.7.6 Spacing of flowing features	400
6.8 Summary and conclusions	403
Chapter 7: A conceptual model of the structure of the Chalk aquifer and its relation to geomorphology	
	406
7.1 Introduction	406
7.2 The structure of voids with water flow in the Chalk	406
7.2.1 General distribution of flow	406
7.2.2 Structure, size and lateral extent of dissolutional voids	407
7.2.3 Vertical development of permeability	408
7.3 Connectivity between void types	409
7.4 Surface karst geomorphology and permeability	411
7.4.1 Stream sinks and dolines	411
7.4.2 Permeability and removal of Palaeogene cover	414
7.5 Evaluation of the Chalk as a karstic aquifer	416
7.6 Thesis conclusions	421
References	422

List of Figures

Chapter 1

1.1 The location of the Pang-Lambourn study area and the distribution of the UK Chalk	26
1.2 Scanning electron photomicrograph of a chalk sample	29
1.3 Borehole images of marl and flint layers	30
1.4 Schematic representation of the geometric distinction between conduits and Fissures	35
1.5 Frequency distribution of UK chalk porosity	36
1.6 Distribution of Chalk transmissivity	38
1.7 Topographic control on the development of permeability	40
1.8 Tracer migration through the unsaturated zone matrix	46
1.9 Rapid downward movement of tracer measured using geophysics	49
1.10 Example of a karst landscape	58
1.11 Discharge from a karst spring in Kotor, Montenegro following a thunderstorm	60
1.12 Aerial photo of dolines in South Wales	61
1.13 Mechanisms of doline formation	63
1.14 Lack of continuity between boreholes due to a surface stream and a hidden karst conduit	65
1.15 Relationship between plan patterns of caves and porosity and recharge	67
1.16 Modified version of the four state model of cave development	70
1.17 Subsurface dissolution features	75
1.18 Stream sinks associated with the English Chalk	77
1.19 Chalk spring at Hungerford	78
1.20 Beachy Head Cave entrance	79
1.21 Chalk cave in Ireland	80
1.22 Passage in Caumont Cave, Normandy, France.	81
1.23 Passage in Petites Dalles Cave, Normandy, France	81
1.24 Survey of Petites Dalles Cave, France	82
1.25 Dissolution tubules, Beachy Head	83

1.26 Karst conduits in chalk	83
Chapter 2	
2.1 Topography of the Pang-Lambourn catchments	86
2.2 Solid Geology of the Pang-Lambourn catchments	90
2.3 Drift Geology of the Pang-Lambourn catchments	91
2.4 Springs emerging from Palaeogene and drift deposits in the lower Pang	93
2.5 Scarp slope springs, north of the Pang-Lambourn catchments	94
2.6 Chalk springs in the Pang and Lambourn river valleys	95
2.7 Flow in the River Lambourn at Shaw	96
2.8 Flow in the River Pang at Pangbourne	96
2.9 Location of River Lambourn and Pang gauging sites used by Griffiths et al. (2006)	99
2.10 Flow accretion in the River Lambourn (Griffiths et al., 2006)	100
2.11 Flow accretion in the River Lambourn (Grapes et al., 2005)	100
2.12 Flow accretion in the River Pang (Griffiths et al., 2006)	102
2.13 Groundwater contours in the Pang-Lambourn catchments	107
2.14 Location of licensed abstraction boreholes	108
2.15 Abstraction rates at major public water supplies between 1983 and 2003	110
2.16 Total abstraction from 16 PWS boreholes	110
2.17 Location of LOCAR boreholes with porosity data	112
2.18 Changes in porosity with depth	113
2.19 Porosity of samples from different stratigraphical units	113
2.20 Porosity profiles in LOCAR boreholes with stratigraphic boundaries	114
2.21 Transmissivity from pumping tests in the Pang-Lambourn catchments	116
2.22 Packer test results from Trumpletts Farm	117
2.23 Location of monitoring boreholes discussed in Section 2.8.6.	119
2.24 Long term water level variations in borehole SU 57/153	120
2.25 Water levels in 4 interfluvial boreholes in the Pang catchment between 1997 and 2002	120
2.26 Water levels in 4 interfluvial boreholes in the Lambourn catchment between 1997 and 2002	121

2.27 Examples of river valley borehole water levels	121
2.28 Relationship between borehole water levels and the long profile of the River Lambourn (Grapes et al., 2005)	124
<i>Chapter 3</i>	
3.1 Surface karst and solid geology in the Pang-Lambourn catchments	130
3.2 Seepage sink	133
3.3 Pit sink	134
3.4 Doline sink	134
3.5 Partial sink	135
3.6 Mature doline sink	135
3.7 Stream sink distribution in the Pang-Lambourn catchments	136
3.8 Stream sink cave, Yattendon	137
3.9 Schematic cross section of Yattendon chalk cave	138
3.10 Sediment filled tube, Yattendon cave	138
3.11 Stream sink chemistry sampling sites	140
3.12 Springs in the Lambourn valley and solid geology	144
3.13 Springs in the Lambourn valley and drift geology	144
3.14 Lynchwood springs	146
3.15 Great Shefford springs	146
3.16 Weston springs	147
3.17 Jannaways and Bagnor springs	148
3.18 Maidencourt Farm, the perennial head of the River Lambourn	149
3.19 Springs in the Pang valley and solid and drift geology	151
3.20 Ingle spring	153
3.21 Jewells spring	153
3.22 The Blue Pool	155
3.23 Kimber spring	155
3.24 The Blue Pool outlet channel	155
3.25 Flow data for the Blue Pool and the River Pang upstream of the Blue Pool between 1976 and 1988	156
3.26 Spring and former cress beds on the River Kennet	158

3.27 Doline in the Lambourn catchment	160
3.28 Dolines and geology	161
3.29 Typical solution feature at Chieveley	162
3.30 Vertical open cavity at Chieveley	163
3.31 Exposure of the Palaeogene-Chalk contact in a quarry in Zone 1	164
3.32 Small relic conduits exposed in the quarry	165
3.33 Relationship between transmissivity and surface karst in the Pang and Lambourn catchments	166
<i>Chapter 4</i>	
4.1 Location of stream sink injection sites in the Pang-Lambourn catchments	169
4.2 Breakthrough curve at the Blue Pool (Banks et al. 1995)	174
4.3 A newly formed sink point	176
4.4 Ponding at a sink point	176
4.5 Injection on 07/02/05	176
4.6 Monitoring for main Smithcroft Copse injection	178
4.7 Field Fluorometer and datalogger	178
4.8 Apparent tracer concentrations in the River Pang at Bucklebury following preliminary Sodium Fluorescein injection at Smithcroft Copse	179
4.9 Tracer breakthrough curves at the Blue Pool outlet (2005)	180
4.10 Colour in the Blue Pool	180
4.11 Results from Jewells and Ingle springs and two piezometers in the Frogmore Farm borehole	181
4.12 Monitoring sites for the Mirams Copse Photine C test	183
4.13 Monitoring locations in the Blue Pool spring complex for the Mirams Copse Photine C test	184
4.14 Monitoring sites in Stanford Dingley village for the Mirams Copse Photine C test	184
4.15 Monitoring sites at Bradfield for the Mirams Copse Photine C test	185
4.16 Cotton for detecting Photine C	188
4.17 Variable flow at Mirams Copse stream sink (2003/2004)	190

4.18 Rainfall at Frilsham during 25 g to 200g Photine C injections at Mirams Copse	191
4.19 Rainfall at Frilsham during 400 g and 1000 g Photine C injections at Mirams Copse	191
4.20 Location of bacteriophage sampling sites	193
4.21 River Thames sampler	195
4.22 River Pang sampler	195
4.23 Blue Pool outlet sampler	195
4.24 Frilsham Sink at time of injection	196
4.25 Mirams Copse sink at time of injection	196
4.26 Results of <i>Serratia marcescens</i> at the Blue Pool	197
4.27 Location of Winterbourne injection sinks and monitoring points	199
4.28 Detailed location of sampling sites at Bagnor and Jannaways springs	200
4.29 Low flow during tracer injection into Honeybottom sink	201
4.30 Tracer injection into excavated channel at Cromwells Sink	201
4.31 Results of tracer testing from Cromwells Sink	203
4.32 Results of <i>Serratia marcescens</i> at Bagnor	204
4.33 Results of <i>Serratia marcescens</i> at Bagnor, large volume presence/absence analysis only	204
4.34 Possible catchment area of Bagnor and Jannaways springs	206
4.35 Catchment area of the Blue Pool proven by tracer testing and possible area of extension to the northwest	208
4.33 Correlation between groundwater velocity and Blue Pool discharge	216
Chapter 5	
5.1 Single and Double porosity aquifers	223
5.2 Breakthrough curves of Maloszewski et al. (1999) at a borehole	230
5.3 Breakthrough curves of Maloszewski et al. (1999) at a spring	230
5.4 Location of approximate area of Blue Pool complex and monitoring sites during tracer tests from Smithcroft Copse	233
5.5 Fluorescein tracer injection	235
5.6 Tracer breakthrough curves at the Blue Pool spring, 2006	240

5.7 Breakthrough curves at the Blue Pool spring during the main peak scaled to peak concentration	242
5.8 Breakthrough curves during the secondary peak at the Blue Pool spring scaled to peak concentration	243
5.9 Correlation between tracer molecular weight and the magnitude of the secondary peak at the Blue Pool spring (data scaled to peak concentrations)	244
5.10 The main dye peaks at the Blue Pool spring with data scaled to tracer injection mass	245
5.11 The tail of dye breakthrough curves at the Blue Pool spring scaled to the injection masses of the tracers	246
5.12 Correlation between tracer molecular weight and the magnitude of the secondary peak at the Blue Pool spring using data scaled to injection mass	246
5.13 Comparison of the peak of three Sodium Fluorescein breakthrough curves at the Blue Pool Outlet	248
5.14 Comparison of the tail of three Sodium Fluorescein breakthrough curves at the Blue Pool Outlet	248
5.15 The first 100 hours of the breakthrough curve of <i>Phix 174</i> bacteriophage at the Blue Pool Outlet	250
5.16 <i>Phix 174</i> and dye breakthrough curve peaks at the Blue Pool Outlet	250
5.17 Full breakthrough curves at the Blue Pool outlet for 5 tracers	251
5.18 Comparison between the peak in the breakthrough curves at the River Pang and the Blue Pool outlet	253
5.19 Breakthrough curves tails at the River Pang and the Blue Pool outlet	253
5.20 Comparison of dye breakthrough curves at the Blue Pool spring and the outlet channel	254
5.21 Bacteriophage results at the Blue Pool Spring and the Blue Pool outlet	255
5.22 Diurnal fluctuations in breakthrough curve tails at the Blue Pool outlet	257
5.23 Determination of “background” Amidorhodamine G concentrations during the secondary peak.	260
5.24 Correlation between tracer recovery during the main peak at the Blue Pool Spring and tracer molecular weight	266

5.25 Correlation between secondary peak recovery and tracer molecular weight at the Blue Pool spring	267
5.26 Correlation between the ratio of the main/secondary peaks and tracer molecular weight	267
5.27 Comparison of the Sodium Fluorescein breakthrough curve at the Blue Pool Spring to modelled curves where advection-dispersion or double porosity diffusion dominate	270
5.28 Multiple flowpaths surrounding a main conduit flowpath	274
5.29 Multiple flowpaths surrounding a main conduit with flow divergence	275
Chapter 6	
6.1 Location of SBDT Boreholes in the Pang-Lambourn catchments	282
6.2 Hosepipe and weight at Peasemore Borehole (SU 47/121)	284
6.3 SBDT tracer injection system	285
6.4 Borehole tracer injection system when the water table is above the casing	286
6.5 Tracer injection at Grumble Bottom borehole	287
6.6 Electrical conductance and temperature readings of Probe 1 when submerged in standard solution	292
6.7 Time taken for tracer efflux from entire borehole	298
6.8 Time for most rapid tracer efflux in boreholes	298
6.9 Relationship between transmissivity and tracer efflux times	299
6.10 Results of uniform injection SBDTs in alphabetical order by borehole name	301 to 309
6.11 Hypothetical situations causing a decrease in tracer dilution rate with depth	310
6.12 Repeated SBDTs at Trumpletts A	313
6.13 Repeated SBDTs at Frilsham A	314
6.14 Repeated SBDTs at Frilsham B	315
6.15 Repeated SBDTs at Frilsham C	316
6.16 Borehole schematic showing five different flow situations	319
6.17 Simulation of uniform crossflow	320
6.18 Simulated crossflow in a fracture	321
6.19 Simulation with a reduced initial concentration at a particular horizon	322

6.20 Simulation of stronger crossflow in upper part of borehole than lower part	322
6.21 Simulation of decreased C_o in upper section of borehole	323
6.22 Simulation of decreasing flow rate with depth in 5 borehole sections	324
6.23 Alternative simulation of decreasing flow rate with depth.	325
6.24 Simulation of increasing flow rate with depth	325
6.25 Simulation of upward vertical flow	327
6.26 Simulation of upward vertical flow with increased dispersivity	327
6.27 Simulation of upward vertical flow with uniform crossflow above	328
6.28 Simulation of upward vertical flow with outflows divided equally between two fractures	329
6.29 Simulation of upward vertical flow with crossflow at the outflow point	330
6.30 Simulation of vertical flow with crossflow in the middle	330
6.31 Simulation of upward vertical flow with inflow divided equally between two fractures	331
6.32 Simulation of upward vertical flow with crossflow in which inflow exceeds outflow	331
6.33 Simulation of upward vertical flow with crossflow in which outflow exceeds inflow	332
6.34 Bagnor point injection SBDTs	336
6.35 Barracks point injection SBDT	338
6.36 Bockhampton point injection SBDTs	339
6.37 Frilsham A point injection SBDT	342
6.38 Frilsham B point injection SBDTs	343
6.39 Frilsham C point injection SBDTs	346
6.40 Gibbet Cottages point injection SBDTs	348
6.41 Grumble Bottom point injection SBDT	350
6.42 Trumpletts A point injection SBDTs	351
6.43 Winterbourne Farm point injection SBDTs	354
6.44 Comparison of flow rates obtained from a heatpulse flowmeter and from SBDTs	357

6.45 Relationship between the true number of flowing features in boreholes and those identified using different techniques	366
6.46 Decision tree for identifying flowing features	367
6.47 Class 1 flow horizons in 24 boreholes	370 to 375
6.48 Images of class 1 flow horizons in Trumpletts A	379
6.49 Images of class 1 flow horizons in Trumpletts B	380
6.50 Images of class 1 flow horizons in Gibbett Cottages	381
6.51 Images from Barracks	384
6.52 Distribution of flowing features with depth below ground level	387
6.53 Distribution of flowing features with depth below water table	388
6.54 Location of Frilsham boreholes	389
6.55 Flowing horizons at Frilsham boreholes	390
6.56 Flowing horizons at Trumpletts	391
6.57 Conceptual model for topology of sub-horizontal flow horizons	392
6.58 Distribution of flow horizons with respect to elevation above sea level	394
6.59 Patterns in vertical flow in boreholes	399
<i>Chapter 7</i>	
7.1 Cross section of fracture enlarged to create fissures, tubules and a conduit.	408
7.2 Conceptual model of the nature of groundwater flowpaths suggested by tracer testing between stream sinks and springs	410
7.3 Geomorphological evolution of stream sinks where a surface stream flows over Palaeogene deposits overlying the Chalk	413
7.4 North-south cross section of Palaeogene retreat	415
7.5 Hardware simulation of proto-cave propagation	417
7.6 Initiation of cave systems with multiple ranks of inputs	418

List of Tables

Chapter 1

1.1 Old and new Chalk stratigraphy for the southern geological province	32
1.2 Porosities in four areas of the English Chalk	37
1.3 Regional trends in transmissivity (T) and storage coefficients (S)	42

1.4 Summary of catchment scale tracer tests in chalk	52
<i>Chapter 2</i>	
2.1 Stratigraphical sequence in the Pang-Lambourn catchments	87
2.2 BFI estimates for the River Pang	98
2.3 Average abstraction in 2002 and license rates of PWS boreholes affecting the Pang-Lambourn catchments	111
2.4 Relationship between transmissivity and topographical location of boreholes	116
2.5 River elevation and borehole water levels	123
2.6 Results of Atkins (2003) water balance	125
<i>Chapter 3</i>	
3.1 Carbonate chemistry of stream sinks	141
3.2 Springs visited in the Lambourn catchment	143
3.3 Springs visited in the Pang catchment	152
3.4 Calculated catchment sizes for major springs	159
<i>Chapter 4</i>	
4.1 Comparative data for bacteriophages and dyes during karst groundwater tracer tests	172
4.2 Monitoring for preliminary Smithcroft Copse injection	177
4.3 Monitoring for main Smithcroft Copse injection	177
4.4 Background fluorescence at monitoring sites	181
4.5 Monitoring sites for the Mirams Copse Photine C test	183
4.6 Photine C injection quantities	187
4.7 Summary of Mirams Copse injections	189
4.8 Location of bacteriophage sampling sites	193
4.9 Results of background monitoring for bacteriophage	194
4.10 Sampling during the Pang bacteriophage tracer test	195
4.11 Monitoring sites during the Winterbourne tracer tests	199
4.12 Sampling schedule during the Winterbourne tracer tests	202
4.13 Sample volume and analysis method	202
4.14 Groundwater velocities in the Pang-Lambourn catchments	214
4.15 Tracer recoveries in the Pang-Lambourn catchments	217

4.16 Comparative recoveries of <i>Serratia Marcescens</i> and <i>Enterobacter Cloacae</i> during three tracer tests in the Yorkshire Chalk	219
4.17 Estimated thicknesses of Palaeogene cover and the unsaturated zone at stream sinks	220
Chapter 5	
5.1 Tracer quantities and dye molecular weights	234
5.2 Tracer injection times	235
5.3 Dye interference	236
5.4 Current metre results in 2004/2005	238
5.5 Stage and discharge at the Blue Pool outlet during the 2006 test	239
5.6 Comparison of dye tracer molecular weight and the magnitude of the secondary peak at the Blue Pool spring	243
5.7 Photolytical coefficients of dyes used at Smithcroft Copse	256
5.8 Sodium Fluorescein tracer recovery at the Blue Pool Outlet	259
5.9 Tracer recovery at the Blue Pool outlet (2006)	261
5.10 Apparent tracer recoveries at the Blue Pool spring (2006)	263
5.11 Model parameters	270
5:12 Summary of tailing following main peak and tracer molecular weight	271
Chapter 6	
6.1 Borehole grid references and test dates of uniform and point injection SBDTs	283
6.2 Variability of depth readings within individual profiles using Probe 1	290
6.3 Variability of depth readings within individual profiles using Probe 2	290
6.4 Variability of depth readings at the bottom of boreholes	291
6.5 Electrical conductance readings of probe 1 when submerged in a standard	293
6.6 Electrical conductance readings of probe 2 when submerged in a standard	294
6.7 Borehole tracer efflux times	297
6.8 Transmissivity from pumping tests and tracer efflux times	299
6.9 Summary of flow directions indicated by point injection SBDTs	335
6.10 Upward vertical flow rates at Bagnor	336
6.11 Upward vertical flow rates at Barracks	338
6.12 Upward vertical flow rates at Bockhampton (injection at 77.9 m AOD)	340

6.13 Upward vertical flow rates at Bockhampton (injection at 101.9 m AOD)	341
6.14 Downward vertical flow rates at Frilsham A	342
6.15 Upward vertical flow rates at Frilsham B (injection at 41.5 m AOD)	343
6.16 Downward vertical flow rates at Frilsham B (injection at 50.2 m AOD)	345
6.17 Downward vertical flow rates at Frilsham B (injection at 55.2 m AOD)	345
6.18 Downward vertical flow rates at Frilsham C (injection at 39.3 m AOD)	347
6.19 Downward vertical flow rates at Frilsham C (injection at 51.3 m AOD)	347
6.20 Downward vertical flow rates at Gibbet Cottages	348
6.21 Downward vertical flow rates at Grumble Bottom	350
6.22 Upward vertical flow rates at Trumpletts A (injection at 14.7 m AOD)	351
6.23 Upward vertical flow rates at Trumpletts A (injection at 59.3 m AOD)	353
6.24 Downward vertical flow rates, Winterbourne Farm (injection 83 m AOD)	354
6.25 Downward vertical flow rates, Winterbourne Farm (injection 81.6 m AOD)	355
6.26 Changes in vertical flow rate and tracer mass as tracer passes different types of flow horizons depicted in Figure 6.16	360
6.27 The elevation of flowing features in 24 boreholes from SBDTs	369
6.28 Details of features on image logs at the location of class 1 flowing horizons (Gibbett Cottages and Trumpletts A and B)	378
6.29 Features on the image log at the location of flow horizons at Barracks	383
6.30 The number of flow horizons at different depths below ground level	387
6.31 The number of flow horizons at different depths below the water	388
6.32 Elevation of flowing horizons in the Frilsham and Trumpletts boreholes	390
6.33 Number of flow horizons at different elevations above sea level	395
6.34 Main outflow elevation and maximum and average flow rate down to outflow in the Frilsham boreholes	398
6.35 The spacing of flowing features with other factors for comparison	402

Chapter 1: The Chalk aquifer and karst

1.1 Introduction: Objectives and thesis outline

This thesis is a study of the nature and distribution of karst development and its influences on groundwater flow and transport in the Chalk. It comprises predominantly field investigations in the Pang and Lambourn catchments in Southern England (Figure 1.1).

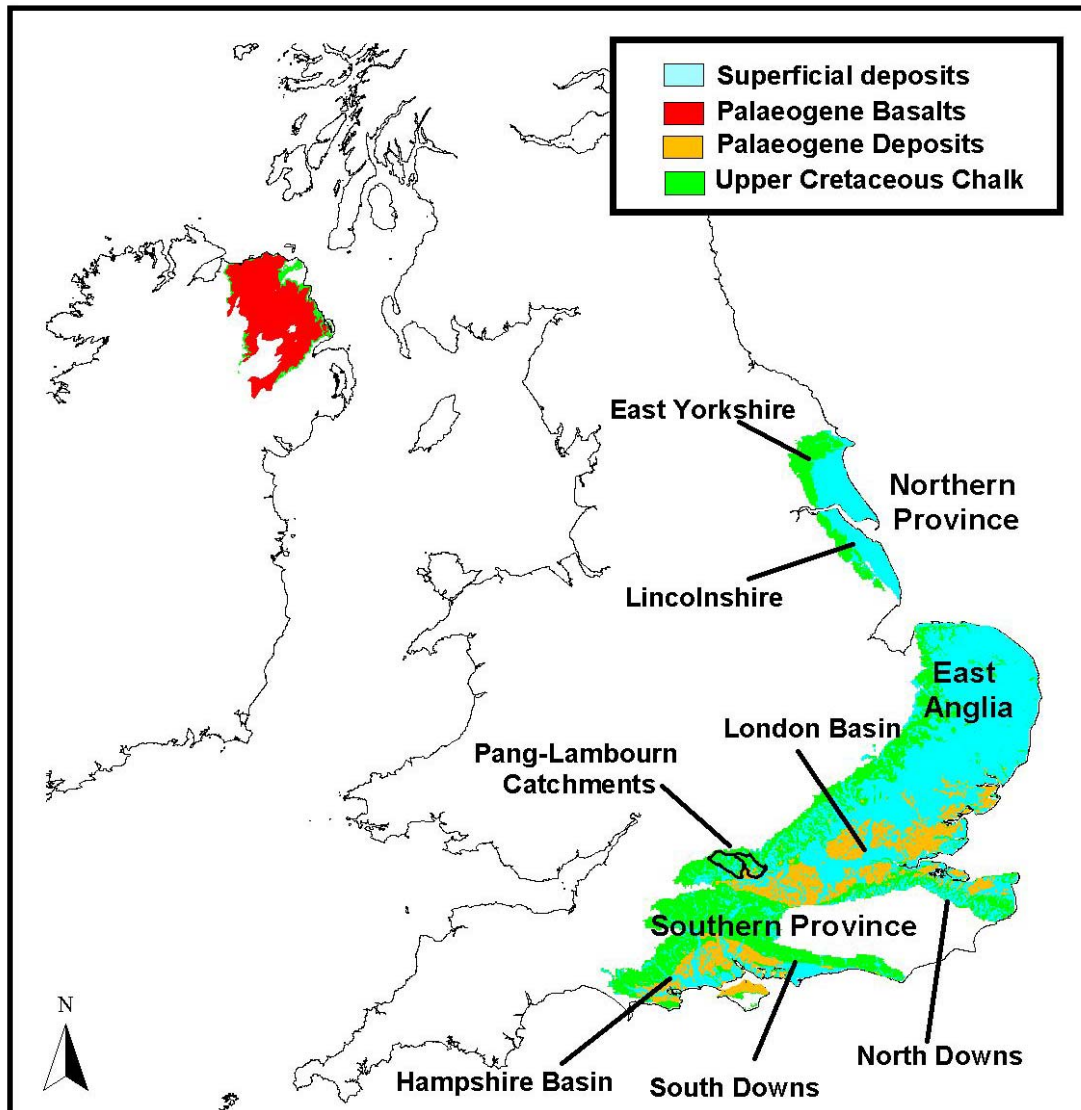


Figure 1.1: The location of the Pang-Lambourn study area and the distribution of the UK Chalk outcrop (green) and areas where the Chalk is present beneath superficial deposits (blue), Palaeogene basalts (red), or other deposits of Palaeogene age (brown)^{BGS}

Specifically the objectives of the thesis are to:

- 1) Establish the nature and distribution of surface karst in the Pang and Lambourn catchments.
- 2) Determine the extent, nature and connectivity of subsurface karst features (i.e. solutional features which provide paths for rapid groundwater flow); and to investigate the controls on the distribution of rapid groundwater flow.
- 3) Investigate contaminant attenuation processes, and their implications for the nature and structure of voids within chalk.
- 4) Produce a conceptual model of the extent and nature of karstification in the chalk of the Pang and Lambourn catchments.
- 5) Consider how applicable this is to chalk in other areas of the UK, and abroad.

The structure of the thesis and the aims of each chapter are outlined below:

There have been many previous hydrogeological studies in the Pang and Lambourn catchments. These are considered in Chapter 2, which provides an overview of the geology, hydrology and hydrogeology of the study area. Although there have been studies of surface karst geomorphology in the Chalk (Section 1.5), there is no coherent conceptual model of the distribution and hydrological function of stream sinks, or the role of karst in chalk springs. These questions are addressed in Chapter 3 which presents the results of a field survey of stream sinks and springs in the Pang and Lambourn catchments, and discusses the controls on the nature and distribution of surface karst in the catchments.

Despite the large number of hydrogeological studies in the Pang and Lambourn catchments (Chapter 2), there have been few investigations of stream sinks and springs, and conduit pathways are largely unknown. The aim of Chapter 4 is to discuss the results of 5 qualitative tracer tests, which were undertaken by the author to establish groundwater flowpaths, and improve the definition of the catchments of major springs. Results of these tests also provided some information on the nature of chalk conduit flowpaths and contaminant attenuation. These questions were investigated further by quantitative tracer tests at one site using multiple tracers (Chapter 5). The high matrix porosity of the Chalk results in diffusional exchange of contaminants between the

matrix and fractures, fissures and conduits (Foster, 1975; Barker and Foster, 1981), but these processes are incompletely understood, and there have been no previous studies of diffusional processes in the Chalk where there is rapid groundwater flow associated with karst conduits. A particular objective of Chapter 5 is to investigate the role of diffusional attenuation mechanisms in the Chalk.

In areas where karst stream sinks are absent, the occurrence of rapid groundwater flow was investigated using Single Borehole Dilution Tests (SBDTs), which are described in Chapter 6. The technique was refined to enable the identification of flowing features in boreholes, and results from 25 boreholes are used to consider the controls on the distribution of these features. Borehole imaging results are used to relate the nature of voids intercepted in boreholes to the flow observed from SBDTs. In Chapter 7 the results of the field survey, natural gradient tracer tests and SBDTs are combined to present a new conceptual model of the role of karst and the distribution of rapid groundwater flow in the chalk of the Pang and Lambourn catchments, with particular consideration of the structure and connectivity of solutional voids in the Chalk.

The purpose of the remainder of Chapter 1 is to set the subsequent field-based studies in the context of existing literature and to evaluate the concept of the Chalk as a karstic aquifer. It begins with a description of the basic characteristics of the Chalk (Section 1.2), and a detailed discussion of chalk hydrogeology (Section 1.3). This is followed by an introduction to karst concepts (Section 1.4), which provides background for the subsequent literature-based discussion of the present understanding of karst in the Chalk (Section 1.5).

1.2 Introduction to the Chalk

1.2.1 Chalk Lithology

The Chalk is a porous marine limestone that was deposited during the Upper Cretaceous period between ~99 and 65 million years ago when much of Northern Europe was submerged beneath a shallow to moderately deep warm sea (Downing et al., 1993). It is a fine-grained very pure limestone typically composed of ~ 98% calcium carbonate (Allen et al., 1997). The carbonate grains making up the rock (Figure 1.2) primarily comprise the skeletal remains of coccolithophores (planktonic algae), but coarser shell fragments are also present (Allen et al., 1997).

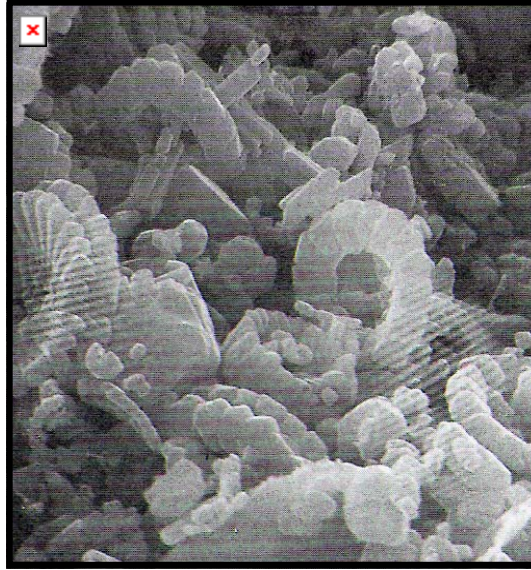


Figure 1.2: Scanning electron photomicrograph of a chalk sample from Berkshire showing coccoliths ~5µm wide. From British Geological Survey (BGS) in Price et al. (1997).

A small proportion of inorganic material forms marl layers (Figure 1.3, left) commonly comprising clays, but occasionally silt or sand. Marl layers are mm to several centimetres in thickness and can be laterally continuous for several hundreds of kilometres (Allen et al., 1997). Some are detrital but smectite dominated marls are thought to be of volcanic origin (Hancock, 1993). The Chalk also contains flint layers (Figure 1.3, right) that are normally parallel to the bedding. Flint is composed of biogenic silica that has been altered during diagenesis to form a hard brittle material. Flints can occur in relatively smooth continuous thin "sheets" often less than 1 cm in thickness, or as layers of discrete irregular nodules between 1 and 30 cm in diameter.

Hardgrounds occur irregularly throughout the Chalk. They are resistant layers with greater bioturbation, greater cementation and reduced porosity. Some are laterally extensive over 10's to 100's of kilometres. They may have formed during falls in sea level or uplift, when there were stronger currents on the sea floor (Hancock, 1993). A reduction in the supply of algal and skeletal material resulted in exposure on the sea floor for longer enabling the chalk to become glauconitised and phosphatised (Kennedy and Garrison, 1975; Hancock, 1993).

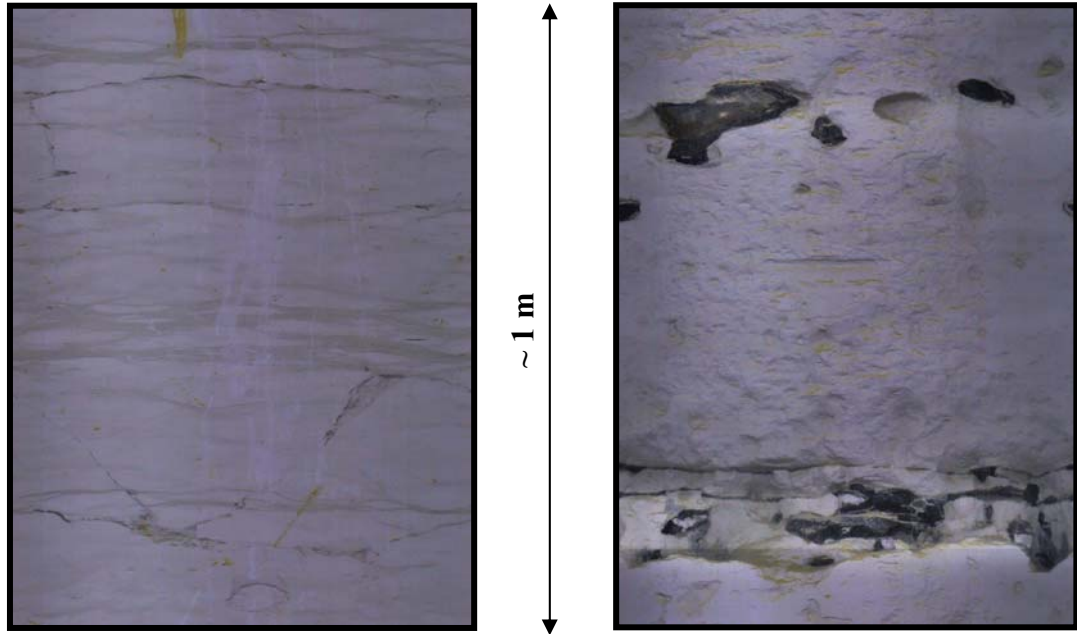


Figure 1.3: Marl layers (left) and flints (right) within the Chalk on borehole TV logs at Trumpletts Farm, Berkshire (from BGS)

1.2.2 The UK Chalk outcrop

The Chalk outcrops over large areas of southern and eastern England (Figure 1.1). It has been divided into the Southern Province including the South and North Downs and the largely confined chalk areas of the Hampshire and London Basins, and the Northern Province comprising Yorkshire and Lincolnshire (Lloyd, 1993). The chalk of East Anglia is in a transitional area where it is mostly covered by low permeability till deposits. The chalk of the northerly province is much harder than that of other areas of England, and this has been attributed to two periods of cementation (Allen et al., 1997) and high palaeotemperatures during post-Cretaceous burial history (Green et al., 1993, cited in Lloyd, 1993). To a lesser degree, the most southerly chalk outcrops in the Hampshire Basin and the South Downs are also harder (Hancock, 1993). These areas have been affected by Alpine tectonics and also have more structural complexity than other areas (Allen et al., 1997). This area and the Thames basin to the northeast were influenced by periglaciation, whilst the East Anglian chalk and the Yorkshire and Lincolnshire chalk have been affected by glaciation. The Chalk is between 200 and 400 m thick in southern England, and increases from 100 to 400 m in thickness in an easterly direction in East Anglia and northern England (Lloyd, 1993).

There is also an Upper Cretaceous chalk outcrop in Northern Ireland (Figure 1.1), known as the Ulster White Limestone Formation that is mostly confined beneath Palaeogene basalts. Whilst the original composition and depositional environment were similar to that of the English Chalk, the rapid burial and heating under the Palaeogene basalts resulted in much greater cementation increasing the hardness and decreasing the porosity (Maliva and Dickson, 1997).

1.2.3 Chalk Stratigraphy

The UK Chalk was originally divided into the Upper, Middle and Lower Chalk. These broad divisions incorporated substantial thicknesses of chalk and during more recent mapping of the Chalk it has been possible to subdivide these formations into smaller mappable units of member status (Bristow et al., 1998). These members are primarily defined in relation to marker horizons (e.g. marl layers, hard grounds and flint layers), although the combination of marker horizons, fossil content, colour, hardness, and geomorphology together define the distinctive characteristics of each unit. Mortimore (1983, 1986) began developing this more detailed stratigraphy. The rationale behind each subdivision and characteristics of each unit are described fully in Bristow et al. (1997).

Table 1.1 shows the relationship between the new and old stratigraphical classifications with respect to the Southern Province, which is relevant to the current study. The units present in the Pang-Lambourn study area are described in detail in Section 2.4.1.

Table 1.1: Simplified relationship between old and new chalk stratigraphy for the southern geological province based on Bristow et al. (1997)

Original subdivisions		New chalk stratigraphy (Southern Province)	
Upper Chalk		Portisdown Chalk	
		Spetisbury Chalk Tarrant Chalk	Culver Chalk
		Newhaven Chalk	
	Barrois' Sponge Bed		
		Seaford Chalk	
	Top Rock Chalk Rock	Lewes Nodular Chalk	
	Middle Chalk		New Pit Chalk
		Holywell Nodular Chalk	
Melbourn Rock Plenus Marls		Zig Zag Chalk	
Grey Chalk			
Tottenhoe Stone			
Chalk Marl	West Melbury Marly Chalk		
Glaucinitic marl			
Upper Greensand/ Gault		Upper Greensand/ Gault	

1.3 Chalk Hydrogeology

1.3.1 The physical structure of the Chalk aquifer

There are four components to the Chalk aquifer; the porous matrix, fractures, fissures (solutionally enlarged fractures) and conduits. The definition of terms relating to openings in rock that carry water is notoriously problematic (Bloomfield, 1996; Worthington, Ford and Beddows, 2000). In this thesis, the term "fracture" will be used to describe discontinuities in the rock that have not been modified by dissolution. Bloomfield (1996) identifies three types of fracture; bedding plane fractures, joints and faults. Bedding plane fractures are the most persistent and are parallel to bedding, often associated with lithological boundaries, marl seams, flint bands and hardgrounds. In chalk these can persist for the full outcrop length which may be > 1km, but may also die out or be absent for tens of metres along an outcrop (Younger and Elliot, 1995). Joints are stress fractures where there is no shear displacement, whilst faults have significant shear displacement of the rock (Hancock, 1985, cited by Bloomfield, 1996). The origin of chalk fracture discontinuities is tectonic (Price et al., 1993), and they usually comprise three near orthogonal fracture sets (Price, 1987); the bedding parallel set, and two roughly perpendicular less persistent joint sets which are predominantly orientated in a NW-SE or NE-SW direction (Downing et al., 1993). The low persistence of joints in chalk was illustrated by Younger and Elliot (1995), who found that all (except one) joints from 11 scanline surveys were less than 3 m in length.

In most areas several metres of chalk near the surface have been weathered resulting in a rubbly structure with a very high fracture frequency and increased permeability (Price, 1987). This is effectively the Chalk "epikarst" zone (Section 1.4.3) and fracture spacing is ~0.05 m (Price et al., 1976). Williams (1987) suggests that the high fracture frequency is due to freeze thaw action under periglacial conditions. Sometimes weathering causes the structure of the bedrock to collapse creating a soft impermeable "putty chalk" layer with low permeability (Williams, 1987; Younger, 1989).

Beneath the near surface weathered zone, fracture spacings of between 0.1 and 1 m have been measured (Price et al., 1976; Bevan and Hancock, 1986; Patsoules and Cripps, 1990). Younger and Elliot (1995) also measured fracture frequency at 11 sites in two regions of Southern England (an area from the Thames to Cambridge, and Kent). They found that bedding parallel fractures had a greater frequency (0.07- 1 m spacing) than

fractures normal to bedding (0.1 to 2 m spacing). They also found that fracture frequency was significantly higher in the Thames-Cambridge area than in Kent, but that within these broad geographical areas there was little variability. At a site in Berkshire in the Thames basin, Bloomfield (1996) found that bedding parallel fractures had a mean spacing of 0.1 m, whilst fractures perpendicular to bedding had a mean spacing of 0.12 m. Scanline surveys in two quarries near Kilham in Yorkshire found average fracture spacings of 0.3 to 0.5 m with more frequent vertical fractures than bedding fractures (Zaidman et al., 1999). Price (1987) reports that few fractures were apparent in chalk caverns constructed at 180-190 m depth and notes that fracture frequency generally decreases with depth below ground level. Observations of rapidly retreating chalk sea cliffs on the English south coast also suggest that bedding parallel fracture frequency decreases with depth (Tim Atkinson, personal communication, 2007). These cliffs are also characterised by vertically extensive fractures, which appear to occur in clusters, sometimes extending the full height of the cliffs.

In this thesis, the term "fissure" is used to mean fractures that have been widened by dissolution. Solutional modifications may take the form of small channels on the fracture surfaces or of a general widening over a substantial proportion of the fracture area. They are distinguished from "conduits" by the fact that they retain the generally planar geometry of unmodified fractures (Figure 1.4). Chalk fissures occur infrequently compared to unmodified fractures (Price et al., 1977, Price et al., 1982, Allen et al., 1997). Fissures develop most commonly from bedding orientated fractures perhaps because as seen at outcrop, they tend to be laterally more continuous. "Conduits" can be defined as tubular voids formed by solution which are distinguished from fissures by the aspect ratio they present in cross section which is ~ 1 in contrast to fissures which have trace length to maximum aperture ratios greatly in excess of 10 (Figure 1.4). The term "cave" refers to conduits that are large enough for humans to enter. It is likely that chalk conduits generally have diameters of ~ 0.1 m to ~ 100 m and lengths of 10's of metres to several kilometres. The frequency and distribution of chalk conduits is very poorly understood because they are concealed beneath the surface and most (in the UK Chalk at least) are not large enough to enter. Chalk conduits and fissures are discussed further in Section 1.5.7.

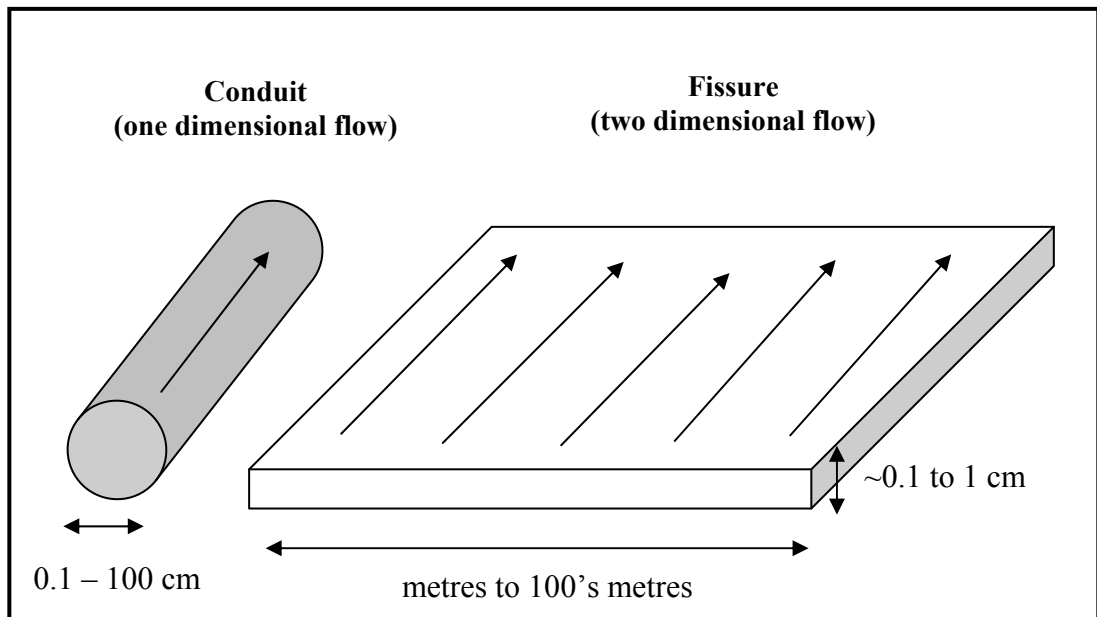


Figure 1.4: Schematic representation of the geometric distinction between conduits (left) and fissures (right)

1.3.2 Aquifer Properties

1.3.2.1 The Chalk matrix

The pores within the matrix are frequent and well connected resulting in high porosity, but they are very small with particularly small pore-throats causing very low permeability (Price et al., 1993). The average permeability of 977 core samples from the English Chalk was only $6.3 \times 10^{-4} \text{ m.d}^{-1}$ (Allen et al., 1997). Allen et al. (1997) found a positive correlation between permeability and porosity of core samples.

Chalk porosity is variable, and is affected by lithology, but primarily determined by the degree and nature of diagenesis; it decreases with depth below the surface because of increased compaction (Bloomfield et al, 1995). Two main diagenetic processes occur: mechanical compaction (the physical reorganisation of fragments into a denser structure), and pressure solution or chemical compaction (the dissolution and reprecipitation of minerals) (Bloomfield, 1997). Porosity is believed to have been between 70 and 80 % following initial accumulation of biogenic sediment (Hancock, 1993). Bioturbation reduced it to ~ 60 % (Bloomfield et al., 1995), before other early diagenetic processes and mechanical compaction during burial of up to 250 m reduced porosity to 35 to 50 % (Hancock, 1993, Bloomfield et al., 1995). With increased overburden chemical compaction processes become more important than mechanical

compaction (Bloomfield, 1997), and burial of up to 1000 m reduced porosity to ~30-40 % (Hancock, 1993). In some areas thermal diagenesis or tectonics caused additional reductions (Bloomfield et al., 1995), and hardgrounds are also associated with the lowest chalk porosities. Chemical compaction processes depend upon pore water chemistry, lithology and clay mineral content and have a more variable effect on porosity than mechanical compaction. This results in more heterogeneous porosity in chalk which has undergone burial of sufficient depths to enable chemical compaction processes to occur (Bloomfield, 1997). Modern day patterns are influenced by the overburden history, with decreased porosity occurring in chinks that were more deeply buried prior to erosion (Bloomfield, 1997).

The Chalk has much higher porosity than other UK limestones (and many elsewhere). Porosities in 2045 core samples taken throughout the English Chalk varied from 3.3 to 55.5 % with an average of 34 % (Bloomfield et al., 1995, Allen et al., 1997). The frequency distribution is shown in Figure 1.5 (based on data presented in Bloomfield et al., 1995). The data were also split into four geographical regions and Bloomfield et al., (1995) found a general trend of increasing porosity from Northern England to Southern England to the Thames and Chilterns area to East Anglia; although samples in the Upper Chalk were similar in all regions. Within each area there is progressively reduced porosity through the Upper, Middle and Lower Chalk (Table 1.2), which is likely to be due to the effects of increased depth beneath overburden.

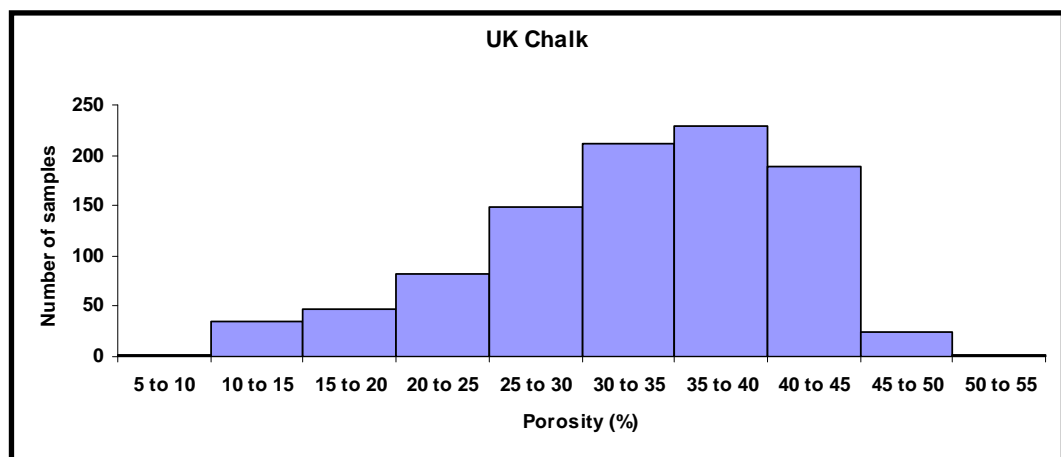


Figure 1.5: Frequency distribution of English chalk porosity (based on data in Bloomfield et al., 1995)

Table 1.2: Porosities in four areas of the English Chalk
(data from Allen et al., 1997)

Porosity %	Max	Min	Average
Northern England Upper Chalk	45.3	3.3	35.4
Northern England Middle Chalk	31.4	6.7	18.9
Southern England Middle Chalk	35.9	20.5	28.4
Southern England Lower Chalk	46.5	9.7	22.9
Thames and Chilterns Middle Chalk	52.6	9.5	31.4
Thames and Chilterns Lower Chalk	39.5	11.6	26.6
Southern England and Thames and Chilterns Upper Chalk	48.9	5.6	38.8
East Anglia Upper Chalk	55.5	24.1	38.4
East Anglia Middle Chalk	47.8	18.4	34.3

1.3.2.2 Hydraulic Conductivity and Transmissivity

Permeability is the capacity of a rock to transmit fluids, and is determined by the nature and connectivity of voids within the rock, but small scale aquifer testing normally measures the hydraulic conductivity which is a measure of permeability for a specified fluid with a given density and viscosity (Price, 1996). In aquifers this fluid is freshwater at ambient temperature. It is measured in units of volume per unit cross sectional area per unit time, or length/time. Larger scale aquifer tests measure the transmissivity, which is the hydraulic conductivity multiplied by the aquifer thickness.

The hydraulic conductivity and transmissivity of unmodified fractures is difficult to assess because aquifer tests measure the fissure and conduit aquifer components as well as unmodified fractures. It is likely that where lower values have been measured the test predominantly sampled an unmodified fracture network that was poorly connected to fissures, and where high values have been obtained, a connected fissure network contributed to the hydraulic conductivity or transmissivity. It has been demonstrated that field measurements in packered sections of boreholes have hydraulic conductivities two orders of magnitude higher than laboratory tests on core samples from the same interval (Price et al., 1977, 1982). This demonstrates that fractures are present fairly uniformly throughout the Chalk and are more permeable than the matrix. Price (1987) suggests that the fracture component of the Chalk aquifer typically has a hydraulic conductivity of $\sim 0.1 \text{ m.d}^{-1}$ and a transmissivity of $\sim 20 \text{ m}^2.\text{d}^{-1}$.

Transmissivity values from 2100 pumping tests in the UK Chalk were reviewed by Macdonald and Allen (2001) and results are in Figure 1.6. These data are biased

towards higher values as most tests were associated with production boreholes. The median value is $540 \text{ m}^2.\text{d}^{-1}$ and the 25th and 75th percentiles are $190 \text{ m}^2.\text{d}^{-1}$ and $1500 \text{ m}^2.\text{d}^{-1}$ respectively (Macdonald and Allen, 2001). The unmodified fracture network cannot account for this high transmissivity.

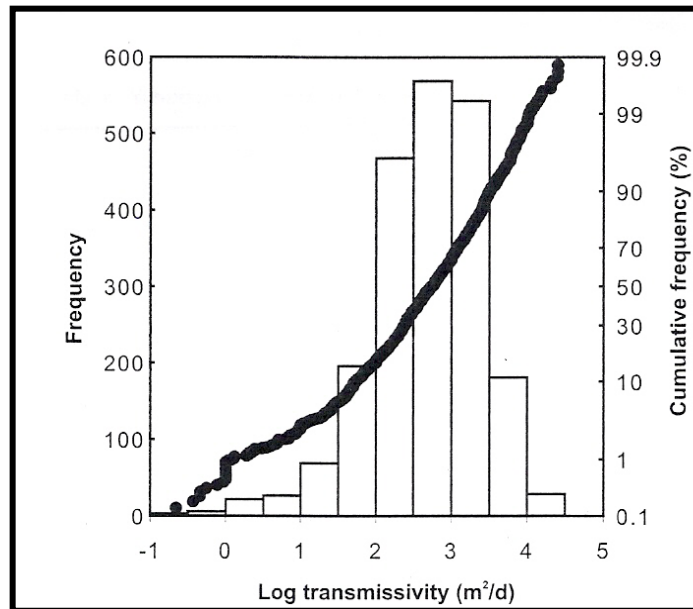


Figure 1.6: Distribution of chalk transmissivity (from Macdonald and Allen, 2001)

Packer testing, logging, and imaging have demonstrated that generally the transmissivity of individual boreholes comes from a small number of fissures (Tate et al., 1970; Price et al., 1977, 1982; Schurch and Buckley, 2002). Tate et al. (1970) found that most of the inflow to a production borehole at Speen in Berkshire occurred through two horizons. At a site in Hampshire there are 4 fissures/ fissure zones in one borehole and 3 at a second site (Price et al., 1977) and at the second site Price et al. (1977) calculated that 99 % of the transmissivity comes from 12 m or 17 % of the saturated thickness. The logging study of Schurch and Buckley (2002) found 6 inflowing fissure horizons in two adjacent 100 m deep boreholes in Berkshire. Whilst most of the flow volume came from the upper 50 m, distinct fissures were identified at ~ 78 and 95 m below ground level at both sites. Price (1987) suggested that an individual fissure may have a hydraulic conductivity of $25000 \text{ m}.\text{d}^{-1}$ and a transmissivity of $500 \text{ m}^2.\text{d}^{-1}$.

There is a well-established conceptual model of the factors affecting the spatial distribution of fissures producing these high transmissivities. This has developed from spatial analysis of pump test results (Allen et al., 1997; Macdonald and Allen, 2001),

investigations of fissure distributions in boreholes using logging techniques (Tate et al., 1970; Headworth, 1978; Schurch and Buckley, 2002), and packer testing (Price et al., 1977; 1982, Williams et al., 2006). Fissures are most commonly found beneath valleys, in the zone of water table fluctuation, and are associated with specific lithological horizons (e.g. hardgrounds, flint layers and marls). They decrease in frequency with depth below ground level, and are more common in unconfined than confined chalk (Allen et al., 1997).

Ineson (1962) noted that transmissivity from pumping tests tends to be highest in river valleys, and most abstraction boreholes are located in river valleys. Macdonald and Allen (2001) statistically compared transmissivity data for the Kennet Valley to 4 parameters; depth to rest water level, saturated thickness of chalk, distance from Eocene deposits and distance from a winter-flowing stream. Although rest water levels are deeper beneath interfluvies than valleys, no correlation between depth to rest water level and transmissivity was found. The best correlation was with distance from winter-flowing streams, but the correlation was not very strong ($r^2=0.43$). Allen et al. (1997) suggest that high transmissivity occurs more consistently in river valleys, but that it also occurs away from river valleys in a less predictable distribution.

It has been suggested that fissures occur frequently under valleys because the structural weaknesses followed by valleys are more fractured (Ineson, 1962; Price, 1987). In contradiction to this, the study by Younger and Elliot (1995) found no correlation between fracture frequency and distance from river valleys. Other factors that are thought to have increased transmissivity under river valleys are concentration of flow through a smaller area of rock (Price, 1987, Figure 1.7), and more consistent dissolutional enlargement of fractures (Younger, 1989; Allen et al., 1997) due to a thinner unsaturated zone or increased mixing of groundwaters (mixing corrosion is discussed in Section 1.4.5). It is also thought that periglacial processes may have increased permeability by freeze-thaw action and increased dissolution under colder conditions (Williams, 1987; Younger, 1989).

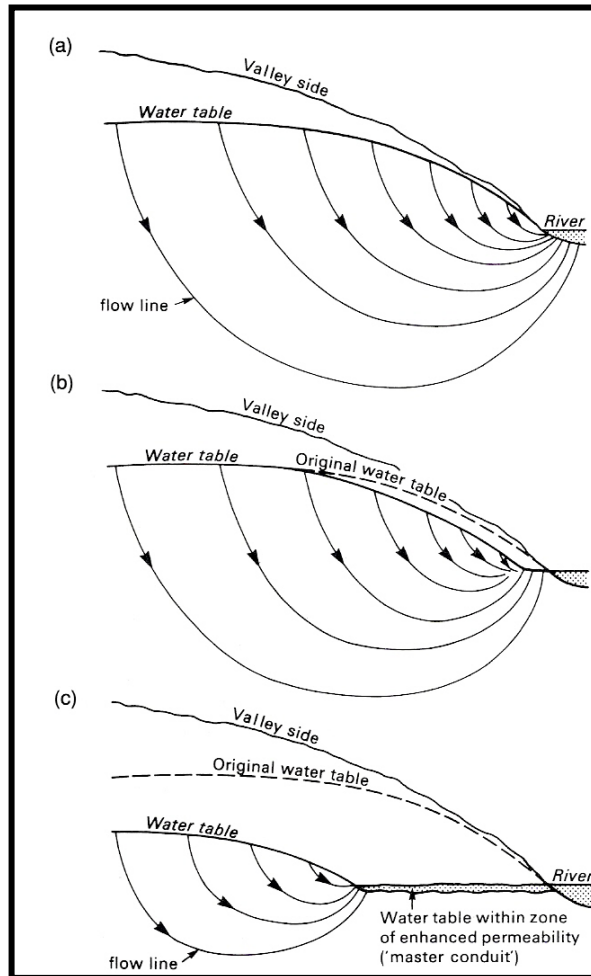


Figure 1.7: Topographic control on the development of permeability. Flow concentration leads to conduit development in river valleys (from Price, 1987)

Fissures are common in the zone of water table fluctuation (e.g. Foster and Milton, 1974; Headworth et al., 1982). Foster and Milton (1974) found transmissivity measured during borehole pumping tests in the Yorkshire chalk to be much lower under low water level conditions indicating that much of the transmissivity was from seasonally saturated fissures. Headworth et al (1982) showed that at an unconfined chalk site in Hampshire, there is a shallow high permeability zone at the water table that results in very little water table fluctuation (3-5 m), and a very low local hydraulic gradient. As pointed out by Price (1987) the process of water table fluctuation does not result in the development of fissures: fissures are found in the zone of water table fluctuation because their presence determines the position of the water table. At many sites fissures are found at greater depths below the water table, but they become less common with depth. It has been suggested that there is generally little flow > 50 m below the water

table because increased overburden results in fewer open fractures, there is less circulation of groundwater, and groundwaters are more likely to have longer residence times and therefore be saturated with respect to calcium carbonate thus preventing dissolution (Allen et al, 1997).

Whilst hydrological processes are largely responsible for the topographical distribution of high transmissivity, lithological factors may determine anomalies such as deep fissures and high transmissivity away from river valleys (Allen et al., 1997). Borehole logging studies have shown that fissures can be associated with hardgrounds (e.g. Schurch and Buckley, 2002). This may be because hardgrounds fracture cleanly (Allen et al., 1997) and are laterally extensive, so providing a well-connected flowpath. However, this may not be the case in all areas. A study of flowing horizons in the East Anglian chalk using TV and geophysical logs by Neil Wooton found no significant relationship between fissures and hardgrounds (Tim Atkinson, personal communication, 2007). Flint layers and marl seams may also be associated with fissure development because they are laterally extensive and have low permeability impeding vertical flow and concentrating lateral flow. Lowe (1992) suggests that the geochemistry of chalk is altered near to flint layers and favours dissolution.

Statistics for regional transmissivity values from Allen et al. (1997) are presented in Table 1.3. Transmissivity is generally higher in Northern England (average $1660 \text{ m}^2 \cdot \text{d}^{-1}$) than Southern England ($754 \text{ m}^2 \cdot \text{d}^{-1}$) and East Anglia (average $439 \text{ m}^2 \cdot \text{d}^{-1}$). This may be because the chalk of the northern province is harder (Section 1.2.2) and more extensively fractured. Some of the areas with low transmissivity are predominantly confined chalk where there is less groundwater circulation due to the depth of the confining strata, and dissolution is impeded because groundwaters are saturated (Macdonald and Allen, 2001).

1.3.2.3 Storage

Storativity values for 1200 tests were collated by Allen et al. (1997) and the regional averages are in Table 1.3. Macdonald and Allen (2001) report that storage coefficients are higher in unconfined chalk (mean of 0.008) than confined chalk (mean of 0.0006). Storage is higher in unconfined aquifers because both elastic storage and drainage under gravity contribute, whilst in confined aquifers there is only elastic storage (Price, 1996).

There is little regional variation in storage (Table 1.3), except that it is considerably lower in Lincolnshire. Lincolnshire data for unconfined chalk are similar to other areas, but data for confined chalk are much lower possibly because the Lincolnshire chalk is harder and has lower porosity reducing elastic storage (MacDonald and Allen, 2001).

Table 1.3: Regional trends in Transmissivity (T in $\text{m}^2.\text{d}^{-1}$) and Storage Coefficients (S) (data from Allen et al., 1997)

	Min T	Average T	Max T	No. T	S	No. S
Southern Province						
South Dorset	0.8	210	3000	38	0.003	19
Salisbury Plain	50	1400	8200	23	0.005	22
Hampshire	0.55	1600	29000	63	0.008	53
South Downs	16	500	9500	45	0.002	22
Kennet Valley	0.5	620	8000	117	0.006	107
The Chilterns	38	820	25000	62	0.004	44
London Basin	1	160	4300	88	0.002	41
North Downs	52	720	7400	57	0.003	35
Average		754			0.004	
East Anglia						
Hertfordshire	26	320	1407	23	0.005	15
Cambridgeshire	10	670	7000	125	0.004	80
West Suffolk	1	680	10000	256	0.004	133
West Norfolk	2	500	9500	45	0.006	22
East Norfolk	1	277	>10000	454	0.002	not provided
East Suffolk	not provided	255	not provided	110	0.003	not provided
North Essex	1	370	7000	415	0.002	not provided
Average		439			0.004	
Northern Province						
Yorkshire	1	1258	>10000	87	0.007	not provided
North Lincolnshire	60	2347	>1000	16	0.0002	not provided
South Lincolnshire	7	1376	4350	39	0.0002	not provided
Average		1660			0.002	

The location of storage in the Chalk is still debated (Allen et al., 1997; Price et al., 2000). MacDonald and Allen (2001) demonstrated a positive correlation between storage coefficient and transmissivity indicating that the fissure network that controls transmissivity is also important in determining storage. However, the volume in fissures is insufficient to account for the high specific yields observed in the Chalk (Allen et al., 1997). The high matrix porosity suggests that the matrix may provide a significant proportion of the storage. Specific yield from the Chalk matrix is limited

because the small pores and pore throats prevent drainage under gravity (Price, 1987). Price (1987) suggests that the usable matrix storage is approximately 3% of the porosity (which is approximately 1 % of the bulk volume of the Chalk). However, Price (1987) concludes that this is still a significant contribution to the overall specific yield. Price et al. (2000) discuss the results of a study by Lewis et al. (1993) that concluded that changes in streamflow were greater than could be accounted for by changes in water table level and that this was due to release of water from storage in the matrix in the unsaturated zone. Price et al. (2000) measured air-water capillary pressure and pore size distribution of different sized chalk blocks and concluded that irregularities on fracture and fissure surfaces may provide a substantial portion of storage.

MacDonald and Allen (2001) suggest that the relatively small difference between storativity values in confined and unconfined chalk is evidence that elastic storage must be important in unconfined chalk implying that the amount of storage held in fractures (which can drain easily under gravity) must be relatively limited. This appears to contradict the evidence from the correlation between transmissivity and storage coefficients that suggests that fissures are important for storage. It appears that fissures, fractures and the matrix are all important components of storage, but that without the presence of the larger fissures the smaller scale features cannot make a significant contribution to the specific yield. The aquifer operates hierarchically with drainage from progressively smaller scale features. Initially the large-scale fissures drain causing a steepened hydraulic gradient from fractures to the fissures, and later from the matrix to fractures and fissures.

1.3.3 Groundwater ages

From the early days of groundwater exploitation, rapid groundwater responses to rainfall, and turbidity and bacterial contamination indicated that chalk groundwaters can be characterised by rapid flow and short residence times of only days or weeks (Price et al., 1993). Tracer testing has proved travel times of <24 hours over distances of several kilometres (Sections 1.3.4 and 1.3.5). Nevertheless, in the late 1960's tritium activity in groundwater was found to be very low indicating that much of the water in the saturated zone had originated before the period of aerial thermonuclear testing from 1953 to 1965 (Price et al., 1993).

Smith et al. (1976) used carbon, oxygen and hydrogen isotope dating techniques to investigate the age of chalk groundwater in the London Basin. They found that in the outcrop area tritium data suggested groundwater was predominantly modern recharge water (post 1953), whereas the oxygen and deuterium isotope data suggested that there was a component of slightly older water. In the central London basin carbon isotope data indicated that the most deeply confined chalk groundwater included water between 20,000 and 25,000 years old, with a progressive increase in the modern day component towards the outcrop.

Downing et al. (1978) investigated seasonal patterns in tritium at three sites in the South Downs and concluded that there are at least two components of groundwater; a modern component with a residence time < 1 year, and an older baseflow which includes 10 % from post 1953 rainfall.

Edmunds et al. (1987), Dennis et al. (1997), and Elliot et al. (1999) also investigated chemical and isotope trends in the London and Berkshire Basins. Carbon, oxygen and hydrogen isotope ratios and noble gas recharge temperature signatures indicate that the oldest groundwaters are Late Pleistocene in origin (20,000 to 25,000 years old) and are located at the centre of the basins, supporting the conclusions of Smith et al. (1976). The study by Elliot et al. (1999) found that abstracted water was either wholly of Holocene age (<11,500 years), or was a mixture of Holocene water and Late Pleistocene palaeowater. They found an apparent lack of groundwater from 13,000 to 17,000 years and suggested this may be due to reduced infiltration during periglacial conditions.

Man-made Chlorofluorocarbon compounds (CFCs) and SF₆ have recently been used to date modern chalk groundwaters (Bateman, 1998; Darling et al., 2005; Gooddy et al., 2006). Data from 21 pumping stations in Hampshire showed relatively recent ages of a few years to a few decades at unconfined and partially confined sites, with CFC contamination at several sites suggesting a component of rapid flowing low residence time groundwaters (Darling et al., 2005). Darling et al. (2005) also note that CFC and SF₆ ages do not include unsaturated zone transit times. Accordingly, CFC-12 and SF₆ samples collected from beneath a 25 m unsaturated zone at a site in Berkshire indicated groundwaters dating from the early to mid 1980's, whilst nitrate in the boreholes was thought to date from fertiliser applications in the mid 1950's (Gooddy et al., 2006).

Groundwaters in shallower boreholes were a mixture of modern and old water in a ratio of approximately 1:3 (Goody et al., 2006).

Groundwater discharging from the Chalk aquifer through abstraction boreholes or springs is clearly a complex mixture of different ages ranging from a low residence time of days to 25,000 year old palaeowaters in the deeply confined sections of the aquifer. The proportion of waters of different ages, and the spatial variations in groundwater ages remain poorly understood, in part because of uncertainties about the mechanisms of groundwater flow through the unsaturated zone.

1.3.4 Unsaturated zone flow

There has been much debate about how much of the flow in the unsaturated zone is through fissures and fractures compared to the matrix. Before 1970, it was believed that all flow occurred through fractures and fissures (Price et al., 1993). However, Smith et al (1970) and Smith and Richards (1972) measured tritium distributions in porewaters from boreholes in Berkshire and Dorset and discovered defined peaks at 4 and 7 m below ground level which originated from recharge during 1963 and 1964, years in which tritium levels in rainfall had been exceptionally high due to nuclear bomb tests in 1962-1963 (Foster and Smith-Carrington, 1980). Smith et al. (1970) suggested that about 85 % of flow in the unsaturated zone occurs through the matrix, and introduced the concept of piston flow whereby water within the unsaturated zone is gradually displaced by new recharge resulting in the oldest, deepest groundwaters being discharged through the bottom of the system. This accounted for the rapid response to rainfall despite the slow migration of tritium. Smith et al. (1970) calculated that average downward rates through the unsaturated zone are 1 m/year. More recent tracer studies (e.g. Wellings, 1984; Barraclough et al., 1994; Haria et al., 2003; Brouyère et al., 2004; Van den Daele et al., 2007), also found that peak solute concentrations move through the unsaturated zone matrix at ~ 1 m/year (Figure 1.8). Foster and Smith-Carrington (1980) found that a tritium peak in a Dorset borehole moved more slowly between 1970 and 1977 than between 1964 and 1970 demonstrating that downward flow rates are not constant. They suggested this was due to variations in rainfall intensities or changes in the physical properties of the rock with depth.

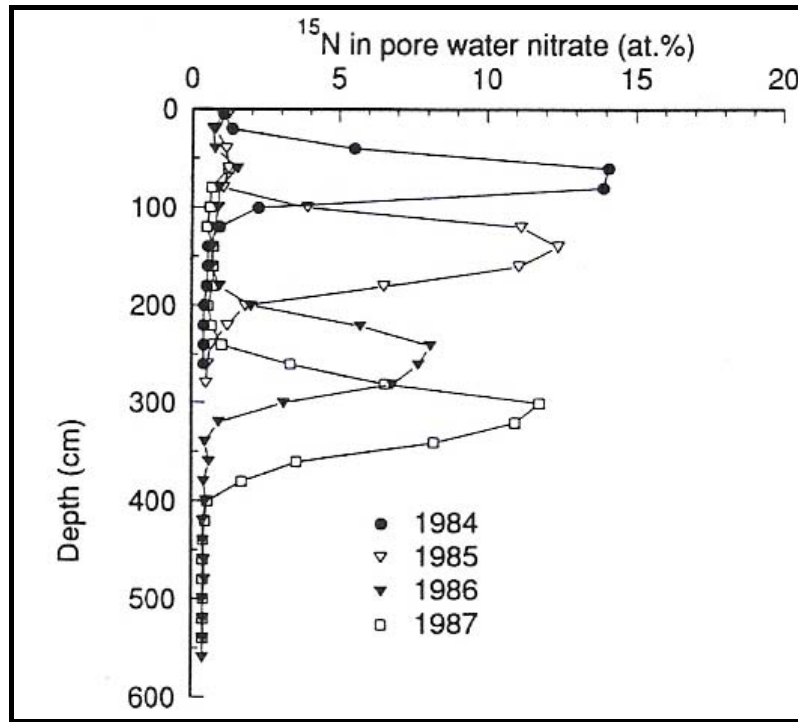


Figure 1.8: Tracer (^{15}N) migration through the unsaturated zone matrix at $\sim 1\text{m}/\text{year}$ in the Chalk at West Ilsley, Berkshire (Barraclough et al., 1994)

Foster (1975) described a mechanism that could explain fissure flow and the slow migration of solutes. He noted that the matrix will be fully saturated in the unsaturated zone, and suggested that during wet periods the concentration gradient would cause diffusion from fractures and fissures into the Chalk matrix slowing the rate of vertical solute movement. This could explain the low levels of tritium in the saturated zone whilst relatively rapid flow was occurring through fractures and fissures in the unsaturated zone.

Downing et al. (1978) measured tritium and β activity in three abstraction boreholes with increased dissolved solids at the beginning of the winter infiltration period. They found that tritium concentrations in groundwater became higher than rainfall concentrations following wet periods, and interpreted this as due to flushing of high tritium water stored in the unsaturated zone. β activity data suggested that there was a time lag of 7 years between recharge and discharge at the abstraction boreholes. They concluded that about 10 % of the total recharge is transmitted rapidly through the unsaturated zone at flow rates of $\sim 50 \text{ m.d}^{-1}$, whereas water in small fractures and large

pores in the rock matrix moves via displacement at a rate of 1-4 m.d⁻¹, with diffusion resulting in the tritium front progressing more slowly at ~ 1 m.a⁻¹.

Near surface field measurements of soil moisture content and matric potential have also been used to investigate recharge mechanisms (e.g. Wellings and Cooper, 1983; Gardner et al., 1990; Mahmood-ul-Hassan and Gregory, 2002; Ireson et al., 2006). These studies generally conclude that flow through the matrix is the dominant process, with fissure flow initiated at some sites when matric potentials exceed a certain threshold. Wellings and Cooper (1983) concluded that at three of the sites they studied in Hampshire matrix flow predominated, whilst at one site fissure flow was initiated during wet periods. However, Mahmood-ul-Hassan (2002) suggested that the frequency of data collection affects the results. He demonstrated that using higher frequency data than that obtained by Wellings and Cooper (1983) there were rapid changes in water content and matric potential in the hours following rainfall, indicating preferential flow through fractures and fissures, whilst low frequency data at the same site indicated matrix flow only. Gardner et al. (1990) measured soil water content and soil water potentials at 7 UK chalk sites. They found that matrix flow was the dominant process and that at most sites fissure flow rarely occurred. Haria et al. (2003) measured soil and chalk water content and water potential at an interfluvial site with a deep unsaturated zone and a dry valley site with a shallow water table and found that at the interfluvial site recharge was through the matrix, whilst at the valley site recharge was both through the matrix and by preferential flow through fissures and fractures.

Combined measurements of CFCs and SF₆ give an indication of whether a groundwater is a mixture of different ages or predominantly derived from piston flow (Darling et al., 2005; Goody et al., 2006). The CFC₁₂ and SF₆ study in Berkshire by Goody et al. (2006) found that deeper samples from further away from a river valley fitted the piston flow model whilst shallow samples close to the river were more mixed suggesting an element of fissure flow.

Modelling studies of Matthias et al. (2005) suggested flow in the matrix was necessary to explain the observed preservation of solute peaks through the unsaturated zone and Matthias et al. (2006) suggested the attenuating effect of a soil layer reduces the rate of infiltration to the underlying chalk sufficiently to enable recharge through the Chalk

matrix, concluding that most flow in the unsaturated zone must be through the matrix, with ~ 17-30% of annual recharge through fractures and fissures on an episodic basis.

Artificial tracer testing studies have demonstrated rapid flow through fissures and conduits in the unsaturated zone. Tracer tests from karst stream sinks (Section 1.3.5) have demonstrated very rapid flow of 4.7 to 20 km.d⁻¹ over distances of several kilometres (Harold, 1937; Atkinson and Smith, 1974; Banks et al., 1995), and must include a proportion of flow through the unsaturated zone. There have also been several tracer tests through the unsaturated zone where the tracer was not injected into a karst feature. Some of these studies (Price et al., 1992; Slater et al., 1997; Zaidman et al., 1999; Bracq and Brunin, 1999; Brouyère et al., 2004; Allshorn et al., 2007) identified rapid fissure flow, whilst others (Barraclough et al., 1994; Van den Daele et al., 2007) did not.

Most of the tracer injected into a soakaway for the M25 in Hertfordshire by Price et al. (1992) was lost, but a very small amount was detected in boreholes 3.5 km away indicating rapid groundwater flow (~1100 m.d⁻¹). Slater et al. (1997) and Zaidman et al. (1999) used cross borehole electrical resistivity imaging to monitor the migration of a salt tracer applied to the surface at a site in Yorkshire. Following tracer application (with an element of artificially induced recharge), tracer moved rapidly through the unsaturated zone in fissures (Figure 1.9). A large proportion of tracer was retained in the upper 4 m (encompassing a thin soil layer and the top of the chalk), and several months later following natural recharge events the tracer again moved rapidly down through the unsaturated zone in fissures (Figure 1.9).

Tracer was injected into the chalk unsaturated zone 57 m above the water table in Escalles in northern France in 1989 (Bracq and Brunin, 1999). It is unclear whether the injection was into a karst feature or if the tracer was applied to the ground surface. The tracer was detected at multiple outlets (abstraction boreholes and springs) with multiple peaks. The fastest velocity was ~ 1 km.d⁻¹ indicating rapid flow. Recoveries were very low (~ 1%).

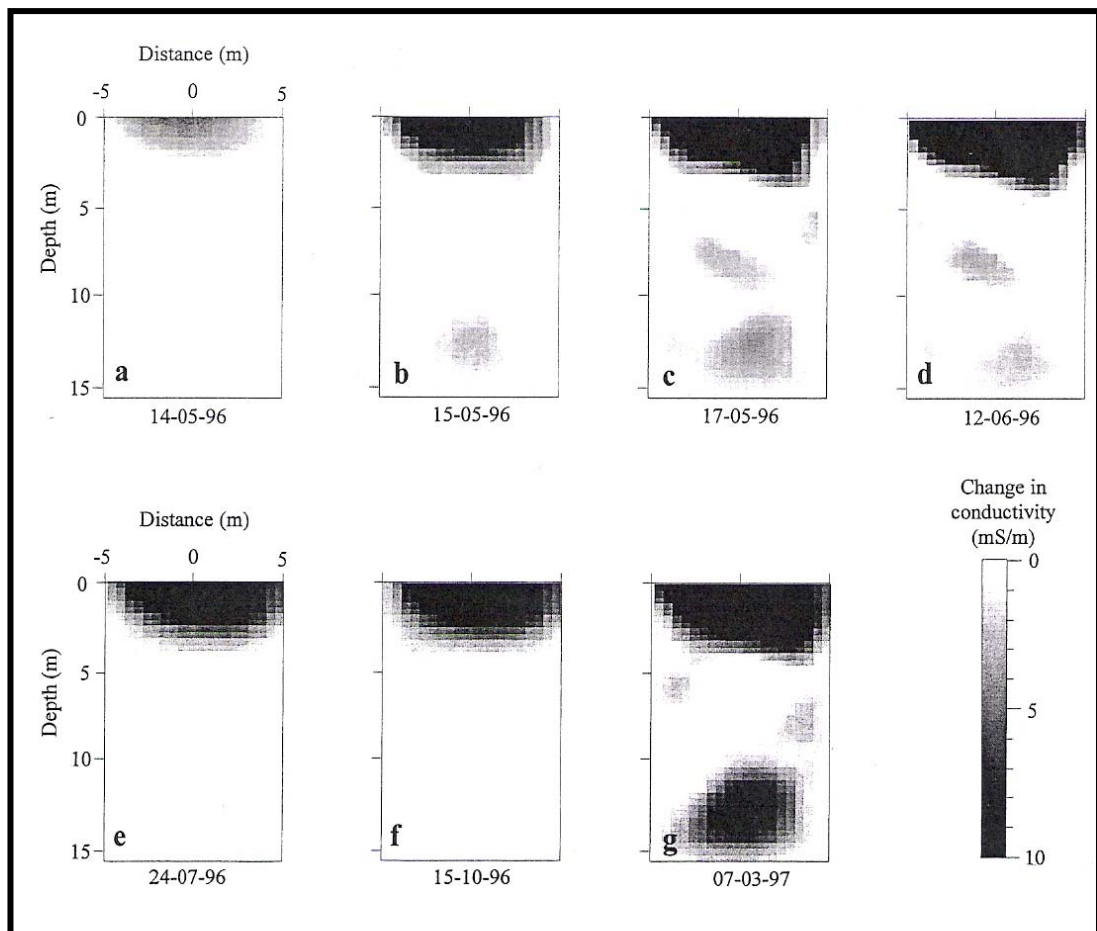


Figure 1.9: Rapid downward movement of tracer following tracer injection (b,c,d) and following heavy rainfall a year later (g), measured using geophysics (Zaidman et al., 1999)

Brouyère et al. (2004) undertook tracer tests through the chalk unsaturated zone in Belgium, and found that under low recharge conditions flow was through the matrix, while high recharge caused fissure flow. They injected tracers into boreholes above the water table and monitored in a borehole extending into the saturated zone that was pumped at 3.2 to $6 \text{ m}^3 \cdot \text{h}^{-1}$. When artificial recharge was induced at the injection borehole tracer moved rapidly through fissures reaching the saturated zone (the pumping borehole) approximately 8.5 m below in 5.15 hours (indicating flow $\sim 40 \text{ m} \cdot \text{d}^{-1}$). No water was added to the injection borehole during a second injection, and tracer took 340 days to reach the saturated zone (in this case the unsaturated zone was $3\text{-}4 \text{ m}$ thick because the water table was higher). They also undertook tracer tests through Quaternary loess deposits overlying the chalk, and did not detect any tracer in the saturated zone even when artificial recharge was used in the injection borehole. They

concluded that where chalk is overlain by soils or other deposits, the recharge rate is attenuated and therefore fissure flow is not initiated during high recharge events.

Allshorn et al. (2007) injected dye tracers into 4 temporary pits dug to bedrock and monitored in a tunnel 12 to 38 m vertically below the injection point. Tracer was detected from 3 of the 4 injections and two subsequent quantitative tests demonstrated groundwater velocities of 9.5-19 m.d⁻¹, and tracer recoveries of 0.004 to 0.0225 %.

A tracer investigation of the top 6 m of the unsaturated zone at a site in Berkshire by Barraclough et al. (1994) did not identify fissure flow. However, the lack of a tritium peak at 15-20 m depth suggested that vertical fissure flow may be more important deeper in the unsaturated zone. Van den Daele et al. (2007) monitored the downward migration of a tracer applied to the ground surface under natural recharge conditions in the Cambridgeshire chalk. No tracer was observed 5 m below the surface indicating an absence of fracture/fissure flow. They concluded that the soil and weathered chalk buffers the effect of high intensity rainfall preventing the onset of rapid flow. They did find secondary tracer peaks at 1.5 and 3.0 m below the surface suggesting limited fracture flow.

Price et al. (2000) measured the properties of chalk blocks and suggested that fissure flow can be generated at any depth in the unsaturated zone, particularly where the matrix hydraulic conductivity is low. They suggest that unsaturated zone fissure flow is initiated in narrow parts of fissures and that it may be more likely to originate near the water table where the pore suctions are lowest.

To summarise the main implications of these different studies, it seems that where karst stream sinks recharge the unsaturated zone, fissure and conduit flow are the dominant mechanisms of unsaturated zone flow. However, most of the unsaturated zone is not connected to stream sinks and many studies suggest that recharge is predominantly through the matrix. Where a connected fracture/fissure network exists, if the infiltration rate exceeds the hydraulic conductivity of the matrix, near surface fissure flow can be initiated (Price et al., 2000). Existing studies have not demonstrated a clear conceptual model of how frequently fissure flow occurs in the unsaturated zone. However, it appears that flow through the Chalk occurs at 3 velocity scales; rapid flow where

recharge is through stream sinks ($\sim\text{km.d}^{-1}$), moderately rapid fracture/ fissure flow ($\sim\text{m.d}^{-1}$), and matrix flow ($\sim 1 \text{ m/year}$).

1.3.5 Tracer investigations of groundwater flow in the saturated zone

Tracer tests that provide insight into the nature of groundwater flow in the saturated zone include local tests such as radial flow tests and single borehole dilution tests; and catchment scale tracer tests from stream sinks, boreholes, dolines and soakaways.

Radial flow tracer tests involve pumping to induce a forced gradient between an injection borehole and the monitoring borehole. They can be used to establish connections between boreholes and travel times under forced gradient conditions; and tracer breakthrough curves can be analysed to determine aquifer parameters. In chalk there have been very variable results. At some sites connections are established and groundwater flow is extremely rapid (Ward, 1989; Ward et al., 1998) whereas at other sites no tracer was detected at the pumping borehole indicating that either there is no connection, or that the tracer was attenuated to below the detection limit (Ward, 1989). Ward (1989) suggested that high tracer attenuation occurred when relative heads in the injection and pumped boreholes indicated that part of the flowpath was along vertical fractures, whereas high tracer recoveries occurred where there was limited drawdown of the pumped borehole and flow was predominantly along horizontal fractures.

Single borehole dilution tests (SBDTs) involve injecting a tracer throughout the saturated zone of a borehole and sampling the water column at intervals following injection to monitor the rate at which the tracer is diluted by aquifer water, and how this varies with depth. Initially the technique was used to determine groundwater velocities using the method outlined in Lewis et al. (1966). However, the method assumes that there is no vertical flow in the borehole and with modern digital instruments and data storage the technique is more useful as a means of identifying preferential flow horizons. One of the aims of this thesis is to investigate the applications of SBDTs and previous studies are reviewed in detail in Chapter 6.

Catchment scale tracer tests are summarised in Table 1.4. There have been relatively few tracer tests from stream sinks in the English Chalk, but in all reported cases tracer was recovered at springs or boreholes several kilometres away in a short time indicating

very rapid groundwater flow (Codrington, 1864; Harold, 1937; Atkinson and Smith 1974; Banks et al., 1995).

Table 1.4: Summary of catchment scale tracer tests in chalk

Location	Distance (km)	Velocity (km.d ⁻¹)	Author
Tracer tests from Stream Sinks			
Wiltshire	1-2	not given	Codrington (1864)
Hampshire	5.8	2-2.6*	Atkinson and Smith (1974)
Hertfordshire	8-20	2.7-5.2*	Harold (1937)
Berkshire	4.7	6.8*	Banks et al. (1995)
N Ireland	0.3-3.6	0.5-2.8^	Barnes (1999)
France	~ 1.5	1.8 - 3"	Massei et al. (2002,2006)
Tracer tests from Dolines			
Surrey	3	2.4*	Richards and Brincker, (1908)
Tracer tests from Soakaways			
Hertfordshire	3.5	2*	Price et al., (1992)
Tracer tests from Boreholes			
Hampshire	not given	0.2-4.7"	Atkinson, personal communication (2007)
Dorset	0.4	0.1"	Alexander (1981), details in Ward et al. (1998)
Yorkshire	0.04 to 5.5	0.05-0.48*	Ward et al. (1997)
Suffolk	not given	not given	Atkinson, personal communication (2007)
Norfolk	1.5	0.4*	Hull (1995)
France	0.7-3.1	2.5-26*	Bracq and Brunin (1999)

*velocity is based on time to first arrival of tracer

^ velocity is minimum velocity

" not specified whether velocity is based on time to first arrival or peak

A dye injected into a stream sink in Wiltshire is reported by Codrington (1864) to have been visible at the monitoring point in "about the time expected" suggesting rapid flow and low tracer attenuation. Similarly tracer was visibly detected in the Hertfordshire tests in up to 7 spring and borehole abstraction sites, up to 6 km apart (Harold, 1931). The Hampshire tracer test (Atkinson and Smith, 1974) is the only quantitative test from a stream sink in the Chalk, and the relatively high recovery of 70 % also suggests low attenuation. In this test tracer was recovered at two groups of outlets with most recovered at one group of outlets and only 0.6% at the other.

Tracer testing from 9 stream sinks in chalk in Northern Ireland also revealed high groundwater velocities of 0.5 to 2.8 km.d⁻¹ (Barnes, 1999). Actual velocities may have been higher as passive detectors were used and minimum values were reported. In four quantitative tests tracer recoveries were between 52% and 94% and tracer breakthrough curves at some sites had multiple peaks (Barnes, 1999).

Scientists at Rouen University have carried out many tracer tests from stream sinks in the French chalk (Joel Rodet, personal communication, 2006). Early work is detailed in Rodet (1991). Much recent work has focused on the Bebec-Hannetot karst system in the Seine Valley, Normandy. Here, groundwater velocities from tracer tests in 1997 were 1.8 to 3 km.d⁻¹, and tracer recoveries were > 90 % (Massei et al., 2002; Massei et al. 2006).

One of the earliest natural gradient tracer tests was from a doline in Surrey (Richards and Brincker, 1908). Salt and a prepared bacterial culture (together with water) injected into a doline were detected ~ 3 km away at the Addington water supply boreholes and adit indicating a velocity of 2.4 km.d⁻¹.

Catchment scale tracer tests from boreholes have been successfully undertaken in the Chalk at 5 sites in the UK (Table 1.4), and results suggest lower velocities and higher attenuation than in tests from stream sinks. In 1976 tracer injected into boreholes in the Candover catchment in Hampshire by Simon Collinson was detected in 3 abstraction boreholes indicating velocities of between 0.2 and 4.7 km.d⁻¹ (Atkinson, personal communication, 2007). At Lulworth in Dorset a test by Alexander (1981) cited by Ward et al. (1998) proved a connection between a borehole and a spring 400 m away on the coast indicating a groundwater velocity of 0.1 km.d⁻¹. A series of tracer tests from boreholes were undertaken in Kilham in Yorkshire (Ward et al., 1997, 2000). Results were very complex and several connections between boreholes and other boreholes or springs were established with groundwater velocities ranging from 0.05 to 0.48 km.d⁻¹ over distances of up to 4 km. In two tests boreholes positioned geographically between the injection borehole and a positive monitoring site were negative (including a pumping PWS borehole), suggesting that there is a discrete conduit/fissure system that is not fully connected throughout the area.

A test in Suffolk in 1987 injected tracer into flow horizons identified from a SBDT and proved a connection between the borehole and springs over a kilometre away, although the tracer arrived at very low concentrations (Atkinson, personal communication, 2007). At a site in Norfolk tracer was also injected into a zone of preferential flow identified from a SBDT, and detected at a spring indicating a velocity of 0.4 km.d⁻¹ (Hull, 1995). The advantage of undertaking a SBDT to determine the feasibility of a catchment scale test from a borehole is illustrated by unsuccessful tracer experiments in Norfolk in 1980 (Ward et al., 1998), and in Berkshire in 2001 (Grapes, personal communication, 2003). In both cases tracer was still present in the injection borehole at the end of the test explaining the absence of tracer at the monitoring points.

Bracq and Brunin (1999) describe the results of three tracer tests from boreholes in the French chalk that demonstrated rapid groundwater flow of 2.5 to 26 km.d⁻¹. Tracer was detected at multiple outlets, the breakthrough curves were characterised by multiple peaks, and recoveries varied between 1 % and 50 %.

1.3.6 Aquifer contamination

The Chalk is the most important aquifer in the UK and provides 15% of the total UK water supply, and 35 % of the water supply in the south and east of England (Gooddy et al., 2006). It provides high yields and water quality is normally good because of the long residence times. In some places there is high attenuation of contaminants by both dispersive and diffusive processes as water moves between the different components of the aquifer.

However, there has been a long history of water quality problems at many abstraction sites. This arises because some of the fissures and conduits which enable the high yields derive a proportion of their water from low residence time groundwater with low potential for attenuation; or because longer residence time groundwaters have been affected by point inputs of high persistence contaminants or the accumulation of persistent contaminants from diffuse pollution.

Point sources of contamination occur due to accidental spillages or poorly managed intentional discharges into soakaways (and in places into natural karst features). The distribution of contaminants in the aquifer from point sources provides information on

the nature of groundwater flow. There are many examples of contamination by chlorinated solvents. Lawrence and Foster (1991) describe two case histories and conclude that once chlorinated solvents enter chalk they persist for many years because solvents are chemically stable and do not biodegrade, and diffusion and sorption causes retention then release of solvents from the matrix. Longstaff et al. (1992) investigated chlorinated solvents in the Dunstable and Luton area and found widespread low-level contamination with several hotspots of higher concentrations. Headworth et al. (1980) investigated the contamination of the Chalk aquifer from mine drainage at Tilmanstone in Kent. Between 1907 and 1974 318,000 tonnes of chloride were discharged onto the Chalk. Borehole investigations in the 1970's demonstrated that in the top 40-50 m the chalk porewaters contained chloride, whilst at greater depths contamination was localised around fissures (Headworth et al., 1980). 10 years after a diesel oil spillage in Eastern England, a study found that the oil was distributed very unevenly through the unsaturated zone (Ashley et al., 1994). Oil reached the saturated zone via fractures and fissures, with some transfer into the matrix within ~ 1cm of the fracture surfaces. In Hertfordshire, a point source of bromate has resulted in a subsurface plume that extends over 10 km from the source and is up to 3 km wide.

Fretwell et al. (2005) investigated the distribution of contaminants in the zone of water table fluctuation (the seasonally unsaturated zone or SUZ) at a site where chlorinated hydrocarbons were disposed of in unlined pits. Using field data and modelling techniques they demonstrated how under high water level conditions contaminants can enter the SUZ from the saturated zone via diffusional processes. This results in initial attenuation of contaminants in the groundwater, but prolongs the duration of the contamination as once the saturated zone is free of contamination, contaminants from the SUZ slowly diffuse back into mobile groundwater under high water level conditions.

Diffuse contaminants are derived from agriculture and include pesticides, fertilisers and microbial pathogens (Foster, 2000). Of these nitrate contamination from inorganic fertilisers has the most significant long-term impact because nitrate generally persists in the environment the longest (Foster, 2000). In situ removal of nitrates by denitrification has been shown to occur in confined chalk, but studies in unconfined chalk suggest that there is limited potential for denitrification (see Foster, 2000 for a review of

denitrification studies). Nitrate contamination of groundwaters was first discussed by Foster and Crease (1974) and appeared to relate to increased application of agricultural fertilisers from the 1950's (Foster, 2000). Limbrick (2003) looked at long-term trends in nitrate concentration at a spring in South Dorset. He found nitrate concentrations (as nitrogen) were consistently $\sim 1 \text{ mg.L}^{-1}$ between 1894 and 1946 whereas data from 1976 to 2001 show a rising trend from ~ 4.5 to $\sim 6.5 \text{ mg.L}^{-1}$. Increases in nitrate since the 1980's have also been demonstrated in chalk abstraction boreholes in the Anglian region (Beeson and Cook, 2004). Beeson and Cook (2004) found short term seasonal fluctuations at some sites with nitrate peaks during late autumn and winter; a decrease in nitrate with depth below the water table, and a small decrease in nitrate with time since onset of pumping during a short term pumping test. Brouyère et al. (2004) note that nitrate concentrations at a chalk site in Belgium increase under high water table conditions and used tracer studies to demonstrate that this can be attributed to flushing out of nitrate stored in the zone of water table fluctuation.

Since the 1960's and 1970's there has been increased use of pesticides and herbicides which were thought to be potentially more serious than nitrates because they are applied to the land surface at much higher concentrations relative to drinking water standards (Foster et al., 1991). Gomme et al. (1992) found that low concentrations of some components of pesticides and herbicides were widespread in chalk groundwaters in one catchment in Cambridgeshire. Low concentrations of pesticide and herbicide compounds have been found in chalk groundwaters at sites in Southern England (Goody et al., 2001; Lapworth and Goody, 2006). However, most compounds in herbicides and pesticides seem to undergo biological and chemical degradation in the soil and unsaturated zone resulting in only very low concentrations occurring in groundwaters (Foster et al., 1991; Goody et al., 2001; Johnson et al., 2001; Chilton et al., 2005). Little is known about the metabolites (breakdown products) of pesticides (Foster, 2000), although a recent study (Lapworth and Goody, 2006) found that in 60% of groundwaters sampled the metabolites of the compound diuron were more prevalent than the parent compound. Due to the high potential for degradation, contamination from diffuse sources of pesticides and herbicides appears to be restricted to places where there is rapid flow through the unsaturated zone, and can be enhanced when associated with transport of colloidal particles (Foster et al., 1997; Goody et al., 2001).

Chilton et al. (2005) note that point sources of pesticides from spillages and soakaways have caused more serious contamination problems.

Contamination of chalk water supplies by microbial pathogens is a long established problem (e.g. contamination of the Addington Well in Croydon, Richards and Brincker, 1908). It is now recognised that faecal coliforms are quite commonly found in groundwaters, and some strains contain harmful viruses (Foster, 2000). Cases of cryptosporidium have been connected to a chalk groundwater supply (Foster, 2000). Most faecal bacteria only survive around 10 days in the aquifer, although some can last up to 100 days (Foster, 2000). Bacterial contamination is often associated with high turbidity.

Contamination of springs and boreholes from pesticides and microbial pathogens only occurs when there is rapid groundwater flow in both the unsaturated and saturated zones (Foster, 2000). In many cases this is likely to be associated with the stream sinks draining agricultural land where the Chalk is overlain by Palaeogene cover (Section 1.5.5). Rapid flowpaths in the unsaturated zone beneath the Chalk outcrop (Section 1.3.4) may also enable rapid transport of pesticides and microbial pathogens following exceptional rainfall. Rapid groundwater flowpaths transport both non-persistent contaminants and persistent contaminants from diffuse and point sources that are held in storage in the Chalk. Diffusion of contaminants into the porous matrix initially results in attenuation (Foster, 1975; Barker and Foster, 1981), but as illustrated by the long-term persistent water quality problems discussed above, contaminants stored in the matrix are later released, prolonging water quality problems.

To conclude, the water quality of abstraction boreholes and springs depends upon the nature of flow and solute transport through the unsaturated and saturated zones, and the degree of connectivity of fissures and conduits. Protection of water resources and springs is difficult because the physical distribution of such features is unpredictable, and modelled source protection zones are often inaccurately defined. An aim of this thesis is to use tracer testing techniques to investigate the physical structure and distribution of fissures and conduits, how and where they are connected, and how attenuation mechanisms operate along rapid groundwater flowpaths.

1.4 General karst concepts

1.4.1 Definition of karst

The term "karst" means stony ground and is the name of an area in Western Slovenia (Klimchouk and Ford, 2000). The landscape is characterised by a lack of surface drainage, bare rock sculpted by dissolution, dolines, stream sinks, and caves. Ford (2004) notes that the term karst was originally adopted to describe similar landscapes by early workers such as Cvijić, (1893), and Sawicki (1909), and that it continued to be defined as a geomorphological term by Sweeting (1972), White, (1988), and Ford and Williams (1989). These authors related the visible karst landscape to the occurrence of rapid groundwater flow in conduits and caves beneath the surface. Figure 1.10 is an example of a typical karst landscape (Picos de Europa, Spain).



Figure 1.10: Example of a karst landscape (Picos de Europa, Spain)

More recently emphasis has moved towards a more hydrogeological definition, and the term karst has been expanded to encompass dissolutional processes in all rocks, the vast majority being carbonates (Klimchouk and Ford, 2000; Ford, 2006). Karst aquifers are now considered to include all aquifers in which initial granular or fracture conditions have been modified by dissolution (Ford, 2006).

Within this hydrogeological definition it is clear that karst occurs across a very wide range of scales depending upon the geological conditions and the history of karstification. Atkinson and Smart (1981) evaluated the carbonate aquifers in the UK, classifying them on a scale of increasing karstification from the Chalk through the Magnesian Limestone and the Jurassic Limestones to the Carboniferous Limestones and Durness Limestones.

1.4.2 Surface karst geomorphology

Karst landscapes may be a mixture of relict features from previous phases of karstification and features that are currently hydrologically active. A distinction can be made between genetically karstic features that are no longer hydrologically active, and functionally karstic features that are hydrologically active and in the process of development. At the extreme end of the karst scale the landscape is entirely dominated by dissolution producing pinnacle karst, cockpit karst, and cone and tower karst landscapes (White, 1988). However, many karst landscapes display much smaller scale geomorphological characteristics; with dry valleys, springs, sinking streams, and dolines being a characteristic at the lower end of the karstification scale. These features are briefly described below, with a more lengthy discussion on dolines because they are important features in chalk landscapes (Section 1.5.3).

Partial or complete capture of surface drainage by an underground network of caves, conduits and fissures occurs in karst landscapes. In karst rocks there is a progression from surface flow within a valley to the eventual formation of a dry valley that is never hydrologically active (Trudgill, 1985; Dreybrodt, 1988; White, 1988). An example of such a dry valley is seen in Figure 1.10. White (1988) describes several stages in the evolution of dry valleys in karst. Prior to dissolutional enlargement of fractures in the subsurface all flow is above ground and surface drainage networks are developed. In the second stage the onset of small scale-fissure and conduit development results in some of the base flow being lost to the underground, but the surface stream flows all year. In the third stage the capacity of the underground conduit system increases to take all the base flow, resulting in a dry stream bed in summer; and in the fourth stage the capacity of the conduits has increased sufficiently to divert all flow underground leaving a remnant valley that is always dry. Over time the structure of the valley may disappear altogether as dolines are developed resulting in an irregular topography.

In karst areas there are many large springs which are functionally karstic features discharging groundwater that has flowed through fissures, conduits and caves. Karst springs tend to be characterised by large and variable discharges (Figure 1.11). They also have high turbidity and a marked change in chemistry following rainfall (Shuster and White, 1971; White, 1988; White, 2006; Toran et al., 2006).



Figure 1.11: Discharge from a karst spring in Kotor, Montenegro following a thunderstorm (note yellow van on right for scale)

There are many discrepancies in the terminology used to describe sinking streams and surface depressions. For example, the term swallow hole is generally used to refer to a sinking stream (e.g. Atkinson and Smith, 1974) but has also been used to refer to hydrologically inactive dolines (e.g. Thomas, 1954; West and Dumbleton, 1972). In this thesis, the term *stream sink* will be used to describe features where a surface stream ends abruptly at a point where the water sinks into the ground, as it is an unambiguous term that clearly implies the presence of water. Stream sinks are functionally karstic features that provide point recharge into the subsurface network of fissures, conduits and caves. The term *doline* will be used to describe surface depressions where there is no surface stream (avoiding the use of the term sinkhole which has been confusingly used to describe both stream sinks and dolines).

Dolines are depressions in the ground surface that are usually circular or oval shaped (Figure 1.12) with diameters normally ranging from <1 m to ~500 m and depths of <1 m to >100 m. The presence of dolines is diagnostic of karst, although their absence does not signify the absence of subsurface karst (Williams, 2004). Hydrological processes in karst dolines are discussed in detail by Gunn (1981) who describes three flow components supplying dolines: overland flow (implying the presence of a sinking stream), throughflow (above the soil-rock interface), and subcutaneous flow (lateral flow in upper weathered part of the rock); and three types of drainage from the base of dolines: shaft flow (films flowing down the sides of shafts), vadose flow (vertical flow down fissures) and vadose seepage (slow vertical flow down fractures or vertical intergranular flow).



Figure 1.12 Aerial photo of Dolines in South Wales (right of quarry)

Understanding how dolines form provides insight into subsurface hydrogeology because some types of doline require the presence of large cavities whilst others can be formed as a consequence of flow down small-scale fissures. Classification of different types of dolines has been widely discussed (Sweeting, 1972; White 1988; Ford and Williams, 1989; Waltham and Fookes 2003; Williams 2004). These studies built on the early work of Cvijić, (see Stevanović and Mijatović, (2005), for details and translations). It can be difficult to determine how a particular doline was formed because dolines

formed by different mechanisms may have similar morphology and many are formed by a combination of processes (Williams, 2004). This has led to some confusion over terminology. Williams (2004) provides an extensive discussion of the different terminology used in the literature and how it relates to the actual mechanisms of doline formation. He distinguishes three different processes; solution, collapse and subsidence. All future references to different types of dolines will adopt the terminology of Williams (2004) described below.

Solution dolines occur where the limestone or soluble rock is exposed at the surface. They form due to lithological and structural variations in fracturing of the bedrock. Diffuse recharge through fractures and fissures in the epikarstic zone concentrates in the more significant fractures and fissures causing watertable drawdown around these flowpaths (Figure 1.13). This further focuses flow and eventually a surface depression is created above the permeable feature where the land surface has been preferentially corroded (Williams 2004).

Collapse dolines occur where rock or sediments in the surface collapse suddenly into a cavity in the underlying karst rock. Williams (2004) subdivides collapse dolines into three categories based upon the surface geology. He suggests that true collapse dolines occur where the karst rock is exposed at the surface, caprock collapse dolines occur where a non-carbonate rock overlies the karst rock, (e.g. dolines in the Millstone Grit overlying the Carboniferous Limestone in South Wales), and dropout dolines occur where unconsolidated sediments are present at the surface (Figure 1.13). Williams (2004) emphasizes the distinction between dropout dolines and subsidence dolines which also occur where sediments overly karst rocks, but do not require the presence of a large void in the karst rock itself. Subsidence dolines (suffosion doline in Figure 1.13) form by the process of suffosion whereby sediments fall or are washed down vertical dissolutional features in the underlying karst rock (Williams 2004). The resulting subsidence can be gradual or rapid. Rapid subsidence occurs in cohesive sediments that can support large voids within the sediment itself as material is removed by suffosion. In non-cohesive cover the removal of sediment occurs more consistently and therefore the subsidence is more gradual.

Williams (2004) also describes buried dolines that have no surface expression but are bedrock dolines that have become filled with sediment. These may be hydrologically inactive palaeokarst features, but can also become reactivated resulting in subsidence. They are analogous to the subsurface dissolution features described in section 1.5.4.

Dolines may be palaeokarst features that are not currently functionally karstic. However, they are genetically karstic and their presence implies that there is or has been a fully connected flowpath between the doline and the aquifer discharge point (Williams, 2004). This can occur across the full spectrum of karst scales but it implies that there is a connected network of fractures of sufficient size to transport solute and/or sediment through the aquifer. As dolines do not occur in fractured aquifers it follows that this network must comprise at the lower end of the karst scale fissures (solutionally modified fractures), and can comprise at the higher end of the karst scale a fully connected cave conduit system.

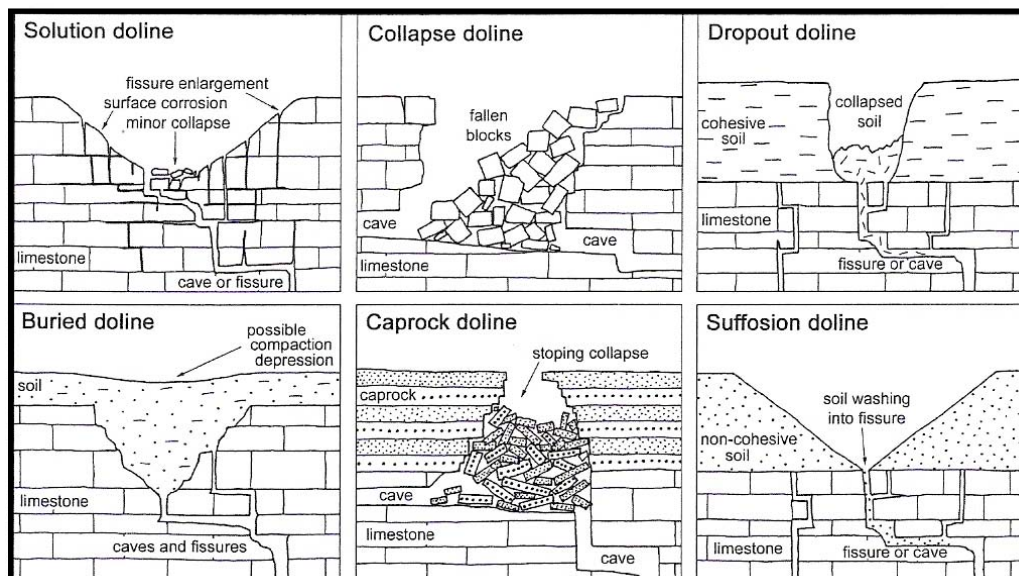


Figure 1.13: Mechanisms of doline formation (from Waltham and Fookes, 2003)

1.4.3 Epikarst

The epikarst (sometimes referred to as the subcutaneous zone) is the near surface area where permeability is higher and more uniformly distributed than elsewhere in the aquifer (Klimchouk, 2000). Physical and chemical weathering widens fractures in a broadly ubiquitous manner. With increased depth below the surface widening of fractures occurs at different rates (Palmer, 2000), and at the base of the epikarst flow is

focused along a few major fissures (Klimchouk, 2000). The epikarst is an important reservoir for groundwater storage (Williams, 1983, Klimchouk, 2000). Klimchouk (2000) notes that Gunn (1983), Klimchouk and Jablokova (1989) and Williams (1983) have demonstrated that epikarst storage can delay groundwater transport through the unsaturated zone by several days to several months. Klimchouk (2000) suggests that groundwater stored in the epikarst is released consistently into the vadose zone supporting baseflow in the phreatic zone during dry periods. He also suggests that the epikarst enables diffuse recharge precluding surface runoff, with flow concentration occurring beneath the surface.

1.4.4 Karst hydrogeology

In karst aquifers flow largely occurs in fissures, conduits and caves. Consequently they are highly heterogeneous and anisotropic. Together with the dominance of turbulent flow this has led authors to suggest that the traditional Darcian approach that treats aquifers as an equivalent porous medium characterised by laminar flow is not applicable to karst aquifers (Ford and Williams, 1989). Models often continue to use the Darcian approach, assuming that if the scale is large enough the effect of fissures and conduits is smoothed out in the same way that differences between pores and grains are assumed to be smoothed out in granular aquifers (White, 2006). Regional scale models based on Darcy's Law sometimes produce reasonable estimates of hydraulic head in boreholes, but there is little justification for assuming that other predictions from the model are correct. For example such models generally under-predict velocity (Smart and Worthington, 2004a).

A further problem in karst aquifers is that groundwater catchments do not necessarily coincide with topography, with conduits carrying water between adjacent surface water basins. (White, 2006). In some cases there may also be significant changes under high flow conditions when overflow conduits transport groundwater in different directions to different basins (White, 2006). A third problem is that conduit and cave development does not always occur in directions that are suggested by borehole groundwater contour maps (Ewers, 2006). Ewers (2006) describes three cases where tracer testing studies demonstrated that groundwater flow in conduits occurred in very different directions from those predicted from the borehole based contour maps. He suggests this can be because underground cave streams control the position of the water table in a similar

manner to surface streams. If boreholes are sited on opposite sites of a conduit or cave groundwater flow will not be from the borehole with the highest head towards the one of lower head, it will be towards the conduit or cave from both boreholes (Figure 1.14)

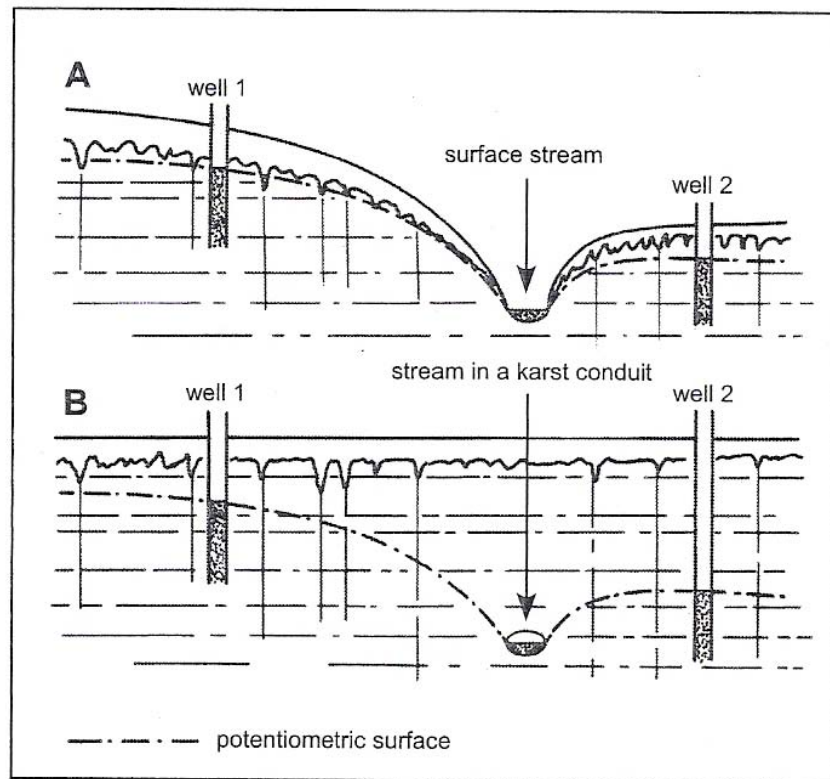


Figure 1.14: Lack of continuity between boreholes due to a surface stream (a) and a hidden karst conduit (b) (from Ewers 2006).

Defining spring and borehole groundwater catchments in karst aquifers and identifying the location of the conduits and caves requires the use of tracer testing or, where possible, direct mapping of cave networks. Catchment scale natural gradient tracer tests have been used in karst aquifers since the end of the nineteenth century (Käss, 1998). Water tracing techniques are reviewed by Ford and Williams (1989) and Käss (1998). Many different types of tracer have been used including spores, salts, bacteria and bacteriophages, but fluorescent dyes and optical brighteners are used most commonly (Käss, 1998). Tracer properties are discussed further in Section 4.2.

Qualitative tracer tests help to delineate groundwater catchments. These use passive detectors that absorb dyes or optical brighteners from a flowing watercourse, and can be collected at intervals of several days. This type of test demonstrates whether a tracer has arrived at a monitoring point and provides a rough indication of travel time.

Quantitative tracer tests and analysis of tracer breakthrough curves provide more extensive information on the nature of groundwater flowpaths (e.g. Atkinson et al., 1973; Atkinson, 1977; Stanton and Smart, 1981; Edwards et al., 1991; Massei et al., 2002; Bracq and Brunin, 1999). Tracer recoveries and the volume of the flow system can be calculated (methods are described in Atkinson et al., 1973), and aquifer parameters can be derived from breakthrough curves (Field, 1997; Käss, 1998).

Tracer testing has shown that groundwater velocities in karst conduits are usually between 0.1 and 10 km.d⁻¹, averaging 1.7 km.d⁻¹ (Worthington, Davies and Ford, 2000, cited by Smart and Worthington, 2004b). Karst aquifers are particularly vulnerable to contamination because of these rapid velocities, and also because stream sinks and dolines enable direct transfer of contaminants into the aquifer. Point source contamination of karst aquifers is discussed by Schindel and Hoyt (2004) whilst dispersed pollution is discussed by Boyer (2004). Martin et al. (2006) note that if contaminants infiltrate the rock matrix, they can have much longer residence times.

Results of tracer tests and mapping of cave passages has resulted in conceptual models of conduit networks relating conduit patterns to geological and hydrogeological factors (e.g. Ford and Williams, 1989; Ford, 2000; Palmer, 2000). For example, Palmer (2000) related cave patterns to porosity and recharge (Figure 1.15). Smart and Worthington (2004b) suggest that most conduit systems are dendritic with a number of tributaries feeding the major trunk conduit although they note there can be distributary flow to multiple outlets, for example in the Mendips, UK (Atkinson, 1977) and in Kentucky, USA (Quinlan and Ewers, 1989). Worthington (2001) discusses the depth of conduit flow in karst aquifers, concluding that deeper conduits occur where there is a high stratal dip, and where there is a long flowpath.

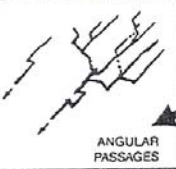

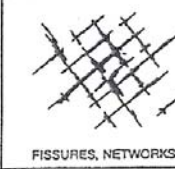
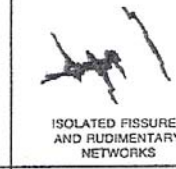
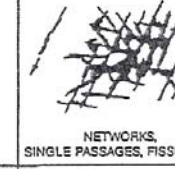
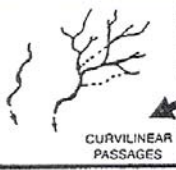

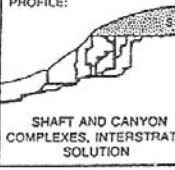
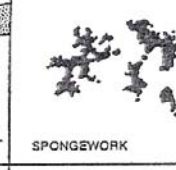
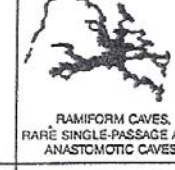
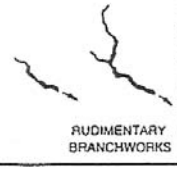
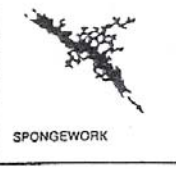
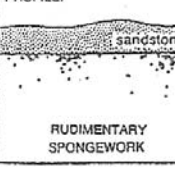
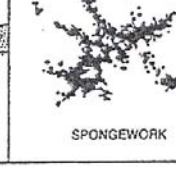
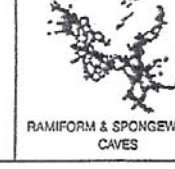
		TYPE OF RECHARGE				
		VIA KARST DEPRESSIONS		DIFFUSE		HYPOGENIC
		SINKHOLES (LIMITED DISCHARGE FLUCTUATION)	SINKING STREAMS (GREAT DISCHARGE FLUCTUATION)	THROUGH SANDSTONE	INTO POROUS SOLUBLE ROCK	DISSOLUTION BY ACIDS OF DEEP-SEATED SOURCE OR BY COOLING OF THERMAL WATER
		BRANCHWORKS (USUALLY SEVERAL LEVELS) & SINGLE PASSAGES	SINGLE PASSAGES AND CRUDE BRANCHWORKS, USUALLY WITH THE FOLLOWING FEATURES SUPERIMPOSED:	MOST CAVES ENLARGED FURTHER BY RECHARGE FROM OTHER SOURCES	MOST CAVES FORMED BY MIXING AT DEPTH	
TYPE OF PRE-SOLUTIONAL POROSITY	FRACTURES	 ANGULAR PASSAGES	 FISSURES, IRREGULAR NETWORKS	 FISSURES, NETWORKS	 ISOLATED FISSURES AND RUDIMENTARY NETWORKS	 NETWORKS, SINGLE PASSAGES, FISSURES
	BEDDING PARTINGS	 CURVILINEAR PASSAGES	 ANASTOMOSES, ANASTOMOTIC MAZES	PROFILE:  SHAFT AND CANYON COMPLEXES, INTERSTRATAL SOLUTION	 SPONGEWORK	 RAMIFORM CAVES, RARE SINGLE-PASSAGE AND ANASTOMOTIC CAVES
	INTERGRANULAR	 RUDIMENTARY BRANCHWORKS	 SPONGEWORK	PROFILE:  sandstone RUDIMENTARY SPONGEWORK	 SPONGEWORK	 RAMIFORM & SPONGEWORK CAVES

Figure 1.15: Relationship between plan patterns of caves and porosity and recharge (Palmer, 2000)

Karst aquifers are now described as having triple permeability (Worthington, Ford and Beddows, 2000; White, 2006) comprising the matrix, fractures and conduits (fissures are included as part of the conduit category in this definition). The frequency and distribution of fissures and small conduits and the interactions between the different components of karst aquifers is still not well understood. It has been suggested that at times of low recharge into stream sinks and dolines, conduits act as drains for the surrounding fractures and matrix, whilst during high flow higher heads in the conduit causes flow from the conduits into the fractures and matrix (White, 1999, cited in Martin et al., 2006). In mature karst aquifers most of the flow is thought to be through conduits and fissures, but with most of the storage in fractures and the matrix (White, 2006). Atkinson (1977) concluded that 60-80 % of groundwater in the Carboniferous Limestone of the Mendip Hills in Somerset is transported in conduits, but that ~ 90 % of the storage was in fractures. White (2006) reports that Hess and White (1989), and Worthington, Davies and Ford (2000) found that ~ 90 % of groundwater flow in the Mammoth Cave system in the Kentucky karst, USA is through conduits.

1.4.5 Controls on subsurface karst development

Factors controlling the development of fissures, conduits and caves are discussed in Ford and Williams (1989), White (1988), Klimchouk and Ford (2000), Lowe (2000), Palmer (2000), Klimchouk (2004), Lowe (2004) and Ford (2004). Karst development depends upon dissolutional processes. The nature of underground voids depends upon lithology, structure, and the length of the period of karstification. Stratigraphical factors can affect the onset of conduit development, and the general geological situation and climate play an important role in determining the rate of karstification.

In carbonate rocks rainwater quickly becomes saturated with calcium carbonate and without more complex chemical processes significant dissolution would not occur (White, 2006). Additional sources of acidity from carbonic acid produced from carbon dioxide in soils, or sulphuric acids from hydrogen sulphide or metallic sulphides are necessary for substantial karst development (Klimchouk, 2004). The importance of dissolution kinetics is discussed in White (1988), Ford and Williams (1989), and White (2006). Calcite dissolution is initially extremely rapid, but when solutions are close to saturation, the rate is several orders of magnitude slower (White, 2006). Mixing corrosion also enhances dissolution where two saturated groundwaters of variable carbon dioxide content mix to form an undersaturated solution (Bögli, 1964, cited by White, 2000). Models based on dissolution chemistry have been used to investigate the initiation and evolution of karst conduits and conduit networks (Dreybrodt and Gabrovšek, 2000; Dreybrodt and Siemers, 2000; and Dreybrodt et al., 2005).

Lithology affects karst development primarily because it determines the initial solubility of the rock (Klimchouk and Ford, 2000). The frequency, distribution and connectivity of fractures and bedding planes affect the nature of subsurface solutional development. For example, Ford (2004) suggests that complex branching conduit networks form more commonly in bedding controlled systems. Faults can result in open voids, or filled features that may form barriers to flow. Rocks with well-connected voids develop solutionally enlarged pathways more quickly. However, rocks with high primary permeability may develop large numbers of small solutional pathways whereas more massive rocks are more likely to develop larger scale caves. Mature karst aquifers where dissolution has occurred for longer periods develop complex conduit networks,

with abandonment of older higher level conduits as new ones develop in response to base level changes.

Ford (2000) presents a modified version of the four state model of cave development in Ford and Williams (1989), (Figure 1.16). It shows the effect of increasing fracture frequency (bedding fractures) on patterns of cave development. It is drawn showing caves draining down dip in steeply dipping rocks, but Ford (2000) notes that states 1 and 2 are more likely to occur if the dip is steep, whilst states 3 and 4 are more likely in strata of near horizontal dip. State 0 (at the top) occurs if fracture frequency or aperture are too low to enable speleogenesis, and State 5 (at the bottom), where fracture frequency or matrix porosity is too high to permit development of caves at an enterable scale.

There can also be stratigraphical controls on fissure and conduit development. Lowe (2000, 2006) proposed the inception horizon hypothesis suggesting that fissures and conduits are preferentially developed along certain stratigraphic horizons. These may be horizons with an in situ source of acidity (e.g. pyrite), or simply horizons where there is a change in the rock properties (e.g. where there is a less permeable layer, flow may be concentrated immediately above it).

The general geological setting is important because if there are impermeable strata that produce acidic soils adjacent to carbonate rocks, these may generate aggressive allogenic surface runoff that recharges the soluble carbonate rock through stream sinks. Climate affects the rate of karst development, which is faster in areas of higher rainfall. Climate also determines the nature of vegetation and soils that provide carbon dioxide increasing the acidity of recharge waters.

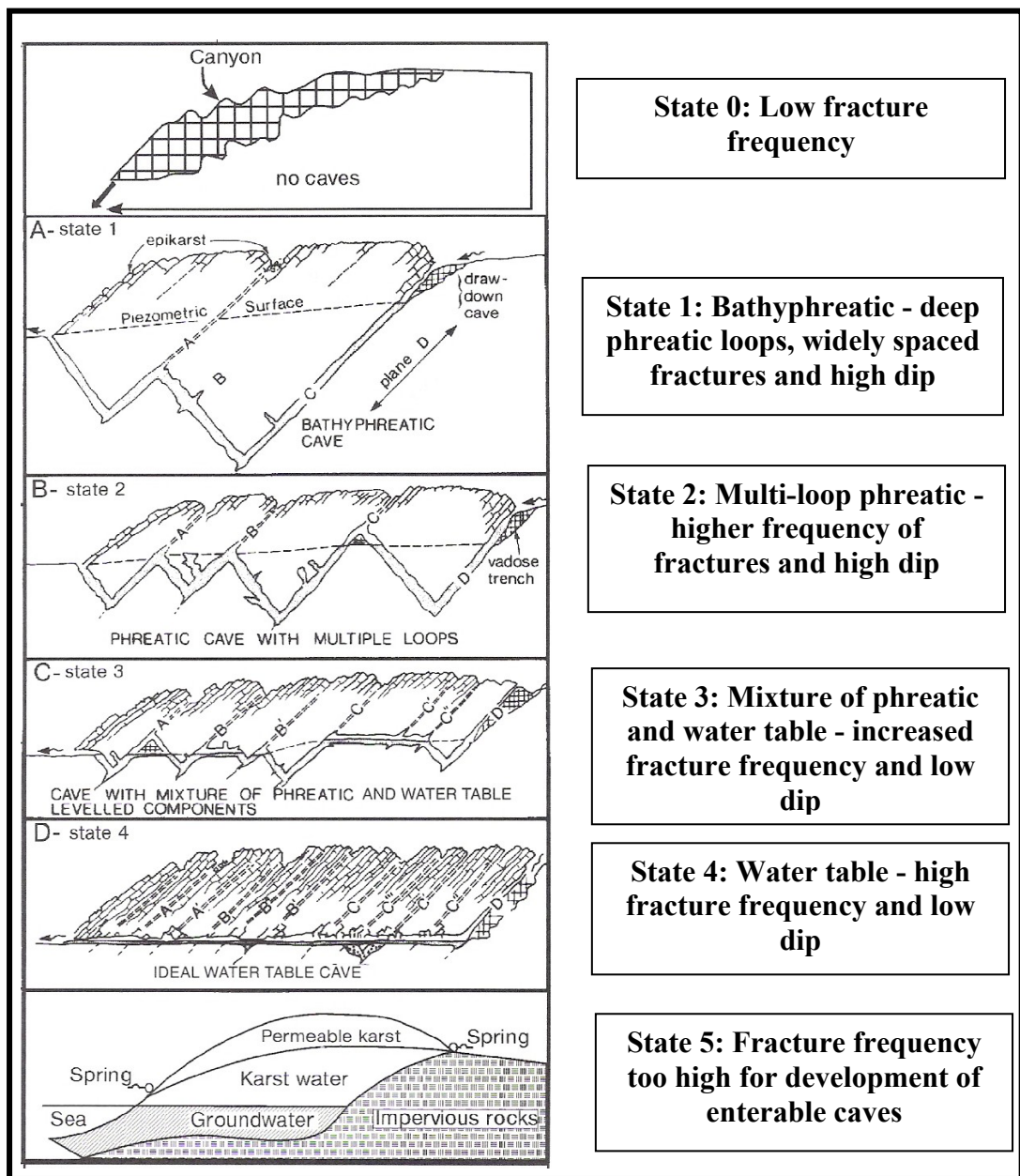


Figure 1.16: Modified version of the four state model of cave development (based on Ford, 2000)

1.5 Chalk Karst Geomorphology

1.5.1 Introduction

Chalk landscapes are weakly karstified compared to landscapes associated with classical karst aquifers. Limestone pavements are absent, and caves are very rarely encountered. Dry valleys are extremely common and dolines, stream sinks and springs are locally abundant but are generally quite small. Large springs (~ 20 to $200 \text{ L}\cdot\text{s}^{-1}$) are relatively common but discharges tend to be much less variable, and the average discharge rather lower than in many fully karstic aquifers. In some areas, subsurface sediment-filled dissolution features are commonly encountered during quarrying or engineering works. This section provides an overview of surface karst features that are observed in the UK Chalk.

1.5.2 Dry Valleys and ephemeral streams

Dry valley networks are the most significant feature in chalk landscapes, but they also occur in other strata in the UK including the Carboniferous Limestones, Jurassic Limestones, and Triassic sandstones (Goudie, 1990). The origin of dry valleys is still debated. Goudie (1990, 2001) discusses theories for the formation of dry valleys in all strata, suggesting that they fall under three broad categories: uniformitarian, marine, and palaeoclimatic. Uniformitarian theories involve gradual evolution of the landscape without any major changes in the environment; and include lowering of the water table in response to erosion of major river valleys, reduction in groundwater catchments due to scarp retreat (Fagg, 1923), river capture, and the "karstic" model of progressive dissolution forming fissures and conduits resulting in increasing amounts of surface water being diverted into the subsurface (Smith, 1975 cited by Goudie, 1990, see also discussion in Section 1.4.2). The marine hypothesis suggests that the valleys were hydrologically active at times in the past when sea levels were higher causing higher groundwater levels. Palaeoclimatic theories are those suggesting that the valleys were hydrologically active under very different climatic conditions than exist at the present time. They include erosion by glaciers or glacial meltwater, erosion during periods of much higher precipitation than currently occurs, and increased runoff during periglacial periods due to decreased permeability.

It was first suggested by Reid (1887) that chalk dry valleys were formed under periglacial conditions because permafrost rendered the ground impermeable enabling

surface runoff in the summer (Goudie, 1990). Many chalk dry valleys are lined with deposits thought to have arisen from solifluction processes (Goudie, 1990; Ballantyne and Harris, 1994), implying that periglacial conditions existed in these areas. Although it is generally agreed that many of the processes described above could have led to the development of the dry valley network in the Chalk, it is thought most likely that they were formed under periglacial conditions due to a combination of decreased permeability and high seasonal runoff (Sparks, 1986; Goudie, 1990; Ballantyne and Harris, 1994). However, very similar dry valleys occur on chalks elsewhere, where periglacial conditions have not occurred, for example in Tasmania and on the Austin Chalk in Texas.

It is likely that karst processes have contributed to the formation of the UK chalk dry valleys. As discussed in Section 1.4.2, fissures and small conduits take time to evolve and prior to their existence there would have been more surface drainage than currently occurs. Also, as major river valleys are downcut, the water table is lowered and new conduits and fissures develop at lower levels resulting in networks of fissures and conduits that previously fed springs (and hence rivers) becoming inactive. Docherty (1971) provides a synthesis on C.C. Fagg's theories that karst processes formed the chalk dry valleys. C.C. Fagg suggested that karstic spring head recession resulted in chalk valleys becoming dry, and that inactive swallow holes and springs in dry valleys have been obscured by recent periglacial features. Field studies of 6 chalk streams in Dorset by Willie Stanton found that ephemeral sections become reactivated at specific points (Dave Buckley, personal communication, 2005). These ephemeral streams may represent an intermediate stage in the abandonment of the valleys (corresponding to the third stage in the development of dry valleys in karst areas described by White (1988) (Section 1.4.2).

It appears that a combination of periglacial conditions and karst processes originally sculpted chalk dry valleys. They are currently hydrologically inactive and there is an absence of surface drainage over much of the Chalk outcrop because the transmissivity (enhanced by the development of fissures) is sufficient to carry most of the recharge in the subsurface.

1.5.3 Dolines

Dolines associated with the Chalk are common, and have been described for more than 150 years. Sperling et al. (1977) discuss early work on Dorset dolines by Stevenson (1812) and the work of Fisher (1859) who suggested that they are formed by dissolution of chalk following percolation of rainwater containing carbonic acid. Dolines are found in the greatest numbers in Dorset, but there are also moderately high densities in Hertfordshire, Buckinghamshire, Wiltshire, Berkshire, Surrey, Kent, and a few parts of the Chilterns (Sperling et al., 1977). However, man-made pits may be mistaken for naturally formed dolines. For example, Prince (1964) noted that many pits in East Anglia are man-made rather than natural dolines. Natural depressions may be distinguished because they have a more regular rounded shape than manmade pits. Dolines appear to be very infrequent in many areas of the Chilterns, on Salisbury Plain and the South Downs (Sperling et al 1977).

Chalk dolines are predominantly found where there is a thin Palaeogene or Clay-with-Flints cover. The largest in England is Culpeppers Dish in Dorset, which is 21 m deep and 86 m in diameter (Waltham et al., 1997). Chalk dolines are small compared to dolines in highly karstic rocks, normally with depths of ~1 to 10 m, and diameters of ~2-50 m.

Sperling et al. (1977) noted that chalk dolines are morphologically similar to dolines studied by Thomas (1954) in the Carboniferous Limestone of South Wales and Mendip. In both studies the internal shape (mean depth to mean diameter ratio) was similar. Sperling et al. (1977) found that doline densities in Dorset on Southover Heath of 99/km², and on Puddletown Heath of 157/km², were comparable to those of 111/km² in South Wales. They also found similarities in the geological situation, with chalk dolines in Dorset where there is Palaeogene cover, and Welsh dolines where the Carboniferous Limestones is overlain by a caprock of Millstone Grit. However, although these similarities suggest a broadly common karstic origin, it does not signify a common genesis. The South Wales dolines are predominantly caprock collapse dolines formed by collapse of the Millstone Grit into cavities in the underlying limestone. In contrast the Dorset and other chalk dolines mostly occur on unconsolidated Clay-with-Flints or Palaeogene deposits, and are probably subsidence dolines formed by suffosion (Section 1.4.2). The nature of the sediments overlying the

Chalk is very variable (Section 2.4), and therefore there may be both rapid subsidence in cohesive sediments to produce the sudden collapses described by Sperling et al. (1977), and slower subsidence in non-cohesive sediments. Subsidence dolines probably occur more commonly in non-cohesive sediments that are more permeable enabling transport of water to the underlying chalk. There are a few shallow dolines present on the Chalk outcrop itself. They may be relict features formed on cover before it was eroded. If they were formed after the removal of cover they must be solution dolines as they are too shallow to be collapse dolines.

Whilst chalk dolines are genetically karstic features that imply a direct recharge mechanism through the overlying sediments when they were formed (Section 1.4.2), they may not be hydrologically active at the present time. House (1992) established a chronology based upon archaeological features on Bronkham Hill, Dorset, and found that most dolines were formed between 1600 and 4000 years ago. He suggested that this may be an indication of higher rainfall during this period increasing dissolution.

1.5.4 Subsurface dissolution features

Subsurface dissolution features are sediment filled voids that differ from dolines because they have no surface expression (Lamont-Black and Mortimore, 1999). The term "dissolution pipe" has been used to describe such features (Lamont-Black and Mortimore, 1999) but confusion arises because it is also used to refer specifically to vertical sediment filled pipes (Thorez et al., 1971). Subsurface dissolution features occur very commonly in areas where the Chalk is overlain by a thin Palaeogene cover (McDowell, 1975; Lamont-Black and Mortimore, 1999; Matthews et al., 2000). They are formed by gradual dissolution of chalk creating voids that are filled by slumping of sediments from the overlying deposits.

Subsurface dissolution features (Figure 1.17) are encountered in quarries, cliffs and during road construction projects (House, 1991; House, 1996; Lamont-Black and Mortimore, 1999). Several studies have used geophysical techniques to identify subsurface sediment filled voids prior to engineering projects (McDowell, 1975; Matthews et al., 2000). They can occur at extremely high densities. Lamont-Black and Mortimore (1999) report up to 265 per hectare at a site in Sussex.

Subsurface dissolution features have very variable morphology, and authors have classified different types (e.g. Thorez et al., 1971; Lamont-Black and Mortimore, 1999). They broadly fall into two categories: dish shaped features with wide diameters relative to their depth, and vertical features which are much deeper than they are wide. Within these categories some features exhibit more complex and irregular structures. Dish shaped features have been described up to 30 m in diameter and vertical features up to 12 m deep (Thorez et al., 1971). The morphology of features encountered in a road construction project within the Lambourn catchment (Mott Macdonald, 2005) is described in more detail in Section 3.6.

Subsurface dissolution features are hydrologically similar to dolines in that they are genetically karstic requiring transport of solutes through the aquifer, although they differ in that they do not require transport of sediments (which would imply turbulent flow). Like dolines they may be relict features that are not currently functionally karstic.

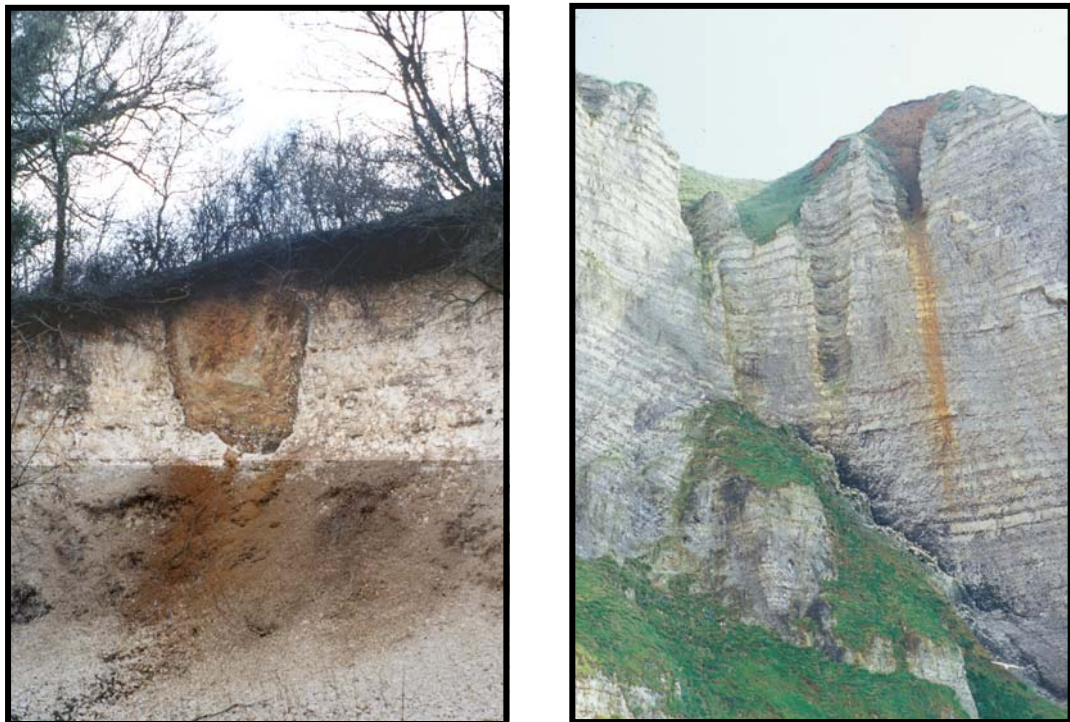


Figure 1.17: Sediment filled subsurface dissolution features in a quarry at Chilton Foliat, Wiltshire (left) and in chalk cliffs at Etretat, France (right) (photos Andy Farrant)

1.5.5 Stream Sinks

The characteristics of stream sinks associated with the Chalk are discussed in the literature in relation to tracer tests in Hertfordshire, Hampshire and Berkshire, (Harold, 1937; Atkinson and Smith, 1974; Banks et al., 1994). There are also geomorphological studies of the stream sinks at Water End in Hertfordshire (Wooldridge and Kirkaldy, 1937; Walsch and Ockendon 1982), and a large stream sink has been observed in the bed of the River Mole in Kent (Banks et al., 1995; Macdonald et al., 1998).

Stream sinks are generally developed on the edge of the Palaeogene cover overlying the Chalk. They tend to be only active during wet periods (Harold, 1937; Atkinson and Smith, 1974; Banks et al., 1994). The streams often sink into a depression and it can be difficult to distinguish stream sinks from dolines (MacDonald et al., 1998).

The best studied features are those at Water End in Hertfordshire where there is an extensive complex of stream sinks in a large depression at the end of the Mimms Hall Brook. Woolridge and Kirkaldy (1937) note that there are also many other sink points along the length of the Mimms Hall Brook and in the general area. The amount of flow into the stream sinks is extremely variable with no flow in exceptionally dry periods, whilst in very wet periods a lake forms over the entire area activating an overflow surface stream (Wooldridge and Kirkaldy, 1937). The exact location of the sink point at Water End varies with hydrological conditions which result in water sinking progressively further upstream as water levels recede (Walsh and Ockendon, 1982). Sink point locations also change as holes become blocked and new holes are eroded.

Recently the British Geological Survey has compiled a database of karst features in the UK (co-ordinated by Andy Farrant). Figure 1.18 shows the distribution of stream sinks associated with the English Chalk recorded in the database. The map shows that in some areas there is a very high density of stream sinks, often near the edge of the Chalk outcrop. The data are biased towards areas that have been recently studied in detail, and it is likely that there are similar densities of stream sinks along the Chalk/Palaeogene margins where none are marked.

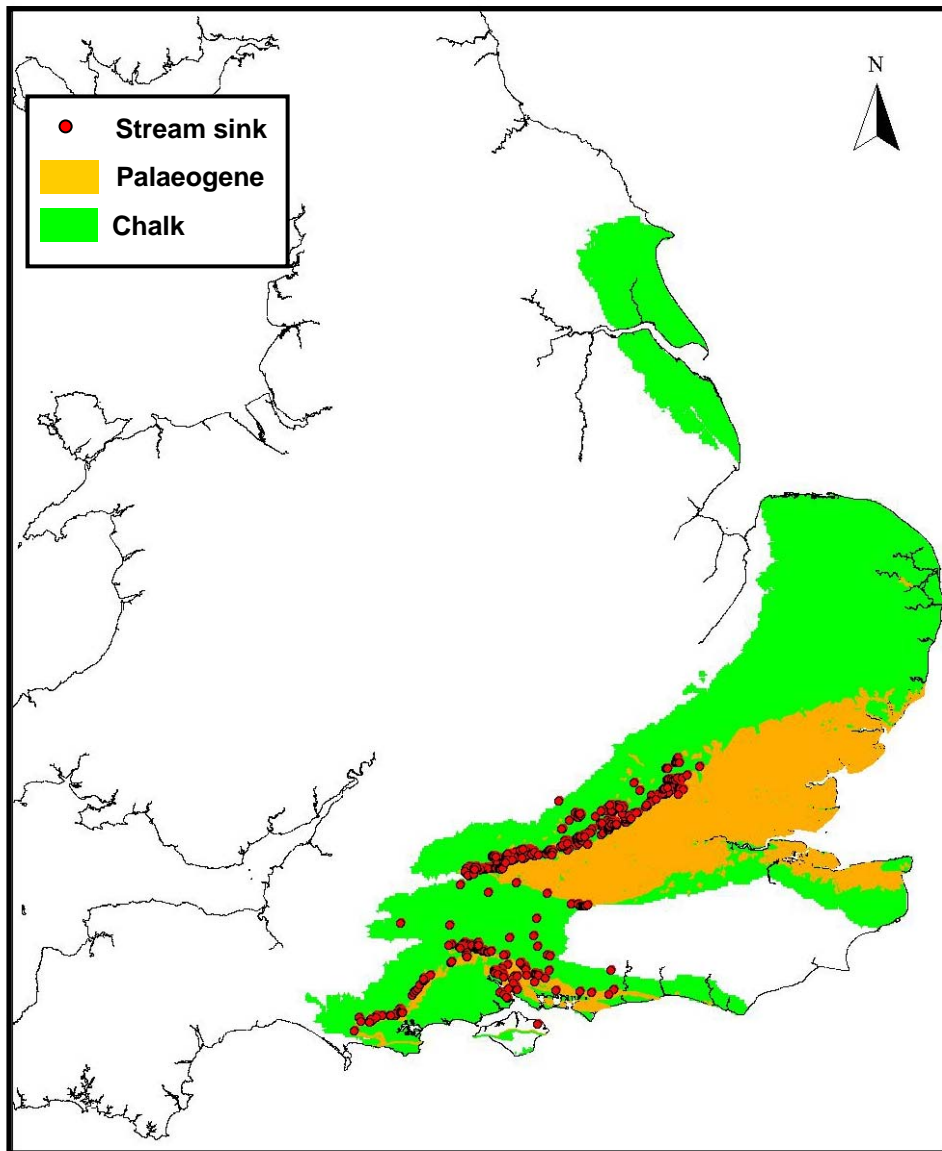


Figure 1.18: Stream sinks associated with the English Chalk recorded in the BGS karst database^{BGS}

1.5.6 Springs

Although large springs (~ 20 to 200 L.s^{-1}) occur frequently in the Chalk, there is no review of their frequency, nature or distribution in the literature. Specifically large springs have been noted in the Kennet valley in Berkshire at Hungerford (SU3187 6797, Figure 1.19) and Kintbury (SU 3741 6709), (Andy Farrant, personal communication, 2004); in Hampshire at Bedhampton (SU 707 064) and Havant (SU 712 063) (Atkinson and Smith, 1974); at Arkley Hole in Hertfordshire (TL 2881 1013), and at the Blue Pool in Berkshire (SU 5829 7148). Docherty (1970) reports that there are large chalk springs at Springhead (TQ 617 726) and Thorncroft (TQ 166 555) in Dorset. There are no records of whether these springs have a variable discharge or become turbid following

heavy rainfall, although turbidity has been reported at the Blue Pool (Banks et al., 1995), and there have been reports of turbidity at the Hungerford springs (Andy Farrant, personal communication, 2004) and Arkley Hole.



Figure 1.19: Chalk spring at Hungerford (left) with outflow channel (right), (photos Andy Farrant)

1.5.7 Chalk caves and conduits

Large cave entrances in outcrops or associated with stream sinks and springs are absent from the UK Chalk, and therefore it is often thought that cave development does not occur. Nevertheless, speleologists have found and explored many small chalk caves in the UK that are reviewed by Bradshaw et al. (1991) and Lowe (1992). Theories that the Chalk is not strong enough to support large cavities (e.g. Sparks, 1986) are countered by descriptions of the chalk sea caves at Flamborough Head in Yorkshire which are 20 m by 30 m (Reeve, 1982; Lowe, 1992), and large sea caves at Cuckmere in Sussex (Bradshaw et al., 1991).

Lowe (1992) notes that the sea caves at Flamborough cannot be wholly formed by wave erosion because they exhibit dissolutional features. Although this may be primarily due to the dissolutional action of seawater rather than meteoric water, freshwater inputs from small conduits associated with bedding planes are present at the landward end of some of the sea caves (Lowe, 1992).

The two most significant purely dissolutional chalk caves in England are Beachy Head and Canterbury Caves in Sussex that are exposed in cliff faces above current sea level and are described by Reeve (1976, 1981). Figure 1.20 shows the entrance to Beachy Head Cave, which is 366 m long. Canterbury Cave is 110 m long. Their location close

to the seashore suggests that mixing between marine and meteoric water may have been involved in their formation although they are generally described as caves formed by freshwater dissolutional processes (Reeve, 1981; Bradshaw et al., 1991; Lowe 1992), and there is a freshwater sump (water filled conduit) at the end of Beachy Head Cave. Both these caves are formed along a tabular flint layer, and dissolution tubules (see below) are also present. There are short sections of passage up to 2 m wide and 2 m high, and in Canterbury cave there is a chamber 9 m x 4 m x 2 m.



Figure 1.20: Beachy Head Cave entrance (photo from http://www.kurg.org.uk/sites/natural_caves.htm)

There are several other examples of short dissolutional caves exposed in sea cliffs in the Beachy Head area and at Seven Sisters in Kent (Reeve, 1977; Lowe, 1992), and at Beer in Devon (Procter, 1984). Although chalk dissolutional caves are mostly fossil phreatic passages, blind avens up to 8 m in height can be found in Beachy Head cave and in the short chalk caves at Beer (Reeve, 1981; Procter, 1984; Bradshaw et al., 1991).

Most stream sinks are in cover materials overlying the Chalk (Section 1.5.5), but there are a few examples where streams can be seen to sink into small chalk caves beneath the cover. Bradshaw et al. (1991) report that such features have been noted at Water End in Hertfordshire (TL 232 044), Lower Ensdon in Kent (TR 07 56), and Warren Row in Berkshire (SU 81 80). A similar feature was identified in Yattendon in Berkshire (SU 5637 7501) during the present study (Section 3.3.4). It is probable that there are other

small chalk caves associated with stream sinks but concealed beneath the cover material.

There are also reports of caves intersected by wells at four sites in Kent that are no longer accessible (Bradshaw et al., 1991). These were Strood (TQ 729 693), Knockholt (TQ 483 597), Chatham (TQ 776 663), and Blackheath (TQ 38 77). Reeve (1976) reports that an early reference by Sill (1907) described an active streamway more than 60 m in length at Strood, whilst Bradshaw et al. (1991) describe the cave at Knockholt as a section of active stream in a passage 10 m long, 5.5 m high and 3.5 m wide.

Campbell (1984) describes a 500 m long active stream cave in the Irish chalk 2 km from the sea (Figure 1.21). Much larger and longer chalk caves have been explored in France, for example Caumont Cave (Figure 1.22) and the Petites Dalles Cave (Figure 1.23 and 1.24) in Normandy. Caumont Cave has been intercepted during mining and comprises more than 7 km of natural passages including large avens up to 30 m in height (Rodet,1991; Rodet et al., 2005). The Petites Dalles Cave is 400 m long with passages up to 10 m in height (Rodet,1991; Laignel et al., 2004). Both caves were largely sediment filled. The Petites Dalles cave was excavated, whereas sediment has been removed from Caumont Cave by recent drainage.



Figure 1.21: Chalk cave in Ireland. Photo by Tim Fogg in Campbell (1984)



Figure 1.22: Passage in Caumont Cave, Normandy, France. Recent stream has eroded a deep channel through a passage previously almost full of sediment, and speleothems are present on roof.



Figure 1.23: Passage in Petites Dalles Cave, Normandy, France

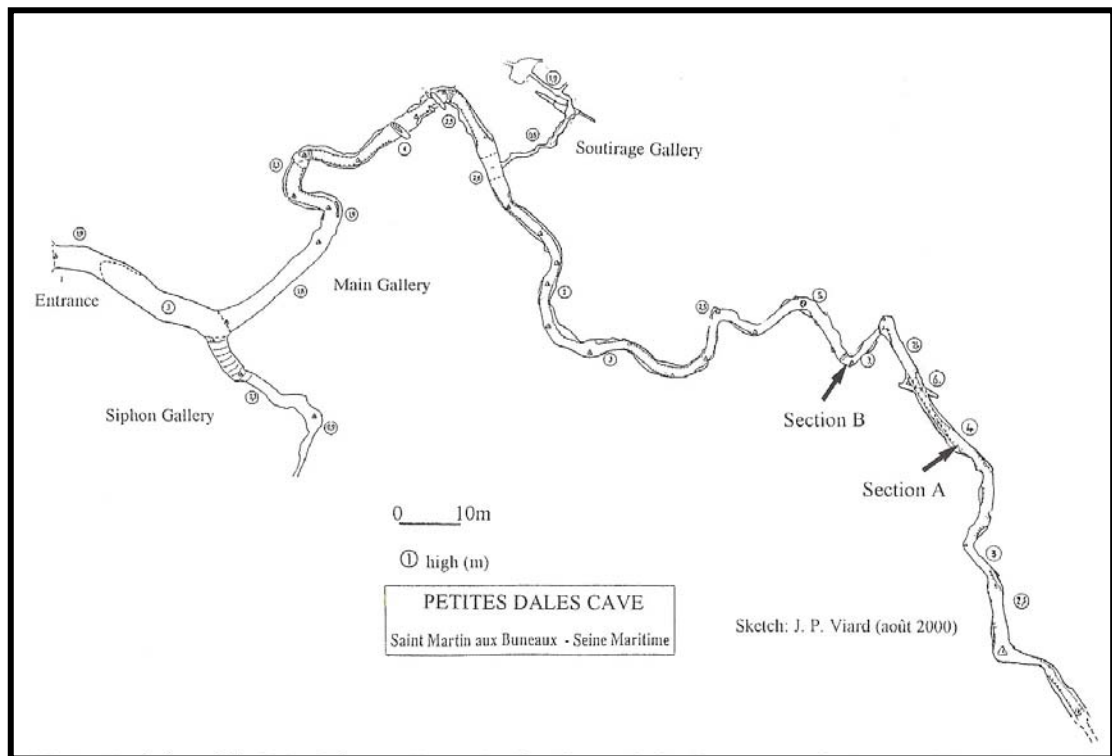


Figure 1.24: Survey of Petites Dalles Cave, France (from Laignel et al., 2004).

It is probable that most conduits in the Chalk are too small to enter. The smallest scale conduit features are the "dissolution tubules" (Figure 1.25) described by Lamont-Black and Mortimore (2000), which have been seen in road cuts and rapidly retreating sea cliffs in England. They are irregular bifurcating voids 1 to 50 mm in diameter, developed along specific stratigraphic or tectonic discontinuities. They are often laterally extensive over many hundreds of metres and result in localised rapid groundwater flow. These tubule horizons are associated with larger scale conduit development at Beachy Head Cave.

Small phreatic conduits have been observed in quarries (Figure 1.26, left). In boreholes cameras have identified circular shaped conduits (Figure 1.26, right). Waters and Banks (1997) also observed conduits in boreholes using a camera, and identified macrobiota living in the conduits.



Figure 1.25: Dissolution tubules, Beachy Head (photo Andy Farrant)

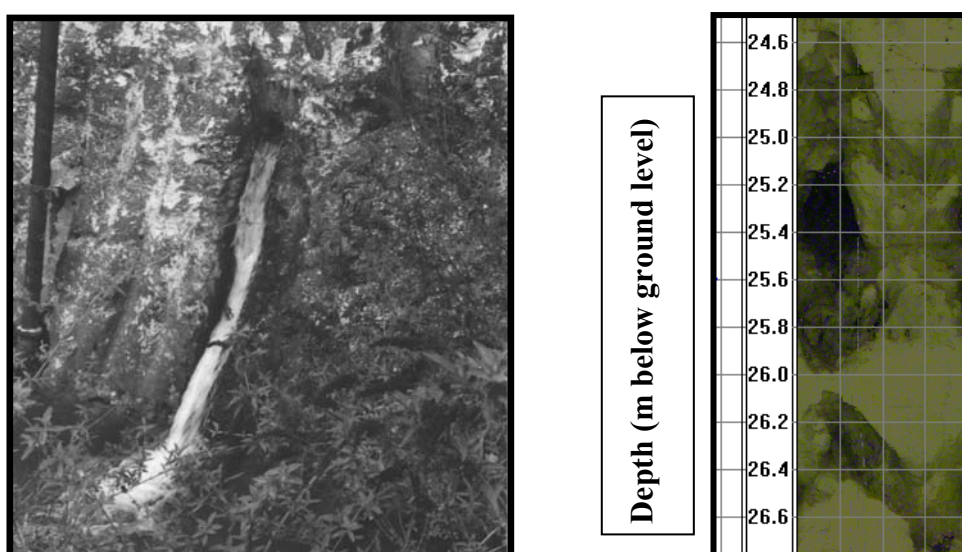


Figure 1.26: Flowing karst conduit 15-20 cm in diameter in a chalk quarry at Swanscombe, Kent (left, photo John Bloomfield), and borehole videoscans image of a conduit ~ 30 cm diameter Frilsham, Berkshire (right, data from BGS)

1.6 Conclusions

It has been recognised for a long time that small-scale surface karst features are commonly associated with the Chalk, particularly where there is a thin Palaeogene cover (Section 1.5). Hydrogeological studies (Section 1.3) have demonstrated that solutional fissures are responsible for the high transmissivity of the Chalk, and that rapid groundwater flow occurs relatively frequently in both the unsaturated and saturated zones. Although some caves have been found in the Chalk (Section 1.5.7), most subsurface dissolution appears to result in small conduits and fissures. In accordance with recent definitions of karst (Section 1.4.1), and as suggested previously

(e.g. Atkinson and Smith, 1974; Banks et al., 1995; Lamont-Black and Mortimore, 2000; Macdonald et al., 1998) the Chalk should be considered as a karst aquifer, but at the lower end of the karstification scale (Atkinson and Smart, 1980). Applying karst principles to the Chalk is useful because karst processes determine the distribution of high transmissivity, and influence the transport and attenuation of contaminants within the aquifer.

Subsurface chalk is characterised by a hierarchy of different types of void with generally increasing permeability from fractures to fissures to tubules to conduits to caves. However, very little is known about the structural organisation of these voids and their relationship to each other. There is no systematic review of the incidence or frequency of tubules, conduits or caves, nor of whether these solution features are isolated from one another or generally linked in continuous networks. Although the distribution of fissures has been investigated (Section 1.3.2.2), it also remains unclear whether they are connected or isolated. The thesis will demonstrate how catchment scale tracer experiments from stream sinks can indirectly shed light on the nature and structure of voids in the Chalk, because solute transport processes are determined by the nature of the voids through which the tracer passes. Overall, the research described in this thesis aims to improve our understanding of how and where karst processes are occurring in the Chalk by applying tracing techniques in the Pang and Lambourn catchments in Southern England.

Chapter 2: The Pang and Lambourn study area

2.1 Introduction

In this chapter past studies in the Pang and Lambourn catchments and recent work undertaken as part of the LOCAR programme are used to present an overview of the general characteristics of the study area. The topography, geology, hydrology and hydrogeology of the catchments are discussed.

2.2 General topography

The Pang and Lambourn river valleys are incised into the dip slope of the Berkshire Downs on the northwestern side of the Thames drainage basin. The Berkshire Downs form a cuesta with a steep north-facing escarpment backed by a complex dip slope on which the principle streams are aligned east, southeast and south. The topographical features of the area are illustrated in Figure 2.1. The River Lambourn has a topographic catchment of 234 km² (Griffiths et al., 2006), and flows 20 km southeast from Upper Lambourn at ~ 150 m AOD to join the River Kennet at Newbury at ~ 70 m AOD. The River Pang has a topographic catchment of 170 km² (Griffiths et al., 2006). It flows in a southerly then easterly direction from Compton at ~ 90 m AOD to where it joins the River Thames at Pangbourne (~ 40 m AOD). In the north of the area the catchments are directly adjacent, but in the south they are separated by high ground within the topographic catchment of the River Kennet.

The highest ground, with elevations of 200-270 m AOD, is in the north and northwest of the catchments. The northerly boundary of the catchments is the crest of the escarpment, from which the scarp slope descends steeply northwards into the Vale of the Whitehorse. To the south and southwest the catchments are bounded by ridges (~ 130 to 150 m AOD), which separate the Lambourn and Pang rivers from the Kennet valley. To the east the catchments are bounded by the drainage divide between the River Pang and the River Thames, which at an elevation of 40-45 m AOD is considerably lower than the upper reaches of the River Pang (~ 90 m AOD at its head).

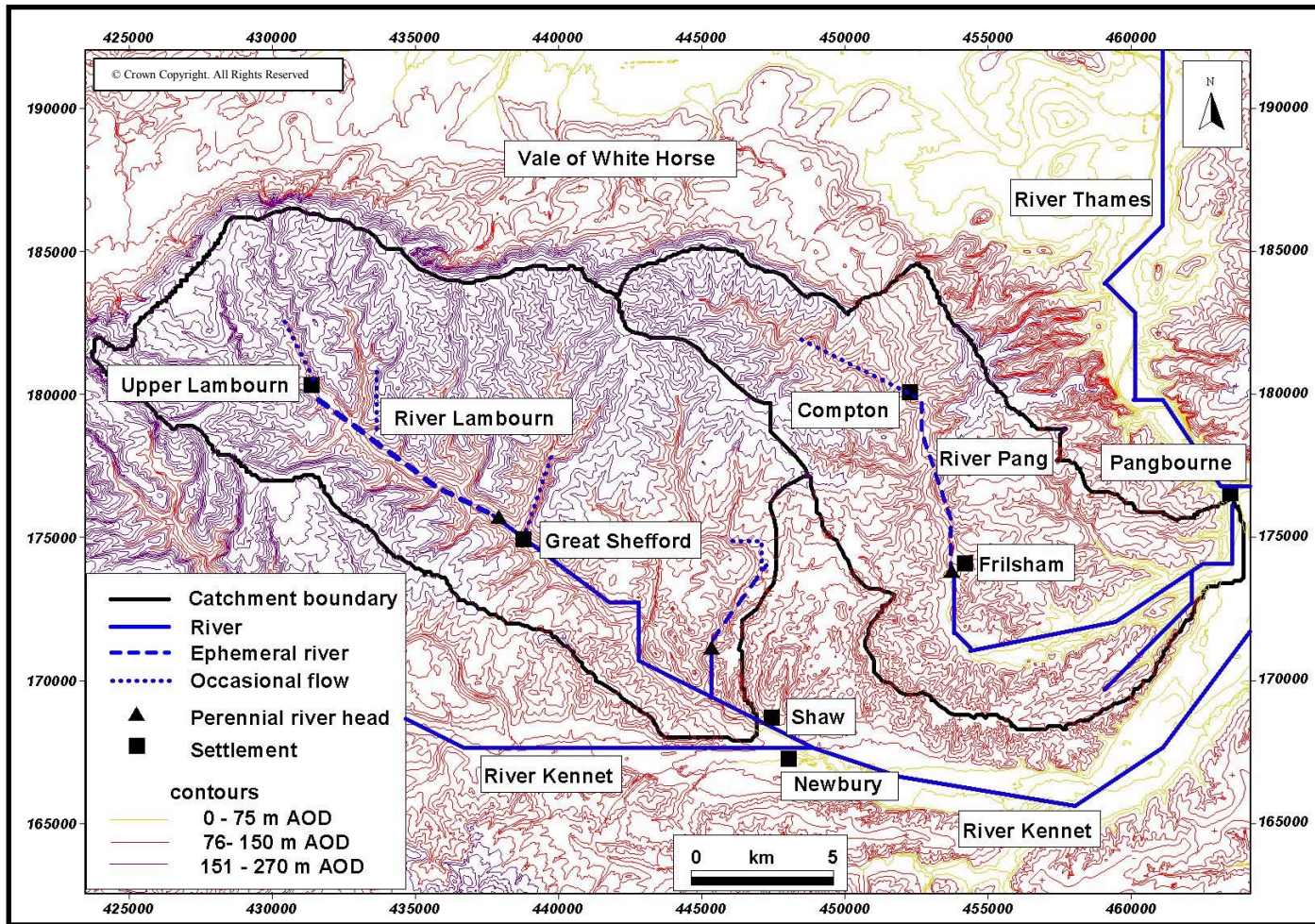


Figure 2.1: Topography of the Pang-Lambourn catchments. Rivers are shown schematically illustrating perennial, ephemeral and occasional flow; detailed river courses are shown on Figure 2.2. Data on dry valleys with occasional flow are from BGS.

2.3 Drainage network

The catchments contain a dense network of tributary valleys (Figure 2.1), which are predominantly dry. Perennial flow only occurs in the lower reaches of the Lambourn and Pang rivers. Ephemeral flow occurs in the upper reaches of these rivers and in tributary streams. There is occasional flow during exceptionally wet periods in the lower reaches of a small number of other dry valleys that intersect the main rivers.

2.4 Geology

2.4.1 Solid Geology

The following outline of the geology of the Pang and Lambourn catchments is largely based upon the report by Aldiss et al. (2002). More detail on the stratigraphical correlation in the area is described in Woods and Aldiss (2004). The oldest strata outcrop at the crest of the escarpment, which forms the north and northwest catchment boundary (Figure 2.2). The strata dip between 0.5 and 2° towards the south-south-east, and the stratigraphic sequence is listed in Table 2.1.

Table 2.1: Stratigraphical sequence in the Pang-Lambourn catchments (from Aldiss et al., 2002)

	Lithological Unit	Thickness (local)
Palaeogene	Bagshot Formation	up to 20 m
	London Clay Formation*	20 to 50 m
	Lambeth Group	20 to 30 m
Cretaceous Chalk	Newhaven Chalk Formation	up to 14 m
	Seaford Chalk Formation	55 to 75 m
	Lewes Nodular Chalk Formation (containing the Chalk Rock)	10 to 28 m
	New Pit Chalk Formation	19 to 46 m
	Holywell Nodular Chalk Formation	15 to 30 m
	Zig Zag Chalk Formation	12 to 55 m
	West Melbury Marly Chalk Formation	20 to 55 m

** This includes the Harwich Formation that underlies the London Clay Formation but has not been mapped separately.*

The oldest formation outcropping within the catchments is the Zig Zag Chalk. The main outcrop of Zig Zag Chalk is outside the Pang and Lambourn catchments on the scarp slope to the north, but there is a small outcrop in the far northwest of the Lambourn catchment, where the overlying Holywell Nodular Chalk has been eroded

away. The Zig Zag Chalk is a soft to medium-hard grey blocky chalk containing limestone hardgrounds, particularly in the lower parts of the formation (Aldiss et al., 2002). These hardgrounds include the Tottenhoe Stone, which is characterised by phosphatic nodules, and the silty fossiliferous Cast Bed (Aldiss et al., 2002).

Stratigraphically and topographically above the Zig Zag Chalk, the Holywell Nodular Chalk outcrops on high ground in the northwest of the Lambourn catchment. It is a medium-hard to very hard, nodular white chalk containing the Plenus marls at its base, which are overlain by the Melbourne Rock hardground (Aldiss et al., 2002). The New Pit Chalk also outcrops on high ground in the upper reaches of the Lambourn and Pang catchments. It is a massive soft to medium-hard smooth white chalk with frequent marls and occasional small flint layers with local hardgrounds at the top of the formation (Aldiss et al., 2002). The Lewes Chalk forms high ground in the upper reaches of the catchment and floors the upper Lambourn and Pang valleys. It is a hard to very hard white chalk with regular nodular flint bands and frequent marl layers. The Chalk Rock (pink on Figure 2.2) is near the base of the Lewes Chalk, and comprises several hardgrounds with an overall thickness of several metres.

Most of the chalk outcrop in the catchments is Seaford Chalk, which covers a wide area on the interfluves extending southwards from the crest of the escarpment. In the main river valleys it is found downstream of the Lewes Chalk outcrop. The Seaford Chalk is a soft to medium hard chalk with frequent nodular flint layers, and occasional tabular flint horizons (Aldiss et al., 2002). Marl layers are largely absent although they can be found in the lower Seaford Chalk (Aldiss et al., 2002). In the upper part of the Seaford Chalk phosphatic chalks and hardgrounds have been identified near Boxford (Jarvis and Woodroof, 1981), and Aldiss et al. (2002), suggest they may be more widespread. The 1 m thick Stockbridge Rock hardground occurs irregularly at the top of the Seaford Chalk, about 5 m below the base of the Newhaven Chalk (Aldiss et al., 2002).

Due to a regional unconformity between the Cretaceous Chalk and the overlying Palaeogene deposits, the Newhaven Chalk is largely absent, but in the south of the Lambourn catchment, there are 4 outliers which overlie the Seaford Chalk, and extend beneath the adjacent and overlying Palaeogene deposits (Aldiss et al., 2002). The base of the Newhaven Chalk is identified by the presence of frequent marl bands that are

absent from the top of the Seaford Chalk (Aldiss et al., 2002). The Newhaven Chalk is a soft to medium-hard chalk with many marl layers and occasional flint bands, and phosphatic chalks and hardgrounds have been observed near Winterbourne (Aldiss et al., 2002).

Where the Newhaven Chalk is absent, the Seaford Chalk is unconformably overlain by Palaeogene deposits. These deposits are present on the high ground bounding the lower reaches of the river valleys. The oldest Palaeogene deposits are the Lambeth Group, which are 20-30 m thick and include the basal Upnor Formation and the overlying Reading Formation. The Upnor Formation is absent in the northern part of the Palaeogene outcrop but where present consists of glauconitic sands and clays between 1 and 2.2 m thick (Aldiss et al., 2002). There is considerable lateral variation in the composition of the Reading Formation but it mainly comprises clays with some beds of fine to medium grained sands up to 7m thick, particularly near the base of the formation (Aldiss et al., 2002).

The Harwich Formation overlies the Reading Formation but despite its distinctive lithological characteristics Aldiss et al. (2002) report that it has been mapped as part of the London Clay Formation. The deposit is quite thin (up to 6 m thick in the east of the Pang and Lambourn area) and is therefore likely to be present on the mapped London Clay Formation outcrop immediately adjacent to the underlying Lambeth Group. The Harwich Formation is described as a basal flint pebble bed overlain by sands and clayey silts (Aldiss et al., 2002). The London Clay Formation itself comprises silty clays and clayey silts with some sand and pebble beds. The London Clay Formation is overlain by the Bagshot Formation in the southernmost part of the Pang catchment. This comprises fine-grained sands with some thin beds of silt and clay.

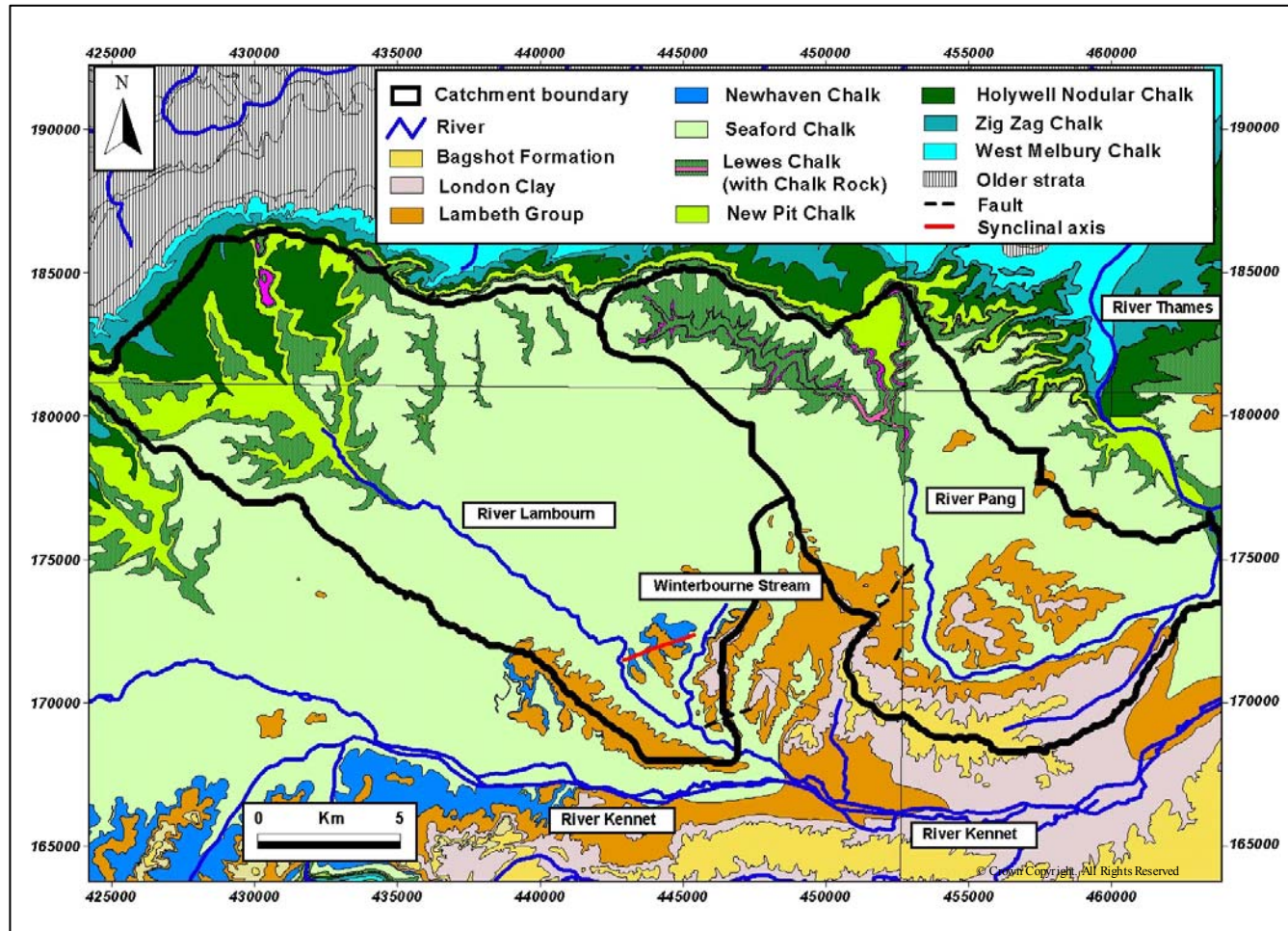


Figure 2.2: Solid Geology of the Pang-Lambourn catchments^{BGS}

2.4.2 Drift Geology

The Drift Geology of the Pang and Lambourn catchments is shown in Figure 2.3. Head, clay-with-flints, alluvium, and sands and gravels (mostly river terrace deposits and plateau gravels) are present in the catchments. Head deposits occur on slopes and on the floors of dry valleys in the upper reaches of the catchments. They consist of stony, sandy and silty clays and clayey gravels that are derived from Clay-with-Flints and chalk that have been moved by solifluction (Aldiss et al., 2002). Head deposits are sandier and contain more flints than Clay-with-Flints, which in turn comprises clays and sandy clays containing flints. Clay-with-Flints are thought to be in-situ weathered remnants of the Palaeogene deposits and underlying chalk (Aldiss et al., 2002). They invariably rest on chalk, and cover the Seaford Chalk on interfluvial areas in the middle reaches of the catchments. Alluvium consists of fine-grained silts and clays with gravel lenses, and is present in the lower reaches of the Lambourn and Pang river valleys. The mapped category of sands and gravels are mostly river terrace deposits and are found in the major river valleys, with plateau gravels present on some interfluvial areas in the south and east of the area.

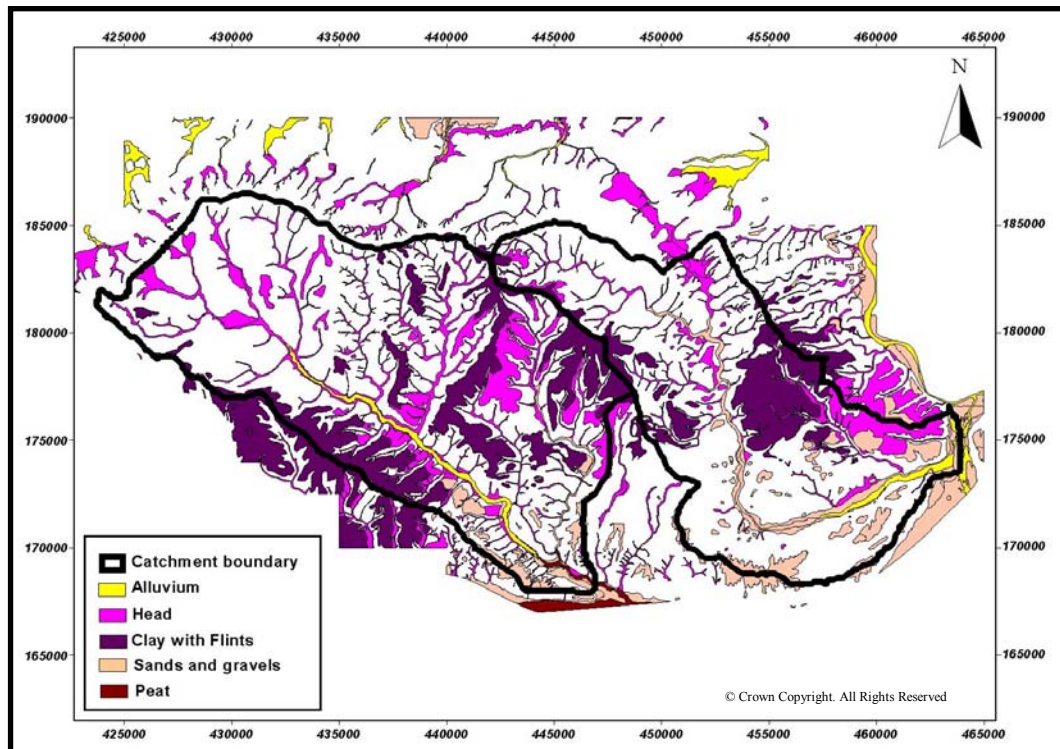


Figure 2.3: Drift Geology of the Pang-Lambourn catchments^{BGS}

2.4.3 Geological structure

Geophysical logs from 60 boreholes were used by Aldiss et al. (2002) to create a three dimensional model to estimate regional dip. Results suggest that the regional dip is generally towards the south-south-east, but in the southeast of the catchments it is more southerly. The dip is generally 0.5 to 1°, locally up to 2°. In the centre of the catchments there are locally reversed dips, and there are several local variations from the regional pattern (Aldiss et al., 2002). Most significant are several NW to SE trending perturbations which Aldiss et al. (2002) attribute to gentle folding. In the southeastern part of the Lambourn catchment between the River Lambourn and the Winterbourne stream tributary outliers of Newhaven Chalk are associated with a small syncline (Figure 2.2). Faults are difficult to identify due to the scarcity of outcrops, and it is likely that there may be many unrecorded faults in the catchments (Aldiss et al., 2002). Aldiss et al. (2002) report that those identified trend NE-SW or ENE to WSW with a downthrow to the SE of 5-10 m. They also suggest that the alignment of valleys in the catchments reflects a dominant fracture orientation from NW to SE with other fractures sets orientated NE-SW and N-S. A study by Bloomfield (1996) of fractures at Play Hatch Quarry outside the catchments 10 km east of Pangbourne (Figure 2.1), also found that the dominant fracture orientation was NW/SE and that faults were extended in a NE/SW direction. These fracture orientations are characteristic of the Chalk in the UK and other parts of Northwestern Europe (Downing et al., 1993).

2.5 Springs

2.5.1 Springs in the Palaeogene and drift deposits

Many small springs with discharges less than 1 L.s⁻¹ emerge from the Palaeogene and drift deposits, and these are often associated with geological boundaries. Figure 2.4 shows an example of the distribution of Palaeogene and drift deposit springs in the lower reaches of the Pang. There is a similar density of springs throughout the Palaeogene outcrop in the catchments. Some springs emerge through the base of sand and gravel drift deposits overlying the Bagshot Formation. Other springs are located near the base of the Bagshot Formation. These discharge groundwater stored in the sandy Bagshot Formation above its contact with the less permeable London Clay Formation. There are however also springs within the London Clay Formation. Those situated on the London Clay Formation close to the boundary with the Lambeth Group are likely to be within the more permeable deposits of the Harwich Formation (which

has been included in the same mapping unit as the London Clay Formation). However, some springs occur in the middle of the London Clay outcrop suggesting that there are locally permeable horizons throughout the formation. There are also some springs within the Lambeth Group (north of the River Pang in Figure 2.4), which are presumably associated with local sandy horizons. In addition to those recorded on Figure 2.4, many other small springs have been observed in the field, suggesting that there are many small bodies of groundwater in locally permeable beds of Palaeogene and drift deposits.

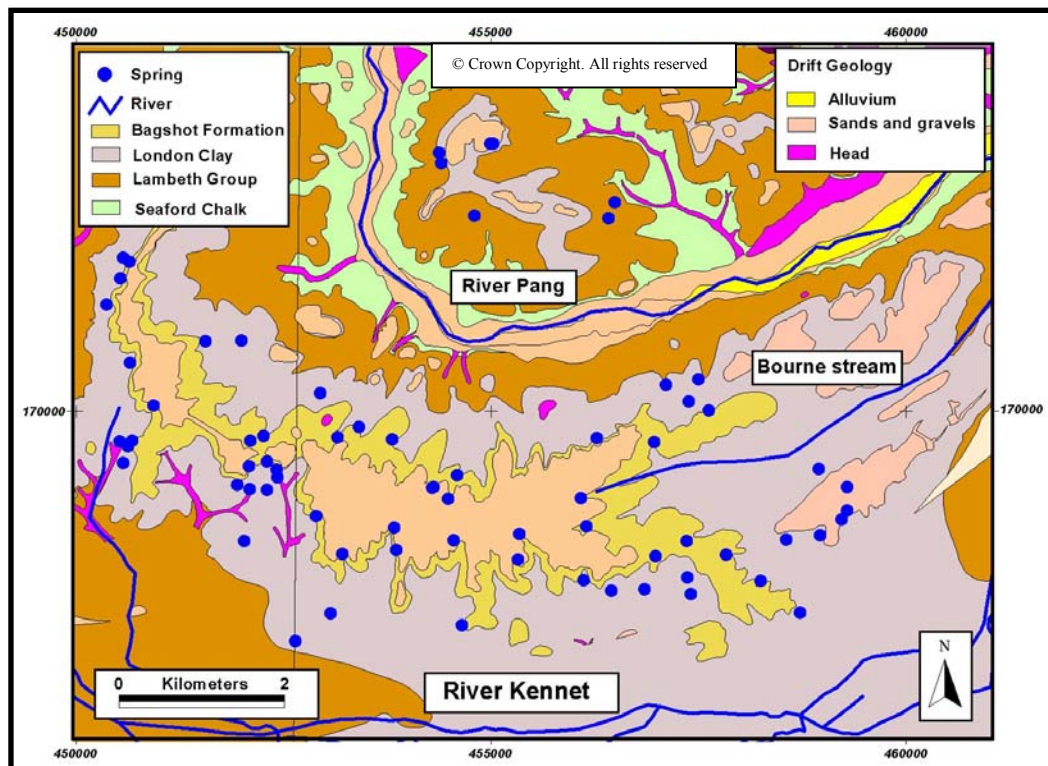


Figure 2.4: Springs emerging from Palaeogene and drift deposits in the lower Pang^{BGS}

2.5.2 Chalk scarp slope springs

There is a distinctive line of springs along the base of the northerly scarp slope (Figure 2.5). Most are at the contact between the Zig Zag Chalk and the West Melbury Marly Chalk. It has been estimated that the scarp slope springs each had a flow of $\sim 1\text{-}5 \text{ L}\cdot\text{s}^{-1}$ in December 2006 following the drought of summer 2006 (Brian Morris, BGS, personal communication, 2007). Although little is known about the seasonal variability in these springs they discharge water that must originate from the upper reaches of the Pang and Lambourn topographic catchments.

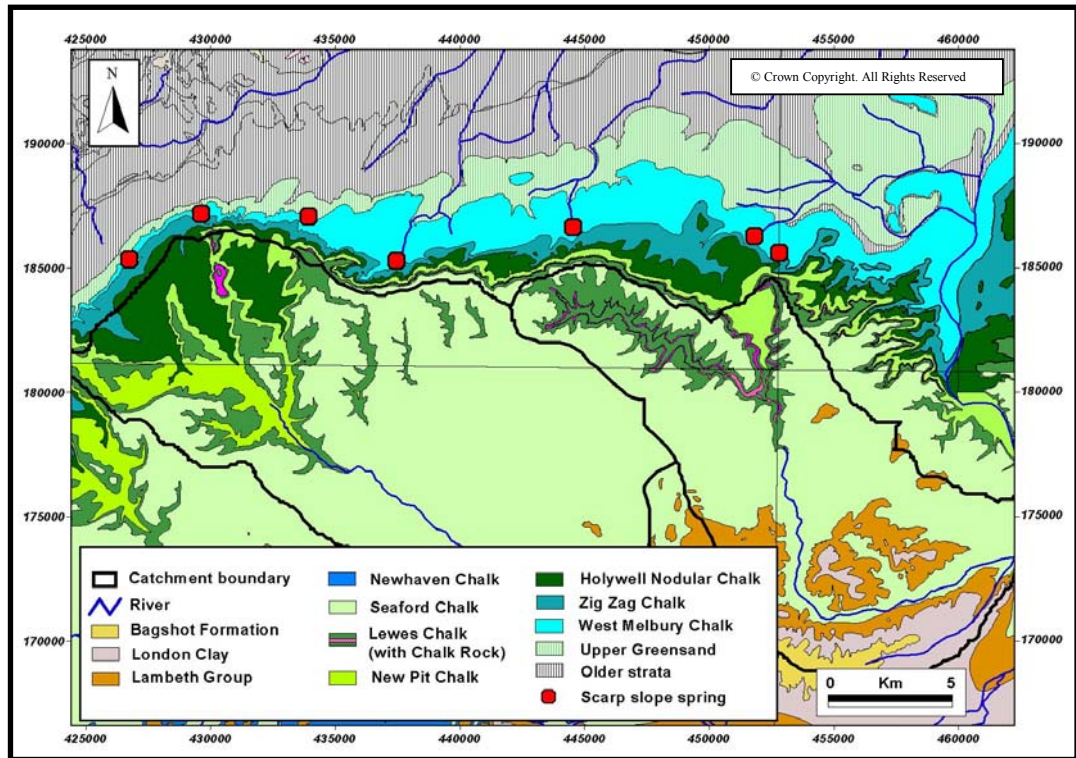


Figure 2.5: Scarp slope springs north of the Pang-Lambourn catchments^{BGS}

2.5.3 River valley chalk springs

There are 14 chalk springs in the Lambourn river valley and 11 in the Pang Valley (Figure 2.6). The smaller springs and seepages (blue triangles on Figure 2.6) have discharges less than 1 L.s^{-1} . The largest of the more significant springs are the Blue Pool in the Pang and Lynchwood springs in the Lambourn which both have an average discharge (when flowing) of $\sim 200 \text{ L.s}^{-1}$. The Blue Pool has a relatively constant flow whereas Lynchwood springs are ephemeral and have substantial discharge variations. The river valley chalk springs are discussed in detail in Section 3.4.

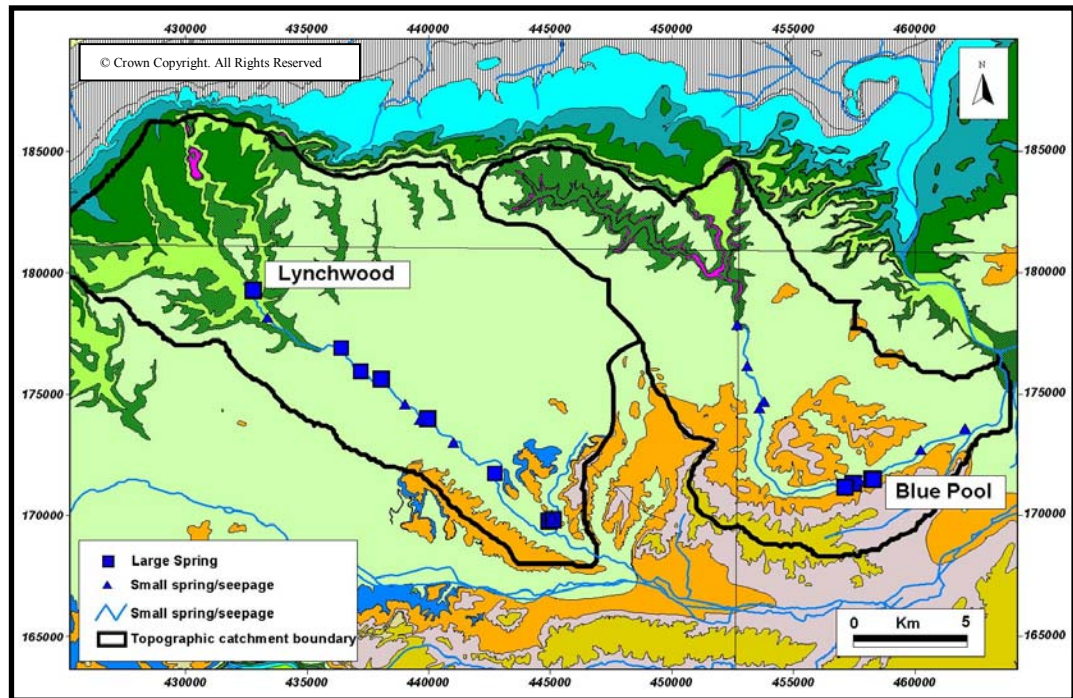


Figure 2.6: Chalk springs in the Pang and Lambourn river valleys (Geology key is as for Figure 2.2) ^{BGS}

2.6 Rainfall and evapotranspiration

Rainfall in the Pang and Lambourn area is highest over the high ground in the north and west, and lower in the south and east (Wheater et al., 2006a). The mean annual rainfall between 1968 and 1997 was 692 mm/year in the Pang and 731 mm/year in the Lambourn (Wheater et al., 2006a). Evapotranspiration rates have been estimated at 525 mm/year in the Pang and 450 mm/year in the Lambourn (Wheater et al., 2006b). Wheater et al. (2006b) do not discuss the difference between the two catchments, or the methods used in the calculation. The work in this thesis does not rely on water balance and therefore more detailed determination of an accurate evapotranspiration rate has not been undertaken.

2.7 Surface hydrology

The mean annual discharge of the Lambourn and Pang rivers between 1968 and 2003 was 1.76 and 0.65 m³.s⁻¹ respectively (Griffiths et al., 2006 based on the National Rivers Flow Archive, 2004). The hydrographs for the rivers (1970-2005) are shown in Figures 2.7 and 2.8 (from Wheater et al., 2006a). Both rivers have a seasonal fluctuation with

groundwater maintaining flow during dry periods, but the River Pang (Figure 2.8) also has a much more flashy response to rainfall, indicating the importance of surface runoff.

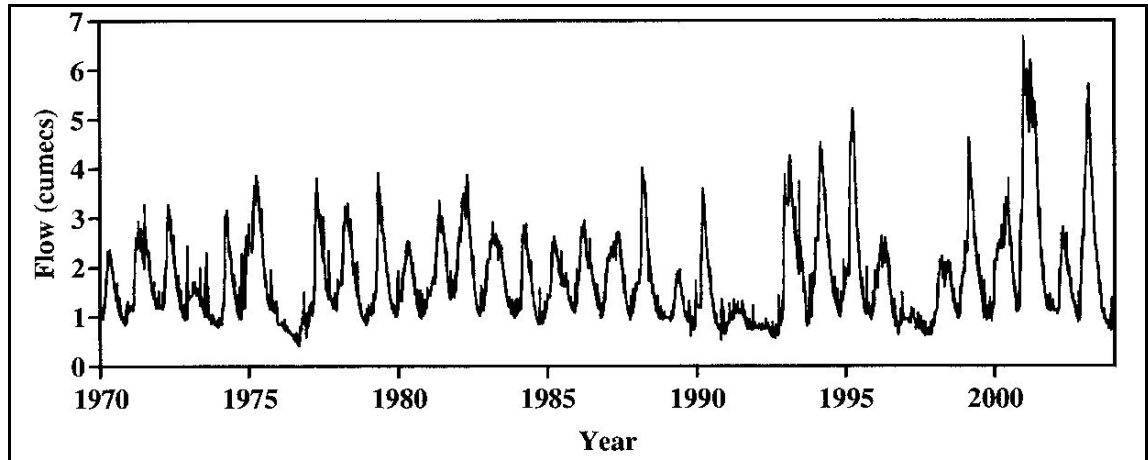


Figure 2.7: Flow in the River Lambourn at Shaw (Wheater et al., 2006a)

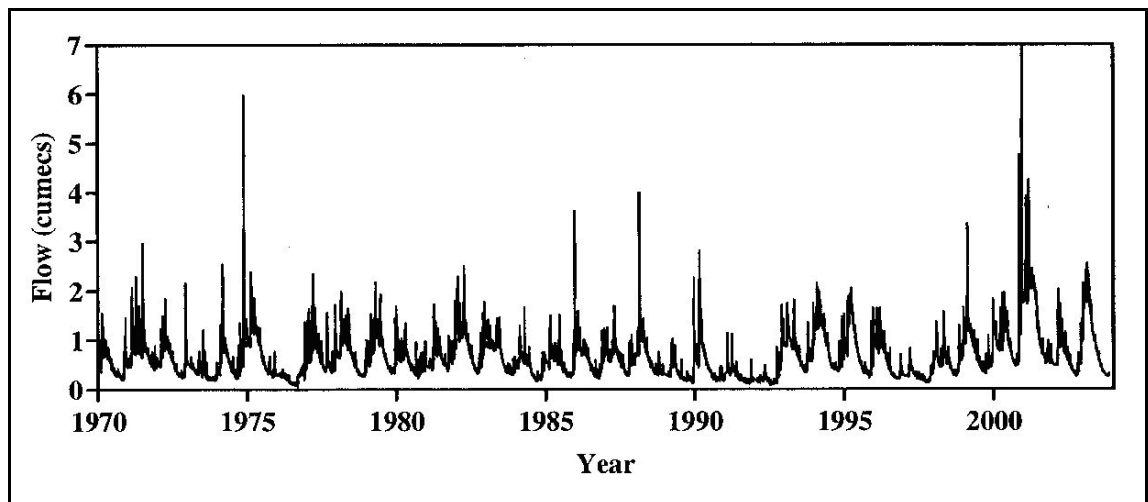


Figure 2.8: Flow in the River Pang at Pangbourne (Wheater et al., 2006a)

In addition to natural inputs from groundwater, interflow and overland flow, there are licensed sewage discharges, other licensed discharges, drains from paved surfaces in villages and towns, and land drains which all contribute to the river discharges. Licensed sewage discharges provide a small relatively consistent discharge. According to Atkins (2003) there are 11 major sewage treatment plants within the Pang and Lambourn catchments and ~ 100 other discharge consents. LOCAR data for a smaller number of discharge consents suggest that license amounts vary between 0.02 and 17 $\text{L}\cdot\text{s}^{-1}$. Thames Water data indicated that the discharge from the Compton sewage works near the seasonal head of the River Pang was 3.25 $\text{L}\cdot\text{s}^{-1}$ during the summer of 2003 (Bricker, 2004). Other surface drains will contribute to the quickflow component of the

rivers although some field drains may also provide a small baseflow component where they drain springs in the Palaeogene deposits.

The baseflow index (BFI) of rivers provides a rough guide to the contribution of groundwater to the discharge, and in chalk streams usually exceeds 90 %. Using the standard Institute of Hydrology (1980), method of numerical baseflow separation from total stream discharge the Pang at Pangbourne has a BFI of 87 % (Peters and Van Lanen, 2004), and the Lambourn at Shaw has a BFI of 96 % (Grapes et al., 2005).

Peters and Van Lanen (2004) have calculated the BFI for the River Pang at Pangbourne and in the upper reaches of the river at Frilsham (Figures 2.1, 2.9), using a new method of baseflow separation involving groundwater levels in a monitoring borehole, total streamflow at the gauging stations, and an estimate of direct runoff based on precipitation data and evapotranspiration data (calculated using the Penman (1948) method). They varied the parameters to produce a range of BFI values. These were then compared to other methods of estimating the BFI at these sites (Table 2.2). The following discussion of these estimates is entirely based upon Peters and Van Lanen (2004).

It is apparent that using all methods the BFI at the Frilsham gauging station is higher than that at Pangbourne. This is because in the upper reaches of the river chalk groundwater provides a substantial proportion of flow, whilst the lower reaches include flow from the Bourne surface stream and other surface runoff from the adjacent Palaeogene strata, as well as drainage from paved areas in Pangbourne. The Kilner and Kněžek (1974) method produces very low BFIs. This method also uses groundwater levels, but unlike the method of Peters and Van Lanen it assumes that the lowest flow observed for a certain groundwater level is the baseflow and it therefore is a minimum estimate that does not take into account the large variability that occurs during baseflow recession (Peters and Van Lanen, 2004). The BFI method of the Institute of Hydrology (1980) produces higher estimates of baseflow than the Peters and Van Lanen method for the Pang gauging station. This method is purely arithmetic and the calculated baseflow includes all runoff from stored sources (not just chalk groundwater). It is likely that these include interflow from Palaeogene deposits in the lower reaches of the river and that this is the cause of the higher BFI at Pangbourne (Peters and Van Lanen, 2004).

The method of Boughton (1993) produces similar results to that of Peters and Van Lanen (2004), but recognises more direct runoff resulting in a slightly lower BFI (Peters and Van Lanen, 2004).

Table 2.2: BFI estimates for the River Pang (Peters and Van Lanen, 2004)

Method	Pangbourne	Frilsham
Peters and Van Lanen (2004)	67.3-77.4	88.5-98.6
Institute of Hydrology (1980)	87	94.3
Boughton (1993)	77.5	88.2
Kilner and Kněžek (1974)	54.8	72.9

The high BFI for the River Lambourn (96 %) reflects the dominance of groundwater in the river. The calculation is based upon the Institute of Hydrology (1980) method, but there is likely to be less interflow included in this baseflow calculation than in the Pang, because the Palaeogene deposits are not so extensive in the lower reaches of the Lambourn.

Hydrological flow accretion studies have been undertaken in the Lambourn (Grapes et al., 2005; Griffiths et al., 2006), and in the Pang (Bricker, 2004; Griffiths et al. 2006). Figure 2.9 shows the location of the flow gauging sites in the Pang and Lambourn rivers used by Griffiths et al. (2006) with grid references supplied by Griffiths (personal communication, 2003). It also shows the location of springs (discussed in Section 3.4).

Figure 2.10 shows the results of the accretion survey in the Lambourn between 2002 and 2005 by Griffiths et al. (2006). Accretion studies reported by Grapes et al. (2005) show a broadly similar pattern (Figure 2.11). These are a combination of archive data compiled by Grapes et al. (2005) and new surveys conducted between 1999 and 2001. The archive data are mainly from three years of above average discharge (1966, 1967 and 1975), but most of Grapes' own current meter data were from the summer months when the discharges were low (Grapes et al., 2005).

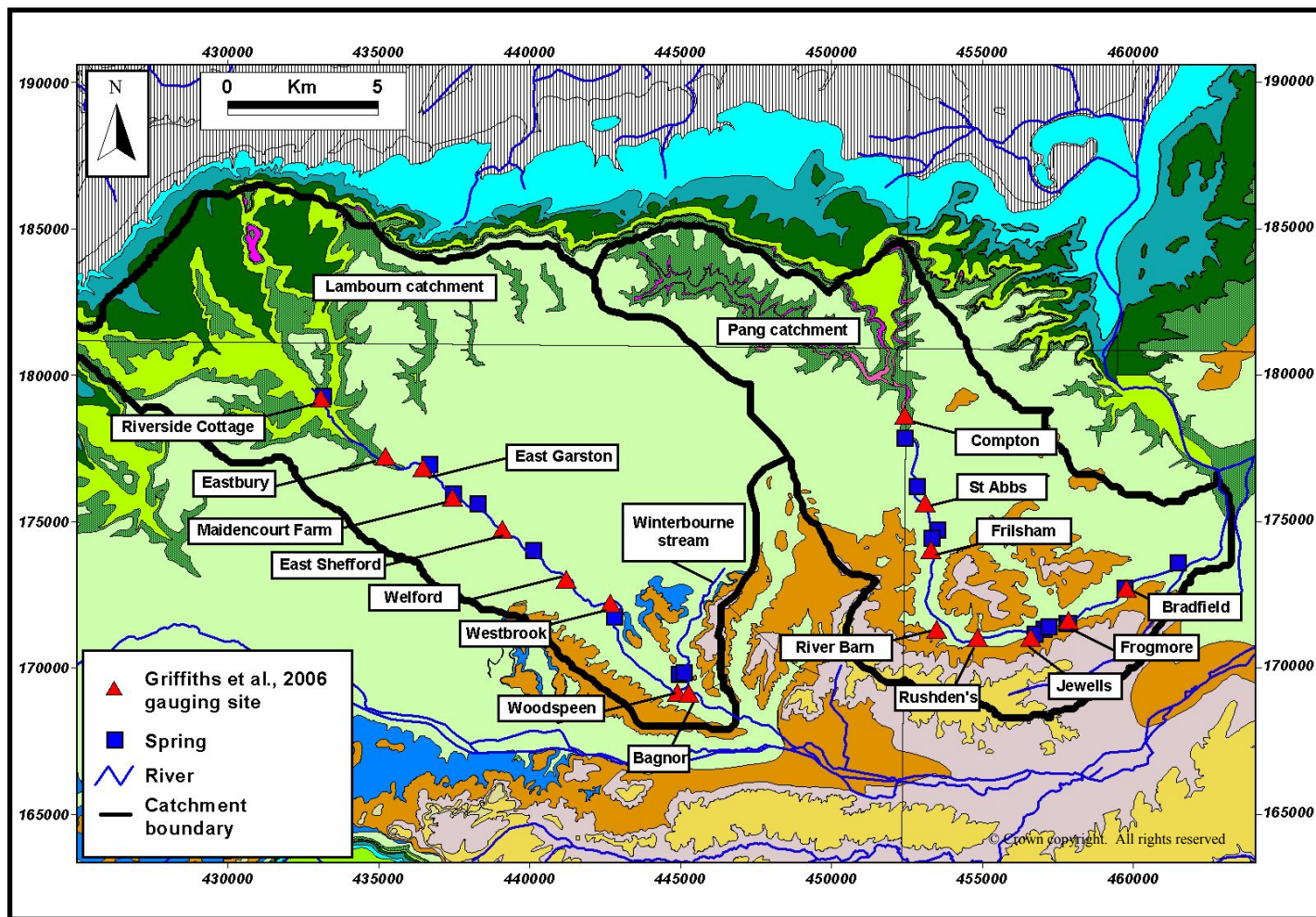


Figure 2.9: Location of River Lambourn and Pang gauging sites used by Griffiths et al. (2006). (Geology key is as for Figure 2.2) ^{BGS}

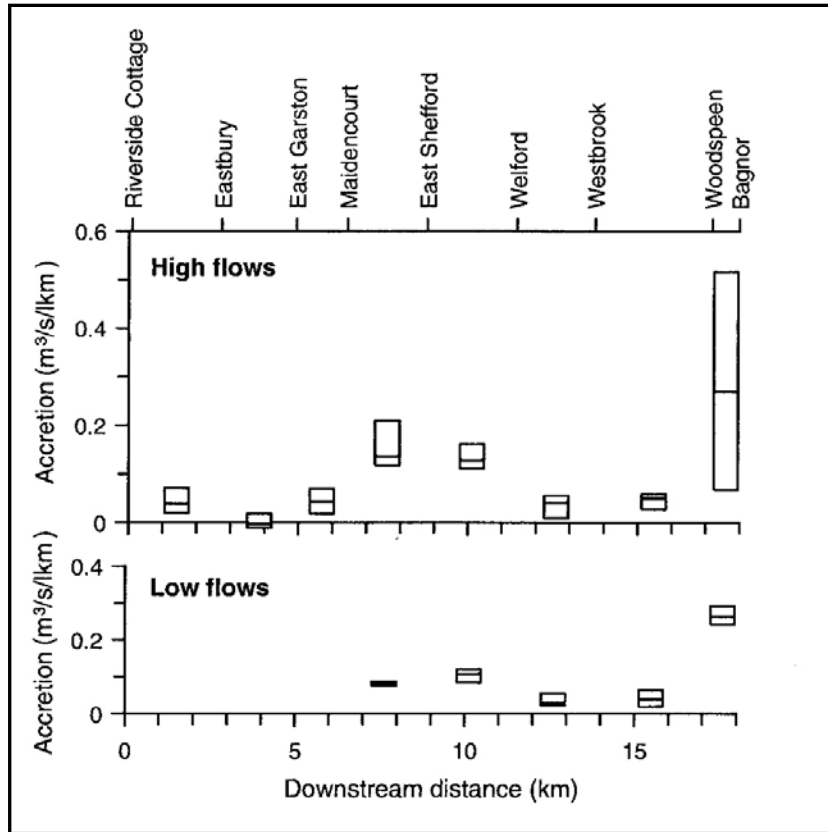


Figure 2.10: Flow accretion in the River Lambourn under high and low flows 2002 to 2005, box plots showing median, Q_{25} and Q_{75} values (Griffiths et al., 2006)

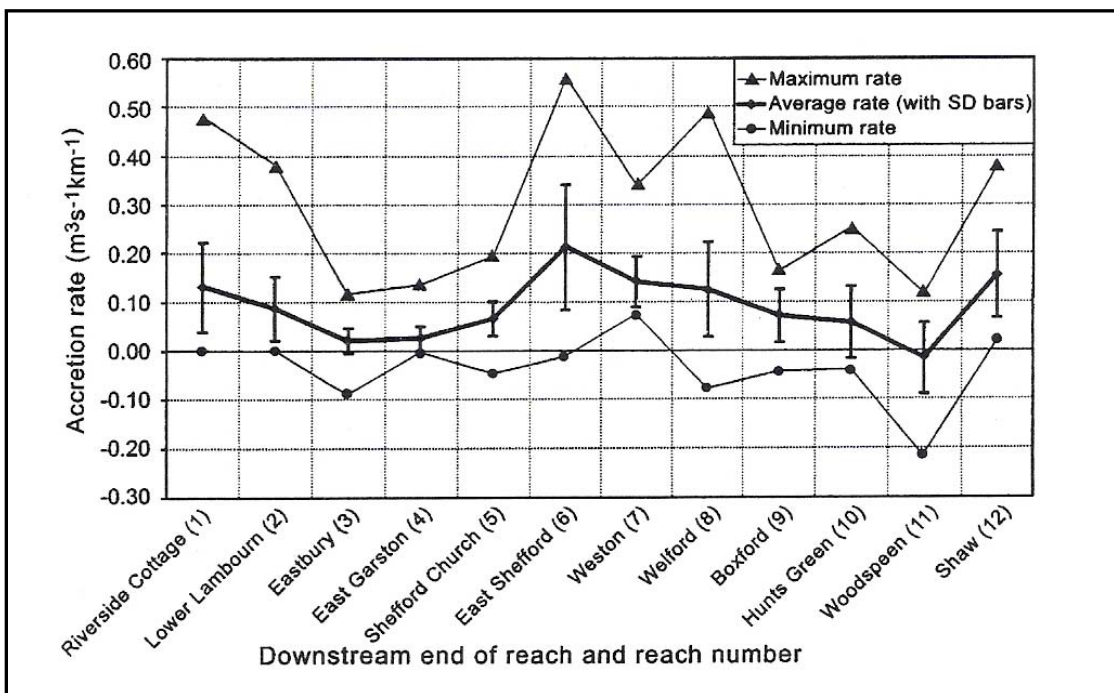


Figure 2.11: Flow accretion in the River Lambourn between 1999 and 2001 (Grapes et al., 2005)

A direct comparison between the actual accretion figures of Grapes et al. (2005) and Griffiths et al. (2006) is not feasible because the data are presented in different forms, the studies were undertaken in different years with different rainfall, and different gauging sites were used (note for example that Woodspeen is the name of a reach in the study by Grapes et al. (2005), but a gauging station name in Griffiths et al. (2006)).

The upper ephemeral reaches of the river begin at Lynchwood springs just upstream of the Riverside Cottage gauging site of Griffiths et al. (2006), whilst the perennial head is normally 6-7 km downstream at Maidencourt Farm (Figure 2.9). Cessation of flow between Lynchwood springs and Maidencourt Farm occurs over a 2-4 week period, whilst reactivation of the Lynchwood springs is very rapid (Grapes, personal communication, 2003).

The middle reaches of the catchment between Maidencourt Farm and Welford provide a large input to the rivers throughout the year (Grapes et al., 2005, Griffiths et al., 2006). Between Maidencourt Farm and East Shefford there is a very consistent input under low flow conditions. The Great Shefford dry valley has been identified as an important source of groundwater within this reach (Bradford, 2002; Grapes et al., 2005). However, more detailed flow accretion surveys over the reach by Griffiths et al. (2006), found that although there is a spring in the Lambourn valley to the northwest of the Great Shefford dry valley, groundwater inputs over the reach are uniform rather than from a single point input. There is also a more variable accretion rate under high flow conditions, suggesting that surface runoff from the settlement of Great Shefford may also contribute. Grapes (personal communication, 2003), noted that the major dry valley at Great Shefford (Figure 2.1) has surface flow under very wet conditions.

In the Woodspeen reach of Grapes et al. (2005) there is flow loss on average. This may be due to groundwater abstraction at the Speen PWS (Section 2.8.4). Accretion rates are generally low in the lower sections of the catchment, except in the final reaches of the surveys (the Shaw reach of Grapes et al. (2005) and the Woodspeen to Bagnor reach of Griffiths et al. (2006)). The extreme variability in accretion in these reaches under high flow suggests surface runoff is important as well as the groundwater that sustains the high accretion throughout the year. The Shaw reach of Grapes et al. (2005) presumably includes the input from the Winterbourne stream (the paper by Grapes et al.

(2005) does not suggest that this input is removed from the data), as well as the surface runoff and drainage entering the river as it passes through the towns of Shaw and Newbury. The Woodspeen to Bagnor reach of Griffiths et al. (2006) does not include the urban areas of Shaw and Newbury, but the input from the Winterbourne stream does lie within the reach. Grapes et al. (2005) report that the average discharge in the Winterbourne stream between 1962 and 2003 was $0.17 \text{ m}^3 \cdot \text{s}^{-1}$. This would constitute a large proportion of the flow in the Woodspeen to Bagnor reach of Griffiths et al. (2006).

Turning to the Pang catchment, Figure 2.12 shows the results of flow accretion surveys undertaken between 2002 and 2005 (Griffiths et al., 2006). Figure 2.9 shows the location of the gauging sites.

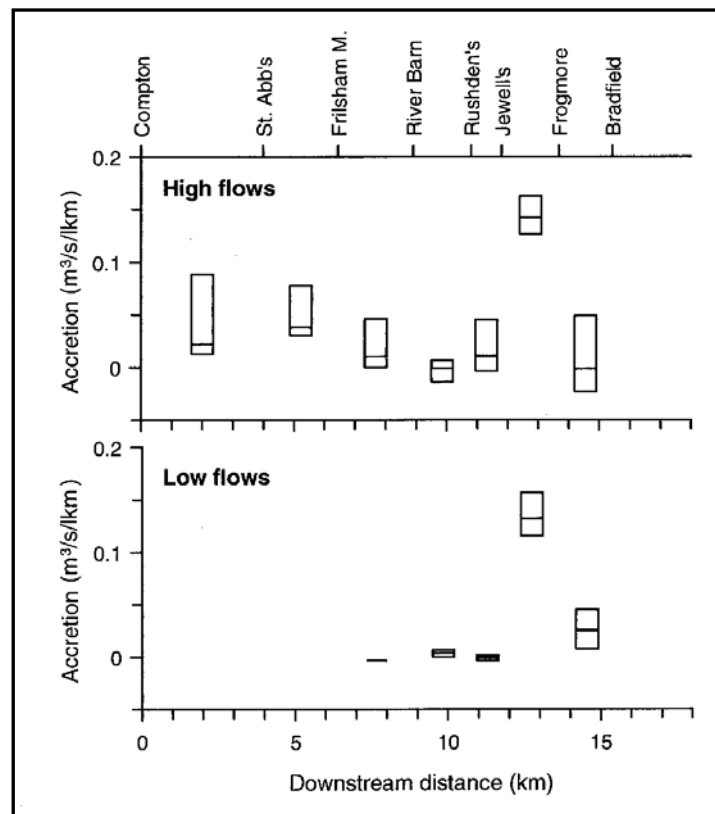


Figure 2.12: Flow accretion in the River Pang under high and low flows between 2002 and 2005, box plots showing median, Q_{25} and Q_{75} values (Griffiths et al., 2006). (Note that the accretion scale differs from Figure 2.10).

The upper ephemeral reaches of the Pang between Compton and Frilsham have relatively high accretion rates in winter. The highest accretion during both high and low flows is between the Jewells and Frogmore gauging sites where there are major spring

inputs, including the Blue Pool spring with a measured discharge of $\sim 200 \text{ L.s}^{-1}$ (Section 3.4.3.2). The accretion survey does not include the lower reaches of the Pang between Bradfield and Pangbourne.

2.8 Hydrogeology

2.8.1 Previous hydrogeological studies in the catchments

There have been a large number of local and catchment scale hydrogeological studies within the Pang and Lambourn catchments by water companies, consultants, the British Geological Survey and university researchers. Many hydrogeological studies are in the form of unpublished reports. Atkins (2003) provide a detailed review of this literature as part of a report on a new Kennet groundwater model that includes the area of the Lambourn and Pang catchments. This report also includes a conceptual model of the hydrogeology of the area. Other recent hydrogeological and hydrological studies of the Pang and Lambourn catchments undertaken during LOCAR are still ongoing although initial publications can be found in a *Journal of Hydrology* Special Issue edited by Wheater entitled "Hydro-ecological functioning of the Pang and Lambourn catchments, UK - Results from the Lowland Catchment Research (LOCAR) initiative" (Volume 330 issues 1-2, October 2006).

The earliest catchment study was part of the Lambourn Valley Pilot Scheme which was undertaken between 1967 and 1969 to determine the feasibility of developing groundwater in the Lambourn for augmentation of river flows in the Thames catchment (Brettel, 1971). The study included a detailed description of the Lambourn catchment, but primarily involved investigating the behaviour of the aquifer and the rivers during and after test pumping. The Thames Groundwater Scheme aimed to use groundwater to augment depleted rivers in the Thames basin (including the Pang and Lambourn catchments) and became operational in 1976 (Morel, 1980). Atkins (2003) report that transmissivity was investigated by Robinson (1976,1978) as part of the Thames Groundwater Scheme. Further work on aquifer properties was undertaken by Rushton et al. (1989) and Allen et al. (1997).

The remainder of this chapter uses the results of these studies to describe the hydrogeology of the Pang and Lambourn catchments.

2.8.2 Recharge rates

Several modelling studies have been undertaken to estimate recharge in the catchments (Morel, 1980; Finch, 2001; Bradford et al., 2002; Christodoulou, 2004; Wheeler et al., 2006a). These studies appear to have obtained contradictory results, which may be due to the difficulties in estimating recharge accurately or may simply reflect annual variations in precipitation because the estimates were made for different years.

Morel (1980) estimated recharge between 1969 and 1975 as ranging from 200 to 425 mm/year with an average of 301 mm/year. Finch (2001) developed a recharge model and calculated that the recharge to the Chalk in the Pang catchment was 105 mm in 1990 and 106 mm in 1997. The model takes into account evaporation (using the Penman-Monteith (Penman, 1948) model), canopy interception, soil moisture processes, overland flow, and interflow.

Bradford et al. (2002) compared four different models used to estimate recharge in the Pang catchment between 1992 and 1995. The models were MORECS (Hough et al., 1996), the Thames Catchment Model (TCM) (Wilby et al., 1994), The Areal Non-point Source Watershed Environment Response Simulation model (ANSWERS) (Bouraoui and Dillaha 1996), and the Root Layers Model (RLM) (Ragab et al., 1997). Bradford et al. (2002) found that the MORECS and TCM models produced lower estimates of recharge than the ANSWERS and RLM models. The differences were much greater in summer months than in winter months and were attributed to the higher complexity of the soil and land use input parameters of the ANSWERS and RLM models. Estimates during a dry year, 1992, ranged from a minimum of 175 mm using a MORECS model to 260 mm using a Root Layer Model (RLM). Estimates during a wet year, 1995, were slightly less variable, ranging from 305 mm using the MORECS model to 385 using the RLM. These results (including the "dry year" of 1992) are consistently higher than those obtained by Finch et al. (2001).

A water balance study of the Pang by Christodoulou (2004) used an average recharge rate of 365 mm/year calculated by the Environment Agency for 1999 to 2003. Average recharge in a distributed recharge model of the Pang used by the BGS is ~ 0.5 mm/day (Chris Jackson, personal communication 2007).

The above review shows that estimated recharge rates for the catchments vary from 105 to 425 mm/year (or 0.3 to 1.2 mm/day), and the true recharge must be considered as uncertain and variable from year to year. The range is broadly compatible with rainfall and evapotranspiration, and the simple differences of annual precipitation and potential evapotranspiration figures given by Wheater et al. (2006a) are 167 mm for the Pang and 281 mm for the Lambourn (Section 2.6).

2.8.3 Groundwater contours

Records from 70 boreholes were used to construct groundwater contours in the catchments as part of the LOCAR programme and are presented in Wheater et al. (2006a). The data were provided by Gallagher (personal communication, 2006). Figure 2.13 shows the contours during a period of low groundwater level (Autumn, 2002) and high groundwater level (Spring, 2003). Comparison of these two maps suggests some limitations, especially at the edges of the contoured area. For example contours indicate a seasonal water level variation of several metres at some points along the River Kennet. However, the main areas of interest are generally better constrained by borehole data.

The contours indicate flow down the Lambourn valley under high and low flow conditions. To the northeast of the River Lambourn flow is from a more northerly direction under high flow conditions. Under low flow conditions some groundwater within the northeasterly part of the Lambourn topographic catchment appears to be lost to the Kennet and Pang rivers to the south and east, and northwards towards the scarp slope. Groundwater also flows from the most northwesterly part of the Pang catchment north and east towards the scarp slope and is probably discharged through the distinctive spring line along the base of the scarp slope (Section 2.5.2).

The contours suggest that in the upper part of the Pang topographic catchment groundwater flows predominantly in a southeasterly or easterly direction, passing across the Pang valley towards the River Thames, which is ~ 50 m lower than the upper reaches of the Pang (Section 2.2). Abstractions at Pangbourne and Gatehampton may also accentuate groundwater flow to the east (Section 2.8.4). Under high flow conditions, flow east of the upper reaches of the Pang is from a more northerly

direction. In the interfluvial area between the lower parts of the Pang and Lambourn catchments, groundwater flow is towards the southeast and the River Kennet.

Groundwater catchments for the Lambourn and Pang are difficult to define because they do not correspond to the topographic catchments and they vary in size and position on a seasonal basis (Wheater et al., 2006a). An additional problem is that because chalk permeability is anisotropic, flow may not always be perpendicular to the groundwater contours. Gains and losses between adjacent catchments are complex. The groundwater contours suggest that the Lambourn groundwater catchment may be reduced under low flow conditions due to increased losses to the Pang and Kennet rivers to the south and east, and to the Vale of the White Horse to the north. The Pang may gain flow from a westerly extension into the Lambourn catchment under low flow conditions, but much water is lost from the Pang catchment by flow to the Thames. Wheeler et al. (2006a) note that the river discharge per unit area of topographic catchment is 50 % less in the Pang than the Lambourn. This may be because of losses from the Pang to the Thames topographic catchment.

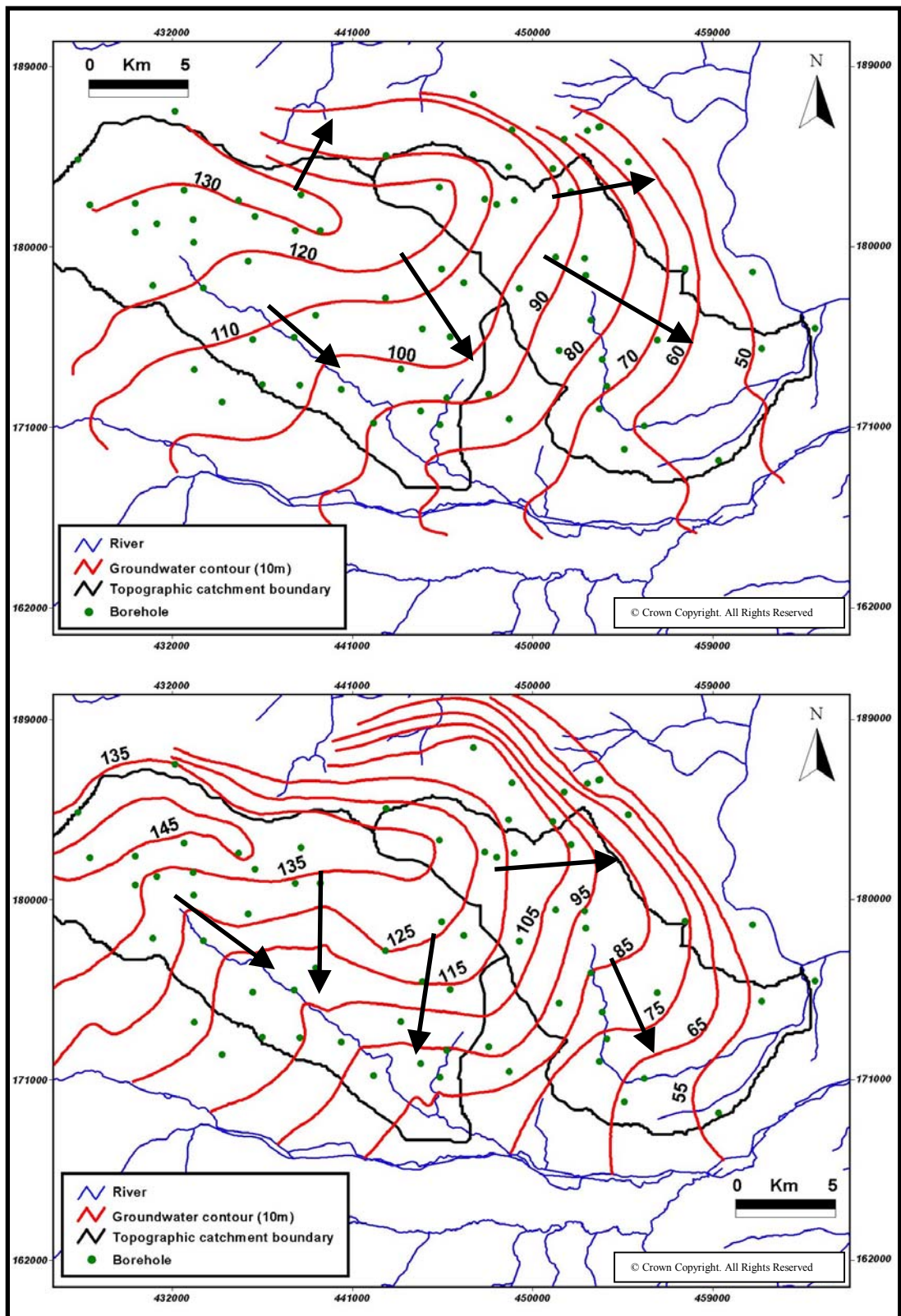


Figure 2.13: Groundwater contours in the Pang-Lambourn catchments in Autumn 2002 (above) and Spring 2003 (below) (supplied by Alex Gallagher, personal communication, 2006). Arrows indicate general flow directions.

2.8.4 Groundwater abstractions

The Pang and Lambourn catchments are both affected by groundwater abstraction, although the impacts are greater in the Pang. Figure 2.14 shows the location of 16 public water supply abstractions for which data were available for from the LOCAR data centre (large red circles on Figure 2.14). Of these 7 are within the Pang and Lambourn catchments, 3 lie close to the topographic boundary of the catchments, and 6 lie a short distance outside the topographic catchment area. Figure 2.14 also shows the location of many small abstractions (small red circles) within the catchments. In the Pang these small abstractions are mainly located along the main river valley, whilst in the Lambourn they are distributed in the upper reaches of the river valley and in the interfluvial area to the northeast. The locations of large abstractions east of the catchments at Cleeve and Gatehampton are also depicted (large black circles).

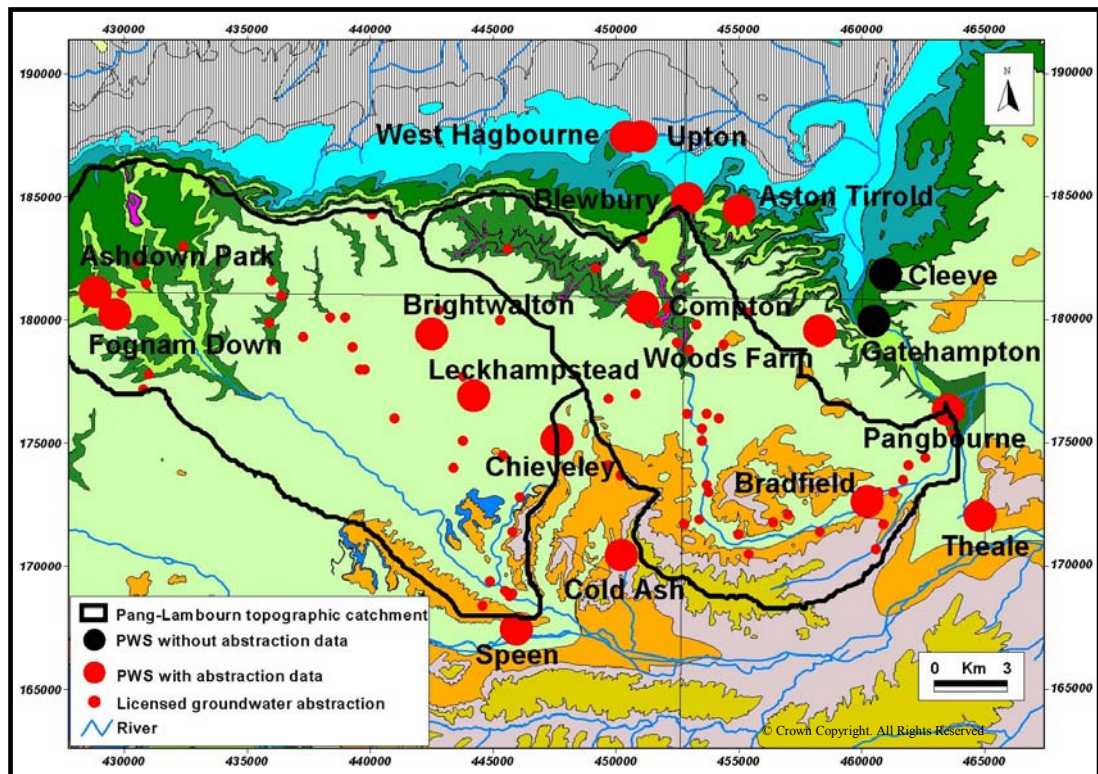


Figure 2.14: Location of licensed abstraction boreholes in the Pang-Lambourn catchments and the adjacent area (geology key is as for Figure 2.2)^{BGS}

Abstraction amounts at the four largest public water supply sites between 1982 and 2002 are presented in Figure 2.15. Figure 2.16 shows the total measured abstraction from all 16 sites shown on Figure 2.14. Table 2.3 shows the license amounts and the actual average abstraction rates in 2002. There has been a decline in the overall

abstraction from $\sim 800 \text{ L.s}^{-1}$ in the early 1980's to $\sim 400 \text{ L.s}^{-1}$ in 2002 (Figure 2.16). The abstraction of $\sim 400 \text{ L.s}^{-1}$ in 2002 is almost two thirds of the average discharge in the River Pang which is 650 L.s^{-1} , and excludes all the private abstractions shown on Figure 2.14. The greatest change during the period between 1982 and 2002 is at Compton, which was a significant abstraction of up to 200 L.s^{-1} in the 1980's (Figure 2.15). Halcrow (1987) report that abstraction from this site appeared to have an impact on the upper reaches of the Pang. This prompted a gradual decline in abstraction until December 1997 when groundwater withdrawals at Compton stopped completely. Despite the decrease in abstraction at Compton, the flow in the River Pang over this period does not appear to show a corresponding increase (Figure 2.8) which suggests that either the previous abstraction was not affecting the flow in the river, or that new abstractions at Gatehampton have affected an equivalent volume of water.

At the present time the most significant abstractions from the Chalk aquifer are those at Pangbourne and Speen, with moderate abstraction from Ashdown Park, Fognam Down, Leckhampstead, Blewbury, Woods Farm and Bradfield. The largest abstraction is at Pangbourne, and with an average discharge of $\sim 200 \text{ L.s}^{-1}$ it is comparable in size to the Blue Pool spring. Assuming a recharge rate of 0.6 mm/day this abstraction would require a catchment area of approximately 30 km^2 , some of which may be within the Pang topographic catchment. However, the actual amount coming from the Pang catchment may be relatively small because some of the abstracted water is thought to come from elsewhere, in particular from the River Thames (Peters and Van Lanen, 2004).

The Pang catchment may also be affected by the very large abstraction at Gatehampton, which is licensed for 1215 L.s^{-1} , and the abstraction at Cleeve licensed for 189 L.s^{-1} . These sites (large black circles on Figure 2.14) are close to the River Thames, on the east bank. Water taken from these sites is derived from both gravel deposits and chalk, and a large proportion may come from the River Thames itself. However, it is possible part of their abstraction may be derived from groundwater flow in the Chalk west of the River Thames, extending into the Pang catchment. Actual abstraction data are not available, although the license amount at Gatehampton is considerable larger than that of other public water supply abstractions in the area (Table 2.3).

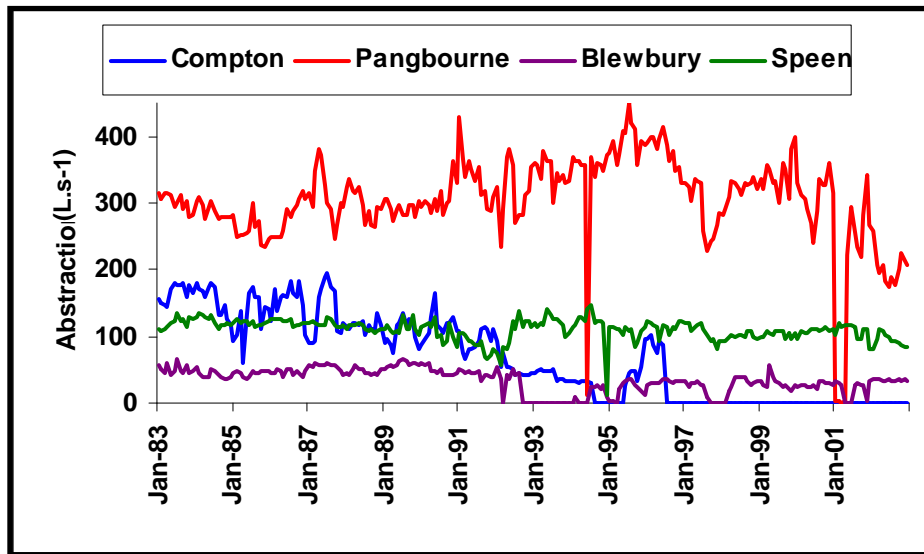


Figure 2.15: Abstraction rates at major public water supplies between 1983 and 2003.

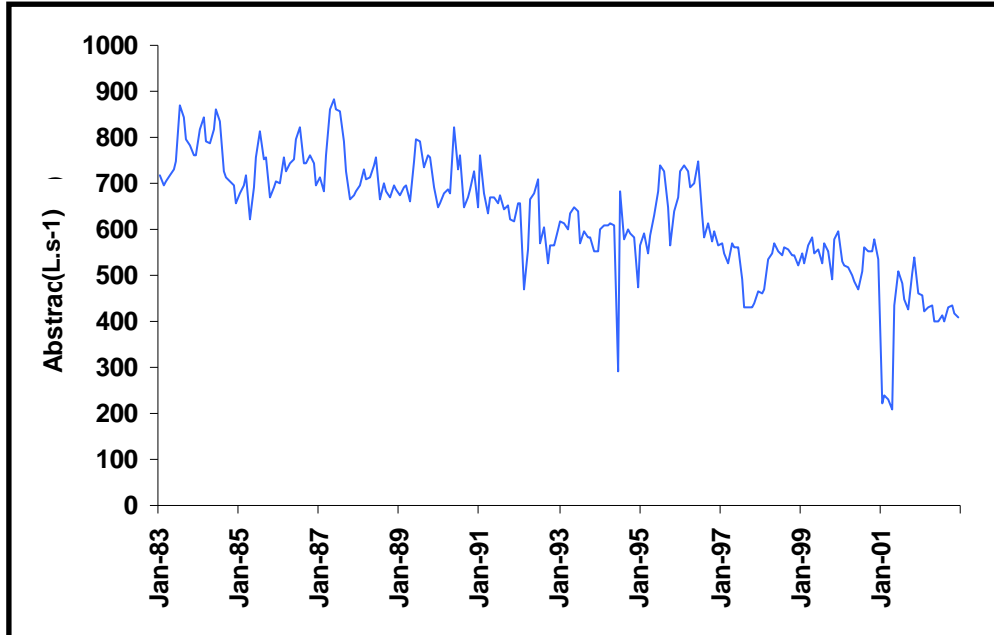


Figure 2.16: Total abstraction from 16 PWS boreholes in and immediately adjacent to the Pang-Lambourn catchments

Table 2.3: Average abstraction in 2002 and license rates of PWS boreholes affecting the Pang-Lambourn catchments

Site	Average abstraction rate in 2002 (L.s ⁻¹)	License (L.s ⁻¹)
Gatehampton	outside LOCAR, data not available	1215
Cleeve	outside LOCAR, data not available	189
Pangbourne	203	447
Speen	94	158
Blewbury	34	105
Fognam Down	26	53
Woods Farm	23	23
Ashdown Park	18	39
Bradfield	11	26
Leckhampstead	9	35
Compton	0	158
Theale	0	210
West Hagbourne	0	24
Aston Tirrold	0	26
Chieveley	0	3.9
Cold Ash	0	21
Brightwalton	0	unknown

2.8.5 Aquifer properties

2.8.5.1 Porosity

Porosity was measured on 112 samples from 5 of the LOCAR boreholes in the Pang and Lambourn by the British Geological Survey. Figure 2.17 shows the location of these boreholes and results are in Figures 2.18 to 2.20. Results follow similar patterns to those found elsewhere in the UK (Bloomfield et al., 1995; Allen et al., 1997) with a gradual decrease in porosity with depth (Figure 2.18, 2.20) due to compaction effects (Section 1.3.2.1).

The average porosity was 38.1% with a standard deviation of 5.2 %. This is slightly higher than the average for the UK Chalk as a whole, which is 34 % (Bloomfield et al., 1995). The maximum porosity was 46.7 % and the minimum was 9.7%. The sample with the lowest porosity is an outlier, presumably taken from a cemented hardground as all other samples had porosities greater than 24 %.

Figure 2.19 relates the distribution of porosities to stratigraphical units. Samples in the Lewes Chalk had lower average porosity (31.6 %) than the Seaford Chalk (39.7 %). This could be a function of the greater depth of samples taken from the Lewes Chalk,

but depth cannot be the only controlling factor, because the 4 samples from New Pit Chalk which is the lowest stratigraphic unit have similar porosity to the modal values in the Lewes Chalk, and are within the range shown by the Seaford Chalk. Figure 2.20 shows the porosity profiles and stratigraphical boundaries and confirms that the middle part of the Lewes Chalk is less porous than the strata above and below it. This is likely to be due to the Chalk Rock hardground, which is present in the Lewes Nodular Chalk (Table 1.1).

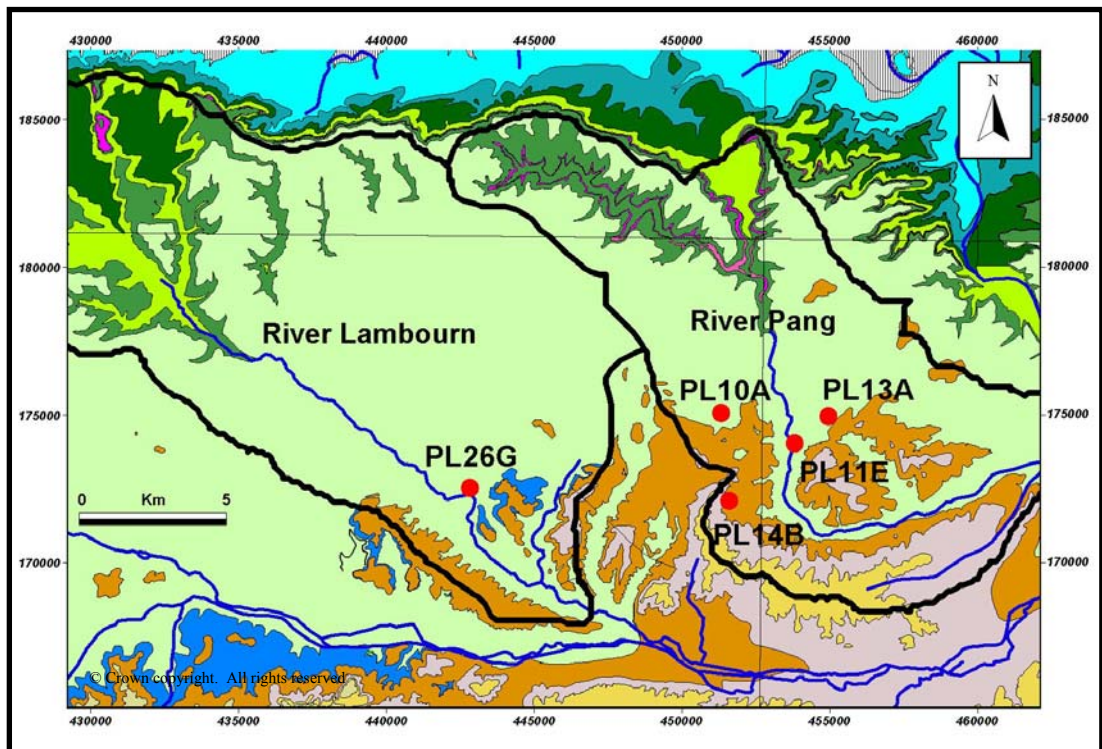


Figure 2.17: Location of LOCAR boreholes with porosity data (geology key is as for Figure 2.2)^{BGS}

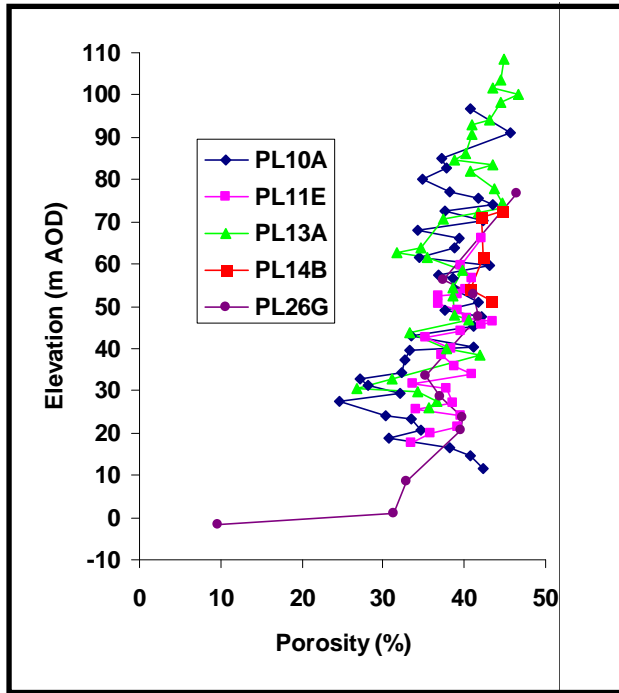


Figure 2.18: Changes in porosity with depth (samples from LOCAR boreholes in the Pang)

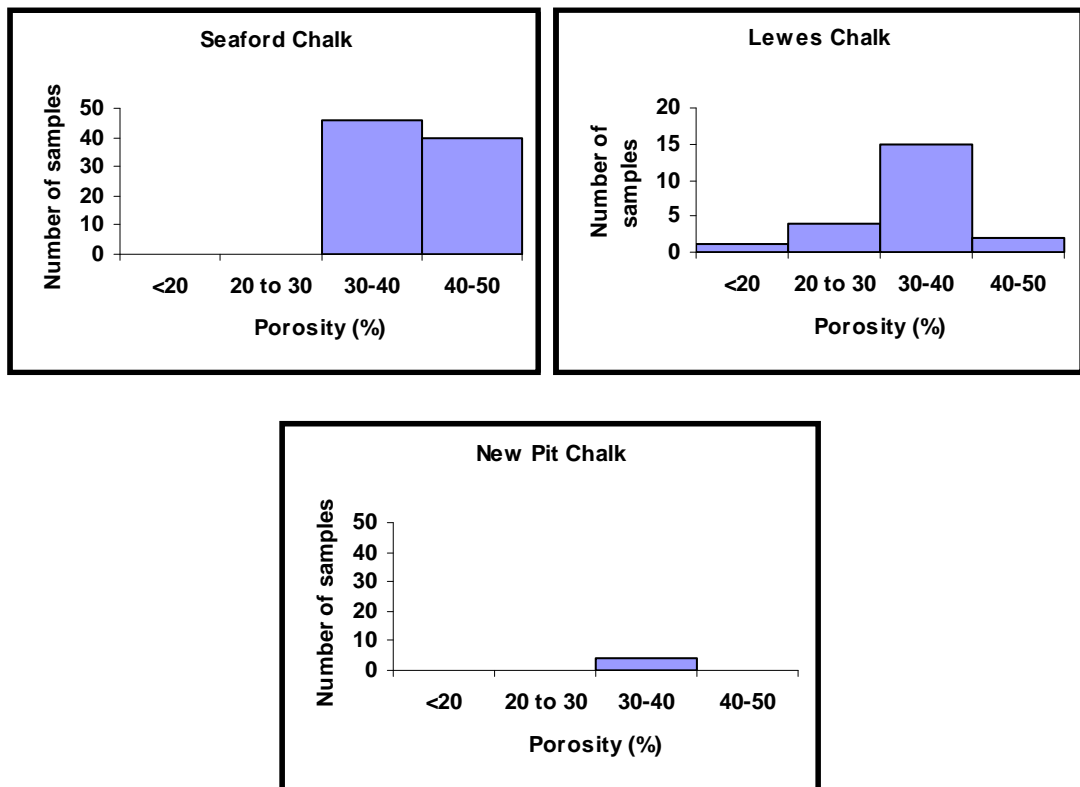


Figure 2.19: Porosity of samples from different stratigraphical units

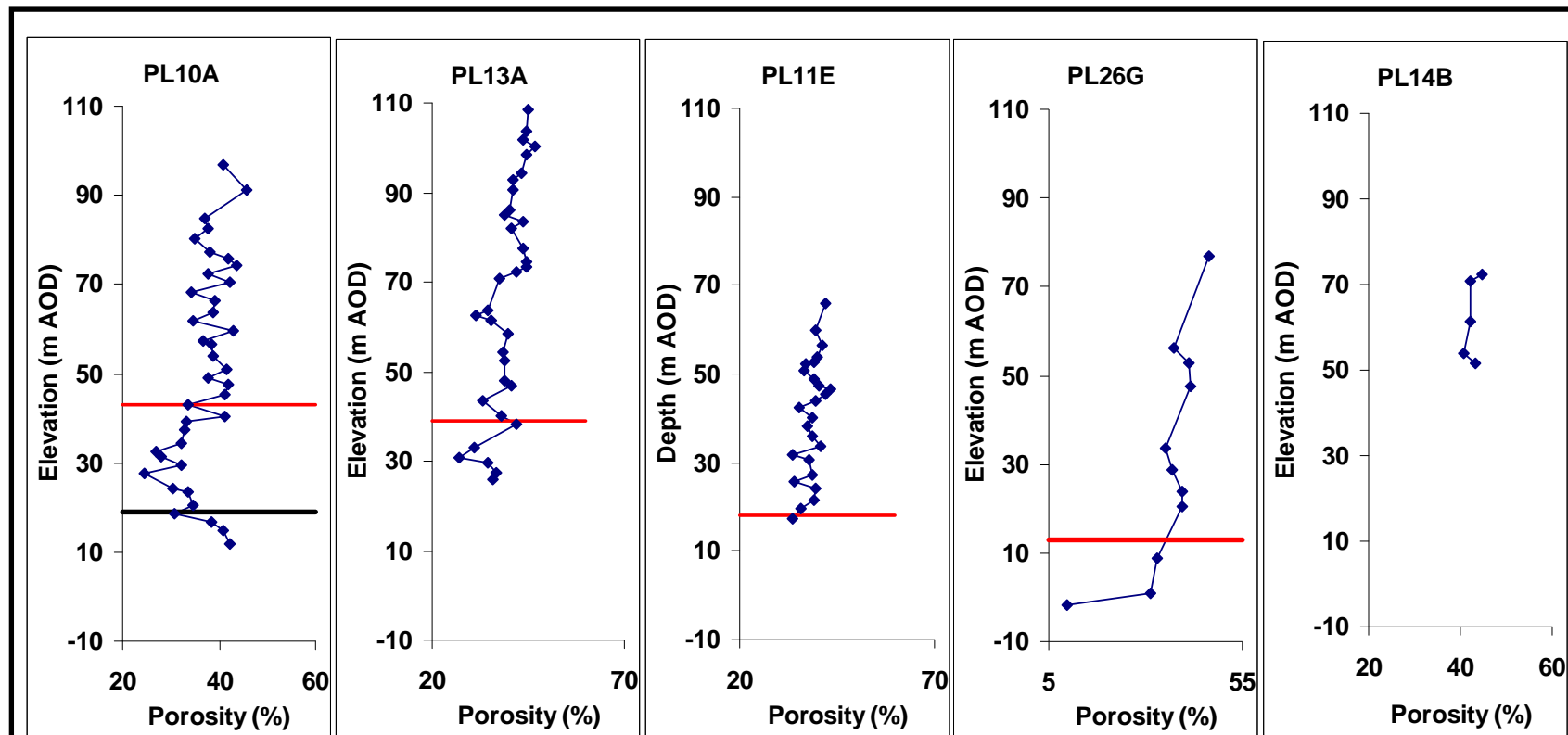


Figure 2.20: Porosity profiles in LOCAR boreholes with boundaries between the Seaford and the Lewes Chalk (red lines), and between the Lewes and New Pit Chalk (Black line)

2.8.5.2 Transmissivity

Results from 117 pumping tests from 74 different boreholes in the Kennet Valley (including the Lambourn and Pang catchments) were reviewed by Allen et al. (1997). The data have a log normal distribution with a slight negative skew (Allen et al., 1997). Transmissivity varied from 0.5 to 8000 $\text{m}^2.\text{d}^{-1}$ with a geometric mean of 620 $\text{m}^2.\text{d}^{-1}$. These values are similar to those in other areas of the Chalk (Section 1.3.2.2).

Extensive work carried out in the Kennet valley as part of the Thames groundwater scheme in the 1970's found that transmissivity was highest in the valleys and lowest in the interfluves (Allen et al., 1997). Borehole geophysical logging suggested that there was a rapid decrease in fracturing with depth, with 90 % of fracture development within 60 m of ground level (Owen and Robinson, 1978 cited by Allen et al., 1997). Analysis of pumping tests conducted in the same borehole under different water level conditions demonstrated the importance of ephemeral saturated fractures in the zone of water table fluctuation (Allen et al., 1997). When the water table fell below these fractures the borehole transmissivity was substantially reduced. Robinson (1976) concluded that transmissivity distributions in the Kennet Valley could be modelled using depth to minimum rest water level, saturated thickness of the aquifer and distance from winter flowing streams (Allen et al., 1997). A more recent modelling study of the Kennet and Pang catchments (Atkins, 2003) has made some additions to this earlier work, concluding that (a) confined chalk has lower transmissivity than unconfined chalk, (b) solutionally widened fractures with enhanced transmissivity occur in deeply confined chalk, and (c) transmissivity can also be greater under valleys than under interfluves in confined chalk.

Transmissivity data for the Pang and Lambourn catchments originally compiled by Allen et al. (1997) were available for LOCAR and values vary between 0.5 and 3400 $\text{m}^2.\text{d}^{-1}$. The patterns in the spatial distribution of the Kennet area first observed by Owen and Robinson, (1978) and reported by Allen et al. (1997) can be seen in the Pang-Lambourn (Figure 2.21). Boreholes with the lowest transmissivity are all located in areas away from the river valleys. However, there are high transmissivity boreholes distributed throughout the catchment, including areas away from the river valleys. There are also high transmissivity boreholes very close to low transmissivity boreholes, which must reflect local heterogeneity in the fractures and fissures causing high

transmissivity. Comparison with topographic contours demonstrates that there is gradually increasing transmissivity from interfluvial to minor dry valleys to major dry valleys, to river valleys (Table 2.4).

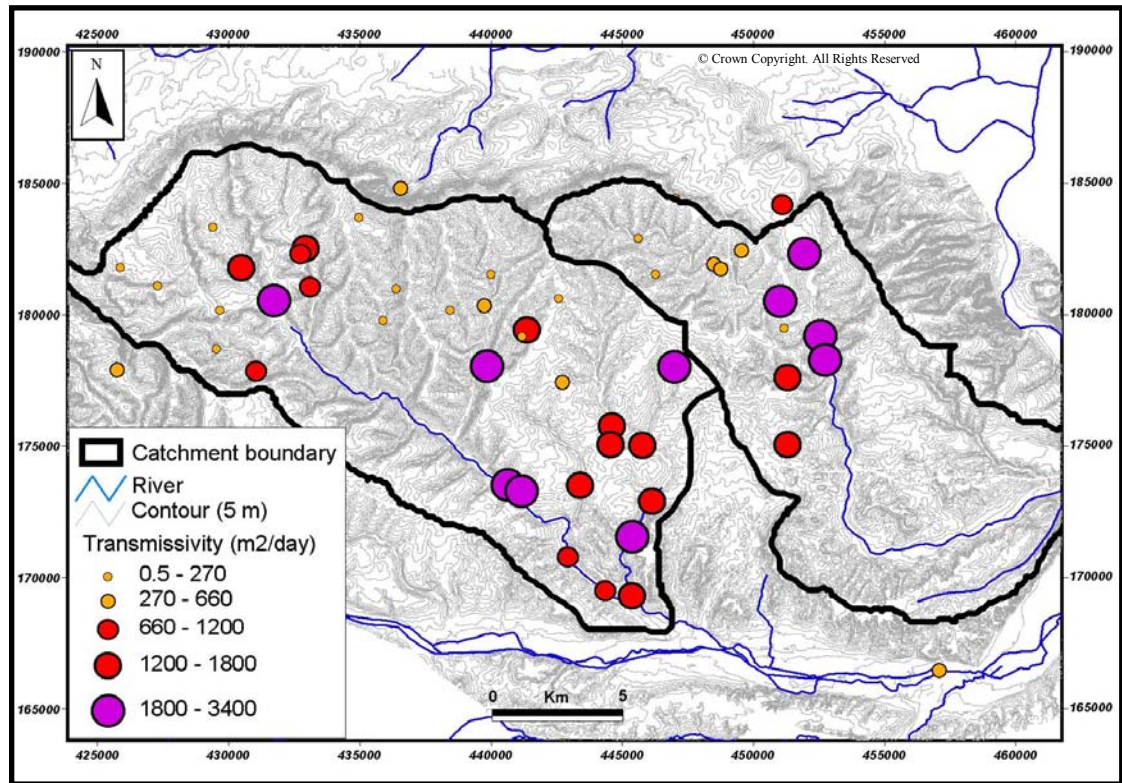


Figure 2.21: Transmissivity from pumping tests in the Pang-Lambourn catchments (data from Allen et al. 1997)

Table 2.4: Relationship between transmissivity, T ($m^2.d^{-1}$) and topographical location of boreholes

Topography	Average T	Max T	Min T	Number of sites
Interfluvial	207	660	1	8
Small dry valley	795	2900	0.5	18
Large dry valley	1372	3400	200	20
River valley	1808	3300	600	12

2.8.5.3 Hydraulic Conductivity

Recently packer testing was undertaken in three adjacent boreholes at the LOCAR interfluvial study site at Trumpletts Farm in the Pang (Williams et al., 2006). The boreholes are on the edge of a dry valley, and there are several shallow karst dolines in the adjacent fields. The location of Borehole 10A at Trumpletts Farm is shown on Figure 2.17. Williams et al. (2006) found that in Borehole PL10A hydraulic conductivity over 3 m long packered intervals varied from 0.04 to 41 m.d^{-1} . There was a strong decrease in hydraulic conductivity with depth although there is also great variability in results from packered layers which were only a few metres apart highlighting the importance of individual fractures or fissures in determining the hydraulic conductivity (Figure 2.22).

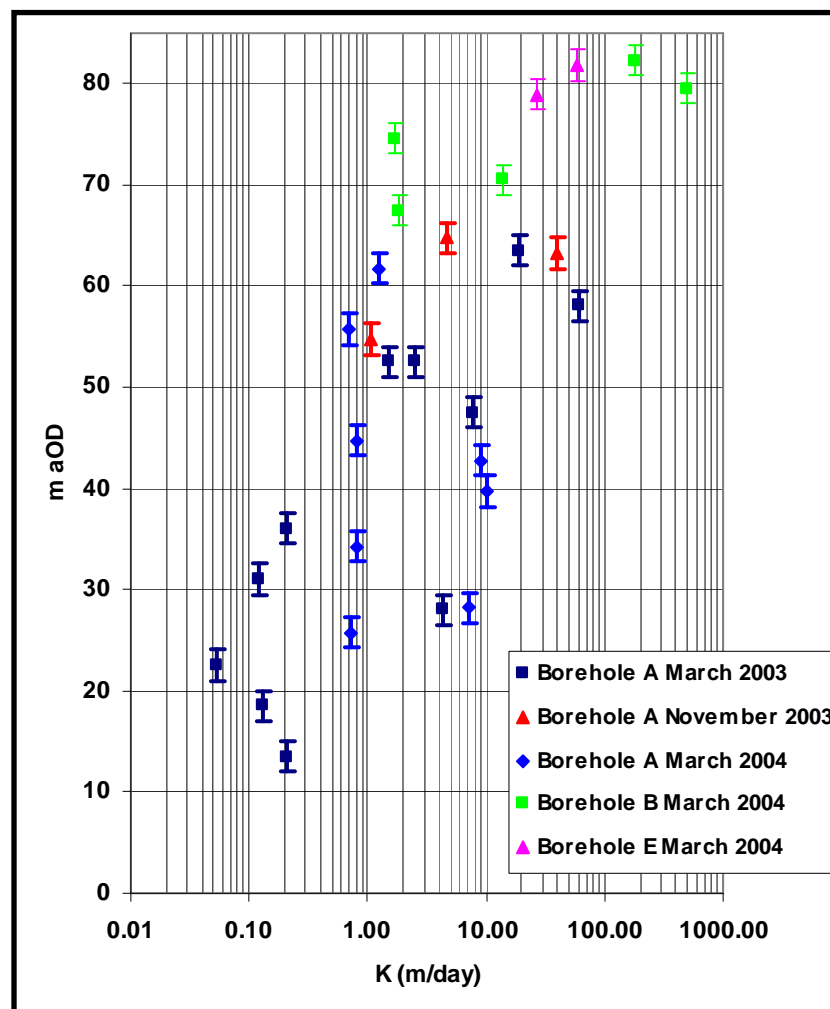


Figure 2.22: Packer test results from Trumpletts Farm. Based on figure and data in Williams et al. (2006)

Results are consistent with previous chalk packer test results from Hampshire (Price et al., 1977) and the South Downs (data from National Rivers Authority (1993) presented in Allen et al. (1997)), which also show a strong decrease in permeability with depth (Section 1.3.2.2). Fewer results were obtained by Williams et al. (2006) from two other boreholes at Trumpletts Farm, but hydraulic conductivities of 180 and $>500 \text{ m.d}^{-1}$ near the top of borehole B were much higher than in borehole A, demonstrating variability in aquifer properties between boreholes only 50 m apart.

2.8.5.4 Storage properties

Storativity values from 107 tests in 74 different boreholes in the Kennet Valley were collated by Allen et al. (1997). The dataset includes the Pang and Lambourn catchments. Storativity values were log-normally distributed with a slight negative skew, and some suggestion of bimodality (Allen et al., 1997). Values ranged from 1×0.0001 to 0.071 with a sample geometric mean of 0.006 and a sample median value of 0.0075 (Allen et al., 1997). Separate data for confined and unconfined chalk are not presented by Allen et al. (1997). However, they do note that values in the Upper Chalk (which is unconfined) were higher than values from boreholes where the stratigraphy data were not available but which were thought to be generally in confined chalk. The storativity values in the Kennet Valley are similar to other areas of the Chalk (Section 1.3.2.3).

2.8.6 Groundwater levels in monitoring boreholes

2.8.6.1 Seasonal fluctuations in groundwater levels

Borehole water levels have been measured at more than 100 sites in the Pang and Lambourn catchments by the Environment Agency. The frequency of monitoring and the length of records are very variable. In this section a selection of boreholes with daily water level data are used to illustrate typical patterns in groundwater levels. The locations of all the boreholes discussed in this section and in Section 2.8.6.2 are shown on Figure 2.23. Borehole water levels fluctuate on a seasonal basis and this is illustrated in Figure 2.24, which shows a long-term record between 1972 and 2002 for borehole SU 57/153 located in the middle reaches of the Pang. It illustrates that both the timing and the magnitude of peak and low water levels varies substantially from year to year. In this example peak water levels varied from March to July, whilst the lowest water levels varied between October and April.

In the upper reaches of the catchments the unsaturated zone is up to 80 m thick and there are seasonal variations in groundwater level of up to 25 m in the Lambourn (Grapes et al., 2005) although 10 m is more typical in the Pang. Figures 2.25 and 2.26 show examples of water levels in boreholes located away from the main river valleys between 1997 and 2002. The figures show that the different boreholes have a broadly similar pattern with respect to the magnitude and timing of peaks and troughs. In boreholes close to the rivers the water level varies seasonally by only 1-3 m (Figure 2.27). There appears to be more variability in the seasonal response of these boreholes.

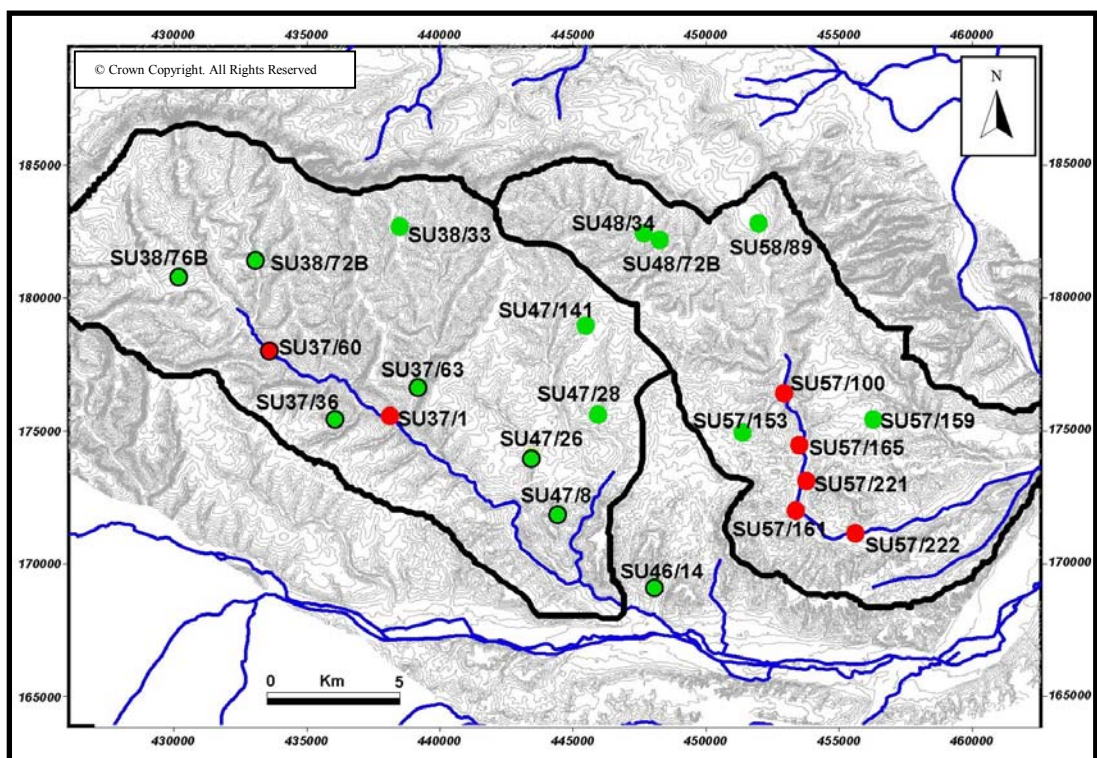


Figure 2.23: Location of Environment Agency monitoring boreholes discussed in Section 2.8.6. Red circles are in river valleys, green are on interfluves, and those with a black outline were used by Grapes et al., (2005) to compare borehole water levels with the elevation of the River Lambourn (Section 2.8.6.2)

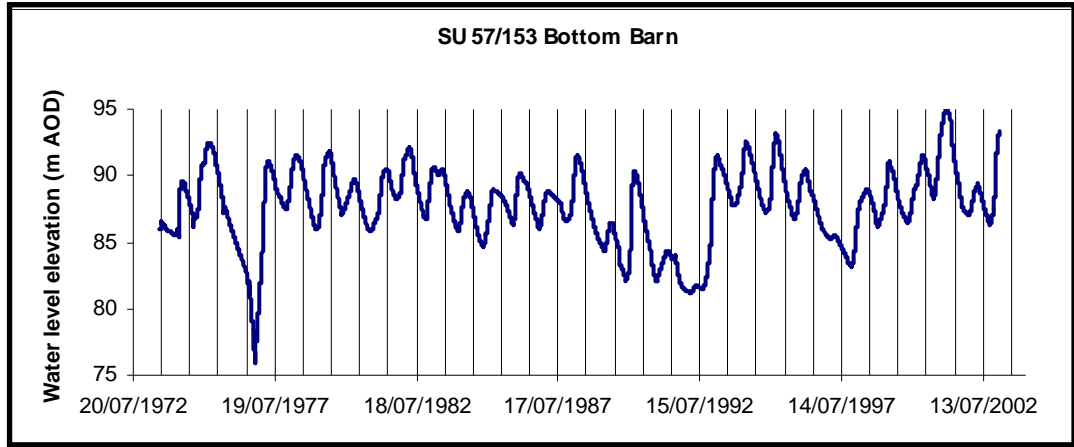


Figure 2.24: Long term water level variations in SU 57/153, Pang catchment

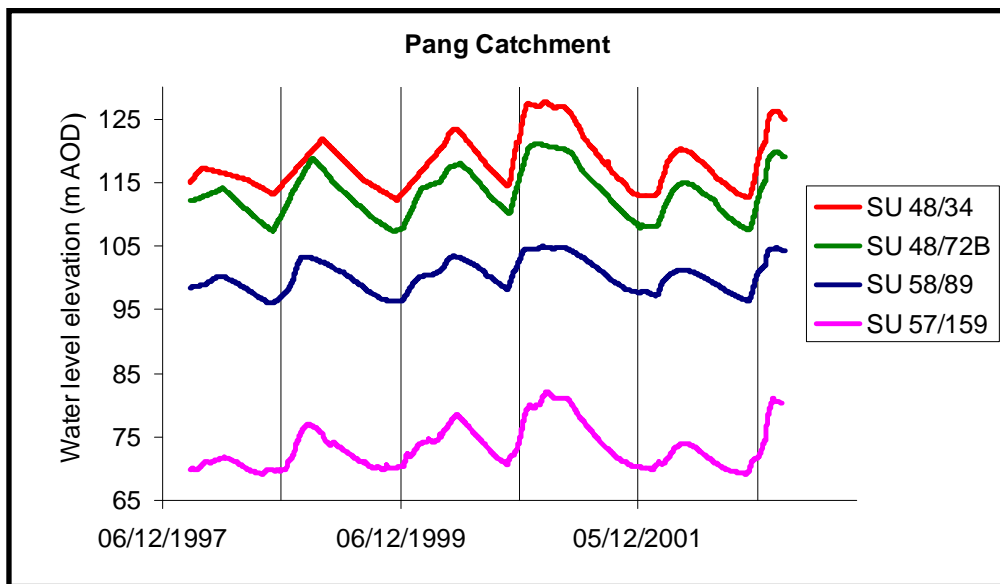


Figure 2.25: Water levels in 4 interfluvial boreholes in the Pang catchment between 1997 and 2002

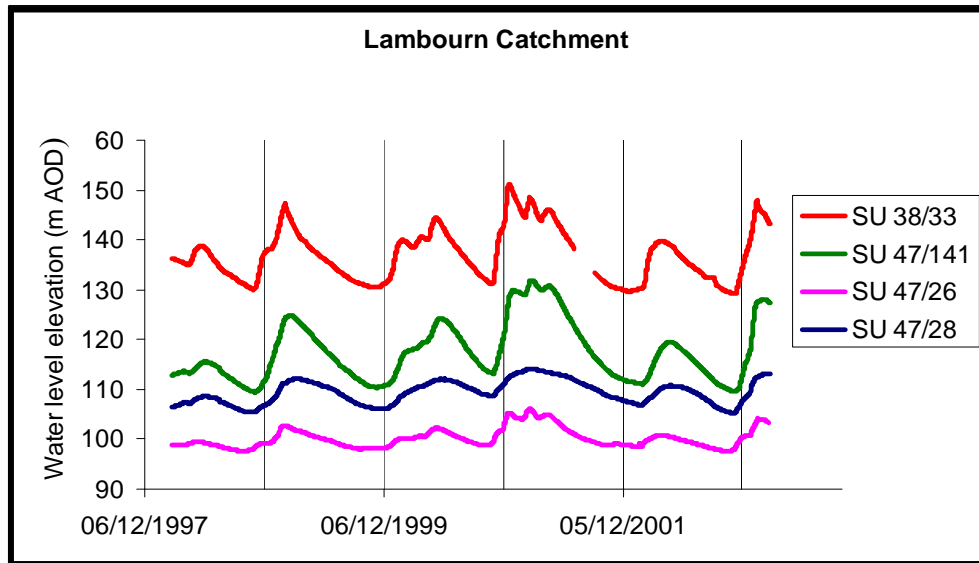


Figure 2.26: Water levels in 4 interfluvial boreholes in the Lambourn catchment between 1997 and 2002

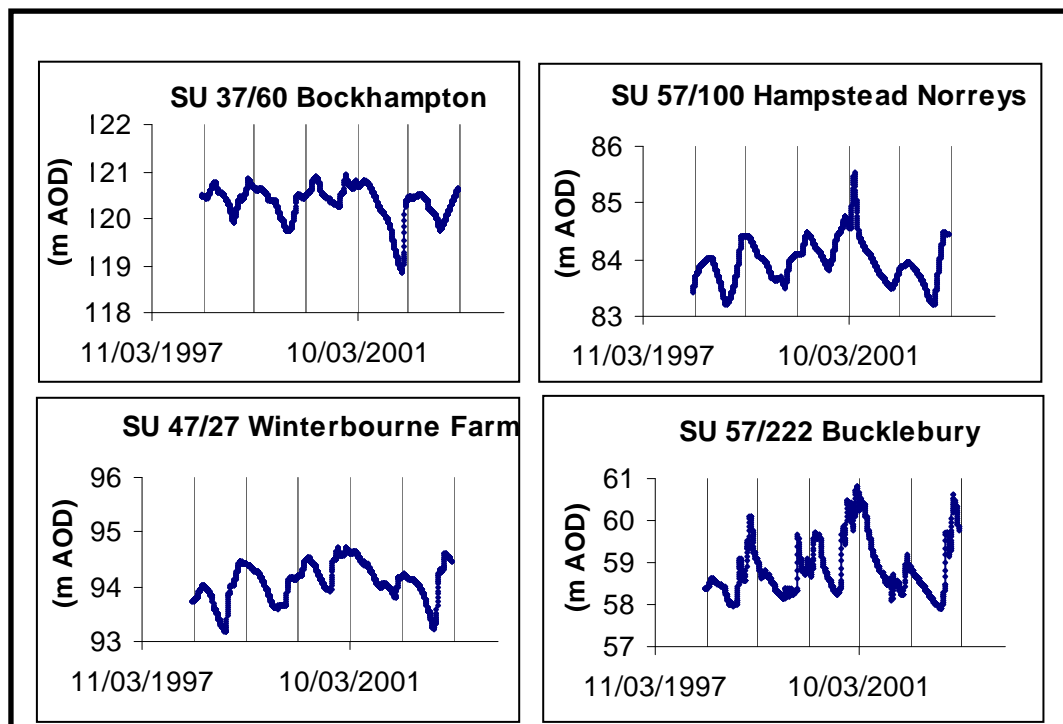


Figure 2.27: Examples of river valley borehole water levels

Atkins (2003) generated daily percolation time series data using the Thames Region catchment model, CATCHMOD which inputs daily rainfall and MORECS evaporation data into a Penman-Grindley type soil moisture model. They smoothed these data using a 31-day moving average and compared the results to borehole water level data collected at intervals of a month or less, and over a minimum period of 15 years. They found 5 different relationships between percolation peaks and peak water levels in boreholes in the Kennet catchment area (borehole water level data were at monthly or more frequent intervals over at least a 15 year period). These were borehole peaks at the same time as percolation peaks, borehole peaks 1,2 or 3 months after percolation peaks, and boreholes with little variation. They found that boreholes in the upper parts of the Pang catchment had a much longer delay before peak water level (3 months) than those in other areas of the Kennet catchment where peak borehole water levels were generally at the same time as percolation peaks or one month after. Atkins (2003) then compared peak borehole water levels to calculated baseflow peaks from the downstream gauging site in each sub catchment. In the Upper Kennet sub-catchments as expected recharge occurred, then groundwater levels peaked, and finally there was a peak in baseflow at the gauging station. However, in the Pang baseflow peaked before peak water levels in boreholes. The boreholes used in the analysis were mainly in the upper reaches of the Pang, and it suggests that these boreholes represent a different groundwater body from that which controls the baseflow. Atkins (2003) suggest that the baseflow may be influenced by faster runoff to large springs (such as the Blue Pool) associated with the Palaeogene cover in the lower reaches of the catchment, where there were very few boreholes that could be used in the analysis.

2.8.6.2 Borehole water levels and river elevations

In both the Pang and the Lambourn there are stretches of river that lie perched above the water table, with water levels in adjacent boreholes lower than the river itself. This demonstrates that the rivers often do not represent the level of the water table, and that they are not fully connected to the groundwater system throughout their length. Water levels in 8 boreholes immediately adjacent to the Pang and Lambourn rivers were compared with estimates of river elevation from 5 m contour data (Table 2.5). The river elevations quoted are the 5 m contour defining the valley at the location of the borehole and the actual river elevation may be slightly lower (although < 5 m lower). The data demonstrate that in the two boreholes in the lower reaches of the Pang, the groundwater

level is 5-10 m below the river level. In the upper reaches of the Pang the data suggest that the river may be perched above the water table under low water level conditions.

Contrastingly, in the Lambourn valley, the upper ephemeral sections of the river appear to be perched above the water table during high water level conditions (borehole SU 37/60), whereas water levels in the two boreholes in the lower perennial sections of the rivers are at, or slightly below river level. Grapes et al. (2005) also show that the river is perched above the water table in the upper ephemeral reaches (Figure 2.28), but that water levels in the lower reaches of the valley are higher than the river level, except under exceptionally low water level conditions in borehole SU 37/63. With the exception of SU 37/60 all the boreholes used for this comparison were some distance from the river and at a higher elevation (Figure 2.23), and therefore might be expected to have higher groundwater levels than the river valley.

Table 2.5: River elevation and borehole water levels

Borehole Number	River elevation (m AOD)	Borehole water level (m AOD)	River perched?
Pang			
SU 57/100	~ 85	83.2-85.5	Possibly perched
SU 57/165	~ 80	~ 78	Possibly perched
SU 57/221	~ 75	72.8-74.2	Possibly perched
SU 57/161	~ 75	68.9-71.7	Perched
SU 57/222	~ 70	57.9-60.8	Perched
Lambourn			
SU 37/60	~ 125	118-120.9	Perched
SU 37/1	~ 110	105.6-106.5	Possibly perched
SU 47/27	~ 95	93.2-94.7	Possibly perched

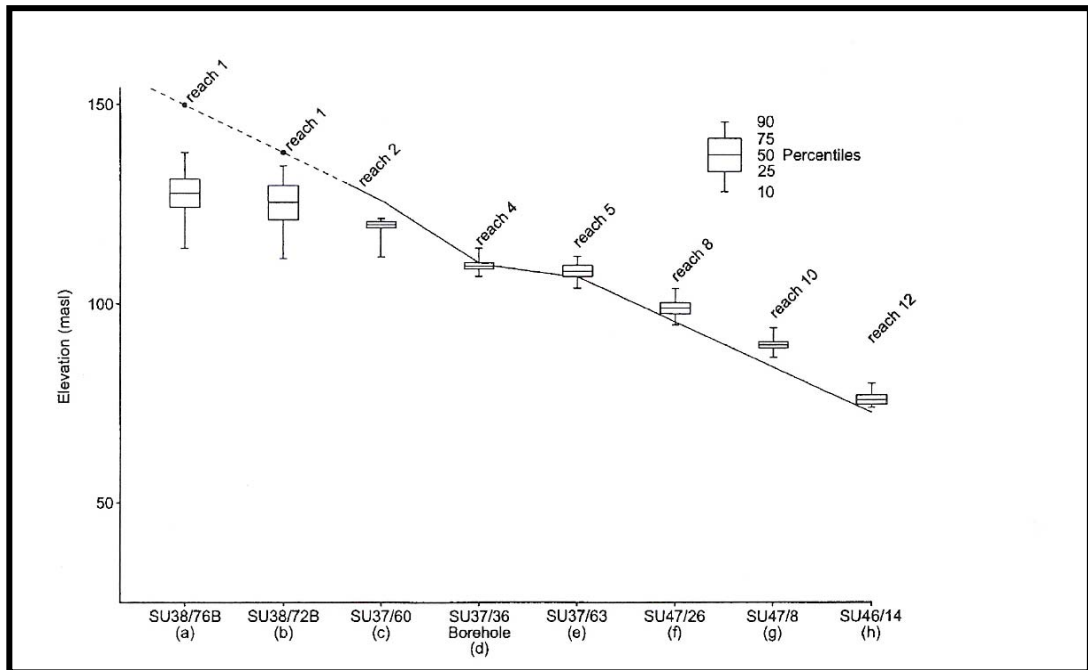


Figure 2.28: Relationship between borehole water levels and the long profile of the River Lambourn (Grapes et al., 2005)

2.8.7 Water Balance

It is extremely difficult to calculate an accurate water balance for the Pang and Lambourn catchments because of the following complications:

- Water falling within the topographic catchments is probably lost by groundwater movement to the catchments of the Kennet and Thames.
- The groundwater catchment area is difficult to define and changes seasonally.
- There are large uncertainties about actual quantities of abstraction and discharge; and the import, consumption and discharge of water within the catchments and export of water out of the catchments is very complex.
- The degree of recharge through Palaeogene deposits to the underlying chalk is not well understood

Atkins (2003) undertook a detailed water balance for groundwater and surface water catchments upstream of the Shaw and Pangbourne gauging stations, and tried to take the above factors into account. The inputs to the groundwater balance were: calculated recharge, sewage discharge to groundwater, and upstream groundwater inputs to the catchment. The outputs of groundwater abstractions and estimated groundwater flow to other catchments were removed to leave an estimated baseflow. The inputs to the surface water balance were runoff (a calculated output of the recharge model) and

sewage discharge to surface water. Surface water abstractions were subtracted to leave an estimated naturalised river flow. Atkins (2003) then used a 10 day smoothed minima technique of baseflow separation (Institute of Hydrology, undated), to calculate a measured quantity of baseflow and surface flow at the gauging stations. This was compared to the calculated groundwater and surface water amounts. The results are shown in Table 2.6, and in all cases the calculated flows were lower than the measured flows. Atkins (2003) thought this was probably due to an underestimation of recharge. Recharge was calculated using the Thames Catchment Model shown by Bradford et al. (2002) to produce lower estimates than other models (Section 2.8.2).

Table 2.6: Results of Atkins (2003) water balance (ML.d⁻¹)

Site	Calculated Baseflow	Measured Baseflow	Calculated surface flow	Measured surface flow
Shaw	136	154	140	160
Pangbourne	33	48	44	55

2.9 Conclusions

The Pang and Lambourn catchments are fairly typical chalk catchments. They have an extensive dry valley network, the rivers are predominantly groundwater fed, boreholes have seasonal groundwater patterns, and they have similar aquifer properties to other areas of the Chalk (in particular other parts of Southern England). In the lower reaches of the catchments Palaeogene strata overlie the Chalk resulting in more surface flow where the deposits are thick and impermeable, whilst there are many small springs where the deposits are locally permeable. The significance of thin Palaeogene strata overlying the Chalk in the development of surface karst features is discussed in Chapter 3.

Flow accretion in both rivers shows extensive spatial variability (Grapes et al., 2005; Griffiths et al., 2006). Both rivers appear to have sections that are normally perched above the water table, demonstrating the complexity of surface-groundwater interactions. In the Pang a very large proportion of groundwater enters the river at a single point at the Blue Pool spring, which with a discharge of $\sim 200 \text{ L.s}^{-1}$ accounts for almost two thirds of the average flow in the river at this point. The importance of point inputs through springs in both rivers is discussed further in Chapter 3. Whilst the Lambourn has a high BFI reflecting the dominance of chalk groundwater inputs, in the

lower reaches of the Pang runoff from adjacent Palaeogene strata and the town of Pangbourne result in a lower BFI than is characteristic of many chalk rivers.

The hydrogeology of the catchments is very complex due to extensive anthropogenic influences, and complex groundwater relationships between adjacent catchments. Groundwater contour maps demonstrate that groundwater flows across the topographically defined boundaries, and the directions of groundwater flow vary on a seasonal basis. The Pang catchment is particularly affected by groundwater flow towards the adjacent River Thames that is at a much lower elevation.

The catchments have been the focus of many hydrogeological studies but there are still uncertainties in particular about the nature and definition of groundwater catchments of springs, rivers and boreholes; and the mechanisms of surface-groundwater interaction. As a result, an accurate water balance has proved impossible to define for the two catchments as a whole. An improved understanding of the role of karst in the catchments may provide insight into some of these uncertainties, and the surface expression of karst features in the catchments is the subject of Chapter 3.

Chapter 3: Karst geomorphic features in the Pang and Lambourn catchments

3.1 Introduction

The objectives of this chapter are to investigate the spatial distribution of surface karst features in the Pang and Lambourn catchments, to describe and catalogue surface and shallow subsurface karst geomorphic features, and to document the nature of groundwater inputs into the river valleys assessing whether any springs have karstic characteristics. The chapter also considers the relationship between surface karst and hydrogeology, providing a framework for the remainder of the thesis that describes tracer tests that investigated the nature and distribution of subsurface karst.

The location of stream sinks, springs, and dolines are recorded in the BGS karst database, which is commercially available from the BGS. The data were available for this research through collaboration with Andy Farrant (personal communication, 2003) who was largely responsible for identifying the karst features in the Pang and Lambourn catchments. Some features were recorded from maps, but most were found during field geological mapping. Some additional stream sinks and springs were identified during the current study. In the first part of the chapter these data are used to provide an overview of the distribution of stream sinks, springs and dolines in the catchments.

As part of the current study most stream sinks and chalk springs in the Pang and Lambourn catchments were visited to investigate their geomorphology and hydrology, and to identify tracer testing injection and monitoring sites. This chapter presents the results of this field survey. The geomorphological and hydrological characteristics of stream sinks are described and their contribution to recharge to the Chalk aquifer is evaluated. Karstic springs are characterised by large discharges and rapid changes in discharge and turbidity following rainfall (Section 1.4.2), and the presence or absence of these characteristics is used to assess whether any of the chalk springs in the Pang and Lambourn river valleys are karstic, providing outlets for subterranean networks of fissures or conduits. Field observations are also used to discuss how much groundwater in the rivers is derived from point inputs through springs and how much enters the rivers through diffuse seepage.

Dolines in the catchment were not specifically visited, and reliance is placed on the BGS karst database in establishing their spatial distribution. A short discussion of doline characteristics and shallow subsurface karst geomorphic features is included. The latter consist of small relic conduits exposed in a quarry, and both small open conduits and large sediment filled dissolution features encountered during a road construction project by Mott Macdonald (2005).

3.2 The distribution of surface karst

Dry valleys are one of the most prevalent geomorphological features and are distributed throughout the catchments on both the Chalk and the Palaeogene (Section 2.3). As discussed in Section 1.5.2, dry valleys are characteristic of karst areas, although in the Chalk they are not wholly karstic, having a complex origin resulting from a combination of processes.

There is a clear spatial pattern in the distribution of surface karst features with three distinctive geomorphic zones as indicated in Figure 3.1. These are characterised by the density of stream sinks and dolines and can be related to the distance from the Palaeogene-Chalk contact.

Surface karst is most intensely developed in the lower reaches of the catchments (Zone 1) where the Chalk is overlain by Palaeogene deposits, which produce acidic soils (Edmond et al., 1992). There are several large and medium sized perennial chalk springs in the river valleys in Zone 1, the biggest being the Blue Pool with a discharge of around $200 \text{ L}\cdot\text{s}^{-1}$. Dolines are common, but stream sinks are the diagnostic feature of Zone 1 and have developed on the edge of the Palaeogene cover where it is thin and composed of sands and gravels, allowing chemically aggressive infiltration to dissolve the underlying chalk (stream sink chemistry is discussed in Section 3.3.5).

Stream sinks are concentrated on Palaeogene deposits of the Lambeth Group (Figure 3.1), which comprises the Upnor and Reading Formations (Section 2.4.1). The Upnor Formation only occurs in the southern part of the Palaeogene outcrop in the area (Section 2.4.1), and is likely to be absent in the areas where stream sinks are present. Aldiss et al. (2002) noted that the Reading Formation often comprise up to 7 m of fine

to medium grained sands and it is probable that stream sinks develop where these predominantly sandy horizons directly overlie the Chalk. During a road construction project north of the lower reaches of the River Lambourn, Mott MacDonald (2005) found palaeochannels in the Reading Formation which were infilled with sands and were < 10 to > 70 m wide and < 3m to > 5 m deep. They found a greater incidence of dissolution features in the Chalk rockhead beneath the Reading Formation where these channels were present (Section 3.6). Where the Lambeth Group is overlain by the London Clay Formation stream sinks are often located on the Lambeth Group close to the boundary, suggesting that runoff over the less permeable London Clay Formation sinks as it reaches the more permeable Lambeth Group.

In the middle reaches of the catchments (Zone 2), characteristic karst landforms are dolines with stream sinks absent. This is the zone where the Palaeogene deposits have recently been almost or completely eroded and much of the area is overlain by Clay-with-flints, providing a low permeability cap on the chalk surface (Figure 2.2). On and around areas covered by Clay-with-flints there are hundreds of karst dolines that may focus recharge at shallow depths beneath the surface. In Zone 2 there are perennial chalk springs at the head of the Lambourn River, and ephemeral springs at the head of the Pang River.

In the upper reaches of the catchments (Zone 3), chalk is exposed at the surface with no cover and little superficial material to concentrate drainage, and recharge is entirely diffuse. There is little evidence of surface karst except that the landscape is characterised by dry valleys and almost all drainage is subsurface. Dolines and stream sinks are absent except for a small cluster of dolines in the northeast of the Pang catchment. There are large ephemeral springs at Lynchwood in the Lambourn valley which when they are active, have an average discharge of about 170 L.s⁻¹ (Grapes et al., 2006).

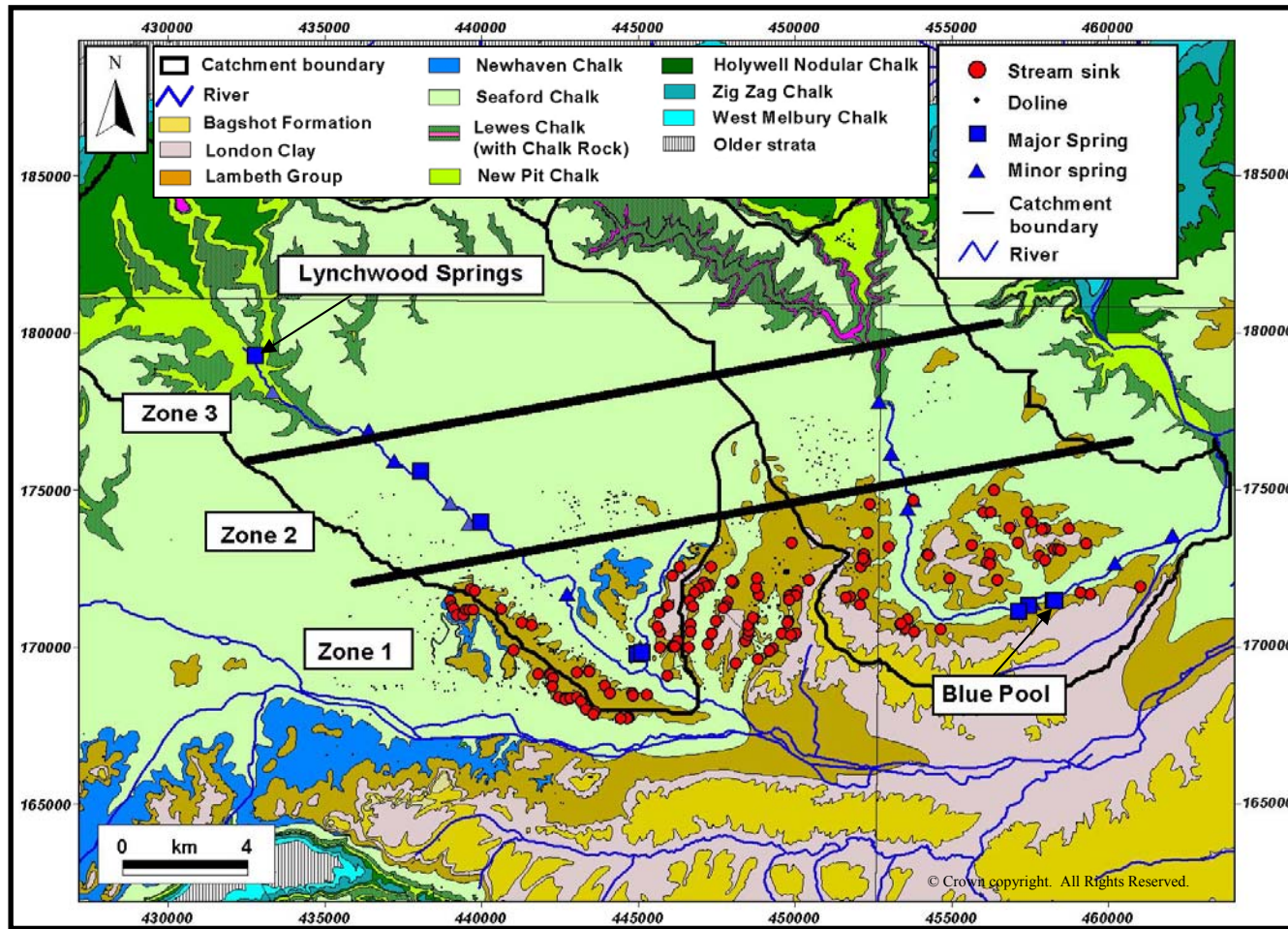


Figure 3.1: Surface karst and solid geology in the Pang-Lambourn catchments (geology key is as for Figure 2.2)^{BGS}

3.3 Stream sinks

3.3.1 Introduction

A field survey of 105 of the stream sinks recorded in the BGS karst database was undertaken to identify potential tracing sites and investigate their geomorphological evolution and hydrological function. During the survey an additional 23 stream sinks were identified. These were all found whilst visiting stream sinks recorded in the karst database and therefore there may be more stream sinks in other areas of the Pang and Lambourn catchments that were not visited as part of this survey. 33 stream sinks recorded in the karst database (as of 2007) were not visited, many of which were additions to the database by other workers after the survey described below had been completed.

Most sites were visited between June and September 2003, and many of the stream sinks are ephemeral features that are dry during the summer except following precipitation. Observation during summer 2003, and information from local residents suggests that ~ 25 of the 128 stream sinks surveyed have a small perennial flow (0.01 to 0.5 L.s⁻¹). Assessments of the likely winter flow were made based upon the presence and depth of distinctive holes in the floor of the depression, the size of the dry channel leading to the sink point, the length of the channel, the likely size of the catchment, and information from local residents. A smaller number of stream sinks were subsequently visited in winter 2003/2004, and sinks that were considered for tracer testing work were visited on multiple occasions.

3.3.2 Stream sink hydrology

The hydrology of stream sinks is determined by the source of water supplying them. This may be surface runoff, Palaeogene spring water, and/or water collected in land/road drains and piped to the stream sink. The response of the stream sinks to precipitation is complex because many are fed by a combination of two or three different types of source, and the sources themselves have variable hydrological characteristics. Most stream sinks have a rapid response to precipitation demonstrating the importance of surface runoff.

Palaeogene springs occur frequently, although except in very wet periods they have very small flows of < 1 L.s⁻¹ (Section 2.5.1). Some stream sinks fed by Palaeogene

springs have a very short channel length and a very rapid response to rainfall suggesting that the springs discharge water from a small groundwater reservoir with a low residence time. Many other stream sinks flow for weeks after rain, flowing almost continuously in winter and also during wet summers, suggesting that they discharge longer residence time groundwater released gradually from storage, and a few Palaeogene springs provide a small perennial flow to stream sinks. Some Palaeogene springs have a variable discharge comprising a small baseflow that is significantly increased following rainfall.

Land drains are commonly discharged into the base of dolines containing natural stream sinks. Some also supply dry dolines, which appear to have no natural water input. In many cases the land drains provide a consistent input ($< 1 \text{ L.s}^{-1}$) under dry conditions, suggesting that drainage is from long residence time Palaeogene springs. Road drains and some land drains have a much more variable discharge with a rapid response to rainfall.

3.3.3 Geomorphological classification of stream sinks

The stream sinks are classified by the following geomorphological categories, which are based on the findings of the field survey:

1) Seepage sinks

Seepage sinks are vegetated areas of marsh often more than 10 m wide, sometimes associated with depressions, sometimes fed by very small streams but with no distinct holes where water sinks (Figure 3.2). It is difficult to estimate the rate of recharge through seepage sinks because the thickness of the deposits overlying the Chalk and the rate of infiltration and flow through these deposits is unknown. However, the very slow flow and marsh at the surface suggest they recharge the aquifer slowly.

Seepage sinks are primarily fed by small Palaeogene springs although infiltration of very local surface runoff may occur following precipitation. They may not have developed into more significant geomorphological features because the catchment is very small and there is insufficient water to propagate extensive fissure or conduit development in the underlying chalk. Many seepage sinks were observed during the field survey but not recorded because they were encountered so commonly. Following

rainfall they were found to occur almost continuously along some sections of the Chalk/Palaeogene boundary. They do not individually provide substantial recharge but their high frequency suggests that collectively they may be an important means of recharge where chalk is overlain by thin Palaeogene cover.



Figure 3.2: Seepage sink, Snelsmore Common, Lambourn catchment, March 2004

2) Ephemeral ponds

There are several ephemeral ponds in the mapped area, sometimes within a doline and sometimes fed by a stream channel. They provide slow recharge via leakage through the base of the pond, usually over weeks or months, occasionally emptying within days.

3) Ditch sinks

These are artificially constructed drainage ditches that terminate abruptly but are not associated with a doline. They were viewed in summer when they were dry but local landowners have observed flows of $\sim 1\text{-}2 \text{ L}\cdot\text{s}^{-1}$ following rainfall and report water sinking into the ground at several of these sites.

4) Pit sink

There are short sections of stream channel and/or drainage pipes from which water sinks within a man-made pit. Recharge may be rapid through holes in the pit floor, or slower were ponding occurs (e.g. Figure 3.3).



Figure 3.3: Ponded pit sink, Pang catchment, January 2004 (photo Tim Guilford).

NGR: 458006 172792

5) Doline sink

Water from a short section of stream channel (or drainage pipe) sinks through holes in the floor of a doline, providing rapid recharge (Figure 3.4). Under high flow conditions the sink points may temporarily pond due to blockages or insufficient capacity in the underlying aquifer. Under low flow conditions some of these streams sink gradually along their length before the main sink point.



Figure 3.4: Doline Sink, Pang Catchment, March 2004 (photo Paul Shand).

NGR: 456270 174310

6) Partial sinks

Partial sinks are eroded holes within streambeds where a proportion of water sinks, but the stream continues to flow beyond the sink point except during dry periods (Figure 3.5).



Figure 3.5: Partial sink, Pang Catchment, January 2006. NGR: 453410 170750



Figure 3.6: Mature doline sink with grassed dry valley continuation at a higher elevation, Lambourn Catchment, March 2004.

NGR: 441823 169170

7) Mature doline sinks

Mature doline sinks have similar hydrological characteristics to doline sinks but are on a larger scale. They are usually associated with a doline between 5 and 20 m deep and 5 and 100 m across, and are often fed by long stream channels within incised valleys. The depressions may form an abrupt end to a valley, sometimes with a dry valley continuation at a higher elevation than the doline indicating past flow prior to the development of the stream sink (Figure 3.6).

Most doline sinks and partial sinks and all mature doline sinks provide rapid point recharge to the Chalk aquifer, and have flows of $\sim 1\text{-}4 \text{ L.s}^{-1}$ following rainfall. There are 37 sites with these characteristics.

3.3.4 The nature and distribution of stream sinks in the Pang and Lambourn

Figure 3.7 shows the distribution of the different types of sinks in the Pang and Lambourn, based upon 128 sites visited as part of this study. At 7 other sites recorded in the karst database no stream sink was identified in the field (small yellow circles on Figure 3.7). At 5 other sites there was a doline but no evidence of water flow (black circles). The 33 stream sinks not visited are included as small blue circles. The stream sinks were divided into areas based upon their geographical and topographical position.

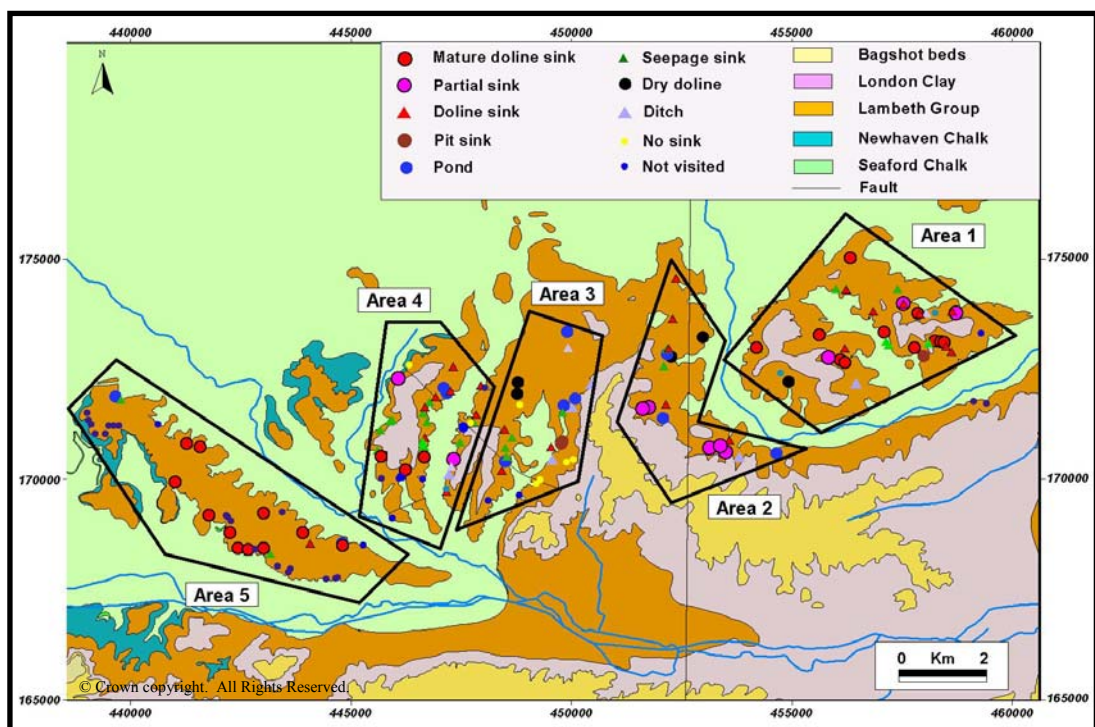


Figure 3.7: Stream sink distribution in the Pang-Lambourn catchments ^{BGS}

Area 1: Yattendon and Frilsham

This is the area north of the lower reaches of the River Pang. It consists of a plateau formed on Palaeogene strata that is divided by a 500 to 1000 m wide dry valley that has been eroded into the Chalk. To the northeast and southwest of this valley Palaeogene deposits cover high ground, and stream sinks are present along the flanks of these ridges.

This area has many well-developed stream sinks (doline sinks and mature doline sinks). The most northerly stream sink (at Yattendon) has eroded through the Palaeogene sediments to reveal a small chalk cave (Figure 3.8). The cave is ~ 30 cm wide, several metres deep and can be seen to extend eastwards for several metres. It is a narrow vadose canyon which appears to have originated on a flint layer ~ 1 m below the contact with the overlying Palaeogene sediments (Figure 3.9). Small relict sediment filled conduits occur along the flint layer (Figure 3.10). This is the only stream sink where it is possible to observe the Chalk directly, and it is possible that there may be similar features beneath the cover material at other sites.



Figure 3.8: Water in a stream sink at Yattendon disappears into a small chalk cave (photo, Paul Shand). NGR: 456372 175009

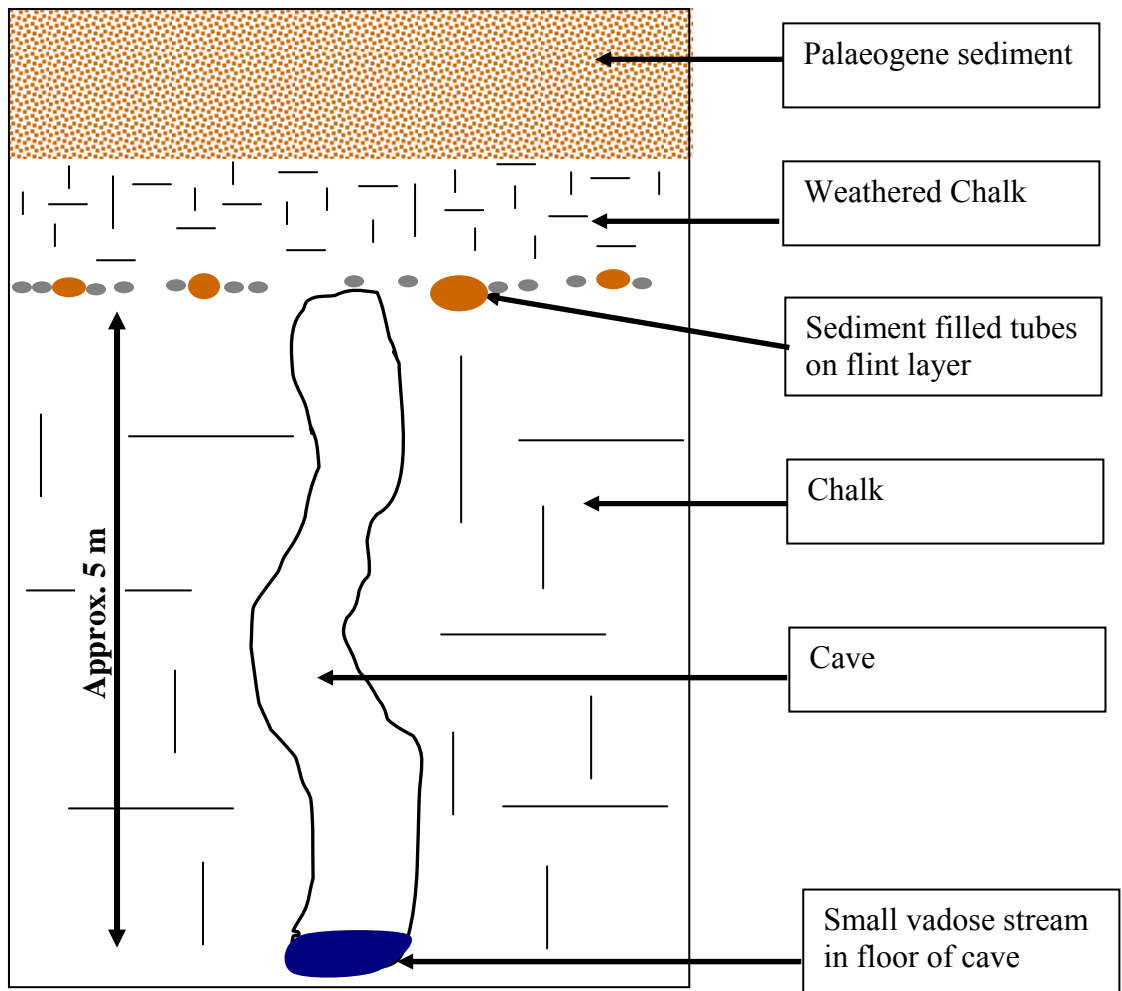


Figure 3.9: Schematic cross section of Yattendon chalk cave (not to scale)



Figure 3.10: Sediment filled tube ~ 10 cm diameter on flint layer near top of chalk, Yattendon cave (photo Paul Shand)

Area 2: Bucklebury and Hermitage

This area includes all the stream sinks along the western side of the Pang valley, although the north and south of this area have very different characteristics.

The 5 partial sinks to the southwest of the Pang provide rapid recharge ($\sim 1-4 \text{ L.s}^{-1}$) following rainfall. They are mature karst features and it is probable that they have not yet developed into mature doline sinks because they are some distance from the Chalk outcrop. Flow has been diverted away from two other sinks in the south of Area 2 (Holly Grove and Tylers Lane stream sinks). These were previously traced to the Blue Pool (Banks et al., 1995), and are discussed in Section 4.3.1. Holly Grove is recorded as a doline sink in Figure 3.7 as there may still be some flow into the doline under high flow conditions. Tylers Lane is recorded as a ditch sink as some of the water may sink through the floor of the ditch dug to divert the flow from the infilled doline sink. The north of Area 2 is considerably less karstic with no development of mature doline sinks.

Area 3: Curridge and Longlane

This area includes stream sinks on the flanks of the Palaeogene high ground that surrounds a broad chalk dry valley extending south-south-west to the River Lambourn. This is the least karstic area. Many stream sinks recorded in the karst database could not be identified or were dry dolines. Others provide small-scale slow recharge via ponds, seepage sinks and ditches. Doline sinks in this area all have small flows ($< 1 \text{ L.s}^{-1}$), even in wet periods.

Area 4: Snelsmore Common

This area includes the Palaeogene/Chalk margins to the east of the Winterbourne valley, and to the east and west of another large dry valley extending southwards to the River Lambourn. In this area there are several doline sinks and seepage sinks and two small partial sinks. Many more small seepage sinks were observed during field visits. Karst development is slight except in the far south where there are three mature doline sinks.

Area 5: Wickham Ridge

There are many mature doline sinks on both flanks of the Wickham ridge, which lies to the southwest of the River Lambourn.

In summary, the most karstic areas with the most geomorphologically significant features (mature doline sinks) are distributed in four areas: the Wickham Ridge to the southwest of the River Lambourn (Area 5), the far south of Area 4, the south of Area 2, and Area 1 to the north of the lower reaches of the River Pang.

3.3.5 Stream sink chemistry

In collaboration with the LOCAR project "Hydrogeochemical functioning of lowland permeable catchments; from process understanding to environmental management" water samples were collected from 8 stream sinks in Area 1. Chemical analysis was conducted by the BGS and data supplied by Paul Shand (personal communication, 2006). Sampling site locations are shown in Figure 3.11 and carbonate chemistry data are presented in Table 3.1. Sampling was undertaken in winter 2005, but during a dry period in which there was very little flow in the stream sinks. The samples generally had low electrical conductance, and low calcium and bicarbonate content. At all sites waters were undersaturated with respect to calcite, with saturation indices of between -0.8 and -4.8. These very low saturation indices demonstrate that Palaeogene runoff into stream sinks will have the capacity to dissolve the underlying chalk.

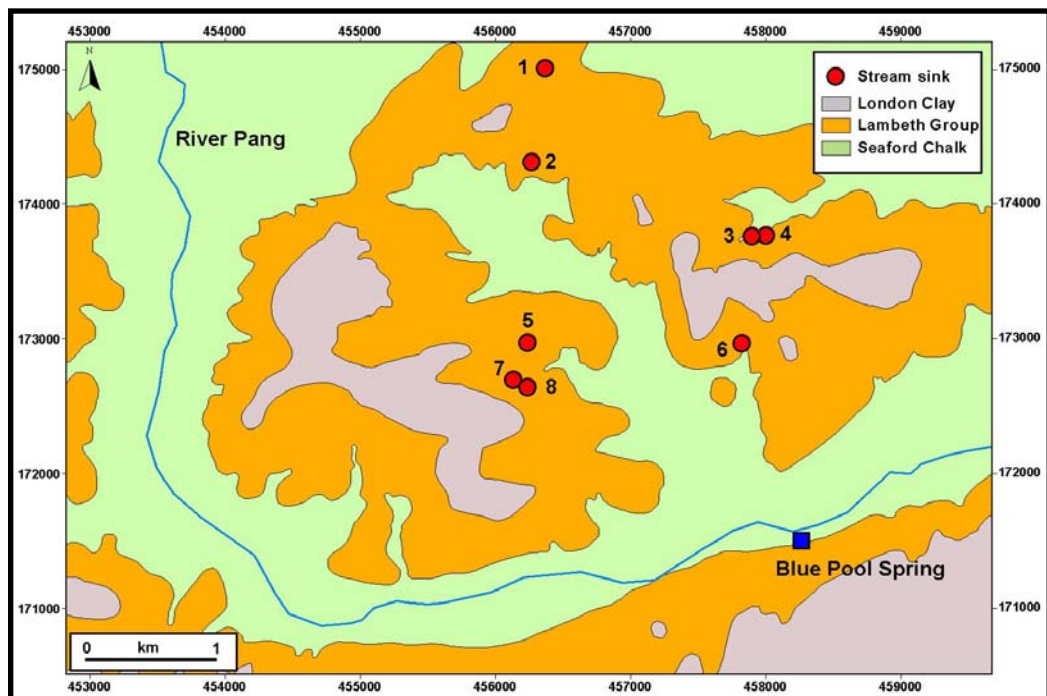


Figure 3.11: Stream sink chemistry sampling sites ^{BGS}

Table 3.1: Carbonate chemistry of stream sinks in winter 2005 (data from Paul Shand, personal communication 2006)

Sink No.	Flow (L.s ⁻¹)	Temperature (°C)	pH	Specific Conductance (µS.cm ⁻¹)	Calcium (mg.L ⁻¹)	Alkalinity as HCO ₃ (mg.L ⁻¹)	Calcite SI*
1	~ 0.2	6	6.9	225	29.6	47	-2.0
2	~ 0.02	6	7.6	577	58.1	72	-0.8
3	~ 1	6	7	173	14.3	14	-2.7
4	~ 0.05	6	6	161	12.2	<3	-4.5
5	~ 0.5	6	6.5	152	13.4	12.6	-3.3
6	~ 0.4	7	7.3	169	18.6	24	-2.1
7	~ 0.5	6	6.6	190	11.8	8.5	-3.4
8	~ 0.3	7	5.7	126	8.06	3.9	-4.8

*The calcite saturation index (SI) was calculated using an automatic calculator found at <http://www.alcochemical.com/products-markets/markets/LSI-Calculator.asp>.

3.3.6 Conclusions of stream sink survey

There are 161 stream sinks in the lower reaches of the catchments at or near the Palaeogene/Chalk contact where the Palaeogene is thin and composed of sands and gravels. Field observation of 128 sites suggests they can be divided into 6 geomorphological categories: seepage sinks, ephemeral ponds, ditch sinks, pit sinks, doline sinks and mature doline sinks. They are fed by springs in the Palaeogene, surface runoff, and land and road drainage pipes. Most stream sinks respond rapidly to rainfall and have no/little flow during dry periods. 37 have more substantial flows that, based on visual observation, were estimated to be ~ 1-4 L.s⁻¹ following rainfall. These stream sinks provide rapid recharge to the underlying chalk. Others provide smaller amounts of recharge often more slowly. Based on qualitative visual observations, a very rough estimate of the total recharge to the Chalk through the 161 stream sinks in the catchments would be ~ 15 L.s⁻¹ during dry periods and ~ 110 L.s⁻¹ in wet periods. This assumes that 30 stream sinks observed to be active during a dry period have an average flow of ~ 0.5 L.s⁻¹ and during wet periods 37 stream sinks have an average flow of ~ 2 L.s⁻¹ and the other 124 stream sinks have an average flow ~ 0.3 L.s⁻¹.

There are many other small seepage sinks around the Palaeogene margin. Field observations suggest that a significant proportion of precipitation falling on the Palaeogene recharges the Chalk aquifer. This occurs either rapidly through surface runoff to stream sinks, or more gradually via local aquifers in the more permeable

Palaeogene deposits which recharge the stream sinks via springs in the Palaeogene, or that simply recharge the Chalk through the subsurface Palaeogene/Chalk boundary.

3.4 Chalk springs

3.4.1 Introduction

Chalk springs listed in the BGS karst database, and sections of river where flow accretion was detected in current meter surveys by Grapes, Griffiths and Bricker (personal communication, 2003) were visited in summer and autumn 2003.

The field survey had three objectives:

- 1) To determine the nature of chalk springs in the catchments and assess how karstic they are.
- 2) To consider the significance of large spring inflows into the rivers compared to smaller or dispersed groundwater inputs.
- 3) To assess site conditions at the springs with a view to monitoring for tracers.

Specific electrical conductance measurements were made at a small number of springs. There appeared to be little variation between springs, with measurements ~ 550 to 600 $\mu\text{S}/\text{cm}$. More detailed investigations of longer-term variability in specific electrical conductance of spring waters were not made during this study.

3.4.2 The River Lambourn

3.4.2.1 Introduction

Table 3.2 details 18 springs in the Lambourn valley shown in Figures 3.12 and 3.13. Five of these springs (bold in Table 3.2) are large point groundwater outflows (1,6,11,15,18). Three other springs (italic in Table 3.2) are large areas of groundwater seepages that provide significant inputs to the river (4,5,14). Six are small groundwater seepages (3,8,10,13,16,17). Four springs recorded in the karst database could not be identified in the field, and may be very small seepages. (Sites 2,7,9,12).

Table 3.2: Springs visited in the Lambourn catchment, including those recorded in the BGS karst database, and new springs identified during the field survey

No.	Name	Easting	Northing	Elevation (m AOD)	Notes	Practical considerations for tracer test monitoring
1	Lynchwood	432782	179257	126	Significant ephemeral spring	Large springs and outlet channel
2	Upper Bockhampton	433012	178614	123	Not identified	
3	Lower Bockhampton	433370	178140	126	Small seepages in riverbed	Very small discharge
4	<i>East Garston</i>	<i>436429</i>	<i>176910</i>	<i>~ 116</i>	<i>Several small springs.</i>	<i>Very small discharge</i>
5	<i>Maidencourt Farm</i>	<i>437233</i>	<i>175923</i>	<i>~ 109</i>	<i>Seepages forming perennial head of River Lambourn</i>	<i>Very dispersed discharge</i>
6	Gt Shefford	438062	175592	107	Seepages over wide area combine to form stream	Dispersed discharge through dense vegetation combine to form outlet channel
7	Gt Shefford2	438705	175483	106	Not identified.	
8	Shefford House	439017	174586	103	Stream rises in grassy field in alluvium	Very small discharge
9		439378	174425	101	Drain in field, no spring.	
10		439628	173928	99	Small stream rises in undergrowth	Very small discharge
11	Weston1	439981	173969	99	Significant perennial spring	Discharge through coarse gravel in unvegetated elongated pool combines to form outlet channel
12	Weston2	440212	173798	98	Not identified.	
13	Welford	440702	173325	~ 98	Small seepages/marsh	Very small discharge
14	<i>Boxford</i>	<i>442749</i>	<i>171718</i>	<i>~ 97</i>	<i>Large marshy area</i>	<i>Very dispersed discharge</i>
15	Jannaways	444967	169761	~ 84	Significant perennial spring	Large springs and outlet channel
16		445081	169991	~ 84	Small seepages in stream bank	Very small discharge
17		445080	169884	~ 84	Small seepages in stream bank	Very small discharge
18	Bagnor	445124	169813	~ 84	Significant perennial spring	Large springs and outlet channel

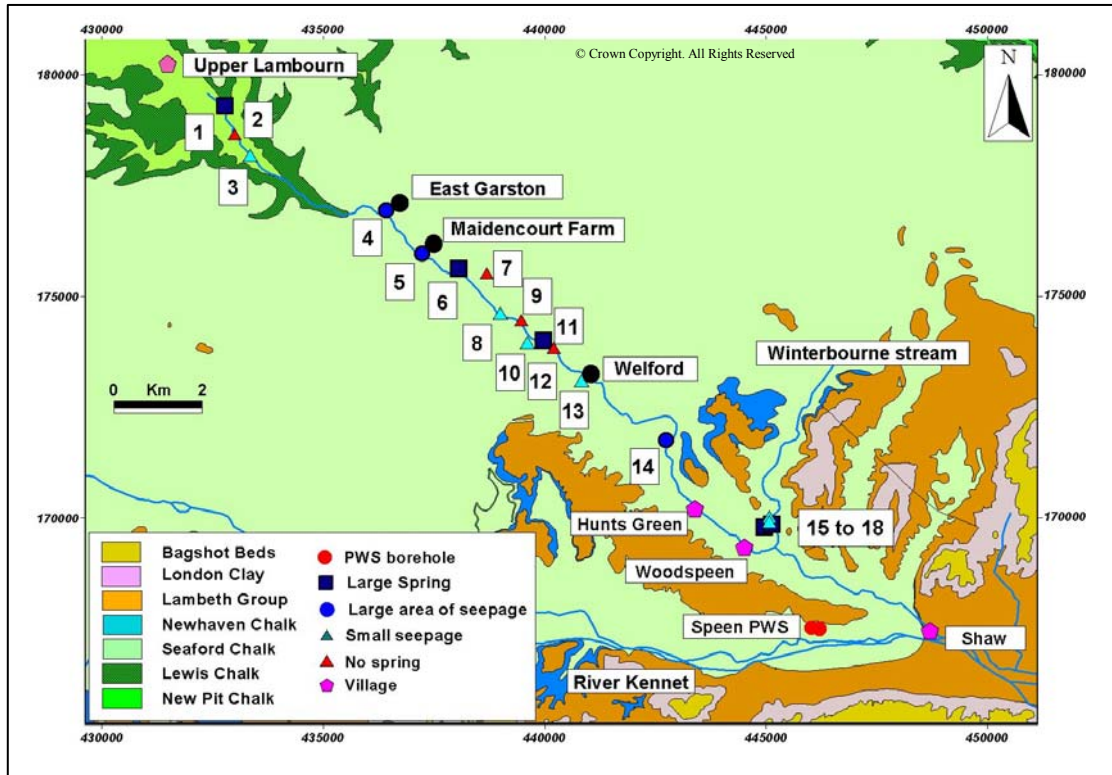


Figure 3.12: Springs in the Lambourn valley and solid geology (numbers refer to Table 3.2)^{BGS}

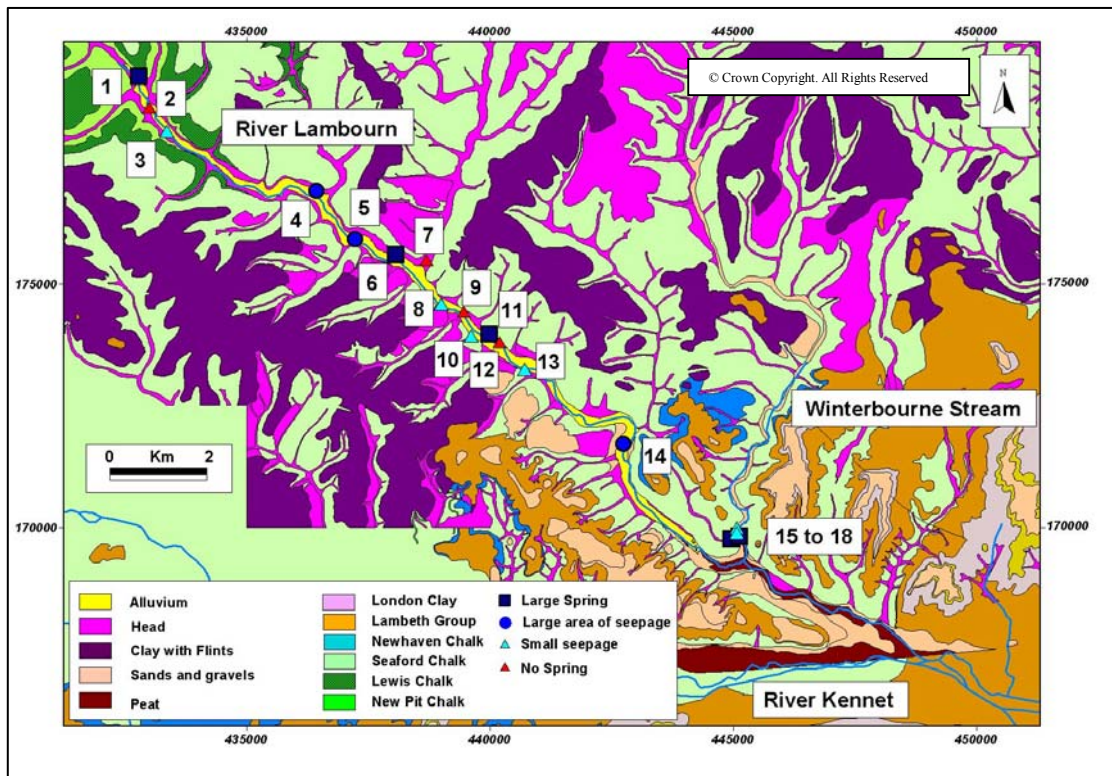


Figure 3.13: Springs in the Lambourn and drift geology (numbers refer to Table 3.2)^{BGS}

3.4.2.2 Major springs (sites 1,6,11,16,19)

Lynchwood springs (site 1) are situated within a large irregular depression. In karst geomorphological terms, they are in "zone 3" away from dolines and stream sinks (Section 3.2). Discharge from the springs occurs along a length of ~ 100 m, with several distinctive outflows both within gravel lined pools in the floor of the depression (left hand photo in Figure 3.14), and from distinctive fracture controlled horizons in the banks of the depression associated with a chalk hardground (right hand picture in Figure 3.14). The springs are located near the top of the New Pit Chalk, close to the boundary with the overlying Lewes Nodular Chalk. The hardground may be the same as that described by Aldiss et al. (2002) in the New Pit Chalk outcrop (also close to the boundary with the Lewis Nodular Chalk) on Warren Down approximately 3.5 km east of Lynchwood. The springs are ephemeral and the exact location of the outflow points varies with the conditions.

The discharge at the springs was measured on 32 occasions between November 1998 and November 2001 (Grapes et al., 2006). Flow varied between 0 and 690 L.s⁻¹ with an average of 170 L.s⁻¹. Grapes et al. (2006) found that the occurrence of flow at Lynchwood springs follows a seasonal pattern reflecting catchment groundwater levels. This suggests that the springs do not have a "karstic" flashy response to rainfall although there are no data on the short-term variability in the discharge. Turbidity has also not been measured, but there are no reports of visually turbid water at the springs following rainfall, and there are no stream sinks in the area that could be connected to these springs. On balance, the evidence suggests that Lynchwood springs are not classically karstic springs with large variable discharges and high turbidity. However, the springs are 7 km upstream of the perennial head of the River Lambourn and they do become active very rapidly. This type of river head migration to springs at specific points is characteristic of karst areas where the capacity of a conduit system is exceeded under high flow conditions resulting in re-activation of ephemeral conduits or fissures which are discharged through the ephemeral higher springs. The rapid migration of the riverhead as Lynchwood springs commence to flow, and speed at which they increase in discharge (Tim Grapes, personal communication, 2003) suggests they may be of this type.



Figure 3.14: The main pool at Lynchwood Springs (left) and an outflow point in the bank of the depression (right). Photos by George Darling.

Great Shefford spring (site 6) is a large marshy vegetated area with several small pools but it is difficult to identify specific groundwater upwellings (Figure 3.15). The combined discharge forms a stream estimated to have a flow of $\sim 20 \text{ L.s}^{-1}$ (although visits were during low flow conditions). The reach including the input from Great Shefford spring was found by Grapes et al. (2005) to have one of the highest accretion rates in the catchment (average accretion of $211 \text{ L.s}^{-1}.\text{km}^{-1}$). The spring is in "Zone 2" and discharges from the Seaford Chalk. The lack of specific upwellings may be due to the presence of head and alluvium deposits overlying the Chalk causing a dispersed outflow (Figure 3.13).



Figure 3.15: Dense vegetation at Great Shefford springs. View of small part of spring area (left) and typical small pool amongst vegetation (right)

Weston spring (site 11) forms an elongated pool along the valley floor with seepages and small upwellings through coarse gravel which combine to form a significant stream channel with an estimated flow of $\sim 20 \text{ L.s}^{-1}$ (Figure 3.16). This perennial spring is also within the Seaford Chalk in "Zone 2". The spring is on the boundary between an area of head deposits and uncovered chalk (Figure 3.13). No flow data are available for Weston springs, but flow accretion studies by Grapes et al. (2005) suggest that accretion in the reach including Weston springs is very consistent, and provides a significant contribution to the catchment discharge under low flow conditions.



Figure 3.16: Weston springs, pool (left) and outlet channel (right)

Jannaways and Bagnor springs (sites 15 and 18) are augmented by shallow boreholes drilled at the site of natural groundwater upwellings. At Jannaways the discharge from the main spring flows through a series of landscaped pools, whilst at Bagnor pools were constructed for watercress production. Natural upwellings are visible within the pools at both sites (Figure 3.17). Adjacent to Bagnor springs, there is also an area of small groundwater seepages along the western bank of the Winterbourne Stream (sites 16 and 17 in Table 3.2).

Jannaways and Bagnor springs are in the Seaford Chalk in the "Zone 1" karst area where adjacent high ground is drained by stream sinks on the overlying Palaeogene deposits. Jannaways springs are at the boundary between head deposits and uncovered chalk. Bagnor springs are mapped as being on peat and sand and gravel drift deposits (Figure 3.13). The surrounding area has a mature carr vegetation, typical of groundwater fed marsh (shown in Figure 3.17).

A rough estimate of flow in the outlet channels is $\sim 15 \text{ L.s}^{-1}$ at each spring, although additional water from Jannaways springs is used for domestic supply. Bagnor springs were observed to have high turbidity and increased flow following a thunderstorm in Summer 2004 suggesting the springs may have a karst component and be connected to stream sinks. Jannaways springs were not turbid.



Figure 3.17: Jannaways (left) and Bagnor (right) springs

3.4.2.3 Smaller springs and groundwater seepages

Several small springs in East Garston (site 4) were identified by Tim Grapes (personal communication, 2003). He found that one spring flowed when the River Lambourn was dry upstream and downstream implying that water from the spring sinks in the riverbed under some flow conditions. Local villagers reported that the spring usually dries up during the summer and reactivates in December/January. East Garston is near the base of the Seaford Chalk in "Zone 3". The Chalk is overlain by head and alluvium drift deposits. There are no discharge measurements. During field visits the flow was $< 2 \text{ L.s}^{-1}$ although there were many other small areas of groundwater seepage in the vicinity.

Maidencourt Farm (site 5) is the normal perennial head of the River Lambourn. During a summer field visit groundwater seepages were observed to occur over a length of $\sim 800 \text{ m}$, with no distinctive upwellings (Figure 3.18). Maidencourt Farm is on the Seaford Chalk, roughly at the boundary between "Zones 1 and 2". The Chalk is overlain by head and alluvium drift deposits (Figure 3.13).



Figure 3.18: Seepage at Maidencourt Farm, the perennial head of the River Lambourn

At Boxford (site 13) field visits failed to find specific groundwater upwellings although there is a large marshy area where groundwater seepages occur. It is difficult to estimate the volume of groundwater inflow at this site because it occurs over a very wide area and there is no outlet channel. Boxford is on the Seaford Chalk in "Zone 1". The Chalk is overlain by alluvium (Figure 3.13).

Small groundwater seepages were observed at 6 other sites (3,8,10,13,16,17), mostly associated with marshy vegetation.

3.4.2.4 The lower reaches of the River Lambourn

Despite high accretion in the lower reaches of the River Lambourn (Section 2.7), no evidence of natural springs was found in the literature, on historic maps, from discussions with local people involved in managing the river, or during two field visits. It is possible that there are groundwater seepages through the riverbed that could not be observed directly.

3.4.2.5 Summary of groundwater inputs to the River Lambourn.

On the basis of accretion of discharge (Section 2.7) and the characteristics of springs present, the River Lambourn can be divided into five sections, as follows:

1) Upper Lambourn to Maidencourt Farm.

High ephemeral accretion dominated by discharge from Lynchwood springs (site 1).

2) Maidencourt Farm to Welford

High perennial accretion includes inputs from large groundwater seepages at Maidencourt Farm (site 5), springs at Weston (site 6) and Great Shefford (site 11), and seepages at Welford (site 13).

3) Welford to Hunts Green

Relatively low accretion. The only observed groundwater inputs are the groundwater seepages at Boxford (site 14).

4) Hunts Green to Woodspeen

No groundwater inputs have been observed in this section, and Grapes et al. (2005) report that there is on average flow loss of 19 L.s^{-1} from the river to groundwater.

5) Woodspeen to Shaw

High accretion dominated by the input from the Winterbourne stream (which has a large groundwater component) and influenced by runoff in the urban areas of Shaw and Newbury.

The major springs identified at Lynchwood, Great Shefford, Weston, Jannaways and Bagnor all occur within reaches with high accretion (Grapes et al. 2005; Griffiths et al., 2006). However the flow from the springs is much smaller than the amount of accretion, and small springs within the riverbed and more diffuse groundwater seepages must provide a very large proportion of the flow in the River Lambourn. It is possible that small, dispersed groundwater outflows occur where diffuse flow within the chalk fracture network comes to the surface over wide areas. Alternatively, head and alluvium drift deposits flooring the river valley may cause dispersion of water

discharged through more significant chalk fissures. The large focused springs generally occur where head and alluvium are absent or at the edge of head deposits.

3.4.3 The River Pang

3.4.3.1 Introduction

Fifteen springs are recorded in the Pang catchment (Table 3.3, Figure 3.19). Of these only four (9,10,12,13) were observed to provide substantial discharges during field visits (bold in Table 3.3). Seven sites (1,3,4,5,11,14,15) are small groundwater seepages (italic in Table 3.3). At four sites recorded in the karst database no springs were found (2,6,7,8).

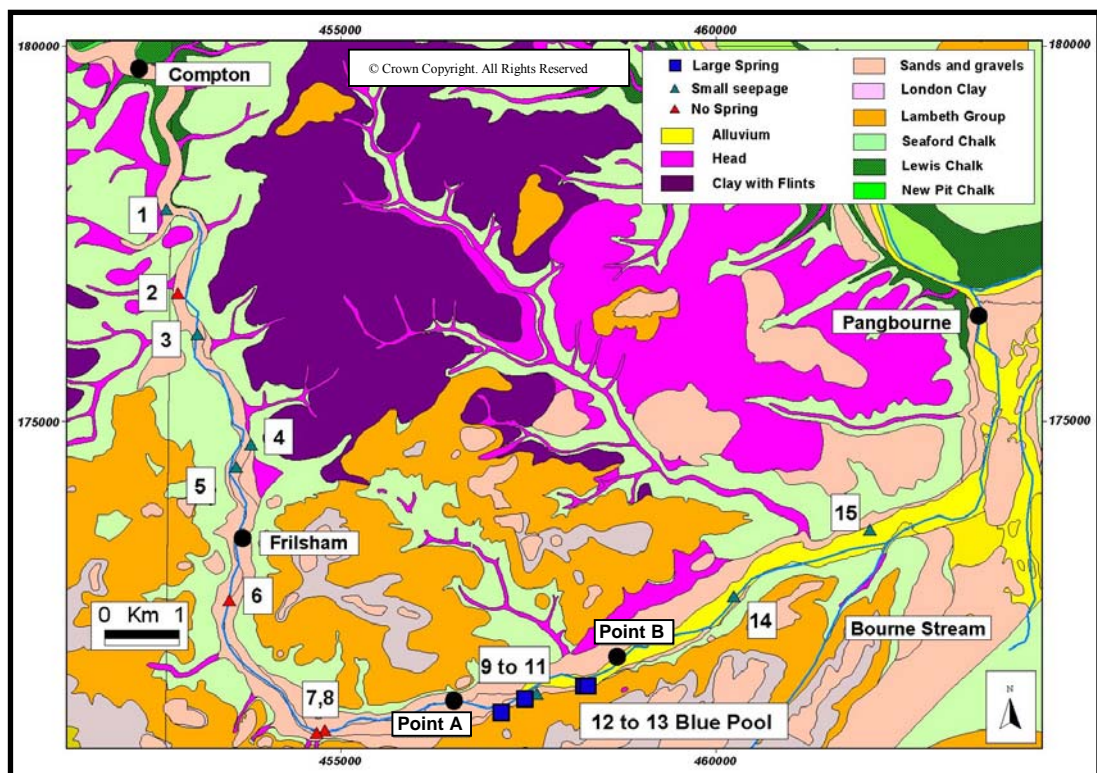


Figure 3.19: Springs in the Pang valley and solid and drift geology

Table 3.3: Springs visited in the Pang, including those recorded in the BGS karst database, and new springs identified during the field survey

No.	Name	Easting	Northing	Elevation	Notes	Practical considerations for tracer test monitoring
1	<i>Floodcross cottage</i>	452688	177831	90	<i>Many seepages in Hampstead Norreys village.</i>	<i>Very small discharge</i>
2	Touchend Pond	452837	176710	84	Not Identified.	
3	<i>Manor Farm</i>	453106	176166	~ 83	<i>Pool</i>	<i>Very small discharge</i>
4		453815	174695	~ 80	<i>Very small seepage through gravel to form pond</i>	<i>Very small discharge</i>
5	<i>Everington</i>	453616	174400	78	<i>Possible dispersed input, standing water in field, no significant spring</i>	<i>Very small and dispersed discharge</i>
6		453522	172620	~ 77	Many land drains in this area but no springs.	<i>Very small and dispersed discharge</i>
7	Bucklebury	454797	170890		Not identified	
8		454689	170855		Not identified.	
9	Ingle	457141	171125	~ 60	Significant perennial spring	Large springs and outlet channel
10	Jewells	457460	171304	~ 62	Significant perennial spring	Large springs and outlet channel
11	<i>Spring cottage</i>	457624	171381		<i>Small spring</i>	<i>Small spring and outlet channel</i>
12	Kimber	458244	171480	~ 58	Significant perennial spring	Large springs
13	Blue Pool	458297	171480	~ 58	Significant perennial spring	Large springs and outlet channel
14	<i>St Andrews Well</i>	460243	172681	~ 54	<i>Groundwater seepage in this area.</i>	<i>Very small and dispersed discharge</i>
15	<i>Maidenhatch Farm</i>	462060	173563	~ 48	<i>Groundwater seepage in this area.</i>	<i>Very small and dispersed discharge</i>

3.4.3.2 Major Springs

At Ingle spring (site 9) groundwater bubbles up through coarse sand deposits within a shallow well and flows into a large pool (Figure 3.20), the floor of which has several other upwellings. The pool feeds an outlet channel that had a gauged flow of 30 L.s^{-1} on 07/02/05. Jewells spring (site 10) rises in coarse gravel deposits forming a substantial stream channel (Figure 3.21) with inflows over approximately 15 m. Flow was gauged at 20 L.s^{-1} on 03/02/05. Flow gauging at both these sites was during a winter of low groundwater levels. At Spring Cottage (site 11), a small pool with groundwater upwellings feeds a very small stream (estimated flow $< 1\text{-}2 \text{ L.s}^{-1}$).

These springs are situated on sand and gravel river terrace deposits overlying Palaeogene Lambeth Group deposits, but at the boundary with the underlying Seaford Chalk. They were not observed to become turbid following rainfall. There are no data on the variability of discharge, but there is some evidence that the flow is fairly consistent. Local residents have not observed cessation of flow, and increases in discharge following rainfall events were not visible during many winter field visits to these springs between 2003 and 2006.



Figure 3.20: Ingle spring



Figure 3.21: Jewells Spring

The Blue Pool spring complex (sites 12 to 13) is the major source of groundwater to the River Pang with a discharge of $\sim 200 \text{ L.s}^{-1}$. Most discharge occurs in the main pool (Figure 3.22), which is several metres deep. Groundwater bubbles up through sand and silt flooring the pool. There are several distinctive upwellings within the main pool and within several other pools in a complex of pools and marshy ground which extends laterally over $\sim 100 \text{ m}$. Kimber spring (site 12) is the most westerly spring at the upstream limit of the complex (Figure 3.23), and groundwater flows from two localised

upwellings on the floor of this pool strongly enough to suspend coarse sand particles. The springs combine to form a substantial stream (Figure 3.24). The Blue Pool springs are on the boundary between Alluvium and River Terrace gravels overlying the Palaeogene/Seaford Chalk margin. The Blue Pool becomes turbid approximately 24 hours after heavy rainfall, reflecting its proved connectivity with stream sinks in the area. Tracer testing in 1988 demonstrated rapid groundwater flow (5.8 km.d^{-1} based on time to peak tracer concentration) from stream sinks 4.7 km west of the Blue Pool (Banks et al., 1995) and this work is discussed in Section 4.3.1.

Although there are no detailed hydrograph data for the Blue Pool to determine spring response to precipitation, flow data were collected on 15 occasions between 1976 and 1988 (Figure 3.25, Banks personal communication, 2005). Discharge varied between 150 L.s^{-1} (05/08/76) and 240 L.s^{-1} (07/01/83). The flow of 150 L.s^{-1} was during the severe summer drought of 1976 and the data suggest that the Blue Pool generally maintains a flow of $150\text{-}200 \text{ L.s}^{-1}$ during summer. The contrast between flow in summer and autumn (times of generally low groundwater level) and winter and spring (when groundwater levels are generally high) is quite small, about $200\text{-}250 \text{ L.s}^{-1}$ in winter and spring compared with $150\text{-}220 \text{ L.s}^{-1}$ in summer and autumn. These limited data suggest that the Blue Pool has a large baseflow, and that the proportion of flow derived from recharge through stream sinks may be quite small.

Figure 3.25 also illustrates the flow in the River Pang downstream of Jewells Farm (upstream of the Blue Pool springs). This has a much more variable flow than the Blue Pool discharge. This may be due to greater seasonal variability in groundwater outflows discharging into the Upper Pang, but it also suggests that surface runoff and drainage may be significant.



Figure 3.22: The Blue Pool



Figure 3.23: Kimber spring



Figure 3.24: The Blue Pool outlet channel

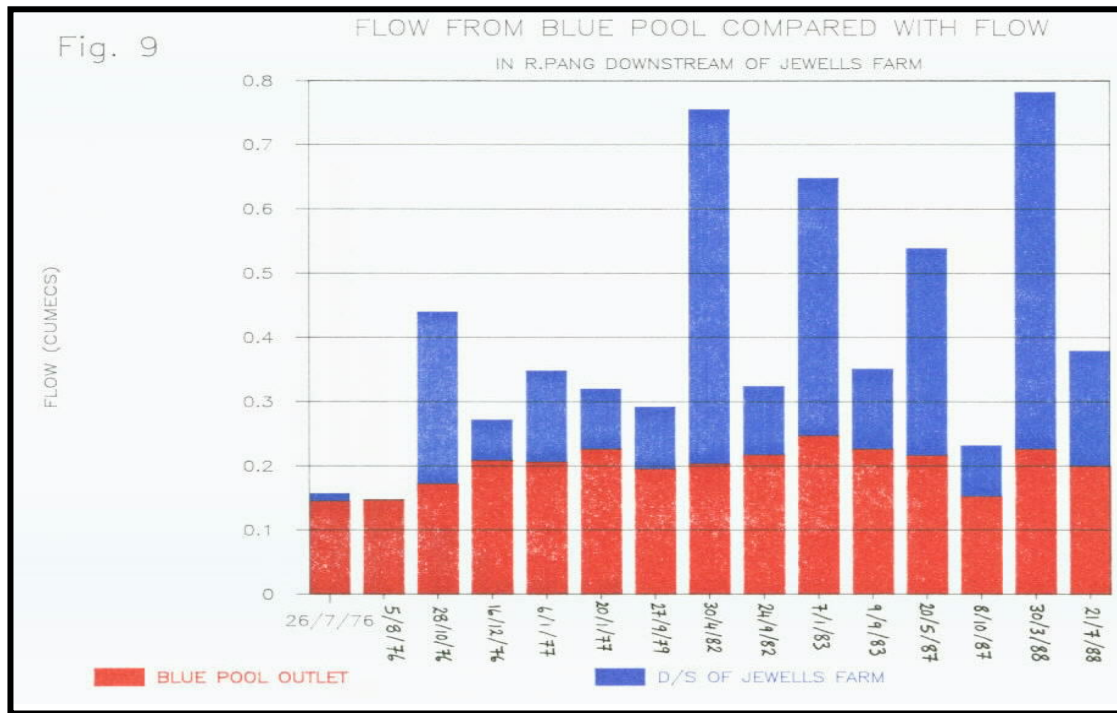


Figure 3.25: Flow data for the Blue Pool (red bars) and the River Pang upstream of the Blue Pool between 1976 and 1988 (blue bars) (Banks, personal communication, 2005). The tops of the blue bars represent the total flow of the River Pang downstream of the Blue Pool.

3.4.3.3 Summary of groundwater inputs to the River Pang

On the basis of flow accretion studies (Section 2.7), and the characteristics of springs, the River Pang can be divided into four sections:

1) The upper reaches between Compton and Frilsham

Many dispersed groundwater inputs contribute to the flow, which predominantly reflects seasonal fluctuations in groundwater levels. The sewage treatment works at Compton provides a small additional discharge that can artificially sustain flow over this reach in summer. This section of the Pang has been affected by groundwater abstraction, and before this there was substantially more flow in the upper reaches of the river (Halcrow, 1987). Halcrow (1987) also describe Manor Farm spring (site 3 on Figure 3.19) prior to the impacts of abstraction when it provided a substantial point input to the Pang. Although abstraction has ceased at the nearest abstraction borehole at Compton (Section 2.8.4), there was almost no flow at Manor Farm spring during field

visits in winter and spring 2004/2005. Flow was observed in winter 2008 (Melinda Lewis, personal communication, 2008).

2) The reach from Frilsham to point A on Figure 3.19

This section of the Pang does not appear to have any significant groundwater inputs. It was observed by Bricker (2004) and Griffiths et al. (2006) to lose water during low flow conditions. It is possible that this section loses flow even under high flow conditions but that accretion from surface runoff is greater than the loss. Several surface drains and ditches have been observed along this section (which also receives the outflow from the Briff Lane Sewage Treatment Works).

3) The area of major springs (sites 9-13 on Figure 3.19)

This is the main area of groundwater inflow to the Pang, and is characterised by large point inputs at distinctive springs (the Blue Pool, Kimber, Ingle, Jewells and Spring Cottage). These springs together contribute a large proportion of the total discharge of the Pang. In low flow conditions they contribute almost all the flow.

4) Point B to Pangbourne on Figure 3.19

Downstream of the Blue Pool there are no major springs discharging into the river although there are some dispersed groundwater seepages in the area around Bradfield and Maidenhatch Farm (sites 14 and 15 on Figure 3.19). At Maidenhatch Farm there is an extensive marshy area including a pond that may be groundwater fed. Very small patches of clean sand were visible amongst the fine brown sediment that flooded the pond. However there was no discernible outlet channel. It is possible that this was a larger spring that has been affected by abstraction at Bradfield and Pangbourne. Much of the accretion in this reach may be from surface flows from the Bourne tributary stream (which crosses the London Clay to the south of the Pang valley) and from surface runoff in the urban area around Pangbourne.

3.4.4 Springs outside the Pang-Lambourn topographic catchments

A spring and cress beds are recorded on historical maps of the River Kennet ~ 1km downstream of the confluence with the Lambourn at Shaw (Figure 3.26). These were visited on 12th March 2004 to determine if they might be potential outlets for stream sinks on Snelsmore Common or the Wickham Ridge (Figure 3.26). The spring is a

small groundwater seepage with little flow ($< 1 \text{ L.s}^{-1}$) at the time of the field visit. The site of the cress beds is a clear pool floored by dark sediment and lighter patches which may indicate groundwater upwellings. There is a channel which could not be directly accessed but which could be an outlet for groundwater discharging into the pool. The former cress beds are on Palaeogene deposits approximately 1.5 km from the boundary with the Seaford Chalk.

There are no springs recorded along the section of the River Thames east of the Pang topographic catchment (Figure 2.1). However it is possible that springs discharge through the riverbed and are not visible due to the large discharge in the river.

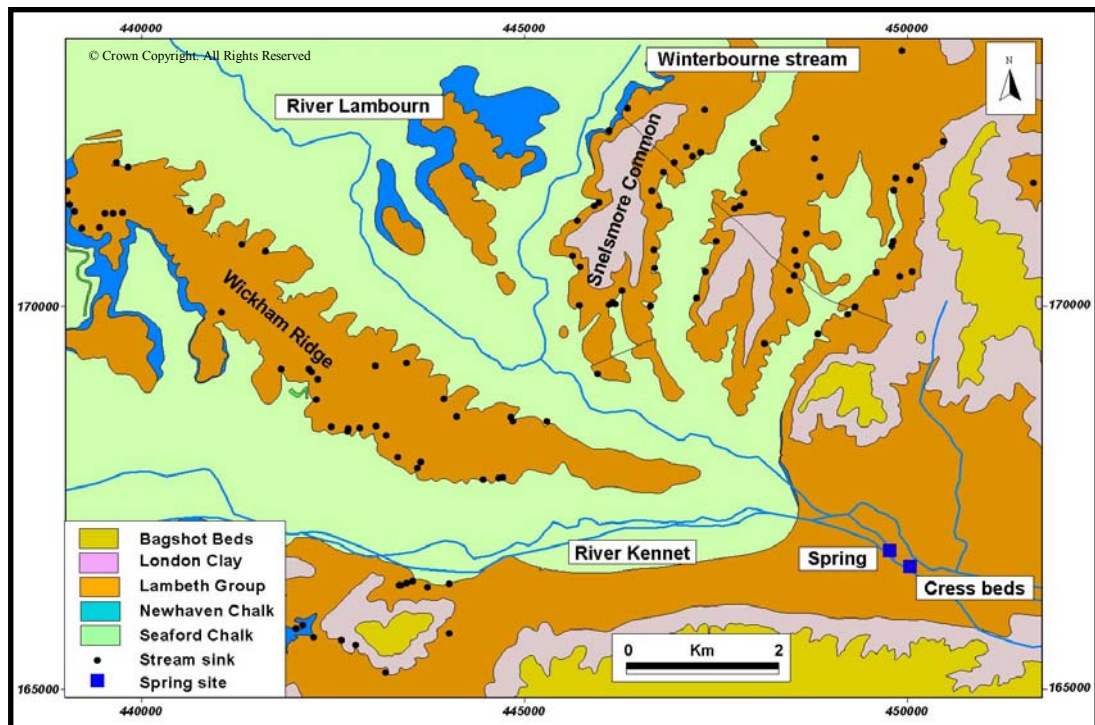


Figure 3.26: Spring and former cress beds on the River Kennet ~ 1 km downstream of the confluence with the River Lambourn

3.4.5 Spring catchment sizes

Table 3.4 shows the calculated catchment sizes of springs in the Pang and Lambourn catchments based upon the spring discharge and the estimated minimum and maximum recharge rates of 0.3, and 1.2 mm.d^{-1} from previous studies in the catchments (Section 2.8.2), and the average recharge rate of 0.5 mm.d^{-1} recently calculated using the BGS distributed recharge model for the Pang and Lambourn catchments (Chris Jackson,

personal communication, 2006, Section 2.8.2). There are no flow data for Weston, Great Shefford, Jannaways and Bagnor springs. At these sites a very rough estimate of flow based on visual observation is used to calculate the spring catchment area, whilst at other sites the average measured flow is used.

If the catchment area of the Blue Pool were 58 km² it would comprise about 33 % of the topographical catchment area of the River Pang. The discharge at the Blue Pool represents about 31 % of the average overall catchment discharge and therefore the upper estimate of a 58 km² catchment area could be accommodated within the Pang topographic catchment. This calculation cannot be performed for Lynchwood springs because they are ephemeral.

Table 3.4: Calculated catchment sizes for major springs

Site	Spring discharge* (L.s ⁻¹)	Catchment (km ²) (1.2 mm.d ⁻¹ recharge)	Catchment (km ²) (0.5 mm.d ⁻¹ recharge)	Catchment (km ²) (0.3 mm.d ⁻¹ recharge)
Blue Pool (Pang)	200	14	35	58
Lynch Wood (Lambourn)	170	12	29	49
Ingle (Pang)	30	2.2	5.2	8.6
Weston/Gt Shefford (Lambourn)/ Jewells (Pang)	20	1.4	3.5	5.8
Bagnor/Jannaways (Lambourn)	15	1.1	2.6	4.3

* Average discharge where flow data are available, estimate based on field observation at other sites

3.4.6 Conclusions of chalk spring survey

Major perennial springs contribute around 40 % of the average discharge in the Pang, whilst in the Lambourn major springs account for only around 15 % of the average discharge. Most of the spring input to the River Lambourn is from ephemeral springs at Lynchwood; therefore almost all the perennial flow is maintained by diffuse and dispersed groundwater inputs to the river. Head and alluvium drift deposits overlying the Chalk in the Lambourn could be the cause of this type of groundwater discharge as outflows from fissures in the Chalk are likely to be dispersed over wide areas as they pass through the drift deposits.

The chalk springs in the catchments provide point inputs to the rivers suggesting flow may be through fissures and small conduits. However, at most sites there is little evidence of strong karst development. At Lynchwood and the Blue Pool the volume of discharge is high ($\sim 200 \text{ L.s}^{-1}$). At the Blue Pool and Bagnor, the springs are characterised by turbidity following rainfall suggesting they are connected to karst stream sinks. Flow data are too infrequent to assess short-term variability in discharge, but field observations and limited flow data for the Blue Pool suggest that despite having turbidity following rainfall, the springs have a high baseflow component.

3.5 Dolines

Dolines in the catchments are up to 10 m deep and between about 1 and 30 m in diameter. Figure 3.27 shows an example of one of the larger dolines in the Lambourn catchment. Many hundreds of dolines are recorded in Zones 1 and 2 where the Chalk is overlain by the Lambeth Group or Clay-with-Flints (Figure 3.1, 3.28). All pits and depressions were included in the BGS karst database, and some of the features may be manmade pits rather than natural karst features. As discussed in Section 1.5.3, the majority of natural dolines are likely to be subsidence dolines formed by suffosion. Most dolines are on high ground between valleys, but a few are within dry valley features suggesting that they may be relict stream sinks.



Figure 3.27: Doline in the Lambourn catchment, $\sim 2 \text{ m}$ deep and $\sim 20 \text{ m}$ diameter

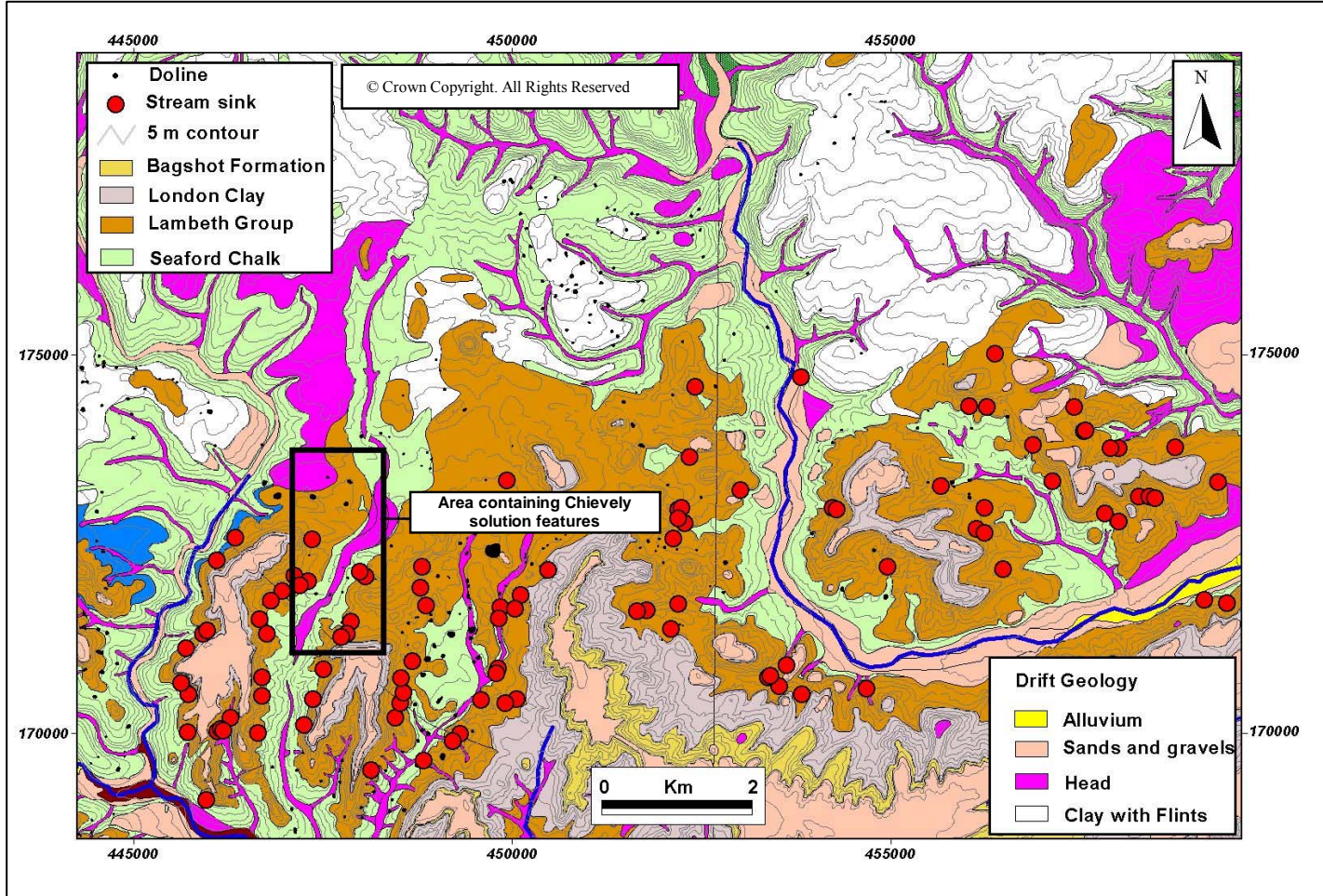


Figure 3.28: Dolines and geology

3.6 Chieveley solution features

During road construction at Chieveley, a large number of subsurface dissolution features were encountered (Jim Gelder, Mott Macdonald, personal communication, 2006). The Chieveley site extends over a large area (approximately outlined on Figure 3.28), which encompasses a northeast southwest orientated dual carriageway and several large roundabouts and slip roads which link into the existing infrastructure. Over much of the site a thin layer of Lambeth Group deposits overly the Chalk, and the site is in karst Zone 1 where many dolines and stream sinks are present. Mott Macdonald (2005) suggest that there are four different types of features, which they categorised as typical solution features, cavity features, deep features and valley features.

Most features encountered were "typical solution features" (Figure 3.29), which Mott Macdonald (2005) describe as steep-sided sediment filled voids 5 to 8 m deep and bounded by chalk in an undisturbed but sometimes weathered state. The infill was a mixture of granular and cohesive material from the Lambeth Group deposits, which had slumped into cavities in the underlying chalk. The infill had a high clay content relative to granular material suggesting that these features may have fairly low permeability. Similar dissolution features are frequently observed in the UK in areas where the Chalk is overlain by a thin Palaeogene cover (Section 1.5.4).



Figure 3.29: "Typical solution feature" at Chieveley, (Mott Macdonald, 2005)

A small number of open cavities were encountered (Figure 3.30). These were 10 to 80 cm in diameter and up to 3.8 m deep (Mott Macdonald, 2005). The cavities were found in one area of the site where there was a continuous flint band very close to the ground surface. They appear to have been formed by focused lateral flow along the impermeable flint layer, which was occasionally penetrated resulting in dissolution of the chalk underneath (Mott Macdonald, 2005). It is not clear how these features connect to the fracture/fissure network in the deep unsaturated zone or below the watertable, or if they are hydrologically active at the present time. It is possible that they were created by small quantities of water running down the sides of the feature in a similar manner to the formation of some types of cave shafts known as “dome pits” (Brucker, Hess and White, 1972; Klimchouk, 2000). In such cases the drain at the base of the shaft often has a much smaller cross sectional area than the shaft (Brucker, Hess and White, 1972). By analogy, the water in the chalk examples may therefore drain away through a relatively small fracture/fissure at the base of the void. It is possible that it is this type of feature that provides the initial drainage through the chalk unsaturated zone beneath stream sinks.

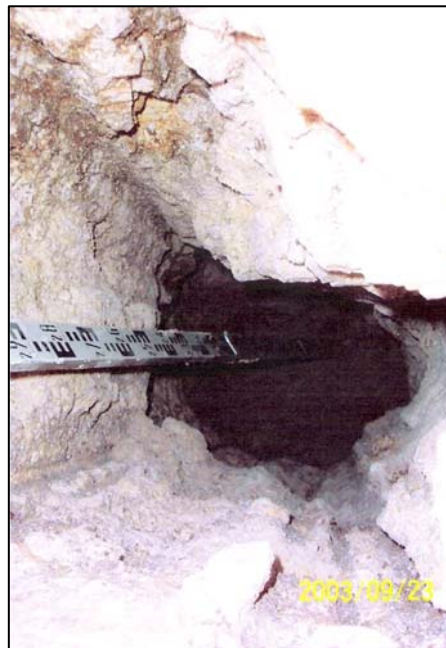


Figure 3.30: Vertical open cavity at Chieveley (Mott Macdonald, 2005)

“Deep features” were not actually observed but at one bridge site during piling there were large grout takes indicating dissolution of the chalk at depth. This occurred over a wide depth range but no large voids were encountered suggesting that it was caused by

the presence of fissures, possibly in the zone of water table fluctuation (Mott Macdonald, 2005).

"Valley solution features" are wider areas of deposits (up to 75 m wide) derived from the Lambeth Group, which extend up to 11 m vertically downwards into the chalk. They are found along the axes of dry valleys. It is thought that they form by a combination of periglacial processes and dissolution (Mott Macdonald, 2005). Mott Macdonald (2005) describe the infill material as including coarse rounded flint gravel deposits and material with a strong subhorizontal fabric and suggest these deposits have been transported some distance by periglacial processes. Clays at the margins of valley features are similar to those found in "typical solution features" suggesting that dissolutional processes have also occurred.

3.7 Relic conduits in zone 1

There is a good exposure of the Lambeth Group-Chalk contact in a quarry in the Pang at NGR 458839 172659 (Figure 3.31). There are seven small conduits within the Chalk ~ 1 m below the Lambeth Group (Figure 3.32). The conduits are about 10-15 cm in diameter, and one of them contains a thin layer of sediment lining the walls (Figure 3.32a). These conduits are currently hydrologically inactive. The conduits are in a similar position with respect to the Lambeth Group as the sediment filled conduits observed at the Yattendon cave stream sink (Figure 3.9).



Figure 3.31: Exposure of the Palaeogene-Chalk contact in a quarry in Zone 1

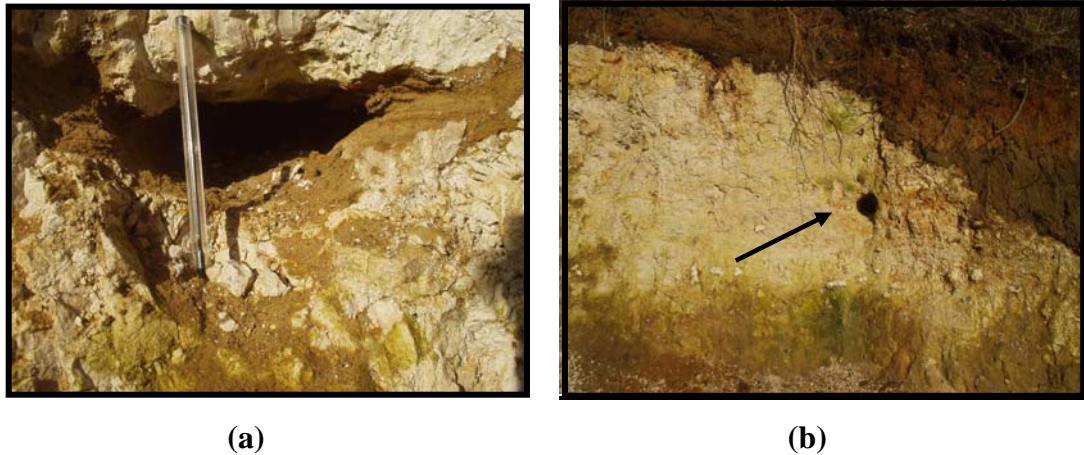


Figure 3.32: Small relic conduits exposed in the quarry, pen in (a) is 14 cm long, conduit in (b) ~ 15 cm diameter.

3.8 Surface karst and groundwater flow

It is clear that in areas of the Pang and Lambourn catchments where the Chalk is overlain by thin Palaeogene deposits dissolution processes are extremely common resulting in high densities of dolines and large, subsurface, sediment-filled dissolution features. The presence of many stream sinks located along the Palaeogene margin suggests that under current hydrological conditions groundwater recharge along fissures and small conduits may also be relatively common in the Zone 1 chalk. Previous tracer testing from two stream sinks in this zone (Banks et al., 1995) indicate very rapid flow (5.8 km.d^{-1} based on the time to peak tracer concentration) to a large regional spring, the Blue Pool, implying that fissures or conduits exist along the whole connecting pathway. It is unclear whether all stream sinks are similarly connected to springs via conduit like pathways, or whether some feed into the regional groundwater body of the Chalk, via smaller fissures and fractures. The tracer testing described in Chapters 4 and 5 was designed to investigate this question, and its implications for contaminant transport and attenuation.

It is much more difficult to investigate the frequency and distribution of fissures and conduits in Zones 2 and 3, because of the lack of stream sinks to provide injection points directly into conduits. There is some evidence that dissolutional voids are important in areas away from the Palaeogene cover. In Zone 2 the occurrence of

dolines suggests that dissolution of the underlying chalk is occurring or has occurred in the past. High transmissivity in the Chalk is thought to be caused by solutional enlargement of fractures (Price, 1987; Macdonald and Allen, 2001), and there is evidence of high transmissivity in Zones 2 and 3 (Figure 3.33). Pumping tests in 18 boreholes in Zones 2 and 3 demonstrated high transmissivity ($> 1200 \text{ m}^2 \cdot \text{d}^{-1}$). The occurrence of major springs (Section 3.4) and abstraction boreholes (Section 2.8.4) in Zones 2 and 3 also suggests high transmissivity associated with flow through fissures. In this study Single Borehole Dilution Tests (SBDTs) in all Zones were used to investigate the spatial distribution of rapid flow and at some sites borehole imaging data were used to determine whether flow horizons identified from SBDTs are associated with dissolutional fissures and conduits (Chapter 6).

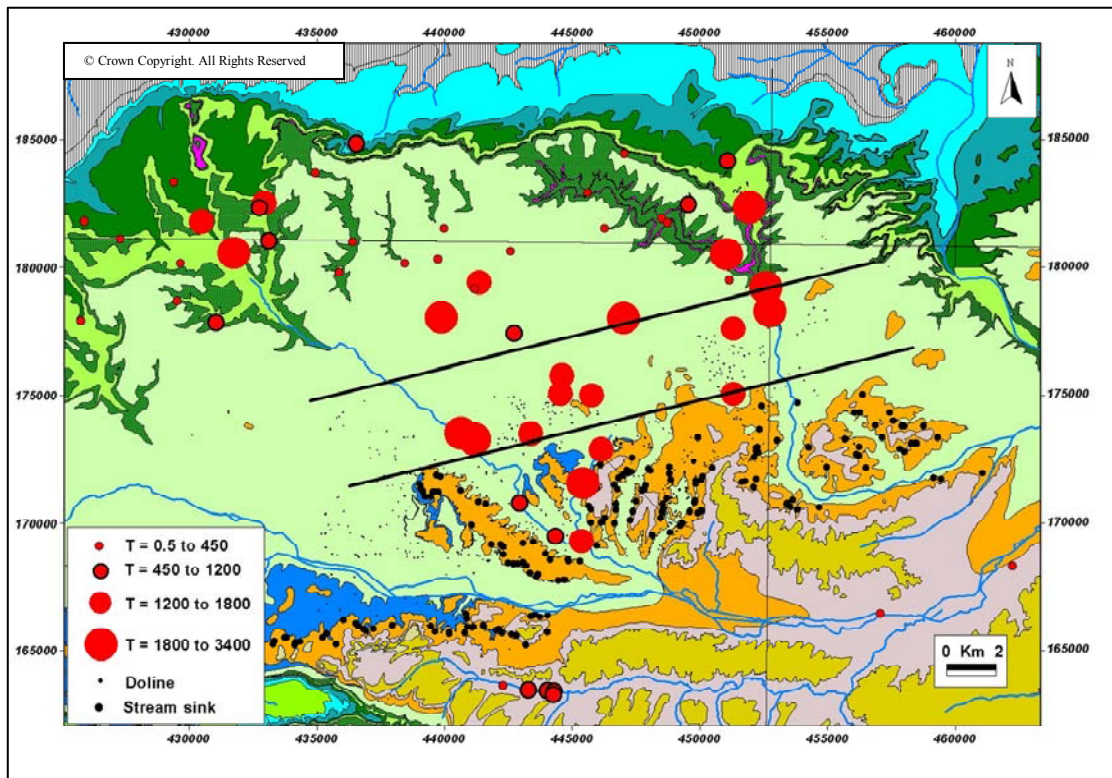


Figure 3.33: Relationship between transmissivity ($\text{m}^2 \cdot \text{d}^{-1}$) and surface karst in the Pang and Lambourn catchments (geology key as for Figure 2.2)^{BGS}

Chapter 4: Investigations of groundwater flowpaths using catchment scale tracer tests

4.1 Introduction

This chapter details qualitative tracer tests undertaken in the Pang and Lambourn catchments to establish groundwater flowpaths. Specifically the aims of the tests were to provide evidence that would help to delineate the catchments of the major springs, to assess the contribution of karstic stream sinks to the springs, and to investigate whether there is connectivity between stream sinks and boreholes and/or smaller groundwater inflows into riverbeds. Similar stream sinks that had been previously tested in the Chalk (reviewed in Section 1.3.5) demonstrated rapid groundwater flow and low attenuation of tracer. A survey of surface karst features in the Pang and Lambourn catchments undertaken as part of the current study (Chapter 3) found a large number of sinking streams on Palaeogene deposits close to the boundary with the Chalk (Figure 3.1). The tracer tests also aimed to investigate whether rapid groundwater flow associated with low attenuation is likely to be common to all stream sinks.

Tracer experiments were designed to investigate the catchments of major springs in the lower reaches of the Pang and Lambourn valleys (Zone 1), where Palaeogene deposits cover adjacent high ground. Much work centred on the Blue Pool spring, which with a discharge of $\sim 200 \text{ L.s}^{-1}$ is substantially larger than any other springs in Zone 1. Previous tracer testing by Banks et al. (1995) from Holly Grove (Figure 4.1) and nearby Tylers Lane stream sinks proved that the catchment of the Blue Pool extends 4.7 km to the west, and this work is reviewed in Section 4.3.1. Tylers Lane stream sink is only about **? m north** of Holly Grove stream sink and for visual clarity is not included in Figure 4.1. These tracer tests could not be repeated because water was diverted away from the stream sinks following the previous tracer tests.

In the current study, to increase the chances of obtaining a positive result, only stream sinks with larger flows following rainfall ($\sim 2\text{-}4 \text{ L.s}^{-1}$) in which water was observed to drain freely through a distinctive hole in the ground were used. The surface karst survey indicated that this occurs at 37 sites (Section 3.3.6). Five of these were selected as injection sites (Figure 4.1). Tracer testing from Smithcroft Copse stream sink

(Section 4.3.2) aimed to determine whether this area is connected to other springs (Ingle and Jewells) in addition to the Blue Pool. Because Smithcroft Copse is near to Holly Grove stream sink which was tested by Banks et al. (1995), it was anticipated that tracer from Smithcroft Copse stream sink would also be discharged at the Blue Pool. Therefore a quantitative test was carried out and breakthrough curves and tracer recoveries are discussed further in Chapter 5 (which also details a second experiment from Smithcroft Copse using 5 tracers to investigate contaminant attenuation processes).

Other tracer tests described in this chapter were not quantitative because it was less certain where tracer would be discharged. Groundwater contours (Figure 2.13), suggest that in the area of the Blue Pool, groundwater flow is predominantly from a west-north-westerly direction, with flow from the north during periods of high water level. This suggests that the Blue Pool may be connected to stream sinks to the north of the Pang, and tracer tests from Mirams Copse and Frilsham stream sinks were designed to test this hypothesis (Section 4.4 and 4.5). In the Winterbourne catchment (a tributary of the River Lambourn) tracer testing was carried out from Honeybottom and Cromwells stream sinks to investigate whether they are connected to nearby Bagnor and Jannaways springs (Section 4.6).

In all tests, monitoring points were chosen to encompass a wide range of possible outcomes. All major springs downgradient or within 5 km of the injection sink were monitored. Where it was not feasible to sample every possible site, a downstream monitoring point in the rivers was included to detect tracer inputs over a large area. Large borehole abstractions downgradient of injection points were also included to investigate connectivity between rapid flowing karstic conduits and water supplies.

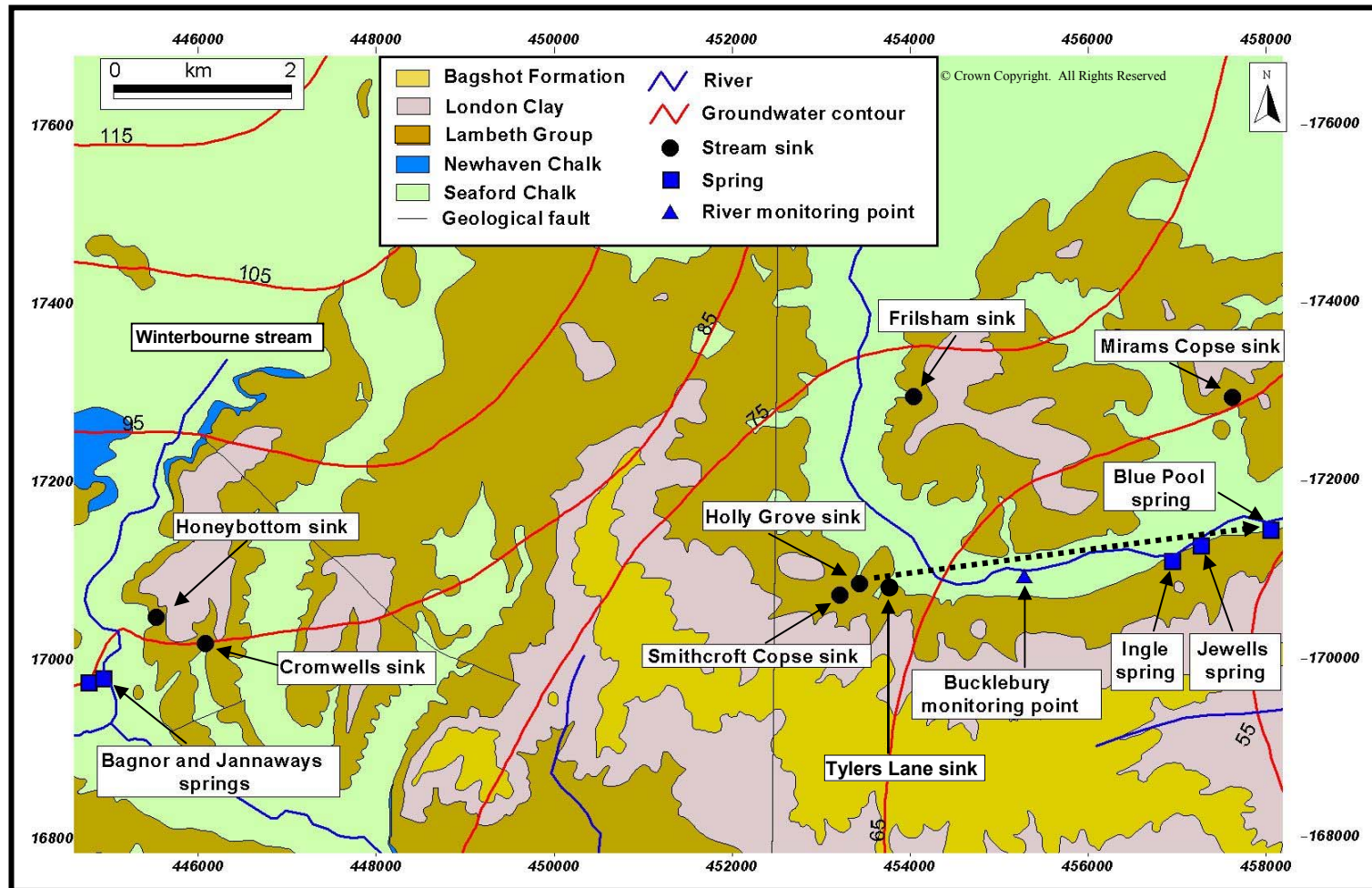


Figure 4.1: Location of stream sink injection sites in the Pang-Lambourn catchments. Black dotted arrow is proven connection between Holly Grove sink and the Blue Pool (Banks et al., 1995). Groundwater contours are from Figure 2.13 (high water table)^{BGS}

4.2 Tracer selection

The properties of groundwater tracers are discussed by Smart and Laidlaw (1977); Käss (1998); and Ward et al (1998). It is important that the tracer is not lost due to chemical reaction, degradation, precipitation, or sorption during transport through the aquifer. Groundwater tracers should be easily detectable and have low background concentrations in the environment. In the preliminary tests in the Pang-Lambourn, some loss of tracer was acceptable because quantitative analysis was not intended. The objective was to establish previously unproven connections, therefore it was most important to maximise the likelihood of unambiguous detection.

Toxicity of groundwater tracers has been extensively investigated (Smart, 1976; Smart, 1984; Field et al., 1995; Käss, 1998; Ward et al 1998; Behrens et al., 2001). Tracers were only considered if they have been proven to have negligible impacts on the environment, and are toxicologically acceptable in tests that might affect water supply boreholes. Two types of tracers were used, fluorescent tracers and bacteriophages.

Sodium Fluorescein dye was used in the initial tests from Smithcroft Copse (Section 4.3.2). It is the most widely used groundwater tracer and has been in use for over a hundred years (Käss, 1998). Despite its non-toxic properties (e.g. Behrens et al 2001), Sodium Fluorescein is visible at low concentrations ($\sim 40 \mu\text{g.L}^{-1}$), and there is often a misplaced perception that it is harmful. Therefore it was not used for the remaining qualitative tests, for which there was more uncertainty about the quantity required and the concentrations which would be present at any positive sites, because no prior work existed for these sites.

The optical brightener Photine C was used for the first qualitative test at Mirams Copse stream sink because it is non toxic (Smart 1976; Aldous et al., 1987) and colourless, and because there were a large number of monitoring sites and it can be easily and quickly detected on cotton receptors that adsorb the dye. Using this cotton detector method, Photine C has been used successfully over 14 km in the Jamaican karst (Smart and Smith, 1976), and over several kilometres in the UK Chalk (Price et al., 1992). Although it has been shown to have poor qualities as a quantitative tracer due to photochemical decay and adsorption onto organic matter (Smart, 1976; Smart and

Laidlaw, 1976), a test in South Wales demonstrated a recovery of 35 % of Sodium Fluorescein and 31 % of Photine during a simultaneous injection (Smart, 1988).

Due to continued concerns from one water company that dyes might persist in water supplies abstracted from the aquifer, bacteriophages were used for all subsequent tracer tests where a water supply might be affected. Bacteriophages are harmless to humans and the natural environment and are suitable for use in tests to public water supply boreholes (Keswick et al., 1982; Drury and Wheeler, 1982; Käss, 1998; Rossi et al., 1998; and Ward et al., 1998). Bacteriophages are small viruses that infect specific bacteria and are incapable of multiplying independently (Käss, 1998). Several different bacteriophage tracers can be used simultaneously because each bacteriophage is unique to a specific host (Rossi et al., 1998) and is assayed by treating a culture of the host and examining it for signs of infection. They are invisible to the naked eye, even at high concentrations, and have a limited lifespan so will not persist or accumulate in the environment. An additional advantage is that bacteriophages are extremely sensitive tracers because they can be injected at high concentrations (10^{12} pfu.ml⁻¹) and detected at levels of <1 pfu/50 mls, a dilution range of almost 10^{14} .

The use of bacteriophages as surface water tracers was first discussed by Wimpenny et al. (1972) and since then they have been widely used in both surface and groundwater tracing. These are reviewed by Käss (1998) and Harvey and Harms (2002). Bacteriophages range in size from ten to several hundred nanometers (Rossi et al., 1998), and as particulate tracers their transport behaviour is different to that of solute tracers. There have been several studies that have compared bacteriophages and fluorescent tracers (e.g. Rossi et al., 1998). Rossi et al. (1998) concluded that in a surface river study dispersion and maximum concentrations were very similar for bacteriophages and dyes. The bacteriophage first arrival time was faster, but this was believed to be due to the higher sensitivity of bacteriophage analysis. Table 4.1 shows the results obtained by Rossi et al. (1998) in a karst groundwater study. They found that under low flow conditions, there were relatively high losses of bacteriophages compared to dyes. Under high flow conditions at the same site, (when travel times were 15 times faster), the bacteriophage H40/1 performed similarly to Sodium Fluorescein dye. Under both high and low flow conditions the bacteriophage H6/1 had lower recovery than the

H40/1 bacteriophage demonstrating that different types of phage may have different characteristics.

Table 4.1: Comparative data for bacteriophages and dyes during karst groundwater tracer tests obtained by Rossi et al. (1998)

Tracer	Quantity	Velocity (arrival, km.h ⁻¹)	Velocity (peak, km.h ⁻¹)	Recovery (%)
LOW FLOW TEST				
Sulfurhodamine G	8.55 kg	0.5	0.4	80
H6/1	1.49 x 10 ¹⁵ pfu.ml ⁻¹	0.6	0.4	1
H40/1	9.18 x 10 ¹⁵ pfu.ml ⁻¹	0.6	0.4	21
HIGH FLOW TEST				
Sodium Fluorescein	5 kg	5.1	4.0	56
H6/1	5.71 x 10 ¹³ pfu.ml ⁻¹	5.1	4.0	25
H40/1	1.68 x 10 ¹⁴ pfu.ml ⁻¹	5.4	4.2	51

Harvey and Harms (2002) provide a summary of retardation factors based on variation in groundwater velocities, between microorganisms and solute tracers. They concluded that in fractured and heterogeneous granular aquifers bacteriophages travel faster than solutes; in karst and homogeneous granular aquifers bacteriophages and solutes travel at about the same velocity; whilst in a study in a granular aquifer with a large unsaturated zone the bacteriophages were extremely retarded.

Bacteriophages do appear to have higher losses than fluorescent tracers. This is likely to be due to the high sorptive properties of bacteriophages (Rossi et al., 1998) and the process of inactivation, whereby the bacteriophage becomes incapable of infecting its host (Käss, 1998).

The properties of bacteriophages are very variable and different types may have different transport behaviour in groundwater. In the current study, three different bacteriophages were used. These are referred to by their host bacteria names: *Serratia marcescens*, *Enterobacter cloacae*, and *Phix 174*. The size of *Serratia marcescens* bacteriophage is ~ 50 nm and that of *Enterobacter cloacae* ~100 nm (Skilton and Wheeler, 1988). *Phix 174* is the smallest at ~ 27 nm (Schijven and Hassanizadeh, 2000). Possible differences in transport behaviour of the three bacteriophages are discussed in Section 4.9 in relation to their attenuation characteristics during the tracer tests.

4.3 Holly Grove, Tylers Lane and Smithcroft Copse

4.3.1 Tracer tests from Holly Grove and Tylers Lane stream sinks, 1988

Tracer testing from Holly Grove and nearby Tylers Lane stream sinks in the Pang catchment (Figure 4.1) was undertaken in 1988 (Banks et al., 1995). The following information is derived from the paper by Banks et al. (1995) and personal communication with David Banks (2005).

The only information about the test from Tylers Lane stream sink is that tracer was detected 4.4 km away at the Blue Pool around 16 hours after injection, indicating a velocity of 6.6 km.d^{-1} . It is not reported whether 16 hours was the time of first arrival or of peak tracer concentration. It is not known if water was pumped into the stream sink, although the site was reported to have a small perennial flow, suggesting that pumping may not have been necessary (Banks, personal communication, 2005).

The tracer test from Holly Grove stream sink, 4.7 km from the Blue Pool spring, was undertaken on 19th July 1988. The gauged flow in the Blue Pool on 21st July 1988 was 199 L.s^{-1} . There was no flow into the stream sink at the time of the test so the tracer was washed down with a bowser of water. 4 litres of Sodium Fluorescein solution was used for the test, although the concentration is not known (Banks, personal communication, 2005). The tracer breakthrough curve is shown in Figure 4.2. First arrival of tracer was 16.5 hours after injection indicating a velocity of 6.8 km.d^{-1} , and peak concentrations occurred 19.5 hours after injection indicating a velocity of 5.8 km.d^{-1} . $1 \mu\text{g.L}^{-1}$ was still present in the final sample taken 31.5 hours after injection. There are no data on background fluorescence and it is not known whether any background fluorescence was subtracted from the values used in Figure 4.2. It is not possible to calculate an accurate tracer recovery because sampling was undertaken in the Blue Pool rather than at the downstream gauging point, and therefore the concentrations measured are not representative of the whole flow from the spring complex. Also the tracer injection mass is not known. However, assuming a discharge of 199 L.s^{-1} and assuming that the concentration measured was representative of all the water flowing from the spring complex, a possible 62 grams of tracer was recovered over the monitoring period. This is a small proportion of the mass likely to have been injected in 4 litres of Sodium Fluorescein solution as these products usually contain more than 20% dyestuff by weight.

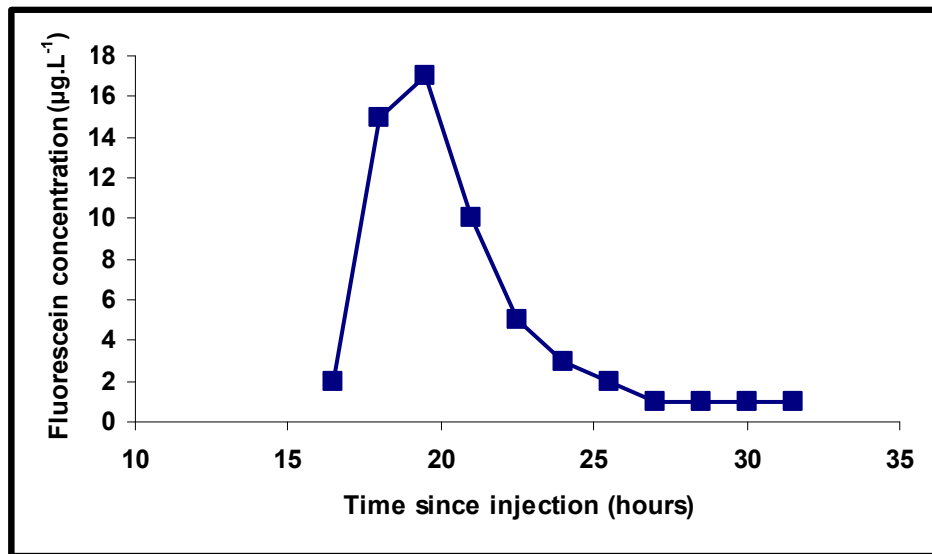


Figure 4.2: Breakthrough curve at the Blue Pool derived from data in Banks et al. (1995)

4.3.2 Tracer testing from Smithcroft Copse stream sink, 2005

4.3.2.1 Objectives

In 2005 two injections were made at Smithcroft Copse stream sink, 5.1 km from the Blue Pool (Figure 4.1). A summary of these tests is published by Maurice et al. (2006) but full details are given here and further interpretation is presented in Chapter 5. The main objective was to undertake a quantitative tracer test to obtain a detailed breakthrough curve and calculate the tracer recovery, and the quantitative aspects of the test are discussed in Chapter 5. The test also aimed to establish groundwater velocities under natural flow conditions, and to determine whether the Smithcroft Copse stream sink is connected to Ingle and Jewells springs (Figure 4.1) and to a borehole located very close to the Blue Pool.

4.3.2.2 Methods

Following its successful use by Banks et al. (1995) Sodium Fluorescein dye was used because it has low toxicity and has been demonstrated to have negligible impacts on the environment (Smart and Laidlaw 1977; Field et al. 1995; Behrens et al. 2001), and is an excellent tracer for quantitative experiments (Käss, 1998).

The previous tracer test from Holly Grove stream sink (Banks et al., 1995) used 4 litres of concentrated Sodium Fluorescein solution which was estimated to contain ~ 800g of Fluorescein dye. This produced a peak of $17 \mu\text{g.L}^{-1}$ 4.7 km away at the Blue Pool. Smithcroft Copse is 300 m further away from the Blue pool (Figure 4.1), and the groundwater velocity from Holly Grove (5.8 km.d^{-1}) was exceptionally rapid. It was considered unlikely that tracer from Smithcroft Copse would arrive at the Blue Pool at concentrations significantly higher than from the previous test by Banks et al. (1995). Therefore, 700 g of Sodium Fluorescein was considered an appropriate quantity. The River Pang passes only 1 km to the northeast of Smithcroft Copse, so a preliminary 70 g injection was undertaken, to determine if there is a rapid connection between the sink and the River Pang.

The Sodium Fluorescein dye used was a liquid product in which the active Sodium Fluorescein component was 70%. Therefore the proposed injection amounts of 70 g and 700 g required ~ 100 g and ~ 1000 g respectively of the liquid product. The preliminary injection of 107 g of the solution took place at 16:55 on 31/01/05. The peak concentration of $5.07 \mu\text{g.L}^{-1}$ at the Blue Pool outlet following this first injection suggested that the proposed 1000 g injection would produce a peak exceeding $50 \mu\text{g.L}^{-1}$. The second injection amount was therefore reduced to 610 grams of the Fluorescein solution which was calculated to produce a peak of ~ $17 \mu\text{g.L}^{-1}$ at the Blue Pool outlet. The second 610 gram injection took place at 10:05 on 07/02/05.

The stream at Smithcroft Copse sinks in a number of places over a channel length of several hundred metres. The position of the sink points was observed to vary from week to week as new depressions and small holes were eroded by the stream in the alluvium over which it was flowing (Figure 4.3). During the tracer testing the total flow was ~ $3\text{-}4 \text{ L.s}^{-1}$. At the time of the first injection there was some degree of ponding in most areas where water was sinking (Figure 4.4). Tracer was poured into the only section of stream that was draining directly into a hole without any surface ponding, although only a small proportion of the total flow was sinking at this point (Figure 4.5). At the time of the second injection a new hole had been formed which was not ponded and drained a larger proportion of the flow, but for consistency the tracer was injected into the same point as the first injection, which was still not ponded.



Figure 4.3: A newly formed sink point (hole diameter is approximately 1 m)



Figure 4.4: Ponding at a sink point



Figure 4.5: Injection on 07/02/05

Details of the sampling following the first injection are listed in Table 4.2 and the location of the River Pang monitoring point at Bucklebury and the Blue Pool are shown on Figure 4.1. Sampling sites following the second injection are listed in Table 4.3 and shown on Figure 4.6. At some sites a Sigma automatic water sampler was used to collect water samples and at others an in situ Field Fluorometer, designed and built at Neuchatel University was used (Figure 4.7).

Standard solutions of 0.1, 1, 5, 10, 20 and 100 $\mu\text{g.L}^{-1}$ were made up using tap water. The Field Fluorometers were calibrated using 5, 10 and 20 $\mu\text{g.L}^{-1}$ standards prior to their installation in the field. Water samples that were collected in the field were measured in the laboratory after the tracer test using a Neuchatel Field Fluorometer adapted using fittings that enable measurement using sample aliquots instead of continuous flow. Standards were measured at the beginning and end of each period of laboratory analysis to ensure that there was no instrument drift.

Table 4.2: Monitoring for preliminary Smithcroft Copse injection

	River Pang at Bucklebury	Blue Pool outlet channel
NGR	455301 171003	458686 17174
Measurement method	In-situ fluorometer	In-situ fluorometer
Sample interval	1 minute	1 minute
Start of sampling	28/01/05 10:25	27/01/05 10:20
End of sampling	04/02/05 11:13	07/02/05 16:09

Table 4.3: Monitoring for main Smithcroft Copse injection

Site	NGR	Measurement method	Sample period	Sample frequency (decreasing as test progressed)
1. Ingle Spring	457141 171125	Automatic water sampler	02/02/05 to 18/02/05	1 to 4 hourly
2. Jewells Spring	457452 171330	Automatic water sampler	02/02/05 to 18/02/05	1 to 4 hourly
3. Blue Pool spring	458290 171482	Hand samples	07/02/05 to 18/02/05	1 to 4 per day
4. Blue Pool outlet channel	458686 171743	In-situ fluorometer	07/02/05 to 21/02/05	1 minute
5. River Pang at Frogmore Farm	458673 171853	Automatic sampler	02/02/05 to 18/02/05	1 to 4 hourly
5. River Pang at Frogmore Farm	458673 171853	In-situ fluorometer	04/02/05 to 14/02/05	1 minute
6. Frogmore Farm borehole	458632 171876	Pumped samples	08/02/05 to 18/02/05	11 samples in each piezometer

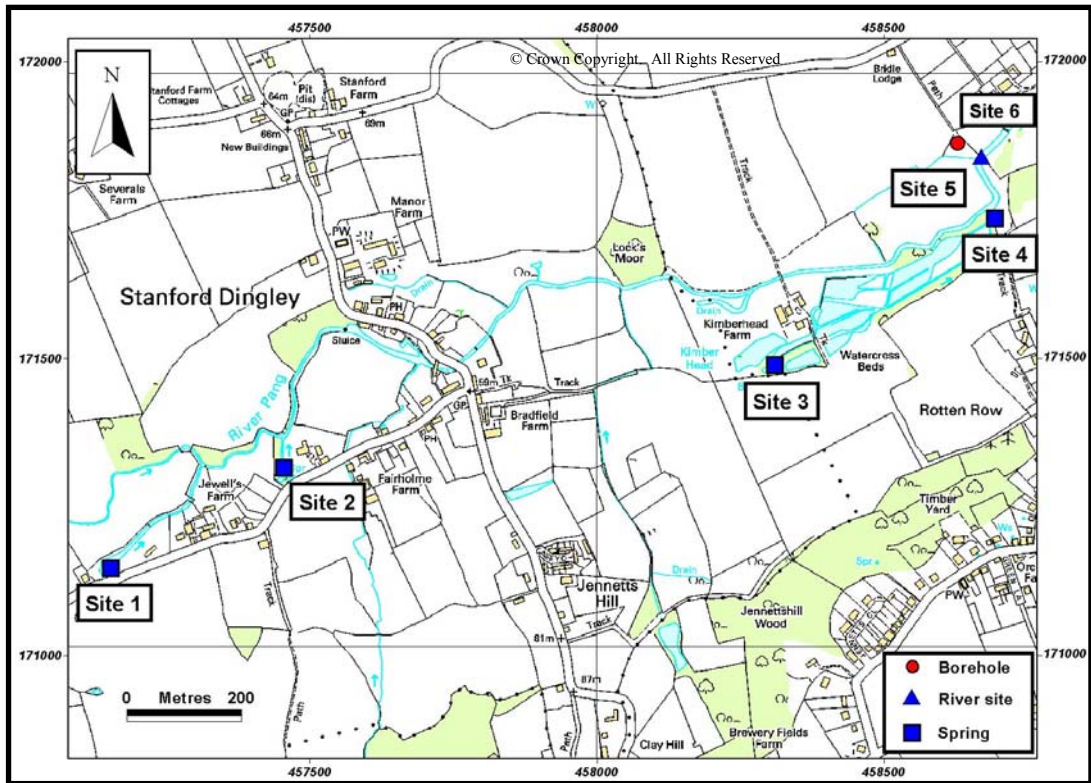


Figure 4.6: Monitoring sites for main Smithcroft Copse injection



Figure 4.7: Field Fluorometer (left) and datalogger (right); from Neuchatel University

4.3.2.3 Results

No tracer from the preliminary injection was detected in the River Pang at Bucklebury (Figure 4.8). Both injections produced breakthrough curves at the Blue Pool outlet (Figure 4.9). Groundwater velocities (based upon time to peak tracer concentration) were 5.1 and 4.7 km.d⁻¹ for injections 1 and 2 respectively.

Visible colouration showed that tracer entered the Blue Pool through all upwellings in the main pool (Figure 4.10), and also at Kimber spring, approximately 100 m to the west. Tracer concentrations in hand samples taken at various different locations in the spring complex had very variable concentrations due to the complex dilution effects in the pools. The peak concentration measured in the Blue Pool was 64.9 µgL⁻¹. This peak concentration was measured in a sample from the site closest to the main upwellings. It is possible that the actual peak concentration in this part of the pool was higher as sampling was very infrequent. There is a considerable dilution effect in the Blue Pool before the tracer reaches the monitoring point at the Blue Pool outlet channel where the peak concentration had reduced to 16 µgL⁻¹.

Figure 4.11 shows the results of monitoring at Ingle Spring, Jewells spring and the two piezometers in the Frogmore Farm borehole. Tracer concentrations did not rise significantly above background at any of these sites.

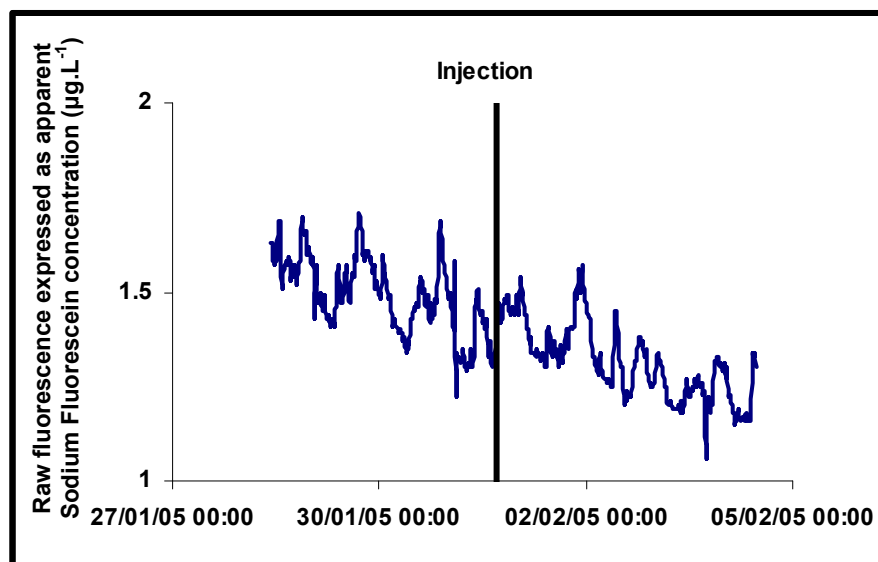


Figure 4.8: Apparent tracer concentrations in the River Pang at Bucklebury following preliminary (70g) Sodium Fluorescein injection at Smithcroft Copse.

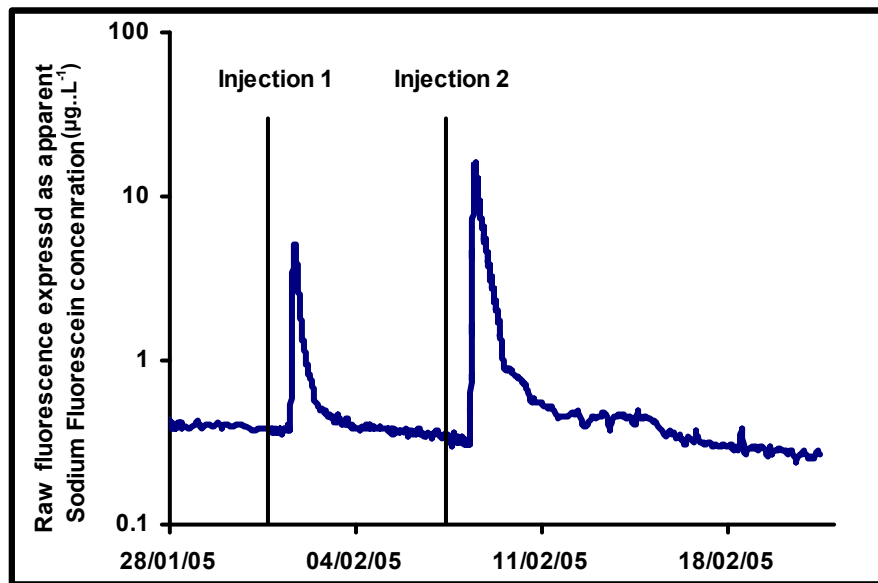


Figure 4.9: Tracer breakthrough curves at the Blue Pool outlet following 70 and 610g injections (2005)



Figure 4.10: Colour in the Blue Pool

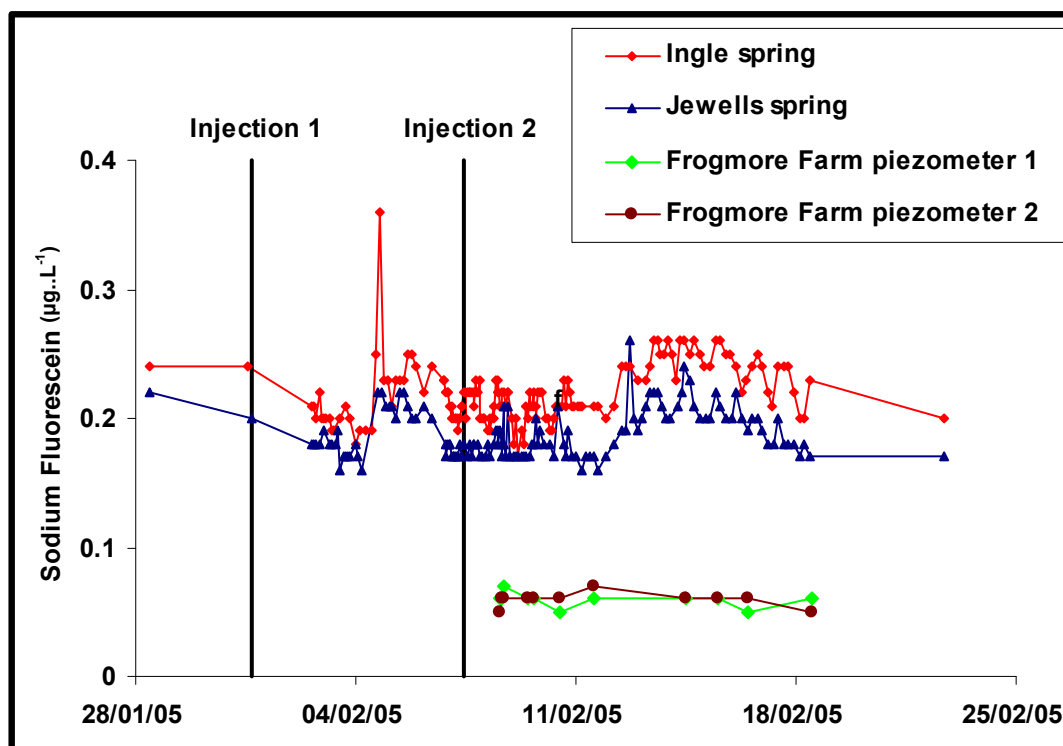


Figure 4.11: Results from Jewells and Ingle springs and two piezometers in the Frogmore Farm borehole

Background fluorescence varied substantially between monitoring sites (Table 4.4). Background fluorescence occurs in springs and rivers from dissolved organic matter, which may be especially high where springs and rivers receive sewage or agricultural effluent (Baker et al., 2003). Variations in background fluorescence between sites can give a rough guide to groundwater characterisation. The very low background fluorescence at the Frogmore Farm borehole suggests a different groundwater source than that of the Blue Pool.

Table 4.4: Background fluorescence at monitoring sites

Site	Average background fluorescence ($\mu\text{g.L}^{-1}$)
River Pang at Bucklebury	1.50
River Pang at Frogmore Farm	0.50
Blue Pool outlet	0.35
Ingle Spring	0.24
Jewells Spring	0.22
Frogmore Farm borehole	0.06

4.4 Photine tracer tests from Mirams Copse stream sink, Pang catchment, 2004

4.4.1 Introduction

The objective of tracer tests from Mirams Copse stream sink was to determine if the Blue Pool catchment extends to the north of the River Pang, in addition to the proven catchment to the west from the Holly Grove/Smithcroft Copse area (Figure 4.1). Mirams Copse stream sink (NGR 457825 172968) is the closest suitable tracing sink north of the Blue Pool.

4.4.2 Methods

The location of 13 spring, river and borehole sites monitored during the tracer test are shown in Figure 4.12 and listed in Table 4.5. In the Blue Pool spring complex two upwellings were monitored in addition to a downstream monitoring point in the Blue Pool outlet channel (sites, 5,6, and 7, Figure 4.13). In Stanford Dingley village, Ingle and Jewells springs (sites 2 and 3) and a third smaller spring (site 4), were monitored (Figure 4.14). The River Pang was monitored in five places to detect any tracer discharged into unknown springs or groundwater inflows through the riverbed. At Bradfield, (site 9), the Pang is divided and three separate channels were monitored (Figure 4.15). Groundwater was monitored at three sites: a borehole at Frogmore Farm near the Blue Pool (site 8, Figure 4.13); the Bradfield PWS (site 10, Figure 4.12); and a private water supply borehole at Maidenhatch farm (site 11, Figure 4.12).

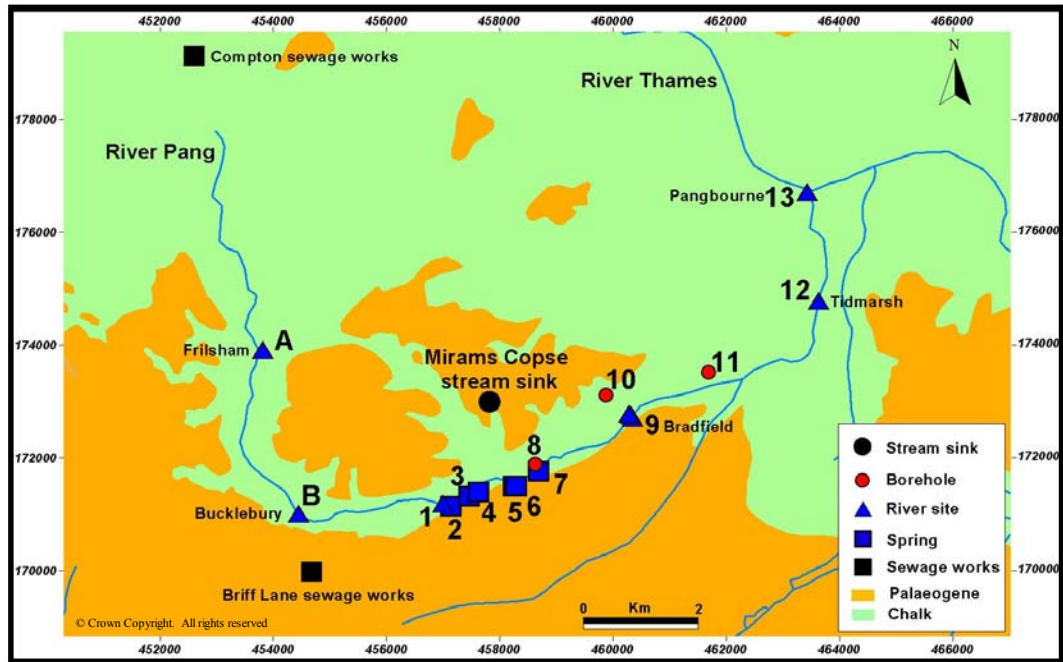


Figure 4.12: Monitoring sites for the Mirams Copse Photine C test^{BGS}

Table 4.5: Monitoring sites for the Mirams Copse Photine C test

Site	Name	Easting	Northing
1	River Pang, upstream of Stanford Dingley springs	456998	171173
2	Ingle Spring	457141	171125
3	Jewells Spring	457460	171304
4	Spring Cottage Spring	457624	171381
5	Kimber spring (westerly Blue Pool uprising)	458244	171480
6	Blue Pool (main spring)	458297	171480
7	Blue Pool Outlet stream	458686	171743
8	Frogmore Farm borehole	458632	171876
9a	R.Pang at Bradfield channel 1	460346	172697
9b	R.Pang at Bradfield channel 2	460325	172742
9c	R.Pang at Bradfield channel 3	460283	172776
10	Bradfield Public Water Abstraction	463635	174771
11	Maidenhatch Farm Abstraction	463431	176698
12	R.Pang at Tidmarsh	459879	173105
13	R.Pang at Pangbourne	461689	173512
A	R. Pang at Frilsham*	453817	173905
B	R. Pang at Bucklebury*	454449	170995

*Additional sites to investigate source of background fluorescence (Section 4.4.3.1)

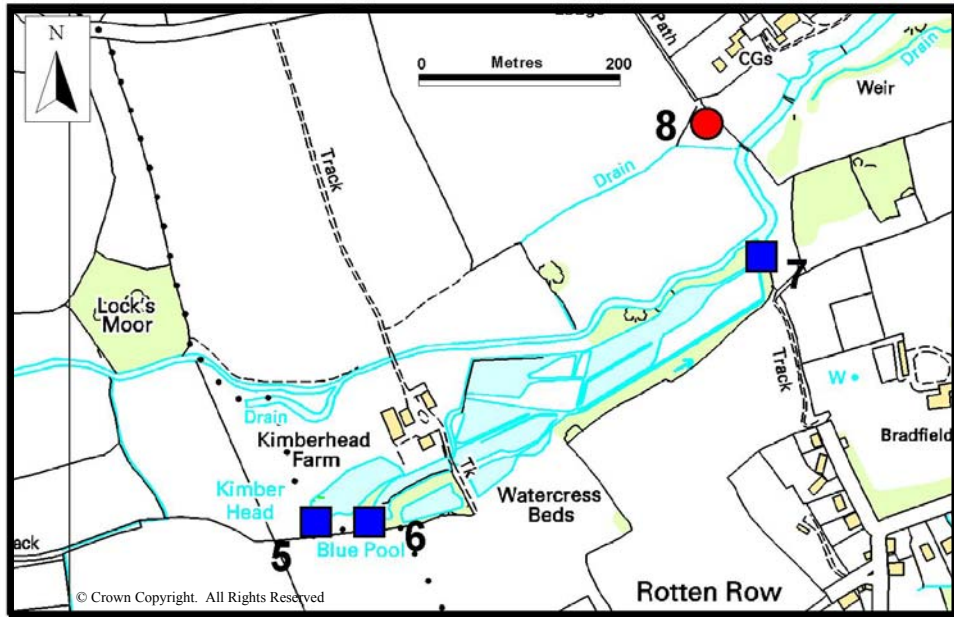


Figure 4.13: Monitoring locations in the Blue Pool spring complex for the Mirams Cope Photine C test

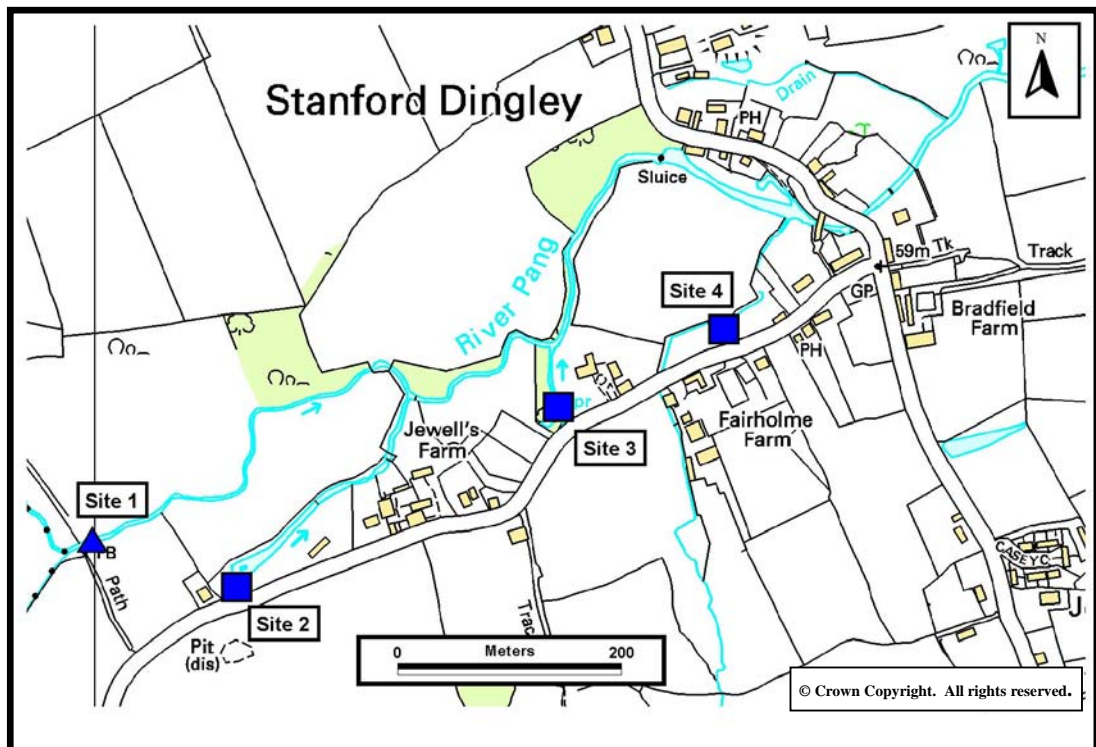


Figure 4.14: Monitoring sites in Stanford Dingley village for the Mirams Cope Photine C test

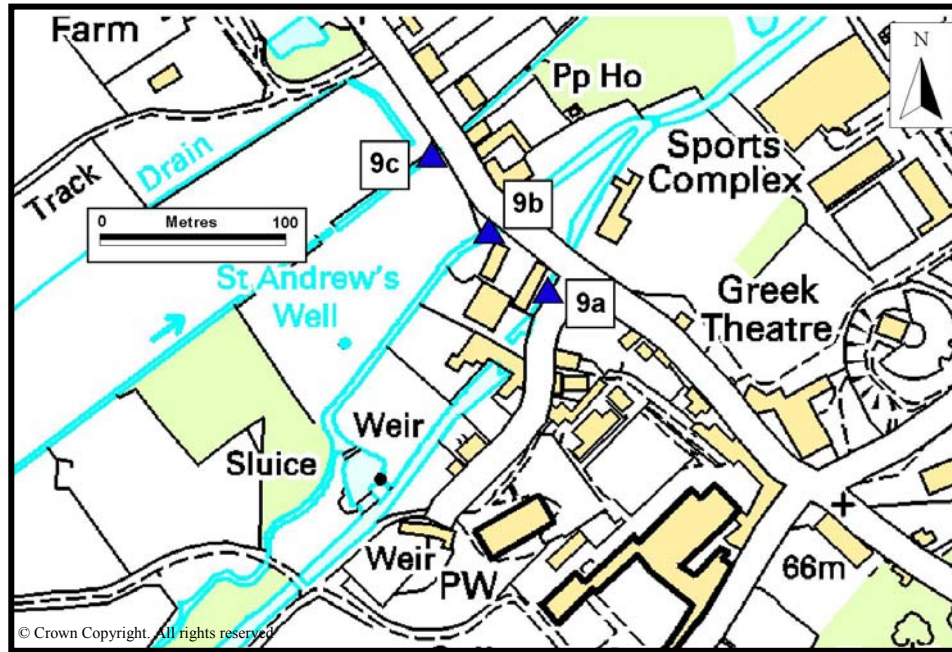


Figure 4.15: Monitoring sites at Bradfield for the Mirams Copse Photine C test

The optical brightener Photine C was used. The product was a 20 % solution. The tracer quantity was calculated to try and ensure that concentrations at the monitoring points would be sufficiently high to obtain unambiguous positive results, but would also remain well below any concentration that would be unacceptable at any possible receptor site. Due to concerns expressed by the water company responsible for the public water supply at Bradfield considerable work was undertaken by the LOCAR project team to demonstrate that tracer injection quantities would not produce a peak at the Bradfield PWS exceeding the $30 \mu\text{g}\cdot\text{L}^{-1}$ threshold suggested by Aldous et al. (1987) as safe for transient consumption in drinking water.

The basic strategy was to use a small injection of dye initially, followed by successively larger injections; either until a positive result was achieved or until a predetermined maximum injection amount had been used. The initial minimum tracer quantity (25 g, equivalent to 125 mls of the 20 % solution) was calculated assuming the worst case scenario that all tracer was recovered at the Bradfield public water supply boreholes, and used the method outlined in Ward et al. (1998):

$$M = CmA\sqrt{4\pi r\alpha}$$

M = injection mass

C_m = maximum peak concentration

A = cross sectional area of the injection pulse

r = distance between injection and sampling point

α = dispersivity

A value of dispersivity of 23 m was estimated from the breakthrough curve published by Banks et al (1995), using the straight line velocity implied by the time to peak and the duration of tracer breakthrough at half peak concentration to solve the advection-dispersion equation (ADE) (Tim Atkinson, personal communication, 2003).

This value gives a likely “worst case” for the effects of dispersion. It was used in combination with various assumed velocities to predict peak concentrations at Bradfield using the ADE. The modelled peak concentration at Bradfield for 25 grams of tracer moving with a velocity of 1000 m.d⁻¹ is about 14 µg.L⁻¹, below the threshold limit of 30 µg.L⁻¹ suggested by Aldous et al (1987).

This quantity of tracer seems small compared with previous experience of tracer testing to boreholes in chalk over much shorter distances (Ward, 1989), and negative results were expected. In the case of negative results it was proposed to double the injection amount and to continue by doubling at each stage. To determine a suitable maximum amount of tracer to be used, it was assumed that a negative result would be obtained at Bradfield, and a positive one at the Blue Pool; and that the velocity and dispersion characteristics of the hypothetical flowpath from Mirams Copse to the Blue Pool could be scaled from the known results of Banks’ (1995) test from Holly Grove.

The basis of scaling is described by:

$$C_{proposed} = C_{Banks} \frac{m_{proposed} \sqrt{x_{Banks}}}{m_{Banks} \sqrt{x_{proposed}}}$$

$C_{proposed}$ = peak tracer concentration in proposed test

m = mass of tracer injected (m_{Banks} = mass in Banks tracer test; $m_{proposed}$ = proposed mass for Mirams Copse tracer test)

x = distance from injection to outlet (x_{Banks} = distance from Holly Grove sink to Blue Pool; $x_{proposed}$ = distance from Mirams Copse to Blue Pool)

This calculation led to the conclusion that an injection of 716 grams of Photine C might lead to a peak tracer concentration of $26 \mu\text{g.L}^{-1}$ at the Blue Pool. Following the selection of a provisional schedule for the test programme (Table 4.6), a more detailed modelling exercise was undertaken to identify likely worst case scenarios for tracer arrival and peak concentrations at Bradfield PWS, should that site prove to be a destination for the tracer from Mirams Copse (Atkinson, 2004). This exercise demonstrated that the combination of a precautionary approach with updating of parameter estimates based on previous negative results should limit concentrations at Bradfield to acceptable levels, and the schedule of tests shown in Table 4.6 was approved by Thames Water plc, who then granted access to their site at Bradfield for monitoring purposes.

Table 4.6: Photine C injection quantities

Stage	Tracer amount*	Duration of monitoring before any further injection
1	25 grams	2 days
2	50 grams	4 days
3	100 grams	1 week
4	200 grams	1 week
5	400 grams	2 weeks
6	716 grams	End of Schedule

**Because Photine C was in the form of a 20 % solution actual injection amounts were five times the mass listed here.*

Cotton detectors were used for passive tracer detection (Figure 4.16). Background monitoring was undertaken prior to tracer injection. During background monitoring, it was found that large amounts of organic biofilm accumulated on the detectors left at sites in the River Pang, and in the Blue Pool outlet. This did not occur on detectors placed directly in the spring upwellings or at the borehole sites. Experiments placing the cotton detectors inside wire mesh and other materials did not reduce the biofilm accumulation. Therefore detectors were changed at 1 or 2 day intervals at all sites for several days following each injection to reduce the influence of biofilm. At the spring and borehole monitoring sites a second detector was changed at 3-day intervals to increase the cumulative affect of tracer adsorption.



Figure 4.16: Cotton for detecting Photine C

Following collection, samples were kept in ziplock polythene bags in a fridge until they were examined under an ultra violet light with a wavelength of 365 nanometers. Standard cotton detectors were used for comparison with field samples. These were soaked in 100 mls solutions of 0.2, 2, 20, 100 and 200 $\mu\text{g.L}^{-1}$ for about 1 hour. Blue fluorescence was clearly visible on these detectors when viewed under the ultraviolet light.

4.4.3 Results

4.4.3.1 Background samples

39 background samples were collected and examined. Background detectors at all monitoring sites in the River Pang were fluorescent. These detectors were often completely smothered in biofilm, but the biofilm itself was fluorescent. The greatest background fluorescence was at site 1, upstream of Ingle and Jewells springs (Figure 4.14). Background presence of optical brightener is often derived from sewage discharges (Käss, 1998), and it was thought that the licensed sewage discharge into the Pang from the sewage works at Briff Lane or Compton might be the source of the background fluorescence (Figure 4.12). Experimental detectors placed at new sites upstream in the Pang at Bucklebury and Frilsham (sites A and B on Figure 4.12) had significantly less background fluorescence than the detectors at site 1. This suggests that the source of the fluorescence may be the sewage treatment plant at Briff Lane. All channels at Bradfield (site 9) had lower background fluorescence than site 1, with the highest fluorescence at site 9a and the lowest at site 9c. The lower fluorescence at site 9c might be due to dilution of the river water by groundwater issues in this area. The general decrease in background fluorescence between site 1 and Bradfield (site 9) is presumably due to dilution in water from Ingle, Jewells and the Blue Pool springs.

Background fluorescence at Pangbourne (Site 13) was higher than Bradfield suggesting that an additional source of fluorescence enters the Pang between Bradfield and Pangbourne.

There was no background fluorescence on any of the detectors from the springs or boreholes; therefore any fluorescence following tracer injection could be interpreted as a consequence of this tracer test.

4.4.3.2 Samples following tracer injections.

No tracer was detected at any of the monitoring sites. Tracer was conclusively absent from all spring and borehole monitoring sites including the Blue Pool and the Bradfield PWS. Due to the high background fluorescence it was not possible to determine conclusively that no tracer was discharged into the River Pang, however there was no noticeable increase in the fluorescence in detectors from the River Pang following any of the injections. Table 4.7 summarises the injections that were made at Mirams Copse between 26/04/04 and 29/11/04. Because no tracer had been detected at any of the monitoring sites following the injections up to 400 grams, it was clear that the flowpath was not similar to that between Holly Grove and the Blue Pool, which had been assumed in calculating the proposed maximum injection of 716 g. The final injection amount was therefore increased to 1000 g (5 litres of the 20% solution). In total 447 detectors were examined following the 6 injections.

Table 4.7: Summary of Mirams Copse injections

Date	Injection time	Injection amount	Samples following injection
26/04/2004	20:25	25 g	48
30/04/2004	13:00	50 g	67
05/05/2004	13:40	100 g	60
11/05/2004	17:50	200 g	119
17/05/2004	no injection, too little flow		
08/11/2004	14:45	400 g	79
29/11/2004	15:50	1000 g	74

4.4.3.3 Flow conditions and rainfall during tracer injections

There was a good flow of $\sim 2\text{-}3 \text{ L s}^{-1}$ entering the stream sink at the time of the 50g and 100g injections. However there was considerably less flow during the other injections with extremely low flow ($<0.5 \text{ L s}^{-1}$) during the 200g and 1000g injections. Figure 4.17 shows the stream sink under high and low flow conditions. Figures 4.18 and 4.19 show

the LOCAR rainfall data from Frilsham (about 2 km from Mirams Copse), and illustrate that the larger injections were all undertaken during dry periods.



Figure 4.17: Variable flow at Mirams Copse stream sink (2003/2004)

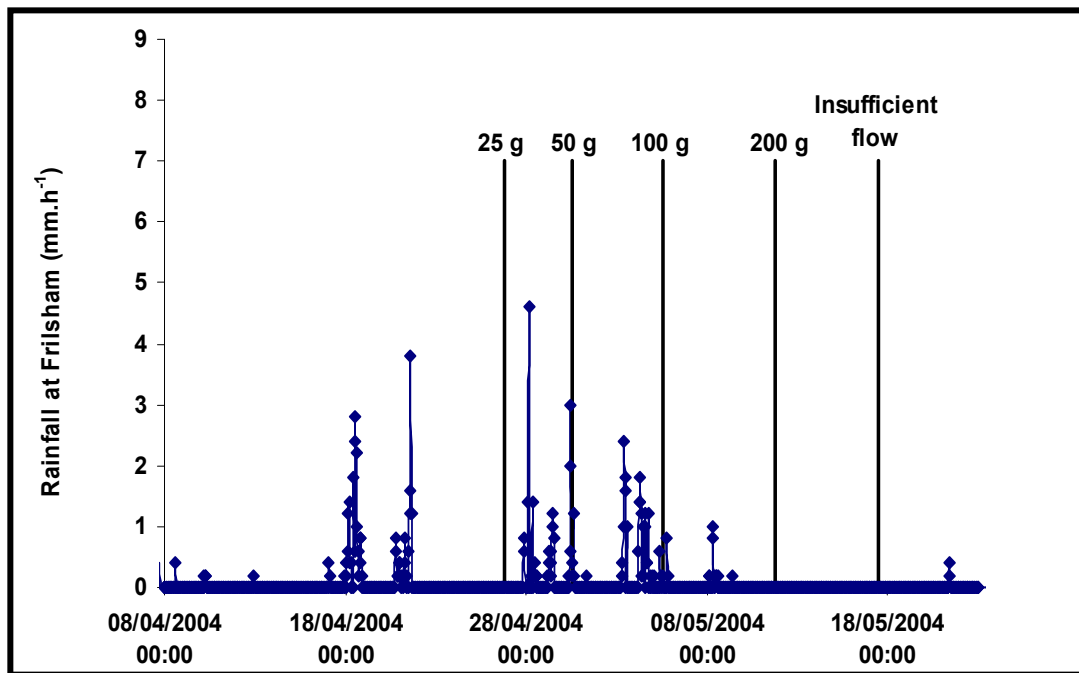


Figure 4.18: Rainfall at Frilsham during 25 g to 200g Photine C injections at Mirams Copse.

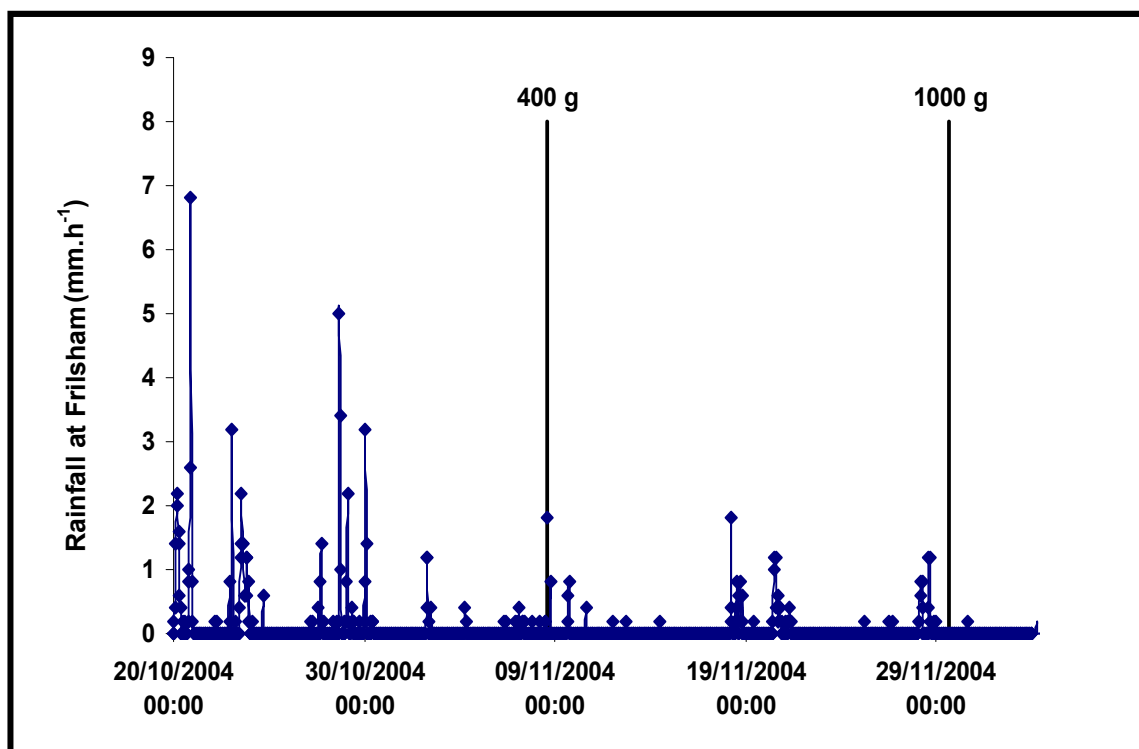


Figure 4.19: Rainfall at Frilsham during 400 g and 1000 g Photine C injections at Mirams Copse.

4.5 Bacteriophage tracer testing from Mirams Copse and Frilsham sinks, Pang catchment, 2006

4.5.1 Introduction

Further tracer testing using bacteriophages was undertaken to determine if the groundwater catchment of the Blue Pool extends to the north of the River Pang. Mirams Copse stream sink was included because it was thought that the negative results using Photine C might have been due to insufficient tracer being used under very low flow conditions. Bacteriophages are much more detectable than Photine C. Frilsham stream sink (NGR 454237 172977) was selected as the second site because it lies at the western boundary of the area of stream sinks to the north of the Pang (Figure 4.20). Groundwater contours (Figure 4.1) suggest that this stream sink is upgradient of the Blue Pool and also that it provides an input into groundwater flows that may have passed beneath the Pang from an area to the west. If Frilsham stream sink feeds the Blue Pool, this area may also be part of the catchment.

4.5.2 Methods

The high cost of analysing for bacteriophages limited the number of sites that could be monitored to three: the Blue Pool outlet channel, and downstream sites in the Pang and Thames rivers (Figure 4.20 and Table 4.8).

The bacteriophages used were single strains with bacterial hosts *Serratia marcescens* and *Enterobacter cloacae*. For each bacteriophage, CREH Analytical, a specialist microbiology laboratory in Leeds, prepared one-litre solutions at concentrations of 2×10^{12} pfu.ml⁻¹. This laboratory also carried out the sample analysis during the tracer test. They used two methods of sample analysis. The first is the presence/absence method that is performed on samples of 50-100 mls. Samples are incubated with the host bacterium and if the bacteriophage is present a lysis is formed (Francis and Watkins 2006). Occasionally, although lysis was evident, the sample was overgrown with contaminating bacteria. To confirm that the lysis was due to the presence of the bacteriophage (and not caused by the contaminating bacteria) a sub sample of the lysis was taken and reanalysed. If lysis was present after further incubation bacteriophage was clearly present. If lysis was absent the sample was classified as negative. However, these samples that were affected by contaminating bacteria are differentiated from negatives and classified as “ambiguous” in the discussions that follow because

they all occur either during periods when the bacteriophage was conclusively demonstrated to be present in other samples, or during periods when it is possible that injected tracer could be discharged at the sample site.

Table 4.8: Location of bacteriophage sampling sites

Sample Site	Easting	Northing
Blue Pool outlet	458686	171743
River Pang	463427	176647
River Thames	463195	176785

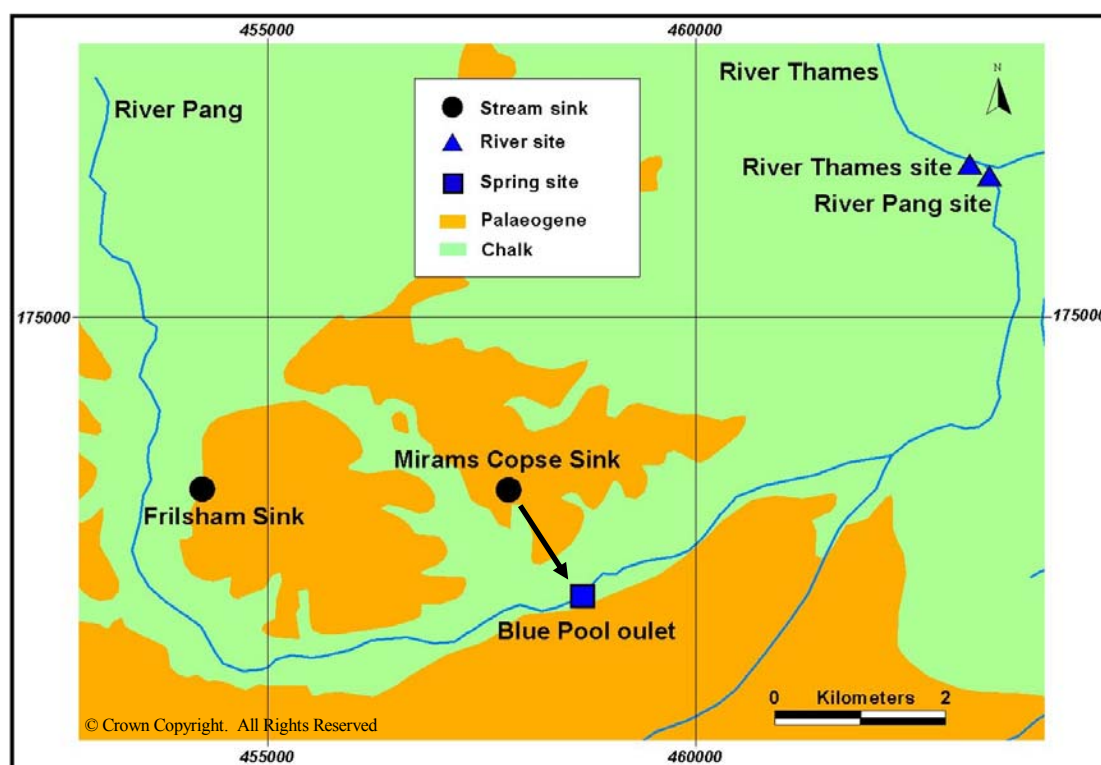


Figure 4.20: Location of bacteriophage sampling sites^{BGS}

The second method of analysis used a much smaller sample (normally 1 ml) to determine the number of pfu (plaque forming units) present after incubation. Due to the ambiguities and high attenuation of tracer during the Winterbourne tracer test which had taken place a year previously (Section 4.6.2), samples were initially analysed using the presence/absence technique which is more sensitive when very low bacteriophage concentrations are present.

Background samples were taken between 27/01/06 and 08/02/06, and results are detailed in Table 4.9. Both bacteriophages were absent from the background samples

from the Blue Pool. *Serratia marcescens* and *Enterobacter cloacae* were also absent from 40 samples from the Blue Pool analysed using the presence/absence technique during the previous tracer test in the Winterbourne (Section 4.6), providing further evidence that these bacteriophages are not normally present at the Blue Pool. Therefore all subsequent samples were analysed using the large volume (~90 ml) presence-absence technique, and any positives following injection could be interpreted as being a consequence of this tracer test.

At other sites in the River Thames and River Pang *Serratia marcescens* and *Enterobacter cloacae* were found in some of the background samples using the presence/absence method (Table 4.9). Each sample that was positive was re-analysed using 1 ml to determine the pfu.ml⁻¹ in the sample. This confirmed that bacteriophages were only present in very low numbers. 1 pfu.ml⁻¹ of *Serratia marcescens* was measured in one of five samples from the Thames, and 1 pfu.ml⁻¹ of *Enterobacter cloacae* was measured in the sample from the Pang. All other samples that were positive using the presence-absence analysis on ~ 90mls of sample had 0 pfu.ml⁻¹ when the 1 ml analysis was performed. Subsequent samples from the River Thames and the River Pang were analysed using 1 ml of sample to determine pfu.ml⁻¹, as positives from presence-absence analysis could not be distinguished from background.

Table 4.9: Results of background monitoring for bacteriophage

	Blue Pool	River Pang	River Thames
Total no. background samples	6	8	8
No. samples positive for <i>S. marcescens</i> using presence-absence	0	2	5
Pfu.ml ⁻¹ <i>S. marcescens</i> in positive samples	0	0	0 to 1*
No. samples positive for <i>E. cloacae</i> using presence-absence	0	1	4
Pfu.ml ⁻¹ <i>E. cloacae</i> in positive samples	0	1	0

* 1 pfu.ml⁻¹ was present in one sample, the other 4 samples contained 0 pfu.ml⁻¹

Samples were collected at all sites using automatic water samplers (Figures 4.21 to 4.23), with a gradual decrease in sampling frequency with time since injection. Table 4.10 summarises the sampling undertaken at each site.



Figure 4.21: River Thames sampler



Figure 4.22: River Pang sampler



Figure 4.23: Blue Pool outlet sampler

Table 4.10: Sampling during the Pang bacteriophage tracer test

	Blue Pool	River Pang	River Thames
<i>Serratia marcescens</i>			
Sample interval at start of test	12 per day	8 per day	8 per day
Sample interval at end of test	~ 3 per day	5 per day	5 per day
Duration of monitoring	21 days	5 days	5 days
Total number samples	120	40	40
<i>Enterobacter cloacae</i>			
Sample interval at start of test	12 per day	8 per day	8 per day
Sample interval at end of test	~ 3 per day	1 per day	1 per day
Duration of monitoring	21 days	20 days	17 days
Total number samples	120	76	73

Tracer injections took place on 15th February 2006. There had been sporadic rainfall in the weeks leading up to the tracer test, and there was significant rainfall during the night preceding the injection. At both sites water was sinking into distinctive holes in the depressions, with a small amount of ponding at Mirams Copse. At 10:30, the *Enterobacter cloacae* bacteriophage was injected into Frilsham stream sink which was flowing at $\sim 2 \text{ L s}^{-1}$ (Figure 4.24). Unfortunately about 1/3 to 1/2 of the tracer was spilt

onto sediments immediately adjacent to the stream. This tracer was washed back into the hole using 10-20 buckets of water, but some tracer may have filtered through the sediments and not reached the sink point. At 11:20 *Serratia marcescens* bacteriophage was injected into Mirams Copse stream sink which was flowing at $\sim 3 \text{ L s}^{-1}$ (Figure 4.25).



**Figure 4.24: Frilsham Sink
at time of injection**



**Figure 4.25: Mirams Copse sink
at time of injection**

4.5.3 Results

4.5.3.1 Results of Mirams Copse injection

Serratia marcescens was conclusively detected at the Blue Pool, 1.6 km from Mirams Copse sink, but it was present at very low levels close to the detection threshold. The results are shown in Figure 4.26. Tracer was first detected at the Blue Pool 8 hours and 53 minutes after the injection, indicating a groundwater velocity of 4.3 km.d^{-1} . Tracer was confirmed present in 13 samples, the last being 4 days and 6 hours after injection (level 3 in Figure 4.26). 1 ml analysis was performed on these positive samples, but all results were negative, indicating the phage levels in the positive samples were lower than 1 pfu.ml^{-1} . A further 21 samples are classified as “ambiguous” (level 2 in Figure 4.26). These all occur after tracer injection, and many are within the period in which the confirmed positives occurred. Throughout the period of positive samples there were also many negative samples indicating that the phage level was lower than 1 pfu/90 mls .

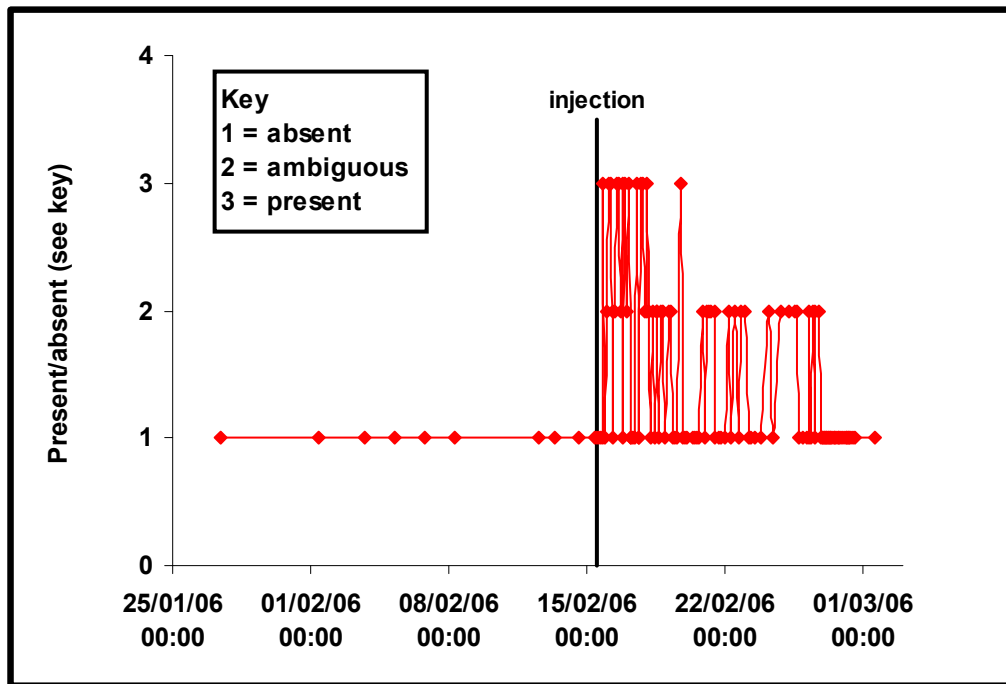


Figure 4.26: Results of *Serratia Marcescens* at the Blue Pool

Figure 4.26 shows four stages of results:

- 1) The background stage, prior to tracer injection when all samples were negative.
- 2) A four-day period following tracer injection when there were many confirmed positives and “ambiguous” samples.
- 3) A subsequent 7-day period when there were “ambiguous” samples
- 4) A period of 3 days at the end of the monitoring period when all samples were negative.

In the River Pang 40 samples were taken between 13/02/06 and 20/02/06. 1 pfu.ml⁻¹ was present in one sample 23 hours after injection. All other samples were negative. The single positive sample was at a time when tracer from the Blue Pool would be expected to be present in the River Pang, and the concentration of 1 pfu.ml⁻¹ was higher than seen in the background samples. However because *Serratia marcescens* was present in the background samples it is not certain that the positive sample was from this tracer test.

In the River Thames 39 samples were taken between 13/02/06 and 20/02/06. 1-2 pfu.ml⁻¹ of *Serratia marcescens* was present in 3 samples between 5 and 17 hours after injection and in 2 samples 2 days after injection. All other samples were negative. The

positive samples are not significantly above background so it is unclear if they were due to the tracer test. The River Thames was responding to rainfall when the samples were taken, and therefore it seems probable that the apparently positive samples are unrelated to the tracer test.

4.5.3.2 Results of Frilsham injection

Enterobacter cloacae was absent from all 120 samples from the Blue Pool. 1 pfu.ml⁻¹ was detected in two samples from the River Thames, but this is not significantly above background. All 1 ml samples from the River Pang were negative.

4.6 Bacteriophage tracer testing from Honeybottom and Cromwells sinks in the Winterbourne catchment, 2005

4.6.1 Introduction

The only significant springs identified in the lower reaches of the Lambourn adjacent to the Palaeogene cover and associated stream sinks are the springs at Bagnor and Jannaways (Section 3.4.2.2). Bagnor spring was observed to have high turbidity following rainfall, suggesting that it may be connected to stream sinks. Honeybottom (NGR 445729 170508) and Cromwells (NGR 446276 170207) sinks on Snelsmore Common (Figure 4.27) were selected because they are the nearest suitable tracing sites to the springs.

4.6.2 Methods

Sites monitored during the tracer test are listed in Table 4.11 and shown on Figure 4.27. At Bagnor and Jannaways springs sampling was at the spring outlet channel downstream of all upwellings, and samples were also taken from the Winterbourne Stream upstream of the inflow from the springs (Figure 4.28).

At the Speen PWS borehole complex, the three boreholes being pumped at the time of the test were monitored. A site in the River Lambourn just upstream of its confluence with the River Kennet was monitored to detect any tracer discharged into unknown springs or groundwater inflows into the riverbed. Flow data for the lower reaches of the River Lambourn (Grapes, 2005) suggest that there may be some accretion in addition to the input from the Winterbourne tributary. The Blue Pool was included despite its distance from the injection sites because it is the largest spring in the area ($\sim 200 \text{ L}\cdot\text{s}^{-1}$),

and tracer testing from Smithcroft Copse, which lies between the Snelsmore Common stream sinks and the Blue Pool, produced positive results at the Blue Pool. Sampling was from the Blue Pool outlet channel.

Table 4.11: Monitoring sites during the Winterbourne tracer tests

Site	Easting	Northing
Bagnor Spring	445170	169792
Jannaways Spring	445064	169744
Winterbourne Stream	445176	169807
Downstream Lambourn	448597	167536
Speen PWS borehole 1	446227	167471
Speen PWS borehole 2	446227	167463
Speen PWS borehole 6	44603	16749
Blue Pool outlet channel	458686	171743

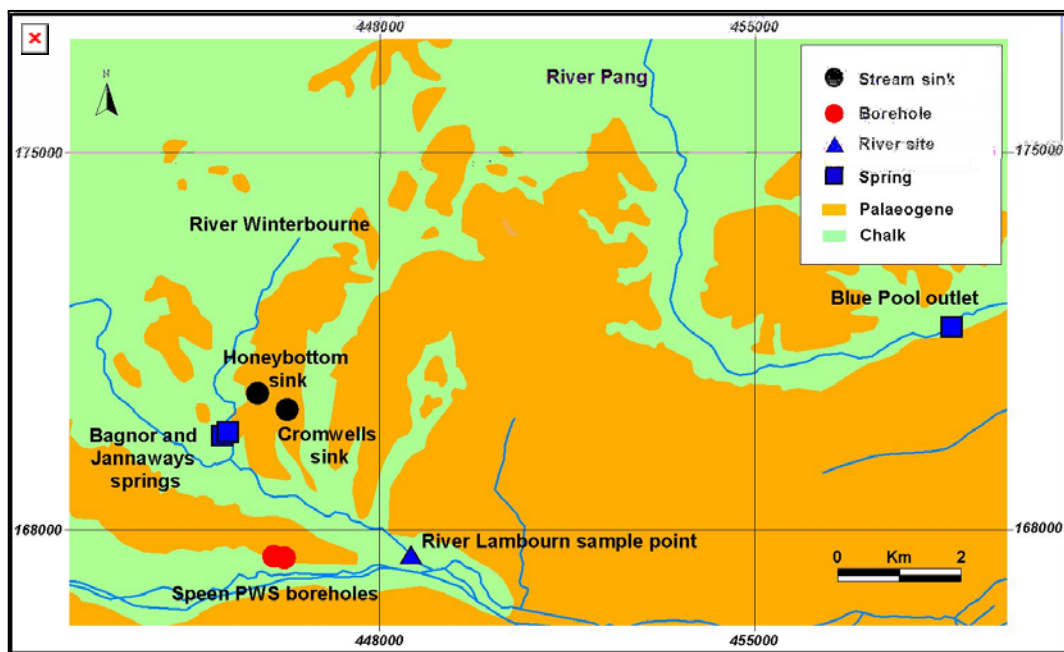


Figure 4.27: Location of Winterbourne injection sinks and monitoring points ^{BGS}

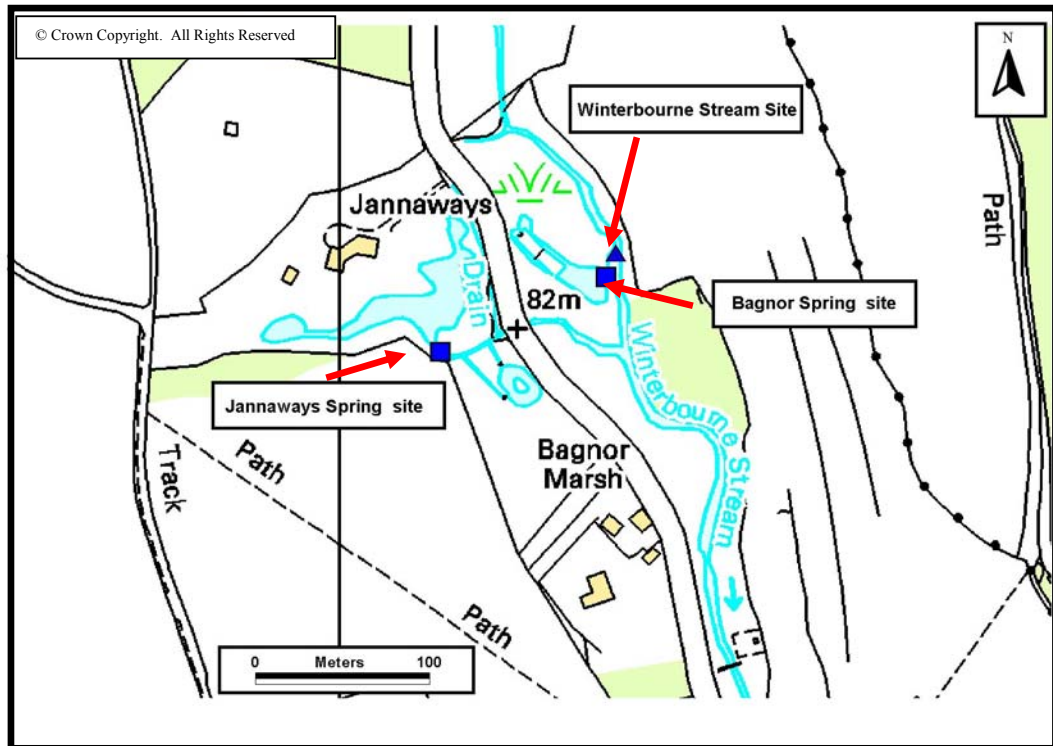


Figure 4.28: Detailed location of sampling sites at Bagnor and Jannaways springs

One-litre bacteriophage solutions with concentrations of 1×10^{12} pfu.ml⁻¹ were injected on 14 March 2005. *Enterobacter cloacae* was injected into Honeybottom stream sink between 14:30 and 14:45. Conditions were poor, with a flow of less than 0.05 L.s^{-1} , although the water was draining directly into a hole in the floor of the depression (Figure 4.29). *Serratia marcescens* bacteriophage was injected into Cromwells stream sink between 15:12 and 15:15. Despite a moderate flow of $\sim 2 \text{ L.s}^{-1}$ in the stream, water was ponded up to 1 m deep in the depression over an area of about 4 m by 6 m. Water drained away slowly through thick fine sediments lining the floor of the depression. It was not possible to excavate a drainhole through the sediment, so a side channel taking approximately half the flow was excavated to a smaller ponded area, which drained away slowly (Figure 4.30).



Figure 4.29: Low flow during tracer injection into Honeybottom sink



Figure 4.30: Tracer injection into excavated channel at Cromwells Sink

Five background samples taken from Bagnor spring, Jannaways spring and the Blue Pool were analysed using presence/absence analysis on ~ 30 to 60 mls of sample. No presence-absence analysis was performed on background samples from the Speen PWS boreholes or the River Lambourn, although 0.1 ml analysis to determine pfu.ml^{-1} was performed on some samples at these sites prior to tracer injection. The sample schedule following the tracer injections is summarised in Table 4.12. These samples were initially analysed using only 0.1 ml of sample to determine pfu.ml^{-1} . This was because CREH Analytical were anticipating large numbers of bacteriophages at any positive site. Later samples (collected after around 17/03/05) were analysed using 1 ml of sample to determine pfu.ml^{-1} . Around 1 week after injection it was clear that large numbers of bacteriophages were not present at any of the sites so all future samples were analysed using the presence/absence method on larger volumes (~65 mls). In

addition, a selection of samples analysed previously using 0.1 or 1 ml were re-analysed using the presence/absence method. Table 4.13 summarises the type of analysis performed on samples based on data provided by CREH Analytical.

Table 4.12: Sampling schedule during the Winterbourne tracer tests

	Method	Frequency	Duration
Bagnor Spring	Automatic water sampler	hourly to 8 hourly	2 weeks
Jannaways Spring	Automatic water sampler	hourly to 8 hourly	2 weeks
Winterbourne Stream	Hand samples	occasional	1 week
Speen PWS boreholes	Hand samples	4-5 times per day to 1 per 2 days	2 weeks
River Lambourn	Hand samples	1 per day	10 days
Blue Pool Outlet	Automatic water sampler	4 hourly to 12 hourly	22 days

Table 4.13: Sample volume and analysis method

Site	0.1 ml	1 ml	presence/absence
Bagnor	14/03/05 15:42 to 17/03/05 08:01	17/03/05 12:41 to 20/03/05 12:41	22/03/05 16:31 to 29/03/05 07:03
Jannaways	14/03/05 16:00 to 17/03/05 08:25	17/03/05 13:19 to 21/03/05 07:51	21/03/05 15:51 to 29/03/05 07:51
Blue Pool	12/03/05 07:50 to 16/03/05 07:36	16/03/06 10:36 to 21/03/06 15:32	21/03/05 16:36 to 06/04/05 12:31
Speen BH1	14/03/05 17:10 to 17/03/05 06:29	17/03/05 10:50 to 21/03/05 06:28	23/03/05 09:58 to 02/04/05 15:29
Speen BH2	14/03/05 17:11 to 17/03/05 06:30	17/03/05 10:54 to 21/03/05 06:29	22/03/05 10:14 to 02/04/05 13:30
Speen BH6	14/03/06 17:19 to 16/03/05 06:33	17/03/05 14:04 to 21/03/05 06:34	22/03/05 10:22 to 06/04/05 17:37
River Lambourn	14/03/05 18:09 to 16/03/05 10:36	17/03/05 11:11 to 20/03/05 11:00	21/03/05 09:54 to 27/03/05 12:44
Winterbourne Stream	14/03/05 17:43 to 16/03/05 09:55	17/03/05 11:56 to 20/03/05 11:35	24/03/05 11:25 to 25/03/05 14:03

4.6.3 Results

4.6.3.1 Background samples

All the background samples were negative, but presence/absence analysis was only performed on samples from Bagnor, Jannaways and the Blue Pool. 0.1 ml background samples for other sites were negative, but it is not certain whether a background tracer presence would have been detected using the more sensitive presence/absence method.

4.6.3.2 Results of Cromwells injection

Serratia marcescens from Cromwells sink was detected and confirmed present at three of the monitoring sites; Bagnor springs (1.25 km from Cromwells Sink), Jannaways springs (1.35 km from Cromwells Sink) and the River Lambourn (Figure 4.31). No tracer was detected in 90 samples from the Speen public water supply boreholes, 11 samples from the Winterbourne stream immediately upstream of Bagnor springs, or 80 samples from the Blue Pool. At Jannaways springs a single sample 9 days after injection was positive, but 93 other samples collected between 14th and 29th March were negative. Three samples collected from the River Lambourn 9 to 13 days after tracer injection were positive.

At Bagnor springs tracer was detected and confirmed present in 9 samples (Figure 4.32). This appears to be the main resurgence point for Cromwells stream sink. The groundwater velocity based on the 1st arrival of the tracer was 0.64 km.d^{-1} . Tracer was first detected on the 16th March 2 days (47 hours) after injection and was last detected on 27th March, 13 days after injection. During this period 39 other samples were negative. 38 samples collected prior to the 16th March, and 4 samples after the 27th March were also negative. Many of the positive results during the periods when only 0.1 ml or 1 ml of sample were initially analysed were detected later when samples were re-analysed using the large volume presence/absence technique. Figure 4.33 only shows results for samples that were analysed using the presence/absence technique.

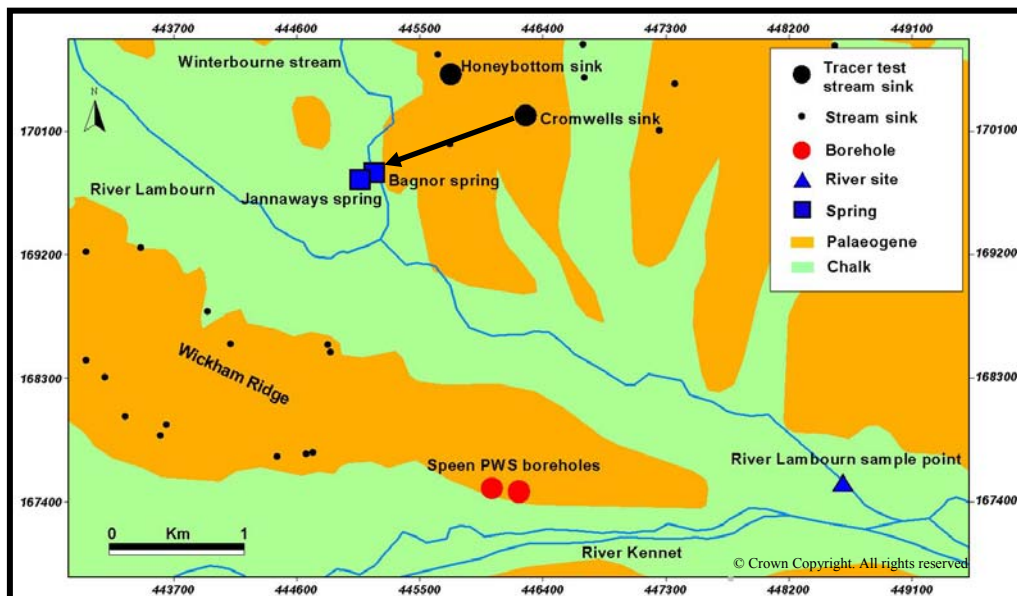


Figure 4.31: Results of tracer testing from Cromwells Sink^{BGS}

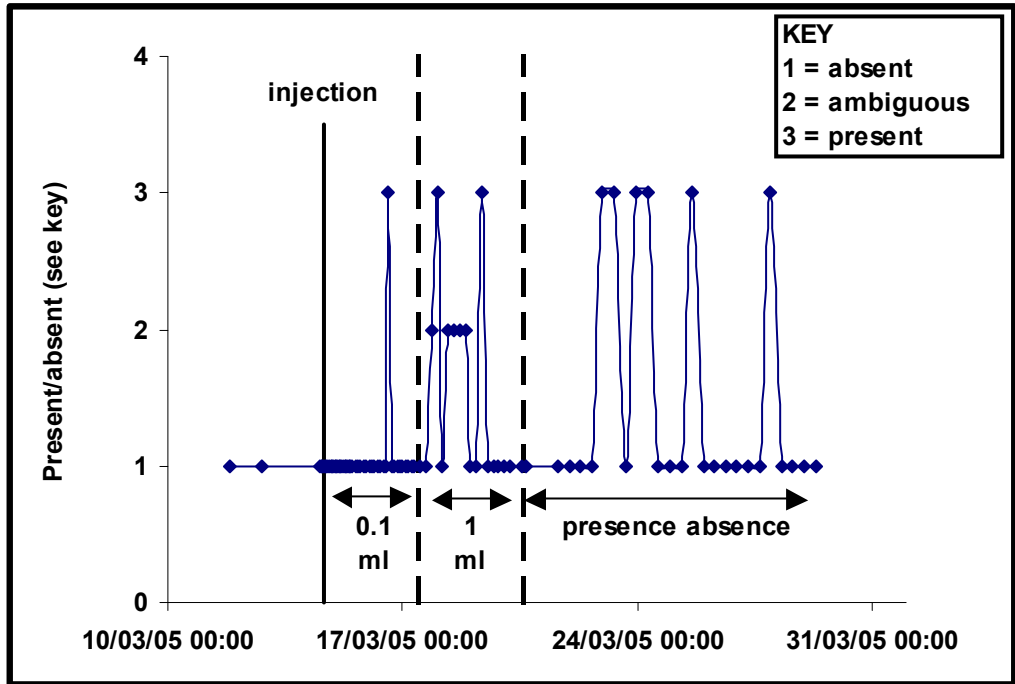


Figure 4.32: Results of *Serratia marcescens* at Bagnor

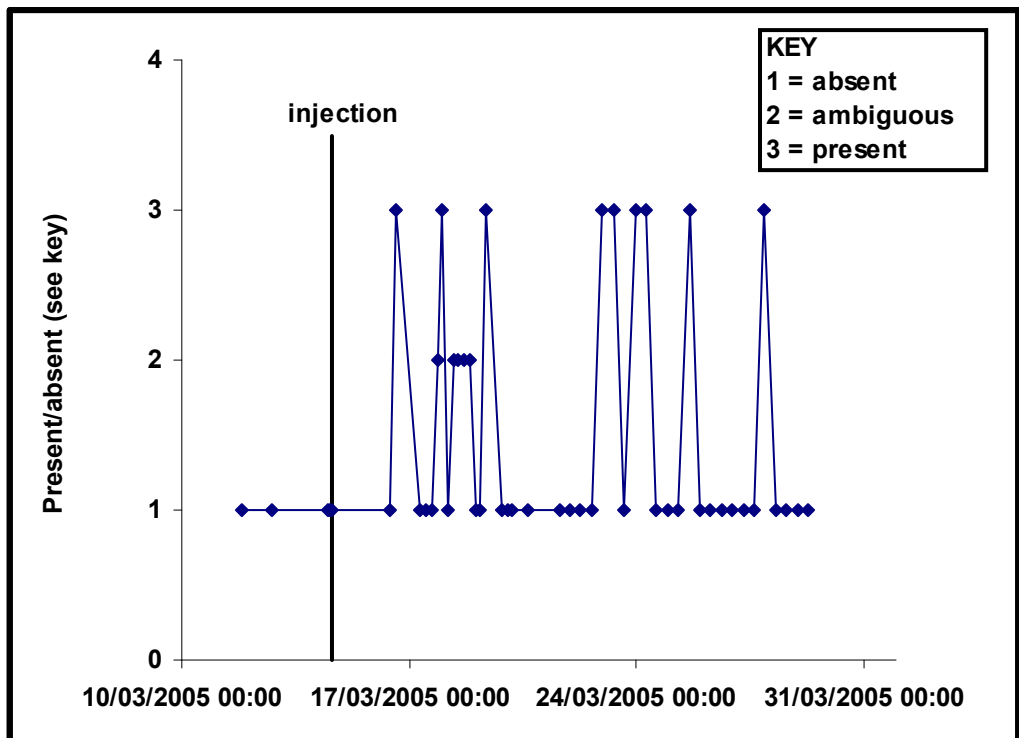


Figure 4.33: Results of *Serratia marcescens* at Bagnor, large volume presence/absence analysis only

4.6.3.3 Results of Honeybottom injection

Enterobacter cloacae was confirmed present in four samples from the River Lambourn on the 22nd, 24th, 25th and 27th March. 3 samples at Bagnor (4 days after injection), and 4 samples at the Blue Pool (5 days after injection) were “ambiguous” (Section 4.5.2). 87 samples from Bagnor and 87 samples from the Blue Pool were negative. No tracer was detected in 90 samples from the Speen public water supply boreholes, 93 samples from Jannaways springs, and 11 samples from the Winterbourne Stream.

4.6.3.4 Comments on sample volumes used in analysis

The results demonstrate that the large volume presence/absence test is required to detect the bacteriophages. Unfortunately this procedure was not used on samples taken in the first week following injection when *Serratia marcescens* was present at Bagnor springs. It is possible that if presence/absence analysis had been used for all samples from the outset:

- The first arrival time of the *Serratia marcescens* at Bagnor Springs might have been earlier.
- *Serratia marcescens* might have been detected in more samples from Jannaways spring.
- Conclusive results might have been obtained for the *Enterobacter cloacae* injected into Honeybottom stream sink.

4.7 Groundwater outlets and their catchment areas

4.7.1 Bagnor and Jannaways Springs

Tracer testing from Cromwells stream sink has conclusively demonstrated groundwater flow west-south-west to Bagnor springs (Figure 4.31), a flow direction that is not indicated by groundwater contours. Positive results were not obtained for the tracer test from Honeybottom stream sink, possibly due to the very small flow at the time of the test. Given that Honeybottom stream sink is very close to Cromwells stream sink it is likely that it is also connected to springs at Bagnor, although a repeat of the tracer test under higher flow conditions would be needed to confirm this.

There are small stream sinks along the Palaeogene/Chalk boundary to the east and west of Snelsmore Common, and it is probable that areas of Snelsmore Common may provide some or all of the catchment for Bagnor springs, although some flow may be

derived from the high ground to the north-north-west which is not characterised by karst stream sinks (Figure 4.34).

The single positive sample from Cromwells Sink at Jannaways springs suggests that Snelsmore Common may also provide some of the catchment for these springs, although it seems likely that most flow may be derived from the high ground to the north-north-west of the springs as this area lies upgradient according to regional groundwater contours. Discharge was not measured at either of the springs, and at Jannaways spring a proportion of the flow is abstracted for domestic use. A very rough estimate of flow would be $\sim 15 \text{ L.s}^{-1}$ at each spring. This would suggest a catchment area of ~ 2 to 3 km^2 for each spring assuming a mean annual recharge rate of 0.5 mm.d^{-1} (Section 3.4.5). The catchment area in Figure 4.34 is $\sim 8 \text{ km}^2$ (outlined in black). Further tracer testing might determine the northerly and easterly extent of the Snelsmore Common contribution to these springs.

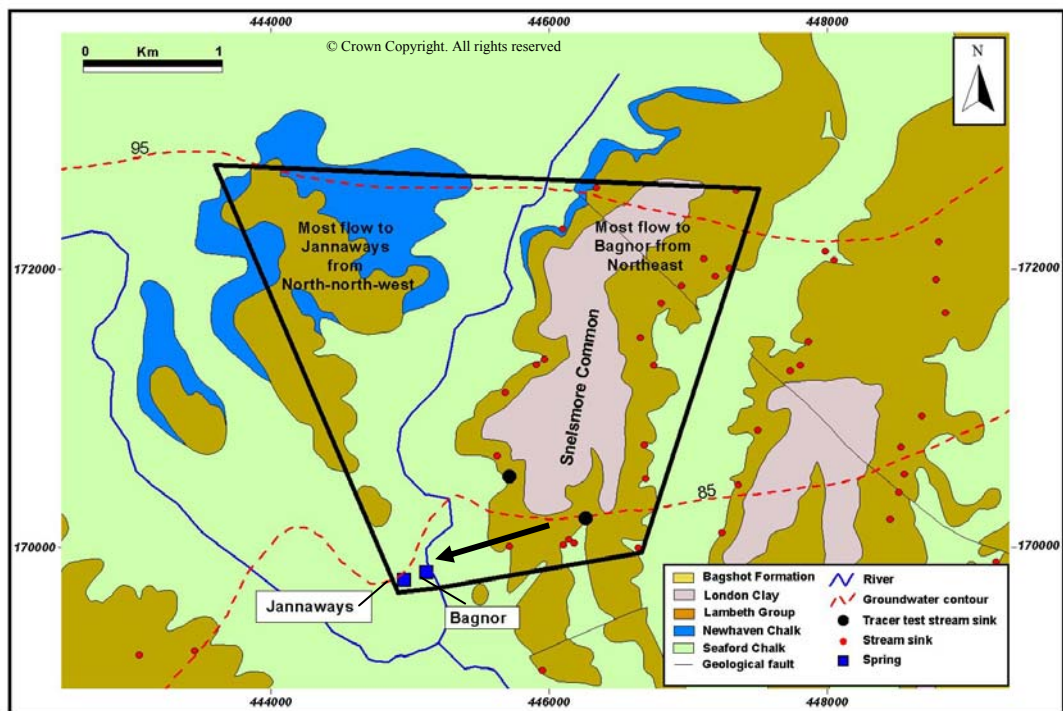


Figure 4.34: Possible catchment area of Bagnor and Jannaways springs (thick black line) with arrow indicating proven connection from Cromwells Sink.

Groundwater contours are from Figure 2.13 (high water table)^{BGS}

4.7.2 The Blue Pool spring

The size of the Blue Pool catchment is estimated at about 35 km² although it could be anywhere in the range of 14 to 58 km² (Section 3.4.5). Although there is no detailed spring hydrograph data for the Blue Pool to determine spring response to precipitation, flow data were collected on 15 occasions between 1976 and 1988 (Banks, personal communication, 2005). Discharge varied between 150 L.s⁻¹ (05/08/76) and 240 L.s⁻¹ (07/01/83). The narrow range of these limited data suggests that there is a large baseflow component to the Blue Pool, and that the proportion of flow derived from point recharge through stream sinks may be quite small, with diffuse recharge playing an important role. This hypothesis is supported by observations of the stream sinks in the catchments. The Smithcroft Copse stream sink only contributes a very small proportion of flow to the Blue Pool (the flow into the sink was approximately 3-4 L.s⁻¹ at the time of the tracer test compared to the Blue Pool flow of 200 L.s⁻¹). The Blue Pool water cannot be derived exclusively from stream sinks, as even if all stream sinks in both the Pang and Lambourn catchments were connected to the Blue Pool they do not provide sufficient flow. (A rough estimate for combined recharge from all stream sinks is ~ 100 L.s⁻¹ following heavy or prolonged rainfall in winter, ~15 L.s⁻¹ in dry periods). More importantly, most stream sinks only flow in winter. The large summer flow from the Blue Pool implies a significant additional source that flows more slowly but consistently throughout the year, and therefore the conduit system must be constantly recharged by water released from storage. One obvious location for such storage is the Chalk aquifer itself, but it is possible that perched groundwater bodies in the Palaeogene also contribute significantly. These hydrological observations suggest that the catchment area is likely to comprise point and diffuse recharge over a laterally extensive area as opposed to isolated stream sink inputs, and that there must be some connectivity between conduits, fissures and fractures.

There is still considerably uncertainty regarding the location of the Blue Pool catchment, but a conceptual model of the likely location in light of the new tracer test results is presented here.

Tracer tests demonstrate conclusively that the catchment comprises Smithcroft Copse stream sink 5.1 km to the west and Mirams Copse stream sink 1.2 km to the north-north-west. Both these groundwater flowpaths are slightly across the gradient as

indicated by the groundwater contours, although the groundwater contours are only based on a small number of widely spaced boreholes in this area. Assuming that these connections do not represent totally isolated conduits it is probable that the catchment extends between these sites (thick black line on Figure 4.35). This area comprises 7 km². The remainder of the catchment is harder to define.

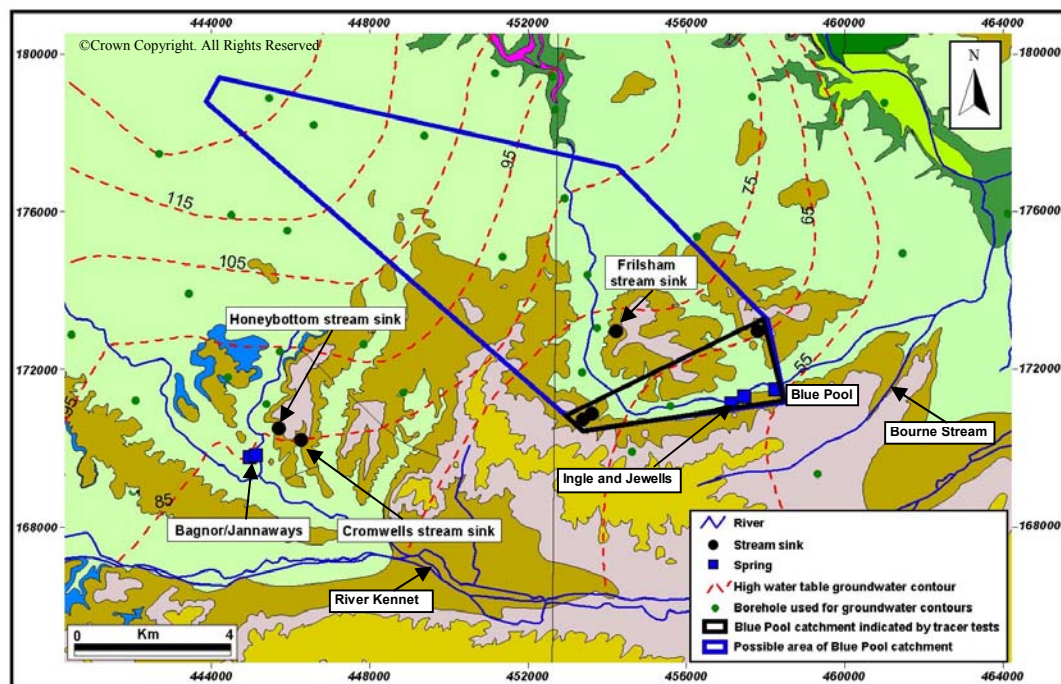


Figure 4.35: The catchment area of the Blue Pool proven by tracer testing (black line) and possible area of extension to the northwest (blue line)^{BGS}

It is unlikely that the Blue Pool catchment extends to the south where the Chalk becomes increasingly confined by Palaeogene strata that appear to be relatively impermeable. There are no surface karst dolines or stream sinks which would provide a recharge mechanism through to the underlying chalk and most of the precipitation falling on this area contributes to surface runoff in the Kennet, Pang and Bourne rivers.

It is possible that the Blue Pool catchment area extends further west beyond Smithcroft Copse, perhaps even as far as Honeybottom stream sink. The timing of the four ambiguous samples (5 days after injection) at the Blue Pool during the Honeybottom tracer test is a surprising coincidence. However such a connection seems unlikely because it would require groundwater flow over a very long distance in a direction aslant the water table gradient. Honeybottom stream sink is very close to Cromwells

stream sink which was demonstrated to be connected to springs to the southwest at Bagnor, and it is much more likely that Honeybottom stream sink is connected to springs at Bagnor (where ambiguous results were also obtained).

It is most likely that the Blue Pool catchment area extends to the northwest (the area outlined in blue on Figure 4.35), although the exact westerly and northerly boundaries are uncertain. The main advantages of this hypothesis are that this would involve an extension of the area proven to be connected to the Blue Pool by the tracer testing, and this extension is directly upgradient in an area of groundwater contours that are relatively well defined by boreholes. The high water table groundwater contours from Figure 2.13 were used in Figure 4.35 because the tracer testing was undertaken in winter. However, Figure 2.13 shows that under low water table conditions there is a much greater easterly flow from the Lambourn catchment across the Pang towards the Thames, and less northerly flow within the Pang towards the Blue Pool, suggesting that the Blue Pool catchment may extend towards the west more than the north.

Comparison of Blue Pool water chemistry data with Palaeogene and Chalk groundwaters shows that the Blue Pool has an intermediate chemistry, closer to pure Chalk than pure Palaeogene waters, with an increased Palaeogene signature following rainfall (Wheater et al., 2006b). This implies that recharge through stream sinks and dolines located on Palaeogene strata is particularly important during wet periods, but also indicates the importance of chalk groundwater storage in maintaining the Blue Pool baseflow. A catchment to the northwest of the Blue Pool incorporates a significant area of Palaeogene where stream sinks and dolines are present, and also a large area of chalk. This would account for the chemistry observations of Wheeler et al. (2006b).

The proposed catchment area extends across the River Pang into the Lambourn catchment. Flow accretion studies in the Pang (Bricker, 2004; Griffiths et al., 2006) indicate that there is no significant accretion downstream of Frilsham until the inputs from Ingle and Jewells springs. A small amount of accretion occurs from surface runoff from constructed land drains and the STW at Briff Lane, but Bricker (2000) and Griffiths et al. (2006) noted that the Pang loses water over this section during low flow periods. It is possible that in high flow the loss still occurs but is less than the gain from surface runoff. These losses from the River Pang are likely to drain into the

groundwater flow system feeding the Blue Pool (and perhaps also Ingle and Jewells springs). Water levels in boreholes adjacent to this section of the River Pang are about 5-10 m below the river level, also indicating the potential for losses from the river to the underlying chalk (Section 2.8.6.2). Above Frilsham there is much greater accretion (Bricker, 2000 and Griffiths et al., 2006) and baseflow index studies suggest that this is derived from groundwater (Section 2.7). The groundwater contours (Figure 2.13) suggest that the influence of the low level aquifer boundary of the River Thames is so great that much groundwater probably flows beneath the Pang even in these upper reaches where flow accretion occurs, and the river itself merely forms an overflow for the uppermost part of the groundwater body. This implies a proportion of recharge in the area to the west and northwest of the upper reaches of the River Pang is discharged in the river rather than at the Blue Pool. The area outlined in blue on Figure 4.35 is $\sim 58 \text{ km}^2$, which at the upper end of the estimated area for the Blue Pool catchment (Table 3.4). It is likely that some of the water within this area is discharged in the upper reaches of the River Pang, and also at Ingle and Jewells springs which have an estimated catchment area of $\sim 9 \text{ km}^2$ (Section 4.7.3).

The main disadvantage of the hypothesized catchment area is that no tracer from Frilsham stream sink was detected at the Blue Pool. However, Frilsham sink is located in the area between Smithcroft Copse and Mirams Copse, and this position suggests that it may be connected to the Blue Pool. Given the extremely high attenuation in the test over 1.6 km from Mirams Copse, it is possible that the tracer from Frilsham sink (a further 3 km from the Blue Pool) could have arrived below the detectable threshold.

In conclusion, it is likely that the Blue Pool is recharged by a mixture of point inputs through stream sinks and dolines, and more diffuse recharge through the Chalk and more permeable parts of the Palaeogene, and that the catchment covers an area extending to the west and north although the exact north and west boundaries are uncertain.

4.7.3 Ingle and Jewells springs

No tracer from the Smithcroft Copse test or the Mirams Copse Photine test was detected at Ingle or Jewells springs and the catchments of these springs remain very uncertain. The combined discharge of the two springs at the time of the Smithcroft Copse tracer test was $\sim 50 \text{ L.s}^{-1}$, which would indicate a catchment area of $\sim 9 \text{ km}^2$, assuming a recharge rate of 0.5 mm.d^{-1} (Section 3.4.5).

Given the likely location of the Blue Pool catchment (Figure 4.35), and the lack of recharge to the Chalk in the area to the south of Ingle and Jewells springs, it seems unlikely that they have a different geographical catchment area. It is most likely that the springs are either fed by groundwater flow from the northwest or the west (both areas also within the likely Blue Pool catchment area). Samples from springs in the Pang and Lambourn were analysed for CFCs and SF_6 in an investigation of groundwater ages undertaken by George Darling and Daren Goody as part of the LOCAR project. CFCs could not be used for age determination because samples were affected by contamination but concentrations at Ingle and Jewells springs were similar to those at the Blue Pool. SF_6 results were also similar at the three sites and suggested a bulk age of 15 years (Darling, personal communication, 2006).

Groundwater contours suggest the springs may be fed by flow from the northwest (Figure 2.13). There are many stream sinks present in this area, which could be connected to the springs (Figure 3.1). Unfortunately, due to the high analytical costs Ingle and Jewells springs were not sampled during the bacteriophage tracer test from Frilsham stream sink that is directly upgradient of the springs. However, during the Sodium Fluorescein tracer test from Smithcroft Copse and the Photine tracer tests from Mirams Copse, Ingle and Jewells springs did not appear to become turbid or have a significantly higher discharge following rainfall. This suggests that there is no fully connected network of larger fissures and conduits between stream sinks and these springs. It seems most likely that the springs are fed by groundwater flow in smaller fractures and fissures.

This also fits with the alternative hypothesis that Ingle and Jewells springs are fed by groundwater flow from the west. Given that the springs lie almost directly along the line of the proven connection between the Smithcroft Copse area and the Blue Pool, it

seems likely that the springs could also be fed by flow from the west. Previous tests in other areas of the English Chalk have demonstrated divergent flow from stream sinks to multiple outlets (Harold, 1937; Atkinson and Smith, 1974). If groundwater flow between the main Smithcroft Copse-Blue Pool flowpath and Ingle and Jewells springs is through smaller fractures and fissures then the Sodium Fluorescein tracer used in the 2005 experiment could have been attenuated to below the detection threshold. The more detectable bacteriophage tracers (without which the connection between Mirams Copse and the Blue Pool would not have been identified) were not monitored at Ingle and Jewells springs during any of the tracer testing. Further bacteriophage tracer testing from Smithcroft Copse stream sink and the closest stream sink to the northwest of the springs might determine whether they are fed by flow from the west or the northwest.

4.7.4 Connectivity between stream sinks and boreholes

Tracer testing provided no direct evidence of connectivity between stream sinks and boreholes. All samples from the Bradfield PWS, Maidenhatch Farm borehole, Frogmore Farm borehole, and the Speen PWS boreholes were negative. This demonstrates that there are no rapid pathways with low attenuation between the stream sinks tested and the boreholes monitored. Background fluorescence at tracer wavelengths at all borehole sites was significantly lower than at spring sites, suggesting that there is a higher degree of attenuation of fluorescent substances in groundwater in boreholes than springs. It is possible that tracer did arrive at one or more of the borehole sites at concentrations below the detection threshold. It is just as likely that groundwater in these boreholes comes from groundwater bodies unconnected to karst conduits and fissures.

The boreholes that were sampled at Speen PWS (Figure 4.31) are not characterised by turbidity following rainfall. However, water in other boreholes at the site are intermittently turbid, perhaps indicating connectivity to stream sinks. The boreholes affected by turbidity are no longer pumped and therefore they could not be sampled during the tracer test. It is possible that these boreholes are connected to stream sinks on Snelsmore Common, however given the results at Bagnor and Jannaways springs, it is much more likely that the Speen boreholes are connected to closer stream sinks identified along the Wickham Ridge to the west of the abstraction site (Figure 4.31).

4.7.5 River-aquifer interactions

The high attenuation observed during the tracer testing suggests that the techniques used are not sensitive enough to detect small groundwater inflows into rivers. *Serratia marcescens* bacteriophage from Mirams Copse sink present at the Blue Pool was not detectable downstream in the River Pang. In the River Thames, it is probable that even a large submerged spring in the river bed would not be identified from tracer testing because of the enormous dilution by the river water into which it would discharge.

There are three explanations for the positive samples in the River Lambourn following tracer injections into Honeybottom and Cromwells sinks:

- 1) Tracer was discharged at Bagnor and Jannaways springs and reached the River Lambourn via the Winterbourne Stream (Figure 4.27).
- 2) Tracer was discharged from another groundwater outlet through the bed of the River Lambourn between the confluence with the Winterbourne stream and the downstream sampling point.
- 3) Apparent positives at the River Lambourn sampling site were actually background tracer not derived from the tracer test.

The first two explanations are unlikely because tracer from Honeybottom sink was not detected at the springs, and tracer from Cromwells Sink was at the threshold of detection, and there would be considerable additional dilution in the River Lambourn. Background presence of the bacteriophages was not measured in the River Lambourn but background samples from the Pang and Thames rivers did contain small amounts of both bacteriophages suggesting that there may also be a background presence of these bacteriophages in the River Lambourn. It is therefore most likely that the apparent positives in the River Lambourn were in fact not a consequence of the injected tracer.

The Winterbourne stream was sampled immediately upstream of its confluence with the outlet from Bagnor Spring (Figure 4.28). The aim was to detect any tracer that was discharged through the bed of the Winterbourne stream upstream of the inputs from Bagnor and Jannaways springs. No samples were positive at this site indicating that there is no significant discharge into the Winterbourne Stream, despite the fact that groundwater flowing from Cromwells stream sink to Bagnor spring must pass underneath it. Insufficient samples were taken to conclude with certainty that no small

groundwater discharges occurred, but it appears that the stream may be hydrologically unconnected to the fissures and conduits that discharge at the springs.

4.8 Groundwater velocities from natural gradient tracer tests

Groundwater velocities obtained from tracer tests in the Pang and Lambourn catchments are very high (Table 4.14).

Table 4.14: Groundwater velocities in the Pang-Lambourn catchments

Injection sink	Spring	Test date	Distance (km)	*Groundwater velocity (km.d⁻¹) (spring)	*Groundwater velocity (km.d⁻¹) (outlet)
Holly Grove	Blue Pool	19/07/88	4.7	6.8 (5.8)	
Tylers Lane	Blue Pool	1988		6.6?	
Smithcroft Copse	Blue Pool	31/01/05	5.1	[7.2]	6.1 (5.1)
Smithcroft Copse	Blue Pool	07/02/05	5.1	[6.6]	5.7 (4.7)
Smithcroft Copse	Blue Pool	26/02/06 [^]	5.1	6.7 (5.9)	5.7 (4.7)
Miramms Copse	Blue Pool	15/02/06	1.6	4.3	
Cromwells	Bagnor	14/03/05	1.25		0.6

**Groundwater velocities are based on time to 1st detection of tracer. For the Blue Pool values in brackets are velocities based on time to tracer peak. Values in square brackets are based on time to first detection at the spring assuming a travel time of 3 hours 10 minutes between the main spring and the outlet (Section 5.4.2.4)*

[^]Groundwater velocities are for Sodium Fluorescein. Three other simultaneously injected tracers indicated the same velocity; a fourth (Amidorhodamine G) arrived and peaked slightly later due to sorption.

Velocities based upon first detection of tracer range from 0.6 to 7.2 km.d⁻¹, although the velocity of 0.6 km.d⁻¹ between Cromwells sink and Bagnor springs is likely to be an underestimate (Section 4.6.3.4). Velocities in the Pang and Lambourn are similar to those obtained from previous tracer tests from stream sinks in the English Chalk (Harold, 1937; Atkinson and Smith, 1974), which varied from 2 to 6.8 km.d⁻¹ based on time to first arrival of tracer (Table 1.4). These chalk groundwater velocities appear to be slightly higher than the average groundwater velocity of 1.7 km.d⁻¹ quoted by Smart and Worthington (2004) for karst aquifers. However, they are similar to those reported for the Carboniferous Limestone in the UK. For example Atkinson (1977) reports that the mean groundwater velocity from 48 groundwater connections between stream sinks

and springs in the Carboniferous Limestone of the Mendips is 6.3 km.d^{-1} (with a range of 0.52 to 21.2 km.d^{-1}). Similar velocities are also found in the Carboniferous Limestone of South Wales (Gascoine, 1989).

Groundwater velocities from three repeated tracer tests during winter from Smithcroft Copse stream sink varied between 6.6 and 7.2 km.d^{-1} , indicating that groundwater velocities from a single site are fairly consistent. Results from nearby Holly Grove and Tylers Lane sink during a summer period were within this range (6.8 km.d^{-1}), suggesting that groundwater velocities may not have substantial seasonal variations. The similarity between velocities from the three stream sinks also suggests that conditions at the individual sink point do not significantly affect the groundwater velocities; and that water sinking at all sites fairly quickly reaches a conduit system that connects this whole area to the Blue Pool. This implies that there is a relatively short distance from each sink through the Palaeogene cover, and through the Chalk unsaturated zone before reaching the main conduit system.

The small variation in velocities may relate to the variation in discharge at the Blue Pool at the time of the tests (Figure 4.33), although the measured variations in the Blue Pool flow are small ($<2\%$). Stanton and Smart (1981) found that in repeated tracer tests over several connections in the Mendips, travel time was inversely proportional to the first power of resurgence output. They concluded that this 1:1 relationship was an indication that flow was in phreatic conduits. The data from Smithcroft Copse appear reasonably consistent with this model. Using the best fit linear relationship depicted in Figure 4.33, which shows a strong correlation between groundwater velocity and flow rate, and considering just the range over which values were actually measured (groundwater velocities of 6.6 to 7.2 km.d^{-1}), the slope of the relationship is 1:1.3. An alternative way of fitting a straight line to these data (minimising residuals of velocity instead of flow) gives a ratio of 1:1.2. Both estimates imply that velocity increases more than would be predicted by the 1:1 relationship expected from a simple phreatic conduit. This might be due to the combination of sparse data with errors in discharge measurement. However, if the conduits were predominantly vadose the ratio of increases in velocity to increases in flow would be expected to be $< 1:1$. Thus it is likely the conduit or fissure systems connecting the Smithcroft Copse area to the Blue Pool are located in the saturated zone through most of their length.

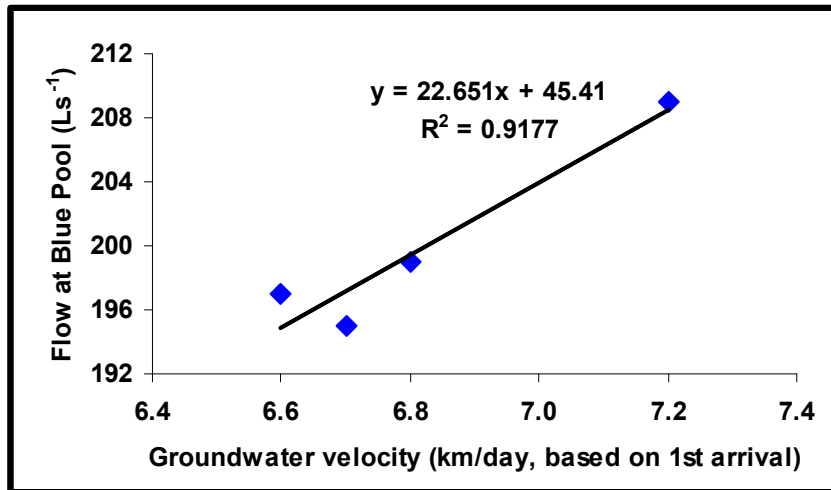


Figure 4.33: Correlation between groundwater velocity and Blue Pool discharge

4.9 Tracer attenuation

Tracer attenuation was extremely variable. Tracer recoveries are discussed in detail in Chapter 5 but summarised here in Table 4.15. Dye attenuation along the Smithcroft Copse-Blue Pool flowpath was lowest, although a significant proportion of dye was lost (~ 75%). Attenuation along the Mirams Copse-Blue Pool flowpath was very high. Recoveries of *Serratia marcescens* bacteriophage were extremely low, and Photine C tracer was completely attenuated. Negative results following *Enterobacter cloacae* injections into Honeybottom and Frilsham sinks appear to be due to complete attenuation as they are likely to be connected to springs that were monitored during the tracer tests (Section 4.7).

Attenuation can be due to tracer related factors or aquifer related factors and in order to draw inferences about the nature of the aquifer it is necessary to eliminate tracer related causes of attenuation. Photine C can be lost due to sorption on organic matter and photochemical decay (Smart and Smith, 1976; Smart and Laidlaw, 1977). It is possible that in the Mirams Copse test some losses occurred due to sorption on organic matter at the stream sink, especially during injections when there was very little flow. Sorption during transport through the Chalk is less likely to have affected the result. Tests by Smart and Laidlaw (1977) indicated that Photine C has low sorption onto inorganic matter, (including limestone), although no sorption tests have been carried out on chalk. Photochemical decay should not have affected the detectors at the Blue Pool as they were placed very close to the upwellings. In the chalk tracer study by Price et al. (1992)

90 kg of a 20 % solution of Photine C was injected into a soakaway and detected in a borehole 3 km away although at extremely low concentrations. *Serratia marcescens* bacteriophage was used along the same flowpath and was also detected at low levels (but with a peak of 6 pfu.ml⁻¹ that is higher than the concentrations of *Serratia marcescens* measured during the Mirams Copse tracer test). In the Mirams Copse test the maximum amount of Photine C injected was 1 kg (4 litres of a 20 % solution). The positive results with *Serratia marcescens* suggest that insufficient quantities of Photine C were used. If dilution of the peak concentration of Photine C was similar to that observed for the bacteriophage, 4 orders of magnitude more would have been needed to produce a positive result. Even assuming that 2 or 3 orders of magnitude could be accounted for in terms of the higher attenuation of bacteriophages compared to dyes, 10 to 100 kg of Photine C would have been needed suggesting that it would not be practicable to obtain a positive result using this tracer, and also that the approach adopted for planning was overly cautious.

Table 4.15: Tracer recoveries in the Pang-Lambourn catchments

Stream sink	Tracer	Recovery at spring (% of injection)
Smithcroft Copse	Dyes*	22-25
Smithcroft Copse	Amidorhodamine G	14
Smithcroft Copse	<i>Phix 174</i> bacteriophage	0.87
Mirams Copse	Photine C	0
Mirams Copse	<i>Serratia marcescens</i> bacteriophage	0.00005 [^]
Cromwells	<i>Serratia marcescens</i> bacteriophage	0.000007 [^]
Frilsham	<i>Enterobacter cloacae</i> bacteriophage	0
Honeybottom	<i>Enterobacter cloacae</i> bacteriophage	0

*Excluding Amidorhodamine G which was sorbed

[^]Assuming 1 plaque per 200 mls for period of tracer discharge (this is likely to be a high estimate of recovery).

As mentioned in Section 4.2, in comparative studies bacteriophages often have higher losses than fluorescent dyes, especially under low flow conditions. This is because bacteriophage tracers are strongly affected by inactivation and sorption. Three different bacteriophages were used in the Pang and Lambourn. *Phix 174* was used in conjunction with four dye tracers enabling a direct comparison in tracer performance (discussed in detail in Chapter 5). Whilst recovery of the bacteriophage was significantly lower than the dyes (Table 4.15), a breakthrough curve with a peak concentration of 1140 pfu.ml⁻¹ was obtained using the bacteriophage. Goyal and Gerba (1979) studied the sorptive

behaviour of five bacteriophages in soils and concluded that sorption of bacteriophages is extremely variable but Phix 174 was one of two bacteriophages found to be the least sorbed. In a review of inactivation and sorption of bacteriophages Schijven and Hassanizadeh (2000) note that *Phix 174* is a relatively conservative bacteriophage tracer because it has low hydrophobicity and high stability. It is therefore important to consider whether higher losses of *Serratia marcescens* and *Enterobacter cloacae* could be because these tracers are more susceptible to sorption and/or inactivation than *Phix 174*.

In the present study positive results were obtained following two injections using *Serratia marcescens* bacteriophage (Mirams Copse and Cromwells stream sinks), but in both cases only very small amounts of the bacteriophage were detected ($< 1 \text{ pfu.ml}^{-1}$). The negative results following the injection of 1 kg of Photine C at Mirams Copse suggest that the high attenuation of the *Serratia marcescens* at this site (and therefore perhaps also that during the test at Cromwells stream sink) is likely to be due to aquifer characteristics as opposed to bacteriophage properties. It appears that the flowpath between Mirams Copse and the Blue Pool is much more attenuating than that between Smithcroft Copse and the Blue Pool, although the same tracer was not used over both flowpaths. There are no other groundwater tracer studies in which *Phix 174* and *Serratia marcescens* were used simultaneously. However there are chalk tracer studies in which *Serratia marcescens* was successfully used and greater concentrations were measured (Skilton and Wheeler, 1988; Price et al., 1992). Although there are no chalk tracer studies in which both Sodium Fluorescein and Photine C were used, a study using both tracers in Carboniferous Limestone demonstrated similar recoveries (Smart, 1988). The evidence therefore suggests that the extremely high attenuation of Photine C and *Serratia marcescens* between Mirams Copse and the Blue Pool is a reflection of the nature of the aquifer. This may also be true for the Cromwells-Bagnor flowpath, although at this site the tracer was injected into a ponded area underlain by fine clay material and organic matter, which may have caused much greater sorption than at Mirams Copse.

Conclusive positive results were not obtained following injection of *Enterobacter cloacae* bacteriophage at two sites and because no other tracers were used at these sites inferences about the nature of the aquifer are more conjectural. However, Skilton and

Wheeler (1988) undertook three tracer tests between observation and pumping boreholes (122 to 366 m apart) in the Chalk in Yorkshire in which both *Serratia marcescens* and *Enterobacter cloacae* were simultaneously injected. Percentage recoveries were similar for both tracers (Table 4.16), suggesting that in the Chalk, *Enterobacter cloacae* may have a similar performance to *Serratia marcescens*.

Table 4.16: Comparative recoveries of *Serratia marcescens* and *Enterobacter cloacae* during three tracer tests in the Yorkshire Chalk (Skilton and Wheeler, 1988)

	% Recovery of <i>Serratia marcescens</i>	% Recovery of <i>Enterobacter cloacae</i>
Experiment 1	0.49	0.12
Experiment 2	0.23	0.34
Experiment 3	0.10	0.18

It is therefore probable that differences in attenuation during the Pang-Lambourn tracer tests are due to differences in the groundwater flowpaths. These may be differences in the thickness of Palaeogene cover or the unsaturated zone, or differences in the nature of the voids through which the tracer is transported in the saturated zone. It is unlikely that thickness of Palaeogene cover is the cause of high attenuation because the site of lowest attenuation (Smithcroft Copse) is furthest from the Palaeogene/Chalk boundary and therefore likely to be underlain by the thickest Palaeogene deposits. However, there does appear to be a thinner unsaturated zone beneath Smithcroft Copse than at other sites (Table 4.17), suggesting that tracer may have been attenuated at other sites during transport through the unsaturated zone. It seems likely that attenuation also occurs in the saturated zone, and that in both zones tracers may have been transported through narrow voids in which dyes were affected by double porosity diffusion and bacteriophages were affected by sorption. Both types of tracer may also have been affected by dispersion.

Table 4.17: Estimated thickness of the unsaturated zone beneath stream sinks

Sink	Miramms Copse	Smithcroft Copse	Frilsham	Cromwell	Honeybottom
Sink elevation (m AOD)	82	78	89	115	114
High water level at sink (m AOD)	65	68	72	85	86
Low water level at sink (m AOD)	58	65	69	81	82
Unsaturated zone thickness (m)	17-24	10-13	17-20	30-34	28-32
Spring elevation (m AOD)	55-60	55-60	55-60	82-85	82-85

4.10 Relationship between attenuation and velocity

The relationship between attenuation and velocity observed in the present tracer tests differs from previous results. In all past chalk tracer tests in which injections were via stream sinks (Coddington, 1910; Harold, 1937; Atkinson and Smith, 1974; Banks et al., 1995; Barnes et al., 1999; Massei et al., 2002, see Section 1.3.5), and in the present Smithcroft Copse test, there was rapid groundwater flow (0.6 to 7.2 km.d^{-1}) combined with low tracer attenuation (visible coloration or recoveries ~ 20 to > 90 %). In contrast, tests from Mirams Copse and Cromwells sinks had high groundwater velocities but very high attenuation of tracer. These tests appear to be similar to previous chalk studies in which tracer was injected into boreholes or soakaways and moderate or high groundwater velocities were combined with very high attenuation (e.g. Price et al., 1992; Ward et al., 1998).

High attenuation would be expected to be associated with lower groundwater velocities because lower groundwater velocities generally occur in narrower voids where more attenuation can occur because there is a greater volume to surface area ratio enabling more diffusion and more sorption. A quantitative tracer test from Smithcroft Copse using multiple tracers was undertaken to investigate tracer attenuation mechanisms further and is the subject of Chapter 5.

4.11 Conclusions of qualitative tracer testing

The results provide some new information regarding groundwater flow directions in the Pang and Lambourn catchments. The Blue Pool catchment has been shown to extend to the north of the River Pang as well as to the west. Bagnor and Jannaways springs are fed by groundwater flow from the east-north-east, rather than the north-north-west as might be predicted from groundwater contours.

In the areas tested there are no flowpaths with rapid groundwater flow and low attenuation between stream sinks and boreholes. Tracer may have reached these sites below the detection threshold. However, very low background fluorescence in borehole waters suggests high attenuation of solutes and a possible lack of connectivity between fractures and fissures supplying these boreholes and voids forming flowpaths associated with stream sinks and large springs. It is possible that some of the boreholes at the Speen PWS that were not monitored during the current study may be connected to stream sinks on the Wickham Ridge to the west of the supply.

The low variability of chalk spring discharges and high BFI of chalk streams indicates they are supported by a very large reservoir of groundwater. Thus the Chalk aquifer has high storage combined with moderate permeability over much of its area and volume. However, tracer connections between stream sinks and springs over distances of several kilometres indicate that embedded within the aquifer are some very much more permeable pathways along which water flow is rapid. Some of these pathways combine rapid flow and low attenuation, a combination well known from cavernous and fissured karst aquifers. Others show rapid flow combined with very high attenuation of particulates and solutes, suggesting that sections of the flowpath have a high surface-to-volume ratio and probably comprise narrow fissures (a few mm to < 1mm wide). Similar degrees of attenuation have been observed previously in tracer tests from boreholes and soakaways in the Chalk (e.g. Price et al., 1992; Allen et al. 1998), but not from sinking streams. Results from Frilsham and Honeybottom tests suggest that there may also be many streams sinks connected to springs by flowpaths along which attenuation is so high that tracers are not detectable using current tracing techniques.

Chapter 5: Investigations of groundwater flow and contaminant attenuation along the Smithcroft Copse-Blue Pool flowpath

5.1 Introduction and background

Tracer testing in the Chalk has demonstrated very rapid groundwater flow between stream sinks and springs (Harold, 1937; Atkinson and Smith, 1974; Banks et al., 1995; and results during the present study from Smithcroft Copse, Mirams Copse and Cromwells stream sinks presented in Chapter 4). The speed of groundwater flow suggests that fully connected systems of conduits have developed in some areas of the Chalk. In karst aquifers such a conduit network would normally result in very low attenuation of tracers and contaminants. However, tracer losses during tests in the Pang and Lambourn catchments suggest that rapid groundwater flow in the Chalk can be combined with moderate to very high tracer attenuation (Sections 4.9 and 4.10). In this chapter quantitative tracer test results are used to investigate the mechanisms that govern contaminant attenuation and to try to determine the process by which tracers (and contaminants) can be transported to groundwater outlets very rapidly but with high losses. It is well established that substances diffuse from fractures and fissures into the porous chalk matrix (Foster, 1975; Barker, 1993). This chapter describes tracer tests designed to investigate whether advection-dispersion or double porosity diffusion (sometimes described as matrix diffusion) is the dominant mechanism of contaminant attenuation along the groundwater flowpath between Smithcroft Copse and the Blue Pool. The main experiment used a simultaneous injection of multiple tracers with different molecular weights (and hence diffusion properties).

In single porosity aquifers with low matrix porosity solutes only move through fractures, fissures and conduits (upper part of Figure 5.1). In contrast the Chalk is a double porosity aquifer in which tracers or contaminants can diffuse from the fractures, fissures and conduits into pores in the surrounding rock matrix (lower part of Figure 5.1).

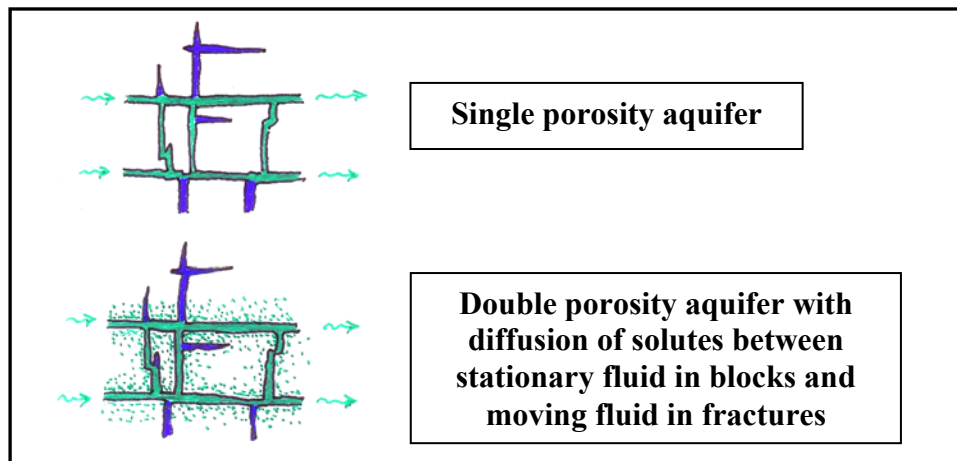


Figure 5.1: Single and Double porosity aquifers (Atkinson, personal communication, 2003)

In single porosity aquifers solute transport is by advection. Attenuation of solutes is by retardation due to sorption and by hydrodynamic dispersion, which includes molecular diffusion and mechanical dispersion. Molecular diffusion is defined by Fick's Laws and is the spreading out of solutes from regions of high to low concentration because of the concentration gradient (Fetter, 2001). Mechanical dispersion is the spreading out of solutes that arises because solute molecules do not all travel along exactly the same path through the aquifer. It comprises longitudinal dispersion along the direction of groundwater flow and lateral or transverse dispersion at 90^0 to the flow direction (Fetter, 2001). In porous media, longitudinal dispersion arises because not all molecules travel along the same length pathway. Fluids travel faster at the centre of pores than near the edges, and faster through large pores than small pores. Lateral dispersion arises because flowpaths can branch out to the side (Fetter, 2001). In fractured or fissured karstic aquifers mechanical dispersion is mainly caused by branching and combining of fractures, although variations in velocity across a single fracture also causes some dispersion (Barker, 1991).

Sorption is the adhesion of a substance transported in water onto solid material and can occur with or without a chemical reaction (Käss, 1998). Adsorption is a term generally used for sorptive processes involving chemical reactions, and these are often irreversible, but can be reversible. In water tracing sorption can cause both losses and retardation of tracers that are affected. The amount of sorption that occurs depends

upon the nature of the substrate material, with increasing sorption from carbonate minerals to clay to organic matter.

The importance of matrix diffusion in the Chalk was first discussed by Foster (1975), and it has been recognised as an important influence on solute transport in many different geological situations (see Jardine et al., 1999; and Meigs and Beauheim, 2001 for a review of previous studies of matrix diffusion). In double porosity aquifers, solutes initially diffuse from fractures and fissures into the immobile pore water in the matrix, delaying transport through the aquifer. They are then further diluted when concentrations in the larger voids become sufficiently low to enable solutes to diffuse back into them from the matrix. Barker (1993) suggests that double porosity diffusion is a significantly more effective attenuation mechanism than dispersion and that where double porosity is occurring dispersion can sometimes be ignored as insignificant.

Double porosity diffusion can cause tracer breakthrough curves to have significant tailing. This was discussed theoretically by Maloszewski and Zuber (1985). A long tail of low tracer concentration was observed in a breakthrough curve from a radially convergent tracer test in the East Anglian chalk which was found to fit models incorporating matrix diffusion better than pure advection-dispersion models (Atkinson et al., 2000). However, non-diffusive processes may also cause long tailing in breakthrough curves. First, Kuntzmann et al. (1997) concluded from numerical modelling of breakthrough curves of sodium chloride in two dipole borehole injection-withdrawal tests that the long tail in the breakthrough curves was caused by transverse dispersivity and rapid exchange between the mobile zone and less mobile water within the fracture system, rather than by matrix diffusion. However, dipole tracer tests inherently cause tailing in breakthrough curves (Novakowski et al., 2004; Einsiedl and Maloszewski, 2005), and it is possible that tailing in the experiment by Kuntzmann et al. (1997) could be an artefact of the tracer injection method. Second, Massei et al. (2006) interpret tailing in a breakthrough curve from a tracer test in the French chalk as being due to slower flow along conduit walls where there is increased friction. However, if tailing in porous aquifers such as the Chalk were caused solely by friction along conduit walls then this process should have a similar effect in non-porous karst aquifers, which does not seem to be the case. For example, breakthrough curves from the low porosity Carboniferous Limestone in the UK generally have considerably less tailing than those

in the Chalk. Third, Meigs and Beauheim (2001) cite Hautjarvi and Vuori (1992) as suggesting that variations in fracture apertures or delayed release of tracer from an injection well could cause tailing in tracer breakthrough curves.

The role of diffusion processes in causing tailing in breakthrough curves therefore remains unclear. The amount of diffusion depends upon the diffusion coefficient of the substance, with greater diffusion of substances with high diffusion coefficients (Jardine et al., 1999). The effects of diffusion in aquifers have been investigated using tracer tests in which tracers with different diffusion coefficients are simultaneously injected (e.g. Garnier et al., 1985; Jardine et al., 1999; Becker and Shapiro 2000; Meigs and Beauheim, 2001; Novakowski et al., 2004; Einsiedl and Maloszewski, 2005) and these studies are considered below.

A long-term natural gradient tracer study in a fractured shale undertaken by Jardine et al. (1999) demonstrated double porosity diffusion using three tracers with different diffusion coefficients at the field scale. The tracers were injected at a steady rate over 180 days into a fractured section of a borehole that had been previously found to have rapid flow during a borehole dilution test. Samples were taken from a piezometer 6 m from the injection borehole that was known to intersect the matrix but not the fracture zone. The tracers with higher diffusion coefficients arrived at the matrix sampling sites faster and their breakthrough curves had higher peaks than those with lower diffusion coefficients indicating that matrix diffusion was a cause of tracer transfer from the fracture network to the matrix. This experiment demonstrates that it is possible to identify differences in tracer behaviour due to double porosity diffusion at the field scale using tracers with different diffusion coefficients. However, sampling from the matrix is probably the optimum experimental design for this.

If the breakthrough curves of simultaneously injected tracers with different diffusion coefficients are identical, then diffusion can be ruled out and an alternative explanation for breakthrough curve tailing is required. The study of Becker and Shapiro (2000) is the only study that conclusively demonstrates the absence of diffusion. Forced gradient weak dipole borehole tracer tests were conducted in a non-karstic fractured aquifer in which the local bedrock comprises a schist with granite intrusions (Becker and Shapiro, 2000). Three tracers with different diffusion coefficients were simultaneously injected

into a fracture isolated by packers (the fracture was identified using borehole logging). The injection borehole was 36 m from the pumping borehole, and 5% of the pumped water was reinjected into the injection borehole. The breakthrough curves of tracer concentration (normalised to injection mass) plotted against the volume of water pumped were identical for the three tracers despite their different diffusion coefficients. Becker and Shapiro (2000) conclude that the significant tailing observed in the breakthrough curves is not due to either diffusional processes or an artefact during the injection process, and propose an alternative explanation for the breakthrough curve tailing involving lateral dispersion. They suggest tracer is predominantly transported by rapid advection in a high conductivity channel but that there is also much slower advection in smaller secondary fractures (perhaps stress features of the larger fractures), and that mass transfer between these two systems causes the breakthrough curve tailing.

Increased diffusion can have various effects on tracer breakthrough curves but in general tracers with higher diffusion coefficients result in breakthrough curves normalised to the injection mass that have lower peaks and longer tails, and higher concentrations during the tail than those of tracers with lower diffusion coefficients (Reimus et al., 2003; Einsedl and Maloszewski, 2005). These types of differences have been observed in four studies (Garnier et al., 1985; Meigs and Beauheim 2001; Reimus et al., 2003; Einsedl and Maloszewski 2005), although the results from the study by Meigs and Bauheim (2001) were inconclusive.

The study of Meigs and Beauheim (2001) involved 25 multi borehole (monopole) convergent flow tracer tests that were conducted in a fractured dolomite using different tracers and different pumping rates. They observe significant tailing in all the breakthrough curves (normalised to the concentration of the injection solution), and interpret this tailing as being due to matrix diffusion. However, despite promoting this interpretation, the authors themselves suggest that breakthrough curves obtained with two different pumping rates that had very similar peak heights were inconsistent with their conceptual model of matrix diffusion because there should be more diffusion with lower pumping rates. They also discuss an example in which they compare the breakthrough curves of two tracers with different diffusion coefficients. The breakthrough curve of the tracer with the higher diffusion coefficient had a lower peak

which they suggest could indicate matrix diffusion, but the authors conclude that this result is ambiguous and may be an artefact caused by the poor quality of the tracer data.

The results from a monopole convergent radial flow tracer test in chalk by Garnier et al. (1985) are presented by Moench (1995) who re-analysed the data. Three tracers with different diffusion coefficients were used (Deuterium, Iodide and Sodium Fluorescein). Breakthrough of iodide was later than that of the other tracers indicating that the iodide was affected by sorption (Moench, 1995). The amount of tailing in the three breakthrough curves (normalised to the maximum tracer concentration) increases with increased diffusion coefficient of the tracer suggesting that diffusion occurred along the flowpath (although the sorption of the iodide could have affected tailing in this tracer). The model developed by Moench (1995) did incorporate diffusion, although a fracture skin providing resistance to diffusion into the matrix was required to model the data.

Einsedl and Maloszewski (2005) discuss a monopole convergent flow tracer test in a fractured granite in which two tracers with different diffusion coefficients were simultaneously injected. The breakthrough curve of the tracer with the higher diffusion coefficient (normalised to the injection mass) had a lower peak and longer tail than the tracer with the lower diffusion coefficient, and the authors interpret this as indicating the existence of tracer diffusion into the matrix.

Although it appears that diffusion can be identified using tracer tests in which multiple tracers with different diffusion coefficients are simultaneously injected, the situation is complicated because substances could diffuse into stagnant water within fractures as well as or instead of into the matrix (Becker and Shapiro, 2000; Reimus et al., 2003). Thus differences in behaviour of tracers with different diffusion coefficients (e.g. the study of Einsedl and Maloszewski, 2005) cannot simply be interpreted as being indicative of diffusion specifically into the matrix. Reimus et al. (2003) argue that it is possible to discriminate between diffusion into the matrix and diffusion into stagnant water by injecting a tracer known to be susceptible to sorption along with two non-sorbing tracers with different diffusion coefficients. Their tracer study included a weak dipole convergent flow test in a volcanic Tuff. The two non-sorbing tracers indicated that diffusion was occurring because the tracer with the higher diffusion coefficient had a breakthrough curve (normalised to the injection mass) with a lower peak than that of

the tracer with the lower diffusion coefficient (Reimus et al., 2003). The breakthrough curve of the sorbing tracer had the lowest peak. Modelling work undertaken by Reimus et al. (2003) using RELAP, a double porosity transport model developed by the authors, suggested that the amount of concentration attenuation in the sorbing tracer was too great to be accounted for solely by diffusion into stagnant water in the fracture system. Tracer must have diffused into the matrix where the greater surface area enabled significant sorption to occur.

Novakowski et al. (2004) conducted two dipole injection-withdrawal borehole tracer tests in a Silurian dolostone. Two tracers with different diffusion coefficients were used (Lissamine and Bromide). The authors suggest that tracers with higher diffusion coefficients would be expected to have delayed peaks, and conclude that the delay in the peak of the tracer with a higher diffusion coefficient (Bromide) is evidence that matrix diffusion is significant at their study site. Delay or retardation of tracers combined with increased tailing (which was also observed in the Bromide breakthrough curve of Novakowski et al., 2004) could also indicate that sorption is occurring (e.g. Reimus et al., 2003). However sorption does not appear to account for the differences in the breakthrough curves of Novakowski et al. (2004) because the retarded tracer, Bromide is not susceptible to sorption (Käss, 1998). Other studies that identified differences in the breakthrough curves of tracers with different diffusion coefficients (Reimus et al., 2003; Einsedl and Maloszewski, 2005) did not observe a delay in the peaks of the tracers with the highest diffusion coefficients, instead finding a decrease in peak height (scaled to injection mass) in tracers of higher diffusion coefficients together with increased tailing. Novakowski et al., (2004) do not present their data in the same way as the studies of Einsedl and Maloszewski (2005) and Reimus et al. (2003) because the breakthrough curves are normalised to peak tracer concentration not injection mass. It is not clear whether if tracer breakthrough curves normalised to injection mass were plotted using the data of Novakowski et al. (2004) there would be a difference in peak height that relates to the diffusion coefficients of the tracers.

It can be difficult to disentangle the effects of diffusion and sorption on breakthrough curves and sorption is not always predictable because the amount of sorption of a particular tracer will vary depending upon the type of substrate that it comes into contact with. Maloszewski et al. (1999) discuss two multi tracer tests undertaken in

Devonian fractured sandstones, quartzites and slates in Germany where sorption was unexpectedly encountered. In the first test Potassium Bromide, Eosin and Deuterium were injected into an exposed fractured rock surface and breakthrough curves were obtained from a borehole 11 m away. The authors suggest that $D_p R_{ap}$ values for Eosin and Deuterium are the same (where D_p = diffusion coefficient and R_{ap} = retardation factor), and therefore because the diffusion coefficient of the Deuterium is five times higher than that of the Eosin, the Eosin must have been significantly sorped (R_{ap} of ~ 5), which they had not been expecting. This result is surprising because the Eosin peak is not delayed (Figure 5.2). However, the Eosin peak is lower than would be expected if no sorption were occurring because the other two non-sorbing tracers (Potassium Bromide and Deuterium) have higher diffusion coefficients than Eosin (and therefore the Eosin (if not sorbed) should have had the highest peak of the three tracers). This study suggests that, if it is assumed that differences in tracer breakthrough curves of simultaneously injected multiple tracers are only affected by diffusion and sorption, then the differences in breakthrough curves that do not appear to relate to the diffusion coefficients of the tracers must be due to sorption.

In a second experiment by Maloszewski et al. (1999) Eosin and Sodium Fluorescein were injected into the borehole where the tracer had been detected in the first experiment. Maloszewski et al. (1999) suggest that breakthrough curves from a spring 225 m from the injection borehole indicate that Sodium Fluorescein was even more sorped than the Eosin. The breakthrough curve of the Sodium Fluorescein (normalised to injection mass) has a lower peak, is slightly delayed, and has higher tracer concentrations in the tail than the Eosin breakthrough curve (Figure 5.3). However, the authors assumed that the diffusion coefficient of these tracers is identical, and in fact Sodium Fluorescein has a lower molecular weight and hence higher diffusion coefficient than Eosin (Section 5.3), and therefore it is possible that the Sodium Fluorescein breakthrough curve was affected by a combination of sorption and diffusion.

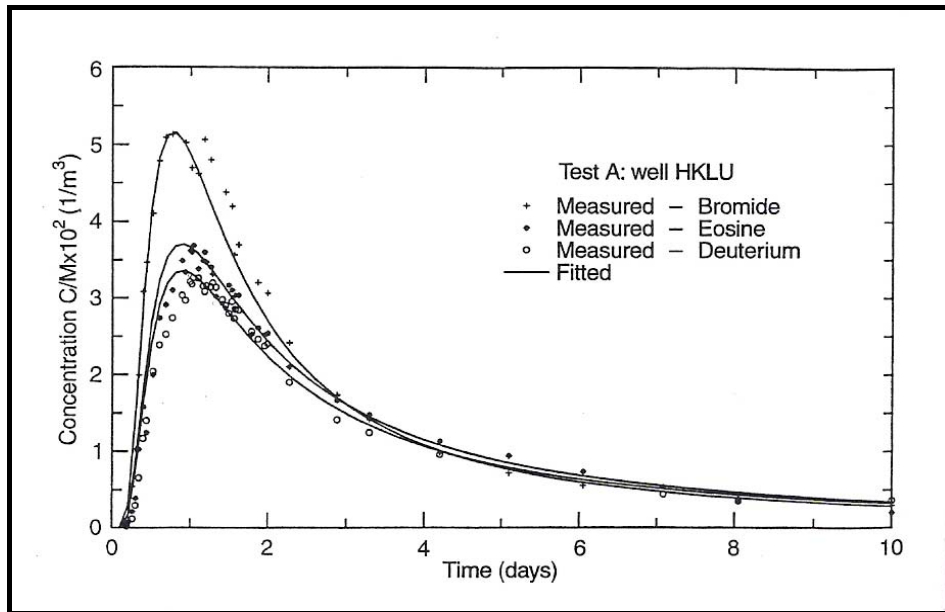


Figure 5.2: Breakthrough curves (normalised to injection mass) obtained from a borehole by Maloszewski et al. (1999) following simultaneous injection of Bromide, Eosin and Deuterium (note that modelled curves do not fit the shape of the peaks very well).

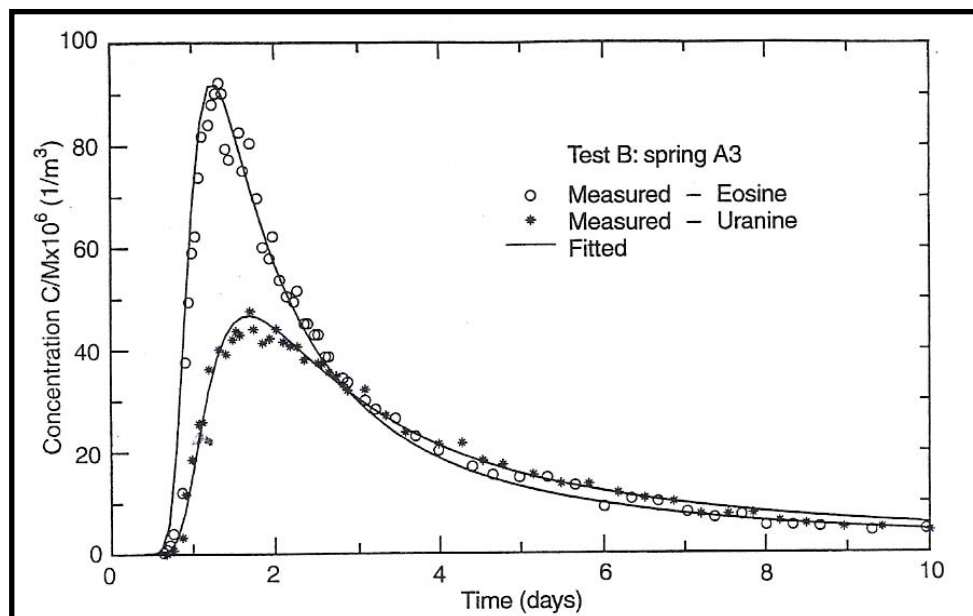


Figure 5.3: Breakthrough curves (normalised to injection mass) obtained at a spring by Maloszewski et al. (1999) following simultaneous injection of Eosin and Sodium Fluorescein

To summarise, there appear to be four main mechanisms that cause tailing in breakthrough curves: diffusion, sorption, artefacts during tracer injection, and an advective transport process in which tracer moves down multiple routes with different flowpath lengths (lateral dispersion). Theoretically tailing due to diffusion can be distinguished if there are differences in the breakthrough curves of tracers injected simultaneously that relate to their diffusion coefficients. However, the situation is complicated because diffusion can be into stagnant water as well as into the matrix. In addition it can be difficult to disentangle the effects of diffusion from sorption because sorption also affects tracers differentially, and the amount of sorption of a particular tracer will vary depending upon the type of substrate that it comes into contact with.

With the exception of the tracer test by Garnier et al. (1985) reanalysed by Moench (1995) that was undertaken in chalk, all the previous studies discussed above were in non-karstic fractured aquifers. They are also almost all borehole tracer tests undertaken over short distances (always less than 250 m, often less than 50 m), and generally under forced gradient conditions. There have been no previous studies of the effects of diffusion in fractured or karstic aquifers with high matrix porosities during catchment scale tracer tests from stream sinks. Double porosity diffusion depends upon the solute in the fracture or fissure remaining in contact with the matrix for sufficient time to significantly affect concentrations in the moving fluid. A parameter t_{cf} can be defined as the characteristic time for diffusion from a fracture to an equal volume of water in the matrix (Barker et al., 2000). Where groundwater flow is rapid, double porosity diffusion has little effect because it occurs too slowly to alter the shape of a rapidly advecting cloud of tracer. It has been suggested that double porosity will only dominate when the breakthrough advection time (t_a) is $\geq 3t_{cf}$ (Barker et al., 2000). It is possible that in karst aquifers the travel time along a conduit pathway will be too rapid for double porosity diffusion to occur to any significant extent. The main experiment described in this chapter was designed to test the importance of double porosity diffusion by obtaining breakthrough curves for 5 simultaneously injected tracers (including four dyes with different diffusion coefficients) over a known karst connection between Smithcroft Copse stream sink and the Blue Pool spring.

5.2 Aims and experimental design

The main aim of this chapter is to use breakthrough curves obtained at the Blue Pool following tracer injections at Smithcroft Copse stream sink to evaluate the relative roles of advection dispersion and double porosity diffusion along this flowpath. Subsidiary aims are to assess any differences in breakthrough curves obtained on different occasions at the same monitoring site, and any differences in the breakthrough curves obtained at three different sites at the Blue Pool. The locations of these sites are shown in Figure 5.4.

Breakthrough curves were obtained following two Sodium Fluorescein injections in 2005 (the experimental methods and qualitative aspects of this test were discussed in Section 4.3.2), and one multi-tracer injection in 2006 (all details in this chapter). The Blue Pool spring complex comprises several groundwater upwellings within a series of pools (Section 3.4.3.2) that combine to form a channel which discharges into the River Pang. Following both 2005 injections breakthrough curves were obtained from this outlet channel (referred to as “the Blue Pool outlet” in this thesis), approximately 20 m upstream of the point at which it joins the River Pang (Figure 5.4). Flow can easily be gauged at the Blue Pool Outlet monitoring site, enabling calculation of % tracer recovery. Following the second tracer injection in 2005 a breakthrough curve was also obtained from the River Pang downstream of the input from the Blue Pool outlet channel (Figure 5.4). Flow was also measured at this site to enable comparison of tracer recovery at the Blue Pool and in the River Pang thereby indicating whether additional tracer was discharged directly into the River Pang.

In the 2006 experiment, breakthrough curves were obtained from the Blue Pool outlet channel but also from the largest, deepest upwelling in the Blue Pool complex (henceforth called “the Blue Pool spring” to differentiate it from the monitoring point in “the Blue Pool outlet channel”). The aim of directly sampling this upwelling (location shown on Figure 5.4) was to obtain breakthrough curves that are not affected by processes within the pools before the tracer reaches the downstream monitoring point in the Blue Pool outlet channel.

The breakthrough curves at the Blue Pool outlet channel in 2005 showed significant tailing (Figure 4.9), but it was not clear whether this was a consequence of double

porosity diffusion. The experiment in 2006 was designed to compare the travel time, breakthrough curves and recovery of four different dye tracers and one bacteriophage tracer and to investigate the role of double porosity diffusion along the flowpath. The diffusion coefficient of solutes scales approximately to the inverse cube root of the molecular weight. Dye tracers of molecular weights ranging from 245 to 691 were used, therefore the relative differential effects between tracers should be about 40 %.

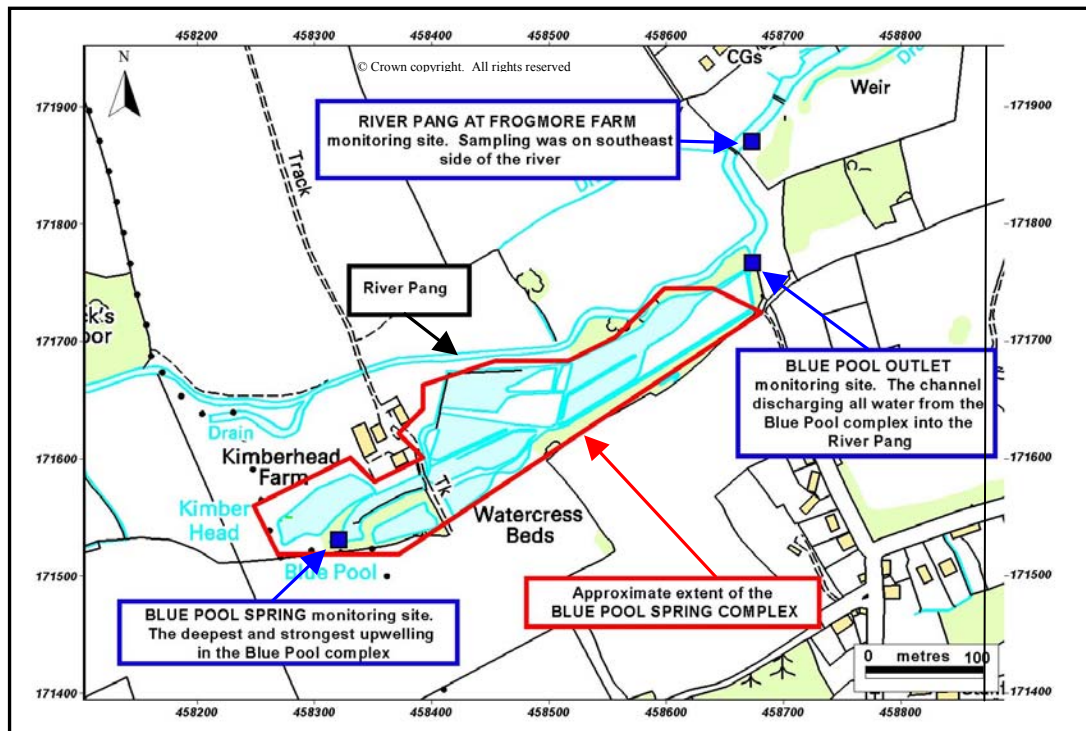


Figure 5.4: Location of approximate area of Blue Pool complex (red boundary) and monitoring sites during tracer tests from Smithcroft Copse (blue squares)

5.3 Experimental Methods

5.3.1 Tracer Methods: Smithcroft Copse 2006 experiment

5.3.1.1 Tracer Selection

Behrens et al. (2001) concluded that there are 7 dye tracers that on the basis of tests of toxicology and ecotoxicology are safe for use in experiments affecting drinking water (although in this case no drinking water supplies are involved in the Smithcroft Copse-Blue Pool connection). Of these, four dyes were chosen to optimise the variability in molecular weight whilst excluding dyes thought to have high sorptive properties. The dyes chosen were Sodium Fluorescein, Amidorhodamine G, Eosin and Sodium Naphthionate. In the bacteriophage tests discussed in Chapter 4, there were very high tracer losses. A bacteriophage (*Phix 174*) was used in the 2006 Smithcroft Copse test to

enable a direct comparison between a bacteriophage and dye tracers over an established groundwater flowpath.

5.3.1.2 Tracer Quantity

Table 5.1 lists the tracers used, the quantity injected and the molecular weights of the dyes. Dye quantities were calculated to produce peaks of $\sim 10 \mu\text{g.L}^{-1}$ above background at the Blue Pool outlet channel. Calculations were based upon the results of the previous tracer test (Section 4.3.2), and the suggestions in Käss (1998) concerning the relative detectability of the dyes. The larger quantity of Sodium Naphthionate (2000 g) was required because there is high background fluorescence at the same wavelength at which this tracer fluoresces.

Bacteriophage specialists CREH Analytical in Leeds made up the bacteriophage injection solution. An initial 1-litre batch of *Phix 174* was at a lower titre than anticipated, (2×10^{11} pfu.ml⁻¹). A second 500 mls batch was at a higher titre (2×10^{12} pfu.ml⁻¹). Both batches were injected.

Table 5.1: Tracer quantities and dye molecular weights

Tracer	Tracer Amount	Molecular weight
Sodium Fluorescein	99.99 g	376
Sodium Naphthionate	2000.07 g	245
Eosin yellow	500.3 g	691.88
Amidorhodamine G	202.98 g	552.59
Phix 174 bacteriophage	1 litre of 2×10^{11} pfu.ml ⁻¹ 500 mls of 2×10^{12} pfu.ml ⁻¹	-

5.3.1.3 Tracer injection

The tracer injections were initially postponed because heavy rainfall caused the stream sink to overflow at all the sink points. A very small (<1 gram) trial injection of Sodium Fluorescein (henceforth termed the “trial injection”) demonstrated that it was not possible to ensure all the tracer entered a sinkpoint with no overflow into the stream beyond. A few days later the water levels subsided. Tracer was injected into the same sink point used in the previous tests in 2005, although again only a small proportion of the total flow was sinking at this point. A length of drainpipe with a funnel on the top was used to direct the tracer into the hole into which the water was draining freely into

the ground (Figure 5.5). The tracer was injected on the night of the Saturday 25th February and injection times are listed in Table 5.2.



Figure 5.5: Fluorescein tracer injection

Table 5.2: Tracer injection times

Tracer	Injection date and time
Sodium Naphthionate	25/02/06 23:42
Eosin	25/02/06 23:46
Amidorhodamine G	25/02/06 23:54
Sodium Fluorescein	26/02/06 00:01
Phix 174 bacteriophage	26/02/06 00:17

5.3.1.4 Sampling schedule

Samples were taken at the Blue Pool spring and the Blue Pool outlet monitoring points using automatic water samplers. 34 background samples were taken over 5 days prior to tracer injection. Following tracer injection samples were taken at 40 minute intervals; this sample interval was gradually reduced to 8 hourly at the end of the test. Sampling continued for 25 days at the Blue Pool spring and 15 days at the Blue Pool outlet following injection.

A selection of samples taken by automatic water sampler at the Blue Pool outlet were also analysed for the bacteriophage *Phix 174*. Twenty background samples from the month preceding injection were analysed. Following injection, samples taken every 80 minutes were analysed, this was gradually reduced to 2-3 samples per day at the end of the test. Twenty samples from the Blue Pool spring between 28/02/06 and 06/03/06 were also analysed for the *Phix 174* bacteriophage.

5.3.1.5 Tracer detection and measurement

For the dye tracers water samples were stored in the dark prior to analysis. Samples were analysed on a Perkin Elmer LS55 spectrofluorometer in the Groundwater Tracing Unit laboratory at University College London. The instrument was calibrated using standard dye solutions. Sodium Naphthionate analysis was conducted using three different methods for concentrations up to $10 \mu\text{g.L}^{-1}$, of 10 to $100 \mu\text{g.L}^{-1}$ and $> 100 \mu\text{g.L}^{-1}$. The standards used for calibration of each dye were measured regularly during sample analysis, and these measurements were used to correct raw fluorescence data for instrument drift.

Fluorescence results were affected by interference between Sodium Fluorescein, Amidorhodamine G and Eosin dyes. Following the method of Käss (1998) standards of each dye were measured using the settings of other dyes. Table 5.3 shows the results of $50 \mu\text{g.L}^{-1}$ standards measured using the three different dye settings. Values in bold are the readings of the $50 \mu\text{g.L}^{-1}$ standard using the settings of that dye. For example the fluorescence intensity of a $50 \mu\text{g.L}^{-1}$ solution of Amidorhodamine G on the Amidorhodamine settings is 490. A $50 \mu\text{g.L}^{-1}$ solution of Eosin on the Amidorhodamine G settings gives a reading of 57.

Table 5.3: Dye interference: fluorescence intensity of $50 \mu\text{g.L}^{-1}$ standards at all settings

Measuring settings	Amidorhodamine G $50 \mu\text{g.L}^{-1}$ standard	Sodium Fluorescein $50 \mu\text{g.L}^{-1}$ standard	Eosin $50 \mu\text{g.L}^{-1}$ standard
Amidorhodamine G	490	1.4	57
Sodium Fluorescein	10	624	36
Eosin	154	39	162

Correlation curves were obtained for all dyes measured using the settings of all other dyes. Conversion of the raw fluorescence intensity to separated dye concentrations for the three dyes was carried out using the following equation set (Käss, 1998):

$$F_1 = k_1C_1 + k_2C_2Z_{21} + k_3C_3Z_{31}$$

$$F_2 = k_2C_2 + k_1C_1Z_{12} + k_3C_3Z_{32}$$

$$F_3 = k_3C_3 + k_1C_1Z_{13} + k_2C_2Z_{23}$$

F is the fluorescence intensity for each of three dyes.

k_i is a constant for converting the fluorescence intensity in a pure dye solution to a concentration (obtained from the calibration curves).

Z_{ij} is the intensity ratio for pure solutions with the settings of a specific dye (obtained from calibration curves of standards measured using different dye settings).

C_i is the final concentration to be calculated

Subscripts refer to the three dyes. The values of k_i and Z_{ij} were obtained from the calibration data and the equations solved for C_1 , C_2 , C_3 by a matrix inversion method on a spreadsheet prepared by John Barker (personal communication, 2006).

CREH Analytical analysed water samples for the bacteriophage *Phix 174*. Samples were stored in brown glass bottles in the fridge prior to analysis, and were analysed not more than a week after collection (and in many cases after only a few days). Sample analysis was conducted on 1 ml samples to determine pfu.ml⁻¹. There was an occasional very low background presence of *Phix 174* at the Blue Pool (1 pfu.ml⁻¹).

5.3.2 Flow gauging and discharge monitoring (2005 and 2006 experiments)

In 2005 and 2006 flow was gauged by current meter and stage was measured from a temporary datum at each site at frequent intervals to determine if the discharge had changed and additional current metering was required. During the 2005 experiment flow was gauged at the Blue Pool outlet and the River Pang at Frogmore Farm on several occasions, and on one occasion at Ingle and Jewells Springs. During the 2006 experiment flow was gauged at the Blue Pool outlet on two days prior to the tracer injections and on the two days following tracer injection.

5.4 Results and Discussion

5.4.1 Flow and stage results

5.4.1.1 Smithcroft Copse 2005 experiment

Flow and stage data at all monitoring sites during the 2005 tracer tests from Smithcroft Copse demonstrated that there was almost no change in flow at any of the sites during the period following the main tracer injection on 7th February. Table 5.4 summarises the flow data ($L.s^{-1}$) obtained by current meter at all sites. At the time of the test the Blue Pool discharge contributed approximately 60% of the total flow in the River Pang downstream of all the springs. Jewells and Ingle springs are considerably smaller than the Blue Pool with flows of $20 L.s^{-1}$ and $30 L.s^{-1}$, respectively, but nevertheless together these springs provide approximately 15 % of the total flow in the River Pang downstream of the Blue Pool.

Table 5.4: Current meter results in 2004/2005 ($L.s^{-1}$)

Date	Blue Pool outlet	Jewells	Ingle	Downstream R Pang
04/11/04				424
03/02/05	209	20		335
07/02/05	197		30	335
09/02/05	185			342
10/02/05	194			
15/02/05	196			

5.4.1.2 Smithcroft Copse 2006 experiment

Table 5.5 summarises the results of the stage readings and current meter data obtained during the 2006 Smithcroft Copse experiment. Following tracer injection on 26/02/06 there was generally little change in the stage reading of 8.1 cm below datum. On the afternoon of the 28/02/06 building work carried out in the Blue Pool complex resulted in the diversion of some of the flow away from the Blue Pool outlet causing stage to decline by 1.5 cm. Current metering was not carried out at this time due to the rapidity of the changes in stage. The change began at ~12:00 on 28/02/06 and stage readings had returned to 8.1 cm by 19:58. It is unlikely that there was any significant change in discharge at the Blue Pool as there was no rain over this period or in the preceding few days and the stage readings consistently remained at 8.1 mm below datum before and after the building works.

Heavy rainfall was observed in the field on the 07/03/06 and 08/03/06. Stage readings on the 08/03/06 and 10/03/06 were elevated to 7.8 and 7.6 cm below datum respectively. Average measured discharge when the stage was 7.4 and 8.1 cm was 203.5 and 192 L.s⁻¹ respectively, suggesting that the increase in stage on the 08/03/06 and 10/03/06 would only have equated to an increase in discharge of a few L.s⁻¹.

Table 5.5: Stage and discharge at the Blue Pool outlet during the 2006 test

Date	Stage (mm below datum)	Discharge (L.s ⁻¹)
23/02/2006 08:54	7.4	
23/02/06 09:00 to 10:30		205
23/02/2006 10:35	7.4	
24/02/2006 11:52	7.4	
24/02/06 11:55 to 13:18		202
24/02/2006 13:18	7.4	
25/02/2006 13:25	7.8	
26/02/2006 11:56	8.1	
26/02/2006 15:56	8.1	
26/02/06 16:03 to 17:00		195
26/02/2006 17:06	8.1	
27/02/2006 08:22	8.1	
27/2/06 08:28 to 09:17		189
27/02/2006 09:23	8.1	
27/02/2006 15:58	8.1	
28/02/2006 09:56	8.1	
28/02/2006 13:12	9.6	
28/02/2006 13:42	9.6	
28/02/2006 13:54	9.2	
28/02/2006 14:58	8.7	
28/02/2006 19:38	8.1	
01/03/2006 13:22	8.1	
01/03/2006 14:25	8.1	
02/03/2006 11:39	8.1	
03/03/2006 13:18	8.1	
04/03/2006 12:58	8.1	
06/03/2006 11:15	8.1	
08/03/2006 11:16	7.8	
10/03/2006 12:06	7.6	

5.4.2 Tracer breakthrough curves

5.4.2.1 Dye breakthrough curves at the Blue Pool spring monitoring point

During the 2006 experiment breakthrough curves were obtained for all four dyes at the Blue Pool spring monitoring point (Figure 5.6).

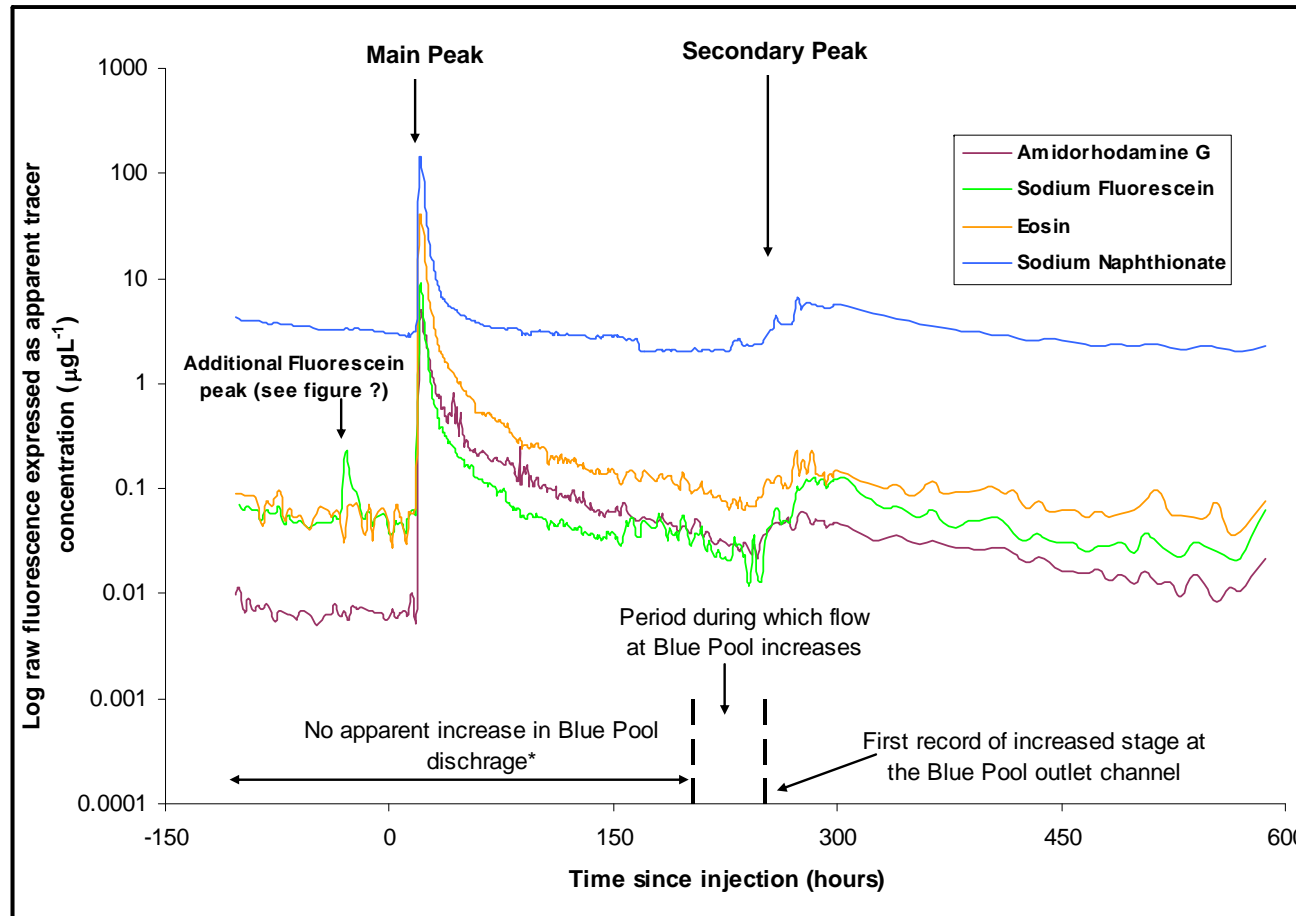


Figure 5.6: Tracer breakthrough curves at the Blue Pool spring, 2006. Plots are apparent tracer concentration (no background fluorescence removed) against time since tracer injection (corrected for small differences between tracers). Increased stage in response to heavy rain occurred sometime between 203 and 251 hours after mean injection time, indicated by the dashed vertical lines.

In addition to the main peak ~ 22 hours after injection, a small secondary peak occurred ~ 280 hours after injection. The peak concentration during the secondary peak was $\sim 6 \mu\text{g.L}^{-1}$ for the Sodium Naphthionate and less than $0.3 \mu\text{g.L}^{-1}$ for all other dyes. This secondary peak coincides with the small increase in discharge noted above. There is also a small peak of $0.2 \mu\text{g.L}^{-1}$ in the Sodium Fluorescein during background sampling (occurring at about 29 hours before the main injection of Sodium Fluorescein and labelled “additional Fluorescein peak” on Figure 5.6). It is probable that this peak is due to the trial injection of $\sim 1\text{g}$ of Sodium Fluorescein on Thursday 23rd February at approximately 21:20 (Section 5.3.1.3). There is no increase in any of the other dyes at the time of the small peak in Sodium Fluorescein, and none of the other dyes had been injected into the stream sink. Interestingly, the time between the trial injection and the small peak is similar to that found in the main experiment (22 hours).

The average of the last five background readings immediately prior to the first tracer breakthrough was subtracted from the data. Time since injection was adjusted to the actual injection time of each individual tracer (which occurred over a 40 minute period). Each breakthrough curve was scaled by its peak dye concentration (the average of the three peak values) to compare the breakthrough curve tailing of the different tracers. Figure 5.7 shows the resultant breakthrough curves during the main peak, whilst Figure 5.8 shows those during the secondary peak.

During the main peak the breakthrough curves for Sodium Fluorescein, Eosin and Sodium Naphthionate are essentially identical (Figure 5.7). Slight differences in peak height occur because the data were scaled to the average of three peak values. The similarities in breakthrough curve tailing suggests that double porosity diffusion is not a significant process along the main flowpath between Smithcroft Copse and the Blue Pool because these tracers all have different molecular weights (Table 5.1). There is a small delay in the Amidorhodamine G peak, and the falling limb is shallower than that of the other three dyes, suggesting that this tracer may have been affected by sorption. There are greater differences between the dyes in the secondary peak (Figure 5.8), which do appear to relate to the molecular weights of the tracers (and hence diffusion). There is a clear correlation between the magnitude of the secondary peak at the Blue Pool spring and the molecular weight of the tracer, with tracers with lower molecular

weights having larger secondary peaks. (Table 5.6, Figure 5.9). This is discussed further in relation to tracer recoveries in Section 5.4.3.5.

By the end of monitoring (600 hours after injection), Sodium Naphthionate, Sodium Fluorescein and Eosin concentrations had returned to background, but Amidorhodamine G concentrations were still above background. There is some suggestion of a further increase in all dye concentrations (except Sodium Naphthionate) at the time monitoring stopped, but this may be background noise (Figure 5.8).

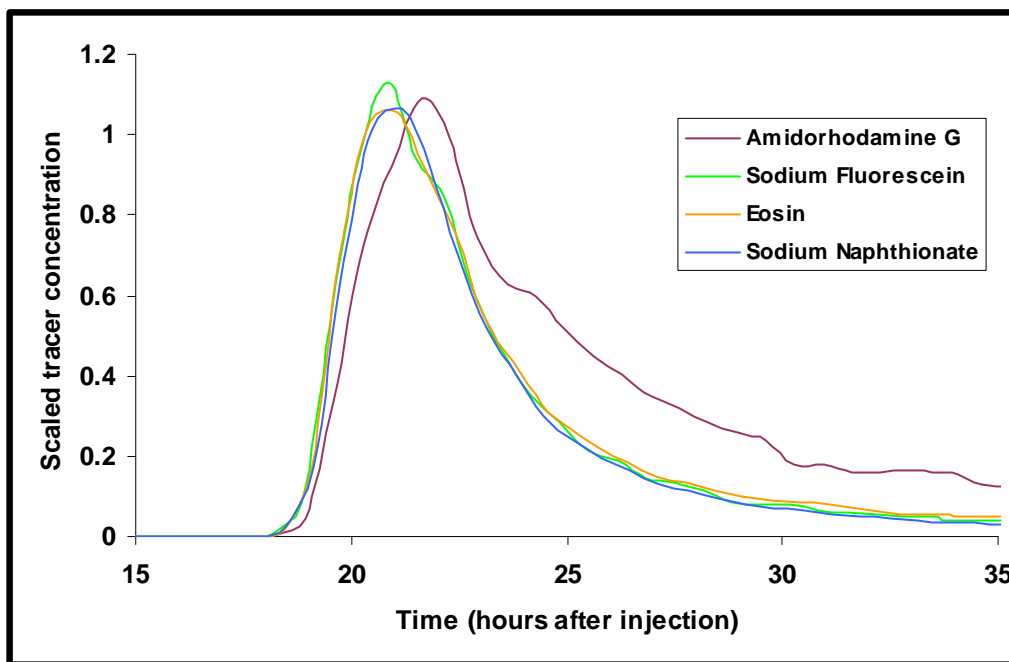


Figure 5.7: Breakthrough curves at the Blue Pool spring during the main peak scaled to the average of the three highest measured tracer concentrations. Background fluorescence (the average apparent fluorescence in five samples prior to tracer breakthrough) has been subtracted from the raw data. Time since injection is corrected for small differences between tracers.

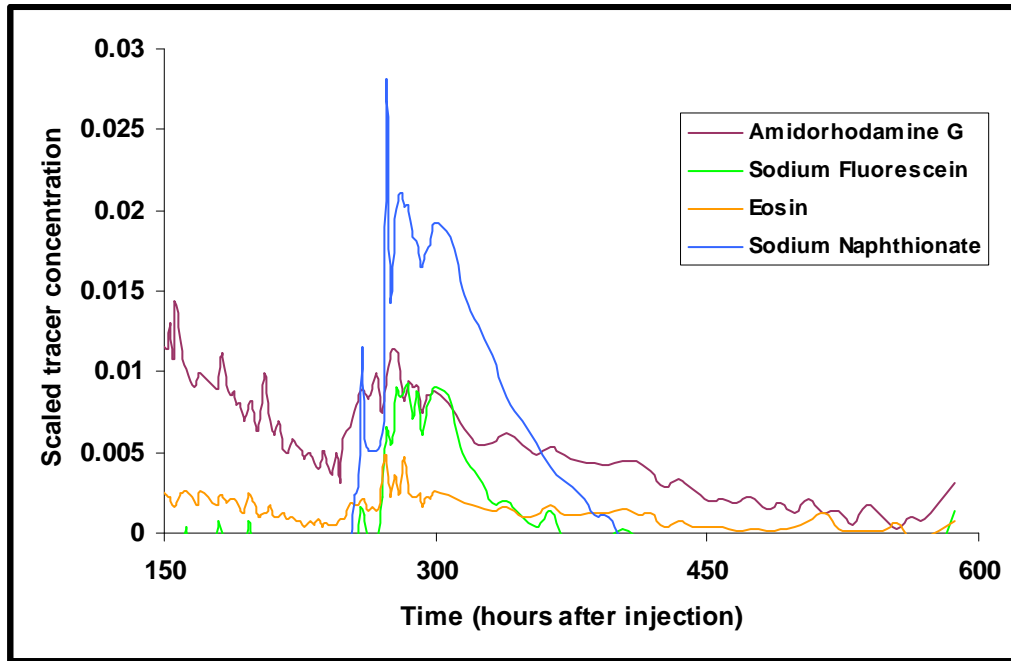


Figure 5.8: Breakthrough curves during the secondary peak at the Blue Pool spring scaled to the average of the three highest measured tracer concentrations (during the main peak). Data treated as for Figure 5.7

Table 5.6: Comparison of dye tracer molecular weight and the magnitude of the secondary peak at the Blue Pool spring (the magnitude of the secondary peak was calculated as the scaled peak concentration during the secondary peak minus the scaled concentration before the start of the secondary peak, using data in Figure 5.8)

	Scaled concentration before start of second peak	Scaled peak concentration of second peak	Magnitude of 2nd Peak	Molecular weight
Eosin	0.00048	0.00478	0.00430	692
Amidorhodamine G	0.00315	0.01143	0.00828	553
Sodium Fluorescein	-0.00473*	0.00479	0.00951	376
Sodium Naphthionate	-0.00472*	0.00926	0.01398	245

* The values for Sodium Fluorescein and Sodium Naphthionate are negative because the tracer has dropped below the original background concentration prior to tracer breakthrough.

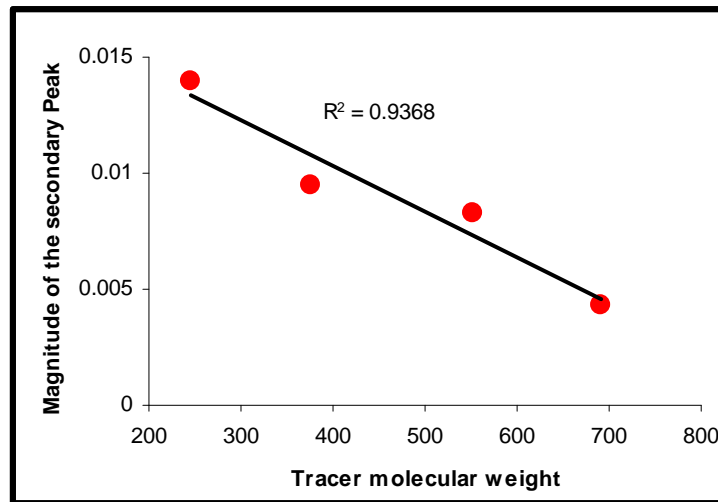


Figure 5.9: Correlation between tracer molecular weight and the magnitude of the secondary peak at the Blue Pool spring using data scaled to peak tracer concentration

In previous studies that used multiple tracers with different diffusion properties (Section 5.1) breakthrough curves were scaled to the injection mass, and differences in peak height that corresponded to the diffusion coefficients of the tracers were interpreted as evidence that diffusion was significant along the flowpath. When the data from this study were scaled in this manner, there are variations in the peak height of the different tracers during the main peak, but even discounting Amidorhodamine G that was sorbed, these differences do not appear to relate to the molecular weights of the tracers (Figure 5.10). This suggests that a process other than diffusion caused the differences in the peak concentrations of the different tracers relative to their injection masses.

Figure 5.11 shows the tail of the breakthrough curves scaled to the injection mass. During the falling limb of the main peak (30 to 130 hours after injection), there is more tailing in the Eosin and Amidorhodamine G than the Sodium Fluorescein and the Sodium Naphthionate (which return to background more quickly). Sodium Naphthionate and Sodium Fluorescein have the lowest molecular weights and would be expected to have falling limbs with more tailing than Eosin and Amidorhodamine G if the differences in tailing were due to diffusion. If it is assumed that diffusion and sorption are the only processes causing differences in the tracer breakthrough curves, then the differences in the heights and falling limbs of the main peak between the tracers that can not be accounted for by diffusion, suggest that Amidorhodamine G may

not be the only tracer affected by sorption. The differences in breakthrough curves scaled to injection mass are considered further in relation to tracer recoveries in Section 5.4.3.5.

Figure 5.11 also shows the secondary peaks scaled to the injection mass. When the data were scaled to the peak tracer concentrations there was a correlation between the magnitude of the secondary peak and the molecular weights of the tracers (Figure 5.9). However, when the data are scaled to the injection mass (Figure 5.11) the correlation only occurs for three of the tracers (Figure 5.12). The secondary peak of the Amidorhodamine G is too small to fit the pattern. This may be because there were much higher overall losses of Amidorhodamine G from sorption that are reflected when the data are scaled to the injection mass, but not when the data are scaled to the peak concentration.

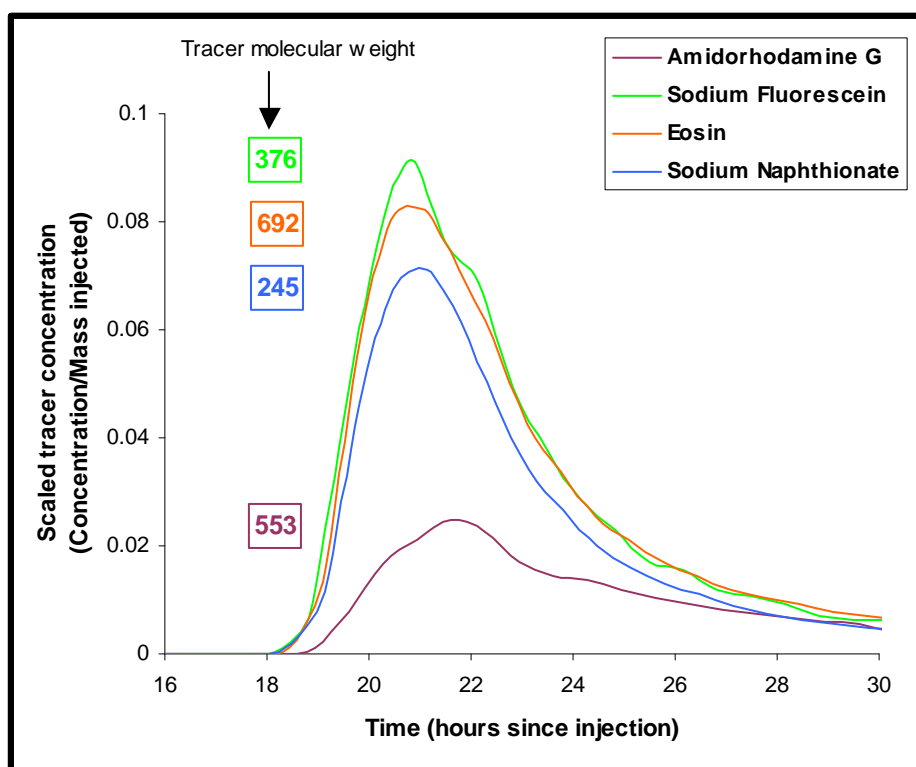


Figure 5.10: The main dye peaks at the Blue Pool spring with data scaled to tracer injection mass. Coloured numbers are tracer molecular weight, which do not appear to correlate with peak height variations.

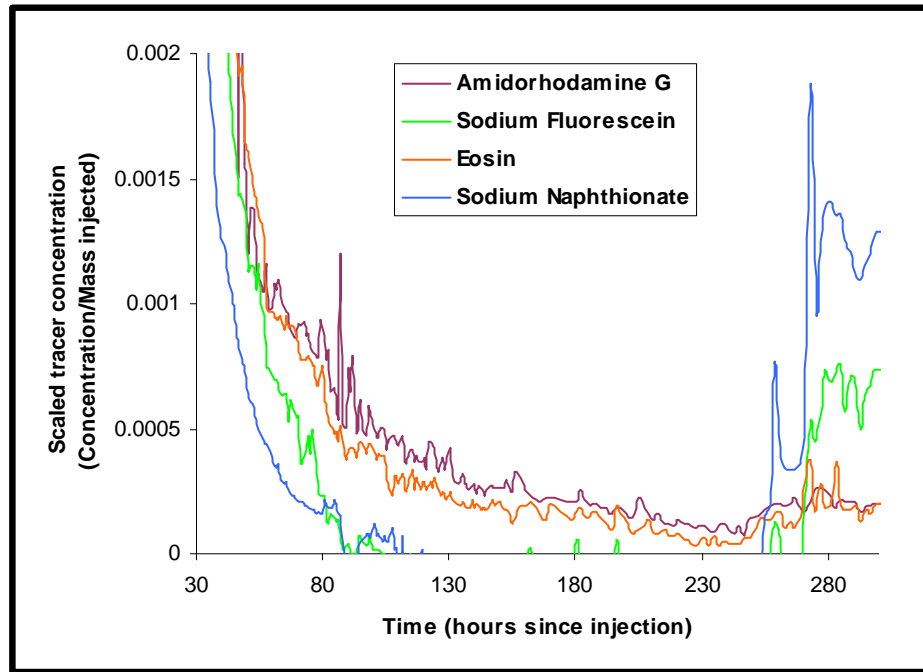


Figure 5.11: The tail of dye breakthrough curves at the Blue Pool spring (including the secondary peak) scaled to the injection masses of the tracers

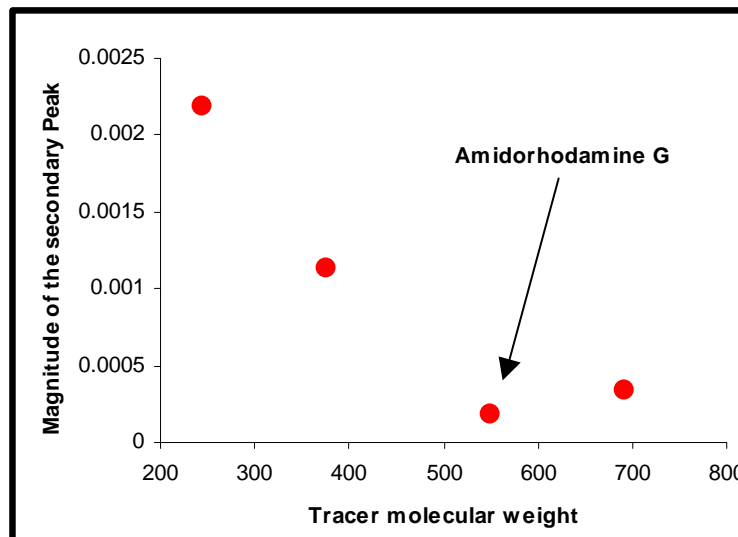


Figure 5.12: Correlation between tracer molecular weight and the magnitude of the secondary peak at the Blue Pool spring using data scaled to injection mass

5.4.2.2 Breakthrough curves at the Blue Pool outlet monitoring point

Sodium Fluorescein breakthrough curves at the Blue Pool outlet were obtained following three tracer injections (two in 2005 and one in 2006). These are directly compared in Figures 5.13 (showing the main peaks) and Figure 5.14 (showing the entire duration of the tests with the tracer concentration scale expanded to show the detail of the breakthrough curve tails). There were minor variations in the breakthrough curves during the main peak with an earlier peak and steeper falling limb during injection 1 in 2005 than for the other injections (Figure 5.13). This injection was undertaken under higher flow conditions (Table 5.4), which may be the cause of the more rapid groundwater velocity (Section 4.8). Tracer concentrations returned to background more quickly following injection 1 in 2005 than following the other tracer injections (Figure 5.14). This could be because less mass was injected during this test and tracer concentrations were generally not elevated as far above background as during tests in which a greater mass was used. Alternatively, the early return to background could be a function of the higher flow conditions during this test reducing breakthrough curve tailing because of the slightly faster travel time.

The latter part of the breakthrough curve tail was only monitored following the second 2005 injection and the 2006 injection. In both cases there are small fluctuations during the tail of the breakthrough curve (Figure 5.14). However the significant secondary peak between 250 and 300 hours after the 2006 injection did not occur over the same time period following injection 2 in 2005. This demonstrates conclusively that the secondary peak in 2006 was caused by the increase in flow, and is not a general/repeatable feature of tracer breakthrough curves over the Smithcroft Copse-Blue Pool groundwater flowpath.

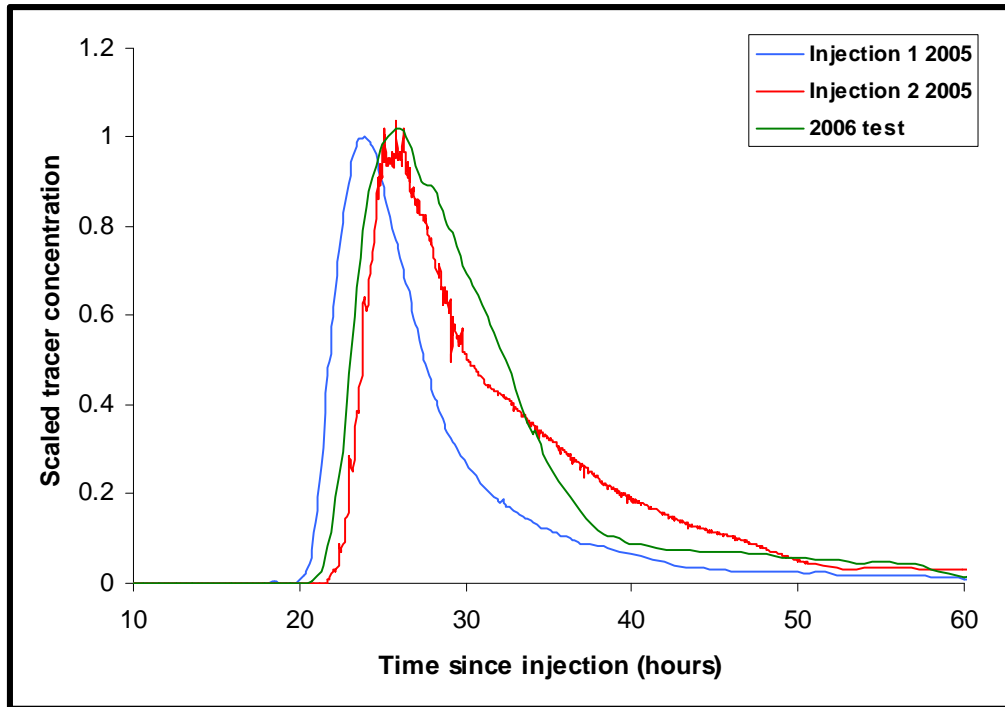


Figure 5.13: Comparison of the peak of three Sodium Fluorescein breakthrough curves at the Blue Pool Outlet (concentrations scaled to the average three peak values to enable direct comparison of the curves)

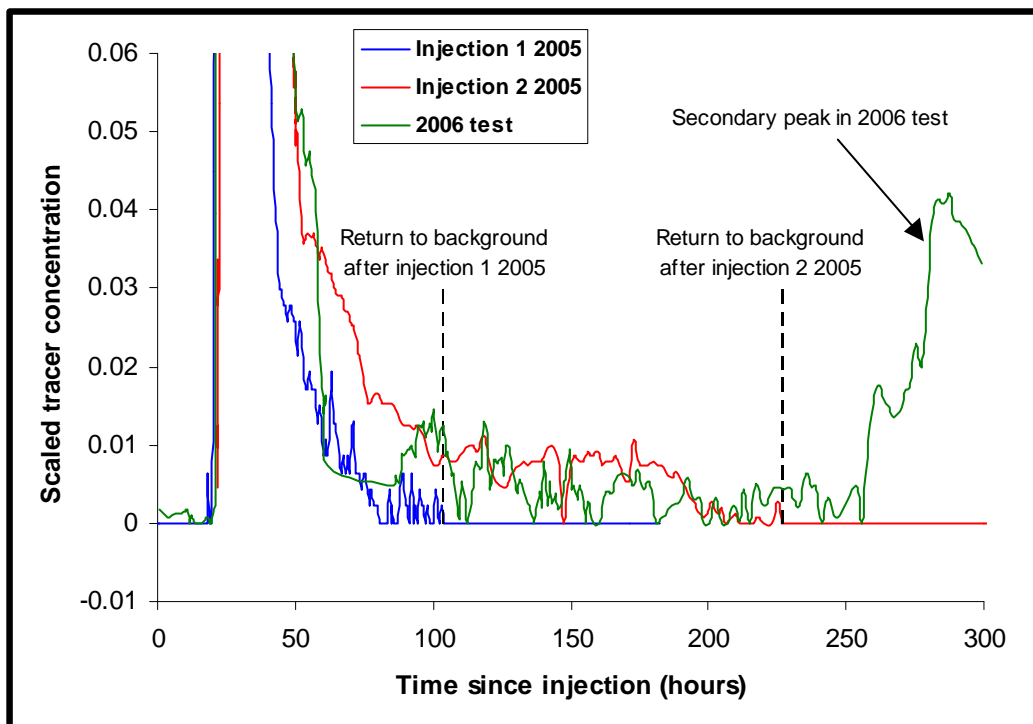


Figure 5.14: Comparison of the tail of three Sodium Fluorescein breakthrough curves at the Blue Pool Outlet (concentrations scaled to the average three peak values to enable direct comparison of the curves).

During the 2006 experiment a breakthrough curve was obtained at the Blue Pool outlet for the bacteriophage *Phix 174* which can be directly compared to the dye breakthrough curves. The main peak of *Phix 174* appears to be divided into 4 subsidiary peaks (Figure 5.15). If these peaks represent true variations in tracer levels in the Blue Pool outlet channel, it could indicate that the bacteriophage tracer travelled down multiple pathways. However the sample density is low and it appears that there are two outliers (circled red on Figure 5.15). If these are removed (dashed line on Figure 5.15), three of the peaks are no longer present and the final smaller peak is only defined by one sample. It seems likely that the multiple peaks are artefacts arising from errors in analytical procedure. The two outliers were omitted from the *Phix 174* dataset in Figure 5.16 which compares the rising and falling limbs of the main peaks of all the tracers (scaled to the average of three peak tracer concentrations), and suggests that the rising and falling limb of the peak in *Phix 174* was very similar to those of the dye tracer peaks. As at the Blue Pool spring (Figure 5.7) the breakthrough curves for Sodium Naphthionate, Sodium Fluorescein and Eosin at the Blue Pool outlet are almost identical (Figure 5.16). The similarity of the bacteriophage breakthrough curve provides further evidence that double porosity diffusion is not significant because it is a particulate tracer unlikely to undergo diffusion. The breakthrough curve for the Amidorhodamine G differed from the other dyes in a similar manner to the Blue Pool spring, with a more gradual return towards background after the main peak.

Figure 5.17 shows all the data for the five tracers at the Blue Pool outlet. Monitoring did not continue as long as at the Blue Pool spring, but the start of the secondary peak is apparent in the dye tracers just before monitoring ended. It is not known whether there was an increase in *Phix 174* during this period because sample analysis for this tracer stopped just before the start of the secondary peak. There are broadly diurnal fluctuations in the tails of all the breakthrough curves except that of Amidorhodamine G, which appear to relate to photochemical decay and are discussed further in Section 5.4.2.5. It is interesting that the diurnal fluctuations are also apparent in the bacteriophage tracer (Figure 5.17), indicating that this tracer was also affected by light.

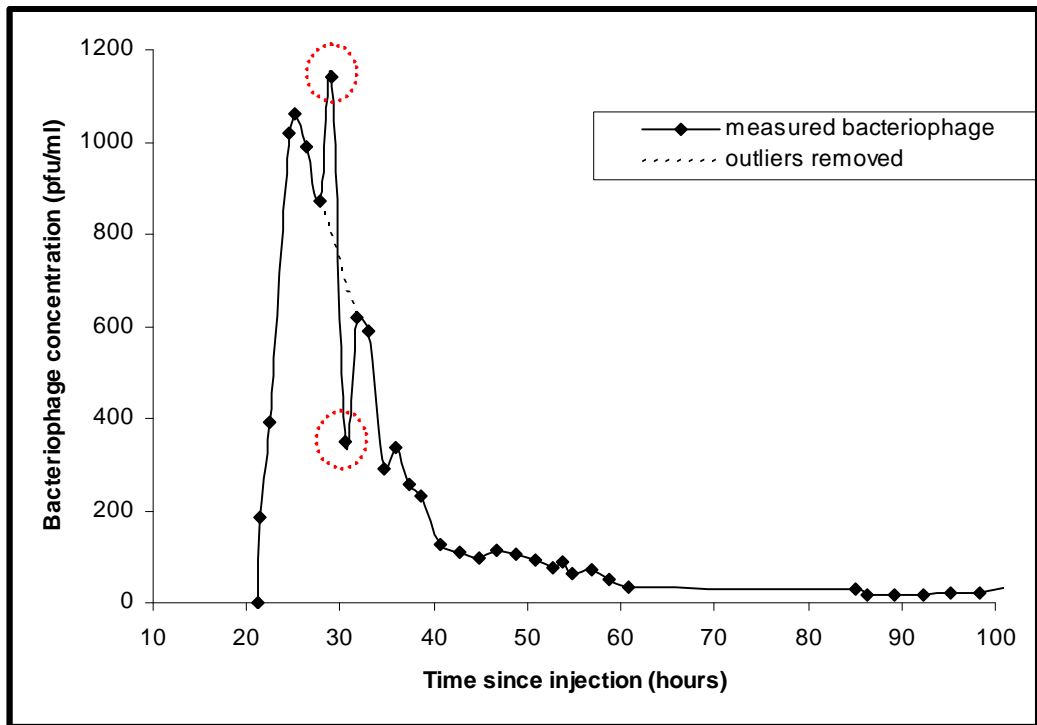


Figure 5.15: The first 100 hours of the breakthrough curve of *Phix 174* bacteriophage at the Blue Pool outlet. Multiple peaks are apparent but are most likely due to errors during analysis of two outliers (circled red).

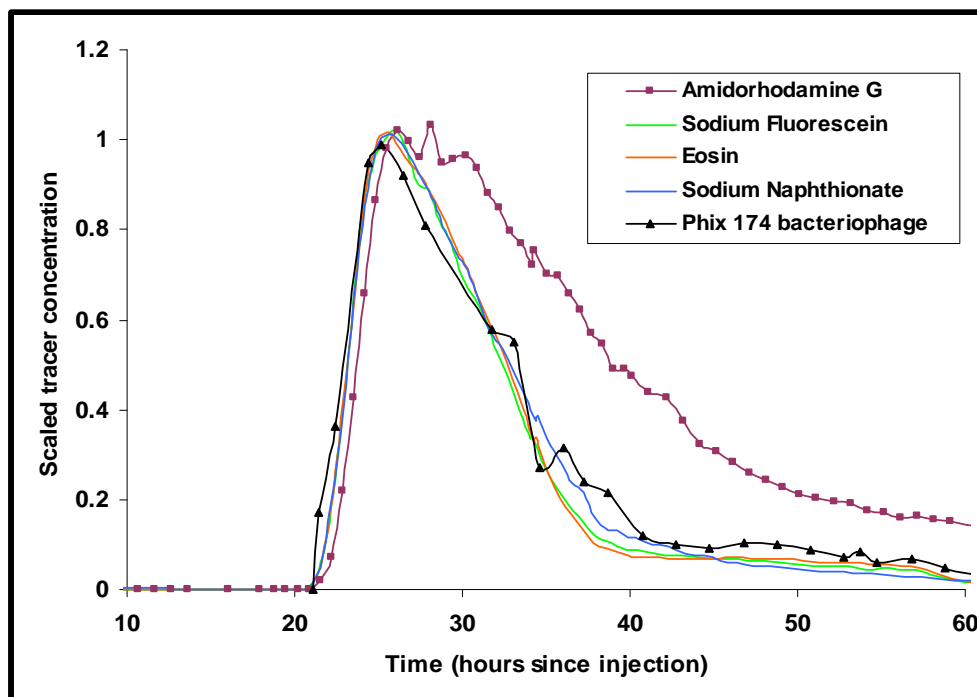


Figure 5.16: Breakthrough curve peaks for the bacteriophage *Phix 174* (outliers removed) and dyes at the Blue Pool outlet. Note that sample times were identical for all dyes and that the sample frequency (shown on the Amidorhodamine G curve) was much higher than for the bacteriophage

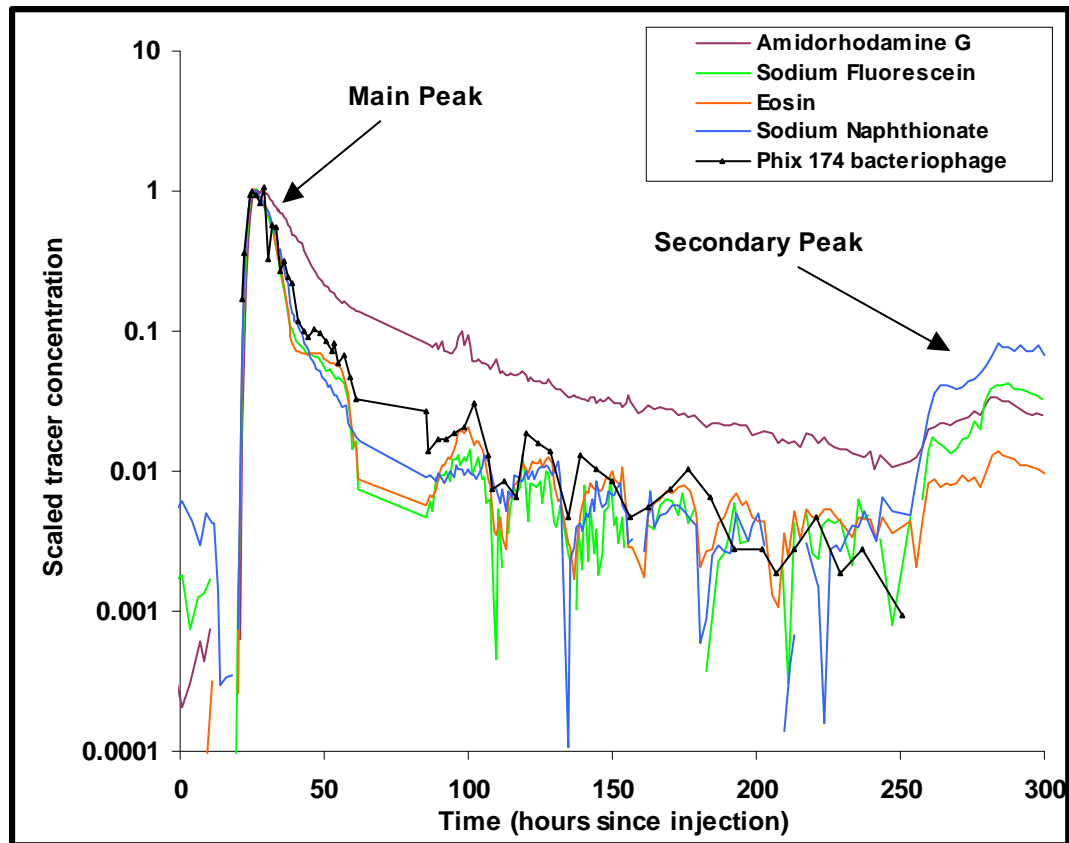


Figure 5.17: Full breakthrough curves at the Blue Pool outlet for 5 tracers (2006)

5.4.2.3 Dye breakthrough curve in the River Pang at Frogmore Farm

Following the second Sodium Fluorescein injection in the 2005 experiment, samples were taken from the River Pang at Frogmore Farm, which is downstream of the input from the Blue Pool outlet channel (Figure 5.4). Figure 5.18 compares the peak in the breakthrough curves in the River Pang at Frogmore Farm and at the Blue Pool outlet using background adjusted concentrations (not scaled values). The data from the Blue Pool outlet were obtained using an in situ field fluorometer that recorded measurements every minute whilst the River Pang breakthrough curve is derived from water samples that were taken at intervals of 1 to 4 hours. Sodium Fluorescein concentrations in occasional water samples taken at the Blue Pool outlet (blue triangles in Figure 5.18) were in good agreement with the data from the in situ field fluorometer.

The peak tracer concentration in the Blue Pool outlet channel was $16 \mu\text{g.L}^{-1}$, which was only slightly higher than that in the River Pang ($13.81 \mu\text{g.L}^{-1}$), despite the increased dilution in the River Pang that had almost twice the flow of the Blue Pool outlet (Table

5.4). During the tail of the breakthrough curve (Figure 5.19) there were slightly higher concentrations in the River Pang than the Blue Pool outlet, and tracer concentrations returned to background earlier at the Blue Pool outlet than in the River Pang. The variation in readings in the tail is very small and may be due to instrument error. However, there was no variation in standard readings on the in situ fluorometer before and after deployment at the Blue Pool outlet and during analysis of samples from the River Pang.

It appears that dye concentrations in the River Pang were higher than might be expected had the Blue Pool outlet been diluted by full mixing with the discharge of the river. This is supported by the higher calculated mass recovery of tracer in the River Pang than in the Blue Pool outlet channel (Section 5.4.3.4). This could be because sampling was on the same side of the river as the input from the Blue Pool outlet channel, and the tracer had not mixed across the width of the channel. To check this, on 10/02/05 hand samples were taken on opposite sides of the River Pang at the location of the sampling point. The sample on the same side as the input from the outlet channel measured $0.72 \mu\text{g.L}^{-1}$ whilst that of the other side measured $0.75 \mu\text{g.L}^{-1}$. This does not support the hypothesis of incomplete mixing, but not enough samples were taken from both sides of the river to determine this conclusively. An alternative interpretation is that there is an additional outlet point for tracer in the channel of the River Pang upstream of its junction with the Blue Pool outlet. The Blue Pool is known to comprise several groundwater upwellings and it seems quite possible that the tracer cloud spreads out through a distributary network that includes a component discharged in the bed of the River Pang alongside the Blue Pool (Figure 5.4).

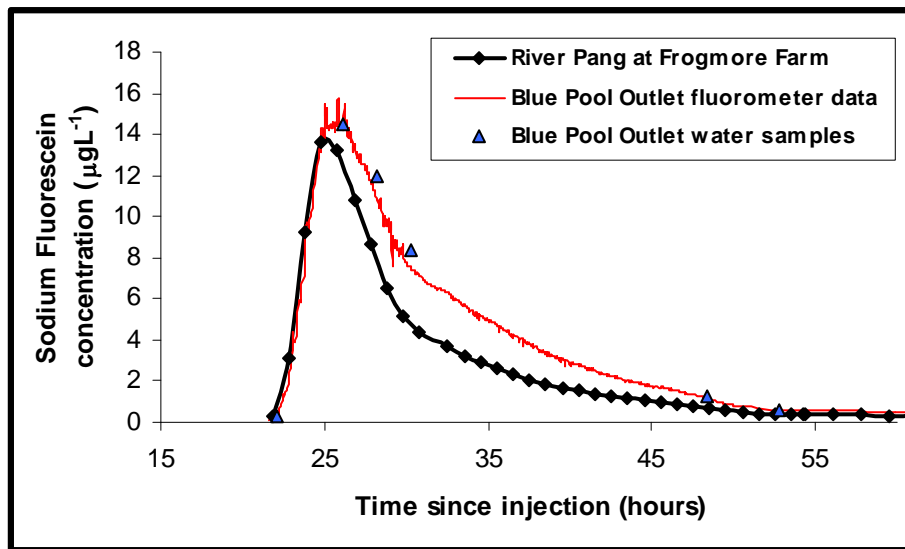


Figure 5.18: Comparison between the peak in the breakthrough curves at the River Pang and the Blue Pool outlet (Injection 2, 2005)

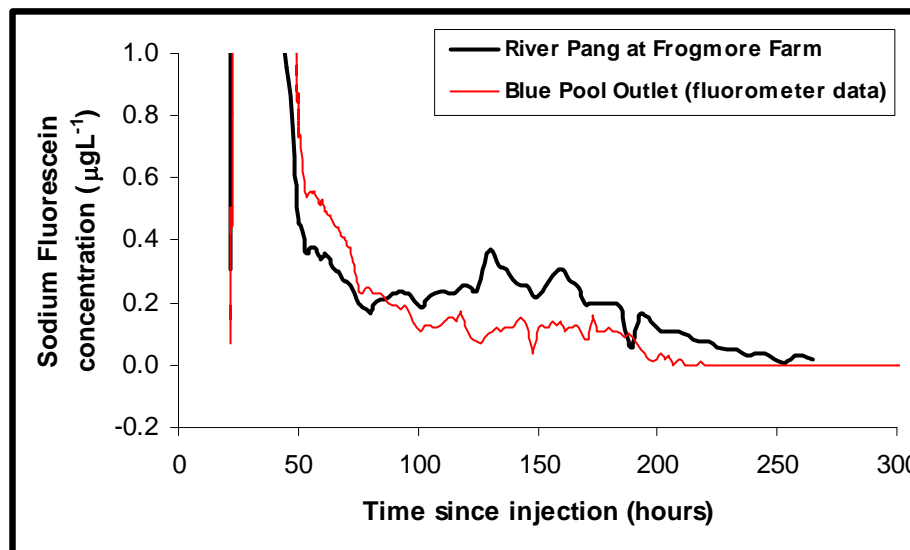


Figure 5.19: Breakthrough curves tails at the River Pang and the Blue Pool outlet (Injection 2, 2005)

5.4.2.4 Comparison of the outlet and the spring monitoring points at the Blue Pool

Figure 5.20 illustrates the differences between dye breakthrough curves obtained from the Blue Pool spring and Blue Pool outlet. Tracer arrived at the Blue Pool outlet channel approximately 3 hours after first arrival of tracer at the Blue Pool spring, and peak tracer concentrations occurred about 5 hours later in the outlet channel. The breakthrough curves from the Blue Pool outlet have a shallower rising limb, smaller peak, and longer falling limb than those from the Blue Pool spring. There is just over a

three-fold dilution in peak concentrations between the Blue Pool spring and the Blue Pool outlet. This is clearly due, at least in part, to mixing and dilution in the pools through which the water flows between the two monitoring points. However, there is some evidence from tracer recovery data (Section 5.4.3), that the tracer concentration may not have been the same in all upwellings in the Blue Pool complex. The upwelling that was sampled directly was the strongest and deepest spring in the complex, and if tracer concentrations do vary between upwellings, it might be expected to have the highest concentration. It is therefore possible that the breakthrough curves obtained at the Blue Pool outlet, which consist of tracer from all upwellings within the complex, may have a reduced peak due to increased dilution from upwellings in which the tracer concentration was lower than at the main spring.

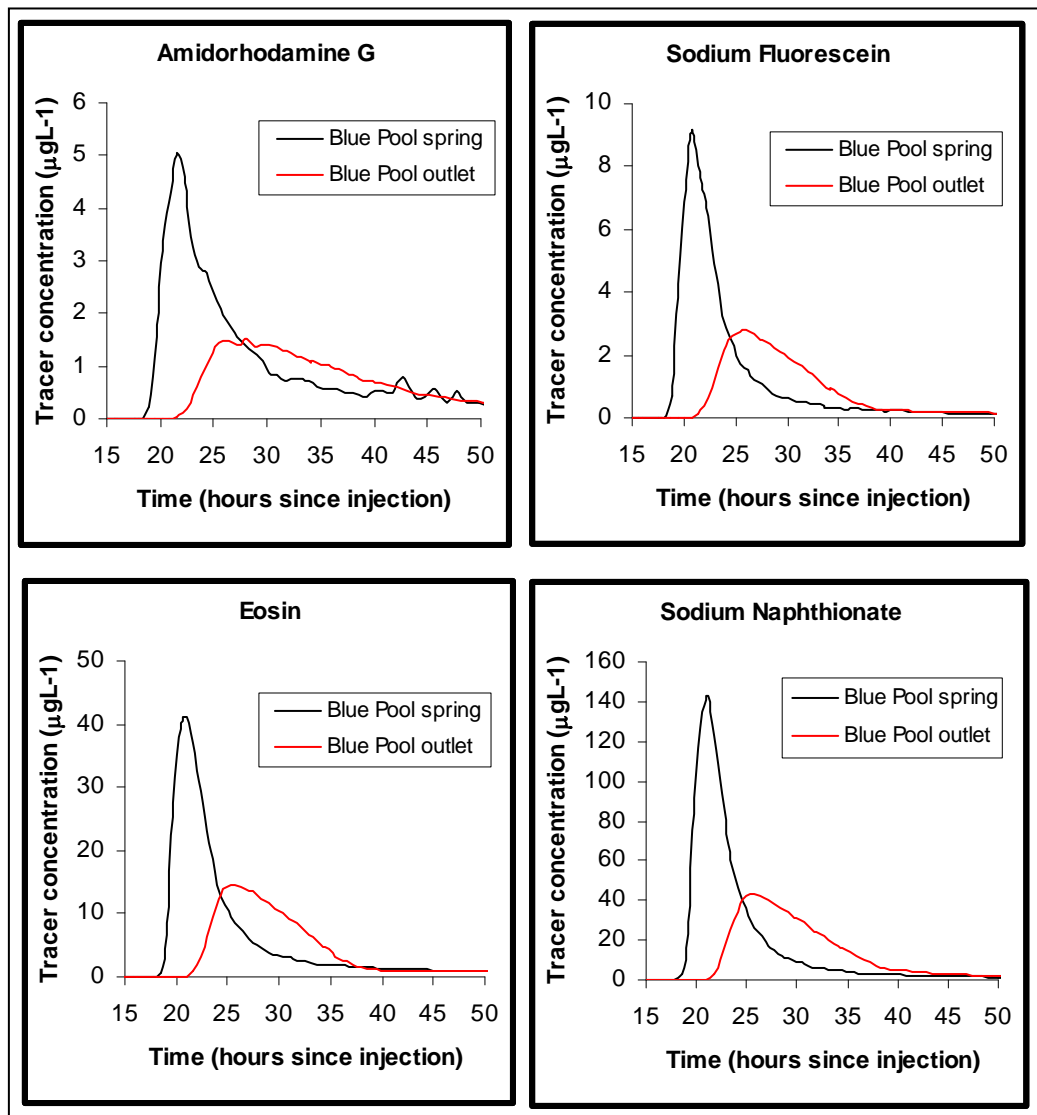


Figure 5.20: Comparison of dye breakthrough curves at the Blue Pool spring and the Blue Pool outlet channel (2006 test)

Few bacteriophage results were obtained at the Blue Pool spring, but during the period for which results are available, bacteriophage levels were generally slightly higher in the Blue Pool spring than at the Blue Pool outlet (Figure 5.21).

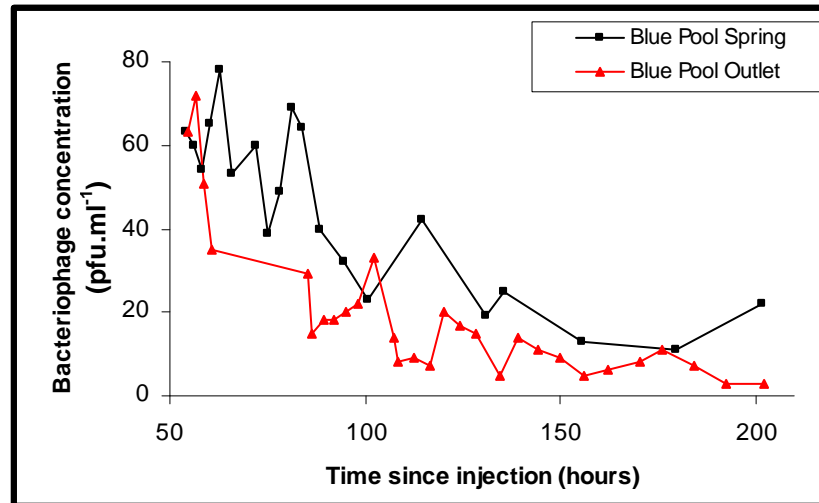


Figure 5.21: Bacteriophage results at the Blue Pool Spring and the Blue Pool Outlet

5.4.2.5 Influence of photochemical decay on tracer breakthrough curves

Many fluorescent dyes decompose in the presence of light. The photochemical decay of dyes used in water tracing has been extensively investigated, and these studies are reviewed in Käss (1998). The breakthrough curves at the Blue Pool spring should not be affected by photochemical decay because samples were taken directly from a discharge point. However, tracer took about three hours to travel between the spring upwellings and the monitoring point in the Blue Pool outlet channel (Section 5.4.2.4), and therefore the breakthrough curves from the Blue Pool outlet (and calculated tracer recoveries) are likely to be affected by photochemical decay. Sodium Fluorescein is particularly susceptible to photochemical decay (Smart and Laidlaw, 1977; Käss, 1998), and it is probable that fluctuations observed in the tail of the Sodium Fluorescein breakthrough curves (Figure 5.14) are caused by photochemical decay reducing tracer concentrations in samples taken during daylight hours whilst those taken at night remain unaffected.

Looking at the 2006 breakthrough curves in more detail (Figure 5.22) it is clear that fluctuations in the tail are diurnal and that all the dyes except the Amidorhodamine G

are affected. The peaks in the fluctuations all occur during the night (the tracers were injected at around midnight on 26/02/06, and therefore each of the vertical black lines on Figure 5.22 are also about midnight). The fluctuations are absent from the Blue Pool spring breakthrough curves (Figure 5.6) confirming that the fluctuations observed at the Blue Pool outlet are likely to be caused by photochemical decay effects between the spring upwellings and the Blue Pool outlet channel monitoring point. Table 5.7 lists photolytical coefficients of the tracers used in the current study (Käss, 1998). A high photolytical coefficient indicates a greater susceptibility to photochemical decay. Amidorhodamine G has a very low susceptibility to photochemical decay explaining the absence of the fluctuations in the breakthrough curve of this tracer. The magnitude of the fluctuations of the Eosin breakthrough curve is higher than that of the Sodium Fluorescein breakthrough curve which might be expected given that Eosin has a higher photolytical decay coefficient. However, the greatest fluctuations occur in the Sodium Naphthionate breakthrough curve, which has a lower photolytical coefficient than Sodium Fluorescein and Eosin, indicating that this tracer may be more susceptible to photochemical decay than suggested by Käss (1998). Although three of the tracers were clearly affected by photochemical decay, it does not appear to have a significant affect on the tracer recovery at the Blue Pool outlet because tracers more susceptible to photochemical decay (with higher photolytical coefficients) do not have lower total recoveries (Section 5.4.3.2). This may be because most of the tracer was discharged during the main peak that has no diurnal fluctuations (Figure 5.16) because it occurred during the night.

Table 5.7 Photolytical coefficients of dyes used at Smithcroft Copse (data from Käss, 1998)

Dye	Photolytical coefficient
Amidorhodamine G	8
Sodium Naphthionate	150
Sodium Fluorescein	550
Eosin	1000

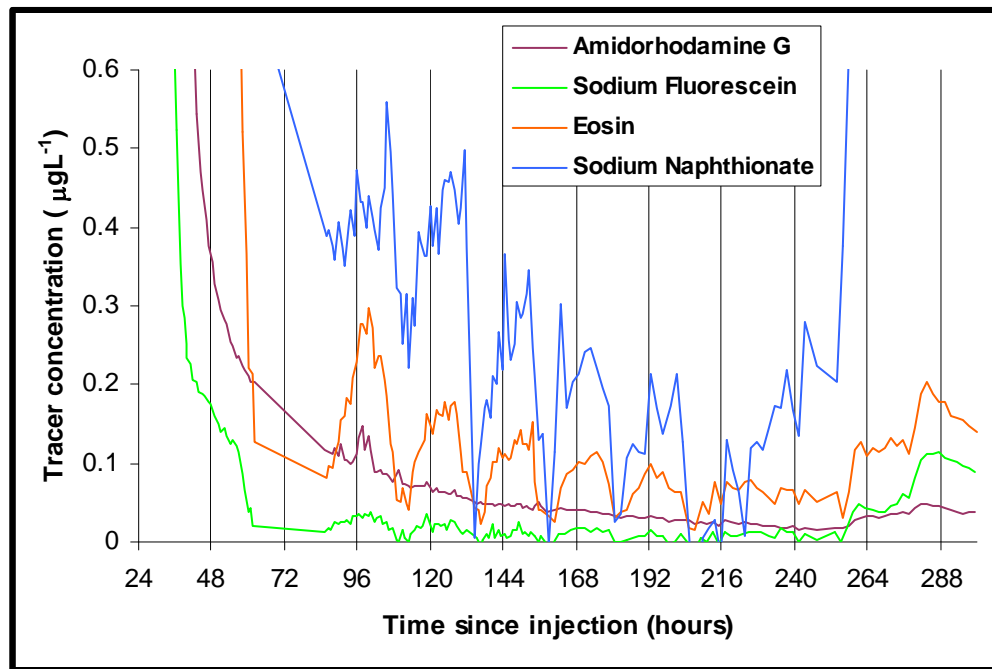


Figure 5.22: Diurnal fluctuations in breakthrough curve tails at the Blue Pool outlet. Data are scaled to peak tracer concentrations with background values removed. Tracers were injected around midnight and vertical lines indicate 24-hour intervals

5.4.3 Tracer recoveries and mass balance

5.4.3.1 Introduction

Where tracer concentration and groundwater discharge are measured the tracer recovery can be calculated. This is the percentage of the injected mass that passed through a monitoring point between breakthrough and the return of tracer concentrations to below the detectable threshold.

The mass of tracer recovered is calculated by:

$$M_o = \int_0^{\infty} C(t) Q(t) dt$$

Where:

M_o = mass of tracer recovered (μg)

C = tracer concentration ($\mu\text{g.L}^{-1}$)

t = time of sample collection

Q = groundwater flow (L.s^{-1})

The tracer concentration is the raw measured apparent fluorescence ($\mu\text{g.L}^{-1}$) minus a background fluorescence (in this study, this was the average fluorescence of 5 samples prior to tracer arrival unless otherwise stated).

5.4.3.2 Tracer recovery at the Blue Pool outlet

The tracer recovery was calculated for three Sodium Fluorescein breakthrough curves that were obtained at the Blue Pool outlet channel in 2005 and 2006, and the breakthrough curves of four other tracers injected during the 2006 experiment. Following the first tracer injection in 2005, stage and flow were not measured at the Blue Pool outlet during the precise period of peak tracer discharge. Flow measured by current meter three days after this injection was used to calculate the tracer recovery. Following the second injection in 2005 stage and discharge at the Blue Pool outlet were measured frequently (Section 5.4.1.1). As there was little change in stage, a constant value of groundwater flow (the average of four current meter measurements that were made during the test) was used to calculate the tracer recovery. Following the 2006 tracer injections, flow at the Blue Pool outlet remained constant during the period of peak tracer discharge but there was a small increase in flow ($\sim 5 \text{ L.s}^{-1}$) which occurred during the latter stages of the breakthrough curves, and coincided with a secondary small peak (Section 5.4.1.2). During this secondary peak, tracer concentrations were very low and calculating the recovery at the Blue Pool outlet using the increased value of flow during this period was found to have no significant effect ($< 0.1 \%$). All the recoveries from the 2006 experiments presented below are calculated using a constant value of flow (the average of two current meter measurements made during the test which was 192 L.s^{-1}).

Table 5.8 shows that the total recovery of Sodium Fluorescein tracer at the Blue Pool outlet following the three injections was similar. Following the 2005 tracer injections, the recovery was slightly higher under higher flow conditions. In the 2006 experiment the flow was almost the same as during the second 2005 injection, and although velocities were identical the recovery was slightly higher in the 2006 experiment. This may be because the time period over which the recovery was calculated was longer in the 2006 experiment. Following the second tracer injection in 2005, concentrations had returned to background 213 hours after injection, whilst in the 2006 injection additional tracer was discharged (during the secondary peak) up to 299 hours after the injection

(Figure 5.14). The recovery of the main peak in the 2006 injection was 21.9 % (excluding tracer discharged in the secondary peak), which is similar to the recovery following the second 2005 injection (21.7 %).

Table 5.8: Sodium Fluorescein tracer recovery at the Blue Pool Outlet

Injection Date	Tracer recovery (%)	Flow [^](L.s⁻¹)	Velocity* (km.d⁻¹)
31/01/05	25.5	209	5.1
07/02/05	21.7	193	4.7
26/02/06	23.95 (21.9 in main peak)	192	4.7

* *Groundwater velocity is based upon the time to peak tracer concentration*

[^] *Flow value used to calculate recovery.*

For the 2006 experiment, the tracer recoveries at the Blue Pool outlet during the main and secondary peaks were calculated separately for the four dyes. The secondary peak recoveries cannot be calculated using exactly the same method for each dye because the breakthrough curves have different patterns prior to the start of the secondary peak, and therefore different methods are required to determine the “background” apparent fluorescence value that would have been measured if the secondary peak had not occurred (and which therefore must be subtracted from measured values to calculate the recovery). At the start of the secondary peak, Amidorhodamine G concentrations had not returned to background. The relatively regular decline in concentrations was used to extrapolate the “background” value that might be expected if the secondary peak had not occurred (Figure 5.23), assuming that tracer concentrations would have continued to decline at the same rate. These extrapolated values were subtracted from measured concentrations during the secondary peak before the tracer recovery was calculated.

Sodium Fluorescein and Sodium Naphthionate concentrations had returned to background before the start of the secondary peak. Raw apparent fluorescence concentrations were lower than before the main peak. A new background (the average of 5 values prior to the arrival of the secondary peak) was subtracted from the measured values in the secondary peak. There are large fluctuations in the tail of the Eosin breakthrough curve (Figure 5.17), but in the 24 hours prior to the start of the secondary peak readings were within, (although at the higher end of), the range of values measured prior to initial tracer breakthrough. The average of 5 readings prior to the arrival of the secondary peak was subtracted from measured values in the secondary peak. It is

however possible that tracer from the first peak was still present and therefore the background value used is higher than the actual background value. If this is the case, the recovery of the secondary peak is slightly underestimated.

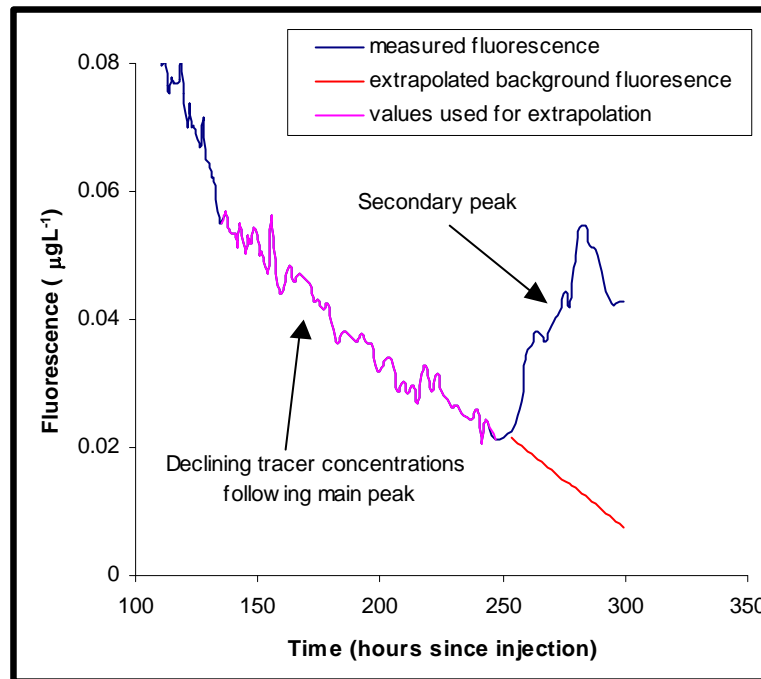


Figure 5.23: Determination of “background” Amidorhodamine G concentrations during the secondary peak. The blue line is the raw data and the red line represents the likely concentrations that would have been measured if the secondary peak had not occurred, based on extrapolation of declining tracer concentrations (pink line depicts values used for extrapolation)

Table 5.9 lists the total tracer recoveries for all the tracers used in the 2006 experiment, and includes a breakdown of the % discharged during the main and secondary peaks. This breakdown is discussed further in Section 5.4.3.5. The total tracer recoveries for the 4 dyes were similar (~ 21-25 %), with the exception of Amidorhodamine G that had a lower recovery (13.66 %). Only 0.87 % of the injected bacteriophage was recovered, indicating that there were very high losses of this tracer compared to the dyes. Bacteriophage losses are generally considerably greater than dye losses (Käss, 1998) and it is likely that die off and sorption were contributing factors to the low bacteriophage recovery.

The photolytical coefficients of the dye tracers (from Käss, 1998) are included in Table 5.9 because some of the breakthrough curves were affected by photochemical decay (Section 5.4.2.5). However, tracers with higher photolytical coefficients (and hence a greater susceptibility to photochemical decay) do not have lower recoveries (Table 5.9), indicating that any effects of photochemical decay on the tracer recoveries at the Blue Pool outlet were extremely small.

Table 5.9: Tracer recovery at the Blue Pool Outlet (2006)

	Total recovery (% mass injected)	1st Peak* (% mass injected)	2nd Peak^ (% mass injected)	Molecular weight	Photolytical coefficient
Sodium Naphthionate	21.40	18.12	3.28	245	150
Sodium Fluorescein	23.95	21.89	2.06	376	550
Amidorhodamine G	13.66	13.23	0.44	553	8
Eosin	24.66	24.12	0.54	692	1000
Phix 174 Bacteriophage	0.87				

* *Background value prior to main peak subtracted from data*

^ *Uses calculated background prior to secondary peak, see above*

5.4.3.3 Tracer recovery at the main Blue Pool spring

In the 2006 experiment breakthrough curves were also obtained at the Blue Pool spring monitoring site (Section 5.4.2.1). The data from these breakthrough curves cannot be used to determine accurate tracer recoveries because the groundwater discharge at the sampling point is not known. Apparent recoveries were calculated using the measured discharge in the Blue Pool outlet channel (192 L.s⁻¹). This assumes that the tracer concentration at the Blue Pool spring sampling point was the same as at all other upwellings in the complex.

There is a better record of the secondary peak at the Blue Pool spring sampling site than at the Blue Pool outlet because sampling continued for a longer period. The recovery during the main and secondary peaks was calculated separately. For the main peak, a background value (the average of five samples prior to breakthrough) was removed from the raw data. Sodium Naphthionate and Sodium Fluorescein had returned to this background level prior to the start of the secondary peak and the average of 5 samples

before the secondary peak was subtracted as a background value for calculation of the secondary peak recovery. Eosin and Amidorhodamine G concentrations were declining steadily prior to the start of the secondary peak; therefore background values were extrapolated using the same method outlined for the Amidorhodamine G at the Blue Pool outlet (Figure 5.23)

The calculated tracer recoveries at the Blue Pool spring are shown in Table 5.10, which includes a breakdown of the percentage recovery during the main and secondary peaks (discussed in Section 5.4.3.5). Comparison of the total tracer recovery at the Blue Pool spring and at the outlet suggests that water discharged through different upwellings in the Blue Pool complex may have had different tracer concentrations. The calculated total tracer recoveries are higher at the Blue Pool spring than at the Blue Pool outlet. Although monitoring continued longer at the Blue Pool spring than at the outlet, this does not appear to account for the higher recoveries. The recovery of Sodium Fluorescein tracer at the Blue Pool spring was recalculated using only data from the period during which the Blue Pool outlet was also monitored (up to 299 hours after injection). This results in a reduction in Sodium Fluorescein recovery at the Blue Pool spring from 40.1 % to 34 %. However, this 34 % recovery is still considerably higher than the 24 % recovery at the Blue Pool outlet suggesting that the length of monitoring period is not the only cause of the difference in recovery at the two sites. It is also unlikely that photochemical decay is the cause of the lower recovery at the Blue Pool outlet because it has been shown to have no significant effect on the recoveries (Section 5.4.3.2), and the Amidorhodamine G, which is not susceptible to photochemical decay, still has a higher recovery at the Blue Pool spring than at the Blue Pool outlet. It is therefore probable that the spring upwelling monitored in the test (the deepest and largest in the spring complex) had a higher concentration of tracer than other upwellings, resulting in an apparently higher recovery when the total discharge from the Blue Pool spring complex was used to calculate the tracer recovery at the upwelling. If different upwellings within the Blue Pool complex have significantly different tracer concentrations, this implies that the tracer discharged at different points within a very small area may have travelled along different flowpaths. The issue of multiple flowpaths is considered further in Section 5.5.

Table 5.10: Apparent tracer recoveries at the Blue Pool spring (2006)

Dye	Total recovery (% mass injected)	1st Peak (% mass injected)	2nd Peak (% mass injected)	Molecular weight
Sodium Naphthionate	34.9	24.26	10.65	245
Sodium Fluorescein	40.1	31.85	8.30	376
Amidorhodamine G	20.7	18.54	2.14	552.59
Eosin	36.4	34.55	1.92	691.88

5.4.3.4 Tracer recovery from the River Pang at Frogmore Farm

The monitoring site in the River Pang at Frogmore Farm is downstream of the Blue Pool outlet channel (Figure 5.4). This site was only monitored following the second injection in 2005. There were no variations in stage measured in the River Pang at Frogmore Farm during the period of peak tracer discharge, and the average of the gauged flow measured on the day of injection and two days later (Table 5.4) was used to calculate the tracer recovery, which was 29.7 %. This is higher than the recovery at the Blue Pool outlet over the same period (21.7 %). The higher recovery in the River Pang might be due to incomplete mixing between the Blue Pool outlet channel and the River Pang (Section 5.4.2.3), but it is more likely that tracer was discharged directly through the bed of the River Pang which when combined with that from the Blue Pool outlet channel, resulted in a greater quantity of tracer passing through the River Pang monitoring point than the Blue Pool outlet. The probable existence of such additional outlet points is consistent with the general layout of the Blue Pool complex itself, with its multiple spring points, and also with the inference made above, that tracer concentrations varied between these outlets.

5.4.3.5 Evidence of diffusion from the tracer recovered in the main and secondary peaks

A clear correlation between the magnitude of the secondary peak and the molecular weight of the tracers was demonstrated in Section 5.4.2.1, although the Amidorhodamine G tracer only fitted the pattern when the tracers were scaled to the peak tracer concentration (Figure 5.9) rather than the injection mass (Figure 5.12). The tracers with lower molecular weights (and hence higher diffusion coefficients) had larger secondary peaks suggesting that a large proportion of the tracer present during the secondary peaks resulted from a process that involved diffusion. This is considered further here, in the light of the tracer recovery data presented above. Although the

patterns described below occur both at the Blue Pool outlet and the Blue Pool spring monitoring sites, only the data from the Blue Pool spring are presented because monitoring at this site continued for the entire duration of the secondary peak, which is not fully recorded in the data from the Blue Pool outlet.

Excluding the data for Amidorhodamine G which are clearly affected by sorption, there appears to be a correlation between the tracer recovery during the *main* peak and the molecular weight of the tracer, with those tracers with higher molecular weight having higher tracer recovery (Figure 5.24, Table 5.10). One interpretation of this result is that diffusion along the flowpath has decreased the amounts of the tracers with lower molecular weight. However, this correlation between the main peak and the molecular weights of the tracers is surprising because when the tracer breakthrough curves were scaled to the injection mass (Figure 5.10) although there were variations in the peak heights of the Sodium Naphthionate, Sodium Fluorescein and Eosin tracers, the peak height did not decrease with decreasing molecular weight as would be expected if diffusion was the sole cause of the variations in the peak heights.

Sodium Naphthionate has the lowest molecular weight of the three and does indeed display the lowest peak concentration (scaled to mass injected). It also has lower peak scaled concentrations than the other two dyes throughout the main peak, and therefore a lower main peak recovery. If molecular weight and diffusion were the sole cause of differences among these tracers, then it would be expected that Sodium Fluorescein would show lower concentrations than Eosin. In fact, Sodium Fluorescein has a higher scaled peak concentration than Eosin, and for much of the descending limb of their main peaks, these two tracers have almost identical scaled concentrations (Figure 5.10). Thus it is superficially not obvious from Figure 5.10 alone why Eosin has a higher main peak recovery than Sodium Fluorescein. The reason can be found by close inspection of the tails of the main peak (Figure 5.11). Here Sodium Naphthionate and Sodium Fluorescein both decline to background values at around 100-110 hours, whereas Eosin displays tailing behaviour very similar to that of Amidorhodamine G. The extra recovery produced by this tail is more than sufficient to compensate for Eosin's lower scaled peak concentrations compared to Sodium Fluorescein, and to give it the highest overall recovery in the main peak. Thus recoveries are ordered in agreement with molecular weight, but peak concentrations and curve shapes are not.

Identifying the process that is responsible for the tailing of Eosin is problematic. The close similarity of the breakthrough curves of all these tracers when scaled by peak height (Figure 5.7) strongly indicates that the major process affecting them are the same, despite their differences in molecular weight. Thus diffusion cannot be a major process affecting curve shape during the first 35 hours of the experiment. When scaled by mass, the peak heights and relative concentrations differ (Figure 5.10) but not in a way predicted from molecular weight, and then only when the tail of the main peak out to 250 hours is included (Figure 5.11). It seems likely that more than one process is involved. Perhaps Eosin is subject to slightly greater reversible sorption than Sodium Fluorescein, which would produce the lower peak and extra tailing seen in Figure 5.10 and 5.11. Sodium Fluorescein sorption on chalk has been measured as slight by Amy Wilkinson (Tim Atkinson, personal communication, 2006). On the other hand diffusion might be involved to explain the much lower concentrations of Sodium Naphthionate. If correct this would imply that all of the dyes were affected by diffusion to different degrees, but none was affected sufficiently to change the shape of the main peak (Figure 5.7). But in fact Sodium Naphthionate (with lowest molecular weight and highest diffusion coefficient) is affected most in the peak (very significantly) and least in the tail, which is inconsistent with diffusion being the dominant cause of the lower peak. It seems likely that Sodium Naphthionate is affected by some other process such as irreversible sorption or other chemical reaction which could result in a lower peak combined with no increase in tailing. The similarity of the dye breakthrough curves to that of the bacteriophage, which is definitely affected by irreversible sorption and die-off, makes this an attractive hypothesis.

Further evidence about the role of diffusion is provided by the quite serendipitous occurrence of a secondary peak, after 250 hours. This was a response to rainfall and increased discharge. The evidence is strong that diffusion is an important process controlling the behaviour of tracers in the secondary peak. There is a very strong linear correlation between % recovery during the secondary peak and tracer molecular weight (Figure 5.25). This correlation ($R^2 = 0.918$) includes Amidorhodamine G (the black circle). As suggested previously by the magnitude of the height of the secondary peaks (Section 5.4.2.1), it appears that the secondary peak recovery was larger for tracers with lower molecular weights. This implies that the secondary peak predominantly

comprises tracer that was previously diffused during transport and which was subsequently flushed out by the increased flow at the time of the secondary peak. This hypothesis is supported by Figure 5.26, which shows that there is a very strong (exponential) correlation between the ratio of the main/secondary peaks and tracer molecular weight ($R^2=0.997$). The implication of this is that there was greater diffusion of the tracers of lower molecular weight as the main peak of the tracer cloud passed through the aquifer resulting in a slightly lower overall tracer recovery at the Blue Pool during the main peak. This diffused tracer was subsequently flushed out by the increase in flow in the aquifer forming the secondary peak that was larger for the tracers that had previously undergone more diffusion. This implies that during the main peak, although the *shape* of the breakthrough curve was not affected by diffusion in a manner that could be distinguished from the sorption processes affecting the dyes, the *mass* may have been affected to a small extent by diffusion. The situation is complicated because irreversible sorption may also have affected the mass recovery during the main peak, and therefore the evidence for tracer mass loss due to diffusion during the main peak is inconclusive. However, the correlations in Figures 5.25 and 5.26 conclusively demonstrate that for all the tracers, diffusion was the most important factor in determining the size (and potentially existence) of the secondary peak.

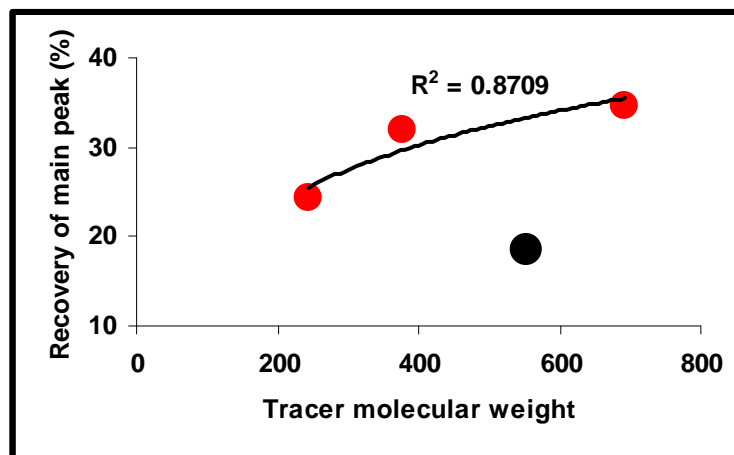


Figure 5.24: Correlation between tracer recovery during the main peak at the Blue Pool Spring and tracer molecular weight (the black circle is the Amidorhodamine G which is excluded from the correlation because it is affected by sorption reducing the recovery relative to that of other dyes)

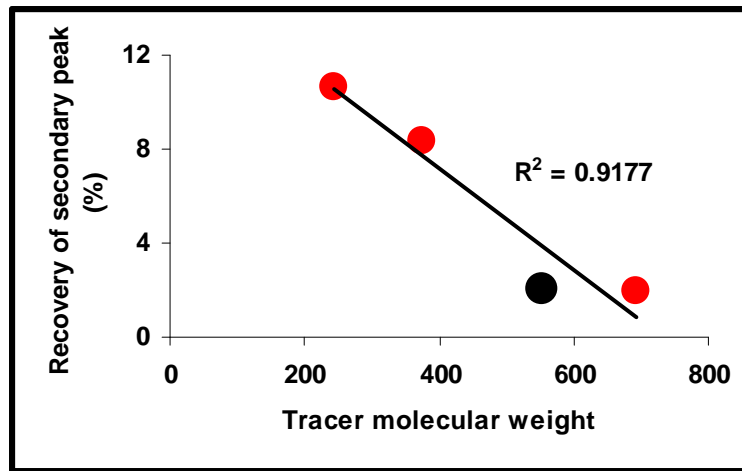


Figure 5.25: Correlation between secondary peak recovery and tracer molecular weight at the Blue Pool Spring (including Amidorhodamine G)

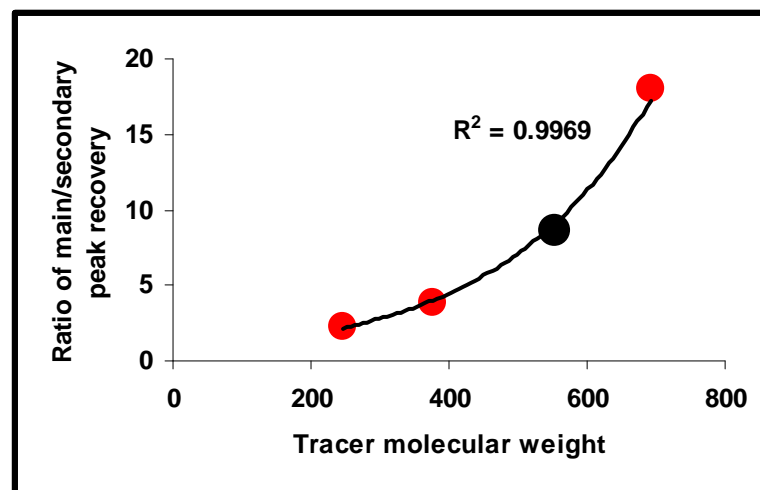


Figure 5.26: Correlation between the ratio of the main/secondary peaks and tracer molecular weight (including Amidorhodamine G)

5.4.4 Discussion of sorption of dyes during the 2006 multi-tracer test

Some tracers are more susceptible to sorption than others. Experiments investigating the sorptive properties of dyes used in water tracing are reviewed in Käss (1998). Several studies have been carried out on Sodium Fluorescein. These found little sorption on mineral matter, but more on organic matter (Smart and Laidlaw, 1997; and German studies by Leibundgut and Lüthi (1976) and Dervey, (1985) that are cited by Käss (1998)). Käss (1998) notes that the study by Dervey (1985) concluded that in

terms of sorption Sodium Fluorescein is a near ideal tracer, closely followed by Eosin, whilst Amidorhodamine G is more sorptive. There is little information on the sorptive properties of Sodium Naphthionate, although there is some suggestion in Käss (1998) that it may be similar to Amidorhodamine G.

Over the Smithcroft Copse-Blue Pool connection it is possible that sorption may occur on organic matter at the stream sink input point, on sediments overlying the Chalk, and on sediments within chalk conduits; but sorption onto the Chalk itself is likely to be most important as most of the flowpath is within the Chalk. A study of Sodium Fluorescein sorption on chalk was undertaken by Amy Wilkinson (Tim Atkinson, personal communication, 2006). This study found that in solutions containing large amounts of suspended chalk particles Sodium Fluorescein was very slightly sorbed suggesting that over a conduit flowpath where there is less contact with chalk there would be no significant sorption of Sodium Fluorescein dye.

There is clear evidence that the Amidorhodamine G tracer was sorbed during the 2006 multi-tracer test from Smithcroft Copse stream sink. The main peak occurred later than the main peaks of the other tracers and the breakthrough curve (scaled to the peak concentration) had higher concentrations during the falling limb (Figure 5.7). The main peak was also much smaller relative to the injection mass than the other three dyes (Figure 5.10), and there was more tailing (Figure 5.11). The total tracer recovery was much lower than that of the other tracers (Tables 5.9 and 5.10), suggesting that sorption caused substantial tracer loss as well as retardation and tailing. The falling limbs of the main peaks in the breakthrough curves for Sodium Fluorescein, Eosin and Sodium Naphthionate (scaled to peak tracer concentrations), and the timing of the peaks are almost identical suggesting that sorption of these tracers did not occur. However, differences in peak height when the tracer is scaled to injection mass (Figure 5.10), which cannot be accounted for by diffusion, suggest that Eosin and Sodium Naphthionate may have been affected by sorption (Section 5.4.3.5). There is also more tailing in the Eosin breakthrough curve than in the other tracers (Figure 5.11), despite the fact that it has the highest molecular weight and would therefore be expected to have the least tailing from diffusion effects. The high tracer recovery (Tables 5.9 and 5.10) suggests that if Eosin was affected by sorption, the process was probably reversible. In contrast, the lack of tailing in the Sodium Naphthionate (Figure 5.10 and 5.11) suggests

if sorption was a cause of the low peak height and low recovery relative to the other tracers, the sorption process was irreversible.

5.4.5 Advection-dispersion and double porosity modelled breakthrough curves

A spreadsheet based forward simulation model was developed by John Barker (personal communication, 2006) to investigate whether the breakthrough curve from the Blue Pool fits an advection-dispersion or a pure double porosity model. The Sodium Fluorescein breakthrough curve from the Blue Pool spring monitoring site was compared to modelled curves that were either defined by an advection-dispersion process or by double porosity diffusion. For advection-dispersion, parameters of t_a (advection time) and t_d (dispersion time) are adjusted and for double porosity t_a and t_{cf} (time for half the tracer in a fracture to be diffused into the matrix) are adjusted to obtain the best fit with the field data. Results are presented in Figure 5.27 with parameter values in Table 5.11. Whilst the advection-dispersion model can fit the rising limb and the peak of the Sodium Fluorescein breakthrough curve at the Blue Pool spring it cannot simultaneously fit the tail. There is significantly more tailing than can be accounted for by advection-dispersion alone. The tail of the breakthrough curve fits the double porosity diffusion model much better. However, in order to fit peak timing and height simultaneously with the tail, the pure double porosity model must use an advection time of 21.7 hours, and so is unable to account for either the rising limb of the actual breakthrough curve or the peak, which occurs earlier at 20.8 hours in the data. In addition a T_{cf} of 133 hours is required to fit the tail, which is many times greater than the advection time. Thus neither of the pure end member processes account for the whole shape of the observed breakthrough curve. A hybrid model, in which advection-dispersion is accompanied by double porosity might do so, but would still require that double porosity diffusion was a major cause of breakthrough curve tailing.

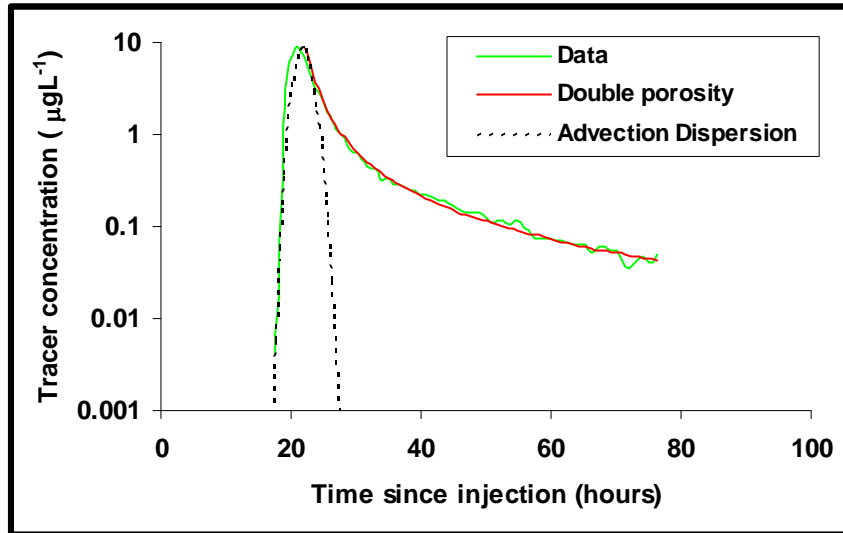


Figure 5.27: Comparison of the Sodium Fluorescein breakthrough curve at the Blue Pool Spring to modelled curves where advection-dispersion or double porosity diffusion dominate

Table 5.11: Model parameters

	Advection-Dispersion	Double Porosity
C_o (Scaling factor between model and data output)	26.7	33.3
T_a (hours)	21.7	21.7
T_d (hours)	0.03	-
T_{cf} (hours)	-	133

As discussed previously, the amount of tailing (following the main peak) does not relate to the molecular weights of the tracers (Figure 5.11, Table 5.12). If the tailing in the breakthrough curves were caused by diffusion, tracers with lower molecular weights should have more tailing. Whilst it is possible that more complicated sorption effects occurred which masked the impact of differential diffusion on the breakthrough curve tails, this is very unlikely because it would require sorption of Sodium Fluorescein to cause higher tailing in this tracer than in the Sodium Naphthionate (the Sodium Naphthionate has the lowest molecular weight and consequently should have undergone the greatest diffusion and had the most tailing, but in fact had the least tailing).

As discussed in Section 1.1, processes other than double porosity diffusion can cause breakthrough curve tailing and the balance of evidence suggests that this is the case along the Smithcroft Copse-Blue Pool flowpath. Injection procedures are unlikely to

affect tailing in a natural gradient tracer test involving a point injection at a stream sink, and it therefore seems most likely that the tailing is due to the effects of lateral dispersion (branching and reuniting of fractures, fissures and conduits in a network with highly heterogeneous permeability and flow velocities), in a similar manner to that suggested by Becker and Shapiro (2000).

Table 5:12 Summary of tailing following main peak and tracer molecular weight

Tracer molecular weight	Tracer in order of increased tailing
245	Sodium Naphthionate
376	Sodium Fluorescein
691	Eosin
553	Amidorhodamine G

5.5 Summary and Interpretation

Quantitative dye tracer tests between Smithcroft Copse stream sink and the Blue Pool have demonstrated that although groundwater flow is very rapid, ~75 to 80 % of the dye is lost over the flowpath. Breakthrough curves scaled to peak tracer concentrations demonstrate that three dyes with variable molecular weights (Sodium Naphthionate, Sodium Fluorescein and Eosin) have almost identical falling limbs following the main tracer peak (Figures 5.7 and 5.16) and that these closely resemble a bacteriophage tracer. This, together with the similar total recoveries of these dyes (Tables 5.9 and 5.10), suggests that double porosity diffusion is not the main cause of the tracer losses.

Tracer breakthrough curves display considerable tailing, but breakthrough curve shape does not appear to relate to the diffusion properties of the tracers and modelled breakthrough curves confirm that double porosity diffusion is unlikely to be the cause of the high degree of tailing.

However, there is also clear evidence from the % recovery of tracer during a secondary tracer peak that diffusion occurs as a minor process along the flowpath. As the main tracer cloud passed through the aquifer diffusion did occur. Although it was not sufficient to affect breakthrough curve shape, it is possible that it affected tracer mass. Increased diffusion of tracers with lower molecular weights may have resulted in very slightly lower recoveries during the main tracer peak at the Blue Pool (although this is

not certain because some dyes also appear to be affected by sorption and it is not possible to fully distinguish the effects of sorption and double porosity diffusion during the main peak). An increase in flow caused a secondary tracer peak to be subsequently discharged. It is clear that the secondary peak was caused by an increase in flow because there was no secondary peak over the same period following tracer injection in a previous test when there was no increase in flow. The secondary peak appears to consist of tracer that had been previously diffused during passage of the main tracer cloud, but which was flushed out by the increase in flow. Consequently, tracers with lower molecular weights, which undergo greater diffusion, had larger secondary peaks.

As discussed in Section 5.1, whilst differences in tracers with different diffusion characteristics can be due to diffusion into the matrix, it can also be due to diffusion into stagnant or slow moving water (Reimus et al., 2003). It is not clear whether over the Smithcroft Copse-Blue Pool connection the diffusion was into stagnant water, the matrix or both. One possibility is that the tracer was diffused into stagnant areas that were later flushed out because of the increased flow creating the secondary peak. This might account for the apparent lack of diffusion effects in the tail of the main tracer peak. However, given the high matrix porosity of the Chalk (Section 1.3.2.1), it is likely that diffusion into the matrix was significant.

The explanation accounting for the most observations from the Smithcroft Copse-Blue Pool tracer tests is that the main flowpath consists of multiple pathways, and the following conceptual model (depicted in Figure 5.28) can be inferred. A proportion of tracer was transported along an open fully connected, small-scale, karst system consisting of small conduits and large fissures (the thick black line in Figure 5.28). Groundwater flow is through large voids in which double porosity effects are minimal and therefore attenuation is low. However, there is also strong lateral dispersion and the overall flowpath consists of a branching network of conduits, fissures and fractures that diverge and converge. Some tracer is transported along multiple pathways of sufficient size that the effects of double porosity diffusion are minimal (thin black arrows in Figure 5.28). This causes tailing in the tracer breakthrough curves due to mechanical dispersion as the pathways diverge and converge. Double porosity diffusion may occur along these flowpaths but is clearly not the major cause of the tailing because tracers of different molecular weights do not display corresponding differences in tailing

following the main peak. However, in addition, a high proportion of the tracer (~ 75%) is transported along much narrower fractures and fissures (red dashed arrows on Figure 5.28). In these narrow fractures and fissures, attenuation of tracer by diffusion into the matrix will be highly effective, and although such tracer would ultimately reach the Blue Pool it would be at concentrations too low to be detected. When flow in the aquifer increases just after the passage of a tracer, as it did in the 2006 experiment, tracer that had previously diffused from narrow fractures and fissures into the matrix (and possibly also into areas of slow moving water in fractures/fissures) will have begun to diffuse back out into the narrow fissures and fractures. These were then flushed out by the increased flow resulting in a second peak at the Blue Pool, the size of which is directly related to the molecular weights (and hence diffusion properties) of the different dye tracers.

The nature of groundwater discharge at the Blue Pool is itself an indicator of flow down multiple pathways. Visible colouration following injection 2 in 2005 (Section 4.3.2) demonstrated that tracer is discharged through a number of upwellings within the Blue Pool complex. This suggests that at least within the local area of the Blue Pool complex, there is a distributary network of fissures and conduits. Comparison of breakthrough curves and tracer recovery in the River Pang at Frogmore Farm and the Blue Pool outlet (Section 5.4.3.4) suggest that the area of groundwater discharge may extend to include small upwellings through the bed of the River Pang. Comparison of tracer recovery at the Blue Pool outlet and the Blue Pool spring suggests that individual upwellings may have had different tracer concentrations, also indicating flow down multiple flowpaths in which there were varied amounts of mixing between tracer labelled water from Smithcroft Copse and diluting water from other sources.

There is some uncertainty regarding the exact cause of the very high tracer losses (~ 75%). Whilst the most likely conceptual model is that depicted in Figure 5.28, it is also possible that divergent flow carried a proportion of the injected tracer out of the Blue Pool catchment area (Figure 5.29). This conceptual model resembles the conceptual and experimental visualisations of the early stages of karstification (e.g. Ford, Lauritzen and Ewers, 2000; Dreybodt and Siemers, 2000). The existence of flow divergence in the Chalk has been conclusively demonstrated at Water End in Hertfordshire (Harold, 1937) where tracer from a stream sink was discharged at outlets several kilometres

apart. However, in the Smithcroft Copse test in 2005 no tracer was detected at any of the additional monitoring points (Section 4.3.2.3) including Ingle and Jewells springs, which are large groundwater outlets located between Smithcroft Copse and the Blue Pool. This demonstrates that divergent flow to these springs is not a cause of low tracer recoveries at the Blue Pool. Flow divergence could also occur to the south and southeast as suggested by groundwater contours (Figure 2.13), but there are no groundwater outlets downgradient and the Chalk becomes increasingly confined by Palaeogene strata. The conceptual model presented in Figure 5.28 therefore seems more probable.

The tracer tests suggest that groundwater flow between Smithcroft Copse and the Blue Pool occurs through a combination of conduits, fissures and fractures, although a proportion of flow is through a fully connected system of larger voids. The nature of voids through which groundwater flow occurs is considered further in Chapter 6 where flowing horizons identified in boreholes using single borehole dilution tests are compared to borehole imaging data to ascertain whether flow is predominantly through conduits, fissures or unmodified fractures.

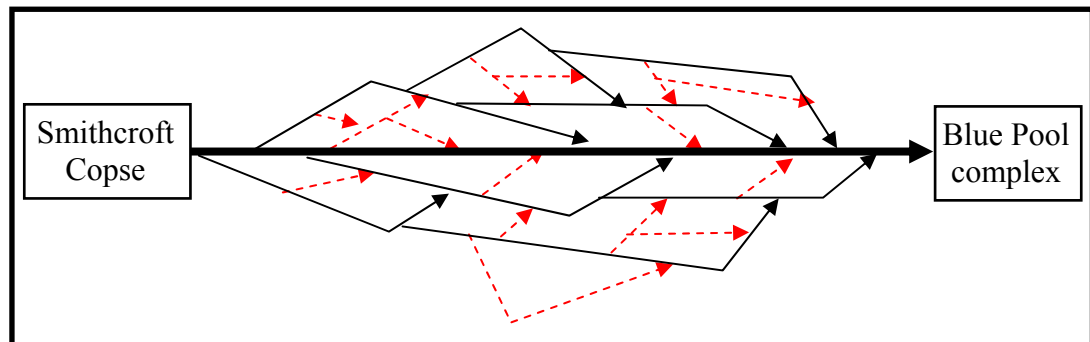


Figure 5.28: Multiple flowpaths surrounding a main conduit pathway (thick black arrow) in which some pathways comprise larger voids (thin black lines) and others include sections of narrow fissures/ fractures (red dashed arrows) in which tracer is effectively attenuated by double porosity diffusion

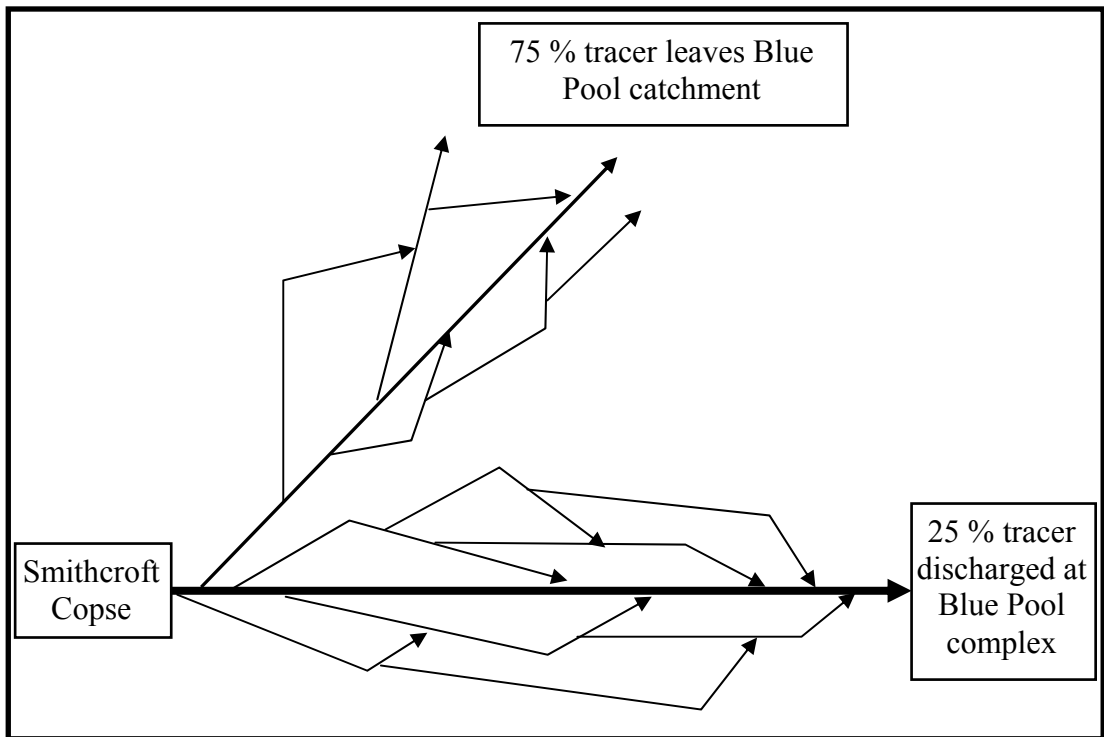


Figure 5.29: Multiple flowpaths surrounding the main conduit with flow divergence out of the Blue Pool catchment area

Chapter 6: Borehole investigations of groundwater flow in the Chalk

6.1 Introduction and background

Catchment scale tracer testing (Chapters 4 and 5) has demonstrated rapid groundwater flow between stream sinks and springs in Zone 1. Rapid groundwater flow implies a fully connected system of conduits between some stream sinks and springs, but attenuation of tracers implies that not all flow between the stream sinks and springs is through conduits, and that there may be considerable connectivity between conduits and voids with smaller apertures such as fissures and fractures. However, the choice of sinking streams as input points dictates that, if successful, these tests investigate flow along particular karst connections and do not provide information on the general distribution of rapid groundwater flow and how this may vary in different parts of the aquifer. Single Borehole Dilution Tests (SBDTs) were used to provide a means of investigating groundwater flow over the whole area of the catchments. SBDTs (under natural gradient conditions) were undertaken in a sample of 25 boreholes representing all three karst zones and three different topographical positions (river valley, dry valley and interfluvium). An important objective was to determine the location of flowing features in boreholes, and their distribution with depth. At a subset of 4 sites, borehole imaging was used to identify the types of flowing features present and determine whether they are associated with solutional fissures or conduits, or if groundwater flow in boreholes is predominantly through unmodified fractures.

SBDTs involve injecting tracer throughout the saturated length of the borehole, and monitoring the dilution of the tracer by groundwater entering and leaving the borehole (Ward et al., 1998; Williams et al. 2006; Pitrak et al., 2007). If there is no vertical flow within the borehole, seepage velocities can be calculated (Lewis, 1966; Gaspar, 1987). In practice variability in hydraulic head in flowing horizons intercepted at different depths often causes vertical flow (Michalski and Klepp, 1990; Church and Granato, 1996; Elci et al., 2001; Shapiro, 2002). SBDTs are therefore best conducted in a short interval of borehole that is isolated using packers (Palmer, 1993; Shreiber et al., 1999; Novakowski et al., 2006). However, SBDTs in long open sections of borehole, even when vertical flow is occurring, can be used to identify the location of flowing horizons

using the shapes of profiles of tracer concentration with depth measured at intervals following tracer injection. Since the 1990's, several authors have used this principle to identify flowing horizons in boreholes and some have developed methods of determining the hydraulic properties of these flow horizons (e.g. Tsang et al., 1990; Löw et al., 1994; Evans 1995; Brainerd and Robbins 2004; West and Odling, 2007). These studies are briefly described below.

The method proposed by Tsang et al. (1990) is carried out whilst a borehole is being pumped. The borehole water is replaced with deionised water and subsequent profiles of electrical conductance with depth (fluid electrical conductance logs) illustrate the depths at which groundwater enters the borehole because there is a sharp increase in the electrical conductance at these depths. Tsang et al. (1990) carried out their experiment in a 1690 m deep borehole in fractured crystalline rocks in Leuggern in Northern Switzerland. A packer was used to exclude flow from a high permeability section at the base of the borehole, and the test was conducted in a low permeability section between 770 and 1637 m below ground level. 9 flow horizons were identified and Tsang et al. (1990) developed a method using an iterative forward modelling technique to derive inflow and outflow rates from the fluid electrical conductance logs, and then used the borehole pumping rate and drawdown during the test to calculate the transmissivity. Löw et al. (1994) developed an analytical method of directly obtaining inflow and outflow rates using the field experimental method of Tsang et al. (1990) without the need for iterative forward modelling. They used field data from the Leuggern borehole used by Tsang et al. (1990), and a second deep borehole in Northern Switzerland in similar strata. Evans (1995) also used the field method of Tsang et al. (1990) at three shallower boreholes (~122 m deep) in a Precambrian gneissic schist in North Carolina. Evans (1995) developed a slightly different analytical method to that of Löw et al. (1994) but which also directly derives inflow and outflow parameters. Evans (1995) notes that in boreholes where flow rates are faster than in the study of Tsang et al. (1990), the fluid electrical conductance may change during the time taken to obtain the log, and therefore the analytical method of Evans (1995) takes into account the time of each individual electrical conductance reading. The field method of Tsang et al. (1990) has also been used simply as a tool for identifying flowing features during general hydrogeological field investigations (e.g. Karasaki et al., 2000).

A slightly different field method was used by Brainerd and Robbins (2004) in a borehole in gneiss and schist in Connecticut. They pumped Sodium Fluorescein tracer into the bottom of the borehole, and then pumped water out of the top at a higher rate. Once steady state conditions were established, inflowing horizons could be identified at depths where tracer concentrations decreased, and an analytical solution was developed to determine the transmissivity of these flowing features.

West and Odling (2007) developed a different field and analytical technique for determining transmissivity values for specific flow horizons in boreholes in which high permeability layers are separated by very low permeability sections of borehole. They undertook SBDTs in three monitoring boreholes in the Chalk in Yorkshire using a saline tracer. The boreholes were not pumped during the tests, but were within 25 to 75 m of a pumping borehole. Abstraction at the pumping borehole induced vertical flow in the monitoring boreholes. Modelling techniques were developed to determine the vertical flow velocity induced by the pumping borehole and the transmissivity of the permeable layers causing the vertical flow.

Matthias et al. (2007) used SBDTs to improve the interpretation of radial flow tracer tests by monitoring the way in which tracer left the injection boreholes. A radial flow tracer test in the Chalk at Trumpletts Farm in the Pang Catchment (one of the sites used in the present study) was conducted in collaboration with the present author as part of the LOCAR programme of work. Sodium Fluorescein and Amino G tracers were injected into two monitoring boreholes 32 and 54 m from the pumping borehole. SBDTs were simultaneously carried out in both injection boreholes using a saline tracer. Tracer breakthrough curves at the pumping borehole from one of the injection boreholes had multiple peaks which the SBDT revealed was due to outflow at different rates from different horizons in the injection borehole. Matthias et al. (2007) used the results of the SBDTs and developed an analytical method to determine a tracer input function (the vertical distribution of tracer flux from the injection borehole during the radial flow tracer test).

The present study differs from previous work in that the objective was to use SBDTs to determine the location and vertical distribution of flowing features across a catchment by testing a large number of boreholes. As the intention was not to determine

transmissivity values for flow horizons, simple SBDTs under natural gradient conditions were performed. A saline tracer was used, and fluid electrical conductance logs were obtained following tracer injection. The study involves both uniform injection tests where the entire saturated column is labelled with tracer, and point injection tests. These involve introducing a slug of tracer at a particular depth. Vertical profiles of electrical conductance are taken to measure the rate at which the slug moves up or down the borehole (Tate et al., 1970; Michalski and Klepp, 1990) and to identify flow horizons (Michalski and Klepp, 1990). Results show that a combination of uniform and point injection SBDTs using saline tracers under natural gradient conditions provides a cheap and easy method of identifying flowing horizons. In the past various borehole logging techniques (calliper logs, imaging logs, fluid temperature/electrical conductance logs and flow logs) were used but some of these techniques are unable to distinguish between flowing fractures and hydrologically inactive fractures, and they may not identify all flowing horizons that are present in boreholes. These techniques are briefly discussed below.

Calliper logs record the variation in borehole diameter with depth. Increases in borehole diameter often occur where a fracture, fissure or conduit is present, but the drilling process may also cause enlargements (for example, in chalk, flints may be plucked out of the borehole walls). Callipers consist of two or three prongs that measure the distance from a centralised point to the borehole wall, and may miss vertical fractures and voids that do not persist horizontally around the circumference. Fractures, fissures and conduits can be seen on borehole imaging logs where cameras are used to view the borehole walls. However neither calliper nor imaging data demonstrate whether the feature is actively flowing. Many hydrologically inactive fractures have been identified by Price et al. (1977), Michalski and Klepp (1990), Paillet (1998, 2000), and Williams and Paillet (2002).

Borehole fluid logs may indicate flow horizons where there is an abrupt change in electrical conductance and/or temperature (e.g. Tate et al., 1970; Price et al., 1977; Williams and Paillet, 2002; Schurch and Buckley 2002). However, the technique fails where flowing features share the same electrical conductance and temperature (Michalski and Klepp, 1990). Price et al. (1982) also suggest that this technique is less likely to detect outflows than inflows because there may be no difference between the

temperature/electrical conductance of the water in the borehole and that of the water leaving the borehole. High sensitivity impeller flowmeters (e.g. Molz et al. 1989, 1994), or heat-pulse flow meters (e.g. Paillet et al., 1987) have proved the most successful method of identifying flow horizons.

Combined fluid logging, flowmeter and imaging techniques were used in 19 boreholes in the Lambourn catchments by Tate et al. (1971). The data from this study are not in a form that could be incorporated into the present study. There is no summary of the location of flowing horizons, and only general conclusions are presented. Tate et al. (1971) identified flowing horizons and concluded that they were commonly associated with bedding planes, and that flow always occurred at the base of the casing. They also determined the stratigraphy from geophysical logging and concluded that there is a stratigraphical control on the location of flowing horizons, but do not specify what this was.

The remainder of this chapter describes and interprets SBDT data that were obtained from 25 boreholes scattered across the Pang and Lambourn catchments. Section 6.3 describes field methods and measurement errors. Section 6.4 presents and discusses uniform tracer injections. Section 6.5 discusses forward modelling and point injection SBDTs which were used to investigate how patterns in the fluid electrical conductance logs obtained following uniform injections relate to flowing features, and the locations of flowing features identified in 24 boreholes are presented. In Section 6.6 borehole imaging data from 4 sites are correlated with flowing horizons and reveals that they are commonly located on dissolutional features. Section 6.7 discusses patterns in the catchment scale distribution of flow horizons and tests the commonly held view that their frequency decreases with depth.

6.2 Site selection and testing schedule

Uniform injection SBDTs were carried out in 6 LOCAR and 19 Environment Agency monitoring boreholes with long uncased sections, diameters of less than 300 mm, and depths of less than 115 m. Boreholes with slotted casing were excluded because it is difficult to interpret the effects of the casing and the gravel pack. In boreholes with a diameter greater than 300 mm it is difficult to mix the tracer across the borehole, and the initial tracer concentration is very dilute. Boreholes more than 115 m deep were not

used because of the physical difficulty of lifting the weight of the tracer injection hosepipe out of the borehole. Within these practical constraints boreholes were selected to provide good spatial coverage across the catchments (Figure 6.1). At the LOCAR interfluvial site (Trumpletts) and river valley site (Firilsham), results were obtained for 2 or 3 boreholes within 50 m of each other to assess local variability. The SBDTs were undertaken throughout the year and therefore to determine if results were affected by differences in water table, tests at 4 sites were repeated at times of different water level. 22 point dilution tests were carried out in 10 of the boreholes. Table 6.1 summarises borehole grid references and dates of the tests.

Borehole logging has been undertaken in 12 of the SBDT boreholes. The 6 LOCAR boreholes were logged as part of the LOCAR programme. Imaging data are available at four of these sites but data from two were not used in the present study because the image resolution is poor. Six Environment Agency boreholes were logged by the British Geological Survey logging team (Dave Buckley and Alex Gallagher). Imaging data are available for five of these sites. Heat pulse flow measurements were made at three sites to compare vertical flow velocities with those obtained from SBDTs.

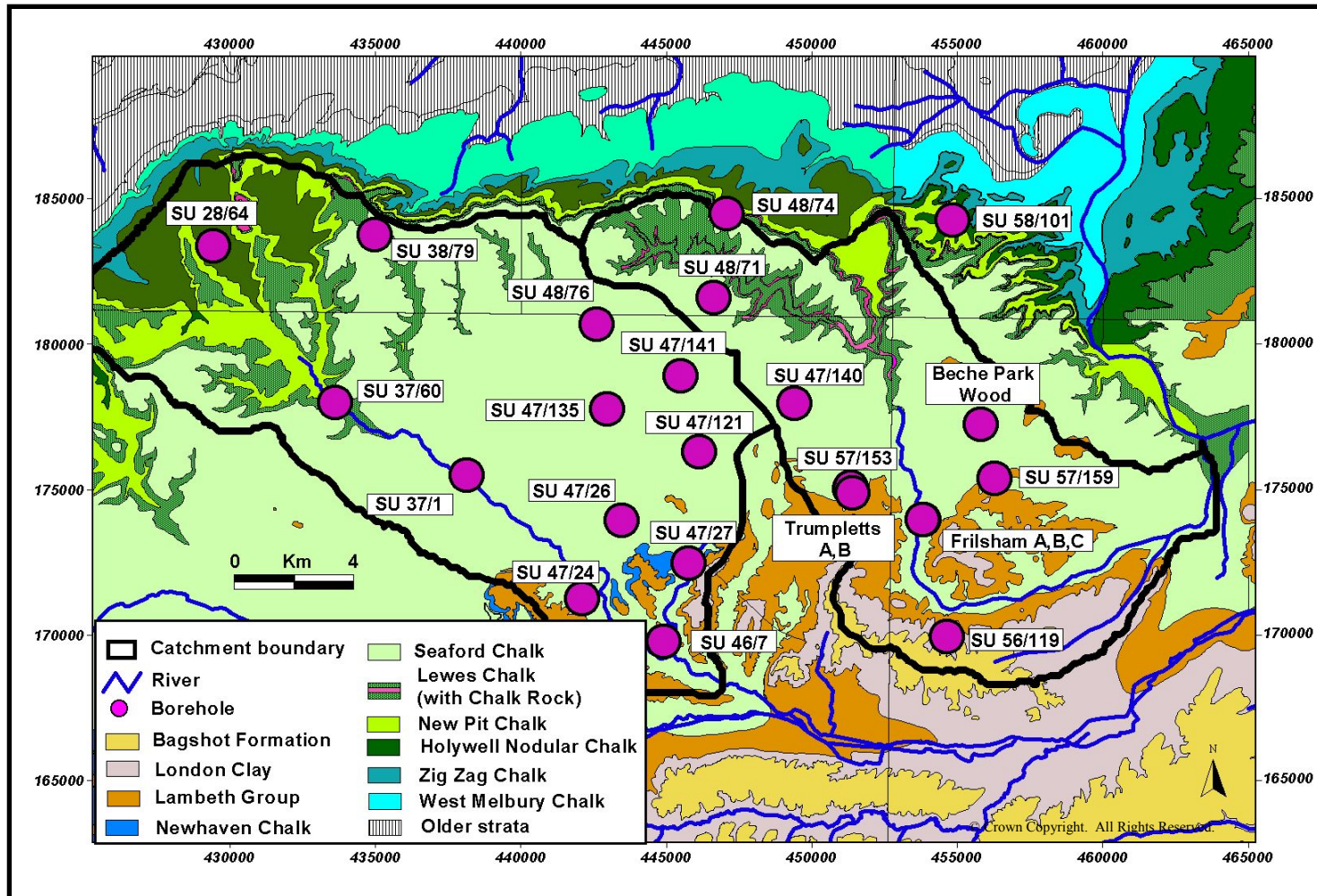


Figure 6.1: Location of SBDT Boreholes in the Pang-Lambourn catchments^{BGS}

Table 6.1: Borehole grid references and test dates of uniform and point injection SBDTs

Name	No.	Easting	Northing	Uniform 1	Uniform 2	Point 1	Point 2	Point 3
Ashridge Wood	SU 47/140	449400	177920	24/08/2005				
Bagnor	SU 46/7	444900	169750	19/08/2005		20/08/2005	20/08/2005	20/08/2005
Barracks	SU 48/71	446620	181560	15/10/2003		22/07/2007		
Beche Park Wood	LOCAR	455800	177200	05/10/2004				
Bockhampton	SU 37/60	433600	177950	01/09/2005		01/09/2005	01/09/2005	01/09/2005
Bottom Barn	SU 57/153	451380	174840	23/08/2004				
Bradley Wood	SU 47/26	443450	173910	25/08/2005				
Briff Lane	SU 56/119	454640	169900	02/08/2005				
Brightwalton Common	SU 48/76	442600	180640	14/08/2003				
Brightwalton Holt	SU 47/135	442960	177730	13/08/2003				
Calversley Farm	SU 57/159	456280	175350	20/09/2004				
Cow Down	SU 48/74	447050	184460	28/09/2004				
Frilsham A	LOCAR	453810	173940	09/12/2003	28/07/2005	08/08/2005		
Frilsham B	LOCAR	453830	173930	10/12/2003	27/07/2005	20/07/2005	21/07/2005	28/07/2005
Frilsham C	LOCAR	453800	173940	16/12/2003	01/08/2005	21/07/2005	21/07/2005	27/07/2005
Gibbet Cottages	SU 47/141	445490	178870	24/08/2004		21/07/2007	21/07/2007	
Great Shefford	SU 37/1	438130	175470	16/08/2005				
Greendown Farm	SU 38/79	434970	183720	14/10/2003				
Grumble bottom	SU 58/101	454820	184230	12/10/2004		24/07/2007		
Highstreet Farm	SU 47/24	442110	171200	18/08/2005				
Knighton Down	SU 28/64	429420	183340	03/08/2005				
Peasmore	SU 47/121	446120	176270	12/08/2003				
Trumpletts A	LOCAR	451320	175000	04/11/2003	16/06/2004	10/06/2004	11/06/2004	14/06/2004
Trumpletts B	LOCAR	451340	175040	05/11/2003				
Winterbourne Farm	SU 47/27	445760	172440	11/08/2005		11/08/2005	11/08/2005	

6.3 Methods

6.3.1 Field Methods

6.3.1.1 Uniform injections

The depth to the water table was measured using a dip meter at the start of each experiment and at least once per day thereafter. At the start of an experiment the bottom of the borehole was plumbed. A background electrical conductance profile was measured prior to tracer injection using a Solinst Levelogger LTC probe, model 3001. Two different probes (a 2003 and a 2005 version of the model 3001) were used. Each probe recorded temperature, specific electrical conductance and depth below the water table. The 2003 probe logged at 2 second intervals, the 2005 model every second. The probe was initially lowered to just below the water table to enable its temperature to adjust to the water temperature. It was lifted out of the water and then lowered slowly to the bottom of the borehole. The logger was programmed and data were downloaded via a cable link to a laptop computer.

Tracer injection was via a weighted hosepipe extending to within 2 m of the bottom of the borehole (Figure 6.2). Hosepipe lengths were joined together using copper tube secured with jubilee clips. The top hosepipe section included a fitting to enable the hose to rest on a plate on top of the borehole (Figure 6.3).



Figure 6.2: Hosepipe and weight at Peasmore Borehole (SU 47/121)



Figure 6.3: SBDT tracer injection system, Grumble Bottom Borehole (SU58/101). Top of hosepipe is resting on a metal plate that spans the top of the borehole casing (photo Alex Gallagher).

Tracer from a stock solution (1.25 kg of table salt dissolved in approximately 10 litres of water) was poured slowly into the hosepipe via a funnel. The volume required (V) was calculated as:

$$V = \pi r^2 h$$

where r is the internal radius of the hosepipe, and h is the length of the borehole between the water table and the bottom of the hosepipe. The volume needed was 0.26 litres of tracer per metre length of hosepipe. If the water table was above the bottom of borehole casing then tracer was only injected into the lower section of hosepipe up to the level of the casing. Water was then injected into the saturated cased section to ensure that the hose was full up to the water table level (Figure 6.4). After the calculated tracer amount (and water if required) was poured into the hosepipe, it was left for a few minutes and then pulled out of the borehole as smoothly as possible (Figure 6.5).

An electrical conductance profile was measured immediately after injection. The data were downloaded to ensure everything was working, and then another profile was measured. The timing of subsequent profiles depended upon the amount of tracer loss

that had occurred. In boreholes where dilution was known to be rapid several profiles were measured before the data were downloaded. In most cases tracer dilution was measured until the electrical conductance had returned to near background levels. In some boreholes where dilution was very slow some tracer was still present in the bottom of the borehole at the time of the last measurement. Standard electrical conductance solutions were measured about once per day to assess instrument drift.

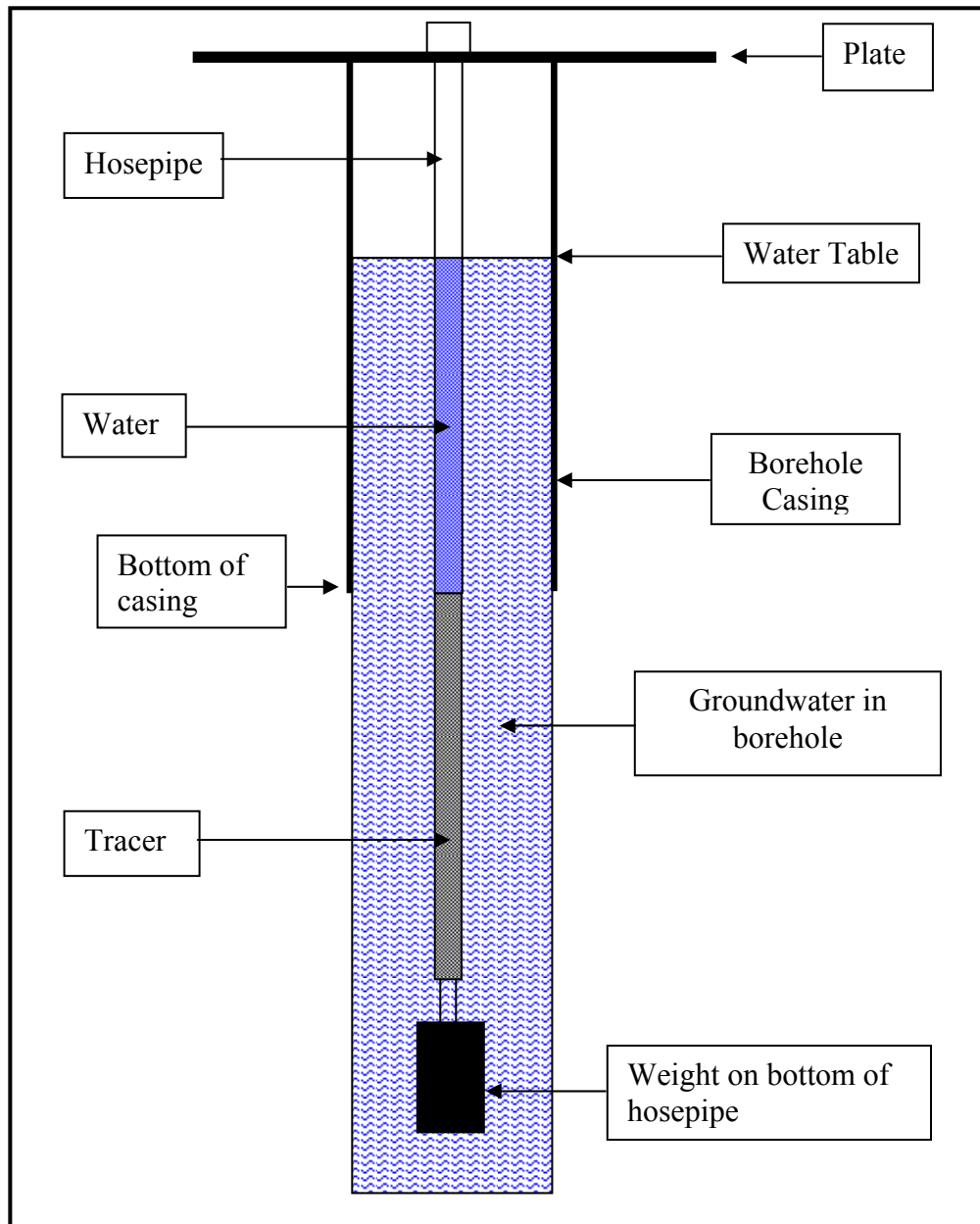


Figure 6.4: Borehole tracer injection system when the water table is above the casing



Figure 6.5: Tracer injection at Grumble Bottom borehole (SU 58/101)

6.3.1.2 Point tracer injections

The procedure for point injections differed only for the tracer injection. The objective was to introduce the tracer at a specific point in the borehole. Initially injections were made using the hosepipe system used for uniform injections. The hosepipe was lowered to the desired injection depth and 250-500 mls of salt solution was poured down the hosepipe followed by an amount of water calculated to fill the hosepipe to the depth of the water table (as in uniform injections with water levels above casing depth, see Figure 6.4). This method was found to produce a very broad spike over up to 15 m of the borehole. Subsequent point injections used a probe filled with salt and lowered to the desired injection depth where a weight dropped down the line triggers the release of the tracer.

6.3.2 Raw data processing

The Solinst Levelogger probe must be connected to a computer to begin and finish logging and therefore data were recorded before and after it was submerged in the borehole, and throughout the temperature adjustment period. Each profile was obtained by selecting a subsection of the raw data between the water table and the bottom of the borehole using the depth readings.

Depth below the water table is measured by a pressure transducer and the readings are affected by changes in atmospheric pressure. Therefore the average apparent depth recorded when the probe was in air before reaching the water table was subtracted from the recorded depth readings below the water table.

The data recorded on the levellogger were at regular time intervals, but for calculation of tracer recoveries, and comparison of electrical conductance values at a specific depth at different times, the electrical conductance data were interpolated to produce profiles of electrical conductance at regular depth intervals. A macro written by Chris Jackson at BGS was used to perform this interpolation and to convert the depth data from cm below the water table to elevations in m AOD. The time of readings was also interpolated; resulting in the following data output for each profile using the macro:

Depth (in m AOD at regular 0.1 m intervals).

Electrical conductance at each depth (interpolated).

Time of each electrical conductance reading (interpolated).

6.3.3 Accuracy and precision of depth readings

There was some variability in the depth readings in air before the probe was submerged. To assess the accuracy of the depth readings during each profile the probe was left on the bottom of the borehole for several readings to obtain a dataset of the variability in depth readings when the probe is submerged at a constant depth. The accuracy of the depth readings was assessed on two different timescales. Firstly the amount of variation when the probe was at a constant depth during an individual profile; and secondly the variation in depth readings between profiles taken at different times during the day or on different days.

The variability during an individual profile was investigated using readings in air and readings at the bottom of the borehole for five tests that used Probe 1 and five tests that used Probe 2. The results are summarised in Tables 6.2 and 6.3. The average air reading is the average of all readings before the probe reached the water table. The total number of data points are also presented. A standard deviation (SD) of the air readings of each individual profile was calculated, and from these a pooled air reading standard deviation was obtained. This procedure was repeated for the readings that were

obtained while the probe rested on the bottom of the boreholes. The combined standard deviation for each test investigated is a combination of the pooled standard deviations for the readings in air and at the bottom of the borehole. For probe 1 the combined standard deviation is less than 5 cm in all five cases (Table 6.2). For probe 2 the combined standard deviations were all less than 7 cm (Table 6.3).

To investigate the variability in depth readings between different profiles, for each individual test the average and standard deviation of the readings on the bottom of the borehole from all the profiles measured during the test were calculated (Table 6.4). It is clear that increased test duration does not cause a greater variability in the depth readings; standard deviations for tests that took place over more than a week were not higher than those from tests over 1 to 2 days. The similar average depth readings from the bottom of the Frilsham boreholes in 2003 and 2005 suggest that the depth readings are consistent over an annual scale (Table 6.4). It is possible that in some boreholes differences in the depth measurements between profiles may be caused by irregularities, blockages or sediment in the bottom of the borehole. This appears to be the case in Peasemore where there was considerable variation in the depth measurement at the bottom of the borehole.

The overall average standard deviation for all the tests is 8.8 cm, which is only slightly higher than the values obtained for individual profiles. This increased variation may be due to irregularities in the bottom of the borehole. It can be concluded that most depth readings are accurate to within +/- 10 cm, and that all are accurate to within +/- 25 cm.

Table 6.2: Variability of depth readings within individual profiles using Probe 1

Borehole	Peasemore	Brightwalton Common	Trumpletts A	Trumpletts B	Frilsham A
Start date	12/08/03	14/08/03	04/11/03	05/11/03	09/12/03
End date	14/08/03	27/10/03	06/11/03	06/11/03	11/12/03
Mean air reading (cm)	82	85	104	105	95
No. of data points in air	756	775	1362	1104	478
Pooled air SD (cm)	1.776	3.834	1.866	1.959	1.585
Mean bottom reading (cm)	1668	2139	7977	7768	4222
No. of data points on bottom	354	233	146	93	133
Pooled bottom SD (cm)	2.44	1.771	1.159	3.465	1.761
Combined SD (cm)	3.018	4.223	2.197	3.981	2.369

Table 6.3: Variability of depth readings within individual profiles using Probe 2

Borehole	Frilsham A	Knighton Down	High St Farm	Ashridge Wood	Bockhampton
Start date	28/07/05	03/08/05	18/08/05	24/08/05	01/09/05
End date	01/08/05	04/08/05	21/08/05	25/08/05	01/09/05
Mean air reading (cm)	78	63	54	3.6	54
No. of data points in air	669	1460	1539	1759	350
Pooled air SD (cm)	5.262	3.988	4.895	2.861	4.204
Mean bottom reading (cm)	4204	2262	2432	1323	4910
No. of data points on bottom	679	345	575	160	350
Pooled bottom SD (cm)	3.134	3.108	3.286	3.412	3.497
Combined SD (cm)	6.125	5.056	5.896	4.453	5.468

Table 6.4: Variability of depth readings at the bottom of boreholes (using all profiles from each individual test)

	Date	Average bottom depth (m AOD)	Range (cm)	SD (cm)	Number
Tests over 1 to 2 days					
Bagnor points	20/08/2005	55.7	30	9	21
Bagnor uniform	19/08/2005	55.8	40	11	15
Bockhampton	01/09/2005	71	10	5	7
Bockhampton point	01/09/2005	71	30	13	6
Bockhampton point	01/09/2005	71.1	30	12	7
Bockhampton point	01/09/2005	71	40	16	8
Frilsham A point	04/08/2005	34.4	20	7	15
Frilsham B	10/12/2003	36.6	20	6	12
Frilsham B	20/07/2005	36.6	20	7	14
Frilsham B point 22	27/07/2005	36.6	40	12	15
Frilsham B point 27	21/07/2005	36.7	30	8	10
Frilsham B point 37	20/07/2005	36.6	30	9	10
Frilsham C	16/12/2003	16.7	10	4	10
Frilsham C	21/07/2005	16.7	10	5	11
Frilsham C point 26	27/07/2005	16.6	10	5	6
Frilsham C point 53	21/07/2005	16.7	20	6	11
Great Shefford	16/08/2005	6.8	20	10	4
Knighton Down	03/08/2005	107.8	20	8	11
Trumpletts A	14/06/2004	7.8	0		10
Trumpletts A point	16/06/2004	7.79	10	3	13
Trumpletts B	05/11/2003	9.7	40	11	12
Winterbourne Farm	11/08/2005	67.9	80	23	10
Tests over 1 week					
Ashridge Wood	24/08/2005	81.48	40	11	10
Bradley Wood	25/08/2005	65.8	0.5	14	10
Calversley Farm	20/09/2004	49	20	7	16
Frilsham A	09/12/2003	34.6	20	5	15
Frilsham A	28/07/2005	34.6	30	9	18
Grumble bottom	12/10/2004	14.9	10	4	10
Highstreet Farm	18/08/2005	65.7	30	10	13
Peasemore	12/08/2003	93.9	150	37	16
Trumpletts A	04/11/2003	7.77	10	5	17
Tests over more than 1 week					
Beche Park Wood	05/10/2004	46	30	10	14
Bottom Barn	23/08/2004	66.5	20	6	16
Briff Lane	02/08/2005	39	50	13	13
Brightwalton Common	14/08/2003	103	20	7	8
Cow Down	28/09/2004	85	10	4	11
Gibbet Cottages	24/08/2004	77.9	30	7	17

6.3.4 Accuracy and precision of electrical conductance measurements

A standard solution of $1.413 \text{ mS}\cdot\text{cm}^{-1}$ was measured most days. The probes were not calibrated to this solution, but the measurements were used to determine the variability of the probe readings, and examples of the data are presented below. As the probe sits in the standard solution there is an apparent change in specific electrical conductance that corresponds to the change in temperature as the probe adjusts to the temperature of the solution (Figure 6.6).

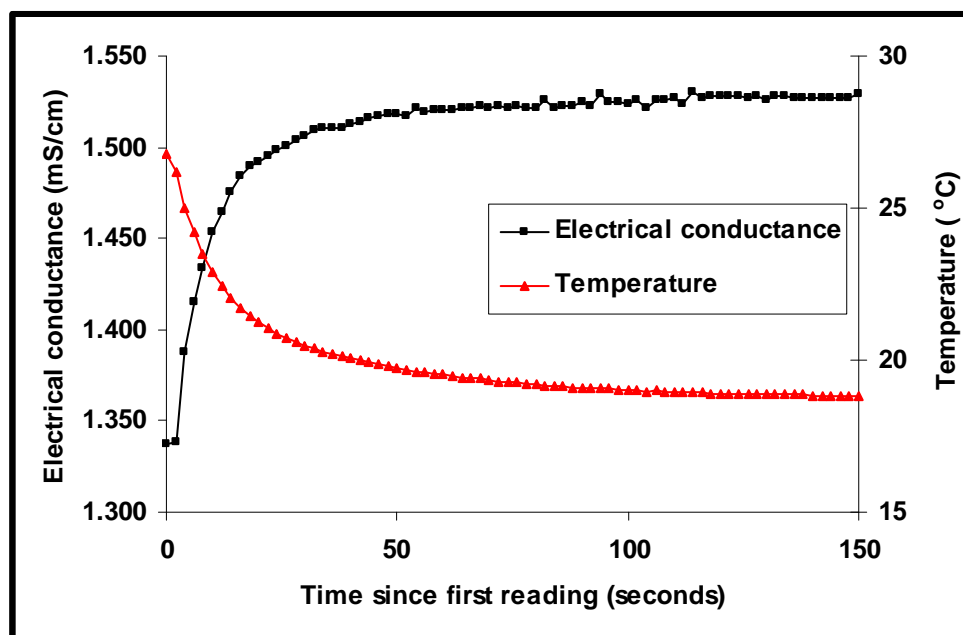


Figure 6.6: Electrical conductance and temperature readings of Probe 1 when submerged in standard solution

Once the probe has adjusted to the temperature of the solution there is very little variability in the electrical conductance measurements. Table 6.5 summarises the measurements of a standard solution between 21/09/04 and 30/10/04 using probe 1 (excluding the data during the period of temperature adjustment). The standard deviations of the readings whilst the probe was submerged in the solution are all $< 0.003 \text{ mS}\cdot\text{cm}^{-1}$. There was greater variability in the readings of the standard solution measured on different occasions. The average reading had a range of $0.039 \text{ mS}\cdot\text{cm}^{-1}$, and a standard deviation of $0.013 \text{ mS}\cdot\text{cm}^{-1}$. Some of this variability may be due to changes in the standard solution because (a) on most occasions the probe was placed in the same bottle of standard solution (and may therefore have altered the electrical conductance of the solution), but on some occasions the probe was placed in a fresh

sample of the stock solution; and (b) there was a general increase in the standard readings over time which was thought to be due to some evaporation of the standard solution. Despite these errors in measurement practice, even the maximum variability in the readings over this period of almost 2 months is generally small relative to changes in electrical conductance recorded during the SBDTs. A fresh sample of a stock solution was measured at the start and end of the period in which probe 2 was used. Probe 2 only measures to 0.010 mS.cm^{-1} (as opposed to probe 1 which measures to 0.001 mS.cm^{-1}). The results are summarised in Table 6.6, which shows that there was very little variation whilst the probe was submerged in the solution (a standard deviation of 0.002 to 0.005 mS.cm^{-1}). There was a 0.010 mS.cm^{-1} difference in the reading of the solution between the start and end of the period in which the probe was used. Overall, the readings of the standard solutions suggest that electrical conductance readings of the probes are accurate to within $\pm 0.010 \text{ mS.cm}^{-1}$.

Table 6.5: Electrical conductance readings of probe 1 when submerged in a standard solution (after a period of temperature adjustment)

Date	Average (mS.cm^{-1})	Max (mS.cm^{-1})	Min (mS.cm^{-1})	SD (mS.cm^{-1})	No. readings
21/09/04 am	1.533	1.537	1.531	0.001	55
21/09/04 pm	1.527	1.530	1.524	0.001	21
22/09/04	1.532	1.534	1.528	0.002	68
23/09/04	1.526	1.530	1.519	0.003	26
27/09/04	1.530	1.535	1.525	0.003	85
28/09/04	1.534	1.536	1.533	0.001	20
02/10/04	1.550	1.553	1.544	0.002	33
04/10/04	1.534	1.538	1.529	0.002	54
05/10/04 am	1.562	1.565	1.558	0.002	36
05/10/04 pm	1.541	1.545	1.537	0.002	25
06/10/04	1.548	1.552	1.544	0.002	20
12/10/04 am	1.556	1.560	1.551	0.003	46
12/10/04 pm	1.548	1.552	1.543	0.003	43
15/10/05	1.565	1.569	1.562	0.002	31
30/10/04	1.529	1.534	1.526	0.003	39

Table 6.6: Electrical conductance readings of probe 2 when submerged in a stock standard solution at the start and end of period in which it was used

Date	19/07/05	08/09/05
Max (mS.cm ⁻¹)	1.040	1.050
Min (mS.cm ⁻¹)	1.020	1.030
Average (mS.cm ⁻¹)	1.030	1.040
Standard deviation (mS.cm ⁻¹)	0.002	0.005
Number readings	179	199

6.3.5 Uniform injection SBDT data analysis methods

The data from the uniform SBDTs were viewed in three ways:

1) The time taken for fresh aquifer water to replace the tracer in the boreholes varied from hours to months. To enable a general comparison of tracer dilution between boreholes, each borehole was assigned a category based upon a tracer efflux time: the time taken for tracer concentrations in most of the borehole to return to background (excluding the few metres at the bottom of boreholes where tracer dilution was often very slow). The categories are (A) efflux times of less than 12 hours, (B) efflux times of 12 to 48 hours, (C) efflux times of 2 days to 1 week (48 to 168 hours), and (D) efflux times of several weeks (more than 168 hours). Because tracer dilution was very variable within some boreholes, this exercise was also undertaken using the fastest efflux time that occurred over a section of borehole. The diameter of the boreholes tested varied from 170 to 300 mm, and therefore a greater volume of water will have been replaced from the wider diameter boreholes. An equivalent flow rate would result in a faster efflux time in a narrower diameter borehole than a wider diameter borehole (although the decreased diameter also results in a decreased borehole surface area and therefore decreased area of flowing horizons). The variability in borehole diameter is not accounted for in the efflux times but based upon the change in cross sectional area for the maximum difference in diameter, efflux times would be affected at very most by a factor of 3 which would result in very little change in the borehole categories assigned.

2) The total decline in tracer concentration through time was considered using plots of summed tracer concentration against the start time of each profile. The summed tracer

concentration was calculated by adding the concentrations (with a background electrical conductance value removed) at each regular depth interval. Because the data were interpolated to regular depth intervals, this method provides a means of integrating electrical conductance with depth.

3) Profiles of electrical conductance plotted against elevation (electrical conductance logs), obtained at different times after tracer injection, were used to show how the dilution of tracer varies with depth in each borehole.

At some sites tracer dilution was extremely rapid and changes in electrical conductance would have occurred during the time taken to obtain the log (as discussed by Evans, 1994). This effect has been ignored in the present analysis because differences in tracer efflux times between boreholes are too great to be corrupted by it, and because interpretation of the position of flowing horizons will be unaffected by such detailed shortcomings of the data. For similar reasons, the data were not adjusted to compensate for vertical variability in borehole diameter (although this would anyway only have been possible at the few sites where calliper data are available)

6.4 Results of uniform injection SBDTs

6.4.1 Tracer efflux times

Tracer efflux times are presented in Table 6.7. The spatial distribution of efflux times for entire boreholes is shown in Figure 6.7, and for the fastest sections in Figure 6.8. In some boreholes there were both sections of very rapid and very slow tracer efflux (e.g. Beche Park Wood and Gibbett Cottages). Boreholes on the same site had similar tracer efflux times (Frilsham A,B,C and Trumpletts A and B). However, Bottom Barn borehole is less than 500 m from the Trumpletts boreholes, but has a much longer tracer efflux time. This borehole is located on elevated ground above the dry valley in which the Trumpletts boreholes are situated.

The regional geographical patterns appear to be explained by varying spatial density of permeable horizons with respect to river valleys, dry valleys and interfluves. In all boreholes that are located in major river valleys tracer efflux from the entire borehole occurred in less than 12 hours. The only other borehole in which this occurred was Knighton Down, which is located on the edge of the major dry valley continuation of

the River Lambourn. There are many boreholes outside major river valleys with sections in which tracer efflux occurred in less than 12 hours. Two of these boreholes are on the edge of a dry valley, and one is on an interfluvial area, but all the others are within dry valleys. Tracer efflux times appear to relate to topography in a similar manner to transmissivity (Section 2.8.5.2). This implies that, as with transmissivity, tracer efflux rate is determined by the presence and density of high permeability fissures. Tracer efflux may therefore provide a rough but simple indicator of borehole transmissivity. Transmissivity data from pumping tests are available for only 4 of the boreholes tested. Table 6.8 compares the transmissivity with the tracer efflux times, and Figure 6.9 shows that there is a reasonable correlation between them, but clearly more data would be required to confirm the robustness of this relationship.

There does not appear to be a strong relationship between rapid tracer efflux and the karst zone in which the boreholes are located. In all three zones there are boreholes in which tracer efflux occurs from the whole borehole or from a section in less than 12 hours (Figures 6.7 and 6.8). Nevertheless, in zones 1 and 2 (where there is most surface karst) all boreholes have sections in which tracer efflux occurs in less than 168 hours, and in all but two boreholes, in less than 48 hours. In addition, all boreholes in which tracer efflux from the entire borehole takes more than 168 hours are located in zones 2 and 3. Together these findings suggest that where less surface karst is present tracer efflux in boreholes is more likely to be slow, but that rapid efflux may occur in all three zones.

Table 6.7: Borehole tracer efflux times

Borehole name	Tracer efflux time (hours)	Fastest tracer efflux time (hours)	Topography	Karst Zone
Highstreet Farm	48 to 168	< 12	edge of minor dry valley	1
Bagnor	< 12	< 12	river valley	1
Frilsham A	< 12	< 12	river valley	1
Frilsham B	12 to 48	< 12	river valley	1
Frilsham C	< 12	< 12	river valley	1
Winterbourne Farm	< 12	< 12	river valley	1
Peasemore	12 to 48	< 12	in major dry valley	2
Gibbet Cottages	> 168	< 12	in minor dry valley	2
Trumpletts A	12 to 48	< 12	in minor dry valley	2
Trumpletts B	12 to 48	< 12	in minor dry valley	2
Beche Park Wood	> 168	< 12	interfluve	2
Great Shefford	< 12	< 12	river valley	2
Knighton Down	< 12	< 12	edge of major dry valley	3
Grumble bottom	48 to 168	< 12	in minor dry valley	3
Bockhampton	< 12	< 12	river valley	3
Barracks	12 to 48	<12	in minor dry valley	3
Calversley Farm	12 to 48	12 to 48	interfluve	1
Ashridge Wood	12 to 48	12 to 48	edge of dry valley	2
Brightwalton Holt	> 168	12 to 48	edge of minor dry valley	2
Bradley Wood	> 168	12 to 48	major dry valley	2
Briff Lane	48 to 168	48 to 168	interfluve	1
Bottom Barn	> 168	48 to 168	interfluve	2
Greendown Farm	> 168	48 to 168	in minor dry valley	3
Cow Down	> 168	48 to 168	interfluve	3
Brightwalton Common	> 168	> 168	interfluve	3

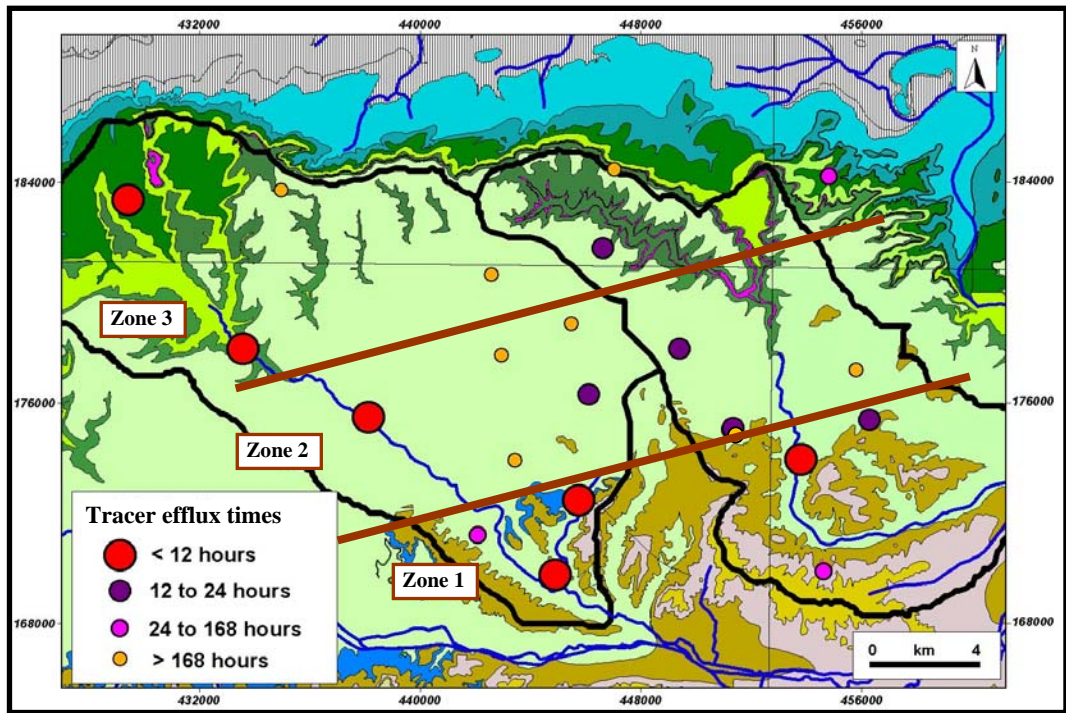


Figure 6.7: Time taken for tracer efflux from entire borehole (excluding impermeable sections at the bottom). Geology key is as for Figure 2.2. Thick brown lines depict boundaries between karst zones 1,2,3.^{BGS}

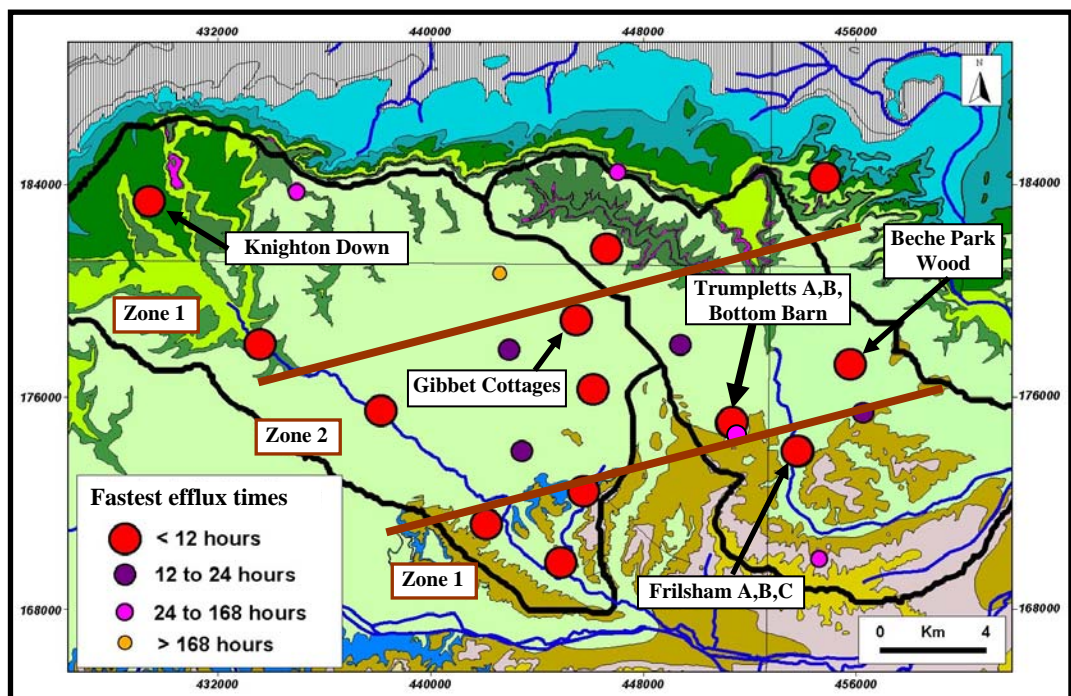


Figure 6.8: Time for most rapid tracer efflux in boreholes

Table 6.8: Transmissivity from pumping tests and tracer efflux times

Borehole	Transmissivity ($\text{m}^2 \cdot \text{d}^{-1}$)	Tracer efflux time (entire borehole)	Tracer efflux time (fastest borehole section)
Greendown Farm	0.5	> 720 hours	< 336 hours
Brightwalton Common	1	> 2520 hours	> 2520 hours
Cow Down	18	480 hours	< 216 hours
Knighton Down	270	< 24 hours	6 hours

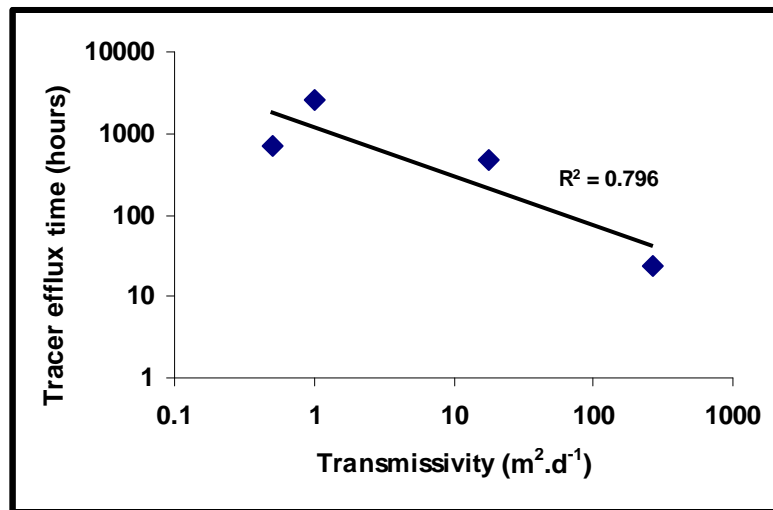


Figure 6.9: Relationship between transmissivity from pumping tests and tracer efflux times

6.4.2 Tracer decline through time

Results of uniform injection SBDTs are shown in Figure 6.10 in alphabetical order by borehole name. The upper graphs show the electrical conductance logs obtained during each experiment, which are discussed in more detail in Section 6.4.3. Categories refer to tracer efflux times (Section 6.3.5). The lower graphs are x-y scatter plots of the summed tracer concentration during each individual profile against time, and form the basis of the discussion in this section about patterns in the decline in tracer through time.

Classical SBDT theory (e.g. Lewis, 1966) assumes that the borehole is well mixed, and that at all levels tracer is diluted by exactly the same groundwater flow. Following

injection, at any particular snapshot in time, tracer concentrations would not vary with depth. This would result in a regular exponential decrease in total tracer in the borehole with time. Departure from this pattern would occur if the tracer were not fully mixed horizontally across the borehole. In general there appears to be good horizontal mixing during the SBDTs, as indicated by the consistency in electrical conductance logs during most tests (upper graphs in Figure 6.10). The exceptions are two boreholes in which tracer dilution was extremely slow (Brightwalton Holt and Brightwalton Common), where tracer concentrations increased following injection indicating poor horizontal mixing. The main departure from classical theory arises due to variability in vertical mixing. This occurs if horizontal groundwater flow varies with depth or if vertical flow is occurring.

A very close approximation to an exponential decrease in summed tracer concentration with time occurs in 10 of the boreholes (e.g. Ashridge Wood, Bagnor and Barracks, lower plots of Figure 6.10). However, these type of plots cannot be used as an indication of consistent horizontal flow during SBDTs. The upper graphs in Figure 6.10 clearly indicate that tracer concentrations within individual profiles varied significantly with depth. In 10 other boreholes there is a general decrease in the rate at which tracer is diluted resulting in concave shaped plots of log summed tracer concentration against time (e.g. Beche Park Wood, Bottom Barn). A probable interpretation is that the initial high rate of decline in tracer is caused by a rapidly diluting section of borehole. Once the tracer in this section has been replaced with aquifer water, the rate of decline in total tracer is determined by the slower dilution in the remainder of the borehole. Within these types of plots there may be two or more straight segments that are “exponential” but only over a limited time interval. The results from Trumpletts A and B are more complex with multiple segments and the plots include convex sections indicating that as the test progressed, there was an increase in the rate at which tracer was diluted.

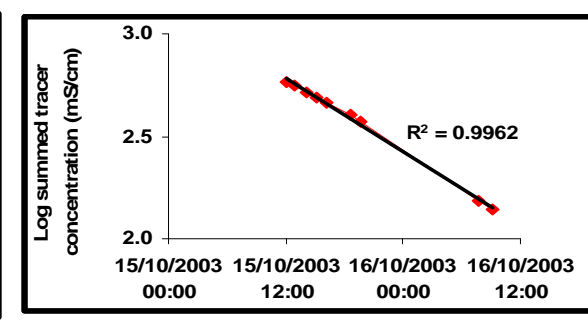
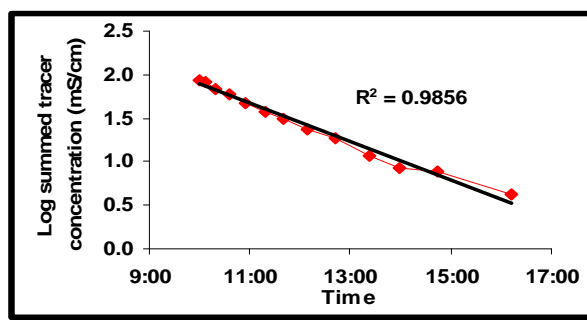
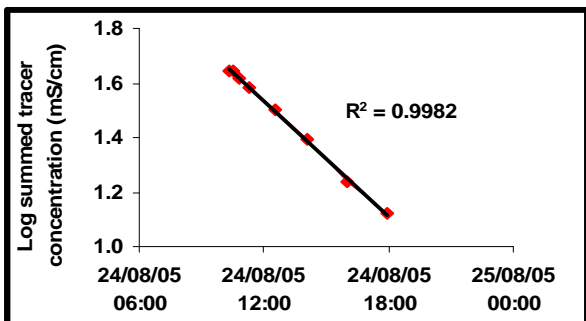
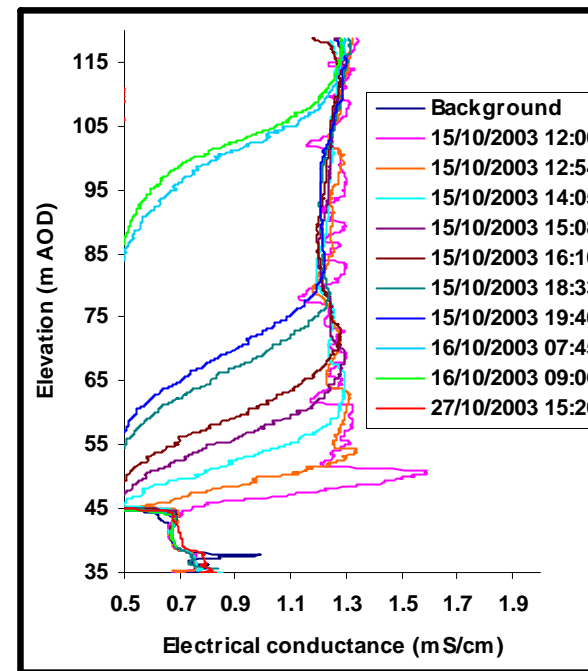
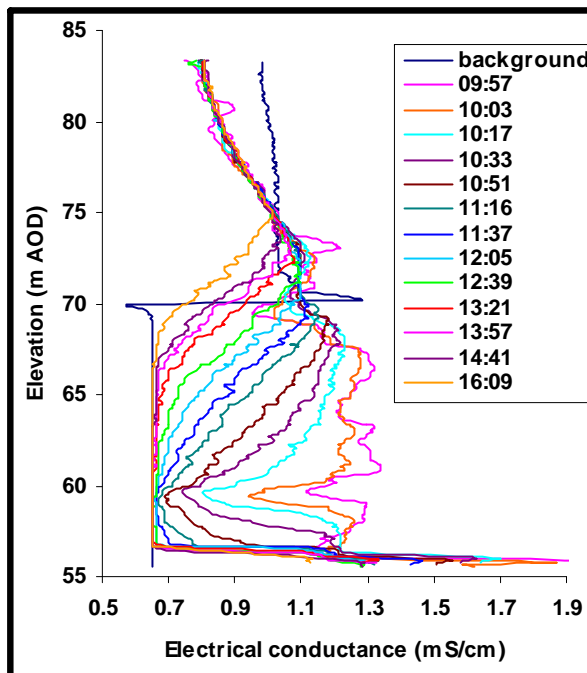
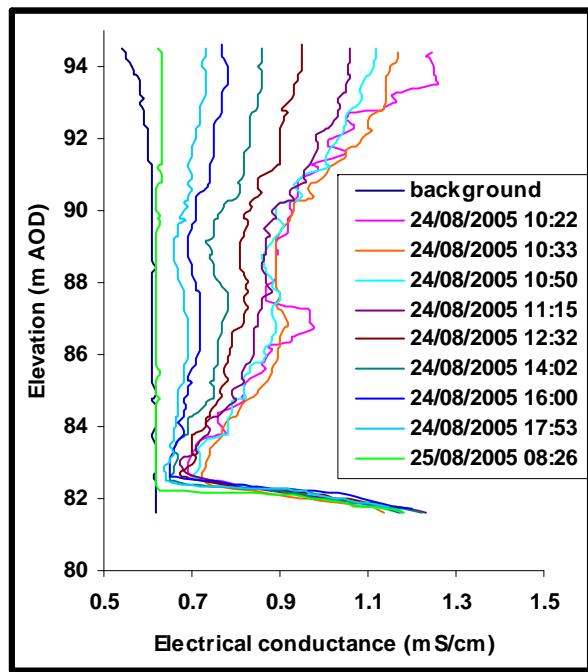
Unfortunately, it is not possible to deduce the flow pattern logically from these plots. Different combinations of, and rates of, vertical and horizontal flow may result in similar plots. Even the straightforward pattern of exponential decay cannot be interpreted as indicating simple horizontal flow. To determine the flow patterns in boreholes, the detail of the electrical conductance logs must be examined (Section 6.4.3).

Figure 6.10: Results of uniform injection SBDTs (in alphabetical order by borehole name)

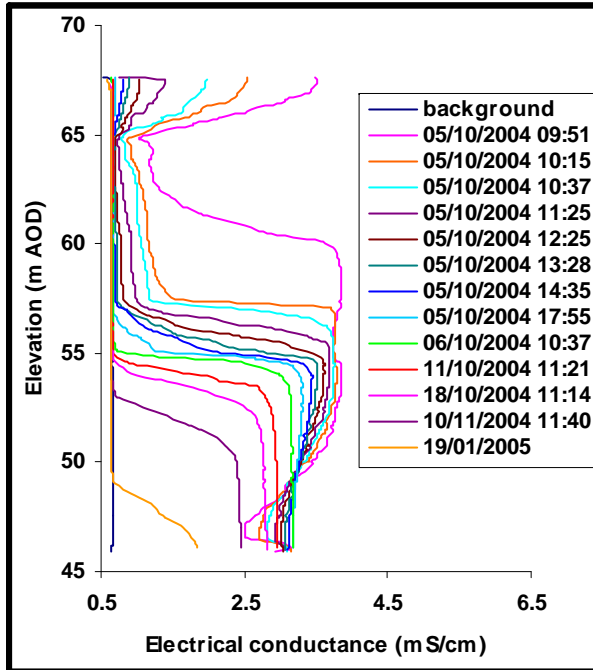
Ashridge Wood (Category B)

Bagnor (Category A)

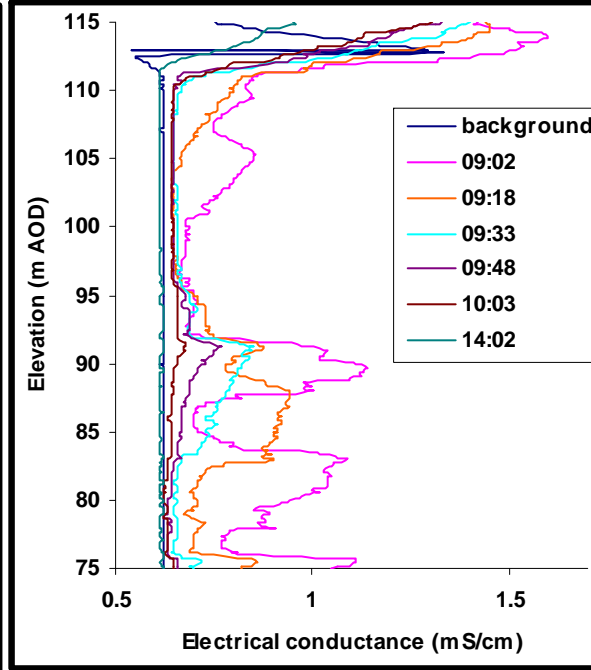
Barracks (Category B)



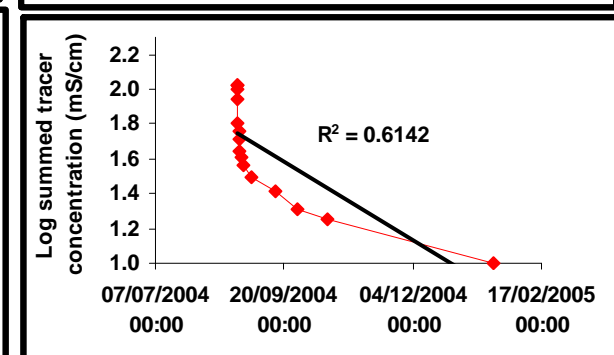
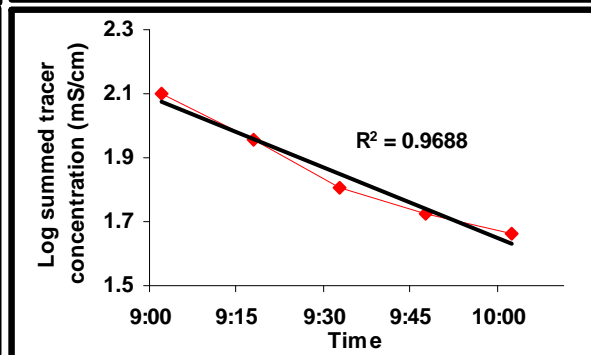
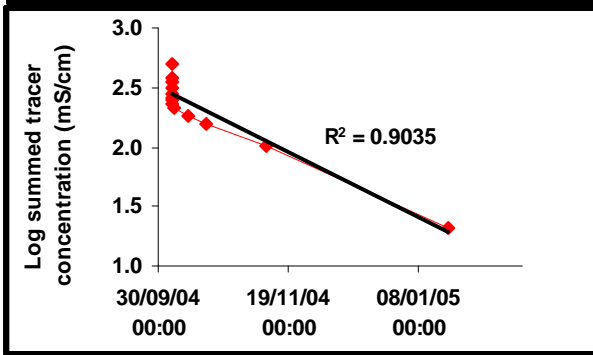
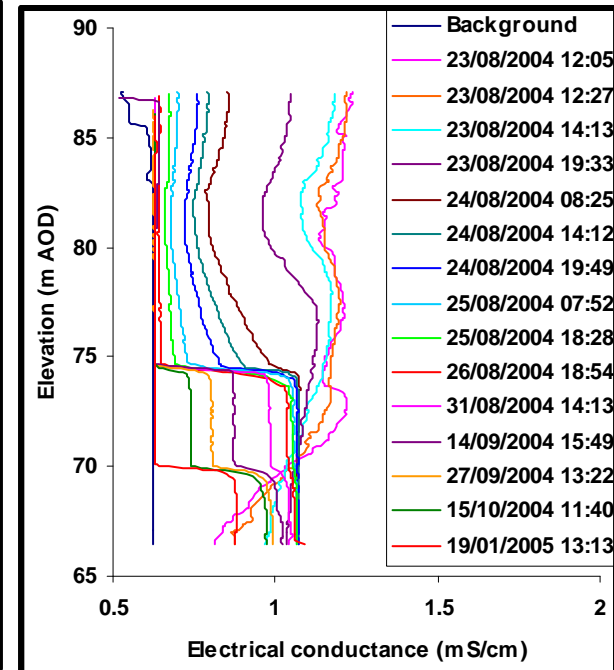
Beche park Wood (Category D)



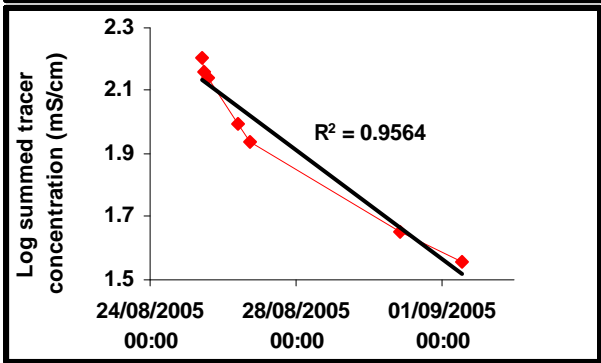
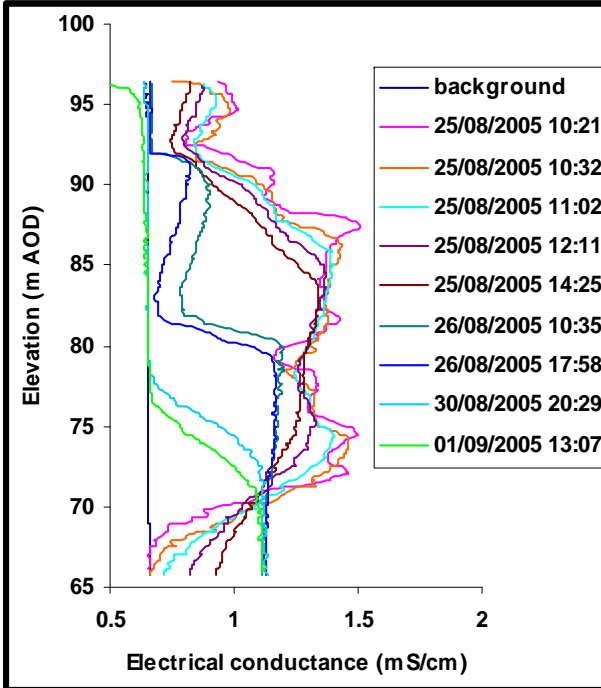
Bockhampton (Category A)



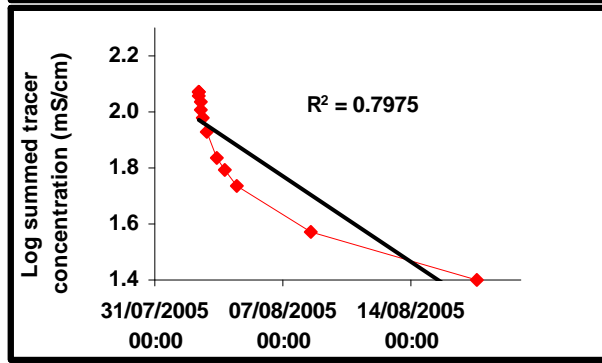
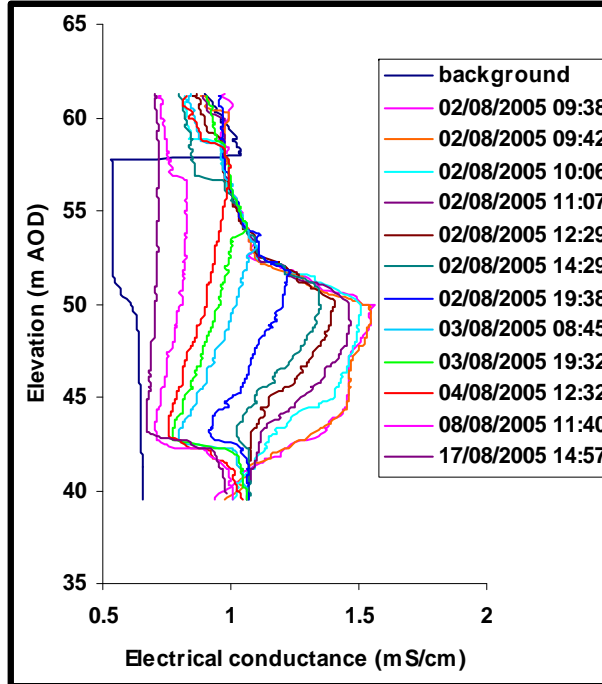
Bottom Barn (Category D)



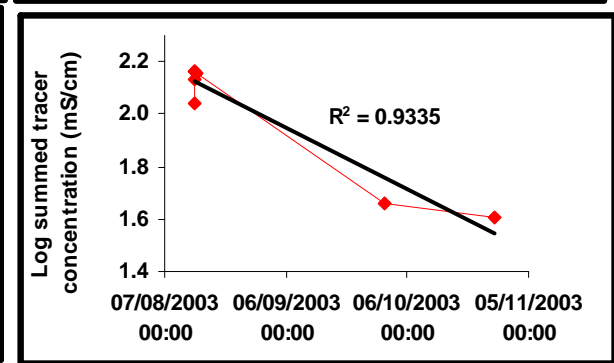
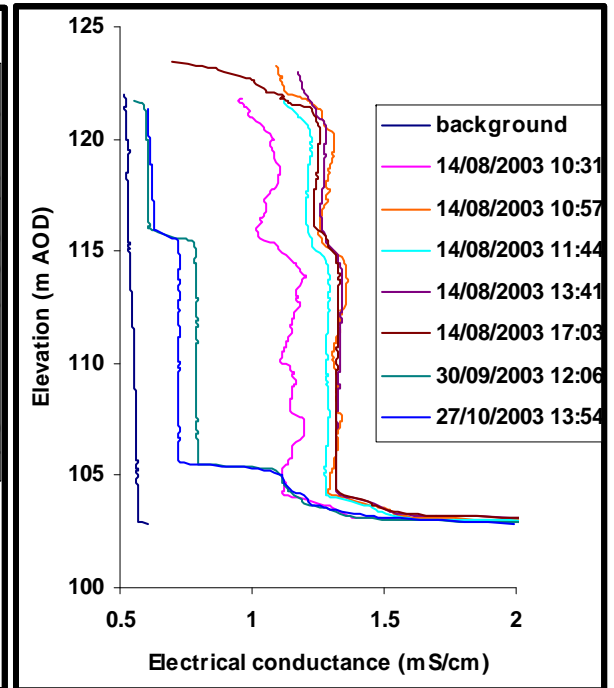
Bradley Wood (Category D)



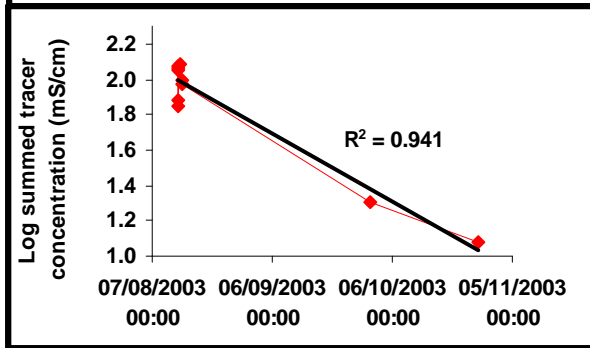
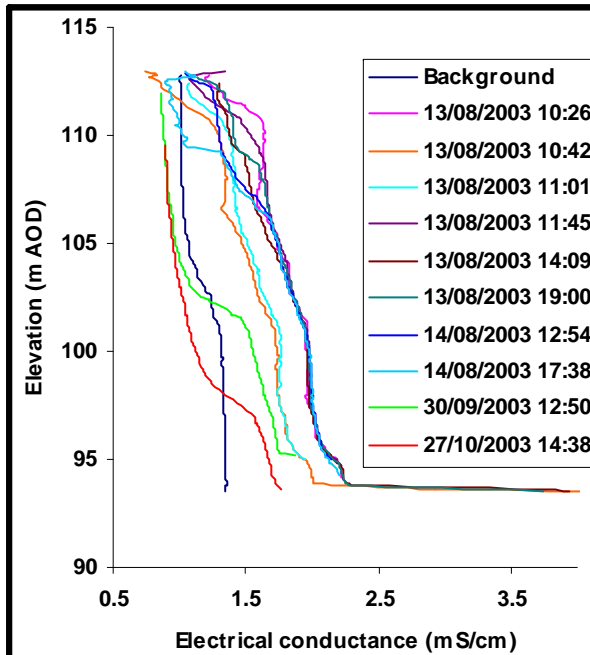
Briff Lane (Category C)



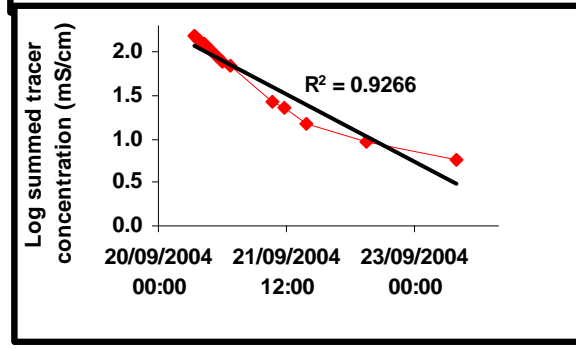
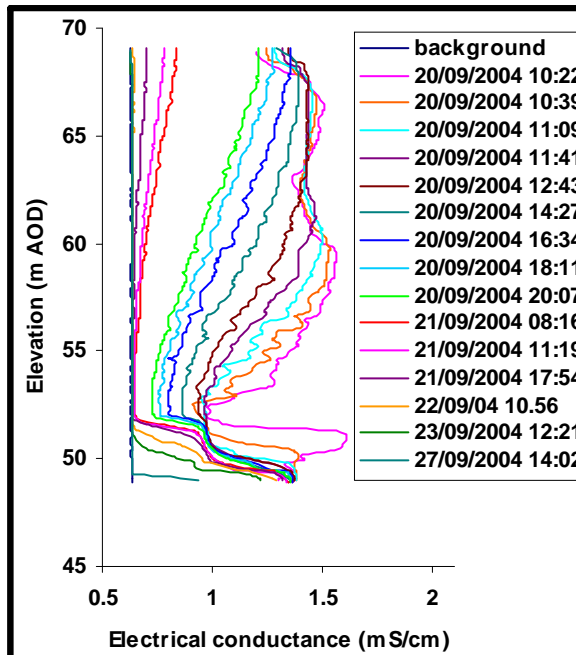
Brightwalton Common (Category D)



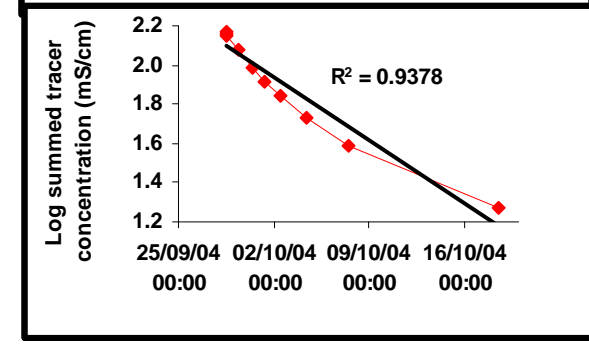
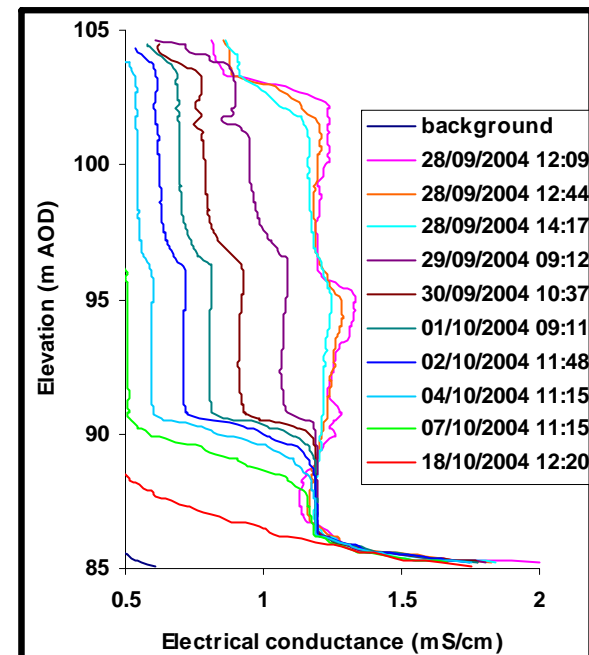
Brightwalton Holt (Category D)



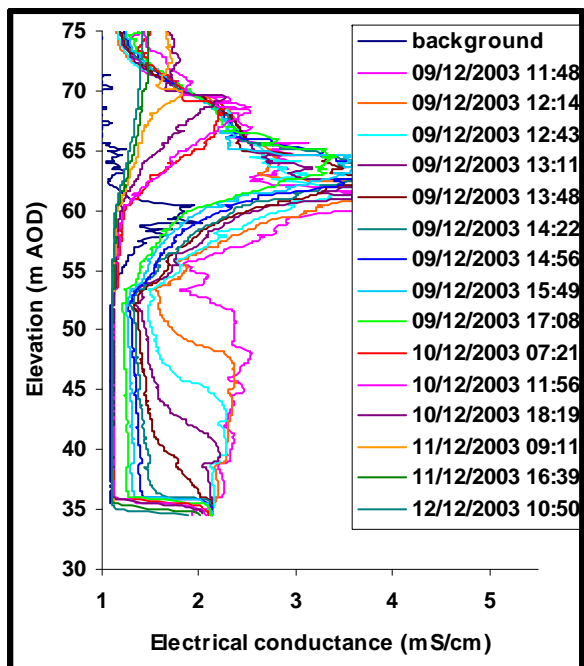
Calversley Farm (Category B)



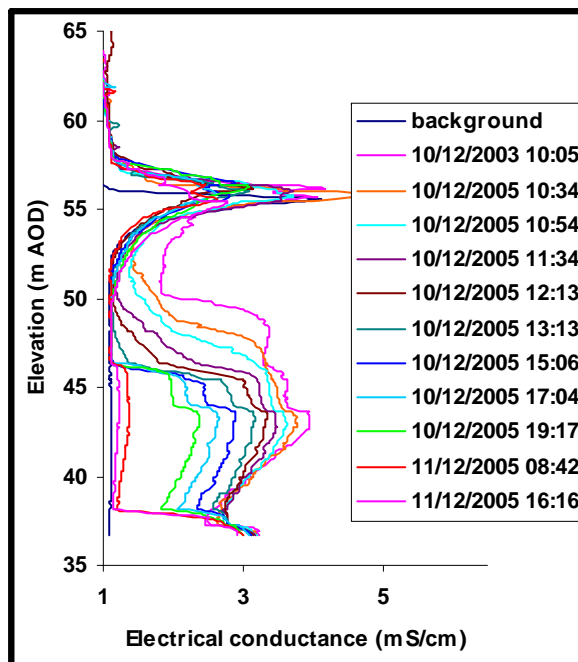
Cow Down (Category D)



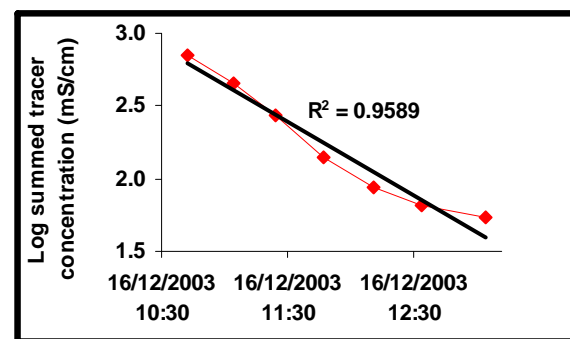
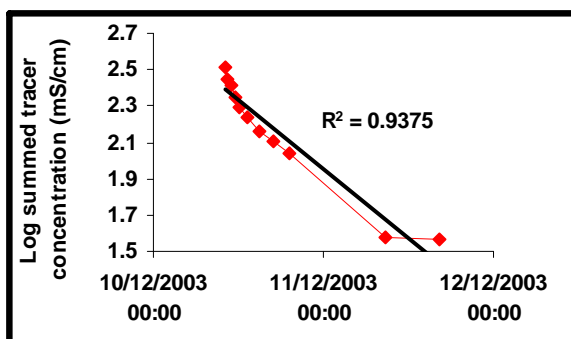
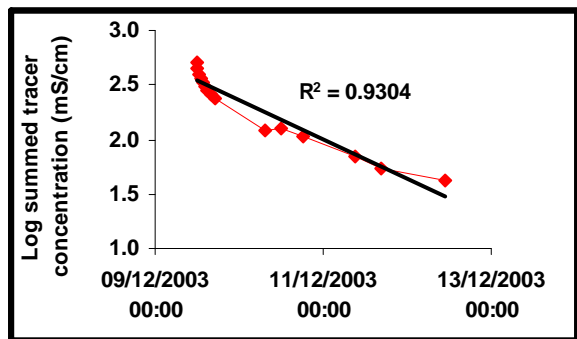
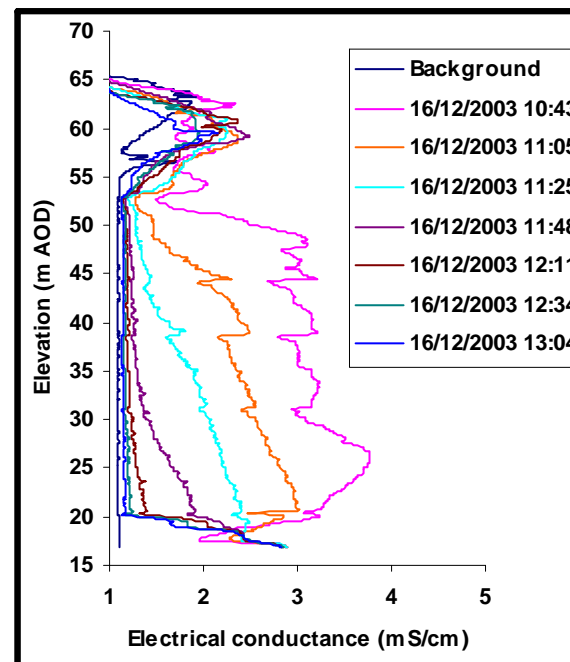
Frilsham A (Category A)



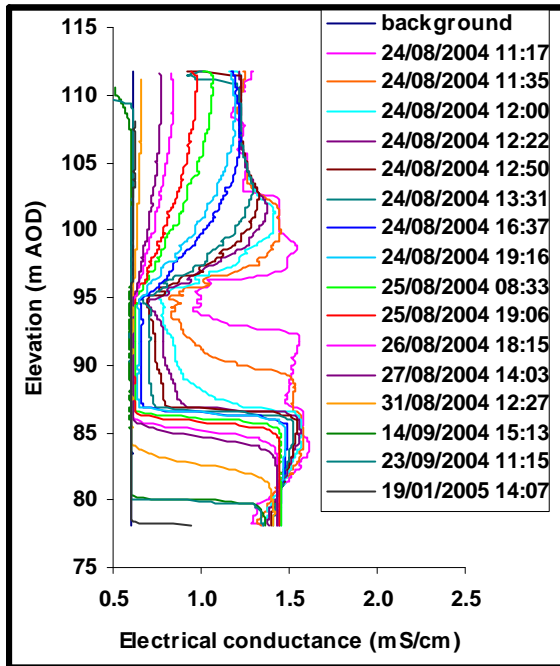
Frilsham B (Category B)



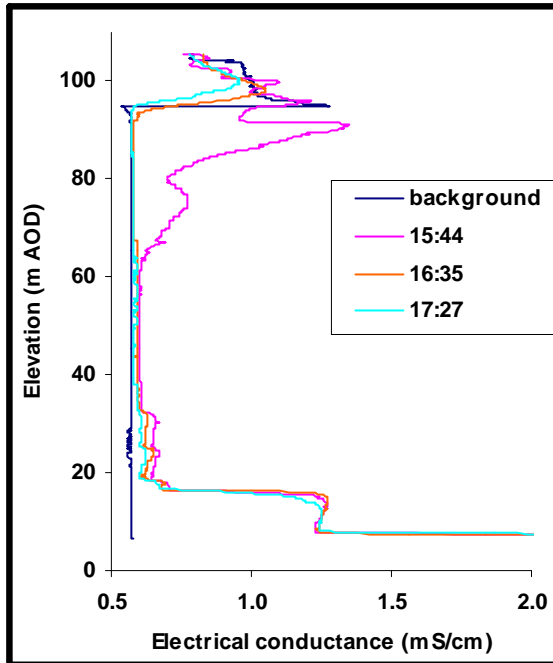
Frilsham C (Category A)



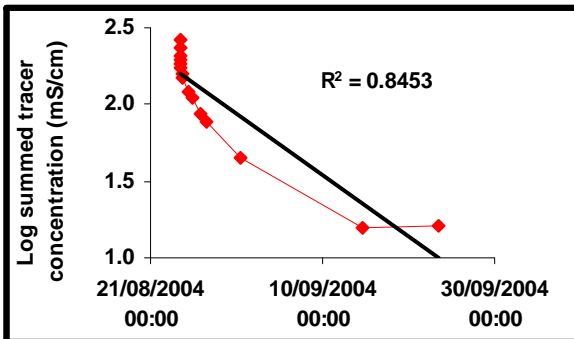
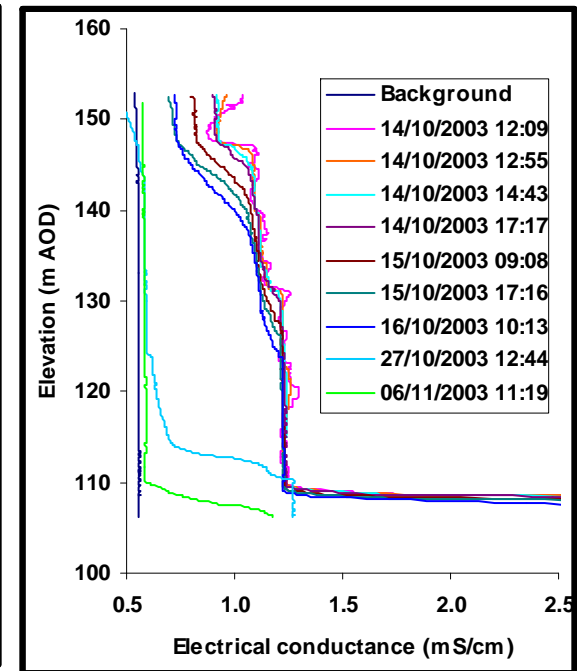
Gibbet Cottages (Category D)



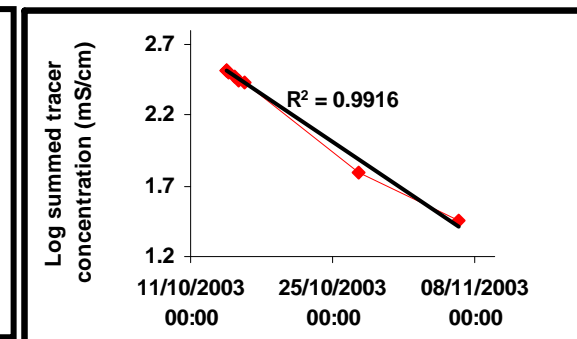
Great Shefford (Category A)



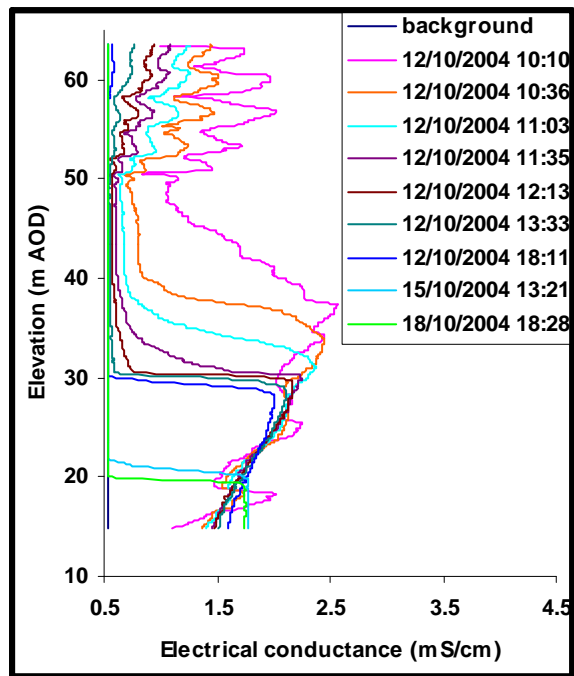
Greendown Farm (Category D)



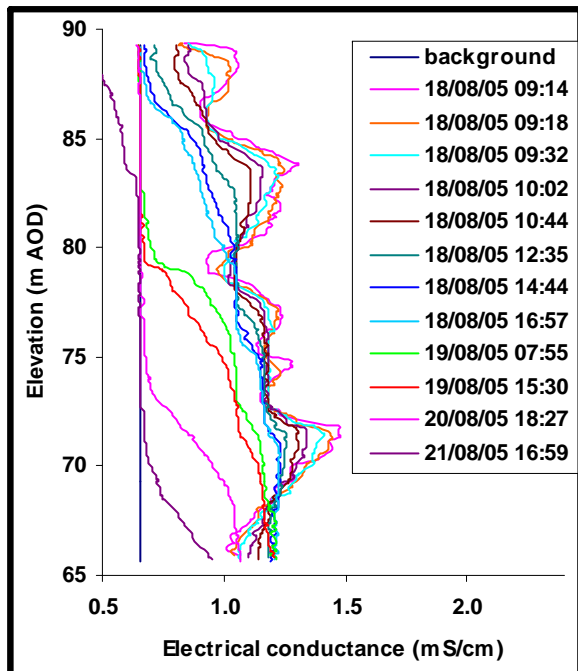
At Great Shefford, as the tracer injection hosepipe was withdrawn at about 10:00 am it became stuck at an unknown depth for several hours. The electrical conductance logs show that dilution of tracer from this borehole was very rapid (< 6 hours), but no other information can be derived from the test.



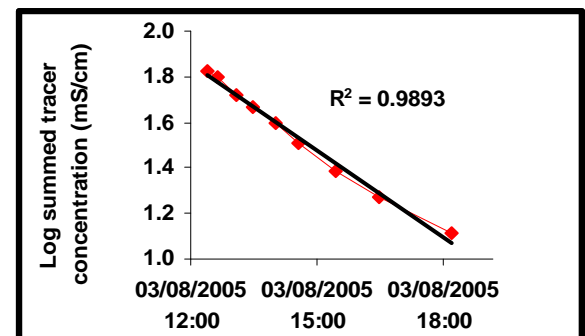
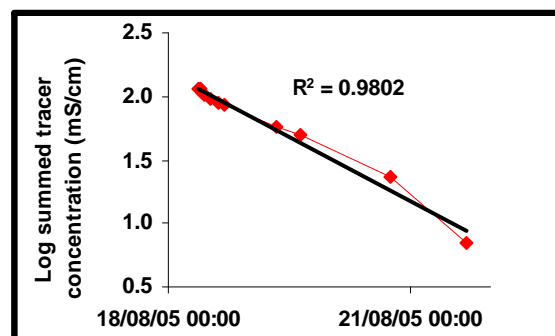
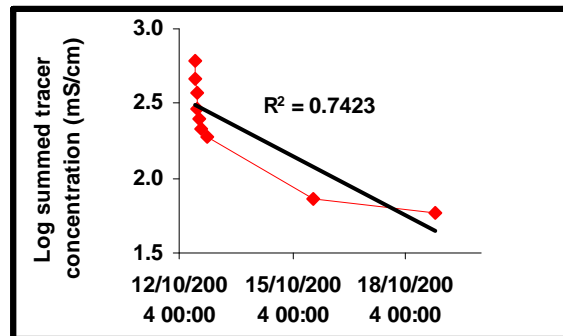
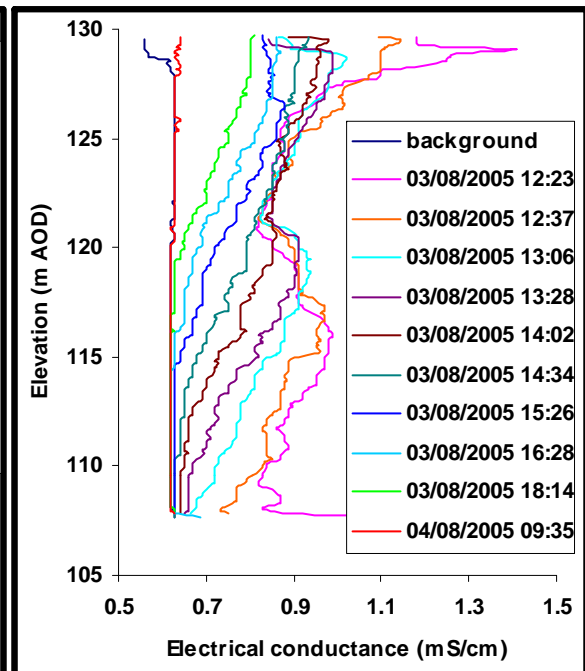
Grumble Bottom (Category C)



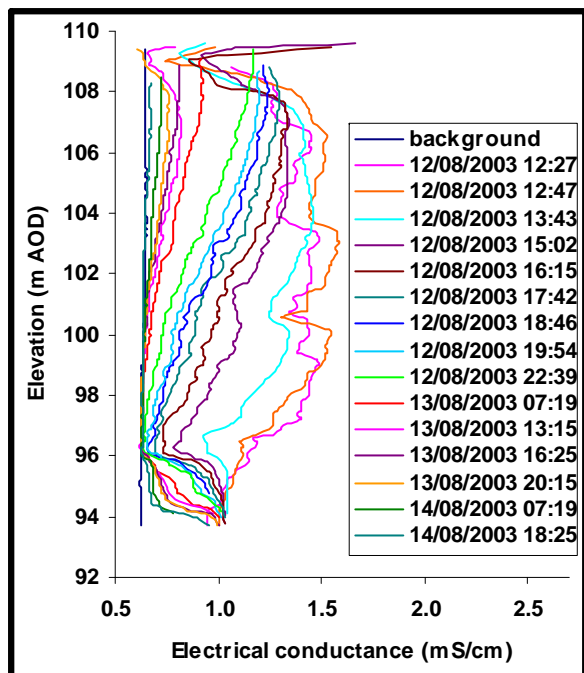
Highstreet Farm (Category C)



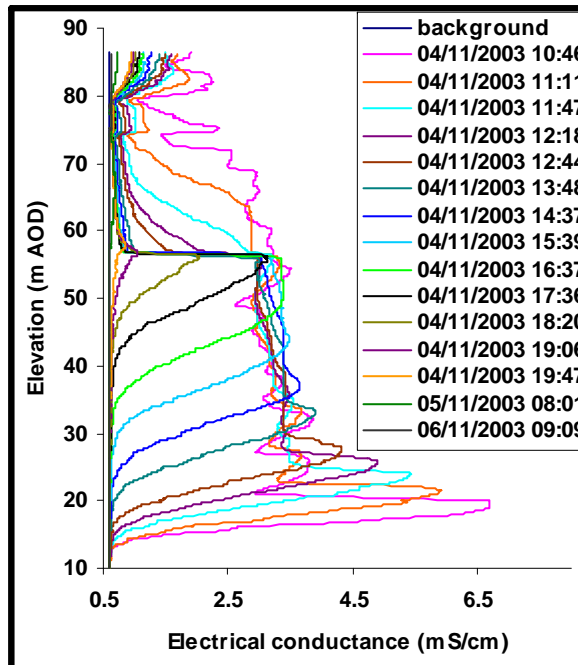
Knighton Down (Category A)



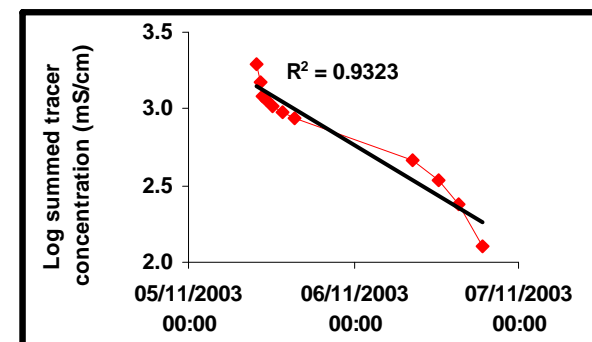
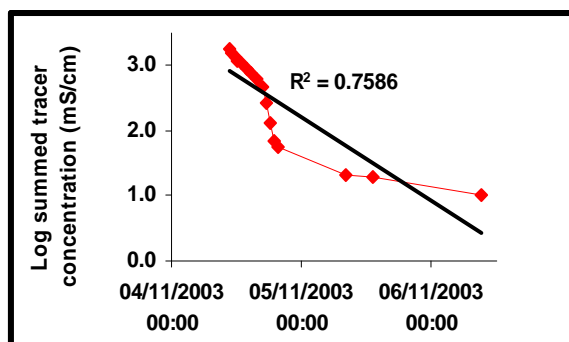
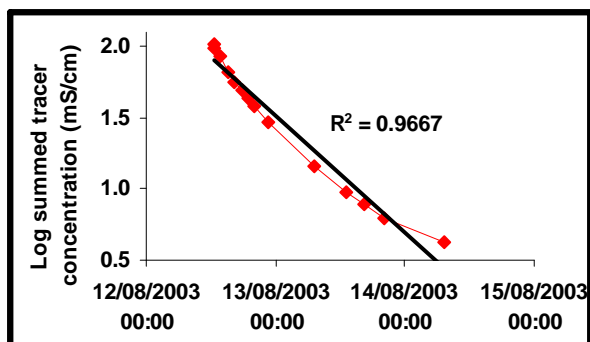
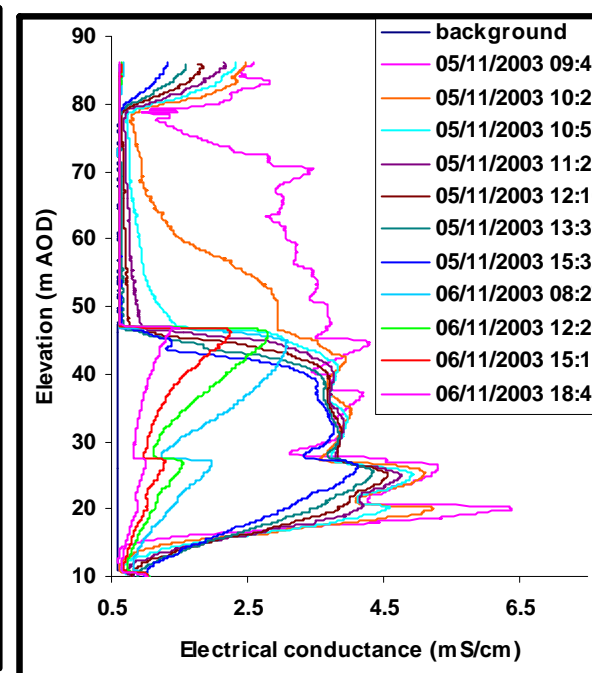
Peasemore (Category B)



Trumpletts A (Category B)



Trumpletts B (Category B)



Winterbourne Farm (Category A)

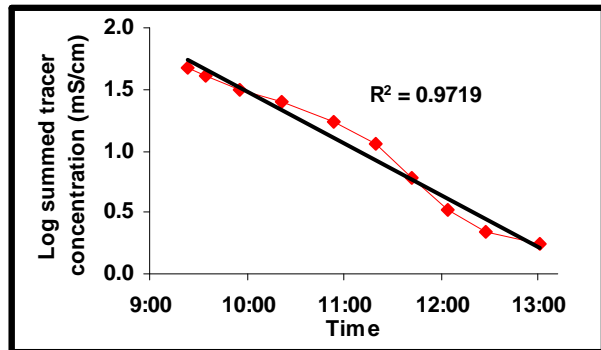
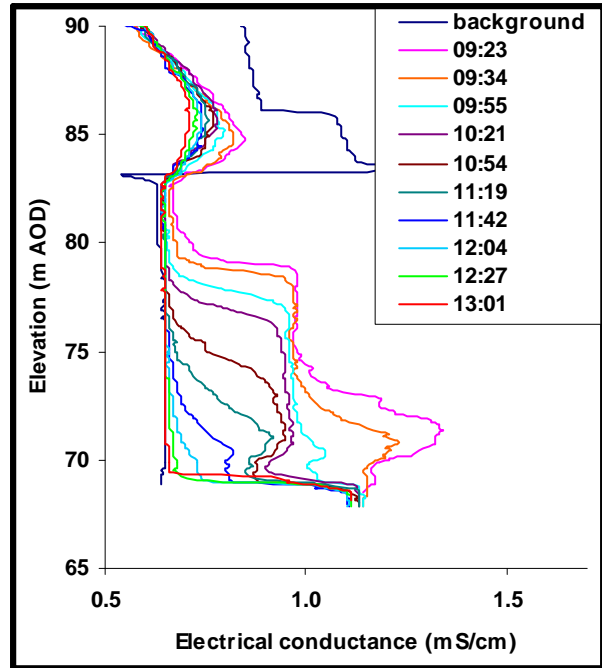


Figure 6.10: Results of uniform injection SBDTs in alphabetical order by borehole name. The upper figures show electrical conductance logs at different times following tracer injection. The lower figures are plots of the log of the summed tracer concentration measured in the borehole during each profile against the start time of the profile. Categories A to D refer to the tracer efflux times (for the entire borehole)

6.4.3 Electrical conductance logs

The patterns in the electrical conductance logs presented in Figure 6.10 (upper graphs) are variable and complex but three general observations can be made:

Firstly, there are often vertical variations in the rate at which tracer is diluted throughout the length of a borehole or over a particular section. In some boreholes there is a more rapid reduction in tracer concentration in the upper part of the borehole/section of borehole than in the lower part. This occurs both when the overall dilution rate is rapid (e.g. Winterbourne Farm below 80 m AOD), or more gradual (e.g. Highstreet Farm throughout the length of the borehole). It was hypothesised that in this situation *either* horizontal flow rates are faster in the upper part of the borehole than the lower part (Figure 6.11a), *or* downward vertical flow is occurring (Figure 6.11b). These hypotheses will be discussed and investigated further using forward modelling in Section 6.5.2 and point dilution tests in Section 6.5.3. In other boreholes there is a more rapid reduction in tracer concentrations in the lower part of the borehole than in the upper part. (e.g. Barracks, Peasemore). In this case it was hypothesised that there is either more rapid horizontal flow in the lower section, or upward vertical flow is occurring. Consistent dilution throughout a section of borehole is relatively rare, but an example occurs above 90 m AOD in the Cow Down test. In many cases more than one of these situations occurs within a borehole (e.g. Bagnor or Gibbett Cottages).

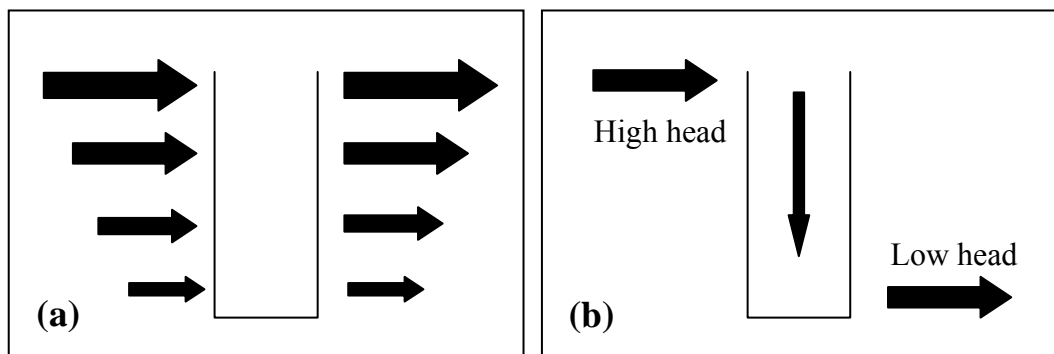


Figure 6.11: Hypothetical situations causing a decrease in tracer dilution rate with depth. (a) shows horizontal flow rates decreasing with depth (thicker arrows indicating faster flow), whilst Figure (b) shows downward vertical flow due to head differences

Secondly, there are often clear features at a particular depth that are consistently present on all electrical conductance logs. For many boreholes, as tracer is diluted there is a sharp boundary between a section with high tracer concentration and a section of much lower tracer concentration (e.g. at 74.5 m AOD in Bottom Barn, at 86 m AOD in Gibbet Cottages, and 56 m AOD in Trumpletts A). There are also horizons at which tracer is diluted more quickly than in the sections of the borehole immediately above and below it (e.g. at 38 and 44 m AOD in Frilsham C, and at several horizons above 50 m AOD in Grumble Bottom). It was hypothesized that fractures/fissures are present where these types of features are observed, and this is investigated further using forward modelling (Section 6.5.2) and point dilution tests (Section 6.5.3).

Thirdly, tracer dilution at the bottom of boreholes is often extremely slow, even if dilution in the borehole is generally rapid. In 21 boreholes tracer was still present in the bottom when the last profile was obtained, and dilution was generally much slower in the bottom few metres than in the rest of the borehole. The profiles often display a sharp boundary between the high tracer concentrations in the bottom of the borehole and water above that had returned to background concentrations earlier in the test (e.g. at 45 m AOD in Barracks). However, in four boreholes (Trumpletts A and B, Bockhampton and Knighton Down) tracer concentrations at the bottom of the borehole returned to background at an early stage.

6.4.4 Seasonal variations in SBDT results

At four sites (three boreholes at Frilsham and Trumpletts A) uniform injection SBDTs were undertaken on two occasions to investigate seasonal variability.

The results are presented in Figures 6.12 to 6.15. The greatest difference in water level was at Trumpletts A where it was 2.11 m higher in June 2004 than in November 2003 (Figure 6.12). The electrical conductance logs are generally very similar following the two injections although the feature at 27 m AOD is more persistently visible under higher water table conditions in June 2004 than in the November 2003 test. Tracer appears to leave the borehole more rapidly under higher water level conditions. On 16th June 2004 there was little tracer left between the bottom and 57 m AOD 5 hours and 24 minutes after the first profile (the green profile at 14:47), whilst in November 2003 it took 7 hours 34 minutes to reach a similar state (the pink profile at 18:20).

In the three Frilsham boreholes there was less difference in water level (12-13 cm), The patterns in the electrical conductance logs were very similar. Most tests are affected by a marked increase in the background electrical conductance between about 55 and 60 m AOD. In Frilsham B and C this appears to be at the bottom of the casing, and in A the spike is 1.4 m below the bottom of the casing. These spikes possibly reflect a zone of distinctive groundwater, but they could also be due to the effect of fluid leaching from the grout used to seal the casing (Song and Atkinson, 1985).

Overall the repeated SBDTs suggest that an increase in water level may cause a small increase in dilution rate, but the patterns in the electrical conductance logs remain very similar. The changes in water level were small, and it is possible that in interfluvial boreholes with water level fluctuations of more than 10 m, SBDTs undertaken at different times of year might display more variation if significant flow horizons were unsaturated under lower water table conditions.

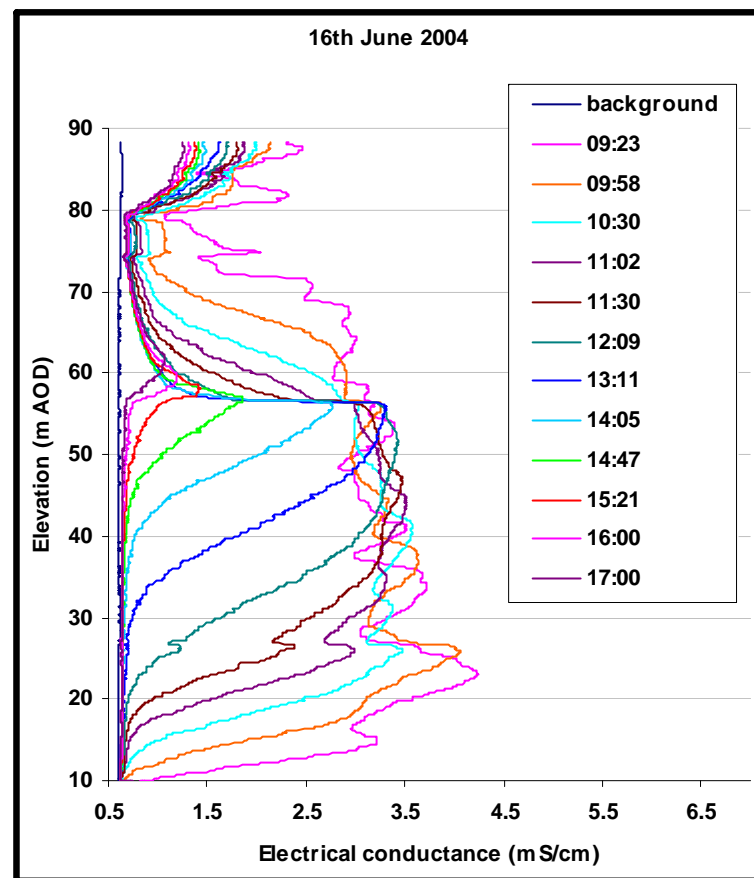
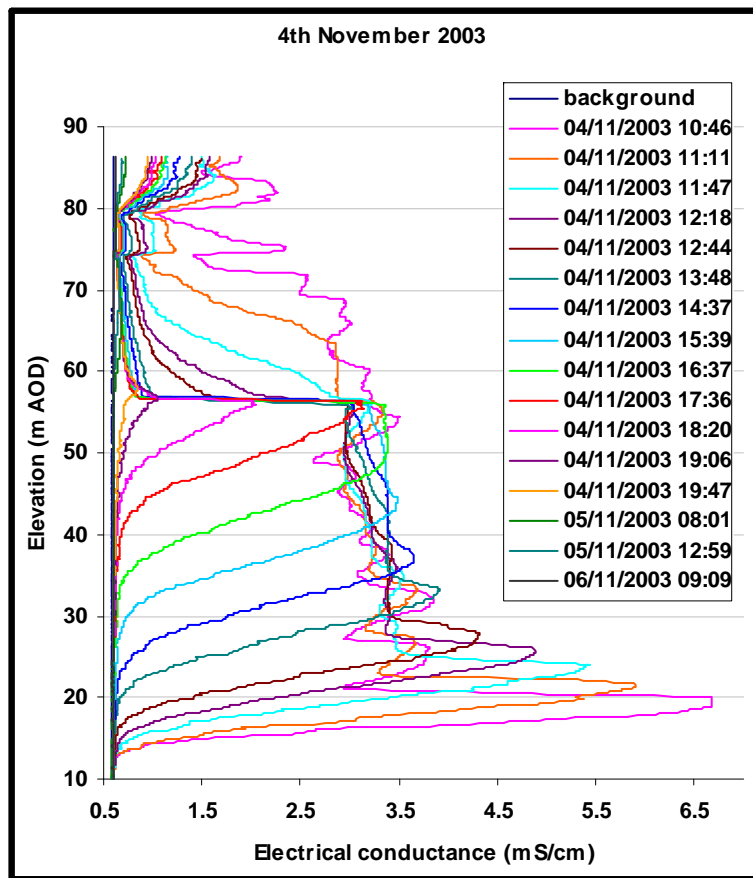


Figure 6.12: Repeated SBDTs at Trumplets A. Water level was 86.44 m AOD on 04/11/03 (left) and 88.56 m AOD on 16/06/04 (right).

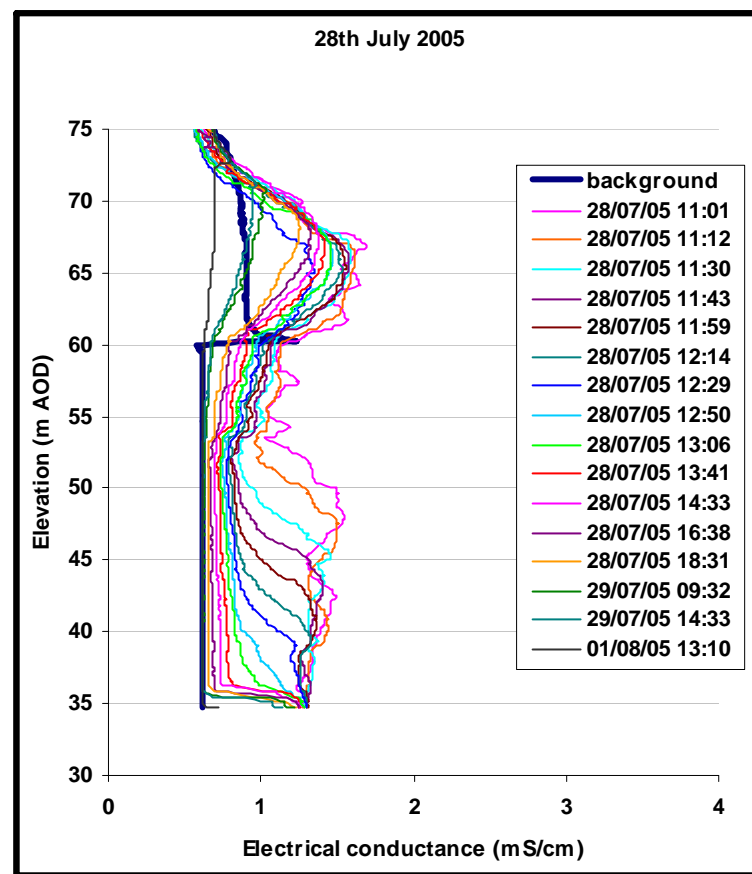
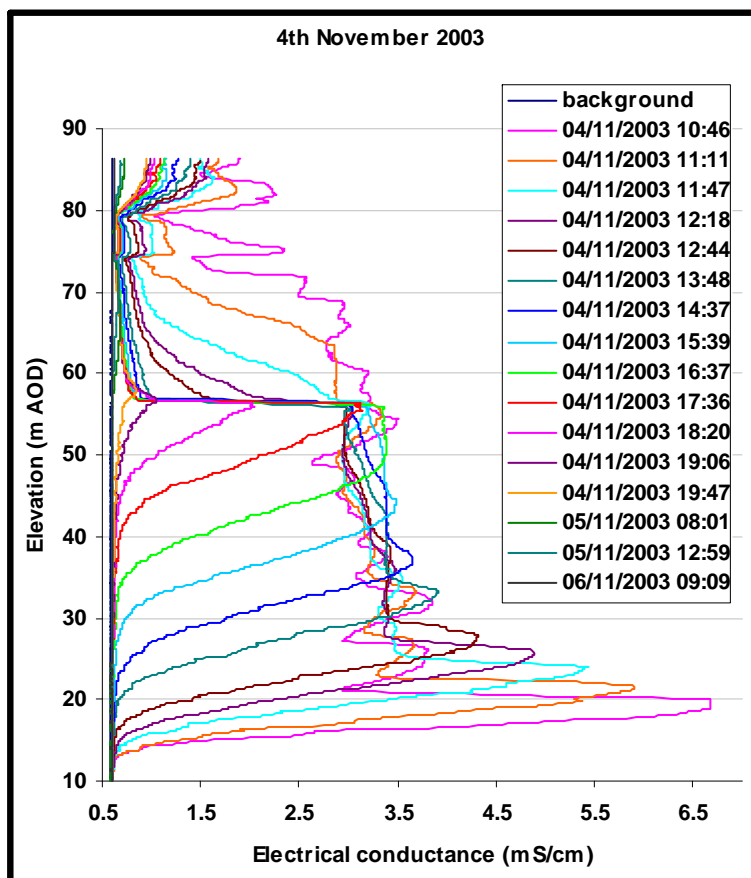


Figure 6.13: Repeated SBDTs at Frilsham A. Water level was 75.95 m AOD on 09/12/03 (left) and 75.82 m AOD on 28/07/05 (right). The borehole is cased to 61.4 m AOD

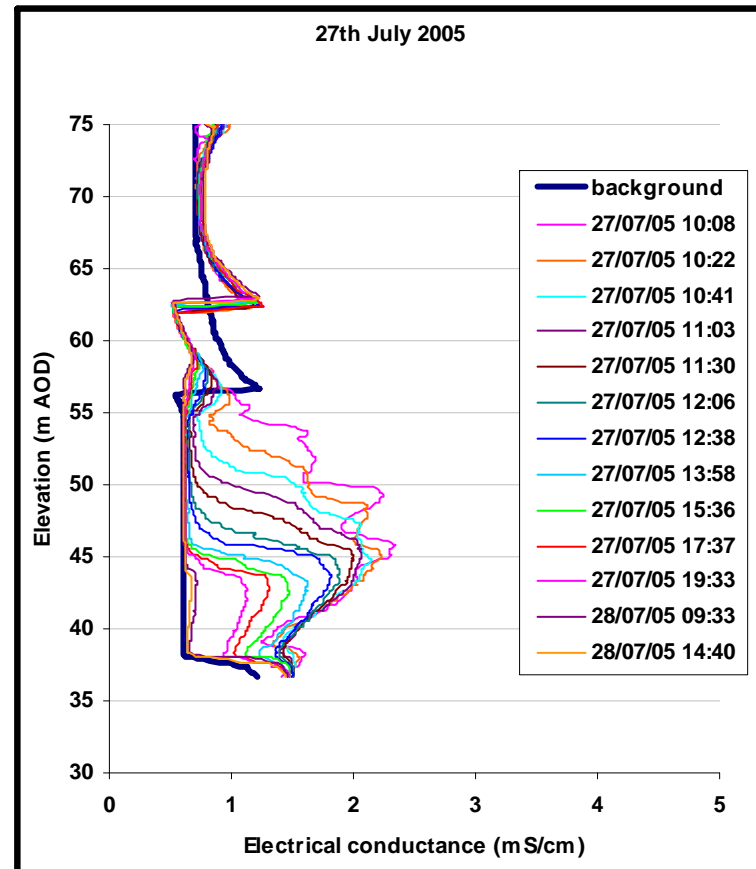
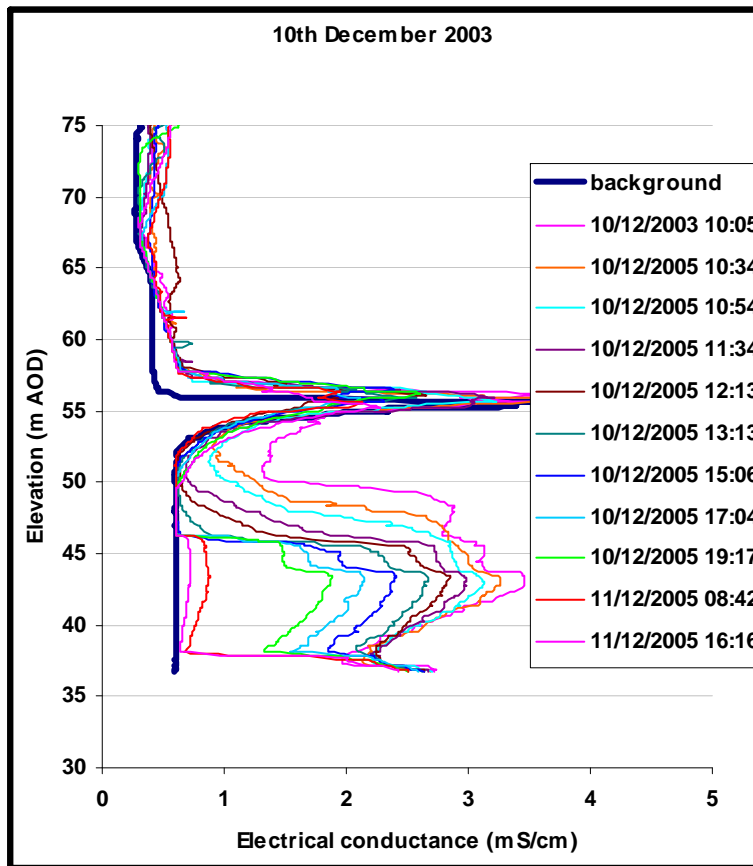


Figure 6.14: Repeated SBDTs at Frilsham B. Water table was 75.90 m AOD on 10/12/03 (left) and 75.78 m AOD on 27/07/05 (right). The borehole is cased to 56.6 m AOD.

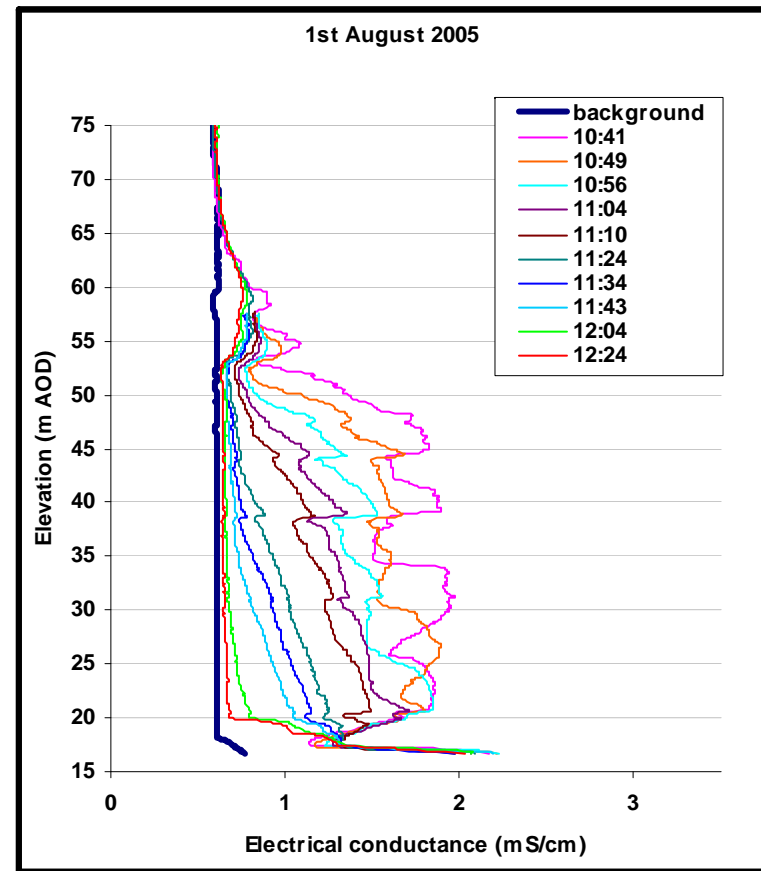
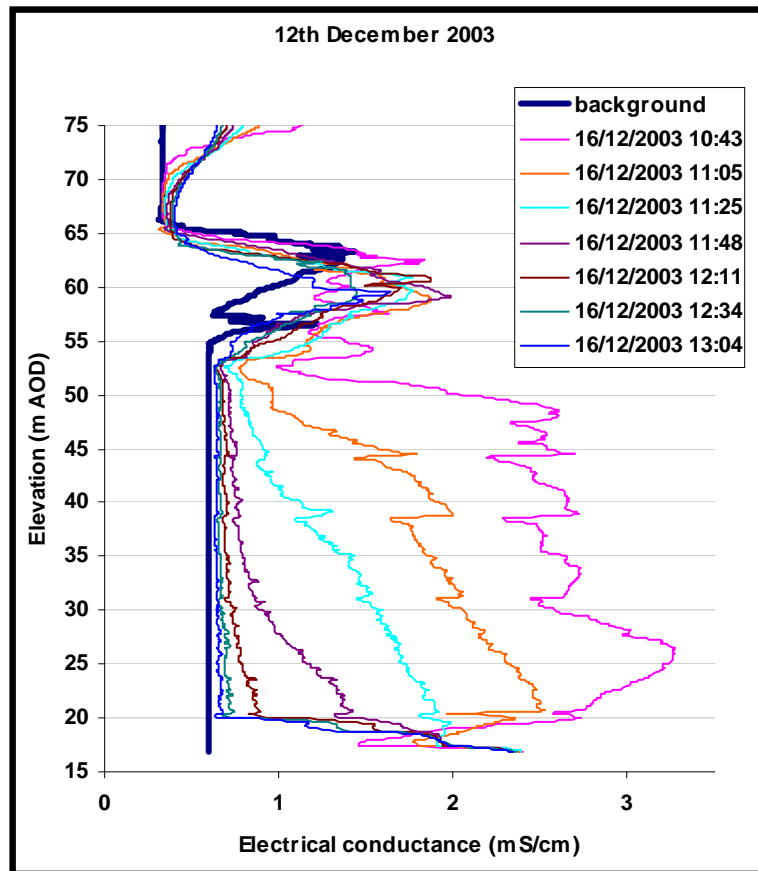


Figure 6.15: Repeated SBDTs at Frilsham C. Water table was 75.93 m AOD on 12/12/03 (left) and 75.79 m AOD on 01/08/05 (right). The borehole is cased to 57.8 m AOD.

6.5 Identifying flowing features from SBDTs

6.5.1 Introduction

As observed in Section 6.4.3, electrical conductance logs obtained during SBDTs have complex and variable patterns. These can in part be attributed to vertical flows within the borehole tested and flow along fractures intercepted by the borehole. The objective of undertaking SBDTs in this study was to determine the location of flowing horizons to investigate their distribution with depth at the catchment scale. The aim of this section is to outline the methods that were used to identify flow horizons from SBDTs. Three types of additional evidence were used to aid their interpretation:

- 1) Forward modelling was undertaken to investigate the types of patterns in dilution profiles that might arise with different combinations of inflows and outflows.
- 2) SBDTs using point injection at a particular horizon were used to confirm vertical and horizontal flows.
- 3) Background electrical conductance and temperature logs were examined because sharp changes in these may indicate the location of a flowing horizon.

The remainder of this section discusses the forward modelling and point dilution SBDTs and then presents the integrated method (incorporating background electrical conductance and temperature logs) that was used to identify flowing features in each borehole.

6.5.2 Forward modelling

6.5.2.1 Introduction and methodology

As part of the LOCAR research programme, an advection-dispersion forward model of SBDTs was developed in Microsoft Excel by John Barker. The objective was to use the model as an exploratory tool to investigate the patterns in dilution profiles during SBDTs. Different flow scenarios were postulated and the model simulated the resulting dilution profiles. This process helped confirm previous insight, and to constrain the possible ways in which the experimental patterns could be interpreted, especially with respect to fissured horizons (with or without vertical flows between them). The model was not used to fit the electrical conductance data from the field results.

The principle of the forward model is that the user specifies an initial tracer concentration (C_o) and a horizontal inflow (Q_{IN}) and outflow (Q_{OUT}) for each model segment. The vertical flow between segments is computed from the differences between (Q_{IN}) and (Q_{OUT}) at a particular horizon (but obviously $\sum Q_{IN}$ must be equal to $\sum Q_{OUT}$). The model runs forward in time and predicts profiles of tracer concentration with depth. Where vertical flows are induced, the advection-dispersion equation is used to calculate the spread of tracer using a dispersivity value supplied by the user.

Figure 6.16 shows five different flow situations that can be induced by adjusting values of Q_{IN} and Q_{OUT} for individual segments. Arrows outside the borehole indicate the segments for which a flow rate is specified with thicker arrows indicating higher flow rates. Many segments are specified to have no horizontal inflow or outflow. Vertical flow occurs between individual segments if inflows and outflows are not equal (in Figure 6.16 arrows depict upward flow within the borehole because at the bottom inflows are larger than outflows, and the reverse occurs at the top). Different, simple combinations of these flow patterns were used to investigate the patterns in tracer concentration profiles with depth that they produce as a tool for identifying flowing horizons in the real boreholes.

Unless otherwise stated, the model was run with the following settings:

The borehole length was set at 50 m and the segment length at 1 m (therefore C_o , Q_{IN} and Q_{OUT} were specified for 50 segments). C_o was set at 100. The diameter of the borehole was assumed to be 0.25 m, and the dispersivity was set at 0.1 m.

For situations without vertical flow, patterns of “diffuse” flow were simulated by assigning small crossflows to every segment. For situations with vertical flow, a small number of segments were assigned Q_{IN} and Q_{OUT} values ($m^3.d^{-1}$) to produce combinations of the flow patterns depicted in Figure 6.16. Q_{IN} and Q_{OUT} were generally set to 0 for all other segments, thereby simulating a situation in which diffuse flow is negligible compared to fracture/fissure flow.

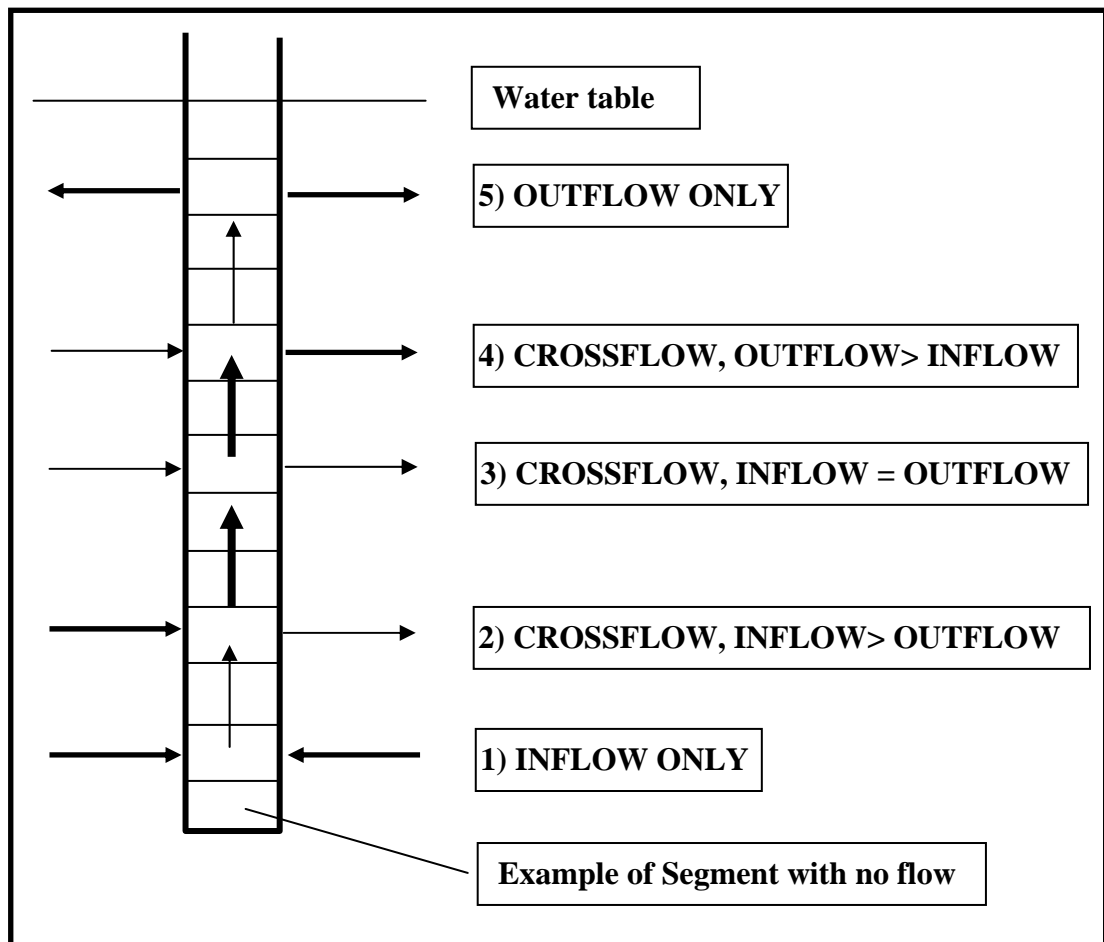


Figure 6.16: Borehole schematic showing five different flow situations

Section 6.5.2.2 presents and discusses simulations without vertical flow and Section 6.5.2.3 details investigations of vertical flow. For each example the output from the model of predicted profiles of tracer concentration at different times following injection are presented. The time units are days (but are affectively arbitrary). Depth is in metres below the water table. Schematic figures are included to show the flow patterns. For simulations incorporating “diffuse” flow, these comprise arrows depicting the general pattern (with thicker arrows indicating higher flow rates), and values of Q_{IN} and Q_{OUT} are specified in the Figure caption. For vertical flow simulations without “diffuse” flow, where only a small number of horizons are assigned Q_{IN} and Q_{OUT} values, they are presented on the schematic figures.

6.5.2.2 Simulations of tracer profiles in the absence of vertical flow

If tracer concentrations decrease and there is no vertical flow then crossflow must be occurring. Figure 6.17 shows the straightforward case of uniform “diffuse” horizontal flow across a borehole. The exponential decrease in the amount of tracer through time is apparent. This pattern is not commonly observed in the current study but it is probable that it occurs below 74 m AOD in Bottom Barn, between 96 and 91 m AOD in Cow Down, and in Brightwalton Common (Figure 6.10).

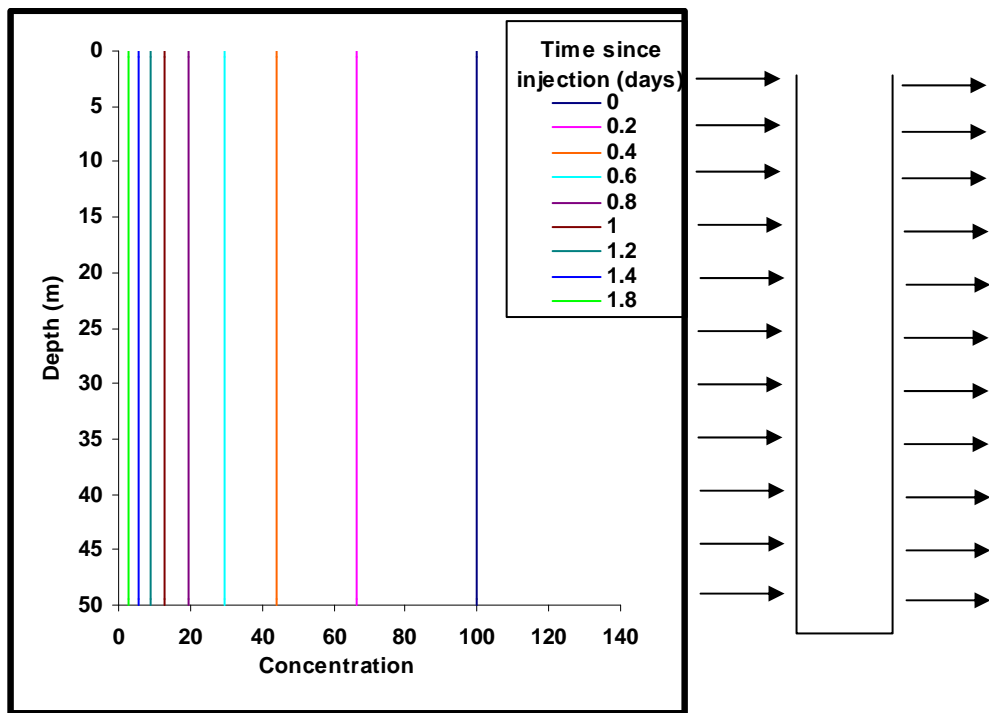


Figure 6.17: Simulation of uniform crossflow (Q_{IN} and Q_{OUT} set to $0.1 \text{ m}^3 \cdot \text{d}^{-1}$ in every segment)

The horizons at which tracer was diluted more quickly than in the sections of borehole above and below (e.g. 38 and 44 m AOD in Frilsham C, and several horizons above 50 m AOD in Grumble bottom, Figure 6.10) can be simulated by including a “fracture/fissure” with a higher inflow and outflow rate than in the surrounding area (Figure 6.18). In this simulation there is no vertical flow (although this may not be the case in the borehole examples listed above). A similar pattern can be created (Figure 6.19) if C_0 at a particular depth is reduced (which is equivalent to simulating a widening in the borehole diameter). However, the feature becomes progressively less significant with time whereas in the simulation with crossflow (Figure 6.18), the feature remains

very pronounced even in late simulations. Generally, where this type of feature is apparent in the SBDT results it persists through all the profiles and is therefore likely to be caused by a flowing fracture/fissure.

The model was used to try and determine the cause of a sharp boundary between areas of higher and lower tracer concentration (e.g. 70 and 74.5 m AOD in Bottom Barn, Figure 6.10). Assuming that there is no vertical flow, a boundary can be created by a change in the rate of crossflow with more rapid flow across the upper section than the lower section (Figure 6.20). A boundary can also be simulated by varying C_o to represent a change in borehole diameter. In Figure 6.21 C_o is set at 80 for 0-23m, and at 100 for 23-50m, but Q_{IN} and Q_{OUT} are set at a constant $0.1 \text{ m}^3 \cdot \text{d}^{-1}$ for every segment. The % difference between tracer concentrations in the upper and lower borehole remains the same, which is not the case in Figure 6.20 where the boundary between the upper and lower borehole remains more pronounced even in later simulations.

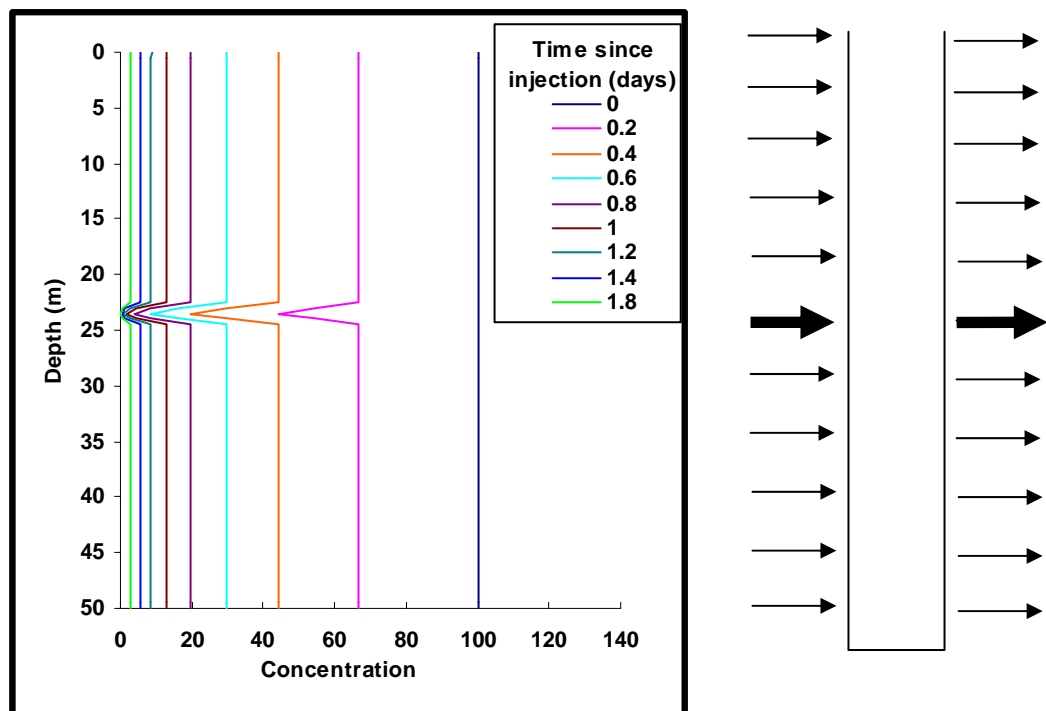


Figure 6.18: Simulated crossflow in a fracture/fissure with a higher inflow and outflow rate than the surrounding rock (Q_{IN} and Q_{OUT} set to $0.1 \text{ m}^3 \cdot \text{d}^{-1}$ in every segment, except at 23-24 m in which Q_{IN} and $Q_{OUT} = 0.2 \text{ m}^3 \cdot \text{d}^{-1}$)

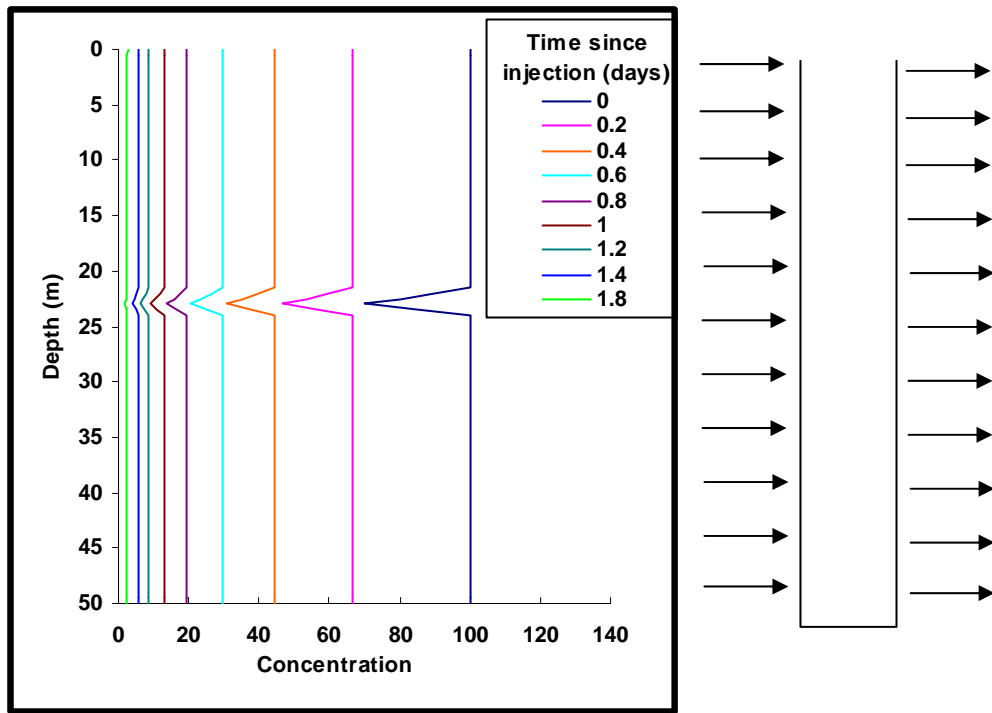


Figure 6.19: Simulation with a reduced C_0 at 23-24 m with Q_{IN} and Q_{OUT} set to $0.1 \text{ m}^3 \cdot \text{d}^{-1}$ in every segment (C_0 was set at 70 at 23-24 m, but kept constant at 100 for all other segments).

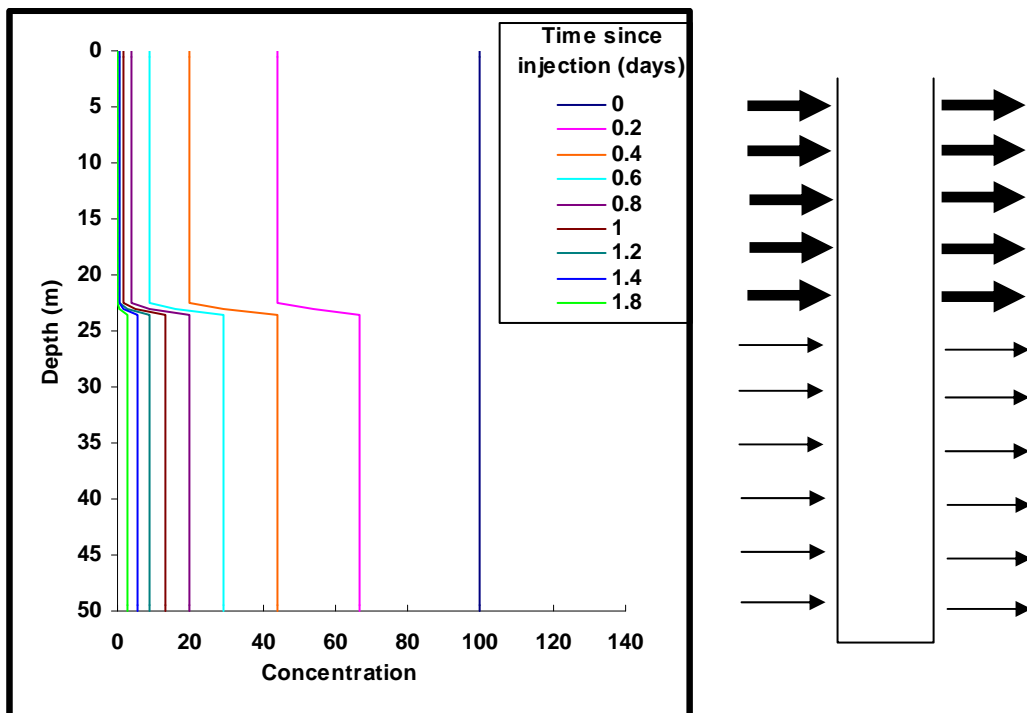


Figure 6.20: Simulation of stronger crossflow in upper part of borehole than lower part (Q_{IN} and Q_{OUT} set to $0.2 \text{ m}^3 \cdot \text{d}^{-1}$ in segments from 0-23 m, and to $0.1 \text{ m}^3 \cdot \text{d}^{-1}$ from 23-50 m)

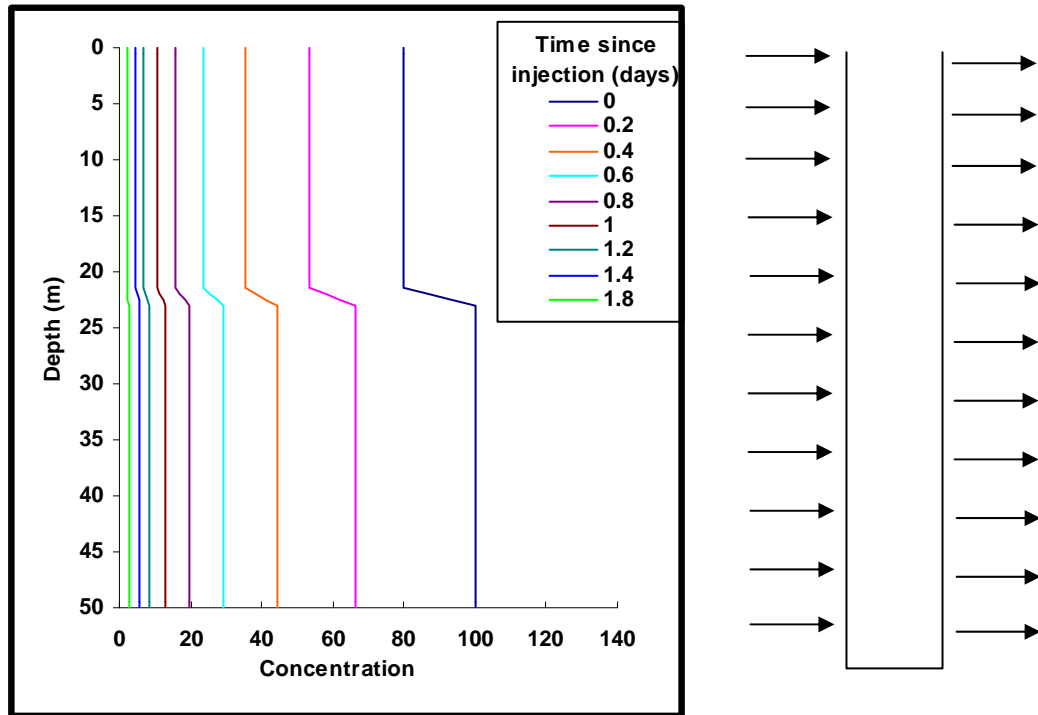


Figure 6.21: Simulation of decreased C_0 in upper section of borehole with Q_{IN} and Q_{OUT} set to $0.1 \text{ m}^3 \cdot \text{d}^{-1}$ in every segment (C_0 was set at 80 in segments from 0-23 m, and 100 for all other segments).

In Section 6.4.3 it was suggested that a reduction (or increase) in dilution rate with depth could be caused by variability in the rate of crossflow (Figure 6.11a). Figure 6.22 shows the results of a simulation in which the rate of crossflow is progressively decreased with depth. The borehole is divided into 5 sections in which all segments are assigned the same values of Q_{IN} and Q_{OUT} . This leads to a stepped profile with sharp boundaries between each section (effectively a multiple case of Figure 6.20). A variant is shown in Figure 6.23. In this case every segment was assigned progressively smaller Q_{IN} and Q_{OUT} values. This leads to more graded profiles that have some similarity to graded profiles in the field data (e.g. High Street Farm and Frilsham A below 50 m AOD, Figure 6.10). Figure 6.24 shows profiles generated with the same settings as Figure 6.23 but with flow rate increasing with depth. These also have some similarities with field data (e.g. Knighton Down and Barracks, Figure 6.10). It is unlikely that real fracturing in the field would produce such a regular variability in flow rates with depth. However, there are also significant differences between the simulations and the field data that strongly suggest that vertical flow is required to account for the patterns observed in the field data. The field data profiles have a sinusoidal shape resulting from

movement of a tracer “front” up or down the borehole that is not apparent in the simulations (the “front” is in fact a boundary between the top/bottom of the tracer plume and the advancing fresh aquifer water above/below). In the simulations, there is a constant rate of change in concentration at any particular horizon. Contrastingly, in the field data there are changes in the rate of concentration change at individual horizons. For example in Frilsham A at 37 m AOD (Figure 6.10) the concentration does not change during the first 4 profiles, and thereafter it changes extremely rapidly. In the following section the patterns seen in the field data are investigated using simulations that incorporate vertical flow, and the effects of the different types of flow patterns shown in Figure 6.16 are considered.

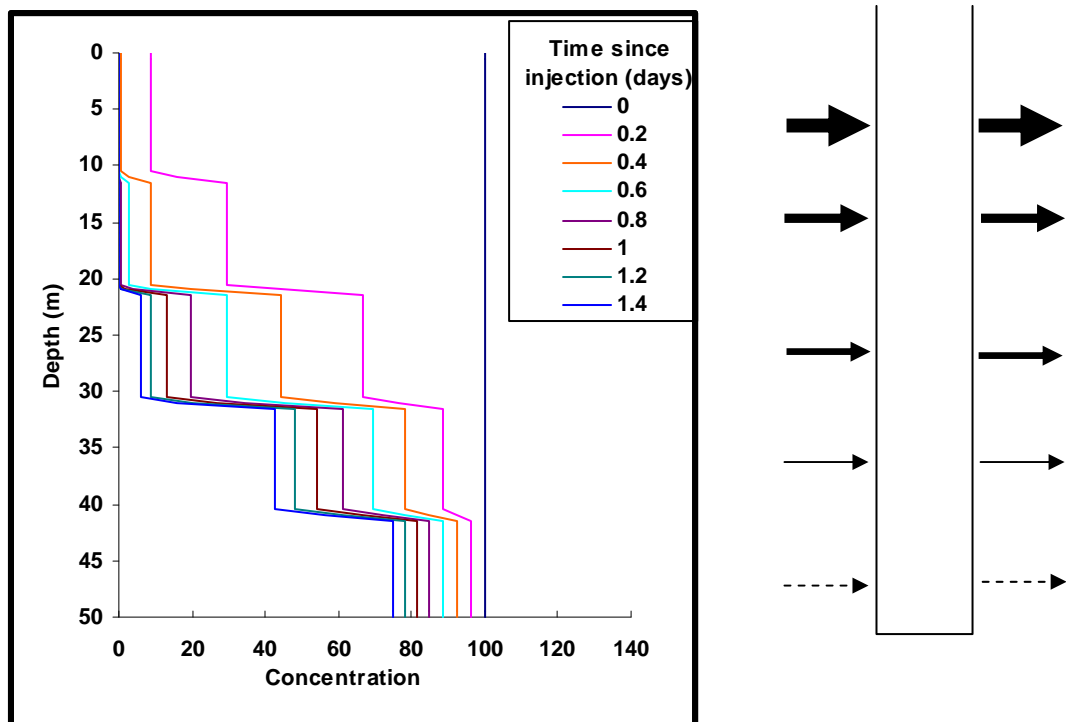


Figure 6.22: Simulation of decreasing flow rate with depth in 5 borehole sections (Q_{IN} and Q_{OUT} set in segments within sections to 0.6, 0.3, 0.1, 0.03 and 0.01 $m^3 \cdot d^{-1}$, simulation ends after 1.4 days).

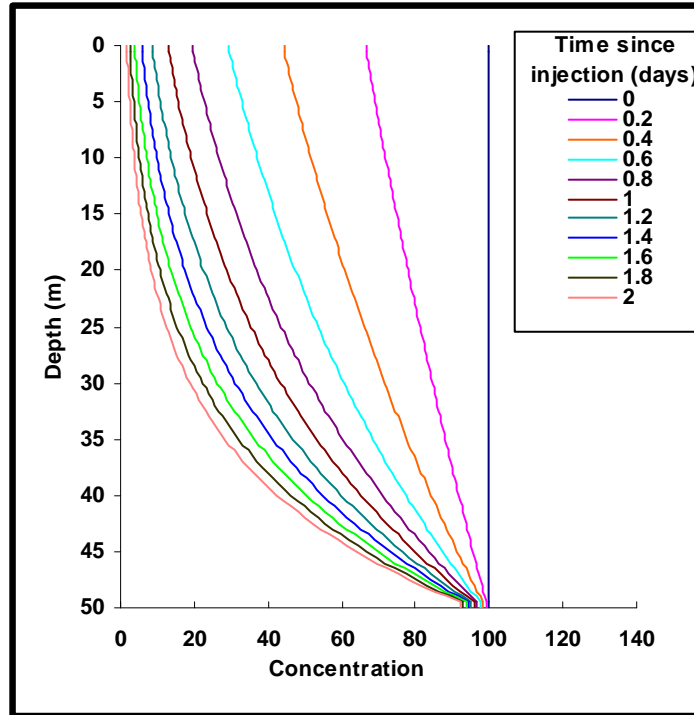


Figure 6.23: Alternative simulation of decreasing flowrate with depth. (Q_{IN} and Q_{OUT} set to decrease by $0.002 \text{ m}^3 \cdot \text{d}^{-1}$ between each segment from $0.1 \text{ m}^3 \cdot \text{d}^{-1}$ for 0-1 m to $0.002 \text{ m}^3 \cdot \text{d}^{-1}$ for 49-50 m, simulation ends after 2 days)

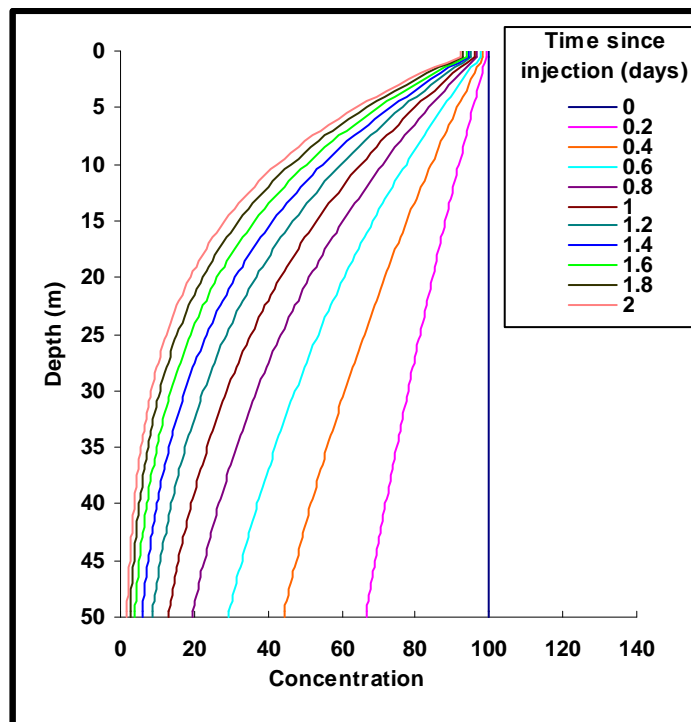


Figure 6.24: Simulation of increasing flowrate with depth (settings as for Figure 6.23 except with increased flow rate with depth).

6.5.2.3 Simulations tracer profiles when vertical flow is occurring

All the simulations presented here are for upwards vertical flow. The patterns in the profiles are the same when downward vertical flow is simulated (although clearly tracer fronts move down the borehole instead of up). The simplest occurrence of vertical flow is the case of a single inlet and a single outlet. In Figure 6.25, as the tracer exits from fracture B it will be replaced by water from below. There is no decrease in tracer concentration at point C in the borehole until the new tracer free water that entered the borehole through Fracture A reaches point C (righthand side of Figure 6.25). The simulated profiles are similar to the field data, (e.g. throughout Barracks and in Trumpletts A from the bottom of the borehole to about 56 m AOD, Figure 6.10), with the same sinusoidal shape and tracer front moving up the borehole. Figure 6.26 shows the simulation results using identical parameters as Figure 6.25 but increasing the dispersivity from 0.1 m to 3 m. This has the effect of spreading the tracer “front” over a greater length of borehole. Similar patterns are seen in many of the SBDT results (e.g. throughout Knighton Down and in Bagnor between about 60 and 70 m AOD).

When vertical flow is occurring, a boundary is created at the exit point or entry point if tracer dilution is much slower or faster in the adjacent borehole section. For example, in Figures 6.25 and 6.26, below 47 m Q_{IN} and Q_{OUT} were set to 0 (representing an impermeable section at the bottom of the borehole) and the fracture inflow point is marked by a boundary. An example of this in the field data is the boundary at 45 m AOD in the Barracks (Figure 6.10). Figure 6.27 shows a simulation of a boundary at the exit point (20 m depth) when upward vertical flow is occurring and there is diffuse crossflow in the section above 20 m.

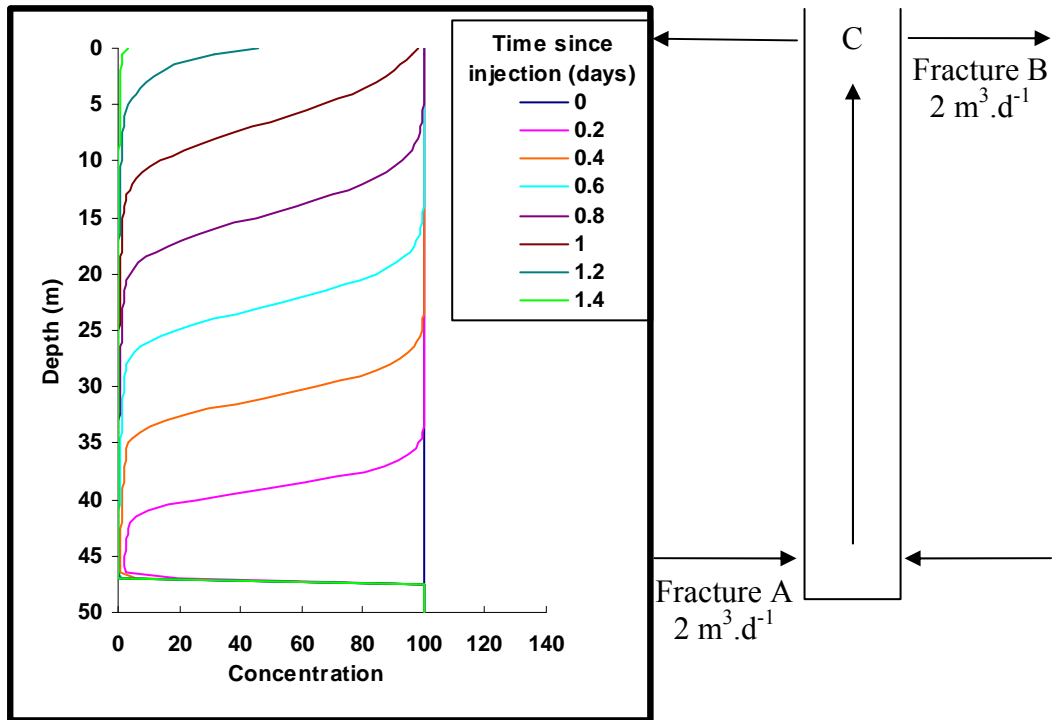


Figure 6.25: Simulation of upward vertical flow with inflow at 46-47 m and outflow at 0-1m

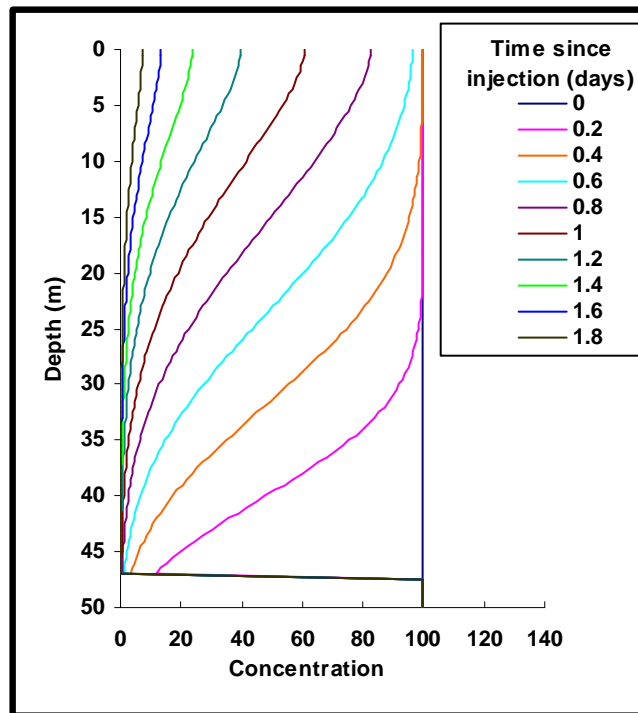


Figure 6.26: Simulation of upward vertical flow with dispersivity increased from 0.1 m to 3m (other settings are identical to those for Figure 6.25)

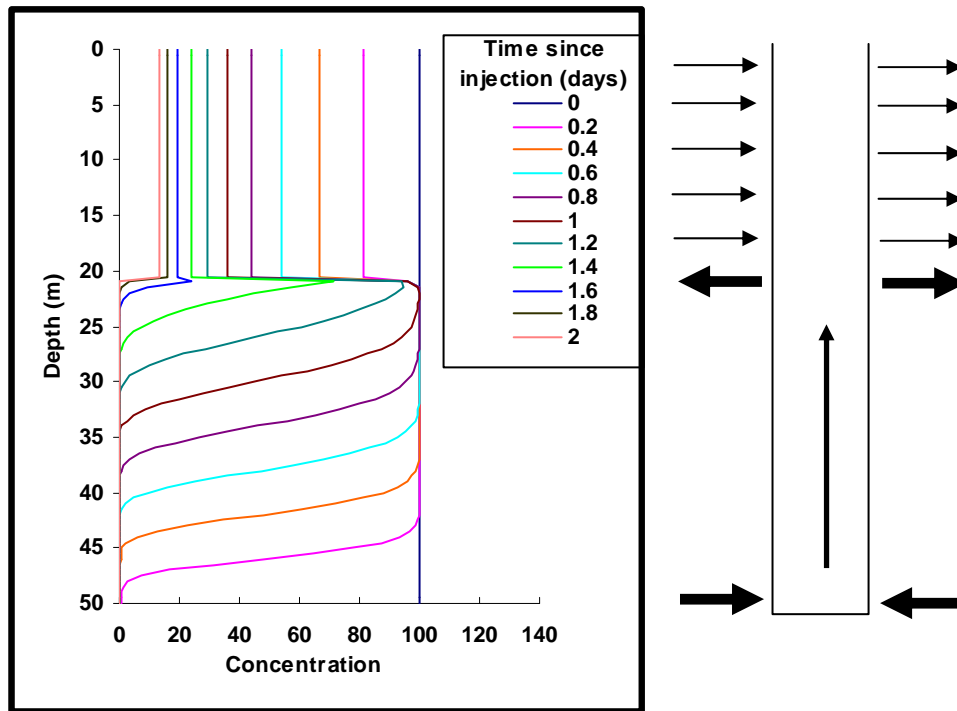


Figure 6.27: Simulation of upward vertical flow between the bottom and 20 m (Q_{IN} and $Q_{OUT} = 1 \text{ m}^3 \cdot \text{d}^{-1}$) with crossflow ($0.05 \text{ m}^3 \cdot \text{d}^{-1}$) in all segments above 20 m

In cases of vertical flow with multiple outlets (Figure 6.28), the rate of vertical flow is slowed as the tracer plume passes the first outlet, but (as in the case of a single outlet) there is no decrease in the tracer concentration until the tracer free water entering through the inflow fracture has reached the second outflow point (fracture C in Figure 6.28). In this simulation the outflows in fractures B and C were set as equal and therefore the rate of vertical flow halved as the plume passed Fracture B. This demonstrates that a decrease in vertical flow rates indicates the presence of an outflowing fracture.

When vertical flow is occurring, if there is crossflow at the outflow point then there is an immediate reduction in tracer at the outflow point (Figure 6.29). However, the concentration then remains at this reduced level as it is replaced by tracer-laden water from below, until the tracer front reaches the outflow point.

Figure 6.30 shows the results of a simulation with crossflow in the middle of a section of vertical flow. The crossflow horizon reduces the tracer concentration, creating a

“sub-front” that moves up the borehole reducing concentrations from 100 to 72, but concentrations do not reduce further until the main tracer front passes the crossflow horizon. As the main tracer front passes the crossflow horizon, a nick point (0.8 days after injection) and a small step (1 day after injection) are visible in the profiles. The vertical flow rate is unaffected by the crossflow horizon. A similar pattern is produced in a simple case of vertical flow in which the inflow is divided between two horizons (Figure 6.31). The difference is that the vertical flow rate increases above the second flow horizon (19-20 m), which does not occur in the case illustrated in Figure 6.30. There is also a more pronounced nick point as the main tracer front passes 19-20 m (1.4 and 1.6 days after injection). The nick point remains pronounced even if Q_{IN} at 19-20 m is reduced from 1 to $0.5 \text{ m}^3 \cdot \text{d}^{-1}$ (not illustrated here). Figure 6.32 shows that similar profiles are also generated in the case of vertical flow with crossflow in which $Q_{IN} > Q_{OUT}$ (case 2 in Figure 6.16). If $Q_{OUT} > Q_{IN}$ (case 4 in Figure 6.16), the same pattern is generated except that the vertical flow rate is reduced above the crossflow horizon (Figure 6.33).

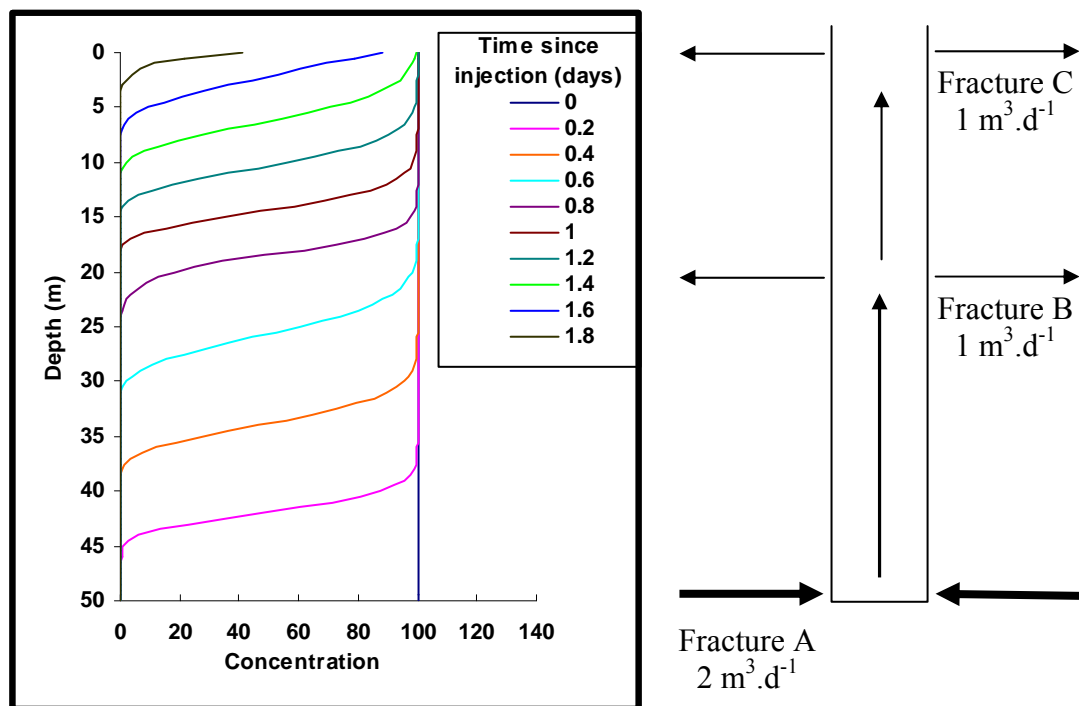


Figure 6.28: Simulation of upward vertical flow from an inflow at 49-50 m (Fracture A) with outflows divided equally between two fractures (B and C) at 19-20 and 0-1 m (Fracture B represents case 5 in Figure 6.16)

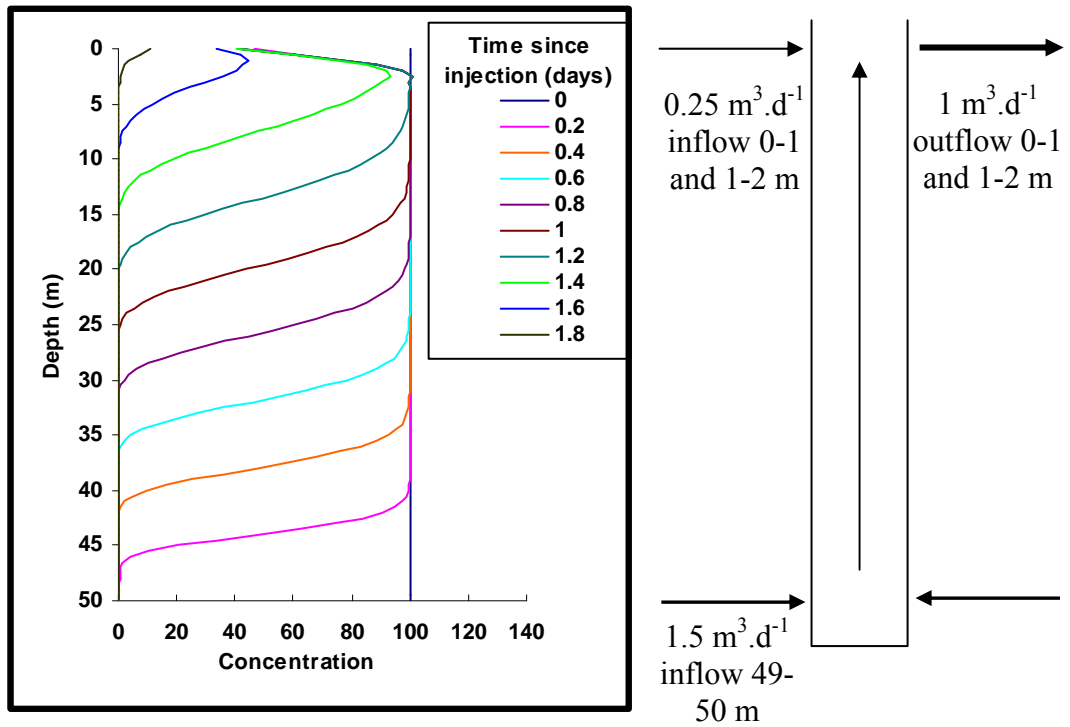


Figure 6.29: Simulation of upward vertical flow with crossflow at the outflow point

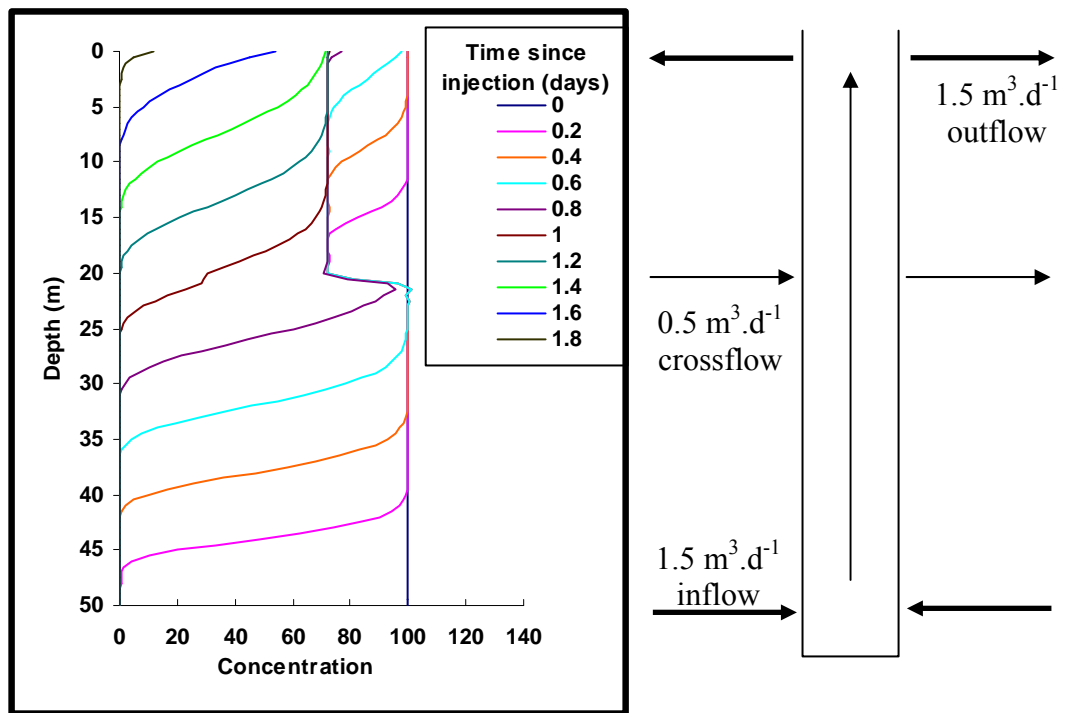


Figure 6.30: Simulation of upward vertical flow with crossflow at 20-21 m (case 3 in Figure 6.16)

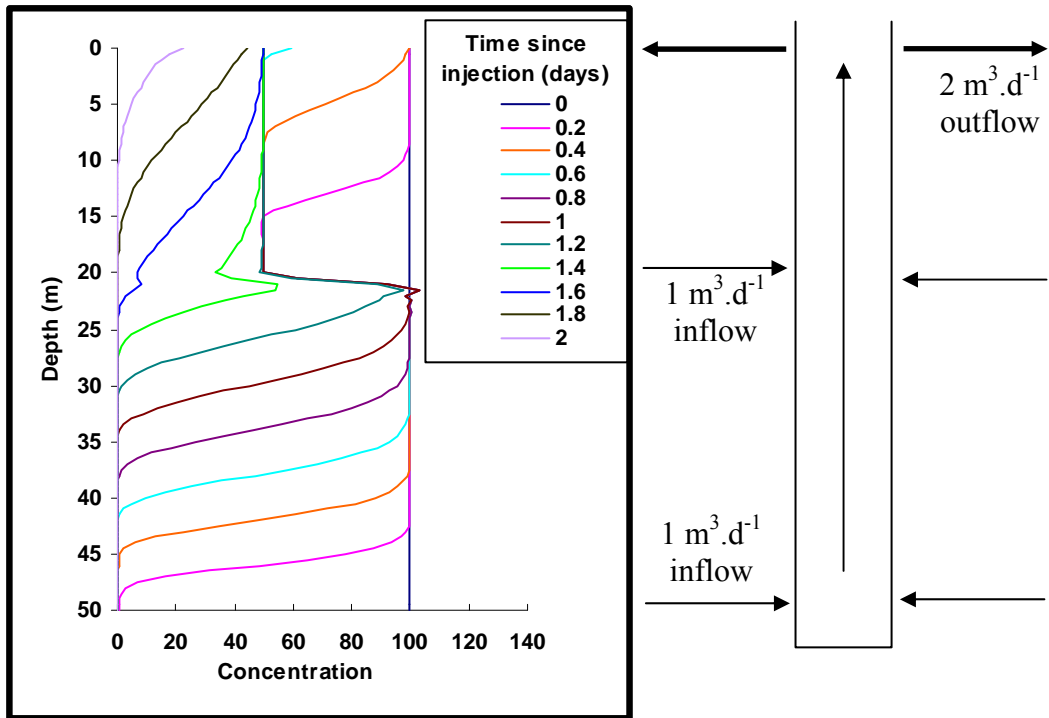


Figure 6.31: Simulation of upward vertical flow with inflow divided equally between two fractures at 49-50 and 19-20 m, and outflow at 0-1m (flow horizon at 19-20m represents case 1 of Figure 6.16)

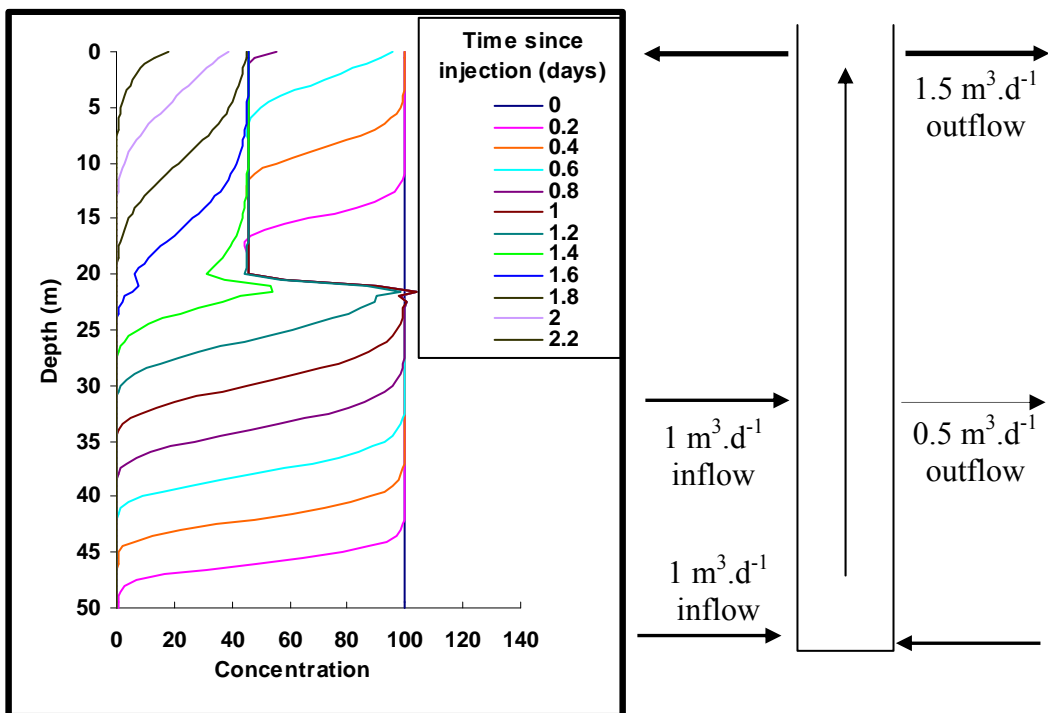


Figure 6.32: Simulation of upward vertical flow from 49-50 m to 0-1 m with crossflow at 19-20 m in which inflow exceeds outflow (case 2 from Figure 6.16)

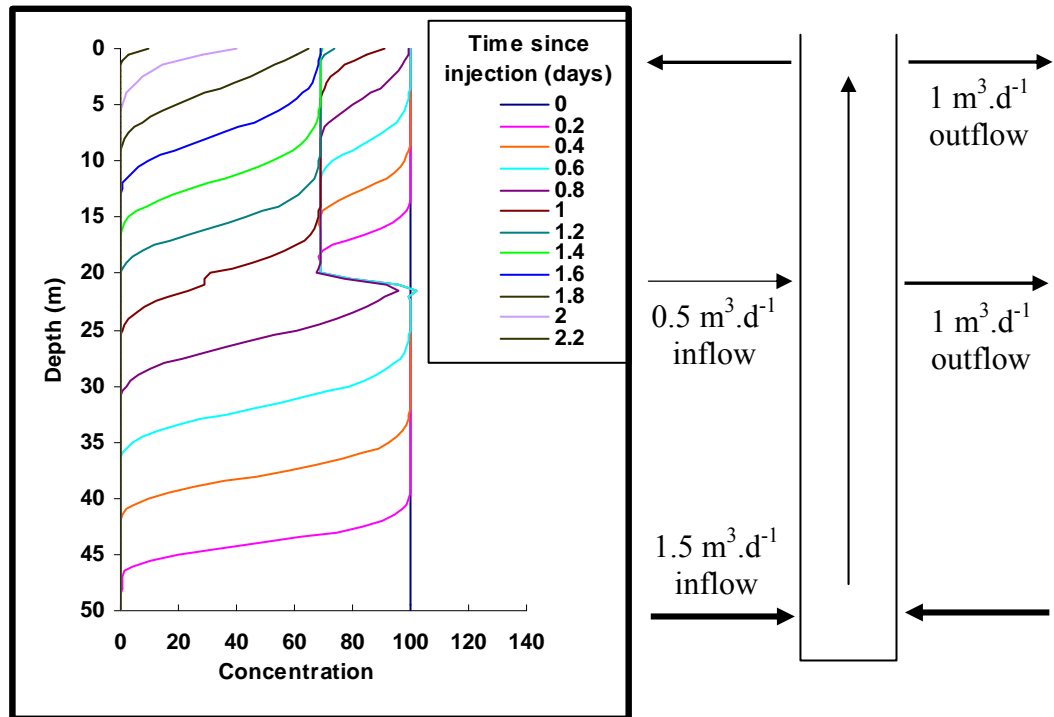


Figure 6.33: Simulation of upward vertical flow from 49-50 m to 0-1 m with crossflow at 19-20 m in which outflow exceeds inflow (case 4 from Figure 6.16)

6.5.2.4 Summary of borehole simulations

The Barker spreadsheet model has been used to simulate some of the patterns that are observed in borehole sections during SBDTs. The field data are more complex because more than one of these different patterns often occurs within one borehole. The simulations assume that all readings within a profile were taken at the same time, and do not take into account the time that is taken in the field to lower the probe down the borehole. Despite these limitations, the simulations suggest that flowing fractures/fissures do cause distinctive features in dilution profiles, and that the experimental results can be used to identify likely flowing horizons at the following locations:

- horizons consistently characterised by lower tracer concentrations than in the area above and below (nick points).
- at the top and bottom of sections where the dilution pattern suggests vertical flow is occurring (which is often marked by a sharp boundary in the tracer dilution profiles).
- within sections of vertical flow if the vertical flow rate changes.

The simulations demonstrate that variations in borehole diameter can affect the patterns, but that effects of increased dilution of the injected tracer in wider sections of borehole become less obvious with time since injection because the % contrast between wider and narrower sections remains constant. In contrast decreases in tracer concentration associated with flowing features are more pronounced even at late stages in the test.

Doughty and Tsang (2005) present results of a similar study that simulates patterns in electrical conductance profiles after borehole water is replaced with deionised water under pumped conditions. They investigate different combinations of inflows and outflows, and variations in flow rates, and they also consider the effect of variations in the electrical conductance of the aquifer water that is entering the borehole. They conclude that inflow points produce distinctive features in the electrical conductance profile but suggest that outflows are harder to identify, a conclusion that seems to be supported in the present study. Outflows (case 5 in Figure 6.16) cause a reduction in vertical flow rate, but there is no decrease in tracer concentration, whereas inflows and crossflow produce distinctive drops in tracer concentration.

The simulations strongly suggest that vertical flow occurred during most of the boreholes tests, because the electrical conductance logs have a sinusoidal shape and tracer “front” which cannot be simulated without vertical flow. This was tested in the field using point injection SBDTs (see below).

6.5.3 Point injection tests

6.5.3.1 Introduction

The results of the uniform injection SBDTs suggested that vertical flow may be occurring at many sites, and forward modelling confirmed that many of the patterns in electrical conductance logs obtained during the uniform injection SBDTs are best accounted for by vertical flow. Point injection SBDTs were undertaken to demonstrate this more conclusively. Loss of tracer mass between tracer profiles was calculated (by summing tracer concentrations) to determine whether dilution was occurring within sections of vertical flow. Vertical flow rates were also calculated based upon the migration rate of the peak tracer concentration with the objective of identifying outflowing horizons where vertical flow rates decreased. The results of point injections

are presented in Section 6.5.3.2. In Section 6.5.3.3 the technique is tested by comparing the calculated vertical flow rates with measurements obtained using a heat pulse flowmeter. Section 6.5.3.4 discusses how point injection SBDTs can be used to identify flow horizons and Section 6.5.3.5 summarises the implications of the point injections for interpreting uniform injection SBDTs.

6.5.3.2 Point injection results

The results of 22 point dilution experiments in 10 different boreholes are presented in Figures 6.34 to 6.44 in alphabetical order by borehole name. There are 4 types of results:

- 1) Graphs of the electrical conductance logs obtained during the uniform injection SBDT for comparison with the point injection data. (If more than one uniform injection was undertaken, the results from the time nearest to the point dilution tests are shown).
- 2) Graphs of the electrical conductance logs obtained during the point injections.
- 3) Plots showing summed tracer concentrations against time (blue line) with the elevation of the peak tracer concentration plotted against time on a second axis (red line).
- 4) A table showing the vertical flow rates based on the change in elevation of the peak tracer concentration between electrical conductance logs.

(3) and (4) are not presented for point injection tests in which the injection was very close to the outflowing end of the vertical flow section.

In most experiments vertical flow was conclusively demonstrated because a plume of tracer focused at or near the injection depth in the first electrical conductance log after injection moves up or down the borehole in subsequent logs. The results are summarised in Table 6.9, which shows that upward flow was demonstrated in 6 borehole sections and downward flow in 7 sections. The injection at 98.17 m AOD in Gibbett Cottages demonstrated horizontal flow suggesting the injection was at a crossflow horizon (Figure 6.40d). At two sites, both upward and downward vertical flow occurred in different sections of the borehole. At Bagnor there is both upward and downward flow *from an inflowing* horizon at 59.5 m AOD (Figures 6.34 b,d,e) and at

Frilsham B there is both upward and downward flow *to outflowing* horizons at 44.1 and 46.5 m AOD (Figures 6.38b,e,h).

The results of each individual test are not discussed in detail because of the large amount of data. In Sections 6.5.3.3 to 6.5.3.5, examples from the results are used for illustrative purposes.

Table 6.9: Summary of flow directions indicated by point injection SBDTs

Borehole	Section (m AOD)	Flow direction	No. point dilution tests
Bagnor	59.5 to 70	Up	1
Bagnor	59.5 to 56.5	Down	2
Barracks	45 to ~115?	Up	1
Bockhampton	74 to ~110?	Up	3
Frilsham A	53 to 35.5	Down	1
Frilsham B	38.3 to 44.1/46.5	Up	1
Frilsham B	55? to 46.5/44.1?	Down	2
Frilsham C	53.7 to 20.3	Down	3
Gibbet Cottages	94 to 99	Horizontal	1
Gibbet Cottages	95.5 to 87.5	Down	1
Grumble Bottom	50.5? to 30.5	Down	1
Trumpletts A	10.24 to 56.5	Up	1
Trumpletts A	56.5 to 74.7	Up	2
Winterbourne Farm	79 to 70	Down	2

Figures 6.34a-e: Bagnor point injection SBDTs

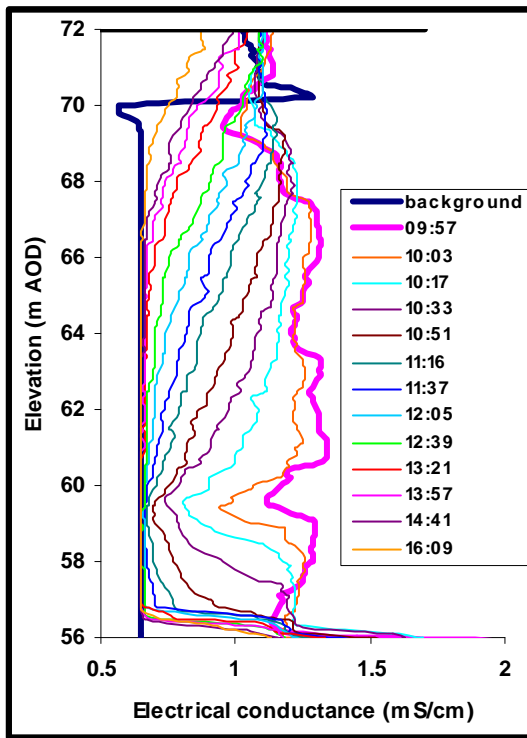


Figure 6.34a: Uniform injection at Bagnor on 19/08/05. The borehole is cased above 72 m AOD as indicated by the black horizontal line

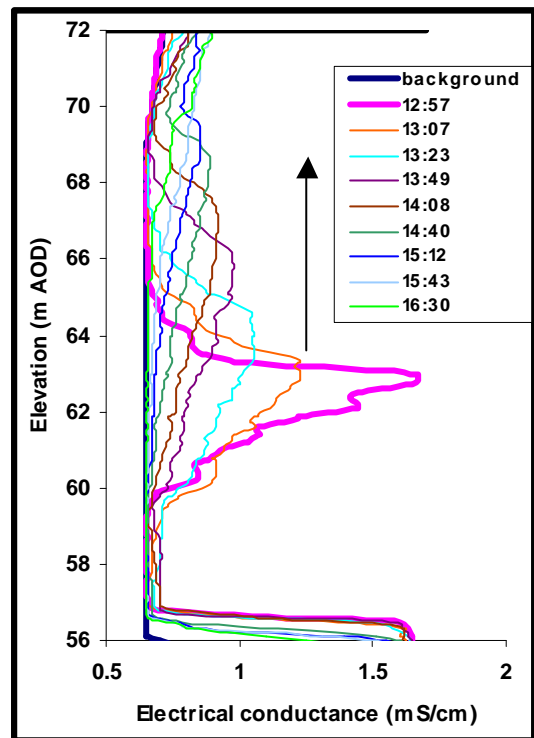


Figure 6.34b: Point injection at 63 m AOD at Bagnor on 20/08/05 indicating upward flow

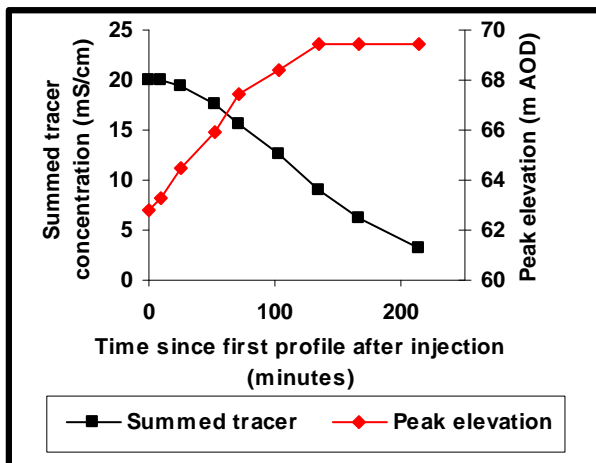


Figure 6.34c: Plot showing upward migration of the peak and decrease in summed tracer concentration following the point injection at 63 m AOD at Bagnor

Table 6.10: Upward vertical flow rates at Bagnor as plume from injection at 63 m AOD moves up the borehole. Note decrease in flow rate after log 5

	flow rate (m/day)
log 1-2	103
log 2-3	157
log 3-4	119
log 4-5	154
log 5-6	65
log 6-7	63

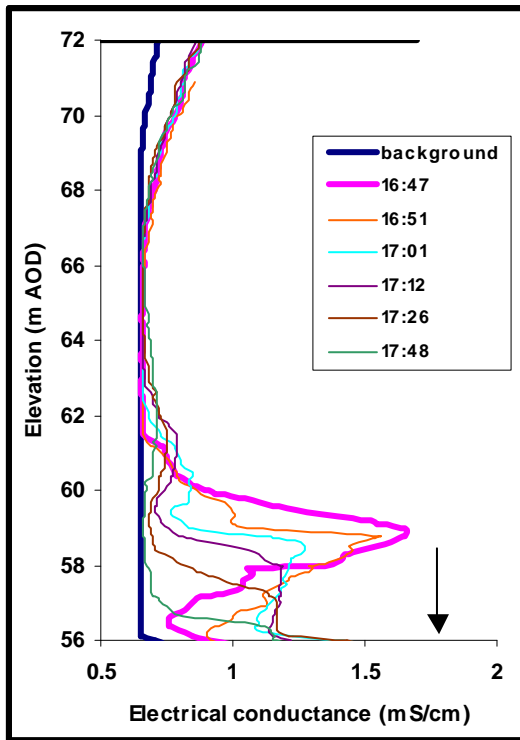


Figure 6.34d: Point injection at 59 m AOD on 20/08/05 at Bagnor demonstrates downward flow

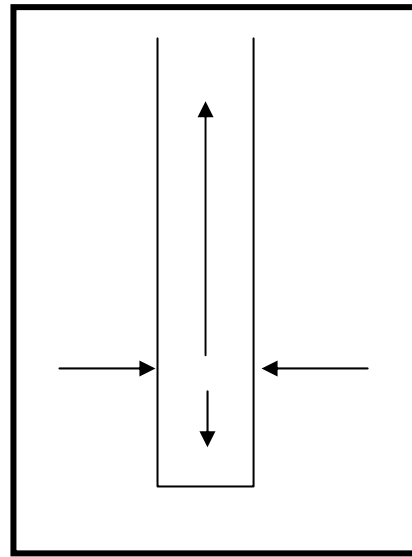


Figure 6.34e: Schematic representation of splitting of flow from an inflowing horizon at about 60 m AOD at Bagnor

Figure 6.35a-c: Barracks point injection SBDT

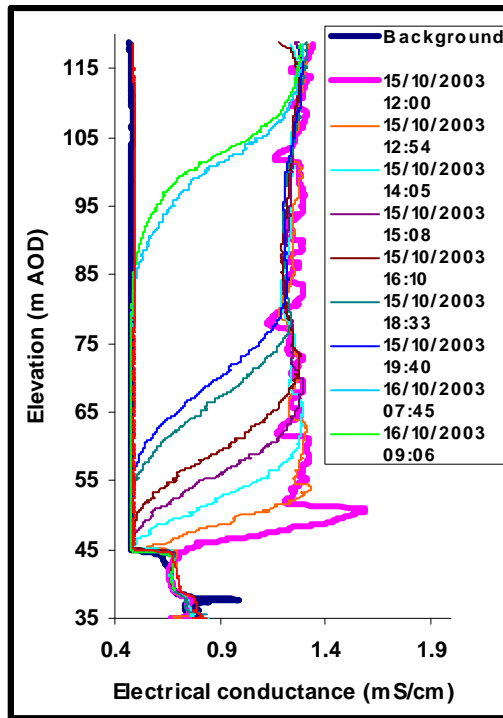


Figure 6.35a: Uniform injection at Barracks on 15/10/03

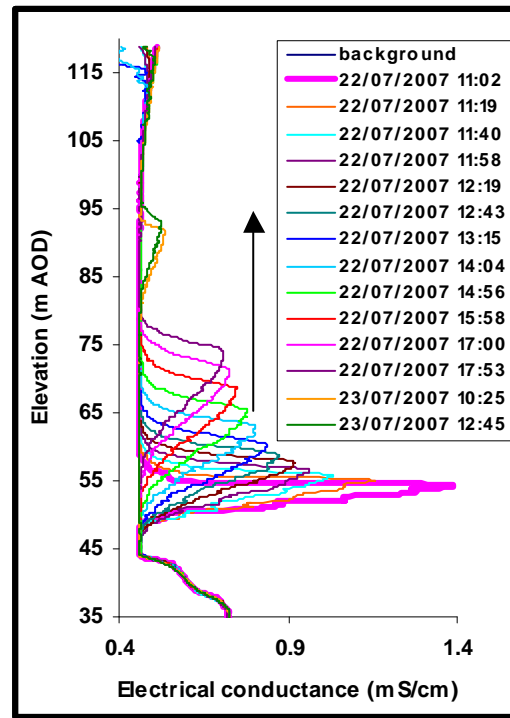


Figure 6.35b: Point injection at 54 m AOD at Barracks on 22/10/07 indicating upward vertical flow

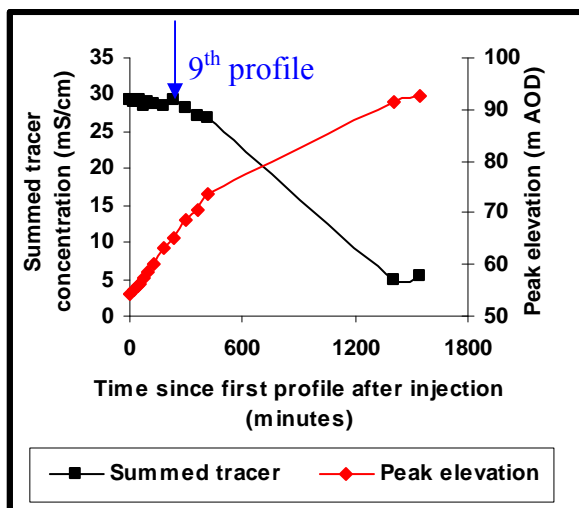


Figure 6.35c: Plot showing upward migration of the peak and decrease in summed tracer concentration following the point injection at 54 m AOD at Barracks.

Table 6.11: Upward vertical flow rates at Barracks as plume from injection at 54m AOD moves up the borehole. Note decrease in flow rate after log 13 (average drops from 66 to 19 m/day)

	flow rate (m/day)
log 1-2	64
log 2-3	48
log 3-4	48
log 4-5	82
log 5-6	72
log 6-7	68
log 7-8	82
log 8-9	58
log 9-10	81
log 11-12	45
log 12-13	80
log 13-14	26
log 14-15	11

Figure 6.36a-h: Bockhampton point injection SBDTs

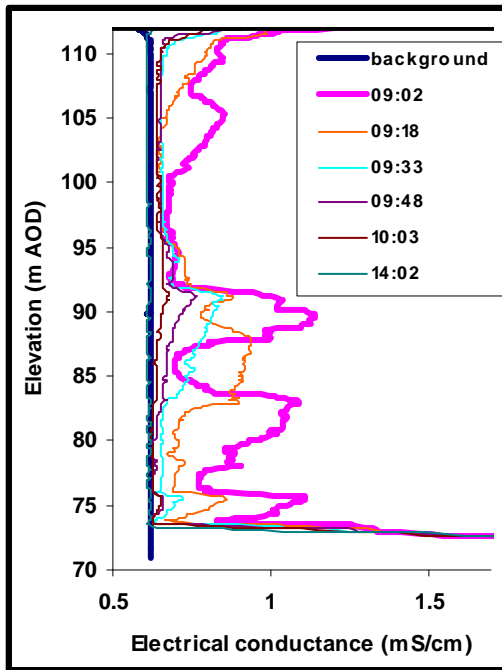


Figure 6.36a: Uniform injection at Bockhampton on 01/09/05. The borehole is cased above 112 m AOD as indicated by black horizontal line

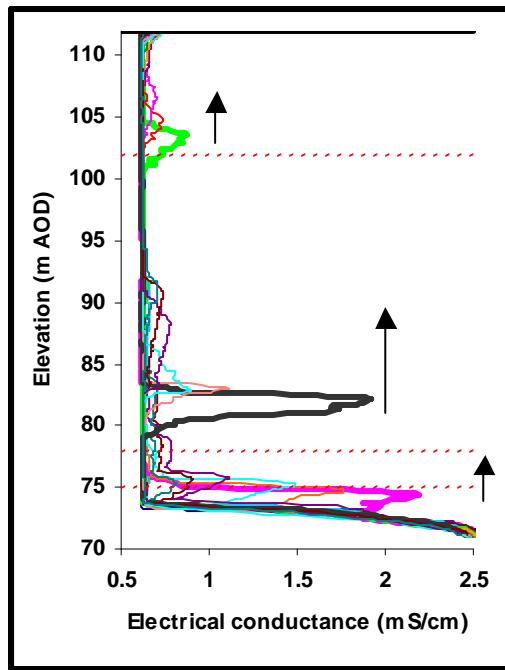


Figure 6.36b: Three point injections (elevations indicated by red dotted lines) at Bockhampton on 01/09/05 indicated upward vertical flow combined with dilution indicating crossflowing horizons

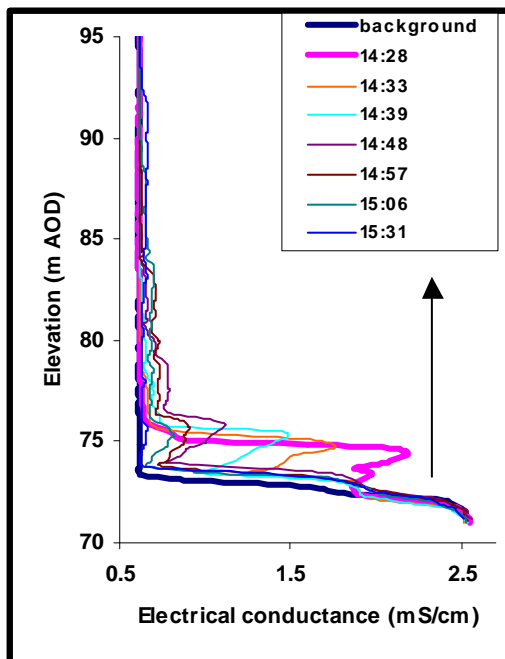


Figure 6.36c: point injection at 74.8 m AOD indicating upward flow and dilution at 76.3 m AOD

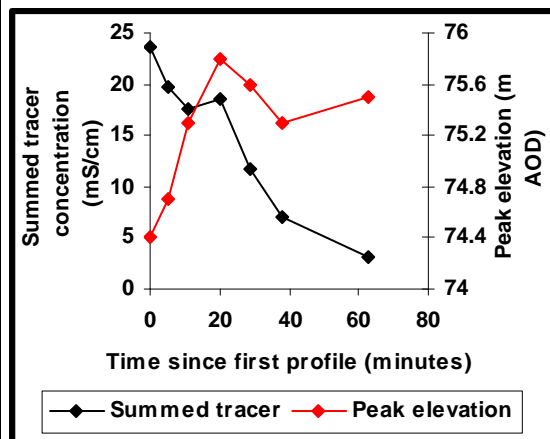


Figure 6.36d: Plot showing upward migration of the peak to about 75.2 m AOD and decrease in summed tracer concentration following the point injection at 74.8m AOD at Bockhampton

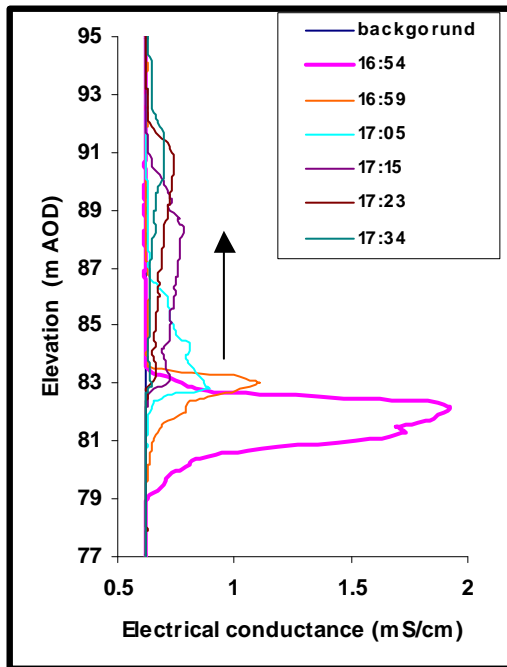


Figure 6.36e: Point injection at 77.9 m AOD indicating upward flow and dilution at 84 m AOD

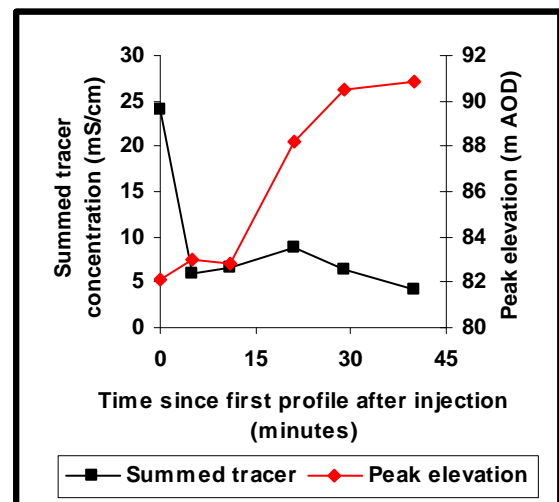


Figure 6.36f: Plot showing upward migration of the peak to about 91 m AOD and decrease in summed tracer concentration following the point injection at 77.9 m AOD at Bockhampton. Note decrease in summed tracer concentration and slowing of upward migration of peak as plume passes flow horizon at 84 m AOD

Table 6.12: Upward vertical flow rates at Bockhampton following point injection at 77.9 m AOD. Note temporary decrease in flow rate between logs 2 and 3 as tracer plume passes flow horizon at 84 m AOD

	flow rate (m/day)
log 1-2	259
log 2-3	0
log 3-4	792
log 4-5	403
log 5-6	43

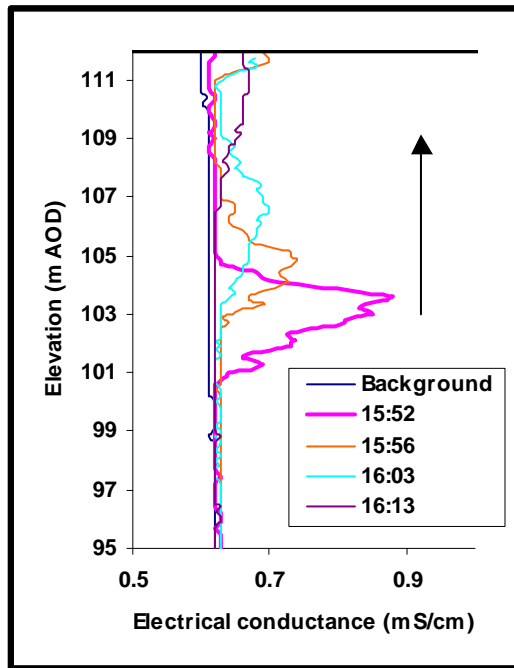


Figure 6.36g: Point injection at 101.9 m AOD indicating upward flow and dilution

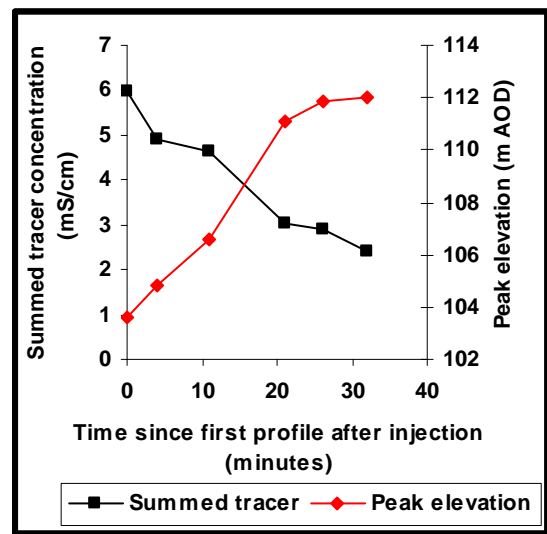


Figure 6.36h: Plot showing upward migration of the peak to about 112 m AOD and decrease in summed tracer concentration following the point injection at 101.9 m AOD at Bockhampton.

Table 6.13: Upward vertical flow rates at Bockhampton following point injection at 101.9 m AOD.

	flow rate (m/day)
log 1-2	432
log 2-3	374
log 3-4	648

Figure 6.37 a-c: Frilsham A point injection SBDT

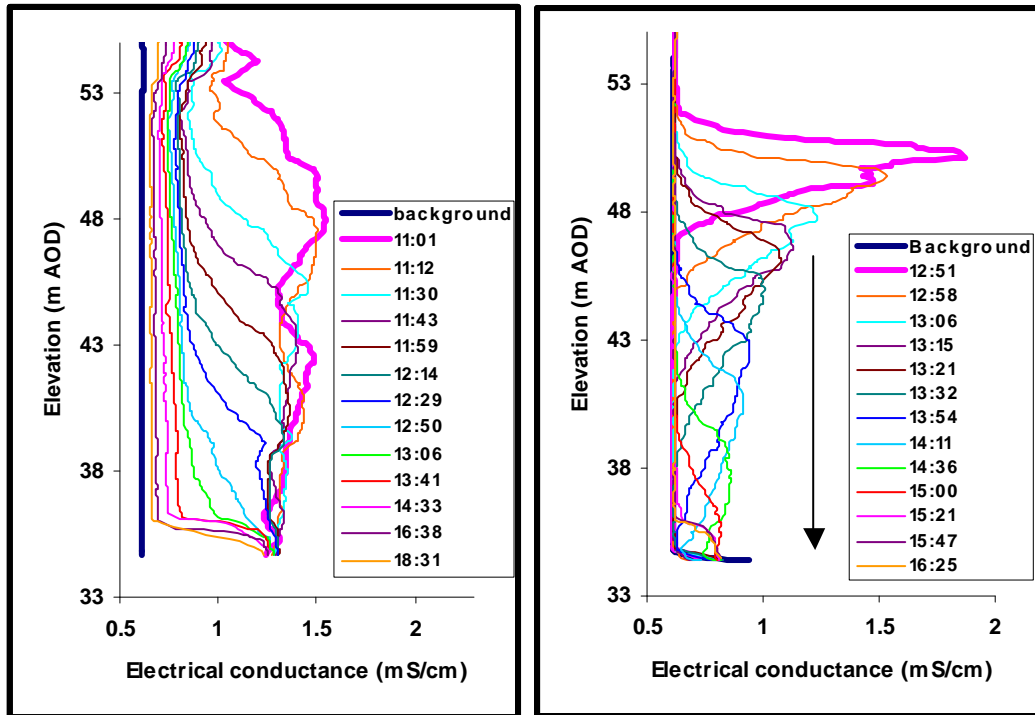


Figure 6.37a: Uniform injection at Frilsham A on 28/07/05.

Figure 6.37b: Point injection at 51.5 m AOD at Frilsham A on 08/08/05 indicating downward flow

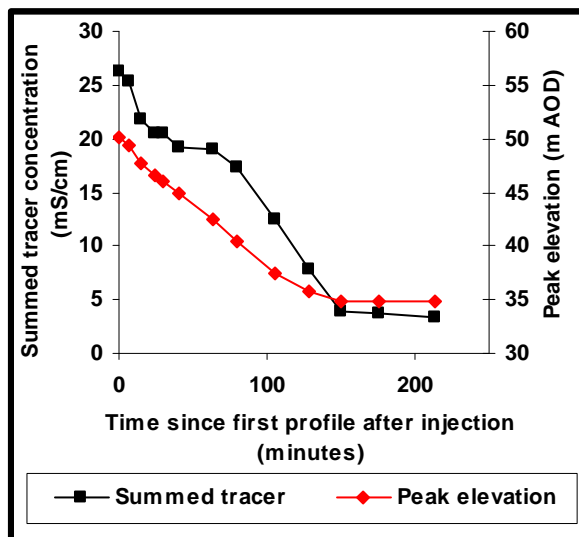


Figure 6.37c: Plot showing downward migration of the peak to about 35 m AOD and decrease in summed tracer concentration following the point injection at 51.5 m AOD at Frilsham A

Table 6.14: Downward vertical flow rates at Frilsham A following point injection at 51.5 m AOD

	flow rate (m/day)
log 1-2	144
log 2-3	297
log 3-4	184
log 4-5	120
log 5-6	144
log 6-7	160
log 7-8	174
log 8-9	99
log 9-10	69
log 11-12	3
log 12-13	-4

Figure 6.38a-g: Frilsham B point injection SBDTs

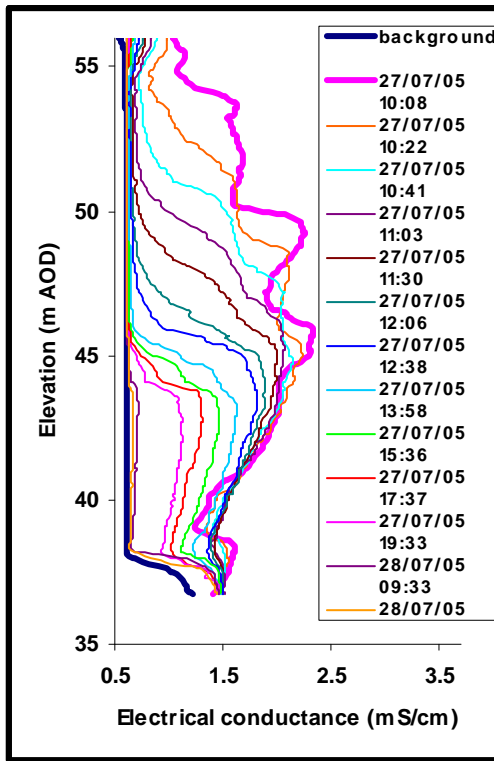


Figure 6.38a: Uniform injection at Frilsham B on 27/07/05.

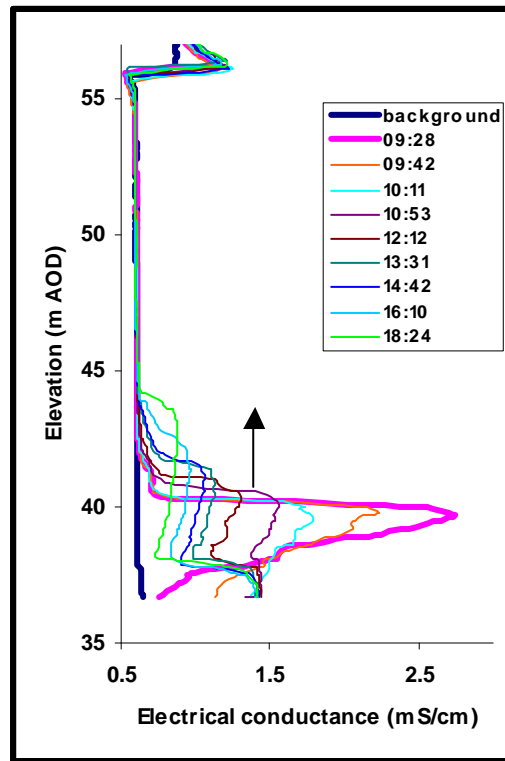


Figure 6.38b: Point injection at 40.1 m AOD at Frilsham B on 20/07/05 indicating upward flow passing a flow horizon at 41.5 m

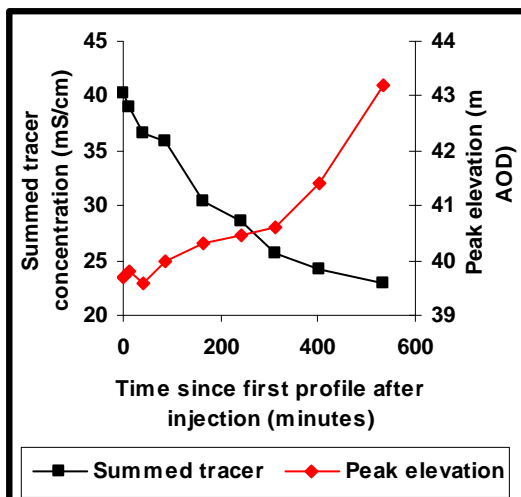


Figure 6.38c: Plot showing upward migration of the peak and decrease in summed tracer concentration following the point injection at 40.1 m AOD at Frilsham B

Table 6.15: Upward vertical flow rates at Frilsham B following point injection at 41.5 m AOD

	flow rate (m/day)
log 1-2	10
log 2-3	-10
log 3-4	14
log 4-5	6
log 5-6	3
log 6-7	3
log 7-8	13
log 8-9	19

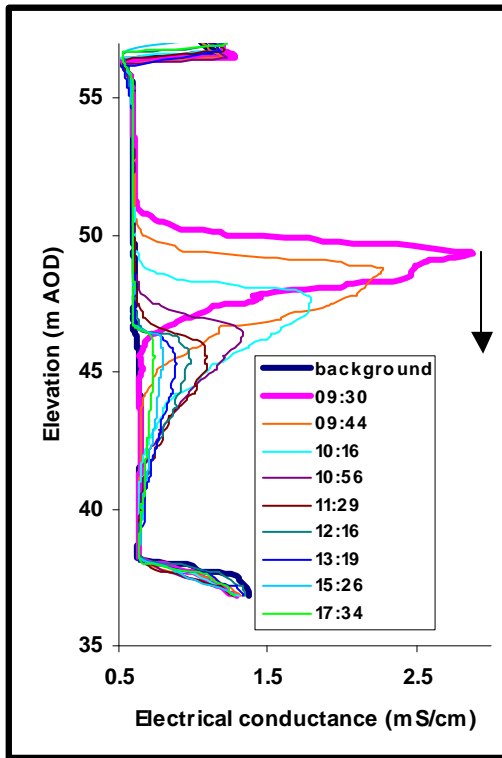


Figure 6.38d: Point injection at 50.2 m AOD at Frilsham B on 21/07/05 indicating downward flow passing a flow horizon at 46.5 m AOD

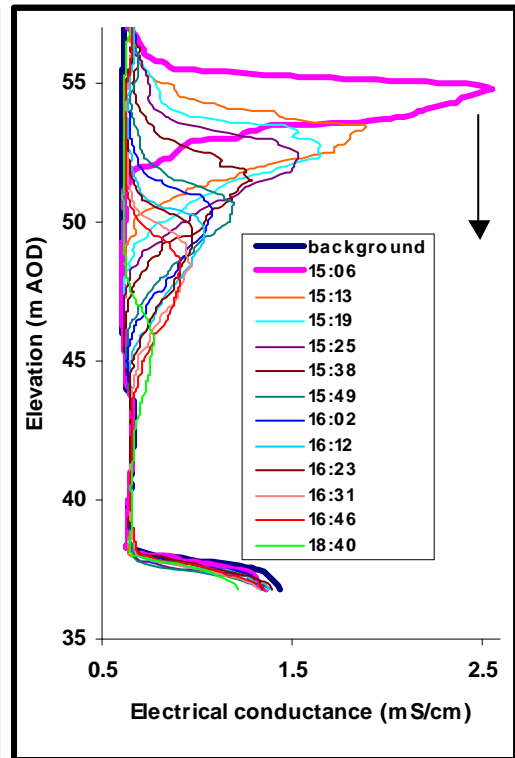


Figure 6.38e: Point injection at 55.2 m AOD at Frilsham B on 28/07/05 indicating downward flow passing a flow horizon at 46.5 m AOD

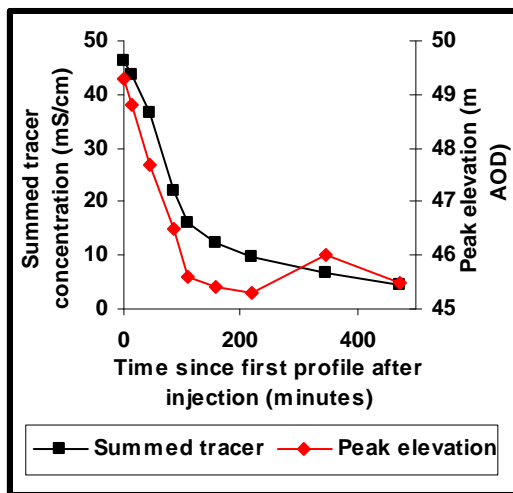


Figure 6.38f: Plot showing downward migration of the peak to about 46 m AOD and decrease in summed tracer concentration following the point injection at 50.2 m AOD at Frilsham B

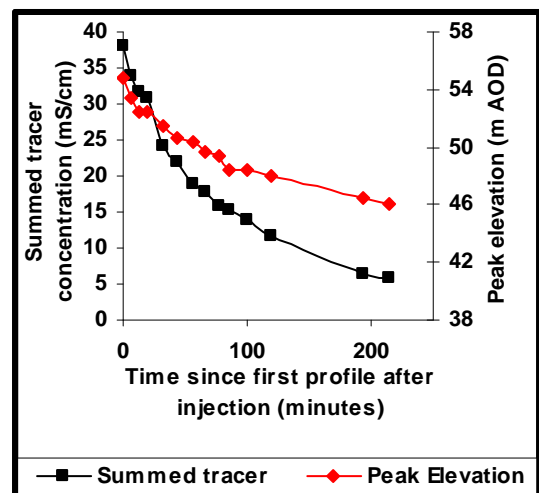


Figure 6.38g: Plot showing downward migration of the peak and decrease in summed tracer concentration following the point injection at 55.2 m AOD at Frilsham B

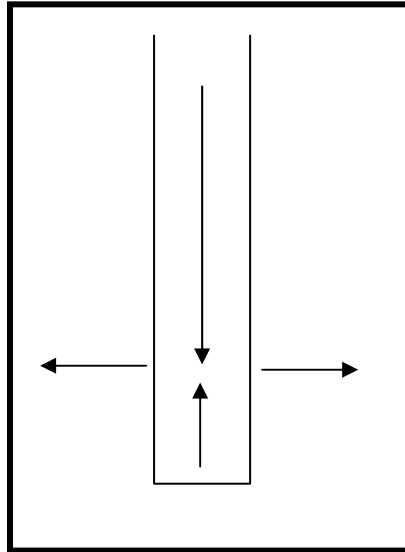


Figure 6.38h: Schematic representation of convergence of upward and downward flow at an outflowing horizon at Frilsham B

Table 6.16: Downward vertical flow rates at Frilsham B following point injection at 50.2 m AOD

	flow rate (m/day)
log 1-2	52
log 2-3	49
log 3-4	43
log 4-5	39
log 5-6	6
log 6-7	3
log 7-8	-9
log 8-9	6

Table 6.17: Downward vertical flow rates at Frilsham B following point injection at 55.2 m AOD

	flow rate (m/day)
log 1-2	288
log 2-3	240
log 3-4	0
log 4-5	99
log 5-6	105
log 6-7	39
log 7-8	108
log 8-9	20
log 9-10	45
log 11-12	-4
log 12-13	33
log 13-14	29

Figure 6.39a-f: Frilsham C point injection SBDTs

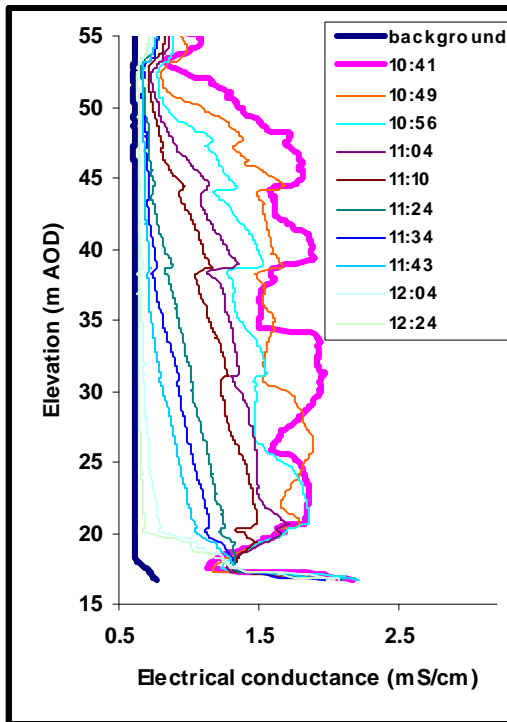


Figure 6.39a: Uniform injection at Frilsham C on 01/08/05

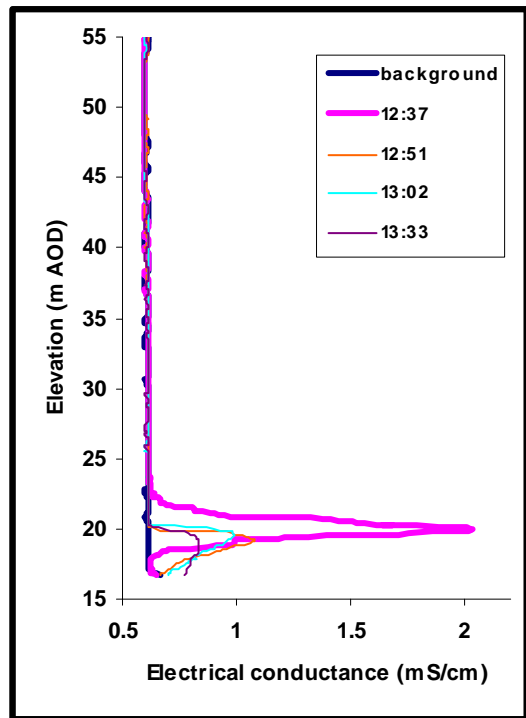


Figure 6.39b: Point injection at 24.3 m AOD at Frilsham C on 21/07/05 indicating dilution from a flow horizon at 20.2 m AOD

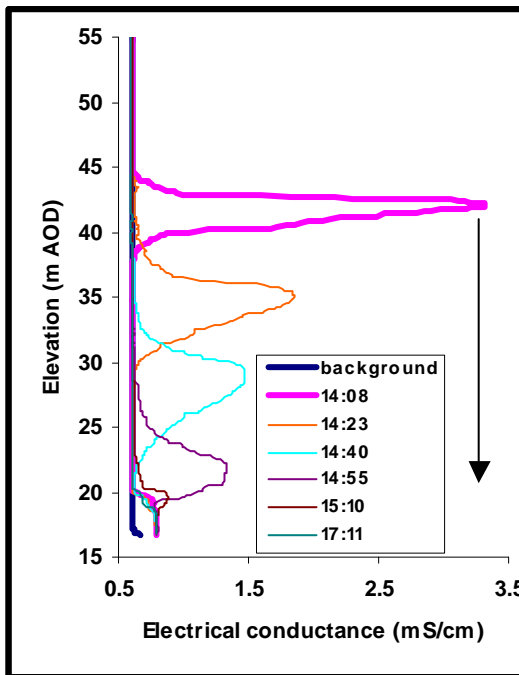


Figure 6.39c: Point injection at 39.3 m AOD at Frilsham C on 21/07/05 indicating downward flow

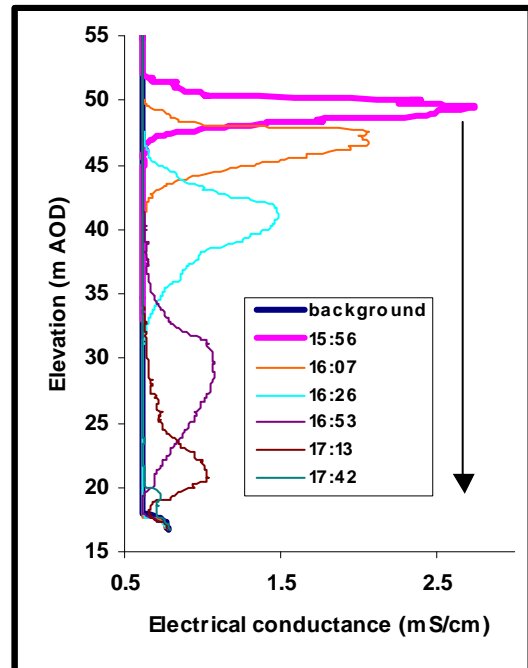


Figure 6.39d: Point injection at 51.3 m AOD at Frilsham C on 27/07/05 indicating downward flow

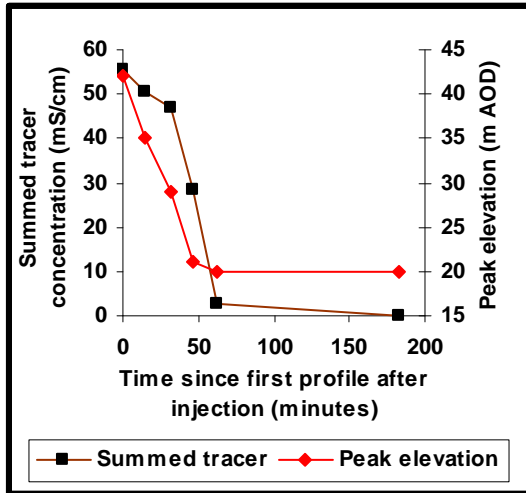


Figure 6.39e: Plot showing downward migration of the peak to about 20 m AOD and decrease in summed tracer concentration following the point injection at 39.3 m AOD at Frilsham C

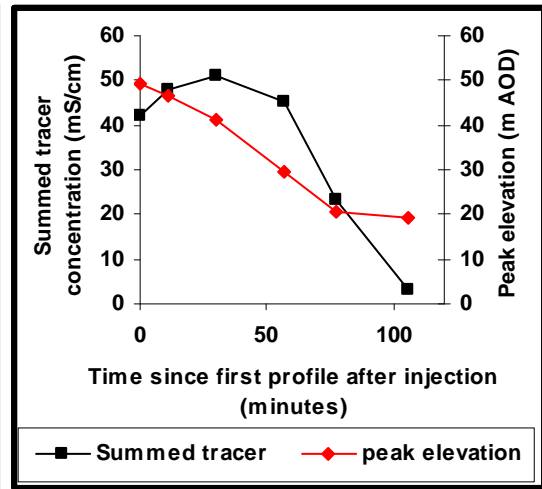


Figure 6.39f: Plot showing downward migration of the peak to about 20 m AOD and changes in summed tracer concentration following the point injection at 51.3 m AOD at Frilsham C. Note apparent increase in summed tracer during first three logs

Table 6.18: Downward vertical flow rates at Frilsham C following point injection at 39.3 m AOD

	flow rate (m/day)
log 1-2	681
log 2-3	508
log 3-4	768
log 4-5	96
log 5-6	0

Table 6.19: Downward vertical flow rates at Frilsham C following point injection at 51.3 m AOD

	flow rate (m/day)
log 1-2	353
log 2-3	416
log 3-4	616
log 4-5	645
log 5-6	72

Figure 6.40a-d: Gibbet Cottages point injection SBDTs

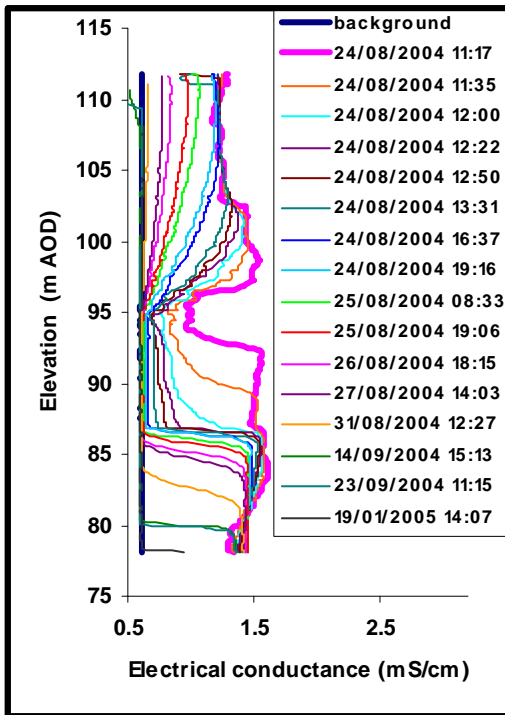


Figure 6.40a: Uniform injection at Gibbet Cottages on 24/08/04

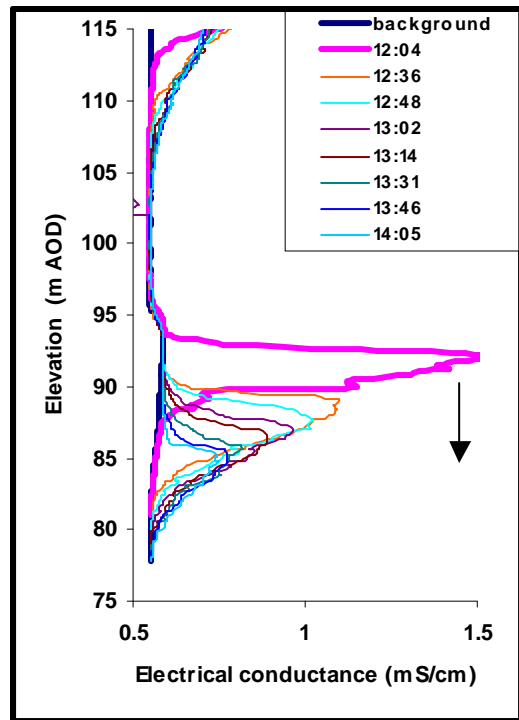


Figure 6.40b: Point injection at 94 m AOD at Gibbet Cottages on 21/07/07 indicating downward flow

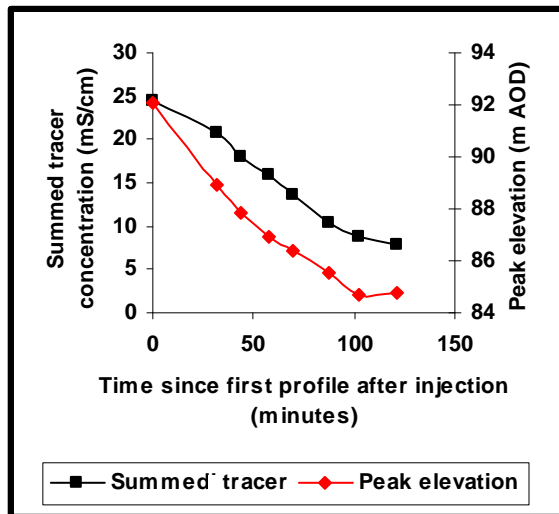


Figure 6.40c: Plot showing downward migration of peak and decrease in summed tracer concentration at Gibbet cottages

Table 6.20: Downward vertical flow rates at Gibbet Cottages following point injection at 94 m

	flow rate (m/day)
log 1-2	140
log 2-3	138
log 3-4	88
log 4-5	72
log 5-6	68
log 6-7	82
log 7-8	-4

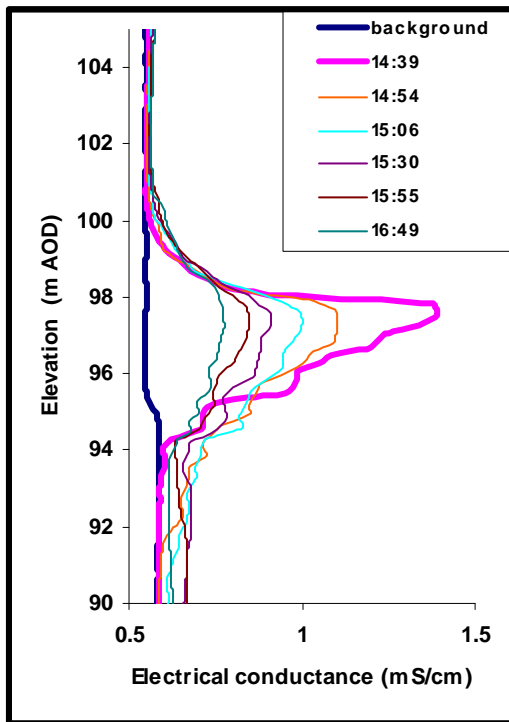


Figure 6.40d: Point injection at 98 m AOD at Gibbet Cottages on 21/07/07 indicating dilution but no vertical flow

Figure 6.41a-c: Grumble Bottom point injection SBDT

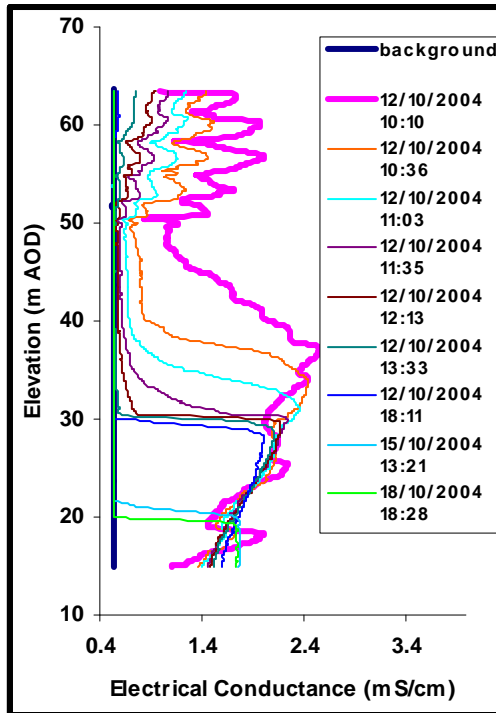


Figure 6.41a: Uniform injection at Grumble Bottom on 12/10/04

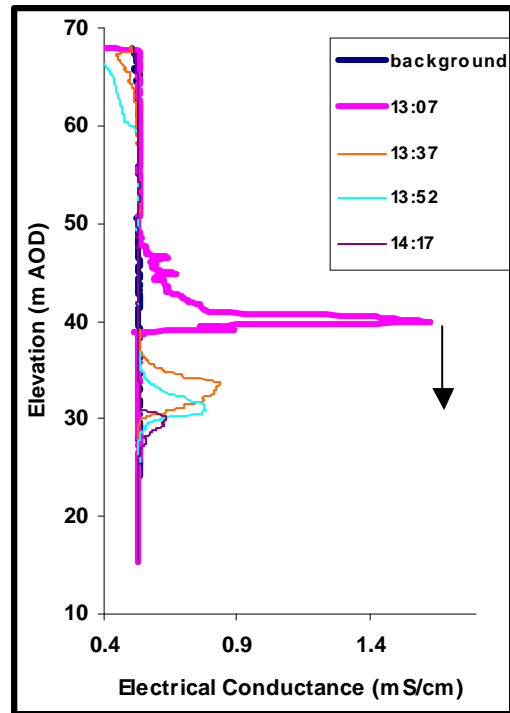


Figure 6.41b: Point injection at 49 m AOD at Grumble Bottom on 24/07/07 indicating downward flow

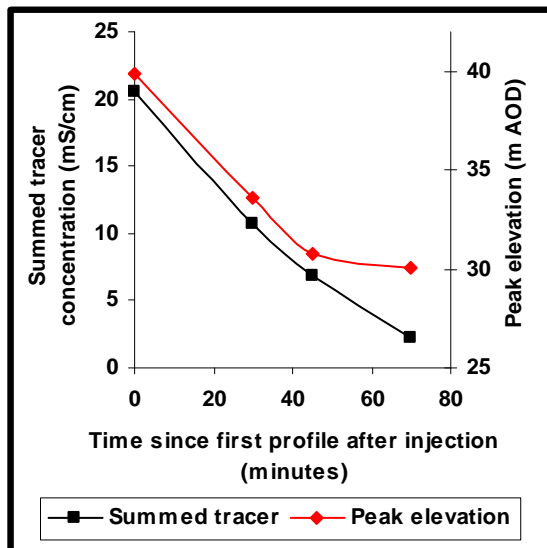


Figure 6.41c: Plot showing downward migration of the peak to about 30 m AOD and decrease in summed tracer concentration following the point injection at 49 m AOD at Grumble Bottom

Table 6.21: Downward vertical flow rates at Grumble Bottom following point injection at 49 m AOD

	flow rate (m/day)
log 1-2	302
log 2-3	269
log 3-4	43

Figure 6.42a-g: Trumpletts A point injection SBDTs

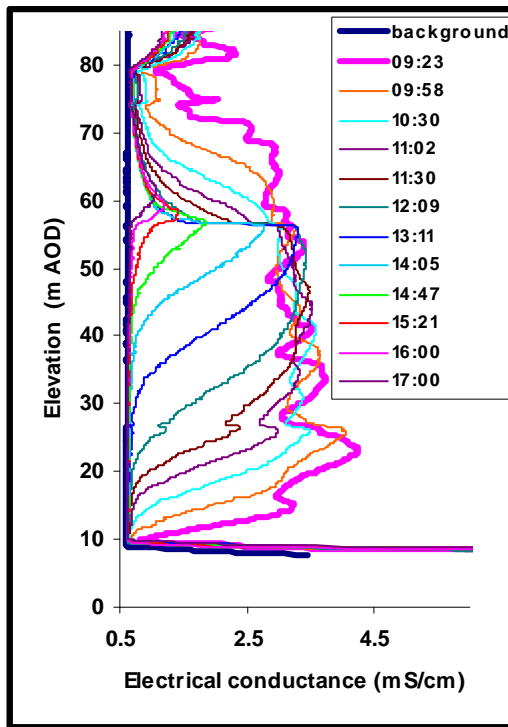


Figure 6.42a: Uniform injection at Trumpletts A on 16/06/04

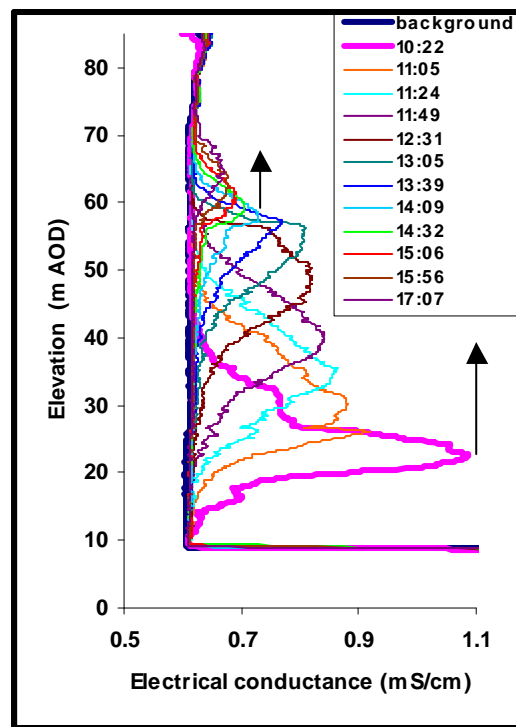


Figure 6.42b: Point injection at 14.7 m AOD at Trumpletts A on 14/06/04 indicating upward flow passing flow horizons at 26.7 and 56.5 m AOD

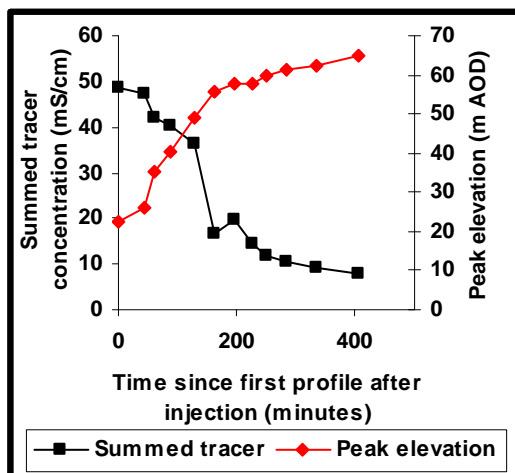


Figure 6.42c: Plot showing upward migration of the peak and general decrease in summed tracer concentration following the point injection at 14.7 m AOD at Trumpletts A

Table 6.22: Upward vertical flow rates at Trumpletts A following point injection at 14.7 m AOD. Note decrease after log 6 from average of 338 to 58 m/day

	flow rate (m/day)
log 1-2	117
log 2-3	697
log 3-4	294
log 4-5	288
log 5-6	292
log 6-7	76
log 7-8	10
log 8-9	82
log 9-10	99
log 11-12	26
log 12-13	55

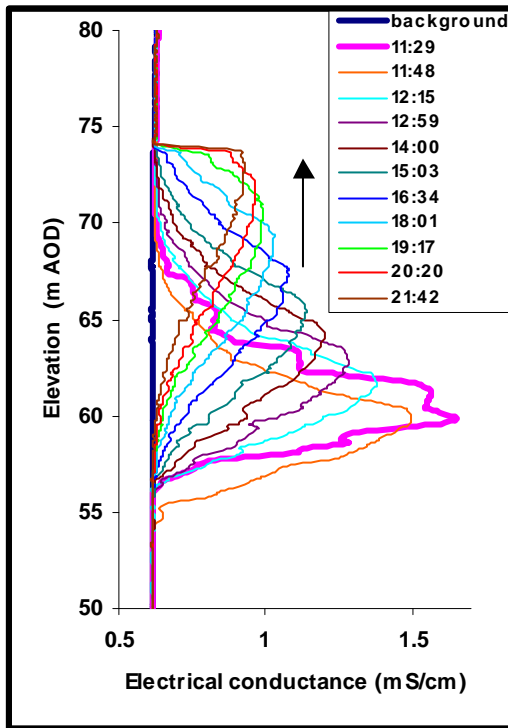


Figure 6.42d: Point injection at 59.3 m AOD at Trumpletts A on 11/06/04 indicating upward flow to 74 m AOD

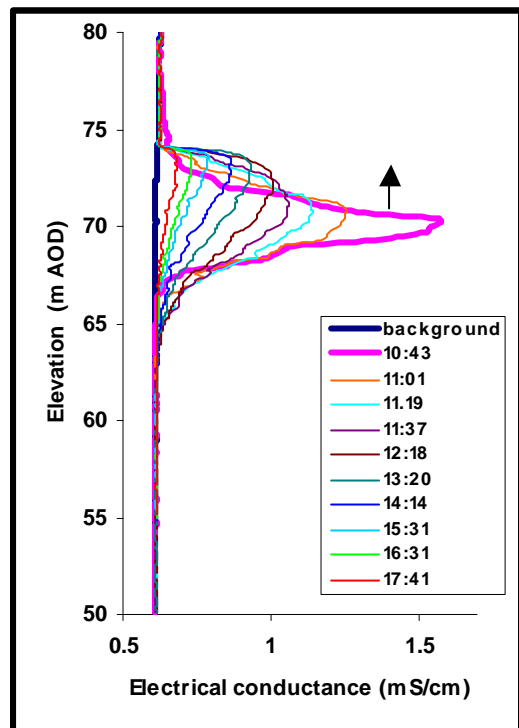


Figure 6.42e: Point injection at 69.3 m AOD at Trumpletts A on 10/06/04 indicating upward flow to 74 m AOD

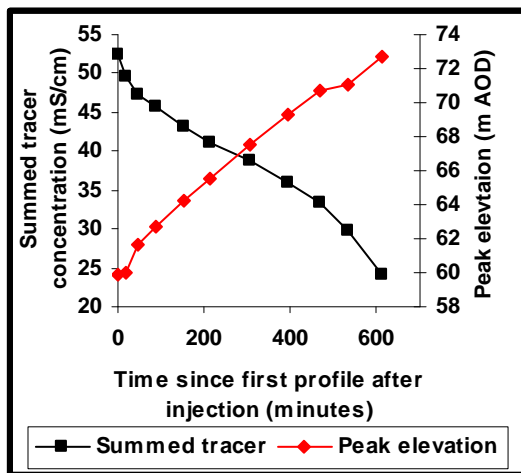


Figure 6.42f: Plot showing upward migration of peak and decrease in summed tracer concentration following injection at 59.3 m AOD at Trumpletts A on 11/06/04

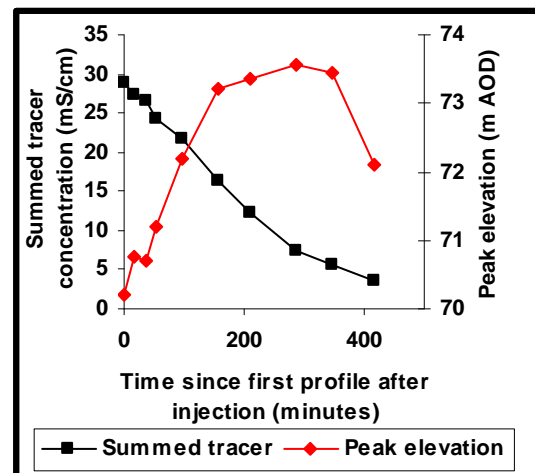


Figure 6.42g: Plot showing upward migration of peak to 73 m AOD and decrease in summed tracer concentration following injection at 69.3 m AOD at Trumpletts A on 10/06/04 74 m AOD

Table 6.23: Upward vertical flow rates at Trumplets A following point injection at 59.3 m AOD. Note flow rates are much lower (average of 32 m.d⁻¹) than those below the flow horizon at 56.5 m AOD (logs 1-6, Table 6.21, average of 338 m.d⁻¹)

	flow rate (m/day)
log 1-2	7
log 2-3	88
log 3-4	36
log 4-5	35
log 5-6	30
log 6-7	32
log 7-8	30
log 8-9	26
log 9-10	9
log 11-12	29

Figure 6.43a-e: Winterbourne Farm point injection SBDTs

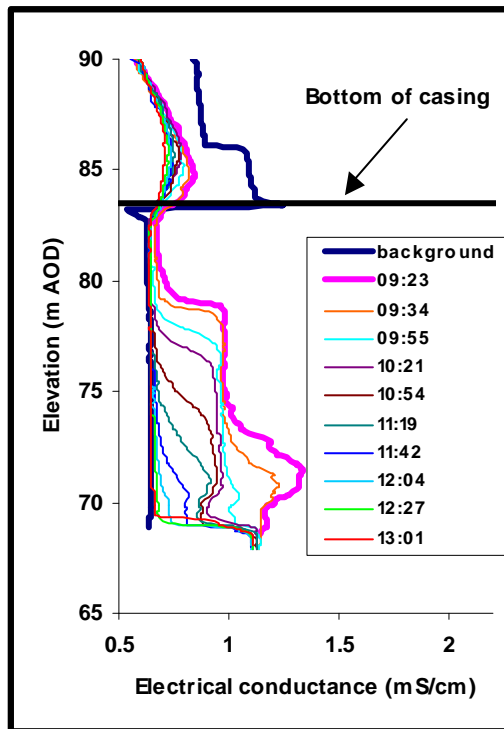


Figure 6.43a: Uniform injection at Winterbourne Farm on 11/08/05. Black horizontal line is the bottom of the casing

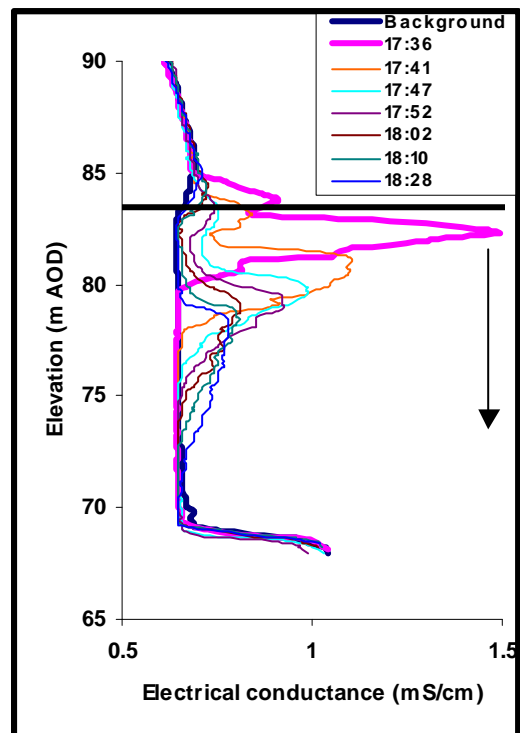


Figure 6.43b: Point injection at 83 m AOD at Winterbourne Farm on 11/08/05 indicating downward vertical flow

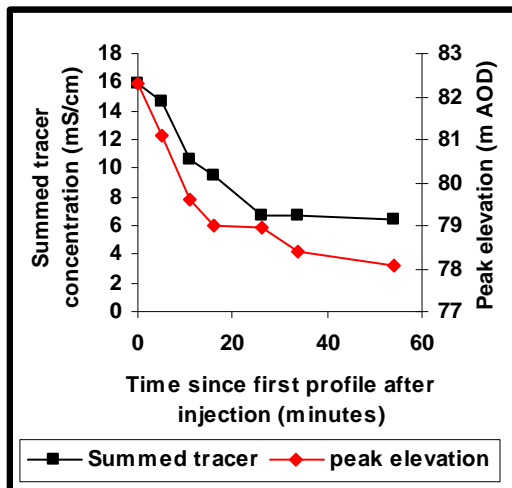


Figure 6.43c: Plot showing downward migration of peak and decrease in summed tracer concentration following injection at 83 m AOD at Winterbourne Farm on 11/08/05

Table 6.24: Downward vertical flow rates at Winterbourne Farm following point injection at 83 m AOD

	flow rate (m/day)
log 1-2	346
log 2-3	360
log 3-4	173
log 4-5	7
log 5-6	99
log 6-7	26

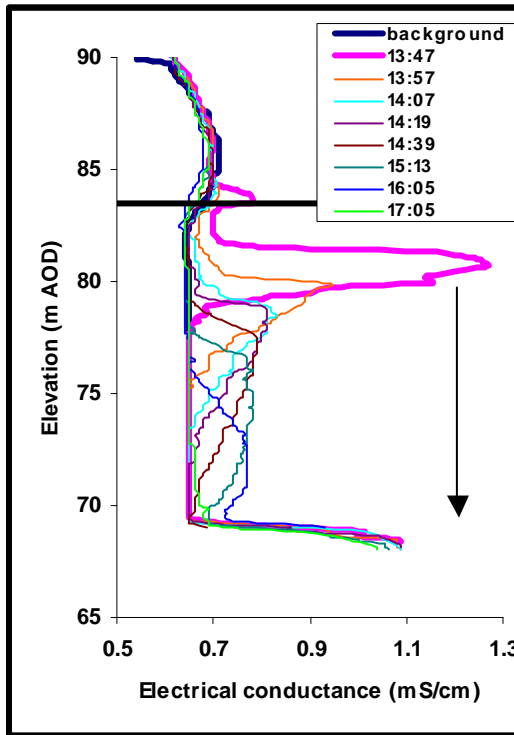


Figure 6.43d: Point injection at 81.6 m AOD at Winterbourne Farm on 11/08/05 indicating downward vertical flow

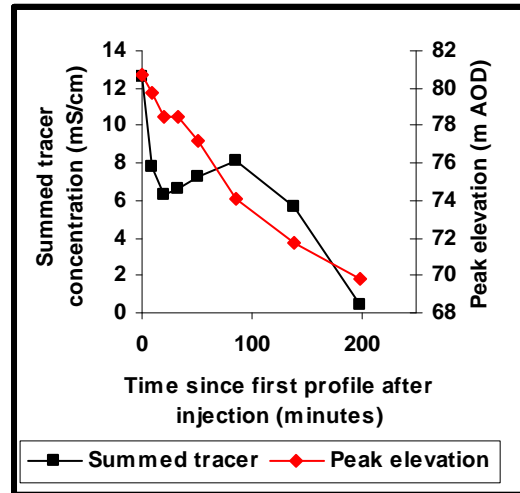


Figure 6.43e: Plot showing downward migration of peak and variation in summed tracer concentration following the point injection at 81.6 m AOD at Winterbourne Farm on 11/08/05. Note apparent increase in summed tracer concentration between 3rd and 6th log.

Table 6.25: Downward vertical flow rates at Winterbourne Farm following point injection at 81.6 m AOD

	flow rate (m/day)
log 1-2	130
log 2-3	94
log 3-4	0
log 4-5	37
log 5-6	52
log 6-7	24
log 7-8	14

6.5.3.3 Vertical flow rates

Vertical flow rates were calculated from 19 point dilution tests. Flow rates based upon the vertical migration of the peak tracer concentration have a very wide range from 3 to 5760 m.d⁻¹. These results are within the range measured by Michalski and Klepp (1990) who conducted point injections in a conglomeratic sandstone. They measured flows of between 4.4 and 22000 m.d⁻¹. The faster flow velocities were measured using a tracer "chasing" technique whereby the electrical conductance probe is left at a constant depth to monitor the passing of the tracer and the procedure is repeated moving the probe to a second depth. They also tried to reduce the effects of the higher density of the saline tracer water by heating the tracer prior to injection.

A pilot study in collaboration with Alex Gallagher (BGS) was undertaken to compare vertical flow rates calculated from point dilution tests with those obtained using a heatpulse flowmeter. At three sites heatpulse flow measurements and point injection SBDTs were performed within 24 hours. The heat pulse flowmeter has only been calibrated for downward flow with calibration points from 172 to 1814 m.d⁻¹. Further calibration of the heat pulse is required, and the effects of the higher density of the saline tracer used in the point injection SBDTs has not been investigated, but preliminary results are discussed here. The measurement range of heatpulse flowmeters is reported as 88 to 8800 m.d⁻¹ (Morin et al. 1988). The lowest flowrate measured using point injection SBDTs was 3 m.d⁻¹ upward flow following an injection at 40.17 m AOD in Frilsham B, (Figure 6.38b, Table 6.14), suggesting that the point injection technique may be more sensitive than the heatpulse flowmeter.

At Barracks the SBDTs clearly demonstrated upward flow (Figure 6.35b). The heatpulse was not calibrated for upward flow but applying the calibration for downward flow to heat pulse data for Barracks gives results of about the same order as those obtained from the point injections (Figure 6.44, left).

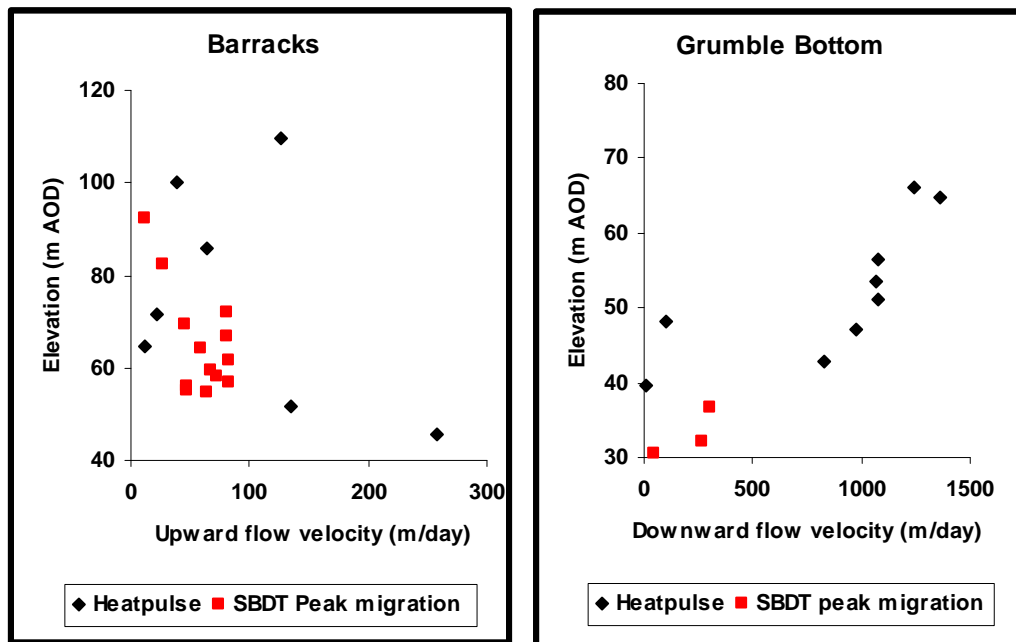


Figure 6.44: Comparison of flow rates obtained from a heatpulse flowmeter and from SBDTs (the vertical migration of the peak tracer concentration) at Barracks (left) and Grumble Bottom (right)

At Gibbett Cottages and Grumble Bottom borehole point injection SBDTs revealed downward flow. Flow rates between 95 and 87 m AOD at Gibbett Cottages were 68-140 m.d⁻¹. At Grumble Bottom the flow rate between 30 and 40 m AOD was 302 m.d⁻¹. Heat pulse measurements obtained at these sites within these depth ranges suggest slow downward flow but flow rates cannot be calculated without further calibration, because of convection effects.

At Grumble Bottom heat pulse measurements indicated very rapid downward flow between 66 and 42 m AOD with the exception of an anomaly at 48 m AOD where downward flow was much slower (Figure 6.44, right). Unfortunately a point injection was not undertaken in the upper section of the borehole between 50 and 66 m AOD. Data over this section of borehole from the uniform injection SBDT in 2004 does not display a clear pattern of downward flow (Figure 6.41a). Instead there appear to be several significant crossflow horizons in this section of the borehole. The water table was 5 m lower during the uniform injection SBDT, and it is possible that downward flow rates were much slower. It is also possible that the inflowing horizon that caused the downward vertical flow measured by the heatpulse in 2007 was unsaturated during

the 2004 uniform injection and that downward flow was therefore not occurring over this section.

Further work is required to enable more accurate flow rates to be calculated using both techniques to enable a comparison between them, but preliminary results suggest that point injection SBDTs may provide an alternative to heatpulse flow measurements which may be able to detect slower vertical flow rates.

6.5.3.4 Identifying flow horizons using point injection SBDTs

Where vertical flow is occurring, there are clearly flow horizons at the top and bottom of the vertical flow section. However, the point injection results were also used to identify flowing horizons within sections of vertical flow.

In this section different methods of identifying flow horizons are discussed:

- 1) Using “nick points” in electrical conductance logs.
- 2) Comparing summed tracer concentrations calculated from each log to identify decreases in tracer mass between logs.
- 3) Using changes in vertical flow rates.

1) Where there are inflows to the borehole the tracer concentration is reduced, causing “steps” or “nick points” within electrical conductance profiles. Where vertical flow is occurring these structures move with the tracer plume and can be difficult to interpret. They were therefore only interpreted as flowing horizons if they are consistently present in multiple profiles. A clear example is the nick point at 26.7 m AOD in Trumpletts A that is seen in the electrical conductance logs obtained following the point injection at 14.7 m AOD and following the uniform injection SBDT (Figures 6.42a and b).

2) Crossflow and outflow horizons cause a decrease in overall tracer mass. Combined plots of summed tracer concentration and peak elevation were used to indicate the depths at which mass loss occurred, with the aim of identifying flow horizons within sections of vertical flow (although the top and bottom of vertical flow sections was also often demonstrated by mass loss). However, because tracer plumes spread out vertically over 10 to 20 m in some tests the plume was in contact with one of the features generating the vertical flow during the period in which most of the electrical conductance logs were obtained. In these cases it was not possible to identify additional

flow horizons within the section of vertical flow. If two or more electrical conductance logs were obtained when a tracer plume was not in contact with the flow horizons at the top and bottom of the vertical flow section, a decrease in summed tracer concentration between profiles indicated the presence of an additional flow horizon. This is illustrated below using the example of the Barracks, but 9 other flow horizons were identified within sections of vertical flow using this method.

In the Barracks borehole there is upward flow from 45 m AOD (Figure 6.35b). The location of this flow horizon is clear from both the uniform and point injections because tracer is not diluted below 45 m AOD. The exact location of the outflow horizon is unclear, but the results from the uniform injection SBDT suggest that it is above 110 m AOD. It is visually apparent from the electrical conductance logs following the point injection that the tracer plume at 10:25 on 23/07/07 (orange on Figure 6.35b) was much smaller than the previous day at 17:53 (purple on Figure 6.35b). The summed tracer concentration (Figure 6.35c) decreased substantially from 27 to 5 mS.cm⁻¹ over this period confirming that the tracer plume passed a flow horizon. The exact location of the flow horizon is unclear because the plume passed it overnight but it must be between 70 and 90 m AOD.

During the period in which the first 9 electrical conductance logs were obtained (the 9th profile is indicated by a blue arrow on Figure 6.35c) there was no substantial decrease in tracer mass suggesting that there are no significant flow horizons over the section of borehole through which the tracer plume passed (50 to 68 m AOD). Small fluctuations in summed tracer concentrations during this period (including small apparent increases) could be due to instrument or measurement errors, variations in borehole diameter or incomplete horizontal mixing. These fluctuations demonstrate the need for caution when using small-scale decreases in mass to identify flow horizons. There was a small but consistent decrease in summed tracer concentration between each of the next four profiles (these are the last four obtained on 22/07/07). This suggests that the leading edge of the plume may have reached the flow horizon, placing it at between 70 and 80 m AOD. However, the losses were very small compared to those overnight, suggesting that it is more likely that the flow horizon is between 80 and 90 m AOD.

3) A change in vertical flow rate is an indication that a tracer plume has passed a flow horizon. Table 6.26 shows the effect of the types of flow horizons depicted in Figure 6.16 on vertical flow rate and tracer mass as a plume of tracer from a point injection passes a flow horizon. For Type 1 (inflow only), an increase in vertical flow rate is the only means of identifying the flow horizon because there is no decrease in mass. The only type in which there is no change in vertical flow is Type 3 (crossflow with an equal rate of inflow and outflow).

Table 6.26: Changes in vertical flow rate and tracer mass as tracer passes different types of flow horizons depicted in Figure 6.16

Type presented in Figure 6.16	Effect on vertical flow rate	Effect on tracer mass in plume
1) Inflow only	Increased	None
2) Crossflow, Inflow > Outflow	Increased	Decreased
3) Crossflow, Inflow = Outflow	None	Decreased
4) Crossflow Outflow > Inflow	Decreased	Decreased
5) Outflow only	Decreased	Decreased

Flow rates within an individual borehole calculated from the migration of a tracer plume during a point injection SBDT are generally quite variable. Results may be affected by variations in the borehole diameter and the effect of the time taken to lower the probe through the water column. The data also suggest that when a tracer plume is in contact with a flow horizon within a section of vertical flow, the vertical flow rate is temporarily slowed. This may be due to eddying as water enters the borehole. For example at Bockhampton, a point injection at 77.9 m AOD demonstrated upward flow passing a flow horizon at 84 m AOD (Figure 6.36e). As the tracer plume passed this flow horizon the vertical flow rate temporarily appeared to cease (between logs 2 and 3, Table 6.12).

Despite the general variability in measured vertical flow rates, there were five examples of sections of vertical flow in which there was a clear change in flow rate as the tracer plume moved up or down the borehole which is likely to be due to the presence of a flow horizon. In four cases (70 to 90 m AOD in Barracks, 56.5 m AOD in Trumpletts A, and both 30.5 and 39.5 m AOD in Grumble Bottom) there was a decrease in flow rate combined with a decrease in tracer mass indicating that the flow horizon is either Type 4 or 5 (Table 6.26).

At Barracks in addition to the decrease in mass as the tracer plume passed a flow horizon between 70 and 90 m AOD (discussed previously) there was also a clear decrease in flow rate from an average of 66 m.d⁻¹ to an average of 19 m.d⁻¹ (Table 6.11).

In Trumpletts A, three point injections clearly demonstrated upward vertical flow from 9.9 m to 74 m AOD (Figures 6.42b,d,e). Two additional flow horizons were identified within this section at 26.7 and 56.5 m AOD. At 26.7 m AOD nick points in the electrical conductance logs indicate a flow horizon (discussed previously). It is not possible to determine whether there was a change in vertical flow rate as the tracer plume from the injection at 14.7 m AOD passed the flow horizon at 26.7 m AOD because the plume was in contact with the flow horizon during the first log after injection (Figure 6.42b), and therefore there are no flow data below the flow horizon. However, the tracer plume also passes a flow horizon at 56.5 m AOD that caused a loss of mass (Figure 6.42b and c), and vertical flow rates were measured above and below this horizon. Flow rates decreased from an average of 338 m.d⁻¹ below 56.5 m AOD to 58 m.d⁻¹ above (Table 6.22). The lower flow rate above 56.5 m AOD is confirmed by the point injection at 59.3 m AOD, which indicated an average flow rate of 32 m.d⁻¹ (Figure 6.42d and Table 6.23).

In Grumble Bottom borehole the combination of uniform and point injection SBDTs and heatpulse data indicate downward vertical flow from 67-68 m AOD to 20 m AOD, and two additional flow horizons within this section at 39.5 and 30.5 m AOD which cause a loss of tracer mass and a decrease in flow rate. The heat pulse data (Figure 6.44, right) indicate rapid downward flow at 66 m AOD implying that the flow horizon at the top of the section of downward vertical flow was between 67 and 68 m AOD (the water table was at 68 m AOD). The flow horizon at 39.5 m AOD is indicated by the point injection (Figure 6.41b). The first electrical conductance log after injection (13:07) has a flat bottom at 39.5 m AOD and there is considerable loss of mass between this log and the next at 13:37 (Figure 6.41c). The heat pulse and point dilution data (Figure 6.44, right) suggest that with the exception of the anomalous heat pulse measurement at 48 m AOD, downward vertical flow rates are much higher above 39.5 m AOD than below it. It is possible that the anomalously low heat pulse measurement at 48 m AOD is due to the presence of a flow horizon temporarily slowing the flow rate

(as discussed above using the Bockhampton example); indeed heat pulse flow measurements below 48 m AOD appear lower than those above, possibly a further indication that there is a flow horizon around 48 m AOD. However, it is also possible that the anomaly is due to a measurement error. The flow horizon at 30.5 m AOD is indicated by both the uniform and point injection SBDTs (Figures 6.41 a,b). There is a clear loss of mass as the plume from the point injection passes 30.5 m AOD (Figure 6.41b). Although there are no data on vertical flow rate from the point injection or the heat pulse, during the uniform injection SBDT the tracer “front” slowed down substantially at 30.5 m AOD.

The fifth example of a change in flow rate within a section of vertical flow is at Frilsham C. Point injections indicate downward flow from above 50 m AOD to 20 m AOD (Figures 6.39c and d). Nick points in the uniform injection SBDT indicate several flow horizons within this section of vertical flow at 52 to 53, 47 to 48, 44, 38, and 30 to 31 m AOD (Figure 6.39a). Results from the point injections are therefore complex because the tracer plume was often in contact with more than one flow horizon. There are also clearly measurement errors in the summed tracer concentration plot for the injection at 51.34 m AOD (Figure 6.39f), which shows an apparent increase in tracer during the first three electrical conductance logs. However, results from the injection at 51.3 m AOD indicate a progressive increase in flow rate as the plume moves down the borehole (Table 6.19). This increase in flow rate combined with the nick points observed in the electrical conductance logs suggest that the flow horizons are Type 2 crossflow horizons in which inflow > outflow (if they were Type 1 inflow only, there would be no nick points in the logs).

There are no examples in the field data in which type 1 inflow only horizons were identified by changes in vertical flow rate (and hence could not have been identified by changes in mass or nick points). However, changes in vertical flow rate provide useful supporting evidence of the location of flow horizons in which there is also loss of mass.

6.5.3.5 Implications of point injection results for interpretation of uniform injection SBDTs

The point injection results confirm that in 12 out of 13 borehole sections tested, electrical conductance logs with a tracer “front” moving up or down the borehole during uniform injection SBDTs indicate vertical flow. For example, the point injection in Frilsham A at 51.5 m AOD confirmed downward flow (Figure 6.37 a and b), and that in the Barracks at 55 m AOD (Figure 6.35a and b), confirmed upward flow. During some uniform injection SBDTs the tracer “front” appears much more spread out than these examples, but point injections confirmed that vertical flow is still occurring. For example, a point injection at 63 m AOD in Bagnor borehole confirmed upward flow between 60 and 70 m AOD (Figures 6.34 a and b). The results at Bockhampton are a little different from those at other sites because there is no single tracer “front” in the electrical conductance logs obtained during the uniform injection SBDT (Figure 6.36a). However there are two independent tracer “fronts” moving up to 92 and 110 m AOD, and three point injections at 64.9, 77.9 and 101.9 m AOD confirmed upward vertical flow (Figures 6.36 b,c,e and g). It appears that in this borehole very high crossflow rates disrupt the tracer front produced by vertical flow.

The upper section of Trumpletts A is the only case in which vertical flow measured in point injection SBDTs appears to contradict the patterns in electrical conductance logs obtained during the uniform injection SBDT. The point injections in Trumpletts A clearly demonstrate upward vertical flow from 9.9 to 74 m AOD (Figures 6.42b and 6.42d). In contrast, the first five profiles after the uniform injection appear to show downward movement of a tracer “front” between 74 and 56.5 m AOD (Figure 6.42a). Careful inspection of the last three profiles following the uniform injection (15:21, 16:00 and 17:00), also confirm that a small amount of tracer moves up from below the flow horizon at 56.5 m AOD. It is unclear why the first few profiles following the uniform injection appear to show tracer moving down the borehole but it suggests that additional flow horizons may occur between 74 and 60 m AOD.

Despite the anomalous result in Trumpletts A, it appears that in uniform injection SBDTs where the electrical conductance logs have a tracer “front”, vertical flow is occurring. For the 12 boreholes in which point injections were not carried out, such patterns in the uniform injection SBDTs were assumed to be indicative of vertical flow,

and on the basis of this, it is probable that vertical flow occurred in at least one borehole section at 11 of these boreholes.

6.5.3.6 Conclusions of point injection SBDTs

Point injection SBDTs clearly demonstrate vertical flow because a tracer plume can be observed moving up or down the borehole. Comparison with heat pulse data suggests this may be the most sensitive field technique for identifying vertical flows in boreholes.

The point injection SBDTs have provided insight into the interpretation of uniform injection SBDTs. Point injection SBDTs demonstrate that when a tracer “front” is observed to move up or down the borehole following uniform injection SBDTs this is usually an indication that vertical flow is occurring, and flowing features can be inferred at the top and bottom of the borehole section. Complex results at Trumpletts A suggest some caution is required in these interpretations.

Flowing horizons can be identified from point injection SBDTs where there are persistent nick points in electrical conductance logs or where there is a loss of tracer mass between profiles. In some boreholes changes in vertical flow rates provided further evidence of flow horizons suggested by nick points or loss of tracer mass. Theoretically, inflow only horizons, which cause an increase in vertical flow rate but no loss of mass can be identified from flow rate data, although this was not demonstrated in the field data from this study.

The point injection SBDT technique could be improved by compensating for changes in borehole diameter using calliper data, and compensating for the effect of the time taken to lower the electrical conductance probe down the borehole. Producing best-fit modelled tracer logs of the field data could be used to determine values of inflow and outflow at each horizon, which would determine which of the five flow types occur. This has not been undertaken because the main objective of the SBDTs was to identify flow horizons at the catchment scale, and it is unlikely that fitting the logs of individual tests would significantly affect the location of flow horizons that have been inferred using qualitative observation of the data.

6.5.4 Integrated method of identifying flowing horizons

The difficulties in identifying flow horizons in boreholes are illustrated in Figure 6.45. The red circle represents the true number of flowing horizons in a borehole. The green circle represents all the features that would be visible in imaging logs. In the Chalk there should be a fracture, fissure or conduit present at the location of flow horizons because there is unlikely to be significant flow through the low permeability matrix, and therefore all flowing features should be visible on image logs. However, as discussed previously there are often features visible on image logs that are not actively flowing. Therefore even where available, features on image logs were not used as a criteria for identifying flow horizons. The black circle represents flowing features that are clearly apparent from the SBDTs. These may not represent all the flowing features that are present. In the diagram it is assumed that there are no errors in the identification of flowing features from SBDTs, and that all features identified from the tests are true flowing features. The blue circle represents flowing features that cause a change in the natural electrical conductance or temperature of water in a borehole. It assumes that all changes represent flowing features and that some are apparent from the SBDTs and some are not. These data were available at all sites using the background electrical conductance log (and temperature measurements recorded at the same time by the Solinst levellogger probe). Additional electrical conductance and temperature logs obtained at 6 sites by the British Geological Survey logging team were also used.

Both SBDTs and changes in the natural electrical conductance/temperature of the borehole fluid were used to obtain the best estimate of the true number of flowing features in each borehole. However, as illustrated in Figure 6.45, even using both techniques, the true number of flow horizons may be underestimated. Figure 6.45 assumes that SBDTs and natural electrical conductance/temperature logs correctly identify flow horizons but in reality there is uncertainty associated with using these techniques due to measurement errors and the subjective nature of interpreting fluid logs. To avoid over interpretation and false identification of flow horizons a decision process was followed (Figure 6.46). Subsequent analyses (Sections 6.6 and 6.7) focus on class 1 flow horizons for which there is the greatest certainty that they have been correctly identified. Class 2 and 3 features were not used to avoid overestimating the number of flow horizons. Further work would be required to confirm whether a flow

horizon is present at these locations. Flow horizons in which tracer took more than one week to be replaced (Class 4) were also omitted from these analyses.

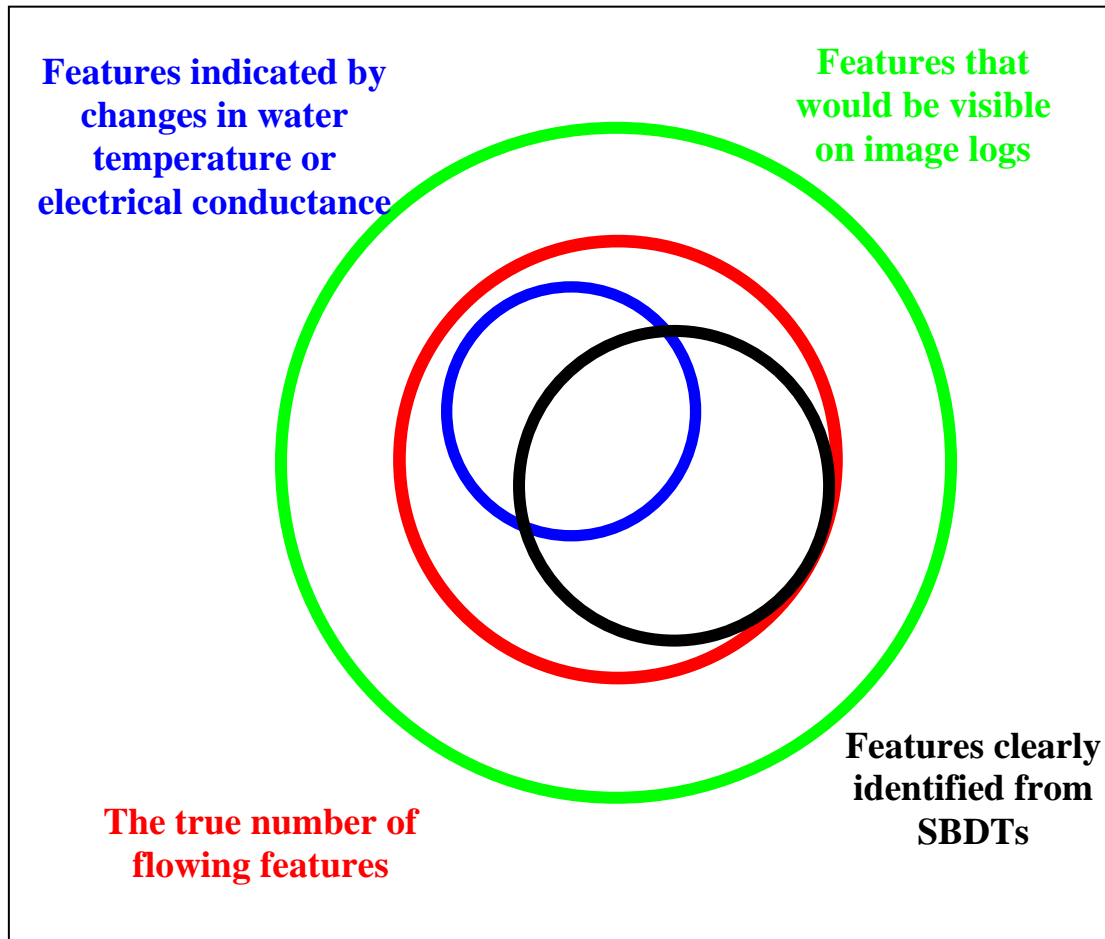


Figure 6.45: Relationship between the true number of flowing features in boreholes and those identified using different techniques

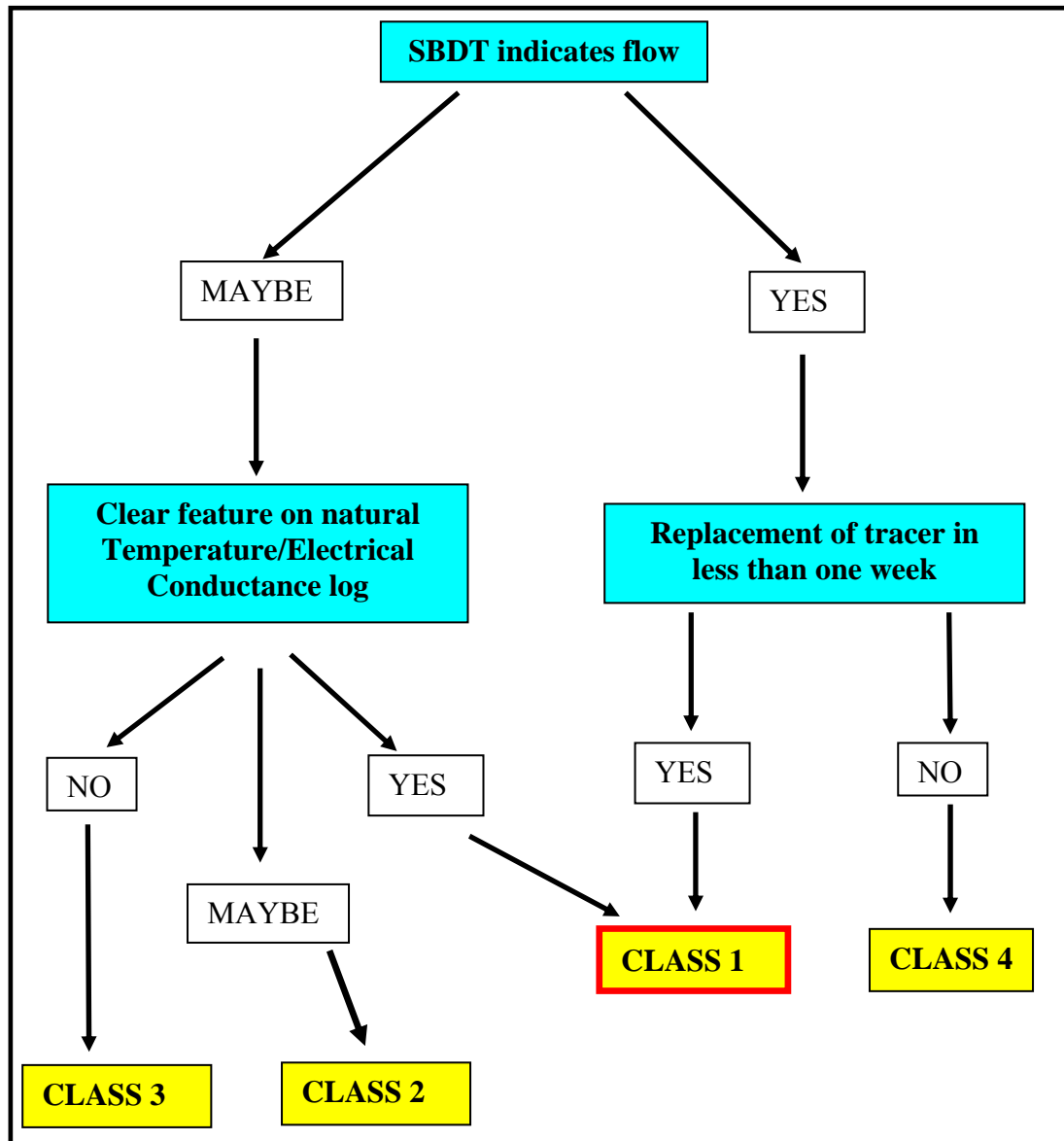


Figure 6.46: Decision tree for identifying flowing features

Flowing horizons were identified from the uniform injection SBDTs using the following criteria:

- If there were nick points or steps in multiple electrical conductance logs.
- If there was a sharp boundary between zones of faster and slower dilution.
- At the top and bottom of vertical flow inferred from the movement of a tracer “front” up or down the borehole

If point dilution data were available flow horizons were confirmed/identified at:

- The top and bottom of a section in which vertical flow was occurring (often confirmed by tracer loss at that depth)
- Depths within sections of vertical flow at which there was tracer loss and/or a change in flow rate.

The "maybe" category in Figure 6.46 includes horizons at which electrical conductance logs displayed very small steps or nick points, or where steps/nickpoints were inconsistently present.

6.5.5 Results: Flowing features in boreholes from SBDTs

Table 6.27 lists the elevation of flow horizons in 24 boreholes (excluding Great Shefford where there are no SBDT data for the middle section that diluted whilst the injection hosepipe was stuck in the borehole). Figure 6.47 shows the location of class 1 flow horizons (black horizontal lines), with boreholes presented in alphabetical order. Solid red arrows indicate vertical flow demonstrated by point injection SBDTs, and dotted red arrows indicate vertical flow inferred from the uniform injection SBDTs. There are 119 class 1 flow horizons, of which 67 do not cause a change in natural fluid electrical conductance/temperature and could therefore only have been identified using the SBDTs.

As discussed previously, the 119 flow horizons is likely be an underestimate of the true number. Flow horizons within sections of vertical flow can be particularly difficult to identify. If tracer is very rapidly replaced by aquifer water it is sometimes not possible to determine from the electrical conductance logs whether there are features contributing to the dilution in addition to those at the top and bottom of the vertical flow (e.g. in Trumplett B between the flow horizons at 78.7 and 47.2 m AOD, Figure 6.47). In slower sections of vertical flow there are sometimes many small-scale steps and nick points which move with the vertical flow and are confusing to interpret so cannot be definitively classified as class 1 horizons (e.g. in the upward flow section between 59.5 and 69.5 m AOD at Bagnor, Figure 6.47). Nevertheless, it is likely that most of the major flow horizons have been identified, and in the following discussion this data set is firstly combined with imaging data to investigate their physical nature, and secondly the

dataset is used to explore the controls on the spatial distribution of groundwater flow at the catchment scale.

Table 6.27: The elevation of flowing features in 24 boreholes from SBDTs

Borehole	Class 1	Class 2	Class 3	Class 4
Ashridge Wood	94, 91.35, 88.75, 85, 82.5	92.5, 90		
Barracks	110-118, 70-90, 45		65-75	
Bagnor	69.5, 59.5, 56.5		67.7, 66.3, 64.3, 62.3, 61.7, 60.7	
Beche Park Wood	67, 64.7, 57.6, 55			45.5 to 48.5
Bockhampton	110.5, 102, 96, 92, 84, 76.3, 73.8		100, 90.2, 88.5, 85.9, 82.3, 80.7, 79.35	
Bottom Barn	86.7, 85.5, 83.2, 81.2, 74.5, 70			
Bradley Wood	94 to 96, 92.5, 82.5, 71		89, 86.5	
Briff Lane	57, 50, 45.6, 42.8			
Brightwalton Common			115.5	105.6
Brightwalton Holt	110 to 113		105 to 109, 93.5 to 97.5	
Calversley Farm	69, 67, 65.6, 61.4, 60.6, 59.2, 51.8, 49	56.4, 54.2	49.8	
Cow Down	104, 101.5, 97.8, 96.5, 90.5			85.9
Frilsham A	60.4, 58.5, 55.3, 53.3, 49, 38.5, 36, 34.7	65.1	42	
Frilsham B	55, 53.4, 46.5, 44.1, 41.6, 40, 38.3			
Frilsham C	57.1, 52.5, 47.5, 43.8, 38.1, 30.5, 20.2		53.3, 26.5	
Gibbett Cottages	109, 97.85, 94.7, 89.5, 87			80, 78.5
Greendown Farm	150			107 to 113
Grumble Bottom	61, 58, 54.5, 51.8, 50.5, 49, 39.5, 30.5, 20			
High Street Farm	88.6, 86.8, 79.3, 67.8			
Knighton Down	128.5, 127.9, 126.9, 126.1, 124.9, 123, 122, 120.8, 108		114.1, 111.7	
Peasmore	109, 103.3, 98.7, 96.1		101.4, 100.6, 97.4, 96.6, 94.5	
Trumpletts A	79.5, 74, 56.5, 26.7, 9.9	65 to 74		
Trumpletts B	84, 81.3, 78.7, 47.2, 27.3, 20.5, 10.6		63.3, 56.	
Winterbourne Farm	83, 79, 69.7			

Figure 6.47: Class 1 flow horizons (horizontal black lines) in 24 boreholes (in alphabetical order)

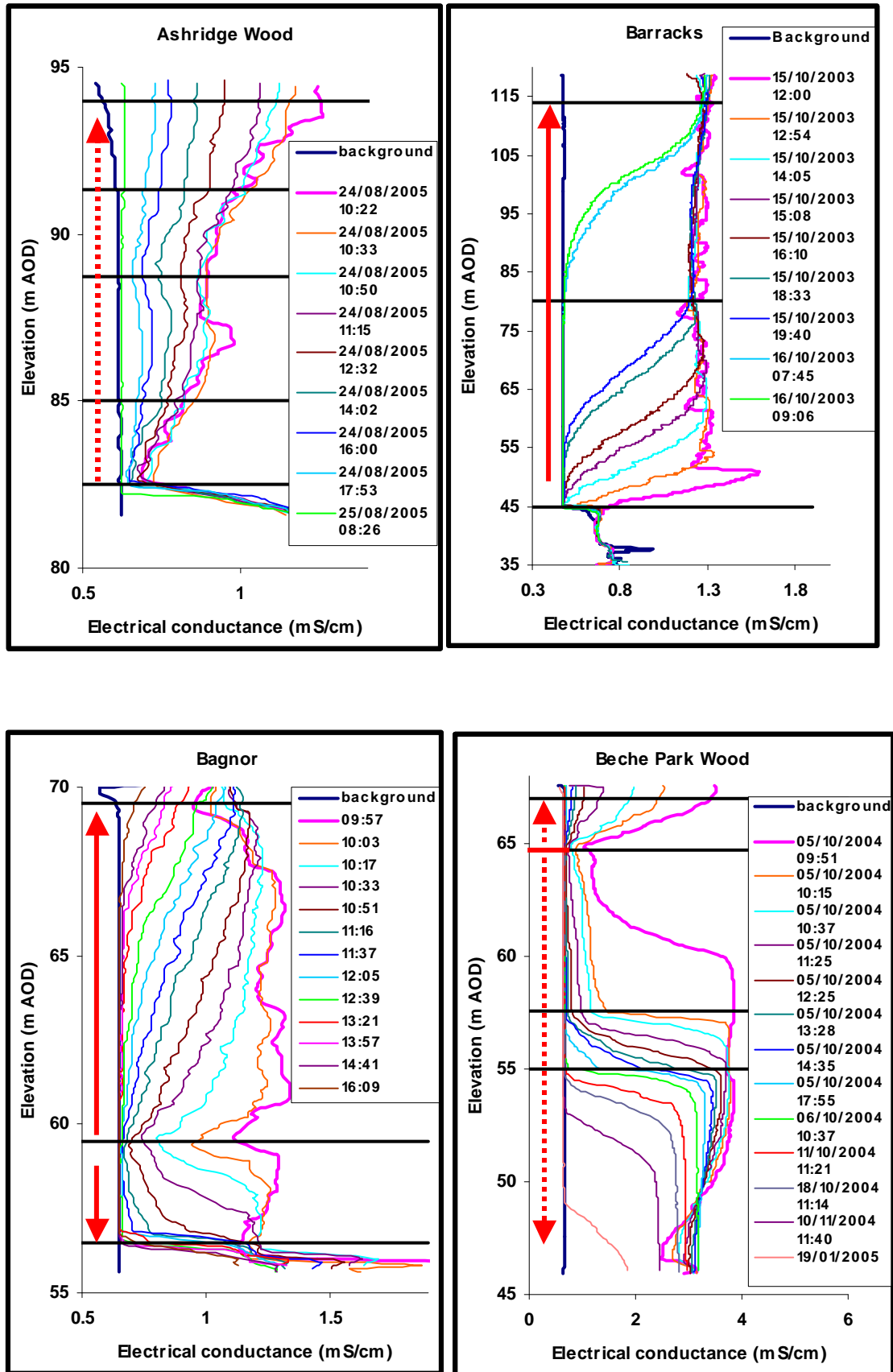


Figure 6.47 (continued)

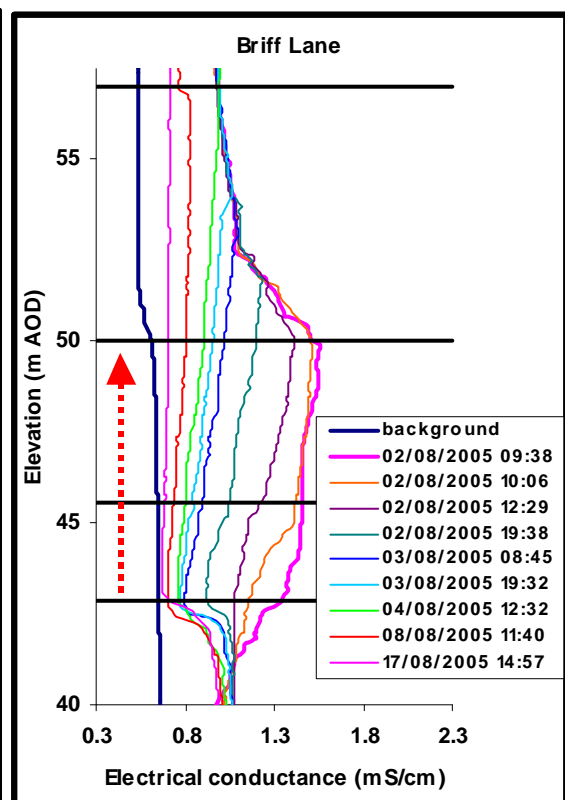
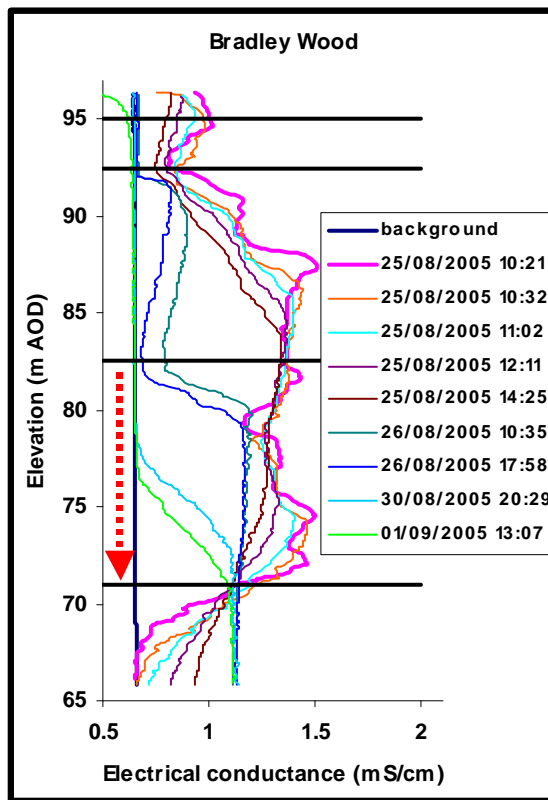
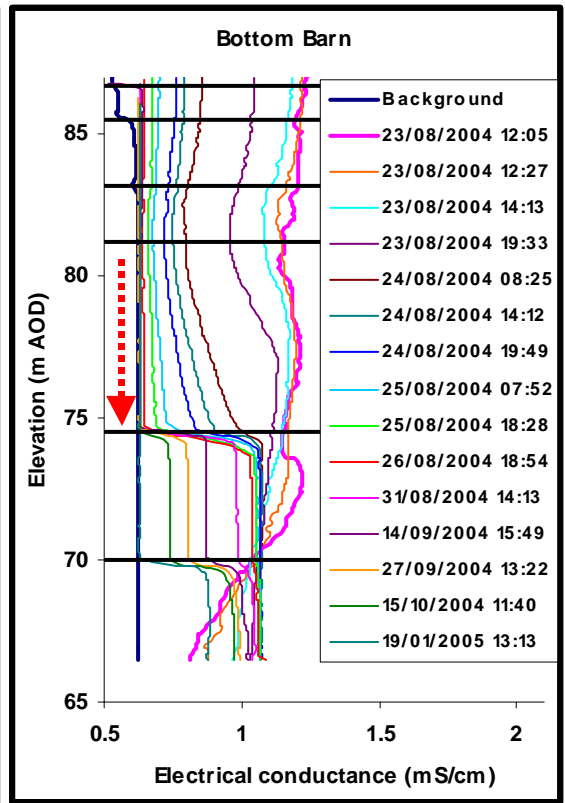
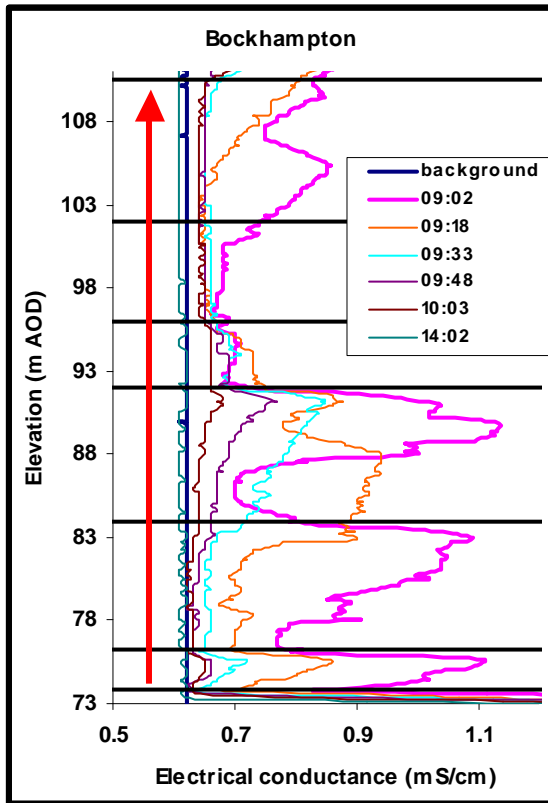


Figure 6.47 (continued)

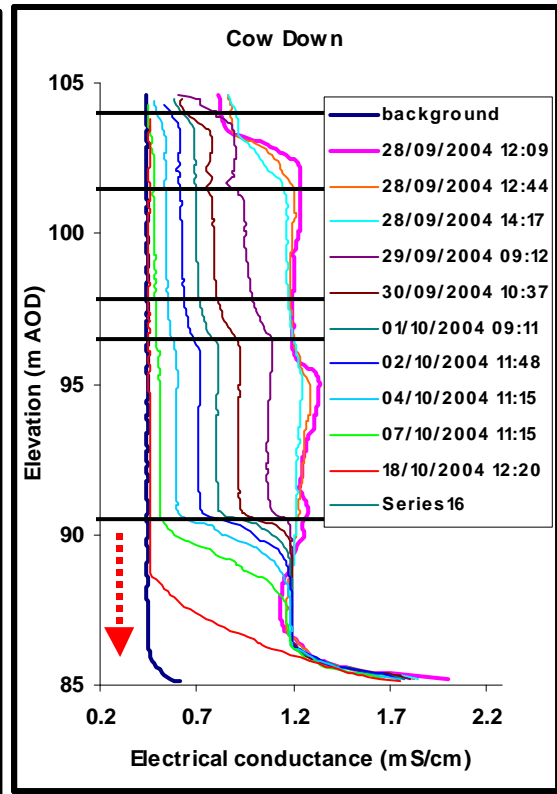
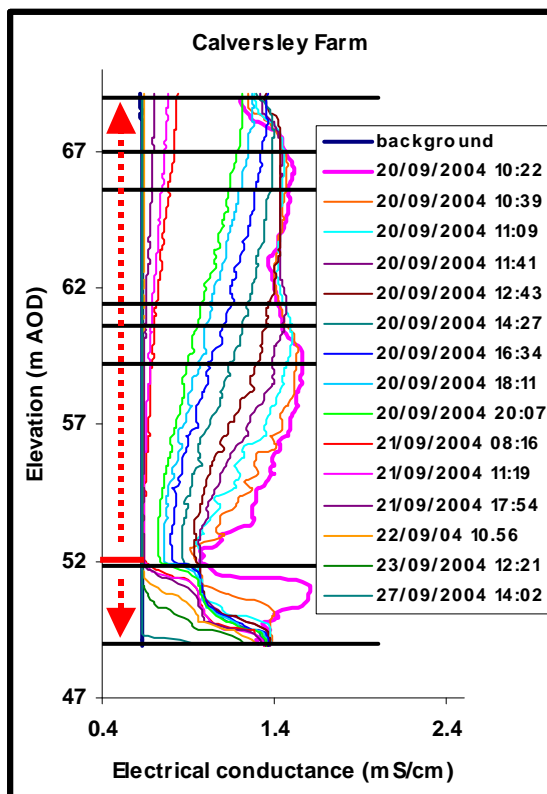
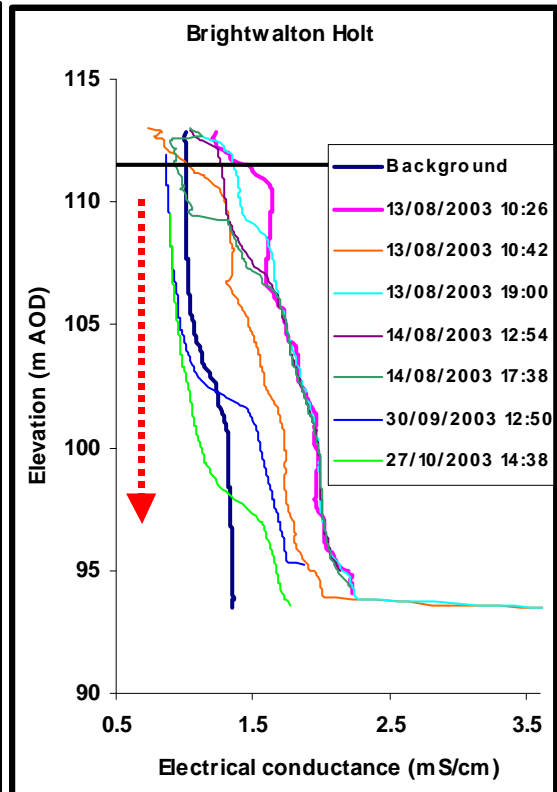
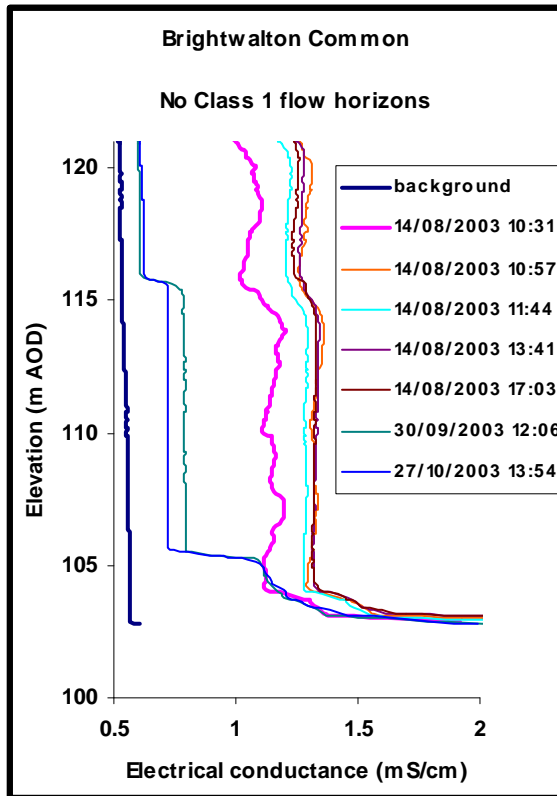


Figure 6.47 (continued)

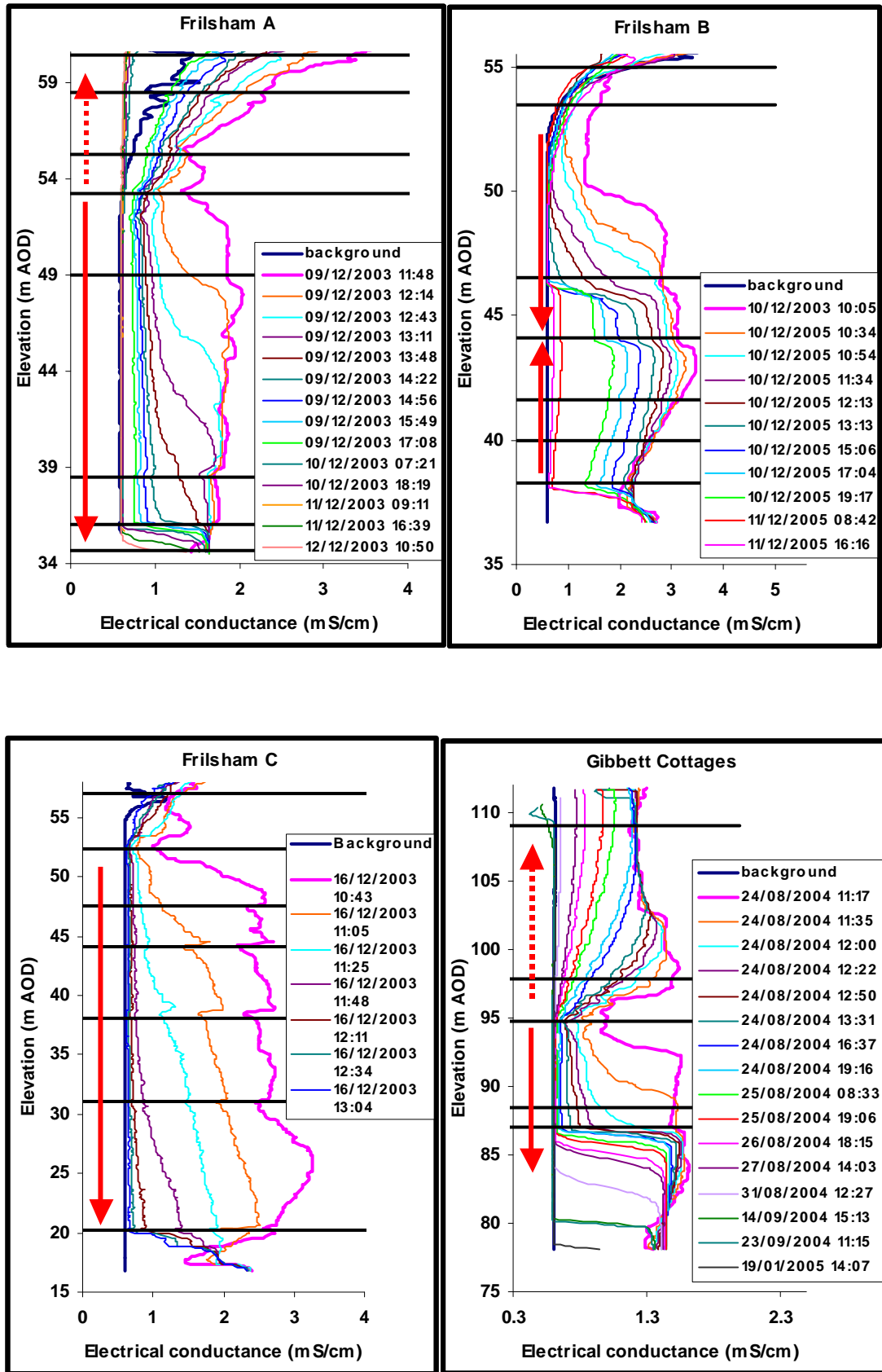


Figure 6.47 (continued)

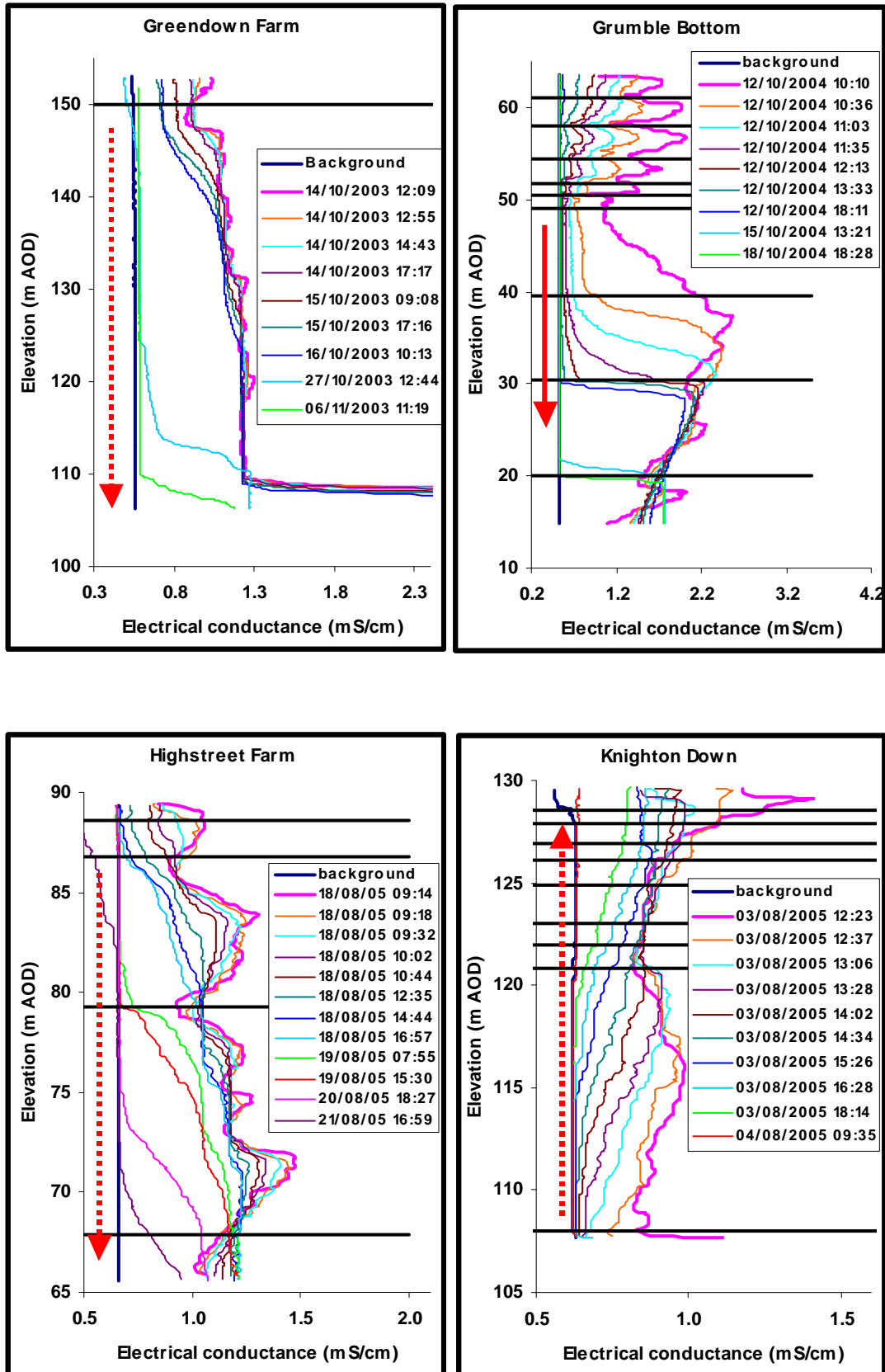
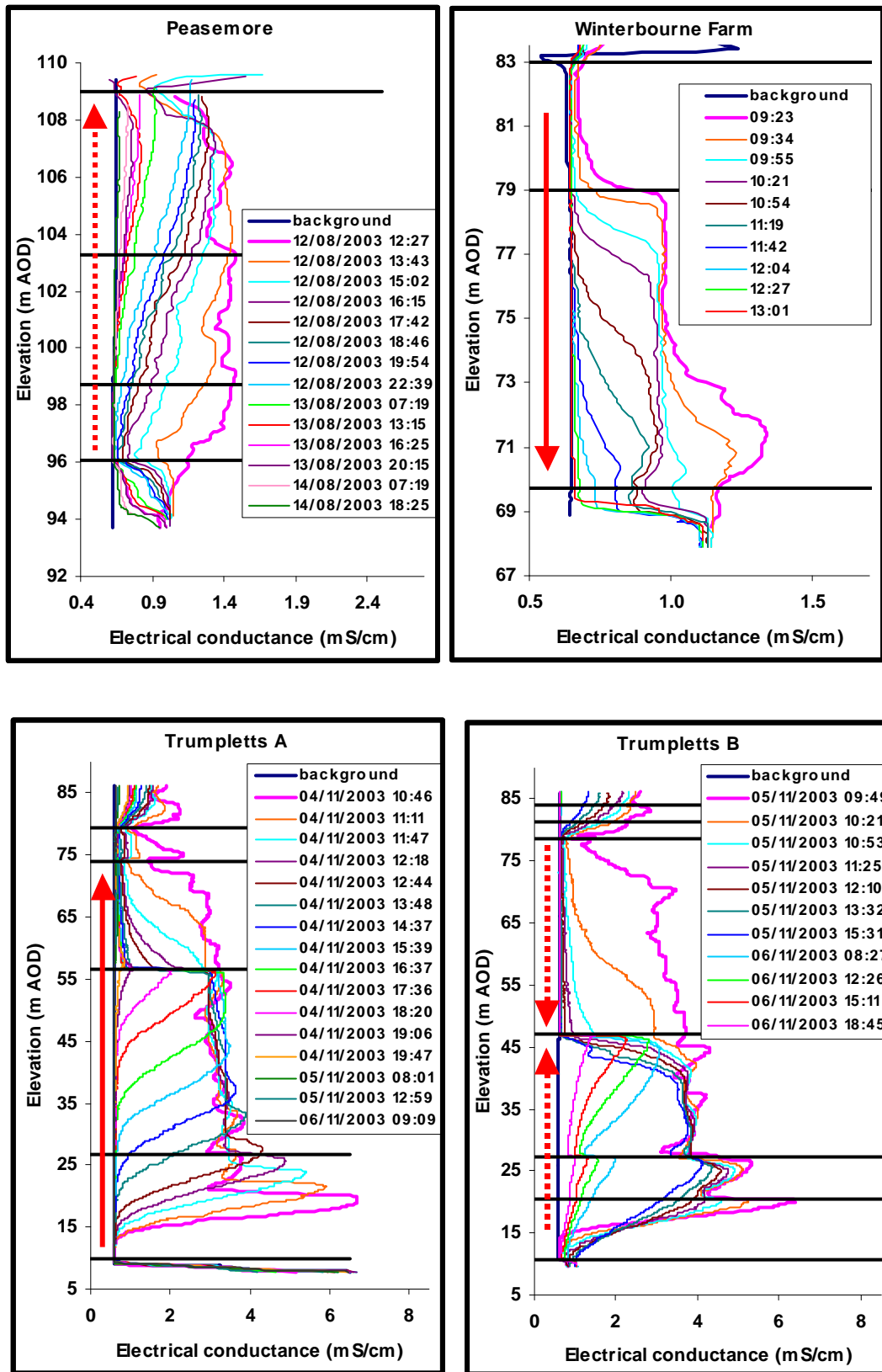


Figure 6.47 (continued)



6.6 The nature of flow horizons

6.6.1 Introduction

Borehole imaging data from 4 sites were used to investigate the types of features present at the location of class 1 flow horizons, and in particular whether dissolutional processes are important. At two of these sites (Trumpletts A and B) the data were obtained for LOCAR using a Makavision optical imager (by Robertson Geologging Ltd.). At the other two sites (Barracks and Gibbet Cottages) data were obtained in collaboration with this study by Alex Gallagher (BGS) using an Electromind optical imager. For each class 1 flow horizon the morphology of the feature and aperture size were recorded and used to determine whether the feature is dissolutional. Features with low aspect ratios or a sinusoidal shape on the image (indicating that the feature was an inclined fracture) were classified as fractures. Features with higher aspect ratios were classified as conduits. Conduits were assumed to be dissolutional. Fractures were classified as dissolutional if there were multiple openings or the aperture was more than 1 cm.

At three other sites (Calversley Farm, Knighton Down and Cow Down), video images were obtained by Dave Buckley and Alex Gallagher (BGS) using a Geovista CCTV sonde. The camera can be switched between a downward and horizontal view of the borehole as it is lowered at a rate specified by the operator (and can be held at a particular depth and panned sideways when in horizontal view). The data consist of a DVD in which there is no scale to enable aperture measurement although many features are clearly visible. It is difficult to investigate the class 1 flow horizons using these data because the camera was not always panned around the borehole at the location of the class 1 flow horizons, and at some, the camera passed the feature very rapidly. Therefore only general observations are made about images from these boreholes.

6.6.2 Visible features on imaging data at class 1 flow horizons

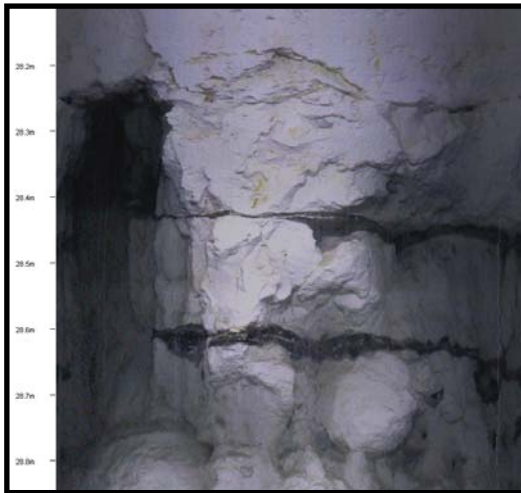
Table 6.28 summarises the morphology and aperture of flow horizons in Trumpletts A and B and Gibbett Cottages. They are also illustrated in Figures 6.48 to 6.50 that are extracts from the image logs at the location of the flow horizons. The results from these three boreholes suggest that small-scale dissolutional processes are important. Of 17 features examined, conduits are present at 7 (41 %), and solutionally enlarged fractures

at 6 (35 %). At 2 (12 %) flow horizons fractures are visible which may be solutionally enlarged and at 2 (12 %) very thin fractures are present.

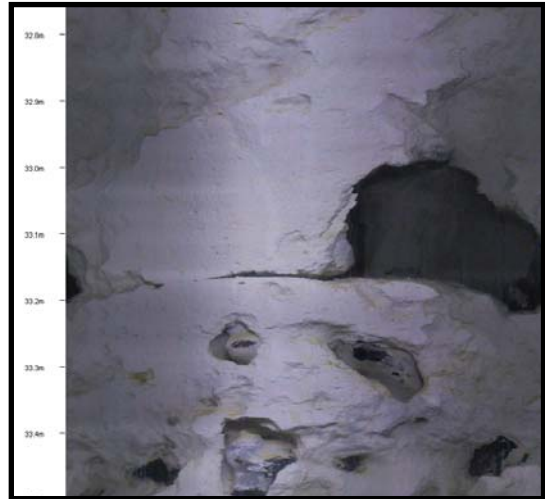
Some general observations can be made about the nature of solutional development at these sites. Individual fractures appear to have very variable apertures and are often characterised by multiple openings suggesting that dissolutional processes have modified the fracture but that this dissolution is erratic and discontinuous. The conduits are on a very small scale. At Gibbett Cottages, solutional features at 95.45 m AOD (about 66 m below ground level) consist of multiple conduits up to 4 cm high on top of a hardground (Figure 6.50c). They resemble the dissolution tubules described by Lamont-Black and Mortimore (2000) that were discussed in Section 1.5.7. The largest conduits are ~ 15 cm high (Figures 6.48 a and b, and 6.50d) and of a similar scale to those observed near the surface in a small quarry (Figure 3.32), and the sediment filled features exposed at Yattendon stream sink (Figure 3.10). The deepest large conduit in Trumpletts A (Figure 6.48b) is about 51 m below ground level, and that in Gibbett Cottages (Figure 6.50d) at about 72 m below ground level demonstrating that conduits can form at considerable depths beneath the surface. At Gibbet Cottages there appears to be sediment in the solutionally enlarged fracture at 87.45 m AOD (Figure 6.50e). This suggests that there is a connected system of fissures and conduits of sufficient size to transport sediment from the surface to this point (about 74 m below ground level).

Table 6.28: Details of features on image logs at the location of class 1 flowing horizons (Gibbett Cottages and Trumpletts A and B)

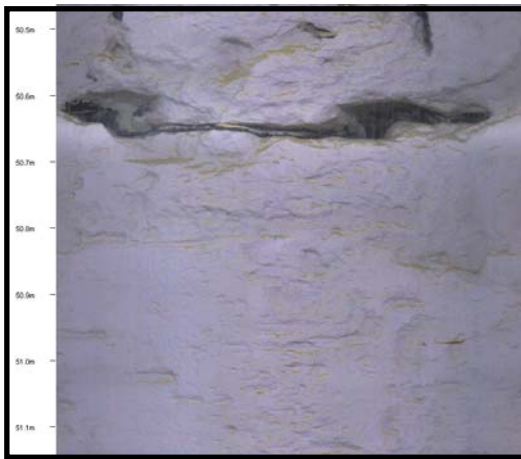
Flow horizon elevation (m AOD)	Image elevation (m AOD)	Morphology	Approximate maximum aperture (cm)	Solutional?
Trumpletts A				
79 to 80	79.4-79.6	Single conduit	15	Yes
74	74.7	Single conduit	15	Yes
56.5	57.2	Fracture, multiple openings	5	Yes
26.7	27.3	Single conduit	1	Yes
9.8 to 10	10.24	Fracture, multiple openings	2	Yes
Trumpletts B				
84	83.7-84	Multiple fractures	0.1	No
81.3	81.3	Fracture, multiple openings	3	Yes
78.7	78.6	Fracture, multiple openings	1	Yes
47.2	47.2	Inclined fracture, multiple openings	1	?
27.3	27.2	Multiple conduits	1	Yes
20.5	20.5	Inclined fracture, multiple openings	1	?
10.6	10.6	Fracture, multiple openings	2	Yes
Gibbett Cottages				
109	109.75	Single conduit	10	Yes
97.85	97.85	Fracture, multiple openings	0.1	No
94.7	95.45	Multiple conduits	4	Yes
89.5	89.25-89.45	Conduit	15	Yes
87	87.45	Fracture, multiple openings	1	Yes



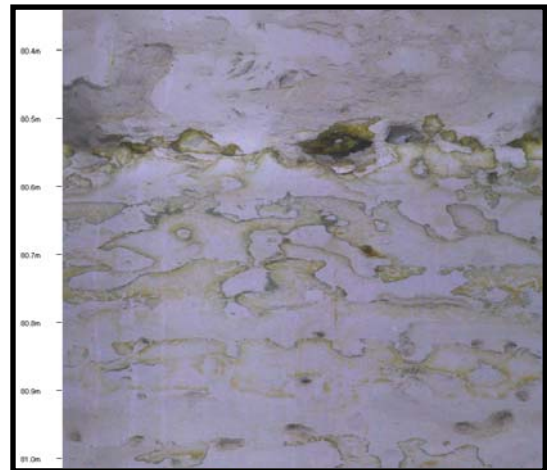
(a) ~15 cm high conduit at 79.4 to 79.6 m AOD on a sheet flint



(b) ~15 cm high conduit at 74.7 m AOD



(c) Solutional fracture (5 cm high) at 57.2 m AOD



(d) ~ 1 cm high conduit at 27.3 m AOD at the top of a hardground



(e) Solutionally enlarged fracture ~ 2 cm high at 10.24 m AOD

Figure 6.48: Images of Class 1 flow horizons in Trumpletts A (tick marks on scale bars are 10 cm apart)



(a) Multiple fractures at 83.7 to 84 m AOD



(b) Solutionally enlarged fracture, up to 3cm high at 81.3 m AOD



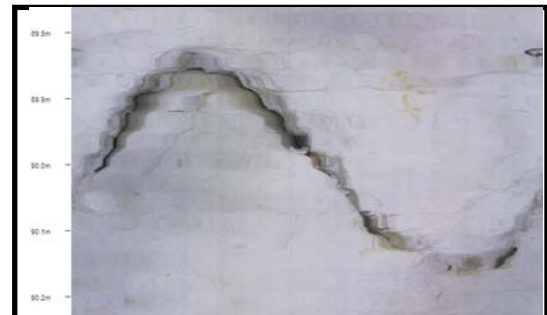
(c) Solutionally enlarged fracture up to 2 cm high at 78.6 m AOD



(d) Inclined fracture possibly solutionally enlarged at 47.2 m AOD



(e) Conduits, aperture ~ 1 cm at 27.2 m AOD on a hardground



(f) Inclined fracture possibly solutionally enlarged at 20.5 m AOD



(g) Solutionally enlarged fracture, up to 3 cm high at 10.6 m AOD

Figure 6.49: Images of class 1 flow horizons in Trumpletts B (tick marks on scale bars are 10 cm apart)



(a) Conduit, ~ 10 cm high at 52.2 m below datum/109.75 m AOD



(b) Thin fracture at 64.1 m below datum or 97.85 m AOD



(c) Conduits up to 4 cm high at 95.45 m AOD on a hardground



(d) Conduit ~ 15 cm high at 89.25 to 89.45 m AOD at a marl horizon,



(e) Solutionally enlarged fracture containing sediment at 87.45 m AOD (~ 74 m below ground level)

Figurer 6.50: Images of class 1 flow horizons in Gibbett Cottages (tick marks on scale bars are 10 cm apart)

At Barracks borehole SBDTs indicate a flow horizon at 45 m AOD, and two others at 110-118 and 70-90 although the exact location of these is not certain. Table 6.29 details the features visible on the image log at these locations. The borehole has upward flow from 45 m AOD, and the location of this inflow is clear because there is no dilution of tracer below 45 m AOD during the uniform injection SBDT (indeed the tracer from the uniform injection in 2003 was still present below 45 m AOD during the point injection in 2007, Figure 6.35b). There are no obvious fractures or solutional features at 45 m AOD on the image log, although there is a feature at 45.4 m AOD that may be a fracture (Figure 6.51a).

As discussed in Section 6.5.3.4, during the point injection SBDT there was little or no tracer loss as the plume moved from 50 to 70 m AOD (Figure 6.35c). Between 45 and 70 m AOD there are only 6 features visible on the image log (Table 6.29) and it is probable that these are either hydrologically inactive or flow through these features is very small. The point injection SBDT demonstrated that there is a flow horizon somewhere between 70 and 90 m AOD because there was a significant loss of tracer mass and decrease in vertical flow rate as the tracer plume passed these elevations (Section 6.5.3.4). However, no single feature can be identified on the image log to account for this. There are 21 small-scale features between 70 and 90 m AOD (Table 6.29). The majority are fractures with multiple openings (e.g. Figure 6.51b) suggesting dissolutional processes have occurred, although the apertures of these multiple openings are sometimes very small (e.g. the top fracture in Figure 6.51b at 86 m AOD). It appears that tracer losses between 70 and 90 m AOD may occur diffusely through many features. Features with multiple openings may be crossflow or outflow only features. The largest feature is a vertical fracture at the top of the zone at 90.7 to 91.4 m AOD (Figure 6.51c), and because this feature comprises a single opening, if active, it must be an outflow only horizon rather than a crossflow horizon.

During the uniform injection SBDT tracer must have been discharged through a flow horizon between 110 and 118 m AOD (Figure 6.35a). The image data suggest that this too may be a zone of diffuse flow through multiple horizons as there are 9 small-scale features present (Table 6.29).

Table 6.29: Features on the image log at the location of flow horizons at Barracks

Flow horizon elevation (m AOD)	Image elevation (m AOD)	Morphology	Approximate maximum aperture (cm)	Solutional?
110 to 118	117	Fracture, multiple openings	2	Yes
	116.2	Fracture	<0.5	No
	115.4	Inclined fracture with multiple openings	1.5	Yes
	115	Inclined fracture with multiple openings	1	Yes
	113.6	Fracture, multiple openings	1.5	Yes
	112-113	Inclined fracture	<0.5	No
	111.6	Fracture, multiple openings	1	Yes
	110.9	Fracture, multiple openings	1	Yes
70 to 90	110.3	Fracture, multiple openings	<0.25	?
	90.7-91.4	Vertical fracture	2	Yes
	87.5	Fracture, multiple openings	<0.5	?
	86	Fracture, multiple openings	<0.5	?
	85.7	Fracture, multiple openings	1	Yes
	84.4	Inclined fracture	<0.5	No
	83.2	Fracture, multiple openings	<0.5	?
	81.9	Fracture, multiple openings	1	Yes
	79.5-79.8	Vertical fracture	1	Yes
	79.1	Fracture, multiple openings	<0.5	?
	78.5	Single conduit	1	Yes
	77.8-78	Inclined fracture, multiple openings	<0.5	?
	77.7	Fracture, multiple openings	1	Yes
	77.2-77.4	Vertical fracture	0.5	?
	77	Fracture, multiple openings	<0.5	?
	76.9	Fracture, multiple openings	1	Yes
	76.3	Fracture, multiple openings	<0.5	?
	76	Fracture, multiple openings	1	Yes
	75.6	Fracture, multiple openings	0.5	?
	74	fracture	<0.5	No
73.7	Fracture, multiple openings	1	Yes	
73	Inclined Fracture, multiple openings	<0.5	?	
45 to 70	66.3	Fracture, multiple openings	1	Yes
	64.4	Inclined fracture, multiple openings	1	?
	59.6	Small opening	0.5	?
	59.2	Fracture, multiple openings	<0.5	?
	56.1	Fracture, multiple openings	1	?
	53.1	Single conduit	1	Yes
45	45.4	Fracture?	<0.5	No



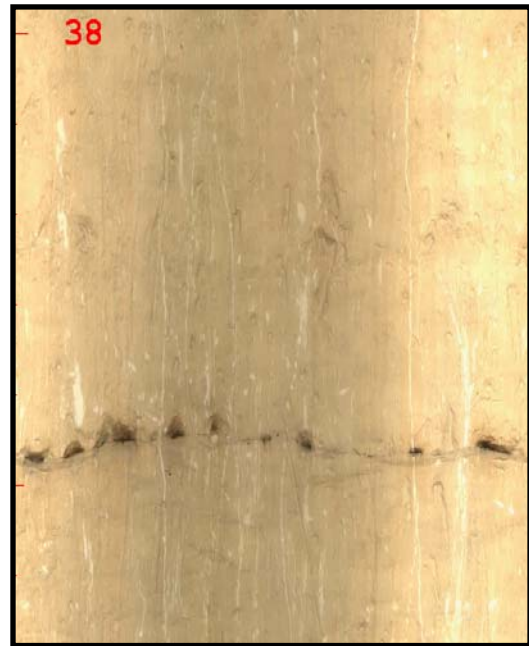
(a) Fracture at 45 m AOD (104 m below datum)



(b) Fractures with multiple openings at 86 and 85.7 m AOD



(c) Vertical fracture at 90.7 to 91.4 m AOD (58 to 58.6 m below datum)



(d) Fracture with multiple openings at 110.9 m AOD (38.45 m below datum)

Figure 6.51: Images from Barracks

Two interesting observations can be made about the DVD images from Calversley Farm and Cow Down boreholes (available from Alex Gallagher, BGS). At Calversley Farm there is a lot of sediment in cavities and protrusions on the borehole walls, and some of the conduits and fissures appear to be sediment floored. The borehole is in karst Zone 1 and is approximately 500 m from the Yattendon stream sink and associated cave passage (Figure 3.8), and is located on a thin layer of Palaeogene cover over the Chalk (the Palaeogene is cased out). It appears that the conduits and fissures in this borehole may be part of the flow system recharged by stream sinks or dolines through which sediment is transported. The sediment-floored features were predominantly up to 4 m above and 7 m below the water table at the time of the imaging log (between 52 and 62 m below ground level). There is also one sediment floored void about 71 m below ground level, although it is not clear from the image whether sediment has fallen down the borehole or been transported through the void. As observed with respect to the feature 74 m below ground level at Gibbett Cottages (Figure 6.50e), the presence of this sediment implies that sediment-laden groundwater recharged through dolines and stream sinks reaches considerable depths in the aquifer, implying that connected systems of fissures and conduits are not restricted to shallow depths.

At Cow Down, imaging data revealed many vertical fractures that extend over several metres of borehole and often appear to be solutionally enlarged. These images demonstrate the occurrence and nature of quite large-scale vertical flow revealing how groundwater can move down through the aquifer. This is rarely observed because vertical boreholes are inherently more likely to intercept horizontally orientated fractures than vertical fractures (Michalski and Klepp, 1990).

6.6.3 Summary

Imaging data demonstrate that dissolutional processes are important at the major flow horizons. At three boreholes groundwater flow in at least 76 % of the major flow horizons identified using SBDTs is through conduits or solutionally enlarged fractures. Dissolutional processes appear to occur up to 100 m below the surface. The largest conduits are about 15 cm high. There are also several examples of horizons or fractures with multiple smaller conduits (4 cm to <1 cm high) that may be similar to the tubule horizons described by Lamont-Black and Mortimore (2000). Many other fractures have very variable apertures, and the images suggest that dissolution occurs in an erratic and

perhaps discontinuous manner. Despite this, there is evidence of sediment at significant depths beneath the surface indicating that a connected system of conduits and fissures of sufficient size to transport sediment is present. Vertical features at Cow Down borehole demonstrate that features exist that can transport groundwater and sediment quite rapidly down through the aquifer, and smaller scale vertical features (e.g. Figure 6.51c) and inclined features (e.g. Figure 6.49f) also reveal vertical aspects of the aquifer structure.

6.7 Catchment scale patterns in the distribution of flow horizons

6.7.1 Introduction

In this section the dataset of class 1 flow horizons is used to investigate the spatial distribution of groundwater flow at the catchment scale. Previous studies suggest that flow horizons decrease with depth below ground level and are more common near the water table (Section 1.3.2.2) and Sections 6.7.2 and 6.7.3 test whether this is supported by the new data. Borehole imaging data show that many of the flow horizons are horizontal features and in Section 6.7.4 the elevations of flow horizons are used to investigate whether they persist laterally both on a local scale and at the catchment scale. Section 6.7.5 considers how catchment scale patterns in upward and downward vertical flow relate to recharge and discharge areas in the aquifer. The data are also used to determine the vertical spacing of flow horizons in the aquifer (Section 6.7.6).

6.7.2 Depth of flowing features below ground level

Table 6.30 lists the number of flow horizons at different depths beneath ground level and the sample size. The sample size for each depth interval was calculated as the number of boreholes in which the entire depth interval was present, uncased and saturated during at least one uniform injection SBDT. Boreholes that only sampled part of the interval were counted by the fraction of the interval each covered. For each 10 m depth interval the number of flow horizons was divided by the sample size to produce a normalised number of horizons per 10 m depth interval. Figure 6.52 shows the distribution of flowing horizons with depth below ground level. The density of flow horizons appears to decrease with depth below ground level as suggested by previous studies (e.g. Allen et al., 1997).

Table 6.30: The number of flow horizons at different depths below ground level

Depth interval (m below ground level)	Number of flow horizons	Sample size	No. flow horizons (normalised)
0-10	0	0.04	0
10-20	11	4.18	2.63
20-30	27	12.37	2.18
30-40	20	11.95	1.67
40-50	18	10.14	1.78
50-60	12	9.78	1.23
60-70	11	8.13	1.35
70-80	8	7.23	1.11
80-90	8	6.3	1.27
90-100	3	4.5	0.67
100-110	1	1	1
110-120	0	0.5	0

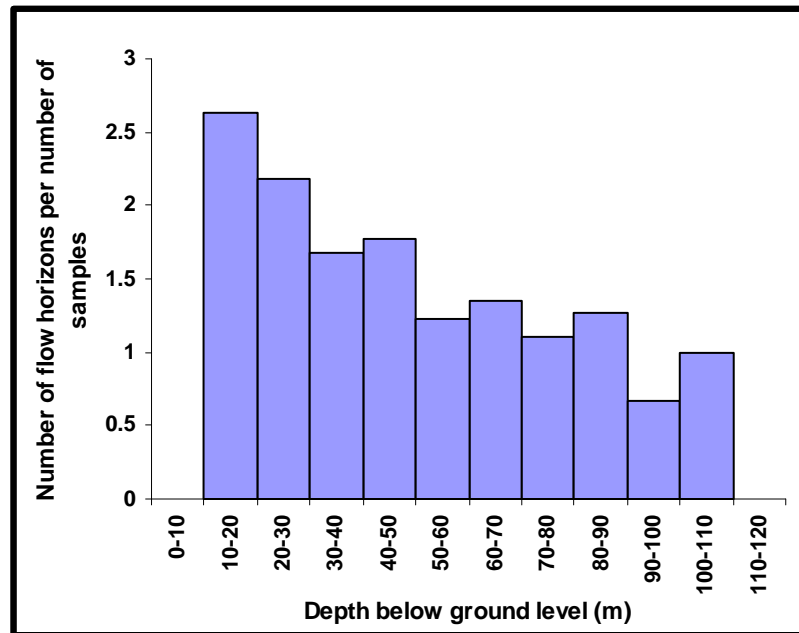


Figure 6.52: Distribution of flowing features with depth below ground level

6.7.3 Depth of flowing features below the water table

Figure 6.53 and Table 6.31 show the distribution of flow horizons with respect to depth below the water table. For each borehole, the water table depth used was an average of the dip measurements during the uniform injection SBDT undertaken under the highest water table conditions. The number of flow horizons within each depth interval was normalised by the sample size (the number of boreholes in which that interval was present and uncased). In general, the density of flow horizons decreases with increased

depth below the water table, as found in previous studies (Allen et al., 1997). The increase between 60 and 80 m may be due to small sample size, as only two boreholes penetrated this interval. More and deeper boreholes extending beyond 80 m below the water table would be required to provide a clearer picture.

Table 6.31: The number of flow horizons at different depths below the water table

Depth interval (m below water table)	No. of flow horizons	Sample size	No. flow horizons (normalised)
0-10	47	15.9	2.95
10-20	28	18.1	1.55
20-30	19	13.1	1.46
30-40	13	9.2	1.41
40-50	5	6.6	0.76
50-60	2	3.9	0.51
60-70	2	3	0.67
70-80	3	2	1.49

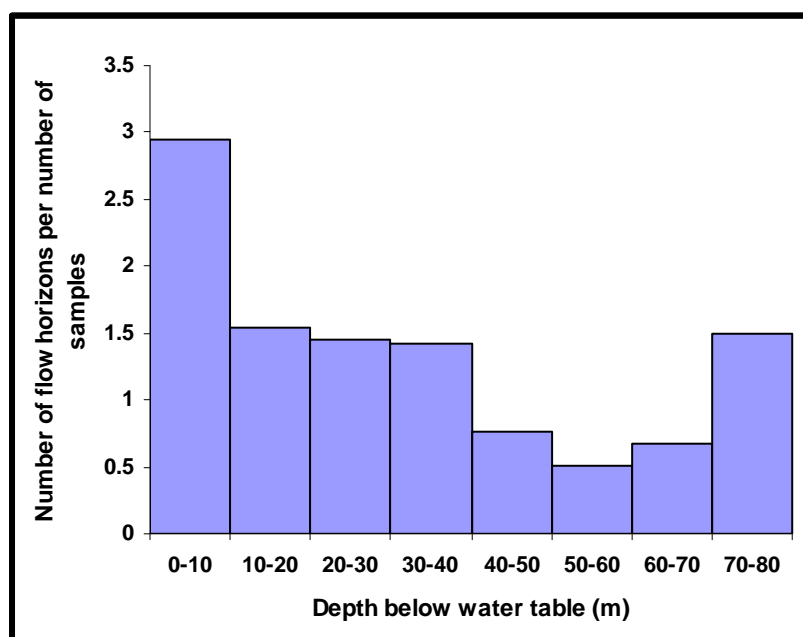


Figure 6.53 Distribution of flowing features with depth below water table

6.7.4 Lateral persistence of flowing features

The elevations of flow horizons were used to investigate whether sub-horizontal flow horizons are laterally persistent. At Frilsham and Trumpletts SBDTs were undertaken in several boreholes less than 50 m apart, providing an opportunity to examine the

persistence of flowing features over this scale. The three Frilsham boreholes are aligned in an approximately ESE-WNW direction with approximately 32 m between C and B (Figure 6.54).

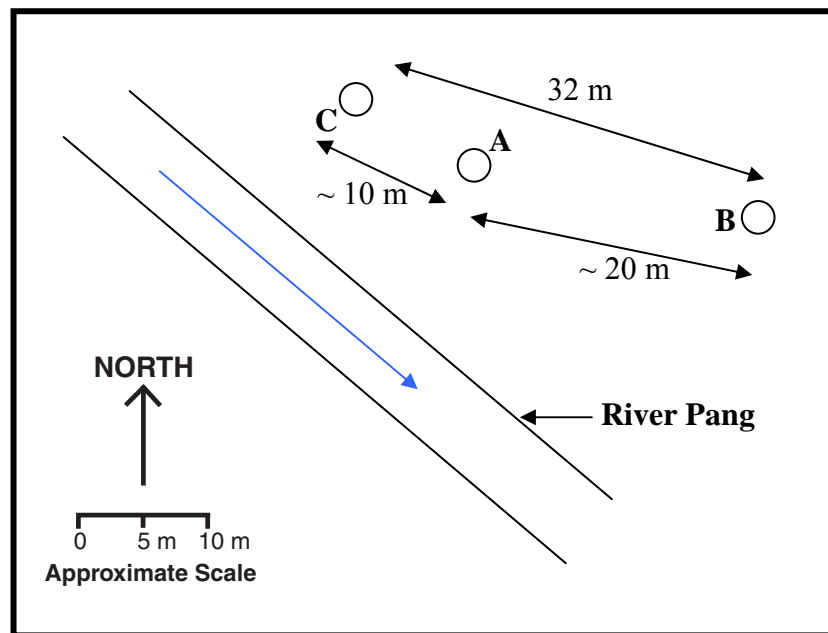


Figure 6.54: Sketch of the layout of Frilsham boreholes (modified from a BGS LOCAR site plan)

Figure 6.55 shows the flow horizons in the overlapping sections of these boreholes (36 to 56 m AOD), colour coded in red, blue and green to indicate those that may persist between boreholes, with black lines representing those that are only present in one borehole. Table 6.32 lists the actual elevations of the flow horizons (also colour coded). Some flow horizons are clearly present at an almost identical elevation in two or three boreholes (e.g. at ~ 38 m AOD in all three boreholes, and at ~ 44 m AOD in Frilsham B and C). Others are at slightly different elevations (e.g. the blue horizon at ~46.5 m AOD in Frilsham B and ~47.5 m AOD in Frilsham C). Three flow horizons are only present in one borehole, but others appear to be present in two or three boreholes suggesting that flow horizons may persist for at least 32 m.

At Trumpletts SBDTs were carried out in two boreholes 45 m apart. There are six flow horizons that appear to be present in one borehole only but three that are at similar elevations in both boreholes (green, red and blue in Figure 6.56 and Table 6.32).

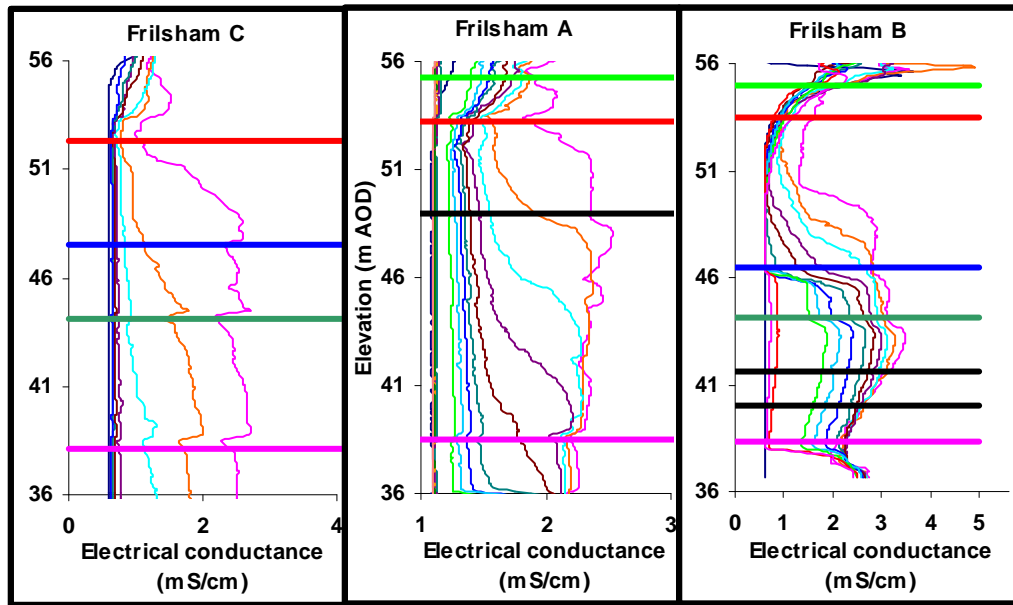


Figure 6.55: Flowing horizons at Frilsham boreholes between 36 and 56 m AOD

Table 6.32: Elevation (in m AOD) of flowing horizons in the Frilsham and Trumpletts boreholes (Within each site elevations in the same font colour may be the same flow horizon and black font represents features only present in one borehole)

Frilsham A	Frilsham B	Frilsham C	Trumpletts A	Trumpletts B
55.3	55	57.1	79 to 80	84
53 to 53.5	53 to 54	52 to 53	74	81.3
48 to 50	46.5	47 to 48	56.5	78.7
38 to 39	44.1	43.5 to 44	26.7	47.2
36	41.5 to 41.7	38.1	9.8 to 10	27.3
	40			20.5
	38.3			10.6

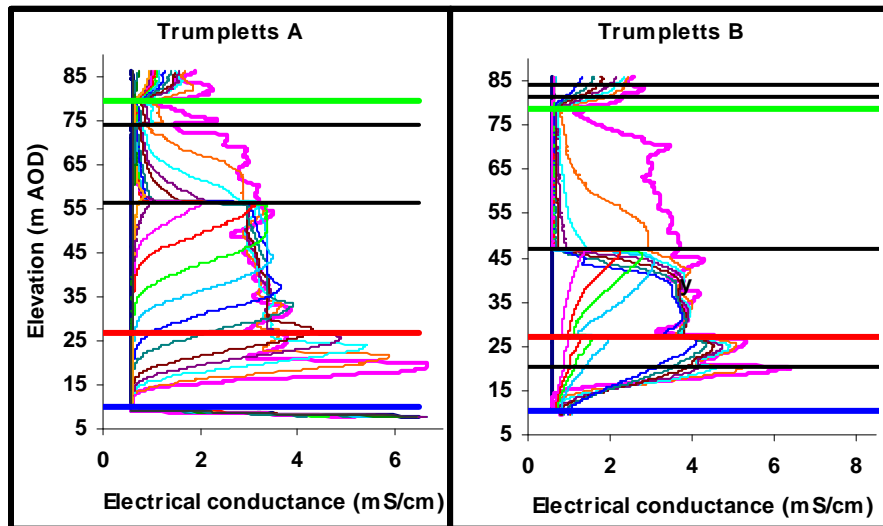


Figure 6.56: Flowing horizons at Trumpletts

The data from Frilsham and Trumpletts suggest that some flow horizons persist laterally for up to at least 45 m. It is probable that these laterally persistent features are bedding controlled. At the catchment scale strata dip approximately $0.5\text{-}2^{\circ}$ towards the SSE. Boreholes at Trumpletts and Frilsham are not orientated down dip, but even assuming the worst case that they were orientated down dip and that the dip were 2° , the downdip displacement between the boreholes would only be 1.6 m at Trumpletts and 1.1 m at Frilsham.

In total 17 features intersecting 1,2, or 3 boreholes were identified. The data suggest that:

- At least 3 (18 %) persist for > 45 m
- At least 7 (41 %) persist for > 30 m
- At least 8 (47 %) persist for > 20 m
- At least 1 (6 %) persists for < 10 m
- At least 3 (18 %) persist for < 20 m

However, at the Frilsham site two flow horizons present in boreholes C and B (at 44 and 47 m AOD) are absent from the intermediate borehole, A (Figure 6.55). This suggests that these opening may be linear or anastomosing.

Taken altogether, the evidence from this sample of 17 flow horizons suggests that sub-horizontal permeable horizons have overall length scales up to at least 45 m. Within each feature there are areas of closed fracture which extend for ~ 10 to 20 m. Borehole imaging evidence suggests that multiple tube-like openings with a variety of diameters (from ~ 0.1 cm to ~ 10 cm) may be common. Figure 6.57 depicts a possible conceptual model of the topology of flowing horizons.

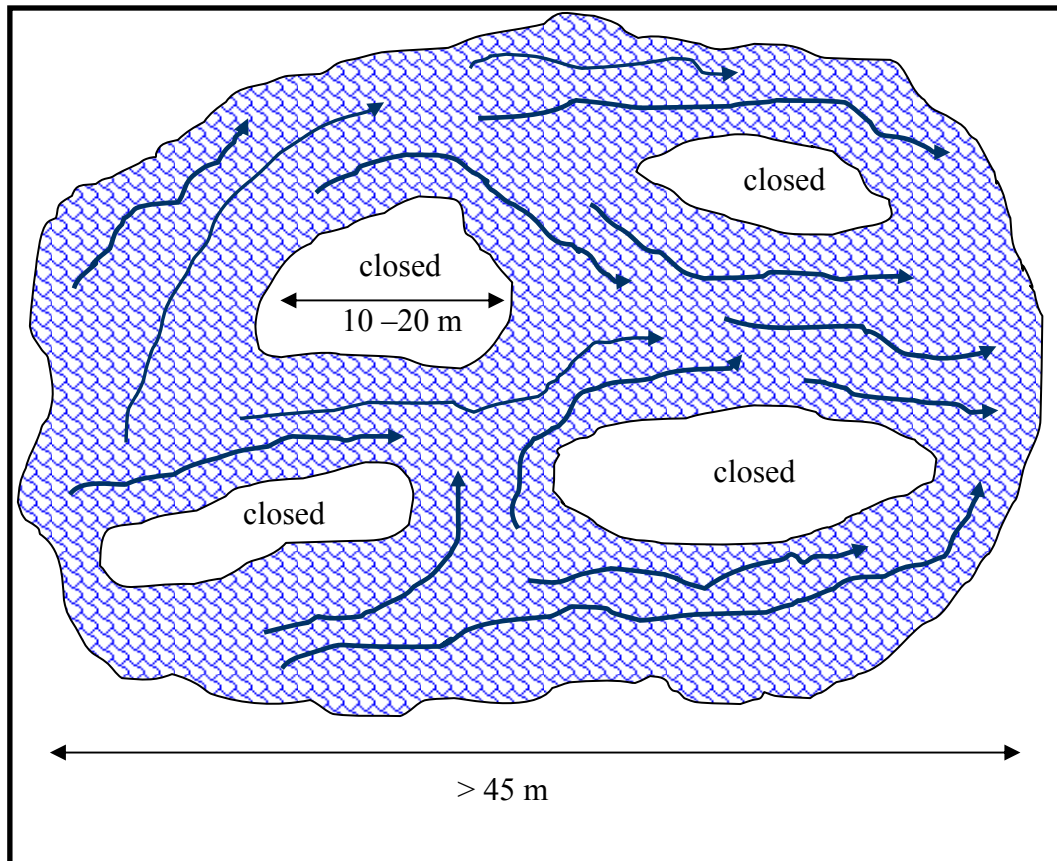


Figure 6.57: Conceptual model for topology of sub-horizontal flow horizons (plan view) showing area of flow persisting at least 45 m (shaded blue with blue arrows) interspersed with areas where fracture is closed (white).

It is not possible to extend this analysis to determine whether there are bedding controlled flow horizons that are laterally persistent at larger scales across the catchments without considering the stratal dip. However, Dave Buckley (personal communication, 2006) has noted a lateral persistence of flow horizons over several kilometres during borehole logging studies. In the current study during field data collection, the most obvious flow horizons immediately apparent from the electrical conductance logs appeared to occur repeatedly at between 55 and 60 m AOD, which is also the elevation of the Blue Pool spring. A previous borehole logging study in the Pang catchment by Schurch and Buckley (2002) also found flowing horizons at 58 m AOD in two boreholes approximately 230 m apart (aligned approximately along the strike) at Banterwick Barn in the Pang catchment. They identified changes in fluid electrical conductance at 58 m AOD, and found solution features on videoscans at these depths. It was one of two flow horizons that persisted between the two boreholes (five other flow horizons were only present in one borehole).

However, when adjusted for sample size, using all the class 1 flow horizons from the present study there is very little difference in the number of flow horizons at particular elevations (Figure 6.58). Sample sizes were very small (≤ 2) between 0 and 15 m AOD, and above 125 m AOD (Table 6.33). Therefore the apparently large number of flow horizons per borehole at some of these elevations is likely to be an artefact of sample size. Between 20 and 115 m AOD there are at least 4 samples in every 5 m interval and the number of flow horizons per sample have a small range from 0.5 to 1.1. There is an apparent slight increase in the number of flow horizons around 55-60 and 90-95 m AOD, but these increases are not significant given the overall small range in the number of flow horizons. It appears that at the catchment scale, there is no clear relationship between flow horizons and elevation.

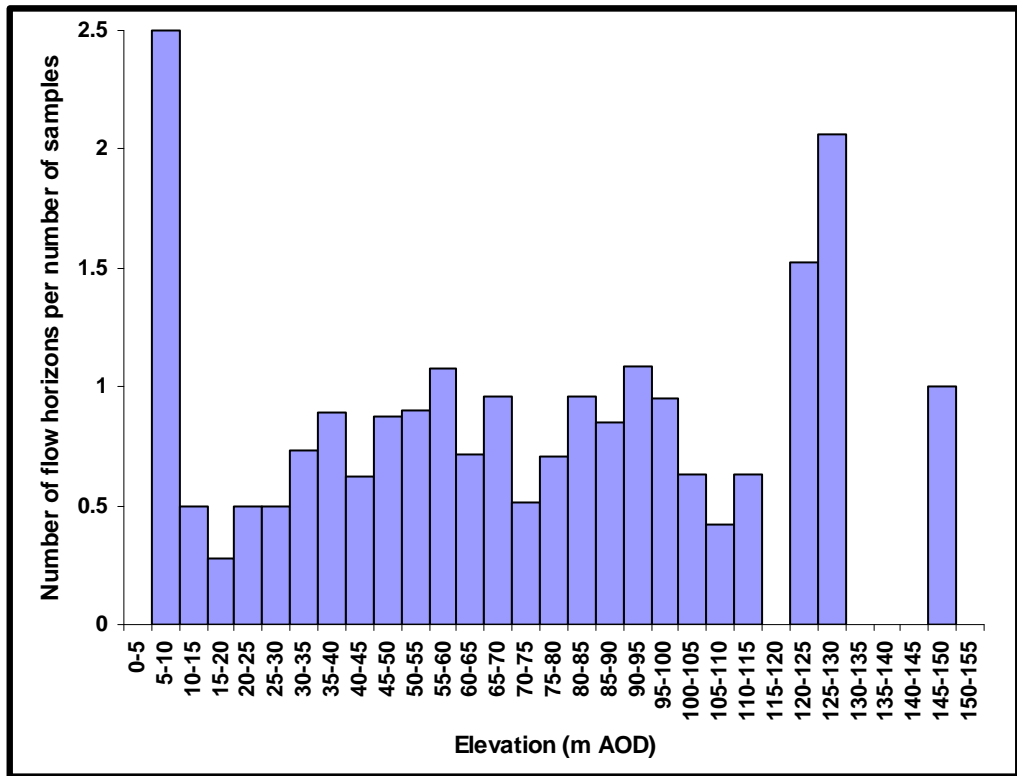


Figure 6.58: Distribution of flow horizons with respect to elevation above sea level

Table 6.33: Number of flow horizons at different elevations above sea level

Depth interval (m AOD)	No. flow horizons	No. Samples	No. flow horizons (normalised)
0-5	0	0	0
5-10	1	0.4	2.5
10-15	1	2	0.5
15-20	1	3.6	0.28
20-25	2	4	0.5
25-30	2	4	0.5
30-35	3	4.1	0.73
35-40	6	6.7	0.9
40-45	5	8	0.63
45-50	8	9.1	0.88
50-55	9	10	0.9
55-60	10	9.3	1.08
60-65	5	7	0.71
65-70	8	8.4	0.96
70-75	4	7.8	0.51
75-80	6	8.5	0.70
80-85	9	9.4	0.96
85-90	7	8.2	0.85
90-95	7	6.4	1.09
95-100	6	6.3	0.95
100-105	4	6.3	0.63
105-110	3	7.2	0.42
110-115	3	4.7	0.64
115-120	0	3.9	0
120-125	4	2.6	1.53
125-130	4	1.9	2.06
130-135	0	1	0
135-140	0	1	0
140-145	0	1	0
145-150	1	1	1
150-155	0	0.54	0

6.7.5 Catchment scale patterns in vertical flow

Vertical flow in boreholes occurs between areas of high and low hydraulic head. Hydrogeological principles suggest upward vertical flow might be expected in discharge areas (river valleys) and downward vertical flow in areas of recharge where groundwater is moving down through the aquifer towards an outlet at a lower elevation with a lower hydraulic head (Michalski and Klepp, 1990). However, this does not seem to be the case in the current study. Figure 6.59 shows the catchment scale patterns in vertical flow identified from the SBDTs. The arrows indicate the direction of vertical

flow, with thick arrows at sites where vertical flow was demonstrated by point injections, and thin arrows where it is inferred from uniform injection SBDTs. The numbers are the elevations of the main outflow horizon with the lowest hydraulic head. In boreholes with several outflow horizons within a section of vertical flow, the elevation of the final outflow horizon is presented because this must be the feature of lowest hydraulic head. The borehole tracer efflux times are also indicated by the size and colour of the circle marking the site.

Eighteen boreholes are in recharge areas (areas away from major river valleys), of which 9 have downward flow, 7 have upward flow, one has both and one has no apparent vertical flow. Upward flow may occur in these boreholes despite being in recharge areas because if they intersect a deep flow horizon with a high hydraulic head upward flow is induced between groundwater bodies that would otherwise be unconnected (and flowing separately down gradient towards groundwater outlets).

It is more difficult to explain why boreholes in river valleys (normally discharge areas) have downward vertical flow because groundwater head should be lowest at the surface. 7 boreholes are in river valleys of which only one has straightforward upward flow towards the river (Bockhampton). The limited data obtained from Great Shefford (Figure 6.10) suggest that there may also be upward flow towards the river at this site, which is adjacent to springs (Section 3.4.2.2).

Bagnor borehole is a few hundred metres from major springs (Jannaways and Bagnor). There is upward flow in this borehole to 69-70 m AOD (just below the bottom of the casing), but there is also downward flow to 56.5 m AOD. This suggests that the flow horizon at 56.5 m AOD is more permeable than that at 69-70 m AOD and may provide a less resistant route to the nearby springs (at ~ 84 m AOD). This would imply that the springs are fed, at least in part, by deep groundwater and also that high permeability vertical features are present in the vicinity of the springs to transmit groundwater up from 56.5 to 84 m AOD. An alternative hypothesis is that the borehole intercepted and joined two isolated flow systems, one discharging at the springs and a deeper system associated with the flow at 56.5 m AOD that discharges elsewhere, perhaps at the Speen public water supply boreholes.

At the three Frilsham boreholes, the situation is also complex. There is rapid downward vertical flow in all three boreholes suggesting the River Pang at Frilsham may be perched above, and not hydraulically connected to the main chalk aquifer. However, flow accretion, probably from groundwater, does occur over the reach that includes the Frilsham site (Section 2.7) although the exact location of groundwater inflows is not clear and no spring discharges have been observed in the vicinity of the Frilsham boreholes. Borehole casing extends to ~ 15-20 m below ground level and it is possible that shallow chalk groundwater within cased out sections of the borehole is in hydraulic continuity with the river. Nevertheless, in Frilsham A the feature with the lowest hydraulic head, (as indicated by the vertical flows in the borehole), is at 35.5 m AOD, and in the deep borehole, Frilsham C, at 20.25 m AOD (Table 6.34). In both boreholes these main outflows are near the bottom. There is both very slow upward and rapid downward flow to the main outflow in Frilsham B at 46.5 m AOD that is 10 m above the bottom of the borehole. It is possible that there are features of lower hydraulic head at depths below the bottom of Frilsham B (36.6 m AOD). For example the borehole is not deep enough to intersect the feature at 35.5 m AOD that is the main outflow horizon in Frilsham A. The data generally suggest that at Frilsham hydraulic head decreases with depth beneath the surface because the boreholes that penetrated deeper elevations had deeper main outflows (Table 6.34). Measured flow rates also suggest that deeper features have lower hydraulic head because downward vertical flow rates are higher in boreholes that intersect deeper flow horizons.

Given the lack of major discharge into the River Pang at this site and the apparent decrease in hydraulic head with depth below ground level it seems unlikely that there is a major vertical flowpath from the lowest major outflow (20.25 m AOD) transmitting water upwards to discharge into the River Pang which is 60 m higher. These experiments appear to demonstrate underflow beneath the River Pang (as suggested by groundwater contours, Figure 2.13) implying that the main flow system is disconnected from the river and that groundwater flow is towards the Blue Pool or the River Thames. Interestingly, in the deepest borehole (Frilsham C) the main outflow (20.25 m AOD) is considerably lower than the elevation of the Blue Pool (~58 m AOD) and the confluence of the Pang and Thames rivers at Pangbourne (~ 40 m AOD). This implies that at the catchment scale groundwater flowpaths develop at depth perhaps along the lines of a Ford (2000) “state 3” model of subsurface karst development (Figure 1.16).

Table 6.34: Main outflow elevation and maximum and average flow rate down to outflow (based on the migration of tracer peak during point tracer injections) in the Frilsham boreholes

Borehole	Bottom of borehole (m AOD)	Elevation of main outflow (m AOD)	Maximum flow rate (m.d ⁻¹)	Average flow rate (m.d ⁻¹)
Frilsham B	36.6	46.5	288	105
Frilsham A	34.5	35.5	297	154
Frilsham C	16.6	20.25	645	508

The Winterbourne Farm borehole is adjacent to the Winterbourne Stream, but also has rapid downward flow to near the bottom of the borehole (69-70 m AOD). There are no springs in the vicinity of the borehole suggesting that there may be poor connectivity between the stream and the underlying Chalk aquifer. The main outflow horizon in the borehole is at the same elevation (69-70 m AOD) as major outflows in the three nearest boreholes (Figure 6.59), possibly indicating that permeability is well developed at this elevation in the area.

Overall, the catchment scale patterns in vertical flow are clearly very complex and a full interpretation is difficult. However, the results do suggest that permeability is developed deep in the aquifer, even to beneath the level of groundwater discharges in the catchments.

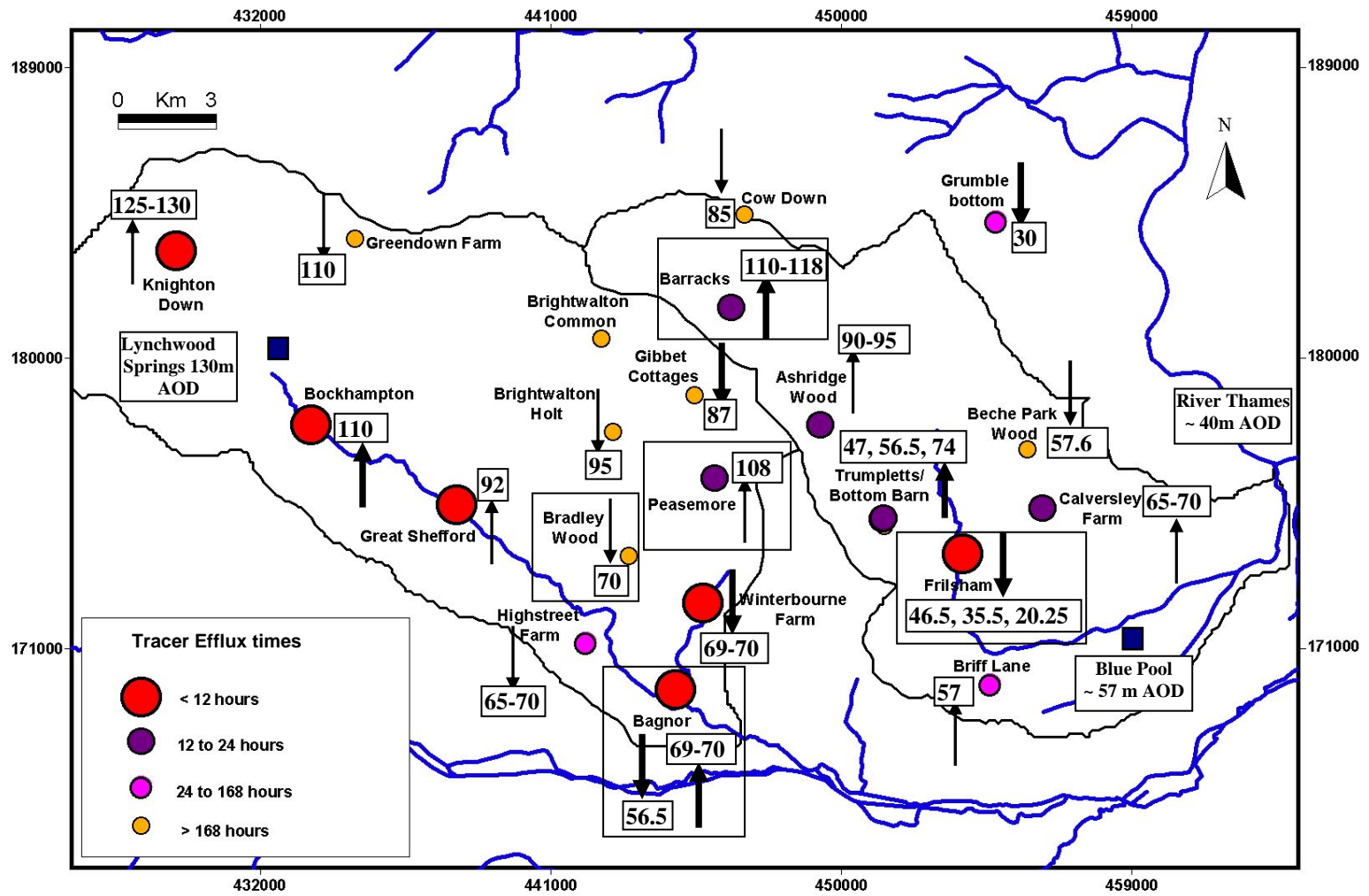


Figure 6.59: Patterns in vertical flow in boreholes. Arrows indicate direction of vertical flow, numbers are elevations of outflow horizon at top/bottom of vertical flow

6.7.6 Spacing of flowing features

The results of the SBDTs suggest that flowing horizons occur relatively frequently (in total 119 flow horizons were identified in 24 boreholes). The results also demonstrate that there is considerable variation in the number of flow horizons present in boreholes. In some there are very few flow horizons (e.g. Brightwalton Common in which there are no flow horizons in a total saturated depth of 20.3 m, and Greendown Farm in which there is one flow horizon in a total saturated depth of 47.2 m). In others there are much higher densities of flow horizons. The highest density occurs in Knighton Down borehole in which there are 9 flow horizons in a total saturated depth of 22.1 m. Previous analyses (Sections 6.7.2 and 6.7.3) showed that the frequency of flow horizons decreases with depth below ground level and depth below the water table. The spacing of flow horizons is clearly not regular and therefore any general estimate of an “average” spacing must be used cautiously. Nevertheless, average spacing is a useful means of aquifer characterisation.

Obtaining an accurate estimate of spacing is difficult because there is an inevitable sample bias towards closely spaced features. This is because the location of the next flow horizons that would be encountered above and below the top and bottom of a borehole is unknown. An average spacing could be derived by measuring the distance between flow horizons, but this increases the bias because boreholes that intercept less than two flow horizons are excluded. The least biased estimate is to divide the total saturated length of each borehole by the number of flow horizons. The spacing of flowing features in the 24 boreholes using this method is presented in Table 6.35. The overall average spacing is 8.8 m. At shallower depths below the surface and below the water table, the spacing is likely to be lower than this, while at greater depths it may be considerably higher.

Table 6.35 also shows the tracer efflux times (discussed in Section 6.4.1) and the topographical situation and karst zone of the boreholes. There is no immediately apparent relationship between the spacing of flow horizons and tracer efflux times. Tracer is not diluted more quickly from boreholes with more Class 1 flowing features. This may in part be because rapid dilution is normally associated with vertical flow and therefore tracer from a long section of borehole flows out through a particular point without the need for a large number of flow horizons. Boreholes with more closely

spaced flowing features occur in all three karst zones. However, boreholes in which the average spacing of flowing features is greater than 7 m all occur in karst zones 2 and 3. The average spacing of flowing features in boreholes in river valleys is always less than 6 m, but the average spacing of flowing features in boreholes in dry valleys and interfluves is extremely variable.

Borehole	Total sample depth	No. flow horizons	Spacing (m)	Efflux time (hrs)	Fastest efflux time (hrs)	Topography	Karst Zone
Knighton Down	22.1	9	2.5	< 12	< 12	edge of major dry valley	3
Calversley Farm	20.75	8	2.6	12 to 48	12 to 48	interfluve	1
Ashridge Wood	13	5	2.6	12 to 48	12 to 48	edge of dry valley	2
Frilsham B	20	7	2.9	12 to 48	< 12	river valley	1
Frilsham A	26.9	8	3.4	< 12	< 12	river valley	1
Bottom Barn	20.4	6	3.4	> 168	48 to 168	interfluve	2
Cow Down	19.5	5	3.9	> 168	48 to 168	interfluve	3
Peasmore	15.7	4	3.9	12 to 48	< 12	in major dry valley	2
Briff Lane	18.2	4	4.6	48 to 168	48 to 168	interfluve	1
Bagnor	13.8	3	4.6	< 12	< 12	river valley	1
Winterbourne Farm	15.4	3	5.1	< 12	< 12	river valley	1
Grumble bottom	48.6	9	5.4	48 to 168	< 12	in minor dry valley	3
Beche Park Wood	21.9	4	5.5	> 168	< 12	interfluve	2
Bockhampton	40.5	7	5.8	< 12	< 12	river valley	3
Frilsham C	41.2	7	5.9	< 12	< 12	river valley	1
Highstreet Farm	23.8	4	6.0	48 to 168	< 12	edge of minor dry valley	1
Gibbet Cottages	32	5	6.4	> 168	< 12	in minor dry valley	2
Bradley Wood	30.7	4	7.7	> 168	12 to 48	major dry valley	2
Trumpletts B	76.25	7	10.9	12 to 48	< 12	in minor dry valley	2
Trumpletts A	80.6	5	16.1	12 to 48	< 12	in minor dry valley	2
Brightwalton Holt	18.3	1	18.3	> 168	12 to 48	edge of minor dry valley	2
Barracks	83.8	3	27.9	12 to 48	<12	in minor dry valley	3
Greendown Farm	47.2	1	47.2	> 168	48 to 168	in minor dry valley	3
Brightwalton Common	20.3	0		> 168	> 168	interfluve	3

Table 6.35: The spacing of flowing features (sorted in ascending order), with other factors for comparison

6.8 Summary and Conclusions

Using SBDTs to identify flow in boreholes

This chapter has demonstrated how the SBDT method can be used to enable flowing fractures to be identified in boreholes. Forward modelling has demonstrated how the location of flow horizons relates to the patterns in tracer logs obtained during uniform injection SBDTs. Point injection SBDTs undertaken in conjunction with uniform injection SBDTs were found to provide useful additional evidence for the location of flow horizons as well as clearly identifying vertical flow in boreholes.

The study demonstrated that flowing horizons can be identified from uniform injection SBDTs using the following criteria:

- If there are nick points or steps in multiple electrical conductance logs.
- If there was a sharp boundary between zones of faster and slower dilution.
- At the top and bottom of vertical flow inferred from the movement of a tracer “front” up or down the borehole

If point dilution data are available flow horizons can be confirmed/identified at:

- The top and bottom of a section in which vertical flow is occurring (often confirmed by tracer loss at that depth)
- Depths within sections of vertical flow at which there is tracer loss and/or a change in flow rate.

The identification of flow horizons using SBDTs could be further developed and improved in future by considering the effects of variable diameter and the time taken to lower the electrical conductance probe down the borehole. The field data could be modelled to obtain actual values of flow and it is probable that a unique solution could be obtained by using the results of both point and uniform injection tests in the same borehole. These modifications were not undertaken in the present study because of time constraints and because flow horizons could be reliably identified without them.

Tracer Efflux Times

Uniform SBDTs were also used to obtain a “tracer efflux time” defined as the time taken for tracer to be replaced by aquifer water. Tracer efflux times were found to relate to topography in a similar manner to transmissivity. Results at four sites where

transmissivity data are available suggest the tracer efflux time may be a function of transmissivity, in which case SBDTs could provide a cheap and easy method of obtaining information on transmissivity. However, more data are required to establish the reliability of the relationship.

The nature and distribution of flow horizons

The identification of 119 flow horizons in 24 boreholes in the Pang-Lambourn catchments enables some inferences to be made about the nature of the aquifer:

- There is a general decrease in the frequency of flow horizons with depth below ground level and below the water table, confirming the results of previous studies of the Chalk (Allen et al., 1997).
- Flow horizons have an average spacing of 8.8 m. However, this number must be treated cautiously because it is an underestimate due to inevitable sample bias, because spacing increases with depth, and because spacing is generally very variable.
- Data from multiple boreholes at two sites demonstrated that some but not all flow horizons persist laterally for up to 45 m.
- Imaging data demonstrated that at least 13 of the 17 flow horizons that could be clearly viewed on image logs are solutionally enlarged fractures or small conduits. This suggests that solutional processes are important in the Chalk and that many of the major flow horizons in chalk boreholes may be solutional.

Vertical development of permeability

Many flow horizons observed on the image logs are horizontal or slightly inclined, suggesting that they may be bedding controlled structures, and that bedding structures may be a major control on flow in the Chalk. This implies that vertical development of permeability in the Chalk may be relatively less important than horizontal development of permeability. However, boreholes are inherently more likely to intercept horizontal flow horizons than vertical flow horizons. The results of this study provide some evidence that vertical development of permeability occurs in the Chalk:

- Solutional vertical features were directly observed in image data at Cow Down borehole.
- At the Frilsham river valley site rapid downward flow to the horizon of lowest head at 60 m below the surface (20 m below the level of the River Thames) suggests

development of permeability at depth in the aquifer and the existence of vertical features transmitting groundwater to and from these depths.

-Flow horizons are sometimes present up to 80 m below the water table and 110 m below ground level, and imaging data indicate that some of the deeper flow horizons show evidence of dissolution. This might imply significant vertical development of permeability to produce a fully connected system of larger voids enabling water undersaturated with respect to calcium carbonate to reach these depths. However, solutional development at depth could also be due to mixing corrosion or possibly *in situ* sources of acidity such as nodular or dispersed pyrite.

- Imaging data show sediment in deep flow horizons. This indicates that there must be a connected system of fissures and conduits of sufficient size to enable transport of sediment from the surface to these depths, and implies that permeability is developed in a vertical as well as horizontal direction.

This study therefore shows that vertical development of permeability does occur in the Chalk but the controls on where this occurs and the extent to which this occurs remain uncertain.

Chapter 7: A conceptual model of the structure of the Chalk aquifer and its relation to geomorphology

7.1 Introduction

In this concluding chapter results from the surface karst survey, tracer testing between stream sinks and springs, and SBDTs will be used collectively to draw inferences about the likely structure of the aquifer and how this relates to surface geomorphology. The aim is not to reiterate full or quantitative details of the experimental inferences, arguments and probabilities developed in the thesis; instead the reader is referred to the relevant sections in earlier pages. The aim here is to provide a broad conceptual overview of how the findings in this thesis contribute to the general understanding of the nature and structure of the Chalk aquifer and to assess the nature and extent of karst development. Three specific questions will be considered:

- What is the structure of voids in the Chalk?
- To what extent are the four components of the aquifer (matrix, fractures, fissures and conduits) connected, between types and among voids of the same type?
- How does subsurface solutional development of voids in the Chalk relate to surface geomorphology?

7.2 The structure of voids with water flow in the Chalk

7.2.1 General distribution of flow

As discussed in Chapter 1, the Chalk aquifer is divided into four components, the matrix, fractures, fissures and conduits although groundwater flow in the matrix is negligible. A network of fractures unaffected by dissolution is thought to increase chalk permeability to $\sim 0.1 \text{ m.d}^{-1}$ and transmissivity to $\sim 20 \text{ m}^2.\text{d}^{-1}$ (Price, 1987). Several UK field surveys (reviewed in Section 1.3.1) suggest that these fractures are spaced at intervals of 0.1 to 1 m. However, the fracture network cannot account for the high transmissivities observed in the Chalk, which are thought to be due to the presence of solutional modification of fractures to form fissures (Price, 1987). Previous investigations (reviewed in Section 1.3.2.2) found that chalk transmissivity is highest in river valleys and also suggested that flowing fissures are most commonly found in the zone of water table fluctuation and associated with specific lithological or

stratigraphical horizons. SBDTs in 25 boreholes in this study aimed to investigate further the distribution of actively flowing horizons. Tracer efflux times, a new parameter obtained from SBDTs that appears to relate to transmissivity, were also found to be consistently rapid in river valley boreholes (Section 6.4.1). The SBDT technique was developed to enable flowing horizons to be identified (Section 6.5) and actively flowing features were found to have an average spacing of ~ 9 m (Section 6.7.6) although as in previous studies the frequency of flow horizons was found to decrease with depth below ground level and depth below the water table (Sections 6.7.2 and 6.7.3).

7.2.2 Structure, size and lateral extent of dissolutional voids

Borehole imaging data were used to investigate the structure of voids present at the location of flow horizons identified from SBDTs. Results suggest that a large proportion of flow horizons are affected by dissolution (of 17 features examined in detail 13 displayed clear signs of dissolution). Dissolutional widenings observed on image logs of borehole walls are on a scale of ~ 0.001 to ~ 0.15 m and may represent irregular widenings of fractures, or more circular shaped tubules and conduits (Figure 7.1). Conduits of ~ 0.15 m are also exposed in a quarry in the Pang (Section 3.7) and at the stream sink cave at Yattendon (Section 3.3.4). Imaging data and field data suggest tubules and conduits may sometimes have a lithological/stratigraphical control because they tend to be associated with flint layers (e.g. Figure 6.48a and b), hardgrounds (e.g. Figure 6.48d and Figure 6.50c), and marl layers (e.g. Figure 6.50d), as suggested by previous chalk studies (Section 1.3.2.2).

Flow occurs through inclined and vertical fissures (discussed below), but many are horizontal or near horizontal suggesting they are bedding plane controlled. These fissures may extend laterally in the x and y direction (Figure 7.1), but estimating their persistence is difficult. It is probable that they extend further in the y direction of groundwater flow than in the x direction. Rapid groundwater flow between stream sinks and springs (past studies reviewed in Section 1.3.5, and new tracer tests described in Chapter 4) suggest conduits/large fissures may on occasion be laterally extensive over several kilometres. SBDTs demonstrated that some flow horizons occur at the same elevation in boreholes up to 45 m apart (Section 6.7.4). However, SBDTs also showed that particular flow horizons do not always occur in all boreholes at the same

site suggesting that there may be closed areas within otherwise laterally extensive areas of flow (Figure 6.57). Borehole imaging data also suggest the lateral extent of solutional enlargement of fractures may be quite limited because openings appear irregular and often do not persist across the entire circumference of the borehole (e.g. Figure 6.48e and Figure 6.49c). A likely explanation is that although in some areas conduits and fissures may be laterally extensive, in many areas the larger solutional voids peter out in the y direction as well as the x direction. The scale at which this occurs is uncertain and is discussed further in Section 7.3.

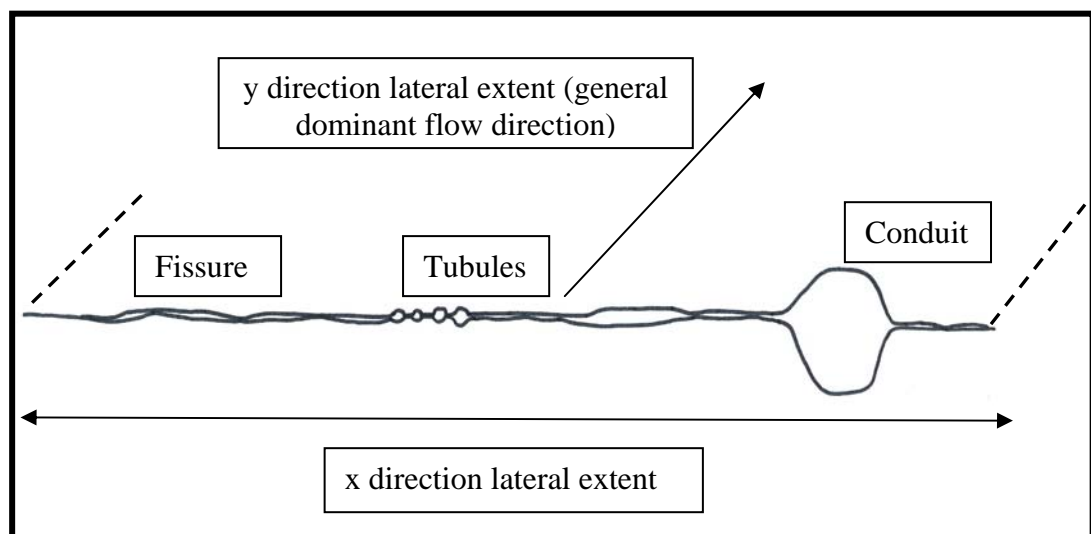


Figure 7.1: Cross section of fracture enlarged to create fissures, tubules and a conduit.

Larger scale conduit development is known to occur in the Chalk although it appears to be fairly rare in the UK (Section 1.5.7). Caves exposed in cliff faces in Sussex have heights and widths up to several metres (Section 1.5.7). In the Pang Lambourn study area the Yattendon stream sink cave is an example of larger scale conduit development (a void ~0.3 m wide, ~ 5 m deep and extending forwards for at least 5 m to a corner). Flow in caves and conduits is one dimensional (in the sense illustrated in Figure 1.4). The longitudinal extent of these larger conduits is uncertain although the Sussex caves are several hundred metres in length.

7.2.3 Vertical development of permeability

Borehole imaging data indicate there are inclined and vertical fractures that could connect horizontal areas of high permeability. Sediment within flow horizons at

considerable depths below the surface also implies the existence of high permeability vertical features. Downward vertical flow in boreholes to outflowing horizons well below the levels of springs and rivers (e.g. at Frilsham, Section 6.7.5) also suggest that vertical permeability must be developed, along which groundwater flow would rise to these outlets. In places fissure pathways may even have some degree of phreatic looping as described in the Ford (2000) “state 3” karst model (Figure 1.16).

7.3 Connectivity between void types

The lack of lateral persistence of many horizontal flow horizons demonstrated by the SBDTs and the imaging data suggest that conduits, fissures and fractures may be well connected to each other. In many instances conduits and fissures may continue for relatively short distances before petering out causing flow to continue in smaller voids. The high attenuation during tracer tests from stream sinks in the Pang-Lambourn (Section 4.9) supports this hypothesis as illustrated in Figure 7.2. In previous tracer tests from Hampshire (Atkinson and Smith, 1974) and Hertfordshire (Harold, 1937), and also in the test from Smithcroft Copse in the current study, tracer attenuation was relatively low suggesting that there is a fully connected network of conduits and larger fissures between the stream sinks and springs (lower part of Figure 7.2). However, in the Smithcroft Copse test ~ 75 % of the tracer was lost and a multi tracer test at this site (Chapter 5) indicated that this is due to transport down multiple pathways with much of the dye tracer being dispersed into smaller fissures and fractures from which it was attenuated, probably by double porosity diffusion into the matrix.

Dye tracer was totally attenuated in the Mirams Copse test but a later test from this site using a bacteriophage demonstrated very rapid groundwater flow (Sections 4.4 and 4.5). This suggests that only a very small amount of tracer was transported down a flowpath comprising conduits and larger fissures, and that many of the pathways include sections through smaller fissures and fractures in which the dye tracer was attenuated (middle part of Figure 7.2).

Bacteriophage show the same contrast in attenuation between Smithcroft Copse and Mirams Copse tests as dyes, but this is presumably due to sorption for which there will be much more opportunity in narrow fissures and fractures. Bacteriophage concentrations following injection at Cromwells stream sink were very low and similar

to those during the Mirams Copse tracer test suggesting that the flowpath may have similar characteristics, although there may have been much greater losses at the Cromwells injection point where tracer had to pass through thick fine organic rich sediments (Section 4.6)

In the most extreme cases it appears that all pathways include one or more sections of flow through smaller fissures and fractures causing total loss of bacteriophage tracer (upper part of Figure 7.2). The evidence that this occurred during the test from Frilsham Sink is fairly convincing because of its' location up gradient and in between Smithcroft Copse and Mirams Copse which are both connected to the Blue Pool (Figure 4.1). It is however possible that attenuation of tracer injected into Honeybottom stream sink was due to losses in the Palaeogene and/or the unsaturated zone because of the extremely low flow in the stream sink at the time of the test (Section 4.6.2).

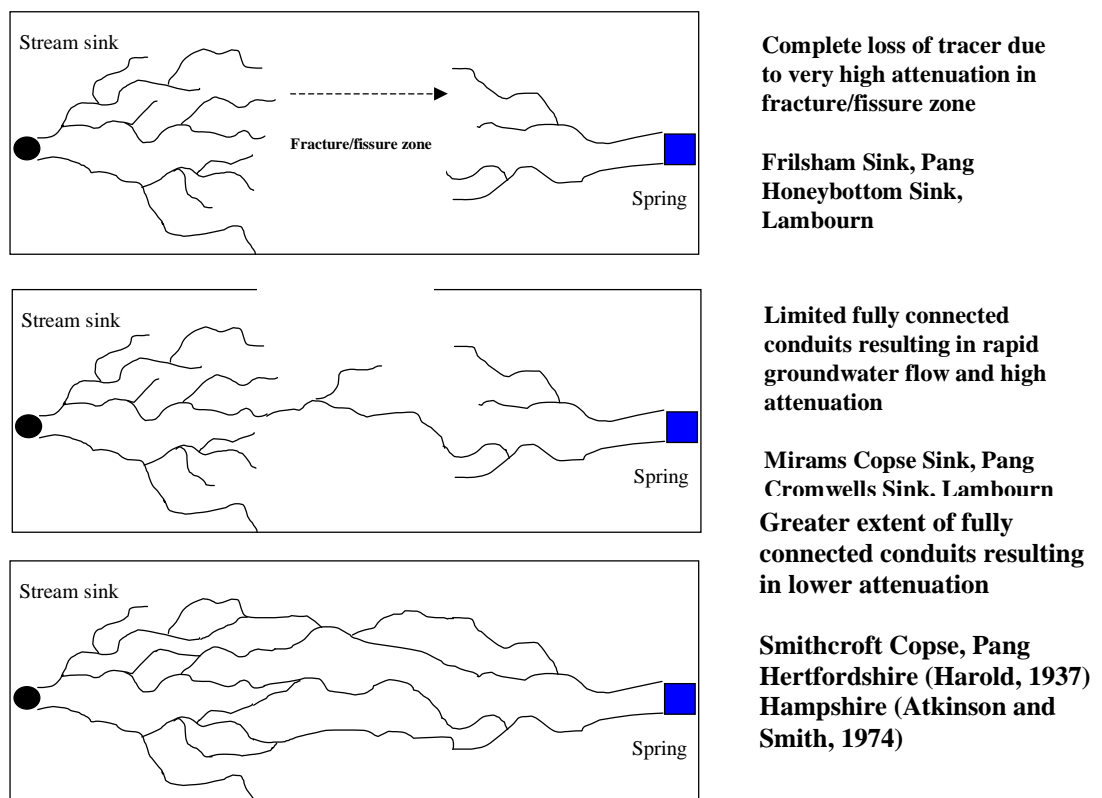


Figure 7.2: Conceptual model of the nature of groundwater flowpaths suggested by tracer testing between stream sinks and springs

Occasionally fully connected networks of conduits and fissures develop between stream sinks and springs. However much of the aquifer appears to comprise localised areas of largely bedding controlled conduits and fissures embedded within a network of fractures. In these areas, the scale over which conduits and fissures persist and are fully connected is very uncertain. One possibility is that heterogeneity occurs at an intermediate scale of 10s or 100s metres. In this case fractures are solutionally enlarged to form conduits and fissures in particular areas (perhaps because groundwaters of different chemistries meet causing local dissolution due to mixing corrosion) separated by areas of lower permeability. These bedding controlled areas of conduits and fissures may occur at vertical intervals ~ 9 m (Section 6.7.6) but it is likely that they become less common with depth below the surface. The degree of vertical connectivity through fissures between these areas is very uncertain, but clearly does occur in some places. There are also probably variations in the degree of connectivity at larger scales across the catchments. It is likely that conduits and fissures are more connected and persistent in river valleys and dry valleys where transmissivity has been demonstrated to be high (Sections 1.3.2.2 and 6.4.1). It is also possible that the distribution of conduits and fissures relates to surface karst geomorphology and this is considered below.

7.4 Surface karst geomorphology and permeability

7.4.1 Stream sinks and dolines

In the Pang and Lambourn catchments, the density of dolines is highest where there is a thin Palaeogene or Clay-with-Flints cover overlying the Chalk (Section 3.5). Some of these dolines may be relict stream sinks that have subsequently become dry as the Palaeogene cover eroded leaving insufficient impermeable ground to generate surface runoff. However, many dolines are likely to be suffosion dolines (Section 1.5.3) that can form if there is a connected network of relatively small fissures. The high density of dolines suggests that there may be fairly frequent networks of these smaller fissures.

There is also a high density of stream sinks focused along the Palaeogene/Chalk boundary (Figure 3.1). Some of these are “seepage sinks” (Section 3.3.3) from which only a very small amount of water enters the ground and there is no distinct hole through which water sinks. These appear to form in areas away from surface streams by very local infiltration of surface runoff or discharge from small Palaeogene springs. The water is aggressive enabling some dissolution of the underlying chalk, but a mature

connected fissure or conduit system does not develop because there is insufficient water entering the ground at a single point. Many seepage sinks are not associated with a doline suggesting that they are immature features.

Most larger stream sinks are located within small valleys that form tributaries to the major river valleys or larger dry valleys they flank. It is likely that before the stream sink was formed, the streams would have provided surface runoff to the major valleys. Field observations suggest several phases in the evolution of the more significant stream sinks. Initially there was a thick Palaeogene cover overlying the Chalk (as in the area to the south of the Pang). Surface streams flowed on the impermeable strata (a present day example is the Bourne stream, Figure 2.4). When the Palaeogene eroded sufficiently to leave only a thin cover overlying the Chalk, stream sinks developed in locally permeable areas as illustrated in Figure 7.3.

The stream flowed over the Palaeogene (stage 1) until it eroded through the deposits sufficiently to become hydrologically connected to the underlying chalk (stage 2). At this stage there were small seepage losses through the streambed, but comprising a small proportion of the total water in the stream. Water infiltrating the Palaeogene gradually dissolved the underlying chalk until small fissures and conduits began to drain water from the stream. This may have led to the development of partial sinks (stage 3). Over time the fissure/conduit system developed sufficiently to capture all the flow from the stream. Doline sinks evolved as material was eroded from the area surrounding the sink point and transported away through the aquifer (stage 4). Initially the stream may have overflowed down the valley in wet weather periods, but eventually the doline deepened creating a stream sink in which all water sinks (stage 5). The now dry valley beyond may be at a higher elevation than the upstream active valley reflecting incision of the active valley since the abandonment of the downstream dry valley (e.g. Figure 3.6). These stages will only be completed if there continues to be a supply of water to the stream sink. Note also the direction of groundwater flow may be different to the direction of the surface stream.

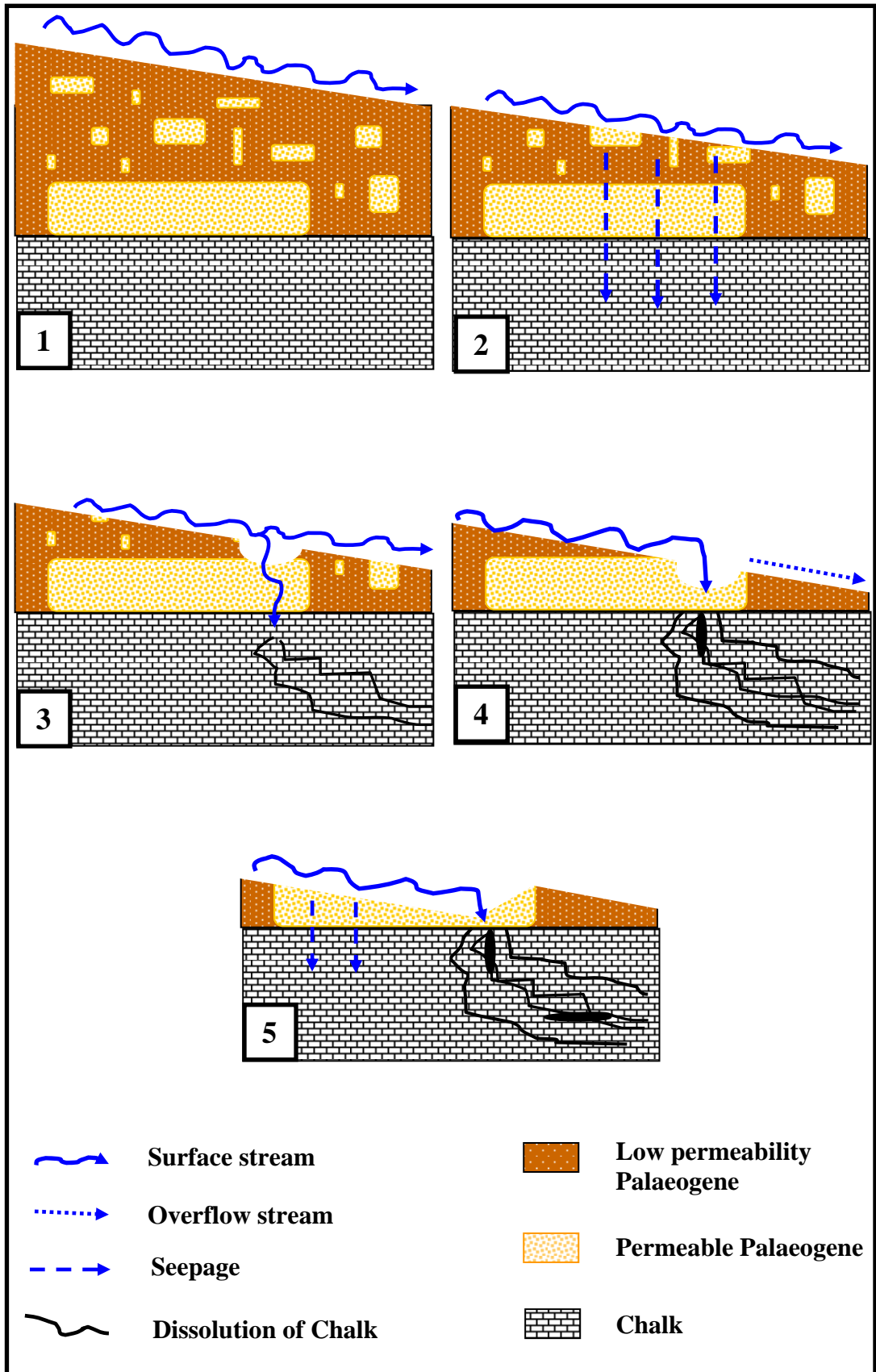


Figure 7.3: Geomorphological evolution of stream sinks where a surface stream flows over Palaeogene deposits overlying the Chalk

7.4.2 Permeability and removal of Palaeogene cover

In Section 3.2 the Pang Lambourn catchments were divided into three zones reflecting the distribution of surface karst that becomes progressively less prevalent with distance from the Palaeogene margin. A key question is whether subsurface solutional development also differs in the three zones. The presence of active stream sinks in Zone 1 and the proven connections to springs suggest that small-scale subsurface fissure/conduit development occurs in Zone 1. It is possible that solutional fissures and conduits become less common with distance from the Palaeogene margin. However, the Palaeogene once covered these areas of the Chalk, and depending upon how quickly erosion caused the edge of the former cover to retreat down-dip, fissure/conduit systems fed by stream sinks may have once been common in Zones 2 and 3 (Figure 7.4). If the depth of solutional development exceeded the thickness of rock removed by erosion in the period since the Chalk was locally exposed, these conduits and fissures could still exist. The modern hydrogeological function of such relict conduits is unclear but they could potentially provide rapid flowpaths in the unsaturated zone, and perhaps through parts of the saturated zone. SBDTs and imaging data from the present study suggest that fissure and conduit development does occur at considerable depths in the aquifer and that fissures and conduits are present in the saturated zone of Zones 2 and 3. Some of these features may be relict features that were initiated in the past by stream sinks providing aggressive point recharge to the Chalk. However, it is also possible that solutional features could develop without stream sink inputs due to the effects of mixing corrosion (which might occur fairly frequently if the aquifer comprises a dense network of multiple pathways made up of fractures, fissures and small conduits).

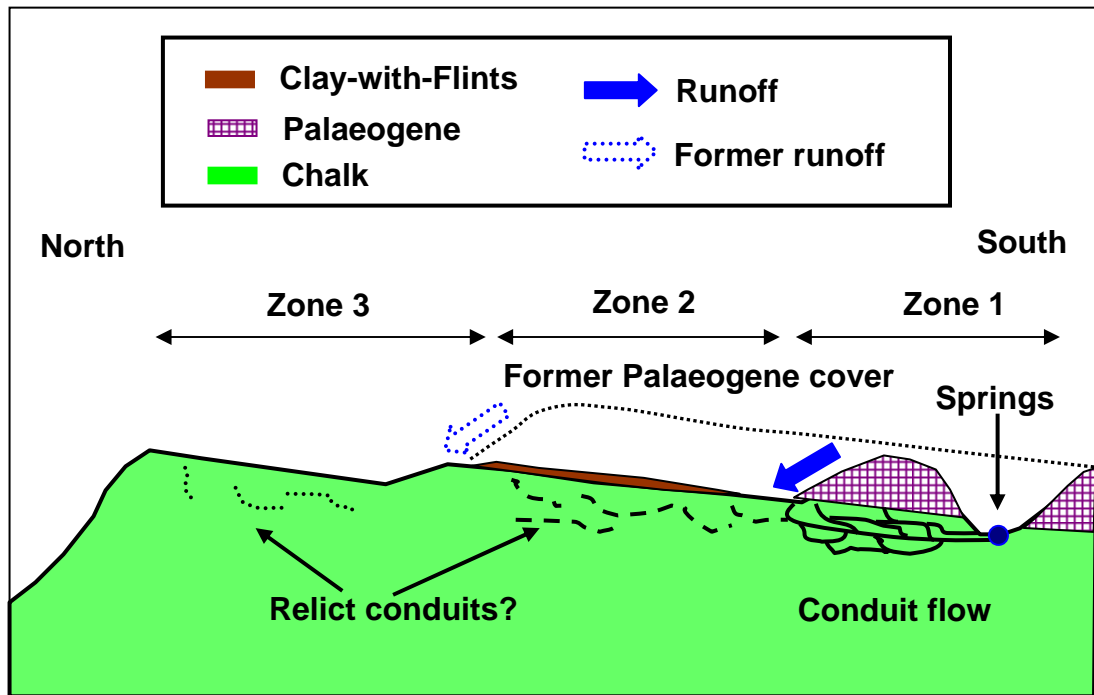


Figure 7.4 Schematic north-south cross section of Palaeogene retreat

In zones 2 and 3 there have been very few catchment scale tracer tests because there are no stream sinks and the location of rapid flowpaths are unknown. A single tracer test has been reported from the equivalent of Zone 2 from a soakaway in the Chalk, around 4 km from the Palaeogene margin at Bricket Wood in Hertfordshire (Price et al., 1992). Although tracer injection was not into a surface karst feature, velocities of 2 km.d^{-1} proved rapid groundwater flow can occur in the absence of surface karst. Very low recoveries ($<0.01\%$) imply a very high degree of attenuation for both dye and bacteriophages as seen in some of the Pang-Lambourn tracer tests in Zone 1. There have been no tracer tests from Zone 3 areas in unglaciated chalk, but two unpublished results from the formerly glaciated Chalk aquifer in East Anglia indicate velocities $\sim 0.1 \text{ km.d}^{-1}$ over distances of up to 1.5 km (Atkinson, personal communication, 2005). Attenuation was extremely great, as in the test in Zone 2 by Price et al., (1992). The high attenuation in both zones probably reflects flow in fractures and fissures with relatively small apertures.

It appears that subsurface karst may be fairly similar in all three zones. Very high attenuation during tracer tests from stream sinks in Zone 1 during the present study is similar to that observed by Price et al (1992) in Zone 2 suggesting that conduit

development in Zone 1 may be relatively limited and similar to Zones 2 and 3. The main karst spring, the Blue Pool, has a high base flow and no apparent significant increase in discharge following rainfall also implying only a small proportion of flow is supplied by a connected conduit network. Conduits and fissures clearly occur in the saturated zone of Zones 2 and 3 and rapid groundwater flow demonstrated by Price et al (1992) suggests that small-scale subsurface karst may be developed in Zones 2 and 3 in a similar manner to Zone 1. However, new tracer tests in Zones 2 and 3 are needed to investigate this further.

The primary difference between the Zones is that stream sinks in Zone 1 provide point recharge to the aquifer and enable likely connected systems of fissures and conduits between the surface and springs or boreholes to be identified. The presence of these connected flowpaths also suggests that there is a higher risk of turbidity and transient pollutants affecting abstraction boreholes and springs in Zone 1 than in Zone 2 and 3 where risk may be locally high but difficult to predict.

7.5 Evaluation of the Chalk as a karstic aquifer

Chalk landscapes have clear signs of karstification with frequent stream sinks, dolines, dry valleys, and large springs, some of which are characterised by turbidity following rainfall. Groundwater flow between stream sinks and springs can be extremely rapid indicating a fully connected local network of conduits and large fissures. However, there is also clear evidence that the extent of karstification is slight compared to classical karst aquifers. Springs, although sometimes large, have high baseflows and do not have variable discharges or rapid responses to precipitation. Tracer tests from stream sinks often show very high attenuation of tracer indicating flow down smaller pathways. The Chalk aquifer seems to comprise a network of fractures, fissures and conduits that are connected to each other. Subsurface dissolution is very common, but perhaps because it occurs so frequently the aquifer comprises lots of fractures displaying small-scale solution enlargement, sometimes in the form of tubules and small conduits, whilst the development of larger caves is extremely rare. Chalk karst resembles the early stages in speleogenesis (e.g. Ford, Lauritzen and Ewers, 2000; Dreybodt and Siemers, 2000; Ford and Williams, 2007) when there are many inputs and pathways and dissolution has not concentrated along a very small proportion of possible flowpaths to create large-scale cave development. Figure 7.5 shows the results of a

gypsum model of the early stages of speleogenesis along a single flowpath by Ewers (1982). Figure 7.6 shows a conceptual model of speleogenesis with multiple inputs (Ford and Williams, 2007) that is similar to the situation in the Pang-Lambourn where there are large numbers of stream sinks and dolines providing multiple inputs to the aquifer. Both these figures depict flow systems comprising multiple pathways in which not all conduit systems connect between the input and output point as appears to be the case in the Chalk.

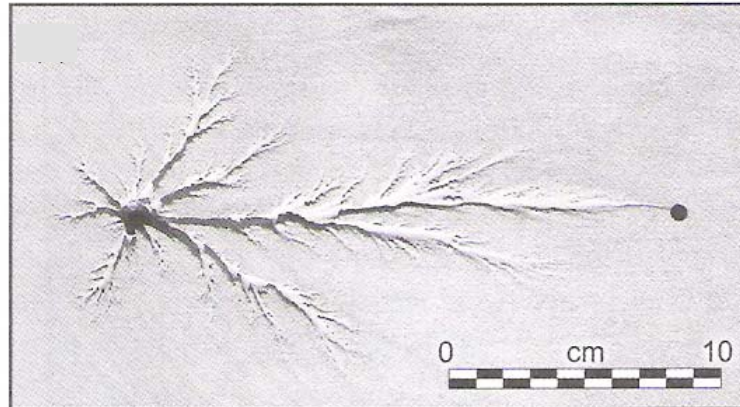


Figure 7.5: Hardware simulation of proto-cave propagation through a bedding plane fissure using plaster of Paris (gypsum). From Ford and Williams (2007) but originally from Ewers (1982)

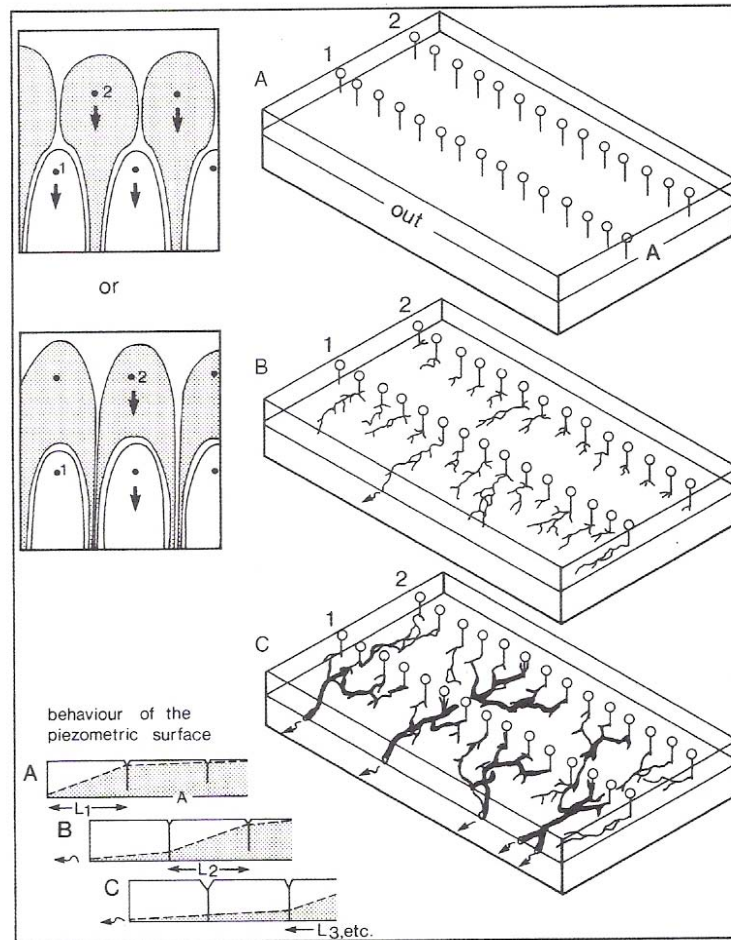


Figure 7.6: Initiation of cave systems with multiple ranks of inputs (From Ford and Williams, 2007)

In summary, the findings of this thesis confirm and re-emphasise some aspects of our existing understanding of the Chalk:

- Field survey of karst features in the Pang and Lambourn catchments highlights the importance of the Chalk/Palaeogene margin in the development of stream sinks. The implication of this is that there is a higher risk of contamination of groundwater by short residence time non-persistent contaminants (e.g. microbial pathogens and pesticides) in Zone 1 Chalk karst areas than in Zones 2 and 3
- Groundwater flow between stream sinks and springs can be extremely rapid over many kilometres and comparable to flow velocities in highly karstic aquifers. This implies the presence of a fully connected system of conduits/large fissures along the flowpath.
- Attenuation of tracers/contaminants along flowpaths between stream sinks and springs can be very low.

- Occasional small-scale cave development occurs in the Chalk in England but large-scale caves do not occur.
- SBDTs and imaging logs have confirmed that solutional processes can occur deep in the Chalk aquifer (up to 80 m below the water table and 110 m below ground level).

This thesis has improved our knowledge and understanding of the Chalk by demonstrating that:

- The density of stream sinks around the Palaeogene/Chalk margin is much higher than previously thought. Recharge of the Chalk through the Palaeogene is an important process that should be considered in any conceptual or mathematical models of chalk catchments.
- Rapid groundwater flow between stream sinks and springs can be combined with very high attenuation and low tracer recoveries. Tracer test results from this study suggest that flowpaths comprise multiple pathways enabling some tracer to be transported rapidly whilst much of the tracer is attenuated to below the detection limit as it travels along flowpaths comprising smaller voids.
- Low tracer attenuation appears to be less common than previously thought, and it is likely that many flowpaths between stream sinks and groundwater outlets include sections of smaller voids in which high attenuation can occur.
- Small-scale karst conduits and fissures probably occur more frequently in the Chalk than was previously thought, and results of SBDTs suggest that they are common in Zones 2 and 3 where there is less surface karst as well as in Zone 1 where there is a high density of surface karst.
- SBDTs and imaging logs have suggested that there is some vertical development of permeability in the Chalk, but the controls on where this occurs and how extensively it occurs remains poorly understood.
- Solutional modification of fractures to form fissures and small conduits appears to be commonly discontinuous. This implies that mixing corrosion or possibly in-situ sources of acidity must be important to enable solutional enlargement in isolation, particularly at depth in the aquifer.

This conceptual model of karst development in chalk is mainly applicable to areas of the UK Chalk where there are adjacent Palaeogene strata that lead to stream sink development as in the Pang and Lambourn study area. It seems probable that in chalk areas where stream sinks have not developed in this manner, there may be less subsurface dissolution, although the role and effectiveness of mixing corrosion in creating small-scale localised fissures and conduits in the Chalk is poorly understood and mixing corrosion may be an important process in the Chalk.

The Chalk is clearly very mildly karstic compared to the main karst aquifers in the UK (the Carboniferous Limestone and the Durness Limestone). Small-scale surface karst features (stream sinks and dolines) appear to be more common in the Chalk than in the Magnesian and Jurassic Limestones although this may be in part due to the presence of adjacent relatively low permeability strata producing acidic soils (the Palaeogene). Subsurface karst (fissures and small conduits) may be developed to a similar degree in the Chalk as in the Magnesian and Jurassic Limestones. However, both these aquifers have lower storage than the Chalk and small caves are more commonly encountered suggesting that karst development may have progressed further than in the Chalk.

It is unclear why the scale of karst development is so much greater in France (Section 1.5.7). The French chalk is overlain by loess which results in the formation of similar stream sinks to those observed in the Pang and Lambourn and other areas of the UK. The chalk in Caumont Cave and the Petite Dalles Cave (Figures 1.22 and 1.23) appears quite hard and it is possible that this has enabled larger scale cave development. It is also possible that there is a lower fracture frequency in the French chalk enabling flow to focus along a smaller number of flowpaths. Further work to compare the characteristics and geomorphological history of the French and English chalks would be required to understand the apparent differences in the degree of karstification.

7.6 Thesis conclusions

This thesis has demonstrated a number of features of groundwater flow in the Chalk aquifer. Groundwater flow is very rapid between stream sinks and springs, but is accompanied by attenuation that in many cases is extremely high. The causes of the attenuation are complicated. A multi-tracer test along the Smithcroft Copse-Blue Pool connection (the first experiment of its kind over a long distance) showed that diffusion is a minor process of attenuation along the main rapid flowpath and suggested that there are multiple flowpaths comprising a connected network of conduits, fissures and fractures. Tracer losses are due to distributary flow from conduits or larger fissures into narrower fissures and fractures from which diffusion and sorption occurs. Tracer tests from other stream sinks confirm aspects of this model.

The single borehole dilution technique was developed to enable the identification of flowing horizons in boreholes to investigate groundwater flow in all areas of the catchment. SBDT results and borehole imaging data suggest that solutional enlargement of fractures to form fissures, tubules and small conduits is common in all areas of the Chalk of the Pang and Lambourn catchments, but in many cases sections of conduits and fissures may have quite limited lateral extent.

There is a clear spatial pattern in the density of surface karst that relates to the distance from the Palaeogene cover. However there are fissures and conduits in Zones 2 and 3 away from the Palaeogene margin and rapid groundwater flow has been demonstrated from a tracer injection into a soakaway in the equivalent of Zone 2 in Hertfordshire (Price et al., 1992). This suggests that the subsurface permeability structure of the Chalk may be similar in all three Zones. The main difference is that in Zone 1 stream sinks provide point recharge to the aquifer and may be actively connected to springs thereby increasing the risk of turbidity or poor water quality in springs and boreholes. In zones 2 and 3 subsurface solutional development may be relict (having developed when stream sinks were present) but it plays an active role in the modern groundwater flow system.

References

- Aldiss, D. T., Marks, R.J., Newell, A.J., Royse, K.A., Hopson, P.M., Farrant, A.R., Aspden, A.J., Napier, B., Wilkinson, I.P., Woods, M.A., 2002. The geology of the Pang-Lambourn catchment, Berkshire. *British Geological Survey commissioned report CR/02/298N*. 38 pp
- Aldous, P.J., Fawell, J.K., and Hunt, S.M., 1987. The application of Photine C when used as a groundwater tracer. *Wrc report PRU 1544-M*. 14 pp
- Allen, D.J., Brewerton, L.J., Coleby, L.M., Gibbs, B.R., Lewis, M.A., MacDonald, A.M., Wagstaff, S.J., and Williams, A.T., 1997. The physical properties of the major aquifers in England and Wales. *BGS Technical Report WD/97/34, Environment Agency R&D Publication 8*. 312 pp
- Allshorn, S.J.L., Bottrell, S.H., West, L.J., and Odling, N.E., 2007. Rapid karstic bypass flow in the unsaturated zone of the Yorkshire chalk aquifer and implications for contaminant transport. In *Natural and Anthropogenic Hazards in Karst Areas: Recognition, Analysis and Mitigation*. *Geological Society of London Special Publication 279*, 111-122
- Ashley, R.P., Lerner, D.N., and Lloyd, J.W., 1994. Distribution of diesel oil in the unsaturated zone following an oil spill on a chalk aquifer. *Journal of Hydrology* **159** (1-4), 43-59
- Atkins, 2003. *Kennet Valley groundwater model*. Draft report by Atkins consultancy (held at BGS)
- Atkinson, T.C., 1977. Diffuse flow and conduit flow in limestone terrain in the Mendip Hills, Somerset (Great Britain). *Journal of Hydrology* **35**, 93-110
- Atkinson, T.C., Smith, D.I., Lavis, J.J., and Whitaker, R.J., 1973. Experiments in tracing underground waters in limestones. *Journal of Hydrology* **19**, 323-349

Atkinson, T.C. and Smith D.I., 1974. Rapid groundwater flow in fissures in the Chalk: An example from South Hampshire. *Quarterly Journal of Engineering Geology* **7**, 197-205

Atkinson, T.C., and Smart, P.L., 1981. Artificial tracers in hydrogeology. In *A survey of British Hydrogeology 1980: London, Royal Society*. 173-190

Atkinson, T.C., Ward, R.S., O'Hannelly, E., 2000. A radial flow tracer test in Chalk: comparison of models and fitted parameters. In *Tracers and Modelling in Hydrogeology, Proceedings of TraM'2000 Conference, Liege, May 2000*. Edited by Dassargues, A. IAHS publication no. **262**, 7-15

Atkinson, T.C., 2004. *Proposed groundwater tracer testing in the River Pang Catchment: Estimation of tracer concentrations at Bradfield PWS, using worst-case assumptions*. Report prepared for Thames Water.

Baker, A., Inverarity, R., Charlton, M.E. and Richmond, S., 2003. Detecting river pollution using fluorescence spectrophotometry: case studies from the Ouseburn, NE England. *Environmental Pollution* **124**, 57-70

Ballantyne., C.K., and Harris, C. 1994. *The periglaciation of Great Britain*. Cambridge University Press, Cambridge. 330 pp

Banks, D., Davies, C., and Davies, W., 1995. The Chalk as a karstic aquifer: evidence from a tracer test at Stanford Dingley, Berkshire, UK. *Quarterly Journal of Engineering Geology* **28**, S31-S38

Barker, J.A., and Foster, S.S.D., 1981. A diffusion exchange model for solute movement through fissured rock. *Quarterly Journal of Engineering Geology*. **14**, 17-24

Barker, J.A., 1991. Transport in fractured rock. In *Applied Groundwater Hydrology*. Edited by Downing, R.A., and Wilkinson, W.B. Oxford University Press. 199-216

Barker, J.A., 1993. Modelling groundwater flow and transport in the Chalk. In *The hydrogeology of the Chalk of North-West Europe*. Edited by Downing, R.A., Price, M., and Jones, G.P. 59-66

Barker, J.A., Wright, T.E.J., and Fretwell, B.A., 2000. A pulsed-velocity method of double-porosity solute transport modelling. In *Tracers and Modelling in Hydrogeology, Proceedings of TraM'2000 Conference, Liege, May 2000*. Edited by Dassargues, A. IAHS publication no. **262**, 297-302

Barnes, S. 1999. Karstic groundwater flow characteristics in the Cretaceous Chalk aquifer, Northern Ireland *Quarterly Journal of Engineering Geology* **32**, 55-68.

Barracough, D., Gardner, C.M.K., Wellings, S.R., and Cooper, J.D., 1994. A tracer investigation of fissure flow in the unsaturated zone of the British Upper Chalk. *Journal of Hydrology* **156**, 459-469

Bateman, A., 1998. *Chlorofluorocarbons in groundwater*. Unpublished PhD thesis. School of Environmental Sciences, University of East Anglia

Becker, M.W., and Shapiro, A.M., 2000. Tracer transport in fractured crystalline rock: Evidence of nondiffusive breakthrough tailing. *Water Resources Research* **36** (7) 1677-1686

Behrens, H., Beims, U., Dieter, H., Dietze, G., Eikmann, T., Grummt, T., Hanisch, H., Henseling, H., Käss, W., Kerndorff, H., Leibundgut, C., Müller-Wegener, U., Rönnefahrt, I., Scharenberg, B., Schleyer, R., Schloz, W., and Tilkes, F., 2001. Toxicological and ecotoxicological assessment of water tracers. *Hydrogeology Journal* **9**, 321-325

Beeson, S., and Cook, M.C., 2004. Nitrate in groundwater: a water company perspective. *Quarterly Journal of Engineering Geology and Hydrogeology* **37**, (4) 261-270

Bevan, T.G., and Hancock, P.L., 1986. A late Cenozoic regional mesofracture system in Southern England and northern France. *Journal of the Geological Society of London* **143**, 355-362

Bloomfield, J.P., Brewerton, L.J., and Allen, D.J., 1995. Regional trends in matrix porosity and dry density of the Chalk of England. *Quarterly Journal of Engineering Geology* **28**, S131-S142

Bloomfield, J.P., 1996. Characterisation of hydrogeologically significant fracture distributions in the Chalk: An example from the Upper Chalk of Southern England. *Journal of Hydrology* **184 (3-4)**, 355-379

Bloomfield, J.P., 1997. The role of diagenesis in the hydrogeological stratification of carbonate aquifers: An example from the Chalk at Fair Cross, Berkshire, UK. *Hydrology and Earth System Science* **1**, 19-33

Bocker, T., 1973. Dynamics of subterranean karstic flow. *Karszt-es Barlangkutatas* **8**, 107-145

Bögli, A., 1964. Mischungskorrosion: Ein Beitrag zur Verkarstungsproblem. *Erdkunde* **18**, 83-92.

Bouraoui, F and Dillaha, T.A., 1996. ANSWERS-2000: runoff and sediment transport model. *Journal of Environmental Engineering* **122**, 493-502

Boughton, W.C., 1993. A hydrograph based model for estimating the water yield of ungauged catchments. In *Hydrology and Water Resources Symposium*, Institution of Engineers, Australia, Newcastle, NSW 317-324

Boyer, D.G., 2004. Groundwater pollution: dispersed. In *Encyclopaedia of caves and karst science*. Edited by Gunn, J. 403-404

Bracq, P., and Brunin, A.S., 1999. Approche des relations tectonique-karst-hydrodynamisme par l'analyse de traçages réalisés dans l'aquifère crayeux du Boulonnais (Escalles, Nord de la France). *Geodinamica Acta* **12**, 359-370.

Bradford, R.B., 2002. Controls on the discharge of chalk streams of the Berkshire Downs, UK. *The Science of the Total Environment* **282-283**, 65-80

Bradford, R.B., Ragab, R., Crooks, S.M., Bouraoui, F., and Peters, E., 2002. Simplicity versus complexity in modelling groundwater recharge in chalk catchments. *Hydrology and Earth Systems Sciences* **6 (5)**, 927-937

Bradshaw J., Caiger N., Halpin M., Le Gear R., Pearce A., Pearman H., Reeve T. and Sowan P., 1991. *Kent and East Sussex Underground*. Kent Underground Research Group. Meresborough Books. 128pp

Brainerd, R.J., and Robins, G.A., 2004. A tracer dilution method for fracture characterisation in bedrock wells. *Groundwater* **42 (5)**, 774-780

Brettel, E.J., 1971. Report on the Lambourn Valley Pilot Scheme, 1967-1969. *Thames Conservancy Report TWA15*. 172 pp

Bricker, S., 2004. *Groundwater influences on the Chalk fed River Pang*. BSc. Thesis. Earth Sciences, University East Anglia. 40 pp

Bristow, C.R., Mortimore, R.N., and Wood, C.J., 1997. Lithostratigraphy for mapping the Chalk of Southern England. *Proceedings of the Geologists' Association* **108**, 293-315

Brouyère, S., Dassargues, A., and Hallet, V., 2004. Migration of contaminants through the unsaturated zone overlying the Hesbaye chalky aquifer in Belgium: a field investigation. *Journal of Contaminant Hydrology* **72**, 135-164

Brucker, R.W., Hess, J.W., and White, W.B., 1972. Role of vertical shafts in the movement of groundwater in carbonate aquifers. *Ground Water* **10 (6)**, 5-13

- Campbell, M., 1984. Surprise finds in the Irish Chalk. *Caves and Caving* **26**, 26
- Codrington, T. 1864. The geology of the Berks & Hants extension, and Marlborough Railways. *Wiltshire Archaeological and Natural History Magazine* **9**, 167-193.
- Chilton, P.J., Stuart, M.E., Goody, D.C., Williams, R.J., and Johnson, A.C., 2005. Pesticide fate and behaviour in the UK Chalk aquifer, and implications for groundwater quality. *Quarterly Journal of Engineering Geology* **38**, 65-81
- Christodoulou, E., 2004. *Investigation of the source of water for the Blue Pool springs, Berkshire, UK*. MSc Thesis, Water Resources Technology and Management, University of Birmingham. 125 pp
- Church, P.E., and Granato, G.E., 1996. Bias in groundwater data caused by well-bore flow in long-screen wells. *Groundwater* **34** (2), 262-273
- Cvijić, J., 1893. Das Karstphänomen. *Geographische Abhandlungen herausgegeben von A. Penck* **5** (3) 218-329.
- Darling, W.G., Morris, B., Stuart, M.E., and Goody, D.C., 2005. Groundwater age indicators from public supplies tapping the Chalk aquifer of Southern England. *Water and Environment Journal* **19**, 30-40
- Dennis, F., Andrews, J.N., Parker, A., Wolf, M., 1997. Isotope and noble gas study of chalk groundwater in the London Basin. *Applied Geochemistry* **12**, 763-773
- Dervey, A., 1985. *Beitrag zum sorptionsverhalten von fluoreszenzfarbstoffen*. Diplomarb. (Ms) Bern. 80 pp
- Docherty, J., 1971. Chalk karst. A synthesis of C.C. Fagg's theories of chalkland morphology in the light of recent hydrological research. *Proceedings of the Croydon Natural History Society* **15** (2), 21-34

Doughty, C., and Tsang, C., 2005. Signatures in flowing fluid electric conductance logs. *Journal of Hydrology* **310**, 157-180

Downing, R.A., Smith, D.B., and Warren, S.C., 1978. Seasonal variations of tritium and other constituents in groundwater in the Chalk near Brighton, England. *Journal of the Institute of Water Engineers and Scientists* **32**, 123-136

Downing, R.A., Price, M., and Jones, G.P., 1993. The making of an aquifer. In *The hydrogeology of the Chalk of North-West Europe*. Edited by Downing, R.A., Price, M., and Jones, G.P. 1-14

Dreybrodt, W., 1988. *Processes in karst systems: physics, chemistry and geology*. Berlin, Springer-Verlag. 288 pp

Dreybrodt, W and Gabrovšek, F., 2000. Dynamics of the evolution of single karst conduits. In *Speleogenesis. Evolution of Karst Aquifers*. Edited by Klimchouk, A.B., Ford, D.C., Palmer, A., and Dreybrodt, W. 184-193

Dreybrodt, W., and Siemers, J., 2000. Cave evolution on two-dimensional networks of primary fractures in limestone. In *Speleogenesis. Evolution of Karst Aquifers*. Edited by Klimchouk, A.B., Ford, D.C., Palmer, A., and Dreybrodt, W. 201-211

Dreybrodt, W., Gabrovšek, F., and Romanov, D., 2005. *Processes of speleogenesis: A modelling approach*. ZRC publishing, Karst Research Institute at ZRC SAZU. 375 pp

Drury D.F. and Wheeler, D.C., 1982. Applications of *Serratia Marcescens* bacteriophage as a new microbial tracer of aqueous environments. *Journal of Applied Bacteriology* **53**, 137-142

Edmunds, W.M., Cook, J.M., Darling, W.G., Kinniburgh, D.G., Miles, D.L., Bath, A.H., Morgan-Jones, M., and Andrew, J.N., 1987. Baseline geochemical conditions in the Chalk aquifer, Berkshire, UK: a basis for groundwater quality management. *Applied Geochemistry* **2**, 251-274

Edwards A.J., Hobbs S. and Smart P.L., 1991. Effects of quarry dewatering on a karstified limestone aquifer: A case study from the Mendip Hills, England. In: *Proceedings of the third conference on hydrogeology, ecology, monitoring, and management of groundwater in karst terranes*, National Water Well Association **77**, 77-91

Einsiedl, F., and Maloszewski., P., 2005. Tracer tests in fractured rocks with a new fluorescent dye – pyrene-1,3,6,8-tetra sulphonic acid (PTS). *Hydrological Sciences Journal* **50 (3)**, 543-555.

Elci, A., Molz, F.J., and Waldrop, W.R., 2001. Implications of observed and simulated ambient flow in monitoring wells. *Groundwater* **39 (6)**, 853-862

Elliot, T., Andrews, J.N., and Edmunds, W.M., 1999. Hydrochemical trends, palaeorecharge and groundwater ages in the fissured Chalk aquifer of the London and Berkshire Basins, UK. *Applied Geochemistry* **14**, 333-363

Evans, D.G., 1995. Inverting fluid conductivity logs for fracture inflow parameters. *Water Resources Research* **31 (12)**, 2905-2915

Ewers, R.O., 2006. Karst aquifers and the role of assumptions and authority in science. In *Perspectives on Karst Geomorphology, hydrology and geochemistry - a tribute volume to Derek C Ford and William B White*. Geological Society of America special paper 404 (edited by Harmon, R.S., and Wicks, C.M). 235-242

Fagg, C.C., 1923. The recession of the Chalk escarpment and the development of Chalk valleys in the regional survey area. *Proceedings and Transactions of the Croydon Natural History and Scientific Society* **9**, 93-112

Fetter, C.W., 2001. *Applied Hydrogeology*. 4th edition. Prentice Hall, Upper Saddle River, NJ. 691 pp

Field, M.S., Wilhelm, R.G., Quinlan, J.F., Aley, T.J., 1995. An assessment of the potential adverse properties of fluorescent tracer dyes used for groundwater tracing. *Environmental Monitoring and Assessment* **38**, 75-96

Field, M.S., 1997. Risk assessment and methodology for karst aquifers 1: estimating karst conduit-flow parameters. *Environmental Monitoring and Assessment* **47**, 1-21

Finch, J.W., 2001. Estimating change in direct groundwater recharge using a spatially distributed soil water balance model. *Quarterly Journal of Engineering Geology and Hydrogeology* **34**, 71-83

Fisher, O., 1859. On some natural pits on the heaths of Dorsetshire. *Quarterly Journal of the Geological Society of London*. **15**, 187-188

Ford, D.C., and Williams, 1989. *Karst geomorphology and hydrology*. London, Unwin Hyman. 601 pp

Ford, D.C., and Williams, 2007. *Karst hydrogeology and geomorphology*. John Wiley and Sons Ltd. 562 pp

Ford, D.C., 2000. Speleogenesis under unconfined settings. In *Speleogenesis. Evolution of Karst Aquifers*. Edited by Klimchouk, A.B., Ford, D.C., Palmer, A., and Dreybodt, W. 319-324

Ford, D., Lauritzen, S., and Ewers, R., 2000. Hardware and software modelling of initial conduit development in karst rocks. In *Speleogenesis. Evolution of Karst Aquifers*. Edited by Klimchouk, A.B., Ford, D.C., Palmer, A., and Dreybodt, W. 175-183

Ford, D.C., 2004. Karst. In *Encyclopaedia of caves and karst science*. Edited by Gunn, J. 473-475

Ford, D.C., 2006. Karst geomorphology, caves and cave deposits: A review of North American contributions during the past half century. In *Perspectives on Karst*

Geomorphology, hydrology and geochemistry - a tribute volume to Derek C Ford and William B White. Geological Society of America special paper 404 (edited by Harmon, R.S., and Wicks, C.M). 1-13

Foster, S.S.D., 1975. The Chalk groundwater tritium anomaly - a possible explanation. *Journal of Hydrology* **25**, 159-165

Foster, S.S.D., 2000. Assessing and controlling the Impacts of Agriculture on Groundwater - from Barley Barons to Beef Bans. *Quarterly Journal of Engineering Geology and Hydrogeology* **33 (4)**, 263-280

Foster, S.S.D., and Crease, R.I., 1974. Nitrate pollution of Chalk groundwater in East Yorkshire - a hydrogeological appraisal. *Journal of the institute of Water Engineers* **25**, 178-194

Foster, S.S.D., and Milton, V.A., 1974. The permeability and storage of an unconfined Chalk aquifer. *Hydrological Sciences Bulletin* **19**, 485-500

Foster, S.S.D., and Smith-Carrington, A., 1980. The interpretation of tritium in the unsaturated zone. *Journal of Hydrology* **46** 343-364

Foster, S.S.D., Chilton, P.J., and Stuart, M.E., 1991. Mechanisms of Groundwater Pollution by Pesticides. *Journal of the Institute of Water and Environmental Management* **5 (2)**, 186-193

Francis, C., and Watkins, J., 2006. *Report on the results of bacteriophage analysis undertaken for British Geological Survey*. CREH Analytical. 17 pp

Fretwell, B.A., Burgess, W.G., Barker, J.A., and Jefferies, N.L., 2005. Redistribution of contaminants by a fluctuating water table in a micro-porous double-porosity aquifer: Field observations and model simulations. *Journal of contaminant hydrology* **78**, 27-52

Gardner, C.M.K., Cooper, J.D., Wellings, S.R., Bell, J.P., Hodnett, M.G., Boyle, S.A., and Howard, M.J., 1990. Hydrology of the unsaturated zone of the chalk of south-east England. In *Chalk* Thomas Telford, London 611-618

Garnier, J.M.N., Crampon, C., Préaux, G., Porel, G., Vreulx, M., 1985. Traçage par ^{13}C , ^2H , Γ et Uranine dans la nappe de la craie sénsonienne en écoulement radial convergent (Béthune, France) *Journal of Hydrology* **78**, 379-392

Gascoine, W., 1989. The hydrology of the limestone outcrop north of the coalfield. In *Limestones and Caves of Wales*. Edited by Ford, T.D. 40-55

Gaspar, E., 1987. *Modern Trends in Tracer Hydrology, Volume II*. CRC Press, Inc., Boca Raton, FL, USA, 137 pp.

Gomme, J., Shurvell, S., Hennings, S.M., and Clark, L., 1992. Hydrology of pesticides in a Chalk Catchment. *Journal of the Institute of Water and Environmental Management* **6 (2)**, 172-178

Goody, D.C., Bloomfield, J.P., Chilton, A.C., and Williams, R.J., 2001. Assessing the herbicide concentrations in the saturated and unsaturated zone of a Chalk aquifer in Southern England. *Groundwater* **39 (2)**, 262-271

Goody, D.C., Darling, W.G., Abesser, C., and Lapworth, D.J., 2006. Using chlorofluorocarbons (CFCs) and sulphur hexafluoride (SF_6) to characterise groundwater movement and residence time in a lowland Chalk catchment. *Journal of Hydrology* **330**, Special Issue "Hydro-ecological functioning of the Pang and Lambourn catchments, UK - Results from the Lowland Catchment Research (LOCAR) initiative" edited by Wheeler. 44-52

Goudie, A., 1990. *The landforms of England and Wales*. Blackwell, Oxford. 394 pp

Goudie, A., 2001. *The nature of the Environment*. Blackwell, Oxford. 544 pp

Goyal, S.M., and Gerba, C.P., 1979. Comparative adsorption of human enteroviruses, Simian Rotavirus, and selected bacteriophages to soils. *Applied and Environmental Microbiology* **38** (2), 241-247

Grapes, T.R., Bradley, R.B., and Petts, G.E., 2005. Dynamics of river-aquifer interactions along a chalk stream: The River Lambourn, UK. *Hydrological Processes* **19** (10), 2035-2053

Grapes, T.R., Bradley, C., and Petts, G.E., 2006. Hydrodynamics of floodplain wetlands in a chalk catchment: The River Lambourn, UK. *Journal of Hydrology* **320**, 324-341

Green, P.F., Duddy, I.R., Bray, R., 1993. Elevated palaeotemperatures in the Late Cretaceous to Early Tertiary throughout the UK region identified by AFTA: implications for hydrocarbon generation. In *Petroleum Geology of North-west Europe: Proceedings of the 4th conference*. (ed J.R. Parker). Geological Society, London. 1067-1074

Griffiths et al., 2006. Streamflow generation in the Pang and Lambourn catchments, Berkshire, UK. *Journal of Hydrology* **330** (1-2) Special Issue "Hydro-ecological functioning of the Pang and Lambourn catchments, UK - Results from the Lowland Catchment Research (LOCAR) initiative" edited by Wheeler. 71-83

Gunn, J., 1981. Hydrological processes in karst depressions. *Zeitschrift für geomorphologie* **25** (3), 313-331

Gunn, J., 1983. Point recharge of limestone aquifers - a model from New Zealand karst. *Journal of Hydrology* **61**, 19-29

Halcrow, 1987. *River Pang discussion paper* (held at BGS). 35 pp

Hancock, P.L., 1985. Brittle microtectonics: principles and practice. *Journal of Structural Geology* **7**, 437-457

Hancock, J.M., 1993. The formation and diagenesis of chalk. In *The hydrogeology of the Chalk of North-West Europe*. Edited by Downing, R.A., Price, M., and Jones, G.P. 14-35

Haria, A.H., Hodnett, M.G., and Johnson A.C., 2003. Mechanism of groundwater recharge and pesticide penetration to a chalk aquifer in southern England. *Journal of Hydrology* **275**, 122-137

Harold C., 1937. The flow and bacteriology of underground water in the Lee Valley. *Metropolitan Water Board 32nd Annual Report*, 89-99.

Harvey, R.W., and Harms, H., 2002. Tracers in groundwater: use of microorganisms and microspheres. *Encyclopaedia of Environmental Microbiology* **6**, 3194-3202

Hautojärvi, A., and Vuori, S., 1992. Comments on tracer tests and data interpretation. *Rep TCO/KPA Turvallisuus Ja Tekniika Työraportti 92-01, Helsinki*.

Headworth, H.G., 1978. Hydrogeological characteristics of artesian boreholes in the Chalk of Hampshire. *Quarterly Journal of Engineering Geology* **11**, 139-144

Headworth, H.G., Puri, S, and Rampling, B.H., 1980. Contamination of a chalk aquifer by mine drainage at Tilmanstone, East Kent, UK. *Quarterly Journal of Engineering Geology* **13 (2)**, 105-117.

Headworth, H.G., Keating, T., and Packman, M.J., 1982. Evidence for a shallow highly-permeable zone in the Chalk of Hampshire. *Journal of Hydrology* **55**, 93-112

Hess, J.W., and White, W.B., 1989. Water budget and physical hydrogeology. In *Karst Hydrology: concepts from the Mammoth Cave Region* (edited by White, W.B., and White, E.L.) 105-126

Hough, M.N., Palmer, S.G., Lees, M.J., Barrie, I.A., and Weir, V., 1996. *The United Kingdom Meteorological Office rainfall and evaporation calculation system: MORECS version 2.0 (1995)*. Meteorological Office, Bracknell, UK

House, M.R., 1991. Dorset Dolines: Part 1, The higher Kingston road cutting. *Proceedings of the Dorset Natural History and Archaeological Society* **112**, 105-108

House, M.R., 1992. Dorset Dolines: Part 2, Bronkham Hill. *Proceedings of the Dorset Natural History and Archaeological Society* **113**, 149-155

House, M.R., 1996. Dorset Dolines: Part 3, Eocene pockets and gravel pipes in the Chalk of St Oswalds Bay. *Proceedings of the Dorset Natural History and Archaeological Society* **117**, 110-116

Hull, J., 1995. *A study of the Chalk aquifer of West Norfolk using groundwater tracing techniques and the single borehole tracer dilution method*. Unpublished MSc. thesis. School of Environmental Sciences, University of East Anglia. 86 pp

Ineson, J., 1962. A hydrogeological study of the permeability of the Chalk. *Journal of the Institute of Water Engineers* **16**, 449-463

Ireson, A.M., Wheater, H.S., Butler, A.P., Mathias, S.A., Finch, J., and Cooper, J.D., 2006. Hydrological processes in the Chalk unsaturated zone - insights from an intensive field monitoring programme. *Journal of Hydrology* Special Issue "Hydro-ecological functioning of the Pang and Lambourn catchments, UK - Results from the Lowland Catchment Research (LOCAR) initiative" edited by Wheater. **330**, 29-44

Institute of Hydrology. 1980. *Low Flow Studies*. Technical Report, Institute of Hydrology, Wallingford, UK.

Jardine, P.M., Sanford, W.E., Gwo, J.P., Ready, O.C., Hicks, D.S., Riggs, J.S. and Bailey, W.B., 1999. Quantifying diffusive mass transfer in fractured shale bedrock. *Water Resources Research* **35** (7), 2015-2030

Jarvis, I., and Woodruff, P.B., 1981. The phosphatic chalks and hardgrounds of Boxford and Winterbourne, Berkshire – two tectonically controlled facies in the late

Conacian to early Campian (Cretaceous) of Southern England. *Geological Magazine* **118**, 175-187

Johnson, A.C., Beison, T.J., Bhardwaj, C.L., Dixon, A., Gooddy, D.C., Haria, A.H., and White, C., 2001. Penetration of herbicides to groundwater in an unconfined chalk aquifer following normal soil applications. *Journal of Contaminant Hydrology* **53 (1-2)**, 101-117

Karasaki, K., Freifeld, B., Cohen, A., Grossenbacher, K., Cook, P., and Vasco, D., 2000. A multidisciplinary fractured rock characterisation study at Raymond field site, Raymond, CA. *Journal of Hydrology* **236 (1-2)**, 17-34

Käss, W., 1998. *Tracing technique in Geohydrology*. Rotterdam, Netherlands: A.A. Balkema. 581 pp

Kennedy, W.J., and Garrison, R.E., 1975. Morphology and genesis of nodular chalks and hardgrounds in the Upper Cretaceous of southern England. *Sedimentology* **22**, 311-286

Keswick, B.H., Wang, D.S., and Gerba, C.P., 1982. The use of microorganisms as groundwater tracers: a review. *Groundwater* **20 (2)**, 142-149

Kilner, K., and Kněžek, M., 1974. The underground runoff separation method making use of the observation of groundwater table. *Journal of Hydrology and Hydrodynamics* **22 (5)**, 457-466

Klimchouk, A., 2000. The formation of epikarst and its role in vadose speleogenesis. In *Speleogenesis. Evolution of Karst Aquifers*. Edited by Klimchouk, A.B., Ford, D.C., Palmer, A., and Dreybodt, W. 91-99

Klimchouk, A., 2004. Speleogenesis. In *Encyclopaedia of caves and karst science*. Edited by Gunn, J. 666-668

Klimchouk, A., and Jablakova, N.L., 1989. Evidence of hydrogeological significance of the epikarst zone from study of oxygen isotope composition of water, Arabika Massif, western Caucasus. *Proceedings of 10th International Congress of Speleology, Budapest* **3**, 798-799

Klimchouk, A., and Ford, D., 2000. Types of karst and evolution of hydrogeologic setting (45-53) and Lithologic and structural controls of dissolutional cave development (53-64). In *Speleogenesis. Evolution of Karst Aquifers*. Edited by Klimchouk, A.B., Ford, D.C., Palmer, A., and Dreybodd, W. 45-64

Kuntsmann, H., Kinzelbach, W., Marschall, P., and Guomin, Li., 1997. Joint inversion of tracer tests using reversed flow fields. *Journal of Contaminant Hydrology* **26**, 215-226

Laignel, B., Dupuis, E., Rodet, J., Lacroix, M., and Massei, N., 2004. An example of sedimentary filling in the chalk karst of the Western Paris Basin: Characterisation, origins and hydrosedimentary behaviour. *Zeitschrift für Geomorphologie* **48 (2)**, 219-243

Lamont-Black, J., and Mortimore, R., 1999. Predicting the distribution of dissolution pipes in the chalk of southern England using high resolution stratigraphy and geomorphological domain characterisation. *Hydrogeology and Engineering Geology of Sinkholes and Karst: Proceedings of the Seventh Multidisciplinary Conference on Sinkholes and the Engineering and Environmental Impacts of Karst*. Balkema, Rotterdam 97-102

Lamont-Black J. and Mortimore R., 2000. Dissolution tubules: A new structure from the English Chalk. *Zeitschrift für Geomorphologie* **44**, 469-489.

Lapworth, D.J., and Goody, D.C., 2006. Source and persistence of pesticides in a semi-confined chalk aquifer of southeast England. *Environmental Pollution* **144**, 1031-1044

- Lawrence, A.R., and Foster, S.S.D., 1991. The legacy of aquifer pollution by industrial chemicals: technical appraisal and policy implications. *Quarterly Journal of Engineering Geology* **24 (2)**, 231-239
- Leibindgut, C.H., and Luthi, B., 1976. Bestimmung des seihvermögens von grundwasserleitern mittels tracer. *Proceedings 3rd International Symposium on underground water tracing, Ljubjana*. 141-148
- Lewis, D.C., Kriz, G.J., and Burgy, R.H., 1966. Tracer dilution sampling technique to determine the hydraulic conductivity of fractured rock. *Water Resources Research* **2 (3)**, 533-542
- Lewis, M.A., Jones, H.K., Macdonald, D.M.J., Price, M., Barker, J.A., Shearer, T.R., Wesselink, A.J., Evans, D.J., 1993. Groundwater storage in British aquifers: Chalk. *R&D Note 169*, National Rivers Authority, Bristol.
- Limbrick, K.J., 2003. Baseline nitrate concentrations in groundwater of the Chalk of South Dorset, UK. *The Science of the Total Environment* **314-316**, 89-98
- Lloyd., J.W., 1993. United Kingdom. In *The hydrogeology of the Chalk of North-West Europe*. Edited by Downing, R.A., Price, M., and Jones, G.P. 220-250
- Longstaff, S.L., Aldous, P.J., Clark, L., Flavin, R.J., and Partington, J., 1992. Contamination of the Chalk Aquifer by Chlorinated Solvents: A Case Study of the Luton and Dunstable Area. *Journal of the Institute of Water and Environmental Management*. **6 (5)**, 541-550
- Löw, S., Kelley, V., Vomvoris, S., 1994. Hydraulic borehole characterisation through the application of moment methods to fluid conductivity logs. *Journal of Applied Geophysics* **31**, 117-131
- Lowe, D.J., 1992. Chalk caves revisited. *Cave Science, Transactions of the British Cave Research Association* **19**, 55-58

Lowe, D.J., 2000. Role of stratigraphic elements in Speleogenesis: The speleo inception concept. In *Speleogenesis. Evolution of Karst Aquifers*. Edited by Klimchouk, A.B., Ford, D.C., Palmer, A., and Dreybodd, W. 65-75

Lowe, D.J., 2004. Inception of Caves. In *Encyclopaedia of caves and karst science*. Edited by Gunn, J. 437-441

Macdonald A.M., Brewerton L. and Allen D.J., 1998. Evidence for rapid groundwater flow and karst type behaviour in the Chalk of Southern England. In: *Groundwater pollution, aquifer recharge and vulnerability*, Robins NS (Ed), Geological Society of London special publication No. **130**, 95-106.

MacDonald, A.M., and Allen, D.J., 2001. Aquifer properties of the Chalk of England. *Quarterly Journal of Engineering Geology* **34**, 371-384

Mahmood-ul-Hassan, M., and Gregory, P.J., 2002. Dynamics of water movement on Chalkland. *Journal of Hydrology* **257**, 27-41

Maliva, R.G., and Dickson, J.A.D., 1997. Ulster White Limestone Formation (Upper Cretaceous) of Northern Ireland: effects of basalt loading on chalk diagenesis. *Sedimentology* **44**, 105-112

Maloszewski, P and Zuber, A., 1985. On the theory of tracer experiments in fissured rocks with a porous matrix. *Journal of Hydrology* **79**, 333-358

Maloszewski, P., Herrmann, A., and Zuber, A., 1999. Interpretation of tracer tests performed in fractured rock of the Lange Basin, Germany. *Hydrogeology Journal* **7**, 209-218

Martin, J.M., Sreaton, E.J., and Martin, J.B., 2006. Monitoring well response to karst conduit head fluctuations: Implications for fluid exchange and matrix transmissivity in the Floridian aquifer. In *Perspectives on Karst Geomorphology, hydrology and geochemistry - a tribute volume to Derek C Ford and William B White*. Geological

Society of America special paper 404 (edited by Harmon, R.S., and Wicks, C.M). 209-217

Massei, N., Lacroix, M., Wang, H.Q., Mahler, B.J., and Dupont, J.P., 2002. Transport of suspended solids from a karstic to an alluvial aquifer: the role of the karst/alluvium interface. *Journal of Hydrology* **260**, 88-101

Massei, N., Wang, H.Q., Field, M.S., Dupont, J.P., and Rodet, J., 2006. Interpreting tracer breakthrough tailing in a conduit-dominated karstic aquifer. *Hydrogeology Journal* **14** (6), 1431-2174

Mathias, S.A., Butler, A.P., McIntyre, N., and Wheater, H.S., 2005. The significance of flow in the matrix of the Chalk unsaturated zone. *Journal of Hydrology* **310**, 62-77

Mathias, S.A., Butler, A.P., Jackson, B.M., and Wheater, H.S., 2006. Transient simulations of flow and transport in the Chalk unsaturated zone. *Journal of Hydrology* **330** Special Issue "Hydro-ecological functioning of the Pang and Lambourn catchments, UK - Results from the Lowland Catchment Research (LOCAR) initiative" edited by Wheater. 10-29

Mathias, S.A., Butler, A.P., Peach, D.W., and Williams, A.T., 2007. Recovering tracer test input functions from fluid electrical conductivity logging in fractured porous rocks. *Water Resources Research* **43** W07443

Matthews, M.C., Clayton, C.R.I., and Rigby-Jones, J., 2000. Locating dissolution features in the Chalk. *Quarterly Journal of Engineering Geology and Hydrogeology* **33**, 125-140

Maurice, L., Atkinson, T.A., Barker, J.A., Bloomfield, J.P., Farrant, A.R., and Williams, A.T., 2006. Karstic behaviour of groundwater in the English Chalk. *Journal of Hydrology* **330** Special Issue "Hydro-ecological functioning of the Pang and Lambourn catchments, UK - Results from the Lowland Catchment Research (LOCAR) initiative" edited by Wheater. 53-62.

McDowell, P.W., 1975. Detection of clay filled sinkholes in the chalk by geophysical methods. *Quarterly Journal of Engineering Geology* **8**, 303-310

Meigs, L.C., and Bauheim, R.L., 2001. Tracer tests in a fractured dolomite 1. Experimental design and observed tracer recoveries. *Water Resources Research* **37** (5), 1113-1128

Michalski, A. and Klepp, G.M., 1990. Characterisation of transmissive fractures by simple tracing of in-well flow. *Groundwater* **28** (2), 191-198

Moench, A.F., 1995. Convergent radial dispersion in a double-porosity aquifer with fracture skin: Analytical solution and application to a field experiment in fractured chalk. *Water Resources Research* **31** (8), 1823-1835

Molz, F.J., Morin, R.H., Hess, A.E., Melville, J.G., and Guven, O., 1989. The impeller flowmeter for measuring aquifer permeability variations. Evaluation and comparison with other tests. *Water Resources Research* **25**, 1677-1683

Molz, F.J., Bowman, G.K., Young, S.C., and Waldrop, W.R., 1994. Borehole flowmeters – field application and data analysis. *Journal of Hydrology* **163**, 347-371

Morel, E.H., 1980. The use of a numerical model in the management of the Chalk aquifer in the Upper Thames Basin. *Quarterly Journal of Engineering Geology* **13**, 153-165

Morin, R. H., Hess, A. E., and Paillet, F. L., 1988, Determining the distribution of hydraulic conductivity in a fractured limestone by simultaneous injection and geophysical logging. *Groundwater* **26**, 587-595.

Mortimore, R.N., 1983. The stratigraphy and sedimentation of the Turonian-Campanian in the southern province of England. *Zitteliana* **10**, 27-41

Mortimore, R.N., 1986. Stratigraphy of the Upper Cretaceous White Chalk of Sussex. *Proceedings of the Geologists Association* **97**, 97-139

Mott Macdonald, 2005. *Chieveley construction report*.

National Rivers Authority, 1993. *Chichester Chalk investigation, double packer testing*. Report by the National Rivers Authority, Southern Region

Novakowski, K.S., Bickerton, G., and Lapcevic, P., 2004. Interpretation of injection-withdrawal tracer experiments conducted between two wells in a large single fracture. *Journal of Contaminant Hydrology* **73**, 227-247

Novakowski, K., Bickerton, G., Lapcevic, P., Voralek, J., and Ross, N., 2006. Measurements of groundwater velocity in discrete rock fractures. *Journal of Contaminant Hydrology* **82**, 44-60

Owen, M., and Robinson, V.K., 1978. Characteristics and yield in fissured Chalk. *Institution of Civil Engineers, Symposium on Thames Groundwater Scheme, Paper 2* 33-49

Paillet, F.L., Hess, A.E., Cheng, C.H., and Hardin, E.L., 1987. Characterisation of fracture permeability with high-resolution vertical flow measurements during borehole pumping. *Groundwater* **25**, 28-40

Paillet, F.L., 1998. Flow modelling and permeability estimation using borehole flow logs in heterogeneous fractured formations. *Water Resources Research* **34**, 997-1010

Paillet, F.L., 2000. A field technique for estimating aquifer parameters using flow log data. *Groundwater* **38**, 510-521

Palmer, C.D., 1993. Borehole dilution tests in the vicinity of an extraction well. *Journal of Hydrology* **146**, 245-266

Palmer, A.N., 2000. Hydrogeologic control of cave patterns. In *Speleogenesis. Evolution of Karst Aquifers*. Edited by Klimchouk, A.B., Ford, D.C., Palmer, A., and Dreybodt, W. 77-90

- Patsoules, M.G., and Cripps, J.C., 1990. Survey of macro and micro faulting in Yorkshire chalk. In *Chalk: proceedings of the International Symposium, Brighton, 1989*. 87-93
- Penman, H.L., 1948. Natural evaporation from open water, bare soil and grass. *Proceedings of the Royal Society* **A193**, 120-146
- Peters, E., and Van Lanen, H.A.J., 2004. Separation of base flow from streamflow using groundwater levels – illustrated for the Pang catchment (UK). *Hydrological Processes* **19**, 921-936
- Pitrak, M., Mares, S., and Kobr, M., 2007. A simple borehole dilution technique in measuring horizontal groundwater flow. *Groundwater* **45 (1)**, 89-92
- Price, M., 1987. Fluid flow in the Chalk of England. *Geological Society Special Publication* **34**, 141-156
- Price, M., Bird, M.J., and Foster, S.S.D., 1976. Chalk pore size measurements and their significance. *Water Services* **80**, 596-600
- Price, M., Robertson, A.S., and Foster, S.S.D., 1977. Chalk permeability - a study of vertical variation using water injection tests and borehole logging. *Water Services* **81**, 603-610
- Price, M., Morris, B.L., and Robertson, A.S., 1982. A study of intergranular and fissure permeability in Chalk and Permian aquifers using double packer injection testing. *Journal of Hydrology* **54**, 401-423
- Price M., Atkinson T.C., Barker J.A., Wheeler D and Monkhouse R.A., 1992. A tracer study of the danger posed to a chalk aquifer by contaminated highway run-off. *Proceedings of the Institution of Civil Engineers: Water, Maritime, & Energy* **96**, 9-18

Price, M., Downing, R.A., and Edmonds, W.M., 1993. The Chalk as an aquifer. In *The hydrogeology of the Chalk of North-West Europe*. Edited by Downing, R.A., Price, M., and Jones, G.P. 35-59

Price, M., 1996. *Introducing groundwater*. Published by Chapman and Hall. 278 pp

Price, M., Low, R.G., and McCann, C., 2000. Mechanisms of water storage and flow in the unsaturated zone of the Chalk aquifer. *Journal of Hydrology* **233** (1-4), 54-71

Prince, H. C. 1964. The origin of pits and depressions in Norfolk. *Geography* **49**, 15-32

Procter, C., 1984. Chalk caves in Devon. *Caves and Caving* **26**, 31

Quinlan, J.F., and Ewers, R.O., 1989. Subsurface drainage in the Mammoth Cave area. In *Karst Hydrology: Concepts from the Mammoth Cave area*. Edited by White, W.B., and White, E.L. 65-103

Ragab, R., Finch, R.W., and Harding, R., 1997. Estimation of groundwater recharge to chalk and sandstone aquifers using simple soil models. *Journal of Hydrology* **190**, 19-41

Rawson, P.F., Allen, P., and Gale, A.S., 2001. The Chalk Group – a revised lithostratigraphy. *Geoscientist* **11** (1), 21

Reeve, T.J., 1976. Cave development in the chalk in St Margerets Bay, Kent. *British Cave Research Association Bulletin* **11**, 10-11

Reeve, T.J., 1977. Chalk caves in Sussex. *British Cave Research Association Bulletin* **18**, 3-4

Reeve, T.J., 1981. Beachy Head Cave. *Caves and Caving* **12**, 2-4

Reeve, T.J., 1982. Flamborough Head Cave. *Caves and Caving* **17**, 23

Reid, C., 1887. On the origin of the Chalk dry valleys and of the coombe rock. *Quarterly Journal of the Geological Society of London* **43**, 364-373

Reimus, P.W., Haga, M.J., Adams, A.I., Callahan, T.J., Turin, H.J., and Counce, D.A., 2003. Testing and parameterizing a conceptual solute transport model in a saturated fractured tuff using sorbing and nonsorbing tracers in cross-hole tracer tests. *Journal of Contaminant Hydrology* **62-63**, 613-636

Richards, H.M., and Brincker, J.A.H., 1908. The potential dangers of water derived from wells in the Chalk. *Proceedings of the Royal Society of Medicine vol i, Epidemiological Section*, 191-203

Robinson, V.K., 1976. *The hydrogeological model of the Kennet Chalk aquifer*. Thames Water Internal Report 125

Robinson, V.K., 1978. *Thames Groundwater Scheme, Test pumping of regional observation boreholes in the Kennet Valley Chalk*. Thames Water Internal Report 64

Rodet, J., 1991. *Les Karsts de la Craie. Etude Comparative*. Unpublished PhD thesis. Universite de Paris-Sorbonne

Rodet, J., Laignel, B., Massei, N., Fournier, M., and Dupont, J., 2005. The 'karstic delta' concept, as a morphological expression of climatic variations of the base level in coastal areas - the example of the Eastern English Channel region (Normandy, France). In *Proceedings of the 14th International Congress on Speleology, Athens, Greece*

Rossi, P., Dörfliger, N., Kennedy, K., Müller, I., and Aragno, M., 1998. Bacteriophages as surface and groundwater tracers. *Hydrology and Earth System Sciences* **2**, 101-110.

Rushton, K.R., Connorton, B.J., and Tomlinson, L.M., 1989. Estimation of the groundwater resources of the Berkshire Downs supported by mathematical modelling. *Quarterly Journal of Engineering Geology* **22**, 329-341

Sawicki, L., 1909. Ein Beitrag zum geographischen Zyklus im Karst. *Geographisches Zeitschrift* **15**, 185-204

Schindel, G and Hoyt, J., 2004. Groundwater pollution: point sources. In *Encyclopedia of caves and karst science*. Edited by Gunn, J. 404-405

Schijven, J.F. and Hassanizadeh, S.M., 2000. Removal of viruses by soil passage: overview of modelling, processes, and parameters. *Critical reviews in Environmental Science and Technology* **30** (1), 49-127

Schreiber, M.E., Moline, G.R., and Bahr, J.M., 1999. Using hydrochemical facies to delineate groundwater flowpaths in fractured shale. *Groundwater Monitoring and Remediation* **19** (1), 95-109

Schurch, M., and Buckley, D., 2002. Integrating geophysical and hydrochemical borehole log measurements to characterise the Chalk aquifer, Berkshire, United Kingdom. *Hydrogeology Journal* **10** (6), 610-627

Shapiro, A.M., 2002. Cautions and suggestions for geochemical sampling in fractured rock. *Groundwater Monitoring and Remediation* **22** (3), 151-164

Shuster, E.T., and White, W.B., 1971. Seasonal fluctuations in the chemistry of limestone springs: a possible means for characterising carbonate aquifers. *Journal of Hydrology* **14**, 19-128

Skilton, H. and Wheeler, D., 1988. Bacteriophage tracer experiments in groundwater. *Journal of Applied Bacteriology* **65**, 387-395

Slater, L., Zaidman, M.D., Binley, A.M., and West L.J., 1997. Electrical imaging of saline tracer migration for the investigation of unsaturated zone transport mechanisms. *Hydrology and Earth System Sciences* **1**, 291-302

Smart, C.C., 1988. Artificial tracing techniques for the determination of the structure of conduit aquifers. *Groundwater* **26**, 445-453

Smart, C.C, and Worthington. S.R.H., 2004a. Groundwater in karst. In *Encyclopaedia of caves and karst science*. Edited by Gunn, J. 394-397.

Smart, C.C, and Worthington. S.R.H., 2004b. Water tracing. In *Encyclopaedia of caves and karst science*. Edited by Gunn, J. 769-771

Smart, P.L., 1976. The use of optical brighteners for water tracing. *Transactions British Cave Research Association* **3 (2)**, 62-76

Smart, P.L., 1984. A review of the toxicity of twelve fluorescent dyes used for water tracing. *NSS Bulletin* **46**, 21-33

Smart, P.L., and Smith, D.I., 1976. Water tracing in tropical regions; the use of fluorometric techniques in Jamaica. *Journal of Hydrology* **30**, 179-195

Smart, P.L., and Laidlaw, I.M.S., 1977. An evaluation of some fluorescent dyes for water tracing. *Water Resources Research* **13 (1)**, 15-33

Smart, P.L., and Maurice, L., 2000. *Water Tracing at Penderyn, South Wales. Report for Mineral Industry Research Organisation*. 7 pp

Smith, D.B., Wearn, P.L., Richards, H.J., and Rowe, P.C., 1970. Water movement in the unsaturated zone of high and low permeability strata using natural tritium. In *Proceedings of IAEA Symposium on Isotope Hydrology, Vienna*. 73-87

Smith, D.B., and Richards, H.J., 1972. Selected Environmental studies using radioactive tracers. *Proceedings of IAEA Symposium on peaceful uses of atomic energy, IAEA, Vienna, 14* 467-480

Smith, D.B., Downing, R.A., Monkhouse, R.A., Otlet, R.L., and Pearson, F.J., 1976. The age of groundwater in the Chalk of the London Basin. *Water Resources Research* **12**, 392-404

Smith, D.I., 1975. The problem of limestone dry valleys - implications of recent work in limestone hydrology. In *Processes in Physical and Human Geography* (edited by Peel, R., Chisholm, M., and Haggett, P). 130-147

Song, L., and Atkinson, T.C., 1985. Dissolved iron in chalk groundwaters from Norfolk, England. *Quarterly Journal of Engineering Geology and Hydrogeology* **18** (3), 261-274

Sparks, B.W., 1986. *Geomorphology*. 561 pp

Sperling, C.H. B., Goudie, A.S., Stoddart, D.R., and Poole, G.G., 1977. Dolines of the Dorset chalklands and other areas in southern Britain. *Transactions of the Institute of British Geographers* **2**, 205-223

Stanton, W.I., and Smart, P.L., 1981. Repeated dye traces of underground streams in the Mendip Hills, Somerset. *Proceedings of the University of Bristol Speleological Society* **16** (1), 47-58

Stevanović, Z and Mijatović, B., 2005 (editors). *Cvijić and Karst*. Serbian Academy of Science and Arts. 405 pp

Stevenson, W., 1812. *General view of the agriculture of the county of Dorset* (London)

Sweeting, M.M., 1972. *Karst Landforms*. London, Macmillan 362 pp

Tate, T.K., Robertson, A.S., and Gray, D.A., 1970. The hydrogeological investigation of fissure flow by borehole logging techniques. *Quarterly Journal of Engineering Geology* **2**, 195-215

Tate, T.K., Robertson, A.S., and Gray, D.A., 1971. *Borehole logging investigations in the Chalk of the Lambourn and Winterbourne valleys in Berkshire*. Natural Environmental Research Council Research Report No. 5. Institute of Geological Sciences. 23 pp

Thomas, T.M., 1954. Swallow holes on the Millstone Grit and Carboniferous Limestone of the South Wales Coal-field. *Geographical Journal* **120**, 468-475

Thorez, J., Bullock, P., Catt, J.A., and Weir, A.H., 1971. The petrography and origin of deposits filling dissolution pipes in the Chalk near South Mimms, Hertfordshire. *Geological Magazine* **108**, 413-423

Toran, L., Tancredi, J.H., Herman, E.K., and White, W.B., 2006. Conductivity and sediment variation during storms as evidence of pathways to karst springs. In *Perspectives on Karst Geomorphology, hydrology and geochemistry - a tribute volume to Derek C Ford and William B White*. Geological Society of America special paper 404 (edited by Harmon, R.S., and Wicks, C.M). 169-176

Trudgill, S.T., 1985. *Limestone Geomorphology*. London, Longman. 196 pp

Tsang, C., Hufschmied, P., and Hale, F.V., 1990. Determination of fracture inflow parameters with a borehole fluid conductivity logging method. *Water Resources Research* **26 (4)**, 561-578

Van den Daele, G.F.A., Barker, J.A., Connell, L.D., Atkinson, T.C., Darling, W.G., and Cooper, J.D., 2007. Unsaturated flow and solute transport through the Chalk: Tracer test and dual permeability modelling. *Journal of Hydrology* **342 (1-2)**, 157-172

Walsh, P.T., and Ockenden, A.C., 1982. Hydrogeological observations at the Water End swallow hole complex, North Mimms, Hertfordshire. *Transactions of the British Cave Research Association* **9 (3)**, 184-194

Waltham, A.C., Simms, M.J., Farrant, A.R., and Goldie, H.S., 1997. *Karst and caves of Great Britain*. Geological Conservation Review Series. 358 pp

Waltham, A.C., and Fookes, P.G., 2003. Engineering classification of karst ground conditions. *Quarterly Journal of Engineering Geology and Hydrogeology* **36**, 101-118

Ward, R.S., 1989. *Artificial tracer and natural ²²²Rn studies of the East Anglian Chalk aquifer*. Unpublished PhD thesis, School of Environmental Sciences, University of East Anglia.

Ward, R.S., Williams, A.T., and Chadha, D.S., 1997. The use of groundwater tracers for assessment of protection zones around water supply boreholes - A case study. In *Tracer Hydrology. Proceedings of the 7th International symposium on water tracing*. Edited by A Kranjc. 369-376

Ward, R.S., Williams, A.T., Barker, J.A., Brewerton, L.J., and Gale, I.N., 1998. Groundwater tracer tests: a review and guidelines for their use in British aquifers. *British Geological Survey Technical Report WD/98/19, Environment Agency R & D Technical Report W160*.

Ward, R.S., Fletcher, S., Evers, S., and Chadha, 2000. Tracer testing as an aid to groundwater protection. In *Tracers and modelling in hydrogeology*. Edited by A Dassargues. IAHS publication no. **262**, 85-90

Waters, A., and Banks, D., The Chalk as a karstified aquifer: closed circuit television images of macrobiota. *Quarterly Journal of Engineering Geology* **30**, 143-146

Wellings, S.R., 1984. Recharge of the Upper Chalk aquifer at a site in Hampshire, England 2. Solute Movement. *Journal of Hydrology* **69**, 275-285

Wellings, S.R., and Bell, J.P., 1980. Movement of water and nitrate in the unsaturated zone of Upper Chalk near Winchester, Hants, England. *Journal of Hydrology*. **48 (1/2)**, 119-136

Wellings, S.R., and Cooper, J.D., 1983. The variability of recharge of the English Chalk. *Agricultural Water Management* **6**, 243-253

West, G., and Dumbleton, M.J., 1972. Some observations on swallow holes and mines in the Chalk. *Quarterly Journal of Engineering Geology* **5**, 171-177

West, L.J., and Odling, N.E., 2007. Characterisation of a multilayer aquifer using open well dilution tests. *Groundwater* **45** (1), 74-84

Wheater, H.S., Neal, C., and Peach, D., 2006a. Hydro-ecological functioning of the Pang and Lambourn catchments, UK: An Introduction to the special issue. *Journal of Hydrology* **330** (1-2), 1-10

Wheater, H., Butler, A., McIntyre, N., Whitehead, P., Johnes, P., Peach, D., Neal, C., Shand, P., Goody, D., Gallagher, A., Jarvie, H., Kennedy, M., Wade, A., Lloyd, A., Franklin, P., Jackson, B., Mathias, S., and Ireson, A., 2006b. Hydrogeochemical functioning of lowland permeable catchments: from process understanding to environmental management. *British Geological Survey Report*. 287 pp

White, W.B., 1988. *Geomorphology and hydrology of Karst Terrains*. New York and Oxford, Oxford University Press. 464 pp

White, W.B., 1999. Conceptual models for karstic aquifers. In *Karst Modelling* (edited by Palmer, A.N., Palmer, M.V., and Sasowsky, I.D.) 11-16

White, W.B., 2000. Development of speleogenetic ideas in the 20th century: the modern period, 1957 to the present. In *Speleogenesis. Evolution of Karst Aquifers*. Edited by Klimchouk, A.B., Ford, D.C., Palmer, A., and Dreybodt, W. 39-43

White, W.B., 2006, Fifty years of karst hydrology and hydrogeology: 1953-2003. In *Perspectives on Karst Geomorphology, hydrology and geochemistry - a tribute volume to Derek C Ford and William B White*. Geological Society of America special paper 404 (edited by Harmon, R.S., and Wicks, C.M). 139-152

Wilby, R., Greenfield, B., Glenny, C., 1994. A coupled synoptic hydrological model for climate change impact assessment. *Journal of Hydrology* **153**, 265-290

Williams, A., Bloomfield, J., Griffins, K., Butler, A., 2006. Characterising vertical variations in hydraulic conductivity within the Chalk aquifer. *Journal of Hydrology* **330** Special Issue "Hydro-ecological functioning of the Pang and Lambourn catchments,

UK - Results from the Lowland Catchment Research (LOCAR) initiative" edited by Wheater. 53-62.

Williams, P.W., 1983. The role of the subcutaneous zone in karst hydrogeology. *Journal of Hydrology* **61**, 45-67

Williams, P., 2004. Dolines. In *Encyclopaedia of caves and karst science*. Edited by Gunn, J. 304-310

Williams, R.B.G. 1987. Frost weathered mantles on the Chalk. In *Periglacial processes and landforms in Britain and Ireland*, Cambridge University Press, Cambridge, edited by Boardman, J. 127–133

Williams, J.H., and Paillet, F.L., 2002. Using flowmeter pulse tests to define hydraulic connections in the subsurface: a fractured shale example. *Journal of Hydrology* **265** (1-4), 100-117

Wimpenny, J.W.T., Cotton, N., and Stratham, M., 1972. Microbes as tracers of water movement. *Water Research* **6**, 731-739

Woods, M.A. and Aldiss, D.T., 2004. The stratigraphy of the Chalk Group of the Berkshire Downs. *Proceedings of the Geologists' Association* **115**, 249-265

Wooldridge, S.W., and Kirkaldy, J.F., 1937. The geology of the Mimms Valley. *Proceedings of the Geological Association* **28**, 31-38

Worthington, S.R.H., Davies G.J., and Ford, D.C., 2000. Matrix, fracture and channel components of storage and flow in a Paleozoic limestone aquifer. In *Groundwater Flow and Contaminant Transport in Carbonate Aquifers*, I.D. Sasowsky and C.M. Wicks, Eds., A.A. Balkema, Rotterdam, pp. 113-128.

Worthington S.R.H., Ford, D.C., and Beddows, P.A., 2000. Porosity and permeability enhancement in unconfined carbonate aquifers as a result of solution. In *Speleogenesis*.

Evolution of Karst Aquifers. Edited by Klimchouk, A.B., Ford, D.C., Palmer, A., and Dreybodt, W. 463-471

Worthington, S.R., 2001. Depth of conduit flow in unconfined carbonate aquifers. *Geology* **29** (4), 335-338

Younger, P.L., 1989. Devensian periglacial influences on the development of spatially variable permeability in the Chalk of southeast England. *Quarterly Journal of Engineering Geology* **22**, 343-354

Younger, P.L and Elliot, T., 1995. Chalk fracture system characteristics: implications for flow and solute transport. *Quarterly Journal of Engineering Geology*. **28**, S39-S50

Zaidman, M.D., Middleton, R.T., West, L.J., and Binley, A.M., 1999. Geophysical investigation of unsaturated zone transport in the Chalk in Yorkshire. *Quarterly Journal of Engineering Geology and Hydrogeology* **32(2)** 185-198